

**Synthesis, Analytical Profiles and Receptor Pharmacology of Methoxylated Derivatives and
Regioisomers of the NBOMe series of Hallucinogenic Drugs**

by

Ahmad Jarallah Almalki

A dissertation submitted to the Graduate Faculty of
Auburn University
in partial fulfillment of the
requirements for the Degree of
Doctor of Philosophy

Auburn, Alabama
April 04, 2019

Keywords: NBOMe, Synthesis, Analysis, GC-MS, Identification, Pharmacology

Copyright 2019 by Ahmad Jarallah Almalki

Approved by

Jack DeRuiter, Chair, Professor of Medicinal Chemistry
C. Randall Clark, Co-Chair, Professor of Medicinal Chemistry
Forrest Smith, Professor of Medicinal Chemistry
Tim Moore, Professor of pharmacology

Abstract

The potential for designer analogue development in the NBOMe series of drugs of abuse is very high based on the methods used to synthesize this class of compounds, and the availability of a wide variety of precursor chemicals which would allow for significant structural variation. Also, since derivatives and isomers of the NBOMe drug class are difficult to differentiate by routine analytical methods, the production of designer analogues would pose significant challenges for those involved in drug detection and identification. In this study several series of NBOMe derivatives and regioisomers were synthesized with varying substituents and substitution patterns in the phenethyl aromatic ring, the N-benzyl aromatic ring, the ethyl side chain and nitrogen atom. These compounds were prepared using the basic synthetic methods reported in the literature. GC-MS and other analytical methods were then explored to identify the specific NBOMe analogues and differentiate regioisomers within series of derivatives.

All NBOMe derivatives prepared underwent the same fragmentation pathway in the electron ionization-mass spectrum (EI-MS) giving a base peak by the cleavage of the benzylic C-N bond to yield a benzyl cation, and ions of secondary abundance from dissociation of the phenethyl C-N bond to form an iminium cation, and from loss of CH₂O from the methoxy benzyl cation. Derivatives of different molecular weight and atomic composition were readily differentiated by CI-MS and other spectroscopic means. Regioisomeric NBOMe derivatives with a single methoxy group in the N-benzyl ring could be differentiated based on the relative abundances of the benzyl cation formed in the EI-MS. Regioisomeric NBOMe derivatives with two methoxy groups in the N-benzyl ring were differentiated by EI-MS only after derivatization with TFA. TFA-derivatization resulted in the formation of unique ions in the EI-MS as well as significant differences in the relative abundance of other key fragment ions. In addition to MS methods,

regioisomeric NBOMe derivatives were also separated and identified by gas chromatographic methods.

The new NBOMe compounds synthesized were tested for their receptor affinities in a variety of assays and several were found to have nanomolar affinities and high selectivity for 5-HT₂ receptor subtypes.

Acknowledgements

First and foremost, I would like to thank ALLAH, the Almighty, the greatest of all, to give me the power, patience, and determination to accomplish this work, without his guidance in my prayers I would not be able to stay in the right track all the time.

I dedicate this thesis to my mother, Nuhair Abdulrahman Surrati, my father, Jarallah Sa'eed Almalki, my brother, Malik Jarallah Almalki for their continuous support and their endless love and care; without them I could not achieve what I achieve today.

I would like to express my gratitude to my research advisors Dr. Jack DeRuiter and Dr. C. Randall Clark, whom supported me in every step through my research career, prepared me to be a good scientist in the future and armed me with the knowledge and experience to discover the mysteries of science.

My appreciation is extended to my committee members Dr. Forrest Smith and Dr. Tim Moore for their valuable lessons and always welcoming my questions at any time.

I would like to acknowledge the important role of Dr. Douglas Goodwin as the university reader for providing me with critical notes in my dissertation and helping me to improve it.

Also, I would like to extend my gratitude to my colleagues Dr. Younis Abiedalla, for his patience in teaching me experimental research techniques during my stay at Auburn University. Also, my thanks are extended to my friends Mohammed Almaghrabi and Mansour Alturki for their wonderful friendship and letting me to mentor them.

Table of Contents

Abstract	ii
Acknowledgements	iv
Table of Contents	v
List of Tables	x
List of Figures	xiv
List of Schemes	xxii
1 Literature review	1
1.1 Introduction	1
1.2 Legal status	5
1.3 Prevalence	6
1.4 Pharmacology and Structure-Activity Relationships.....	8
1.5 NBOMe Related Toxicities and Mortality.....	13
1.6 Pharmacokinetics (ADME Properties)	15
1.7 Analytical Detection	18
1.8 Mass Spectral Analysis	20
1.9 Gas chromatography with infrared detection (GC-IRD).....	26
1.10 Nuclear magnetic resonance (NMR)	28
1.11 Synthesis and Chemistry of the NBOMes	30
1.12 Project Rationale and Specific Objectives	32
1.13 Design and Synthesis of NBOMe derivatives	33
2 Synthesis of the Target NBOMe Derivatives	35
2.1 Synthesis of N-(Methoxy)-, N-(Dimethoxy)- and N-(Methylenedioxyphenyl)benzyl-Substituted phenethylamines	35
2.2 Synthesis of the N-(Substituted)benzyl-4-Bromo-2,5-Dimethoxyphenethylamines ..	48
2.3 Synthesis of the N-(Bromo-Dimethoxysubstituted)benzyl-monomethoxyphenethylamines (eMOBNs)	54
2.4 Synthesis of the N-(Substituted)benzyl-4-Iodo-2,5-Dimethoxyphenethylamines.....	56
2.5 Synthesis of the N-(Substituted)benzyl-Dimethoxyphenpropylamines (DMPPAs)...	62

2.6	Synthesis of the N-(Substituted)benzyl-Bromo-2,5-Dimethoxyphenpropylamines ...	64
2.7	Synthesis of the N-(Substituted)benzyl-N-Methyl-2,5-Dimethoxyphenethylamines.	68
2.8	Synthesis of the (Substituted)benzyl-N-Methyl-2,5-Dimethoxyphenpropylamines ..	72
2.9	Synthesis of the deuterium and ¹³ C labeled 2,3-Dimethoxybenzaldehydes for mass spectral fragmentation studies.....	73
3	Analysis of the N-(Methoxy)benzyl-methoxyphenethylamine Series.....	77
3.1	Introduction.....	77
3.2	Mass Spectral Analysis.....	78
3.3	Gas Chromatographic Separations.....	87
4	Analysis of the N-(Methoxy)benzyl-dimethoxyphenethylamine and N-(Methoxy)benzyl-methylenedioxyphenethylamine Series	89
4.1	Introduction.....	89
4.2	Mass Spectral Analysis.....	91
4.3	Gas Chromatographic Separations.....	104
5	Analysis of the N-(dimethoxy)benzyl- and N-(methylenedioxy)benzyl-2,5-dimethoxyphenethylamine Series	107
5.1	Introduction.....	107
5.2	Mass Spectral Analysis of the N-(dimethoxy)benzyl-2,5-dimethoxyphenethylamine Series.....	108
5.3	Mass Spectral Analysis of the N-(methylenedioxy)benzyl-2,5-dimethoxyphenethylamine Series	115
5.4	Gas Chromatographic Separations.....	117
6	The N-(Substituted)benzyl-4-bromo-2,5-dimethoxyphenethylamine Series	121
6.1	Introduction.....	121
6.2	Mass Spectral Analysis.....	122
6.3	Gas Chromatographic Separations.....	133
7	The N-(Bromo-Dimethoxy)benzyl-Monomethoxyphenethylamine Series (eMOBN).....	136
7.1	Introduction.....	136
7.2	Mass Spectral Analysis.....	137
7.3	Gas Chromatographic Separations.....	146
8	The N-(Substituted)benzyl-4-iodo-2,5-dimethoxyphenethylamine Series	149
8.1	Introduction.....	149

8.2 Mass Spectral Analysis	150
8.3 Gas Chromatographic Separations.....	159
9 The N-(Methoxy)benzyl-, N-(Dimethoxy)benzyl- and N-(Methylenedioxy)benzyl-dimethoxyphenethylamine Series	163
9.1 Introduction.....	163
9.2 Mass Spectral Analysis.....	165
9.3 Gas Chromatographic Separations.....	182
10 GC-MS Analysis of Trifluoroacetamide Derivatives of the N-(Methoxy)benzyl-4-Bromo-2,5-dimethoxyphenethylamines, N-(Dimethoxy)benzyl-4-Bromo-2,5-dimethoxyphenethylamines and N-(Dimethoxy)benzyl-4-Iodo-2,5-dimethoxyphenethylamines	187
10.1 GC-MS of TFA Derivatives of the N-(Substituted)-4-X-2,5-dimethoxyphenethylamines	187
10.2 Structure-MS Studies and the m/z 263 Ion	196
10.3 GC-MS of TFA Derivatives of the N-(Substituted)-Methoxyphenethylamines	201
11 Pharmacology	212
11.1 Experimental Procedure and Data Analysis	212
11.2 Serotonin 5-HT ₁ Receptor Binding Profiles	217
11.3 Serotonin 5-HT ₂ Receptor Binding Profiles	221
11.4 Serotonin 5-HT ₃₋₇ Receptor Binding Profiles	227
11.5 Dopamine D ₁ -D ₅ Receptor Binding Profiles	232
11.6 Adrenergic Receptor Binding Profiles.....	237
11.7 Histamine Receptor Binding Profiles	241
11.8 Opioid Receptor Binding Profiles.....	245
11.9 Transporter Binding Profiles.....	249
11.10 Other Receptors	252
12 Summary and Conclusions	253
13 Experimental - Synthesis.....	263
13.1 Synthesis of deuterated vanillin	263
13.2 Synthesis of 2,5-dimethoxyphenylnitroethene (2,5-DMPNE).....	263
13.3 Synthesis of 2,5-dimethoxyphenethylamine (25DMPEA)	265
13.4 Synthesis of N-(2'-methoxy)benzyl-2,5-dimethoxyphenethylamine (25DMPEA2MB).....	266

13.5 Synthesis of 4-bromo-2,5-dimethoxyphenethylamine (4Br25DMPEA)	268
13.6 Synthesis of N-(2'-methoxy)benzyl-4-bromo-2,5-dimethoxyphenethylamine (4Br25DMPEA2MB).....	269
13.7 Synthesis of the N-(5'-Bromo-2',3'-dimethoxysubstituted)benzyl-2-methoxyphenethylamine (2MPEA5Br23DMB - eMOBNs)	270
13.8 Synthesis of the N-(Substituted)benzyl-4-Iodo-2,5-dimethoxyphenethylamines by the ICl/AgOCCF ₃ Method	271
13.9 Synthesis of N-(Substituted)benzyl-4-Iodo-2,5-dimethoxyphenethylamines by the I ₂ /Ag ₂ SO ₄ Method.....	272
13.10 Synthesis of 2,5-dimethoxyphenethylamine-N-trifluoroacetamide (Protection)..	273
13.11 Synthesis of 4-iodo-2,5-dimethoxyphenethylaminetrifluoroacetamide.....	273
13.12 Synthesis of 4-iodo-2,5-dimethoxyphenethylamine (Deprotection).....	274
13.13 Synthesis of N-(2'-methoxy)benzyl-4-iodo-2,5-dimethoxyphenethylamine (4I25DMPEA2MB)	274
13.14 Synthesis of 2,5-dimethoxyphenpropylamine (25DMPPA).....	276
13.15 Synthesis of the N-(2'-methoxy)benzyl-2,5-dimethoxyphenpropylamine (25DMPPA2MB).....	277
13.16 Synthesis of 4-bromo-2,5-dimethoxyphenpropylamine Method A (4Br25DMPPA)	278
13.17 Synthesis of 2,5-dimethoxyphenpropylamine-trifluoroacetamide (Protection): Method B	279
13.18 Synthesis of 4-bromo-2,5-dimethoxyphenpropylamine-trifluoroacetamide	279
13.19 Synthesis of 4-bromo-2,5-dimethoxyphenpropylamine (Deprotection).....	280
13.20 Synthesis of N-(2'-methoxy)benzyl-4-bromo-2,5-dimethoxyphenpropylamine..	280
13.21 Synthesis of N-Methyl-2,5-dimethoxyphenethylamine.....	282
13.22 Synthesis of (2'-methoxy)benzyl-N-methyl-2,5-dimethoxyphenethylamine: Method A (Reductive Amination).....	283
13.23 Synthesis of (2'-Methoxy)benzyl-N-methyl-2,5-dimethoxyphenethylamine: Method B (via intermediate benzoyl amides)	283
13.24 Synthesis of N-(2'-methoxy)benzyl-N-methyl-2,5-dimethoxyphenethylamine, Method C (Direct displacement).....	284
13.25 Derivatization of amines with (trifluoroacetic anhydride or pentafluoropropionic anhydride)	285
14 Experimental	286

14.1 Materials	286
14.2 Instruments.....	288
14.3 GC-Columns	290
14.4 Temperature Programs.....	290
References	295

List of Tables

Structural formula of NBOMe Derivatives.....	24
Yields and Crystallization Solvents for the Methoxy (MPNEs)-, Dimethoxy (DMPNEs)- and Methylenedioxy (MDPNEs)- phenylnitroethenes.	37
Yields for the Methoxy (MPNEs)-, Dimethoxy (DMPNEs)- and Methylenedioxy- (MDPNEs)- Phenethylamines.	40
Yields and Crystallization Solvents for the N-(Methoxy)benzyl-methoxyphenethylamines.	46
Yields and Crystallization Solvents for the N-(dimethoxy)benzyl- and N-(methylenedioxy)-benzyl-2,5-dimethoxyphenethylamines.	46
Yields and Crystallization Solvents for the N-(methoxy)benzyl-dimethoxyphenethylamines. ...	47
Yields and Crystallization Solvents for The N-(Substituted)benzyl-4-Bromo-2,5-dimethoxy-phenethylamines.	53
Yields for the N-(bromo-dimethoxy)benzyl-monomethoxyphenethylamines.....	55
Yields and Crystallization Solvents for the N-(Substituted)benzyl-4-iodo-2,5-dimethoxy-phenethylamines.	61
Yields and Crystallization Solvents for the dimethoxy- and Methylenedioxyphenyl-2-nitropropenes.....	63
Yields for the N-(Substituted)benzyl-phenpropylamines.	63
Yields and Crystallization Solvents for the N-(Substituted)benzyl-4-bromo-2,5-di-methoxyphen-propylamines.....	68
Yields for the (substituted)benzyl-N-methyl-2,5-di-methoxyphenethylamines.	71
Yields for the N-(methoxy)benzyl-N-methyl-2,5-dimethoxyphenpropylamines.	73
Common Fragmentation Pathways for the methoxy/dimethoxy substituted NBOMe derivatives.	111
Relative abundance of Fragment ions in the EI-MS of the N-(dimethoxy)benzyl-4-bromo-2,5-dimethoxyphenethyltrifluoroacetamide.	191
Relative abundance of Fragment ions in the EI-MS of the N-(dimethoxy)benzyl-4-iodo-2,5-dimethoxyphenethyl-trifluoroacetamide.....	193
Relative abundance of fragment ions in the EI-MS of 2MMPEADMBs, 3MMPEADMBs and PEADMBs.	206

Cell lines used to prepare membrane pallets for the binding assays.....	214
Experimental conditions used to determine receptor binding profiles of the NBOMe compounds at serotonin receptor subtypes.....	217
Binding Affinity of the 4H25-DMPEA Series at 5-HT ₁ Receptor Subtypes.....	218
Binding Affinity of the 4Br25-DMPEA Series at 5-HT ₁ Receptor Subtypes.	218
Binding Affinity of the 4I25-DMPEA Series at 5-HT ₁ Receptor Subtypes.	219
Binding Affinity of MPEABrDMBz (“eMOBN”) Series at 5-HT ₁ Receptor Subtypes.....	219
Experimental conditions used to determine receptor binding profiles of the NBOMe compounds at serotonin receptor subtypes 2.....	221
Binding Affinity of the 4H25-DMPEA Series at 5-HT ₂ Receptor Subtypes.....	223
Binding Affinity of the 4Br25-DMPEA Series at 5-HT ₂ Receptor Subtypes.	224
Binding Affinity of the 4I25-DMPEA Series at 5-HT ₂ Receptor Subtypes.	224
Binding Affinity of MPEABrDMBz (“eMOBN”) Series at 5-HT ₂ Receptor Subtypes.....	225
Experimental conditions used to determine receptor binding profiles of the NBOMe compounds at different serotonin receptor.....	227
Binding Affinity of the 4H25-DMPEA Series at 5-HT ₃₋₇ Receptor Subtypes.	228
Binding Affinity of the 4Br25-DMPEA Series at 5-HT ₃₋₇ Receptor Subtypes.	229
Binding Affinity of the 4I25-DMPEA Series at 5-HT ₃₋₇ Receptor Subtypes.	229
Binding Affinity of MPEABrDMBz (“eMOBN”) Series at 5-HT ₃₋₇ Receptor Subtypes.	230
Experimental conditions used to determine receptor binding profiles of the 4X25-DMPEA compounds at dopamine receptor subtypes.	233
Binding Affinity of 4H25-DMPEA Series at Dopamine Receptor Subtypes.....	235
Binding Affinity of 4Br25-DMPEA Series at Dopamine Receptor Subtypes.....	235
Binding Affinity of 4I25-DMPEA Series at Dopamine Receptor Subtypes.	236
Binding Affinity of MPEABrDMBz (“eMOBN”) Series at Dopamine Receptor Subtypes.	236
Experimental conditions used to determine receptor binding profiles of the 4X25-DMPEA compounds at adrenergic receptor subtypes.	238
Binding Affinity of the 4H25-DMPEA Series at Adrenergic-2 Receptor Subtypes.	239
Binding Affinity of the 4Br25-DMPEA Series at Adrenergic-2 Receptor Subtypes.	239
Binding Affinity of the IBr25DMPEA Series at Adrenergic-2 Receptor Subtypes.	240

Binding Affinity of MPEABrDMBz (“eMOBN”) Series at Adrenergic-2 Receptor Subtypes.	241
Experimental conditions used to determine receptor binding profiles of the 4X25-DMPEA compounds at histamine receptor subtypes.....	242
Binding Affinity of the 4H25-DMPEA Series at Histamine Receptor Subtypes.	242
Binding Affinity of the 4Br25-DMPEA Series at Histamine Receptor Subtypes.	243
Binding Affinity of the 4I25-DMPEA Series at Histamine Receptor Subtypes.....	243
Binding Affinity of MPEABrDMBz (“eMOBN”) Series at Histamine Receptor Subtypes.	245
Experimental conditions used to determine receptor binding profiles of the 4X25-DMPEA compounds at opioid receptor subtypes.....	246
Binding Affinity of the 4H25-DMPEA Series at Opioid Receptor Subtypes.	247
Binding Affinity of the 4Br25-DMPEA Series at Opioid Receptor Subtypes.	247
Binding Affinity of the IBr25DMPEA Series at Opioid Receptor Subtypes.	248
Binding Affinity of MPEABrDMBz (“eMOBN”) Series at Opioid Receptor Subtypes.....	248
Experimental conditions used to determine receptor binding profiles of the 4X25-DMPEA compounds at transporter subtypes.....	249
Binding Affinity of the 4H25-DMPEA Series at Transporters.	250
Binding Affinity of the 4Br25-DMPEA Series at Transporters.	250
Binding Affinity of the IBr25DMPEA Series at Transporters.	251
Binding Affinity of MPEABrDMBz (“eMOBN”) Series at Transporters.....	251
Yields and Crystallization Solvents for the Methoxy (MPNEs)-, Dimethoxy (DMPNEs)- and Methylenedioxy- (MDPNEs)- phenylnitroethenes.....	264
Yields and Crystallization Solvents for the dimethoxy- and Methylenedioxyphenyl-2-nitropropenes.....	264
Yields for the Methoxy (MPNEs)-, Dimethoxy (DMPNEs)- and Methylenedioxy (MDPNEs)- Phenethylamines.	266
Yields and Crystallization Solvents for the N-(Methoxy)benzyl-methoxyphenethylamines.	267
Yields and Crystallization Solvents for the N-(dimethoxy)benzyl- and N-(methylenedioxy)-benzyl-2,5-dimethoxyphenethylamines.	267
Yields and Crystallization Solvents for the N-(methoxy)benzyl-dimethoxy-phenethylamines.	268
Yields and Crystallization Solvents for the N-(Substituted)benzyl-4-Bromo-2,5-dimethoxyphenethylamines.	270

Yields for the N-(bromo-dimethoxy)benzyl-monomethoxyphenethylamines.....	271
Yields and Crystallization Solvents for the N-(Substituted)benzyl-4-iodo-2,5-dimethoxyphenethylamines.	275
Yields for the N-(Substituted)benzyl-substituted-phenpropylamines.	278
Yields and Crystallization Solvents for the N-(Substituted)benzyl-4-bromo-2,5-di-methoxyphenpropylamines.....	281
List of columns used and their composition.	290
List of temperature programs used for system 1.....	291
List of temperature programs used for system 2.....	292
List of temperature programs used for system 3.....	292

List of Figures

Global emergence of new psychoactive substances up to December 2018.....	1
Proportion of new psychoactive substances by psychoactive effect group as of December 2018. 2	
Structures of LSD, psilocybin, DOB, DOM, mescaline, and 2C-X class.....	4
Structures of 2C-X and 25X-NBOMe hallucinogens.	5
Blotter sheets presenting 3 different artwork patterns containing a mixture of 25I-NBOMe, 25C-NBOMe and 25H-NBOMe.....	7
Plasma membrane monoamine reuptake transporters (DAT, SERT and NET).	8
Serotonin 5-HT ₂ receptors.	10
EI mass spectrum of 25B-NBOM HCL salt	20
EI mass spectrum of 25I-NBOM HCL salt.....	21
EI mass spectrum of 25C-NBOM HCL salt	21
Mass spectra of (a) 2,5-dimethoxy-4-bromo-N-(2'-methoxy)benzyl-phenethylamine (25B-NB2OMe) 4, (b) 2,5-dimethoxy-4-bromo-N-(3'-methoxy)benzyl-phenethylamine (25B-NB3OMe) 5, and (c) 2,5-dimethoxy-4-bromo-N-(4'-methoxy)benzyl-phenethylamine (25B-NB4OMe)	25
FTIR spectra of (a) 2,5-dimethoxy-4-bromo-N-(2'-methoxy)benzyl-phenethylamine HCl (25B-NB2OMe) 4, (b) 2,5-dimethoxy-4-bromo-N-(3'-methoxy)benzyl-phenethylamine HCl (25B-NB3OMe) 5, and (c) 2,5-dimethoxy-4-bromo-N-(4'-methoxy)benzyl-phenethylamine HCl (25B-NB4OMe)	27
NMR spectrum of 25B-NBOMe HCl salt	29
General skeleton of NBOMes derivatives.	33
Mass Spectra of the 2-monomethoxy nitroethene.	38
Mass Spectra of the 2,5-dimethoxy nitroethene.	38
Mass Spectra of the 3,4-methylenedioxy nitroethene.....	39
NMR Spectra of the 2,5-dimethoxy nitroethene.....	39
Mass Spectra of the 2-monomethoxyphenethylamine.....	41
Mass Spectra of the 2,5-dimethoxyphenethylamine.....	42
Mass Spectra of the 3,4-methylenedioxyphenethylamine.....	42

NMR Spectra of the 2,5-dimethoxyphenethylamine.	43
NMR spectrum of N-4-methoxybenzyl-2,5-Dimethoxyphenethylamines.	43
Structures of the N-(substituted)benzyl-4-bromo-2,5-dimethoxyphenethylamine Series.	48
Proton NMR of the 2,5-dimethoxyphenethylamine and 4-bromo-2,5-dimethoxyphenyl-amine intermediates.	51
Structures of the N-(substituted)benzyl-4-iodo-2,5-dimethoxyphenethylamine Series.	56
Proton NMR of the 2,5-dimethoxyphenethylamine and 4-iodo-2,5-dimethoxyphenethylamine intermediates.	59
Structures of the N-(methoxy)benzyl-dimethoxyphenpropylamine Series.	64
Gas chromatography and mass spectrometry of product obtained from reaction of 2,5-dimethoxyphenpropylamine with bromine-acetic acid.	66
Mass spectra of A) 2,3-dimethoxybenzaldehyde, B) 2-OCD ₃ ,3-methoxybenzaldehyde, C) 3-OCD ₃ ,2-methoxybenzaldehyde.	74
Mass spectra of A) 2,3-dimethoxybenzaldehyde, B) 2-O ¹³ CH ₃ ,3-methoxybenzaldehyde, C) 3-O ¹³ CH ₃ ,3-methoxybenzaldehyde.	76
Structures of the N-(methoxy)benzyl-methoxyphenethylamine Series.	77
CI-MS of Mass Spectra of the N-2'-methoxybenzyl-2-methoxyphenethylamines.	78
Mass Spectra of the N-(monomethoxy)benzyl-2-methoxyphenethylamines.	79
Mass Spectra of the N-(monomethoxy)benzyl-3-methoxyphenethylamines.	79
Mass Spectra of the N-(monomethoxy)benzyl-4-methoxyphenethylamines.	80
MS-MS of the 150 ion (top) and 121 ion (bottom) of the N-(methoxy)benzyl-methoxyphenethylamines.	81
Structures of the simplified derivatives.	82
EI-MS of Mass Spectra of the N-benzyl-phenethylamine (Compound 10).	84
EI-MS of Mass Spectra of the N-benzyl-2-methoxyphenethylamine (Compound 11).	84
EI-MS of Mass Spectra of the N-(2'-methoxy)benzyl-phenethylamine (Compound 12).	85
EI-MS of Mass Spectra of the N-benzyl-methylphenethylamine (Compound 13).	85
EI-MS of Mass Spectra of the (2'-methoxy)benzyl-N-methylphenethylamine (Compound 14).	86
EI-MS of Mass Spectra of the N-2-(3'-methoxy)phenethyl-N-phenethylamine (Compound 15)	86
Gas chromatographic separation of the N-(monomethoxy)benzyl-methoxyphenethylamines.	87
Gas chromatographic separation of the N-(monomethoxy)benzyl-methoxyphenethylamines.	88

Structures of the N-(methoxy)benzyl-dimethoxyphenethylamine Series.....	90
Structures of the N-(methoxy)benzyl-methylenedioxyphenethylamine Series.....	90
Representative CI-MS of Mass Spectra of the N-(2'-methoxy)benzyl-2,5-dimethoxyphenethylamines.....	91
Mass Spectra of the N-(2'-methoxy)benzyl-dimethoxyphenethylamines.....	92
Mass Spectra of the N-(3'-methoxy)benzyl-dimethoxyphenethylamines.....	93
Mass Spectra of the N-(4'-methoxy)benzyl-dimethoxyphenethylamines.....	94
MS-MS results of for 23DMPEA2MB and fragment ions m/z 121 and 91.....	96
Structures of the simplified derivatives.....	97
EI-MS of Mass Spectra of the N-benzyl-2,5-dimethoxyphenethylamine (Compound 25).....	97
EI-MS of Mass Spectra of the N-(2',5'-dimethoxy)benzyl-phenethylamine (Compound 26).....	98
EI-MS of Mass Spectra of the (2'-monomethoxy)benzyl-N-methyl-2,5-dimethoxyphenethylamine (Compound 27).....	98
EI-MS of Mass Spectra of the (2'-monomethoxy)benzyl-N-methyl-2,5-dimethoxyphenpropylamine (Compound 28).....	99
Representative CI-MS of Mass Spectra of the N-(2'-methoxy)benzyl-2,3-methylenedioxyphenethylamines.....	101
Mass Spectra of the N-(methoxy)benzyl-2,3-methylenedioxyphenethylamines.....	102
Mass Spectra of the N-(methoxy)benzyl-3,4-methylenedioxyphenethylamines.....	103
Gas chromatographic separation of the N-(monomethoxy)benzyl-dimethoxyphenethylamines	105
Gas chromatographic separation of the N-(monomethoxy)benzyl-2,3-methylenedioxyphenethylamines.....	106
Gas chromatographic separation of the N-(monomethoxy)benzyl-3,4-methylenedioxyphenethylamines.....	106
Structures of the N-(methoxy)benzyl-2,5-dimethoxyphenethylamine Series.....	107
CI-MS of Mass Spectra of the N-2',5'-dimethoxybenzyl-2,5-dimethoxyphenethylamine.....	108
Mass Spectra of the N-(dimethoxy)benzyl-2,5-dimethoxyphenethylamines.....	109
Exact mass determination for the m/z 136 ion using high resolution mass spectrometry (HRMS).....	111
Mass Spectra of ^{13}C labeled N-(2',3'-dimethoxy)benzyl-2,5-dimethoxyphenethylamines.....	114
Mass Spectra of the N-(methylenedioxy)benzyl-2,5-dimethoxyphenethylamines.....	115

CI-MS of Mass Spectra of N-2',3'methylenedioxybenzyl-2,5-dimethoxyphenethylamine.....	116
Gas chromatographic separation of the N-(dimethoxy)benzyl-2,5-dimethoxyphenethylamine regioisomers.....	118
Gas chromatographic separation of the derivatized N-trifluoroacetamide-(dimethoxy)benzyl-2,5-dimethoxyphenethylamines.....	119
Gas chromatographic separation of the N-(methylenedioxy)benzyl-2,5-dimethoxyphenethylamines.....	120
Structures of the N-(substituted)benzyl-4-bromo-2,5-dimethoxyphenethylamine Series.....	121
Mass Spectra of the N-(monomethoxy)benzyl-4-bromo-2,5-dimethoxyphenethylamines.....	122
CI-MS of Mass Spectra of the N-2'-methoxybenzyl-4-bromo-2,5-dimethoxyphenethylamines	123
MS-MS of the 121 ion.....	124
Fragmentation pathway of the 2-methoxy "eMOBN" Derivative.....	125
High mass region of bromine-containing fragment ions in the EI-MS of the N-(monomethoxy)-benzyl-4-bromo-2,5-dimethoxyphenethylamines.....	126
Mass Spectra of the N-(dimethoxy)benzyl-4-bromo-2,5-dimethoxyphenethylamines.....	128
CI-MS of Mass Spectra of N-(dimethoxy)benzyl-4-bromo-2,5-dimethoxyphenethylamine.....	129
Mass Spectra of the N-(methylenedioxy)benzyl-4-bromo-2,5-dimethoxyphenethylamines.....	131
CI-MS of Mass Spectra N-(methylenedioxy)benzyl-4-bromo-2,5-dimethoxyphenethylamine series.....	132
Gas chromatographic separation of the N-(monomethoxy)benzyl-4-bromo-2,5-dimethoxyphenethylamines.....	133
Gas chromatographic separation of the N-(dimethoxy)benzyl-4-bromo-2,5 dimethoxyphenethylamines.....	134
Gas chromatographic separation of the N-(methylenedioxy)benzyl-4-bromo-2,5-dimethoxyphenethylamines.....	135
Structures of the N-(bromo-dimethoxy)benzyl-monomethoxyphenethylamine series.....	136
CI-MS of Mass Spectra of the N-(4'-bromo-2',5'-dimethoxy)benzyl-2-methoxyphenethylamines.....	137
MS-MS of the <i>m/z</i> 229 ion.....	139
Mass Spectra of the N-(5'-bromo-2',3'-dimethoxy)benzyl-monomethoxyphenethylamines.....	141
Mass Spectra of the N-(2'-bromo-4',5'-dimethoxy)benzyl-monomethoxyphenethylamines.....	142
Mass Spectra of the N-(5'-bromo-2',4'-dimethoxy)benzyl-monomethoxyphenethylamines.....	143

Mass Spectra of the N-(4'-bromo-2',5'-dimethoxy)benzyl-monomethoxyphenethylamines. ...	144
Mass Spectra of the N-(3'-bromo-4',5'-dimethoxy)benzyl-monomethoxyphenethylamines. ...	145
Gas chromatographic separation of the N-(5'-bromo-2',3'-dimethoxy)benzyl-monomethoxyphenethylamines.	146
Gas chromatographic separation of the N-(2'-bromo-4',5'-dimethoxy)benzyl-monomethoxyphenethylamines.	147
Gas chromatographic separation of the N-(5'-bromo-2',4'-dimethoxy)benzyl-monomethoxyphenethylamines.	147
Gas chromatographic separation of the N-(4'-bromo-2',5'-dimethoxy)benzyl-monomethoxyphenethylamines.	148
Gas chromatographic separation of the N-(3'-bromo-4',5'-dimethoxy)benzyl-monomethoxyphenethylamines.	148
Structures of the N-(substituted)benzyl-4-iodo-2,5-dimethoxyphenethylamine Series.	149
Mass Spectra of the N-(monomethoxy)benzyl-4-iodo-2,5-dimethoxyphenethylamines.....	150
CI-MS of Mass Spectra of the N-2'-methoxybenzyl-4-iodo-2,5-dimethoxyphenethylamines. .	151
MS-MS of the 121 ion.	152
High mass region iodine-containing fragment ions in the EI-MS of the N-(monomethoxy)benzyl-4-iodo-2,5-dimethoxyphenethylamines.	153
Mass Spectra of the N-(dimethoxy)benzyl-4-iodo-2,5-dimethoxyphenethylamines.....	155
CI-MS of Mass Spectra of N-2,5-dimethoxybenzyl-4-iodo-2,5-dimethoxyphenethylamine.	156
Mass Spectra of the N-(methylenedioxy)benzyl-4-iodo-2,5-dimethoxyphenethylamines.	157
CI-MS of Mass Spectra N-(2,3-methylenedioxy)benzyl-4-iodo-2,5-dimethoxyphenethylamine series.	158
Gas chromatographic separation of the N-(monomethoxy)benzyl-4-iodo-2,5-dimethoxyphenethylamines.	160
Gas chromatographic separation of the N-(dimethoxy)benzyl-4-iodo-2,5-dimethoxyphenethylamines.	161
Gas chromatographic separation of the N-(methylenedioxy)benzyl-4-iodo-2,5-dimethoxyphenethylamines.	162
Structures of the N-(methoxy)benzyl-dimethoxyphenpropylamine Series.	163
Structures of the N-(methoxy)benzyl-dimethoxyphenpropylamine and N-(methoxy)benzyl-methylenedioxyphenpropylamine Series.	164

Mass Spectra of the N-(monomethoxy)benzyl-2,5-dimethoxyphenpropylamines.	166
Mass Spectra of the N-(monomethoxy)benzyl-2,3-dimethoxyphenpropylamines.	167
Mass Spectra of the N-(monomethoxy)benzyl-2,6-dimethoxyphenpropylamines.	168
CI-MS of mass spectra of the N-2'-methoxybenzyl-2,5-dimethoxyphenpropylamines.	169
MS-MS of the 121 ion.	170
Mass Spectra of the N-(monomethoxy)benzyl-3,4-methylenedioxyphenpropylamines.	171
CI-MS of Mass Spectra N-(2'-methoxy)benzyl-3,4-methylenedioxyphenpropylamine series..	172
Structures of the simplified derivatives.	173
EI-MS of Mass Spectra of the N-(2',5'-dimethoxy)benzyl-3,4-methylenedioxyphenpropylamines (Compound 21).	173
EI-MS of Mass Spectra of the N-(4'-Bromo-2',5'-dimethoxy)benzyl-3,4-methylenedioxy- phenpropylamines (Compound 22).	174
EI-MS of Mass Spectra of the N-(2'-monomethoxy)benzyl-2-Bromo-4,5-dimethoxyphen- propylamine (Compound 23).	174
Mass Spectra of the N-(dimethoxy)benzyl-2,5-dimethoxyphenpropylamines.	177
CI-MS of Mass Spectra of N-2,3-dimethoxybenzyl-2,5-dimethoxyphenpropylamine.	178
Mass Spectra of the N-(methylenedioxy)benzyl-2,5-dimethoxyphenpropylamines.	180
CI-MS of Mass Spectra N-3,4-methylenedioxybenzyl-2,5-dimethoxyphenpropylamine series.	181
Gas chromatographic separation of the N-(monomethoxy)benzyl-2,5-dimethoxyphen- propylamines.	182
Gas chromatographic separation of the N-(monomethoxy)benzyl-2,3-dimethoxyphen- propylamines.	183
Gas chromatographic separation of the N-(monomethoxy)benzyl-2,6-dimethoxyphen- propylamines.	184
Gas chromatographic separation of the N-(monomethoxy)benzyl-3,4-methylenedioxyphen- propylamines.	184
Gas chromatographic separation of the N-(dimethoxy)benzyl-2,5 dimethoxyphenyl-propylamines.	185
Gas chromatographic separation of the N-(methylenedioxy)benzyl-2,5-dimethoxyphen- propylamines.	186
Mass Spectra of the N-(methoxy)benzyl-4-bromo-2,5-dimethoxyphenethyltrifluoroacetamide regioisomers.	187

Mass Spectra of the N-(dimethoxy)benzyl-4-bromo-2,5-dimethoxyphenethyltrifluoroacetamide regioisomers.....	190
Mass Spectra of the N-(dimethoxy)benzyl-4-iodo-2,5-dimethoxyphenethyltrifluoroacetamide regioisomers.....	195
Exact mass determination for the m/z 263 ion using high resolution mass spectrometry (HRMS).	196
N-(2',5'-dimethoxy)benzyl-4-bromo-2,5-dimethoxyphenethylpentafluoropropionamide.....	198
N-(2',5'-dimethoxy)benzyl-2,5-dimethoxyphenethyltrifluoroacetamide.....	198
N-(2',5'-dimethoxy)benzyl-4-bromo-2,5-dimethoxyphenethyltrifluoroacetamide.....	199
N-(3'-methyl-4'-methoxy)benzyl-4-bromo-2,5-dimethoxyphenethyltrifluoroacetamide.....	200
N-(3'-methoxy-4'-methyl)benzyl-4-bromo-2,5-dimethoxyphenethyltrifluoroacetamide.....	201
EI-MS of the 2MMPEADMB regioisomers.....	203
EI-MS of the 3MMPEADMB regioisomers.....	204
EI-MS of the PEADMB regioisomers.....	205
Gas chromatographic separation of the derivatized N-trifluoroacetamide-N-(dimethoxy)benzyl-phenethylamines.....	211
Schematic of binding assay plate. Increasing concentrations (0.01 nM to 10 μ M, from left to right) of reference or test compound are added (50 μ L aliquots, in duplicate) from 5x stocks to wells containing 50 μ L of 5x radioligand (fixed concentration, prepared in buffer) and 100 μ L of buffer. Finally, 50 μ L of receptor-containing membrane homogenate (5x suspension in buffer) are added to achieve a final assay volume of 250 μ L.....	215
Dose response curves for the most potent 4X25DMPEA derivatives at 5-HT ₁ receptor subtypes.	220
Dose response curves for the most potent 4X25DMPEA derivatives at 5-HT ₂ receptor subtypes.	226
Dose response curves for the most potent 4X25DMPEA derivatives at 5-HT ₃₋₇ receptor subtypes.	231
Dose response curves for the most potent 4X25DMPEA derivatives at dopamine receptor subtypes.....	237
NBOMe derivatives.....	253
N-(monomethoxy)benzyl-monomethoxyphenethylamine series.....	254
N-(monomethoxy)benzyl-dimethoxyphenethylamine series.....	255
N-(dimethoxy)benzyl-2,5-dimethoxyphenethylamines.....	257

N-(monomethoxy)benzyl- and N-(dimethoxy)benzyl-4-bromo-2,5-dimethoxyphenethylamine series.	258
N-(monomethoxy)benzyl- and N-(dimethoxy)benzyl-4-iodo-2,5-dimethoxyphenethylamine series.	260
TFA-acetamide derivatives of the 4-unsubstituted, 4-bromo- and 4- iodo- N-benzyl-dimethoxy regioisomers of series 3, 4 and 5.....	260
2',3'- or 3', 4'-methylenedioxy N-Benzyl ring Substituted NBOMe derivatives.	261
Alpha and N-methyl substituted NBOMe derivatives.	262

List of Schemes

The metabolic pathways for 25I-NBOMe	17
Proposed EI-MS fragmentation pathway for the N-(monomethoxy)benzyl-4-bromo-2,5-dimethoxyphenethylamines.	22
Proposed EI-MS fragmentation pathway for the N-(monomethoxy)benzyl-4-bromo-2,5-dimethoxyphenethylamines.	22
general synthetic scheme for 25X-NBOMes.	31
Synthetic approach for the methoxy-, dimethoxy- and methylenedioxy-substituted N-benzylphenethylamines.	35
Synthetic approach for the methoxy-, dimethoxy- and methylenedioxy-substituted phenethylamine intermediates.	36
Synthesis of the Methoxy-, Dimethoxy- and Methylenedioxy-N-Benzylphenethylamines.	45
Initial synthetic approach for the N-(substituted)benzyl-4-bromo-2,5-dimethoxyphenethylamine Series.	49
Initial synthetic approach for the 4-bromo-2,5-dimethoxyphenethylamine intermediate.	49
Second synthetic approach for the 4-bromo-2,5-dimethoxyphenethylamine intermediate.	50
Synthesis of the N-(substituted)benzyl-4-bromo-2,5-dimethoxyphenethylamine Series.	52
Synthesis of the N-(bromo-dimethoxy)benzyl-monomethoxyphenethylamines.	54
Initial synthetic approach for the N-(substituted)benzyl-4-iodo-2,5-dimethoxyphenethylamine Series.	57
Initial synthetic approach for the 4-iodo-2,5-dimethoxyphenethylamine intermediate.	58
Second synthetic approach for the 4-iodo-2,5-dimethoxyphenethylamine intermediate.	58
Synthesis of the N-(substituted)benzyl-4-iodo-2,5-dimethoxyphenethylamine Series.	60
Synthesis of the N-(Substituted)benzyl-dimethoxy- and methylenedioxyphenpropylamines.	62
Initial synthetic approach for the 4- bromo-2,5-dimethoxyphenpropylamines intermediate.	67
Synthesis of the N-(Substituted)benzyl-bromo-2,5-dimethoxyphenpropylamines.	67
Initial synthetic approach for the (substituted)benzyl-N-methyl-2,5-dimethoxyphenethylamines series.	69
Synthesis of the N-methyl-2,5-dimethoxyphenethylamine.	69

Initial synthetic approach for the synthesis of (substituted)benzyl-N-methyl-2,5-di-methoxyphenethylamines.	70
Synthesis of the (substituted)benzyl-N-methyl-2,5-dimethoxyphenethylamines.	70
Synthesis of the (substituted)benzyl-N-methyl-2,5-dimethoxyphenpropylamines.	72
Synthesis of deuterated 2,3-dimethoxybenzaldehyde.....	73
Synthesis of deuterated 2,3-dimethoxybenzaldehyde.....	75
Proposed EI-MS fragmentation pathway for the N-(methoxy)benzyl-methoxyphenethylamines.	80
Proposed EI-MS fragmentation pathway for the ring and N-substituted-benzyl-methoxyphenethylamines.	83
Proposed EI-MS fragmentation pathway for the N-(monomethoxy)benzyl-dimethoxyphenethylamines.	95
Proposed EI-MS fragmentation pathway for Compounds 25-27.	100
Proposed EI-MS fragmentation pathway for the N-(methoxy)benzyl-monomethoxyphenethylamines.	104
Proposed EI-MS fragmentation pathway for the N-(dimethoxy)benzyl-2,5-dimethoxyphenethylamines.	110
Proposed Mechanism for the formation of the <i>m/z</i> 136 ion.....	112
Proposed EI-MS fragmentation pathway for the N-(methylenedioxy)benzyl-2,5-dimethoxyphenethylamines.	116
Derivatization technique.	118
Proposed EI-MS fragmentation pathway for the N-(monomethoxy)benzyl-4-bromo-2,5-dimethoxyphenethylamines.	123
Proposed EI-MS fragmentation pathway for the N-(4'-bromo-2',5'-dimethoxy)benzyl-2-methoxyphenethylamine.	126
Proposed EI-MS fragmentation pathway for the N-(monomethoxy)benzyl-4-bromo-2,5-dimethoxyphenethylamines.	127
Proposed EI-MS fragmentation pathway for the N-(dimethoxy)benzyl-4-bromo-2,5-dimethoxyphenethylamines.	130
Proposed EI-MS fragmentation pathway for the N-(methylenedioxy)benzyl-4-bromo-2,5-dimethoxyphenethylamines.	132
Proposed EI-MS fragmentation pathway for the N-(bromo-dimethoxy)benzyl-monomethoxyphenethylamines.	138

Proposed formation of the m/z 214/216 ion from the N-(5'-bromo-2',3'-dimethoxy)benzyl-monomethoxyphenethylamines.	139
Proposed EI-MS fragmentation pathway for the N-(monomethoxy)benzyl-4-iodo-2,5-dimethoxyphenethylamines.	152
Proposed EI-MS fragmentation pathway for the N-(monomethoxy)benzyl-4-iodo-2,5-dimethoxyphenethylamines.	154
Proposed EI-MS fragmentation pathway for the N-(dimethoxy)benzyl-4-iodo-2,5-dimethoxyphenethylamines.	156
Proposed EI-MS fragmentation pathway for the N-(methylenedioxy)benzyl-4-iodo-2,5-dimethoxyphenethylamines.	159
Proposed EI-MS fragmentation pathway for the N-(monomethoxy)benzyl-dimethoxyphenpropylamines.	169
Proposed EI-MS fragmentation pathway for the N-(monomethoxy)benzyl- 3,4-methylenedioxyphenpropylamines.	172
Proposed EI-MS fragmentation pathway for Compounds 25-27.	176
Proposed EI-MS fragmentation pathway for the N-(dimethoxy)benzyl-2,5-di-methoxyphenpropylamines.	179
Proposed EI-MS fragmentation pathway for the N-(methylenedioxy)benzyl- 2,5-dimethoxyphenpropylamines.	181
Proposed EI-MS fragmentation pathway for the N-(methoxy)benzyl-4-Bromo-2,5-dimethoxyphenethyltrifluoroacetamide.	189
Proposed EI-MS fragmentation pathway for the N-(dimethoxy)benzyl-4-bromo-2,5-dimethoxyphenethyltrifluoroacetamide.	191
Structure of the N-(2',5'-dimethoxy)benzyltrifluoroacetamide m/z 263 ion.	196
Proposed conjugation for the N-2',5'-dimethoxybenzyltrifluoroacetamide.	197
preferentially fragmentation of m/z 136 over 263 ion.	197
NBOMe derivatives with modified phenethyl aromatic ring substituents.	202
Mass spectral fragmentation pathways for TFA-derivatives of NBOMe analogs.	207
The m/z 105 fragment.	210

1 Literature review

1.1 Introduction:

The use of illegal drugs continues to increase worldwide with nearly 275 million (5%) of the global population between the ages 15-64 years reported to have used drugs at least once a year [1]. Cannabis, cocaine, ecstasy and amphetamines remain the most frequently used illicit drugs [2]. Mortality related to illegal drug use increased by 60% from 2000 to 2015 [1], with nearly 450,000 deaths reported in 2015 [3].

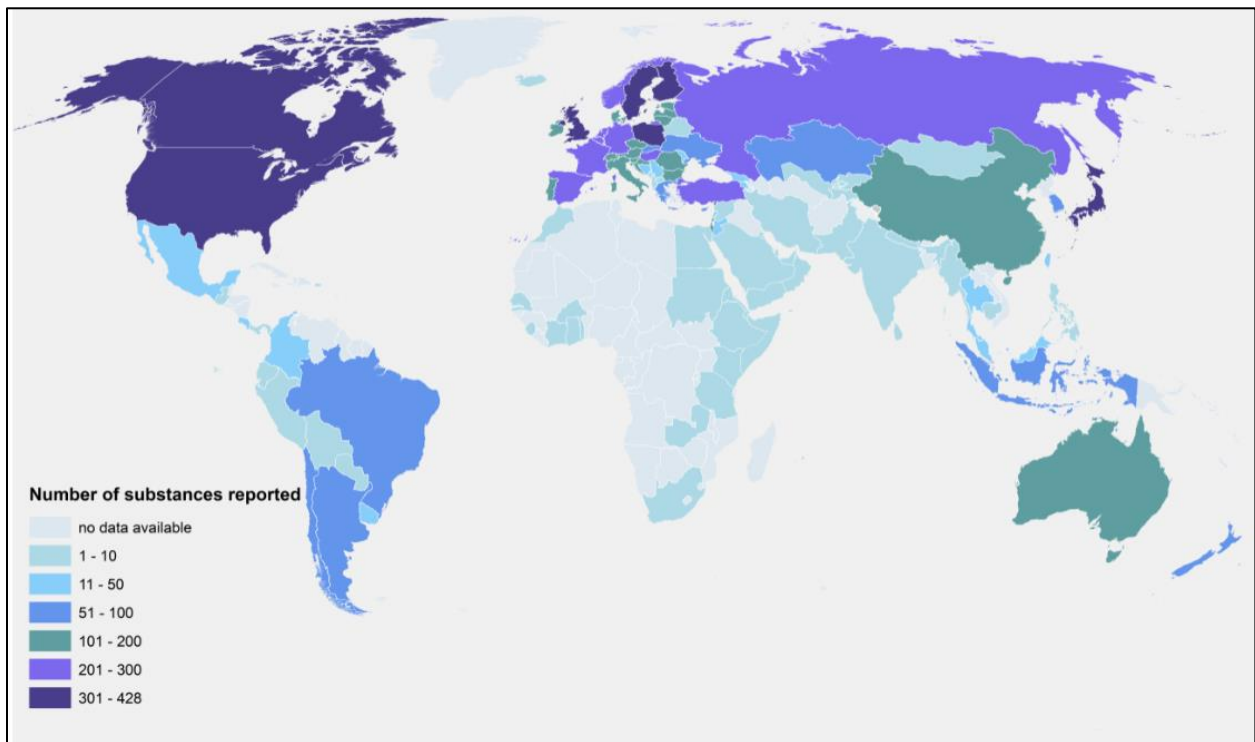


Figure 1 Global emergence of new psychoactive substances up to December 2018 [4].

Over the past decade and to the present, the number of new psychoactive substances (NPSs) identified in the illegal drug market across the globe has continued to grow [5]. For example, every week around one new psychoactive substance is being reported in Europe [6]. A total of 892 NPSs were reported between 2009-2019 with 492 NPS identified 2017 alone (Figure 1) [7]. Among all reported NPSs by the end of 2018, stimulants represented the largest fraction of drugs reported,

followed by synthetic cannabinoid, classic hallucinogens, opioids, and finally dissociatives and sedatives/hypnotics (Figure 2) [8]. The novel psychoactive drug 25I-NBOMe and related substances were reported by the largest number of countries (47) across the globe [3].

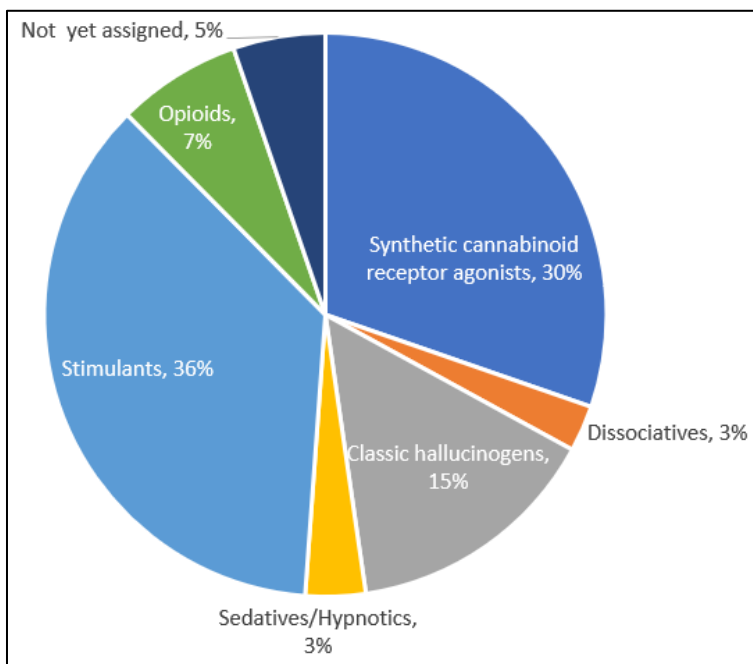


Figure 2 Proportion of new psychoactive substances by psychoactive effect group as of December 2018 [8].

The NPSs category includes a large number of chemical substances from different structural classes that induce biological effects similar to controlled or historically scheduled illegal drug substances [2, 9, 10], In the clandestine market NPSs are often referred as legal highs [11], research chemicals [12], synthetic drugs, bath salts, plant fertilizers [2], designer drugs [13], plant food [9, 10], insect repellents, and air fresheners. These new drugs often carry the disclaimer “for research purposes only” or “not for human consumption” on their packaging [10]. There are four main structural and pharmacologic classes of NPSs which include cannabinoids, psychostimulants, opioids, and hallucinogens. The cannabinoids and psychostimulants remain the most widely abused substances. While less common, hallucinogens continued to be used and novel hallucinogenic drugs such as the NBOMEs continue to appear in the clandestine drug market [14].

The NPSs are defined as “substances of abuse, either in a pure form or a preparation, that are not controlled by the 1961 Single Convention on Narcotic Drugs or the 1971 Convention on

Psychotropic Substances, and which may pose a significant public health threat [13]. While many NPSs are new chemical entities, not all are as the name may imply. For example, a number of NPSs are derivatives of amphetamine and MDMA that were synthesized and reported in the literature decades ago. The designation of “new” in NPS simply refers to the presence of a substance not previously identified in the clandestine market place across the world. Many of these NPSs, old and new, were produced to evade existing scheduling regulations in countries around the globe. [2, 13, 15].

Over the past decade the presence of NPSs have reached unprecedented levels [14] as a result of continuous analog design and ease of availability through cyber networks [12], head shops and from drug dealers [9, 10]. These substances are often promoted as either safe alternative to illicit drugs [9, 15] or were intended as psychotropic agents for the treatment of psychological problems [2]. NPS abuse have become a real problem [11, 12] since these drugs are often associated with serious medical and psychiatric issues [2, 9].

The terms “psychedelics” or “hallucinogens” typically refer to any substance that binds to 5-HT_{2A} receptor and produce agonist effect [16]. Hallucinogen NPS drugs can be divided in three categories based on source and structural class: the ergolines such as LSD, the tryptamines or indoleamines such as psilocybin, and the phenylalkylamines [16]. The phenylalkylamine hallucinogens can be further subdivided in two broad classes: the phenylisopropylamines or “amphetamine class”, such as 2,5-dimethoxy-4-bromoamphetamine (DOB) and 2,5-dimethoxy-4-methylamphetamine (DOM) and the phenethylamine class which includes substances of natural origin like mescaline the active constituent of Peyote cactus [9, 17] and the synthetic 4-substituted-2,5-dimethoxyphenethylamines or so-called “2C-X” compounds (Figure 3) [14]. The phenethylamine core structure is common to a large class of substances including the catecholamine neurotransmitters (dopamine, epinephrine and norepinephrine) as well as a number of stimulant and hallucinogenic drugs of abuse [10]. Interestingly the 2C-X compounds have psychedelic and stimulating effects based on the structure and dose [9-11].

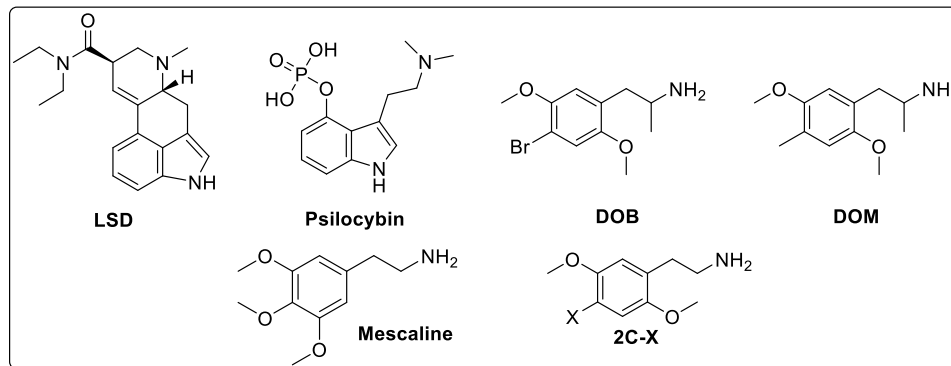


Figure 3 Structures of LSD, psilocybin, DOB, DOM, mescaline, and 2C-X class.

The NBOMes are N-2-methoxybenzyl substituted derivatives of the 2C-X class of hallucinogens. They were originally synthesized by Ralph Heim in 2004 for research purposes as potent agonists of 5-hydroxytryptamine receptor subtype 2A (5-HT_{2A}) [18]. This series of compounds was further developed by Braden and Nichols in 2006 [19] who demonstrated that these compounds were highly potent hallucinogens with activity at microgram scale doses [11, 14, 20]. Because of their high affinity at 5-HT_{2A} receptors, the ¹¹C radiolabel isotope of NBOMes were developed as radioligands [21] to map the distribution of 5-HT_{2A} receptors in the brain by positron emission tomography (PET) [22-24]. The NBOMes were subsequently shown to also act as agonists at α -adrenergic receptors [25] and H₁ histamine receptors [26]. As a result, they can produce both serotonergic and sympathomimetic effects [20, 25]. It has been speculated that the psychotropic features of these drugs reported in the scientific literature triggered the interest of the designer drug producers [11] to use them as recreational drugs in illicit drug market.

The clandestine marketed NBOMes are sold as “research chemicals” under various names N-bomb, Smiles, Solaris, and Cimbi. The 2C-X hallucinogens (for example: 2C-B, 2C-I, etc.) are phenethylamines with methoxy group (OCH₃) substitutions at the 2- and 5-positions [9], that possess structure similarities with MDMA and mescaline, causing physical and psychological effects and hallucinations through serotonergic stimulation. The “2C” series of hallucinogenic phenethylamines were first described by Alexander and Anne Shulgin [27] who used the term “2C” to refer to the two carbons between the benzene ring and the amino group (Figure 4). In 1991, Alexander Shulgin or “the godfather of psychedelics”, published his famous book [27] “Phenethylamines I Have Known And Loved (PIHKAL)”, in which he described the synthesis of many phenethylamines and his own experience while testing these drugs [2]. Chemical structures

of phenethylamine, 2C-phenethylamine, 2 C-C and N-(2'-methoxy)benzyl-2,5-dimethoxy-4-chlorophenethylamine (25C-NBOMe) are given in Figure 4.

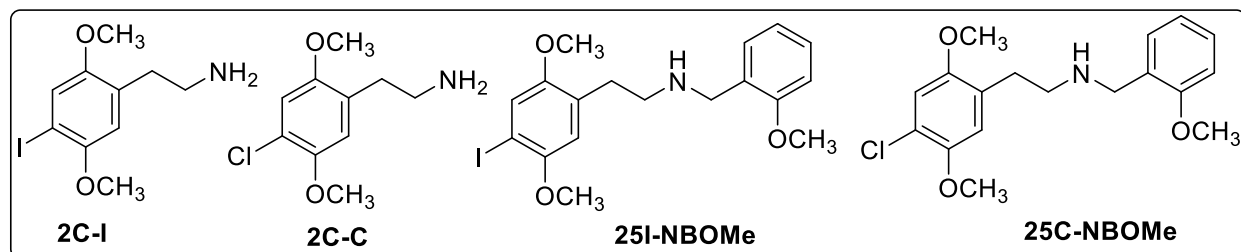


Figure 4 Structures of 2C-X and 25X-NBOMe hallucinogens.

The NBOMe series of drugs has practically no history of human consumption prior to 2010 when they first became available on the internet [28]. Blotter papers and powders containing these new psychedelics were detected on the Polish drug market in 2011. Among others, three representatives of the NBOMe compounds containing alkyl group at position 4 of the phenethyl ring [29] were identified first. Blotter papers impregnated with the chloro derivative 25C-NBOMe also entered the market in 2011. Between 2012-2013, a number of NBOMe exposures were reported to Texas poison centers. Of these 76% involved 25I-NBOMe, 12% 25C-NBOMe, and 12% an unknown NBOMe. The majority (88%) of patients were men and mean age was 17 years (range: 14-25 years) [30]. Currently, the most widely used NBOMe substances are 25I-NBOMe (street names: 25I, INBMeO, N-bomb, Smiles, Solaris and Cimbi-5), followed by 4-bromo derivative (25B-NBOMe) and 4-chloro analog (25C-NBOMe; street names C-Boom, Cimbi-82, Pandora and Dime) [28, 31]. However, a significant number of other 4-substituted NBOMEs have also been reported in the literature.

1.2 Legal status:

The wide variety and increased number of NPS has created significant challenges for regulatory agencies throughout the world [5, 15]. Over the years, designer drug manufacturers have shown great flexibility in altering the chemical structures of existing drugs of abuse to escape both the legal restriction and analytical detection [11]. Often as a new law is enacted to control one novel

NPS, another structurally related but chemically distinct analog appears on the illicit drug market [15]. In any attempt to address this problem some countries like the US and Canada have adopted legislation which attempts to schedule future, new designer drugs “based on chemical similarity to an already controlled substance”, or a generic approach for “controlling a family of substances that are precisely defined” to control substances not explicitly mentioned in the legislation [2]. Other countries have simply attempted to impose a blanket ban on all psychoactive substances [5]. The legal definitions used in such blanket bans are either “effect-based” or “purpose based”. For example, the effects-based ban of the UK [15], Australia and Ireland would in theory cover an NPS with “the capability of a substance to influence the user’s mind, mood, brain or behavior”. The purpose-based ban in countries like Romania and Poland addresses NPS for substances that “may be used instead of, or for the same purpose, as controlled drugs”.

The 2C-X hallucinogens, which can also serve as precursors for the synthesis of NBOMes, have been controlled by countries across the globe for some time. And now the production, distribution and use of NBOMes is regulated in most countries. The US classified 25I-NBOMe, 25B-NBOMe and 25C-NBOMe as a Schedule I controlled substance in 2016 [32]. This designation is reserved for substances that have a high potential for abuse and adverse health effects without any therapeutic benefits. Now 25I-NBOMe, 25B-NBOMe, and 25C-NBOMe are under controlled in Denmark, Slovenia, Russia, Sweden and areas of Australia (Queensland and New South Wales) [33-35] and UK [36]. Further legislative actions may be required to prevent continued spread of these drugs [9], and some countries have called for an international ban of these drugs [20].

1.3 Prevalence:

According to the recent data published from System to Retrieve Information from Drug Evidence (STRIDE) “which is a USA federal database for the seized drugs analyzed by Drug Enforcement Administration (DEA) forensic laboratories” and the National Forensic Laboratory Information System (NFLIS) “which collects drug analysis information from state and local forensic laboratories” indicated that between January 2014 to April 2018, a total of 4326 reports for the NBOMe drugs. This included 2129 reports for 25I-NBOMe, 1273 reports for 25C-NBOMe, and

finally 924 reports for 25B-NBOMe. Some combination of NBOMe drugs have also been encountered in seized materials in US [32].



Figure 5 Blotter sheets presenting 3 different artwork patterns containing a mixture of 25I-NBOMe, 25C-NBOMe and 25H-NBOMe [11].

Similar trends were reported in European Union countries according to the European Monitoring Centre for Drugs and Drug Addiction (EMCDDA). This agency is responsible for collating and distributing information related to drug use in European countries [37]. Interestingly no drugs of the NBOMe category were reported before June 2012 [38].

In an online questioner (Global Drugs Survey or formally known as MixMag) that was conducted in 2012 on 22289 respondents, 2.6% of the respondents reported they had tried one of the main three NBOMe, i.e. 25I-NBOMe, 25B-NBOMe, and 25C-NBOMe. 25I-NBOMe was the most commonly used of the NBOMe (2.0%), followed by 25B-NBOMe (1.2%) then 25C-NBOMe (0.8%). The participants of this survey were mainly from the US, Canada, and UK [31]. In another survey conducted on 2014 [39], the prevalence of use of NBOMe drugs showed a slightly higher result (4.8% compared with 2.6%) than the previous questioner discussed above from the Global Drug Survey.

According to a 2013 online article published on Erowid Extracts [40], with a total of 314 reports on NBOMe use. The number of NBOMe use has increased from 5 reports in 2010 to 126 reports in the first six months of 2013 with more than 8,000 posts containing the word “NBOMe” on the internet discussion forum [41].

1.4 Pharmacology and Structure-Activity Relationships:

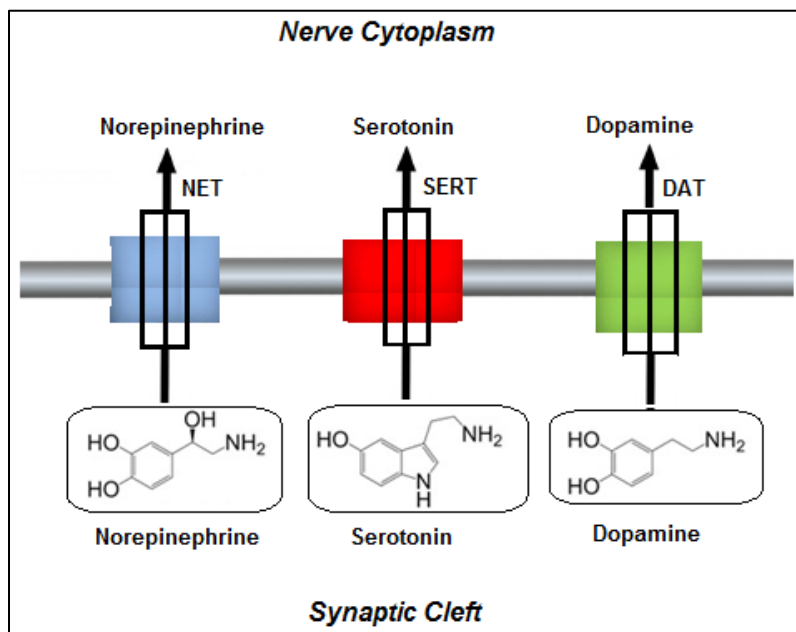


Figure 6 Plasma membrane monoamine reuptake transporters (DAT, SERT and NET).

The primary mechanism of action for many psychotic drugs of abuse involves modulation of central nervous system neurotransmitter activity by actions at pre- or postsynaptic receptors or by inhibition or activation of neurotransmitter reuptake systems. The primary neurotransmitter targets involved in the effects of psychoactive drugs appear to be serotonin (5-HT), norepinephrine (NE) and dopamine (DA) receptor subtypes, and the serotonin (SERT), norepinephrine (NET) and dopamine (DAT) reuptake transporters [2].

Alterations in neurotransmitter levels in the brain often leads to either desirable or undesirable effects [2]. For example, the increases in serotonin levels can lead to entactogenic or hallucinogenic or effects, and in extreme cases to a life-threatening condition, serotonin syndrome [2]. Increases in NE levels can alter the cardiovascular functions (e.g., tachycardia and hypertension) and temperature regulation (hyperthermia) [2]. Finally, increased DA levels are associated with reinforcing and behavioral-stimulating effects of drugs [42-44] in addition to high abuse potential for drugs that affect dopamine reuptake [2, 45, 46] in contrast to high serotonin levels [44, 47].

The monoamine neurotransmitter 5-hydroxytryptamine or serotonin (5-HT) is involved in mediating many physiologic and behavioral processes including mood, emotion, feeding behavior and food intake, sexual behavior, sleep and circadian rhythm, and the neuroendocrine system [48]. Serotonergic neuronal pathways in the CNS have also been reported to play important roles in numerous conditions such as addiction, schizophrenia, obsessive compulsive disorder, pain, inflammation, migraine, cluster headaches, [49] and GI tract function . Therefore, there has been continuing interest in developing ligands for the serotonin receptors and transporters to research and treat many disorders such as schizophrenia, depression, obesity, emesis, and irritable bowel syndrome (IBS) [48]. Serotonin receptors are sub-classified into seven subfamilies (5-HT₁ to 5-HT₇) based on structure and signal transduction mechanism. With the exception of 5-HT₃ receptors, serotonin receptors are considered as G-protein-coupled receptors, while 5-HT₃ receptors are ligand-gated ion channel [50].

The 5-HT₂ subfamily of receptors appears to be involved in many of the CNS actions of serotonin. This receptor family is further subdivided into 3 subtypes, 5-HT_{2A}, 5-HT_{2B}, and 5-HT_{2C} [51]. It is thought that 5-HT_{2A} receptors contribute to both central and peripheral physiological actions, mediating platelet aggregation, vasoconstriction, and intra-ocular pressure in the peripheral tissues, while regulating circadian rhythm, mood, cognitive states and the learning process in the CNS as well as the effects of psychoactive drugs [52]. The 5-HT_{2B} receptors are mainly found in the gut with lower distribution in the lung and the heart and to the least possible extent in the brain. Though 5-HT_{2B} receptors are critical for organ structure development in the heart and the brain, activation of these receptors is also associated with heart disease [51]. Finally, 5-HT_{2C} receptors appear to be responsible for regulating dopamine and serotonin release in the brain and therefore have been targeted for treating stimulant abuse and anxiety, and weight regulation [48]. The 5-HT_{2C} receptors share the closest structural homology to 5-HT_{2A} receptors and have also been proposed to be a target for many psychoactive drugs [48].

Modulation of 5-HT_{2A} receptor function has been linked to complex CNS activities ranging from cognitive process and working memory to affective disorders [9, 11, 20]. Stimulation of 5-HT_{2A} receptors is also strongly associated with the hallucinogenic effects of many illicit drugs [9]. However, hallucinogenic drugs can also interact with other 5-HT receptor subtypes with varying

selectivity and efficacy, as well as other non-serotonin targets. These complex receptor and transporter actions complicates the study of the relationships between receptor occupation and behavioral effects and hallucinogenic drugs after systemic administration [16].

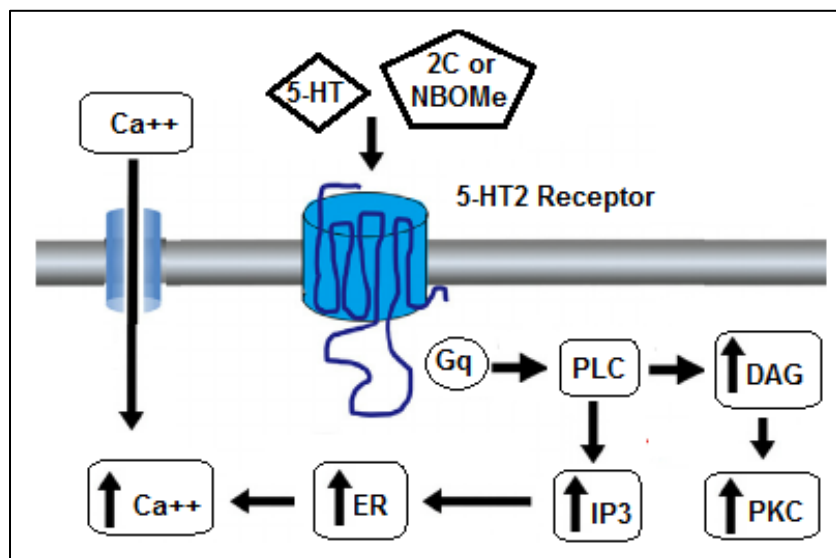


Figure 7 Serotonin 5-HT₂ receptors.

Structure-activity relationship (SAR) studies have led to the development of drugs with low nanomolar affinities for the 5-HT_{2A} receptor, some of which are among the most potent partial agonists with hallucinogenic effects known to date [53-56]. Data suggest that 2C-X drugs interact effectively with serotonin receptors, most of which act as 5-HT_{2A} receptor agonists. Typically, a 2C-X drugs have a lipophilic substituent in the para or 4-position of the aromatic ring, which contributes to further enhance 5-HT_{2A} affinity and partial agonistic action [57, 58]. The most active 2C-X compounds identified to date possess an ether, alkylthio, alkyl, or halogen group at the 4-position and their potency increases in the aforementioned sequence [59, 60]. The results retrieved from SAR studies suggest that N-substitution of common phenethylamines with short alkyl substituents (methyl or ethyl groups) considerably decreases the binding affinity for serotonin receptors compared to the unmodified compounds. However, the addition of an N-benzyl moiety increases the affinity and potency [19]. For example, Braden et al found that substitution of a N-benzyl group to 2,5-dimethoxyphenethylamine (2C-H) resulted in a 13-fold increase in 5-HT_{2A} receptor binding [61]. Furthermore, adding a methoxy or hydroxy functional group to the ortho or 2'-position on the N-benzyl group resulted in further increases receptor binding [9, 11, 14]. For

example, addition of the N-(2'-methoxy)benzyl substituent to 2C-I as in 25I-NBOMe increased 5-HT_{2A} receptor affinity 17-fold; 2C-I has a K_i of 0.73 nM and 25I-NBOMe has a K_i of 0.044 nM. The same trend was observed when adding a N-(2'-methoxy)benzyl substituent to 2C-B as in 25B-NBOMe; 2C-B has a K_i of 6 nM while 25B-NBOMe as a K_i of 0.19 nM at 5-HT_{2A} receptors. Also adding a N-(2-hydroxy) benzyl group to 2C-H as in the 25H-NBOH drugs resulted in an 82-fold increase in affinity. Silva et al prepared a number of NBOMe derivatives in which the phenyl ring was replaced with a heterocycle such as indole and quinazolinone. In these studies, it was also found that the heterocyclic-ethylamines that were substituted with an N-(2'-methoxy)benzyl substituent had the highest 5-HT_{2A} receptor affinity, although as partial agonists [62]. Finally, in addition to high receptor affinity, the NBOMe and NBOH derivatives displayed high selectivity (> 1000-fold) for 5-HT_{2A} receptors over 5-HT_{1A} receptors, and moderate selectivity (up to 35-fold) for 5-HT_{2A} over 5-HT_{2C} receptors [11].

It is reported that the increase in 5-HT_{2A} receptor affinity resulting from the substitution of a N-benzyl group to the 2C-X structure as in the NBOMes is due to additional aromatic pi-stacking interactions between the added benzyl group and a Phe residue at position 339 on the receptor [19]. Furthermore, adding an appropriately positioned oxygenated functionality to the N-benzyl ring increases receptor affinity further by hydrogen bond formation [63]. The ortho or 2'-position appears to be optimal for this hydrogen bonding interaction since moving it to the meta (3') or para (4') position is associated with a gradual and significant decline in affinity [14]. In addition to reduced hydrogen bonding, steric factors also appear to play a role in the reduction of binding affinity that occurs with meta and para methoxy substitution pattern [14]. For example, in NBOMe derivatives substituted with a bromine atom in the N-benzyl ring it was observed that 4'-bromo isomer displayed 10-20 fold reduced affinity (K_i=52.5 nM) compared to corresponding 3'-bromo isomer (K_i=3.98 nM) and 2'-bromo isomer (K_i=2.34 nM) [63]. To further emphasize the importance of steric constraints around the para position of the N-benzyl ring within the binding pocket of the 5-HT_{2A} receptor, Braden et al replaced the N-benzyl ring with N-naphthyl group which lead to reduction in 5-HT_{2A} binding affinity by 20-fold (K_i naphthyl = 4.83 vs K_i benzyl = 0.25 nM) [19]. Finally, when the N-(2'-methoxy)benzyl substituent of 25B-NBOMe was replaced with N-pyridinyl, an electron deficient heterocyclic system, a significant reduction in affinity was

reported, consistent with the observation that electron deficient ring systems have lower aromatic stacking interaction [14].

The NBOMe compounds have a high degree of structural flexibility based on their linear phenethylamine structure. Thus, they can exist in a variety of different conformational forms and adopt different binding poses at their target receptors [14]. To investigate the potential binding conformation of the NBOMe-type compounds Juncosa et al. [48] prepared a series of conformationally restricted analogues of 25B-NBOMes. These restricted derivatives showed the same relative receptor binding profiles as the NBOMes with more than 100-fold selectivity for 5-HT_{2A} versus 5-HT_{2C} receptors, but their 5-HT_{2A} receptor affinity was significantly less than the unrestricted compounds and the data did not support the binding of one conformation versus another.

A number of α -methyl substituted or amphetamine-type NBOMe derivatives have also been prepared and assessed in 5-HT_{2A} receptor binding assays. These derivatives generally have significantly lower 5-HT_{2A} receptor affinity than the corresponding NBOMe parent compound. For example, the addition of α -methyl group to 25I-NBOMe results in a decline in efficacy (E_{max}) and a 12-fold reduction of affinity for 5-HT_{2A} receptors suggesting that substitution in this portion of the NBOMe molecule reduces receptor affinity [14, 19].

While the hallucinogenic effects of the NBOMes and other psychedelic drugs are attributed to agonist action at the serotonin 5-HT_{2A} receptors, there is limited information correlating this receptor action with behavioral responses in animal models. Halberstadt and Geyer studied the effects of several 25I-NBOMe and 2C-I on the head twitch response (HTR) that is induced by activation of 5-HT_{2A} receptor in rats and mice. This model is widely used as a behavioral proxy for hallucinogen effects in humans. In this assay 25I-NBOMe displayed 14-fold higher potency than 2C-I, consistent with the relative 5-HT_{2A} receptor binding affinities of these two compounds [17]. The ¹¹C radiolabeled form of 25C-NBOMe has been studied as a potential ligand to map the distribution of 5-HT_{2A} receptors in the brain by positron emission tomography (PET) [22]. Because this drug has a nanomolar affinity at the 5-HT_{2A} receptor (2.89 nM) *in vitro* it, along with other members of the NBOMe series, has been characterized as “superpotent” agonist [22]. However,

the association between 5-HT_{2A} receptor occupation and the pharmacological effects of these drugs remains to be established.

There are relatively few studies characterizing the pharmacologic actions of NBOMe compounds in humans reported in the scientific literature. However, case reports in the medical literature and anecdotal reporting at internet sites such as Erowid highlight a number of pharmacologic actions experienced by those using these drugs. Reported effects range from relatively mild psychotropic actions to life threatening events [11, 20, 64] based on the route of administration and dose [64]. The CNS reported effects include euphoria, mental and physical stimulation, entactogen effects (feelings of love, empathy, and sociability), mystical experiences, alterations in cognition, audio-visual hallucinations, time distortion, agitation, aggression, confusion and insomnia. Peripheral effects noted include nausea, tachycardia, hypertension, hyperthermia and hallucinations. There are several reports of associating NBOMes use with seizures, cardiac and/or respiratory arrest and death [9, 10, 20, 64]. And in some cases, the use of NBOMe drugs appeared to have triggered “serotonin syndrome” which is life threatening condition if not properly managed [9]. At this time there are no reports concerning the addiction or physical dependence potential of the NBOMe drugs [9, 33-35].

1.5 NBOMe Related Toxicities and Mortality:

Hospital admission data and case reports have described various toxic effects associated with the NBOMe drugs including tachycardia, hypertension, confusion, agitation, aggression, visual and auditory hallucinations, seizures, hyperpyrexia, clonus, metabolic acidosis, rhabdomyolysis and acute kidney injury [65-69]. Elevated creatine kinase and white cell counts were also noted by Hill et al in several patients admitted to the hospital after NBOMe use [68]. Non-fatal intoxications and deaths associated with 25I-NBOMe drug have been reported by Australia (at least 2 deaths), Belgium (3 non-fatal, 1 unconfirmed death), Poland (4 nonfatal, 1 unconfirmed death), Sweden (18 non-fatal), the United Kingdom (7 non-fatal, 1 death) and the USA (19 non-fatal, 11 combined NBOMe deaths, 5 25I-NBOMe deaths) [35]. Many but not all of these cases have been analytically confirmed.

In the US, Kelly et al reported that four males between the ages of 18 and 19 simultaneously presented to the emergency department (ED) after recreational use of 25I-NBOMe [65]. They purchased the drug from another individual who obtained it through the internet. Upon arrival, all patients were tachycardic and displayed varying levels of psychomotor agitation. None were capable of providing a clear history. Three of the patients experienced prolonged seizure activity which required pharmacologic therapy, intubation, and mechanical ventilation.

A single non-fatal intoxication with 25B-NBOMe in the US was reported and there have been two case reports of death associated with 25B-NBOMe ingestion in the UK and Switzerland [34, 70]. In all three cases the presence of 25B-NBOMe was confirmed analytically. For the non-fatal case, a 19 year old male in prior good health was found by his roommates having “jerking movements”. He was taken to the hospital where he was observed to be experiencing tachycardia, hypertension, seizures and hyperpyrexia (Poklis et al. 2013). The patient required intensive medical treatment including intubation and sedation. A serum and urine specimen were obtained 39 hours after admission with 25B-NBOMe concentrations measured to be 180 pg/ml (0.18 ng/ml) in the serum and 1900 pg/ml (1.9 ng/ml) in the urine. This patient recovered and was fully alert and orientated six days after the reported ingestion.

Poklis et al reported the presence of 25I-NBOMe in three emergency room patients [71]. The patients presented with signs and symptoms of drug intoxication including tachycardia, hypertension, severe agitation and seizures. In one case, only 25I-NBOMe was detected at 0.1 ng/ml, with another case involving 25I-NBOMe (2.3 ng/ml) and 25C-NBOMe, and the final case involving 25I-NBOMe (1.2 ng/ml) and 25H-NBOMe. In addition to these reports described above, there are a large number of reports from the US and abroad detailing the toxic effects of NBOMe drugs involving individual patients in various settings.

The Drug Enforcement Agency (DEA) obtained medical examiner and post-mortem toxicology reports from various states implicating some combination of 25I-NBOMe, 25C-NBOMe and 25B-NBOMe in the death of 14 individuals [35]. The average age of these individuals was 20 years (range 15 to 29 years). The circumstances surrounding the deaths included acute toxicity (11 cases), or unpredictable, violent behavior due to 25I-NBOMe toxicity, ultimately leading to death

(3 cases). Within this series, in June 2012 two teenagers fatally overdosed on a substance that was allegedly 25I-NBOMe and a 21-year-old man died of an apparent overdose in October 2012 after taking a liquid drop of 25I-NBOMe nasally at a music festival. Furthermore, an 18-year old died in January 2013 after ingesting 25I-NBOMe that was sold as LSD. With results from a post-mortem toxicology screen, the cause of death in this case was attributed to acute 25I-NBOMe poisoning with no alcohol, prescription drugs or other illicit drugs. Walterscheid et al reported two deaths linked to 25I-NBOMe use in individuals who had recently attended a “rave” party [72]. The first case involved a 21-year-old male driver who had admitted to the passenger in his vehicle that he had taken “acid”. He then experienced a sudden surge of violent behavior that caused him to pull over and destroy the interior of the car, and then he became unresponsive. The post-mortem examination was unremarkable internally despite numerous external superficial injuries consistent with physical aggression. The second case involved a 15-year-old female who was socializing outside a rave party, became ill, and rapidly deteriorated as friends transported her to the hospital. The postmortem assessment showed external contusions but internal injuries were superficial. Comprehensive toxicological screens in both cases revealed the presence of cannabis and 25I-NBOMe.

1.6 Pharmacokinetics (ADME Properties):

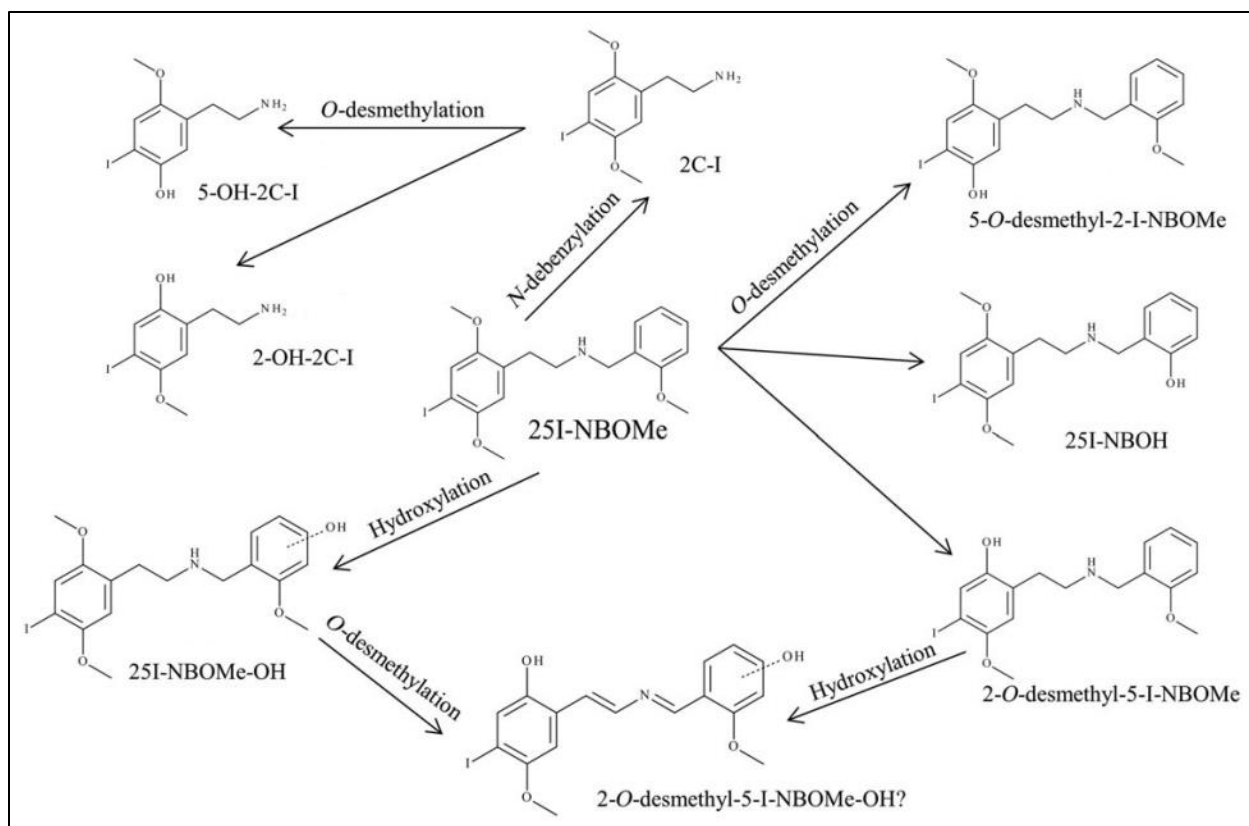
The psychotropic effects of NBOMe substances are route of administration and dose dependent [10]. Due to their high psychotropic potency, NBOMe drugs, similar to LSD, are most commonly distributed on blotter papers [11]. Other forms have been reported including solutions, powder, capsule, and sprays [9, 11, 20, 33-35, 41]. Sometimes these dosage forms contain a mixture of NBOMe drugs [11].

Blotter papers containing NBOMe drugs for sublingual or buccal administration are the most common dosage form [11]. Due to their high potency, very small quantities of the drug can be distributed in large number of doses in blotter form [9, 20]. In an apparent attempt to improve absorption from the oral cavity, NBOMes have been complexed with cyclodextrins in blotter papers in some dosage forms identified to date [9, 10, 38]. Powder dosage forms for sniffing or insufflation [9] and intravenous injectable forms have also been reported [20]. Oral ingestion of

solid dosage forms or foods containing NBOMe derivatives is less common [10] presumably due to the limited oral bioavailability of these drugs due to first pass metabolic degradation [9].

Different NBOMe doses are reportedly used based on the route of administration and specific NBOMe drug administered. It appears that mild hallucinogenic effects are felt at doses as low as 50-250 µg with regular dose range between 500 to 800 µg [10, 11]. The onset and duration of action of the NBOMe drugs also appears to be dependent on routes of administration and the type of drug product used. The onset of hallucinogenic activity appears to range from 5-120 minutes, and the duration of effect is from 3-10 hours depending on whether the drug is insufflated or consumed orally [33-35, 73].

The metabolism of NBOMe drugs has been the subject of a number of studies [69, 74-87]. The commonly abused NBOMe derivatives, 25C-NBOMe, 25B-NBOMe and 25I-NBOMe, reportedly undergo metabolism by common pathways involving primarily O-demethylation, O, O-bisdemethylation, and aromatic ring hydroxylation (Scheme 1). Another minor pathway after buccal administration includes N-dealkylation which can give rise to the corresponding 2C-X metabolite [14, 75, 76, 83]. To date in human and rat metabolism studies over 60 NBOMe metabolites have been detected [14]. While the hydroxylation reaction occurs preferentially at the N-benzylmethoxy ring, all three of the methoxy groups in a typical NBOMe drug are susceptible to O-dealkylation [85]. It appears that the primary enzymes of metabolism are CYP2C9 and CYP2C19 which catalyze O-demethylation, and CYP1A2 and CYP3A4 which are responsible for ring hydroxylation, and CYP3A4 which catalyzes N-dealkylation [14, 75, 83]. A number of these enzymes are heavily expressed in the liver and gut [14]. Most of this phase I CYP metabolites are conjugated with glucuronic acid and sulfate prior to excretion [10, 11, 14, 77, 85].



Scheme 1 The metabolic pathways for 25I-NBOMe [74].

Grumann et al. published a study concluded that the poor oral bioavailability of the NBOMe drugs is likely due to extensive first pass metabolic inactivation as the drugs pass through the intestinal mucosa and liver following oral delivery [14]. Based on their structures and known structure-activity data, most CYP metabolites would be expected to be less active than the parent drug. It was suggested that the N-dealkylation metabolic pathway may be more prominent after oral ingestion of NBOMe drugs in comparison to buccal or nasal administration and that this pathway does lead to formation of the corresponding 2C-X metabolite, itself an active hallucinogen. However, the 2C-X formed metabolically would be significantly less potent than the parent drug by at least 1-2 orders of magnitude [14] based on receptor binding and pharmacologic data.

In another study to assess the low oral bioavailability of NBOMes, Leth-Petersen et al [88] found that the clearance rate for 25I-NBOMe was much higher (4.1 L/kg/h) than that for the corresponding 2C-I phenethylamine (0.20 L/kg/h) and that the NBOMe derivative had a higher hepatic extraction ratio (1.2 L/h/kg) [89]. From this the authors concluded that NBOMes are

subject to extensive first-pass metabolism, explaining why these drugs have low oral activity [14]. These findings were confirmed in another study [14] where it was observed that only subcutaneously administered 25I-NBOMe can produce significant pharmacologic effects while intra-peritoneal administration did not, strongly suggested that NBOMe underwent a first pass metabolism effect.

Since NBOMes are metabolized by CYP enzymes, the potential for drug interactions exist when they are administered with other drugs or substances that are CYP inhibitors or inducers. While there are no literature reports of significant drug-drug interactions to date, co-administration of an NBOMe drug with a CYP inhibitor could result in significantly increased hallucinogenic and other pharmacologic effects [75, 76].

1.7 Analytical Detection:

The specific identification of NPSs presents many analytical challenges. Due to the dynamic nature of the illicit drug market, NPSs are being generated all the time and often analytical reference standards are not available and there are no published spectra available in the literature. For some drugs, the potency is high and therefore the quantity of drug in a sample is so low that only the most sensitive instrumentation can detect its presence. Some NPSs can have stereoisomeric or regioisomeric forms which are not readily differentiated by standard forensic analysis. A number of NPSs can decompose due to thermal instability, complicating analysis.

Electron-impact mass spectrometry (EI-MS) has been a routine analytical detection and identification method for drugs of abuse, however, continuous growth in the NPS market and the great similarities in the physical and chemical properties of NPS substances limits the effectiveness of this analytical method when used alone. Recently, more advanced MS techniques such as gas chromatography/tandem mass spectrometry (GC/MS/MS), liquid chromatography/electrospray ionization quadrupole time of flight mass spectrometry (LC/ESI-QTOF-MS), liquid chromatography/tandem mass spectrometry (LC-MS/MS) have been developed and applied successfully to address many of the challenges in new drug identification. One of the advantages of using ESI-QTOF-MS is great mass accuracy and high resolution. Based on exact mass

measurement of a molecule and its fragments, it's possible to determine the chemical formula of an unknown substance [90]. Also, along with these MS techniques, additional information concerning drug structure can be obtained by using other analytical methods including infrared and NMR spectroscopy, although, these methods lack adequate sensitivity when complex mixtures have to be investigated [90].

While analytical laboratory testing methods are evolving as described above, widespread availability of this instrumentation and standardized testing for NPS drugs is not common in most forensic and clinical toxicology laboratories. However, a number of methods to identify and quantify NBOMe compounds in forensic and biological specimens have been reported in literature. The most commonly methods for detection in biologic samples involve chromatographic separation techniques such as high performance liquid chromatography (HPLC) or ultra-performance liquid chromatography (UPLC) coupled to either tandem mass spectrometry (MS-MS) or high-resolution time-of-flight mass spectrometry (HRTOF-MS). As extraction procedure both liquid-liquid extraction (LLE) and solid phase extraction (SPE) have been reported. In one approach a HPLC-MS-MS method for the detection and quantification of nine NBOMe compounds in urine (25H-NBOMe, 25CNBOMe, 25I-NBF, 25D-NBOMe, 25B-NBOMe, 2CT-NBOMe, 25I-NBMD, 25G-NBOMe and 25I-NBOMe) using a rapid SPE was developed [71]. A similar analytical approach was reported for the identification and quantification of 25B-NBOMe in serum and urine, after a simple LLE technique using 25H-NBOMe as the internal standard [70]. Pasin et al developed and validated a method for the detection and identification of 37 new designer drugs, including 25B-NBOMe, 25C-NBOMe, 25HNBOMe and 25I-NBOMe, in whole blood using LC-QTOF-MS [91].

Identification of 25C-NBOMe and a demethylated and glucuronidated metabolite of 25C-NBOMe in urine and blood samples was achieved by using UPLC-HRTOF-MS. Also, quantification of these drugs in post-mortem specimens (peripheral whole blood, urine, vitreous humor, liver, and gastric content) and in antemortem whole blood sample was performed by UPLC-MS/MS [86]. Stelpflug et al used LC-MS/MS for the quantification of 25I-NBOMe and UPLC-TOF-MS for the identification of excreted metabolites of the same drug in urine samples collected from a clinical case [69].

Forensic analysis of blotters containing NBOMe compounds is normally performed by GC–MS or LC–MS [28, 92]. These techniques require sample preparation which involves extraction of the potential drug analytes by soaking blotters in organic solvents and filtering prior to injection. These methods are time consuming and potentially can in some cases destroy the sample. Coelho reported a method that rapidly detects NBOMes and other NPS by taking ATR-FTIR spectra directly from the blotters [93]. In 39 blotter papers tested (out of 77) three types of NBOMe class (25B-NBOME, 25C-NBOME and 25INBOME) were detected by this method. This analysis is a quick but only preliminary test since each blotter is a mixture of paper and one or more NPS, which reduces the discriminating power of IR spectrometry, therefore confirmation with analytical techniques such as GC–MS or LC–MS is still necessary.

1.8 Mass Spectral Analysis:

Many forensic laboratories use gas chromatography/electron impact mass spectrometry (GC/EI-MS) as the primary tool to identify the active ingredients in seized illicit drugs [90, 94]. The EI-MS of several NBOMe compounds with varying substituents in the 4-position of the phenethyl ring have been published and representative examples are shown in Figure 8-10 below.

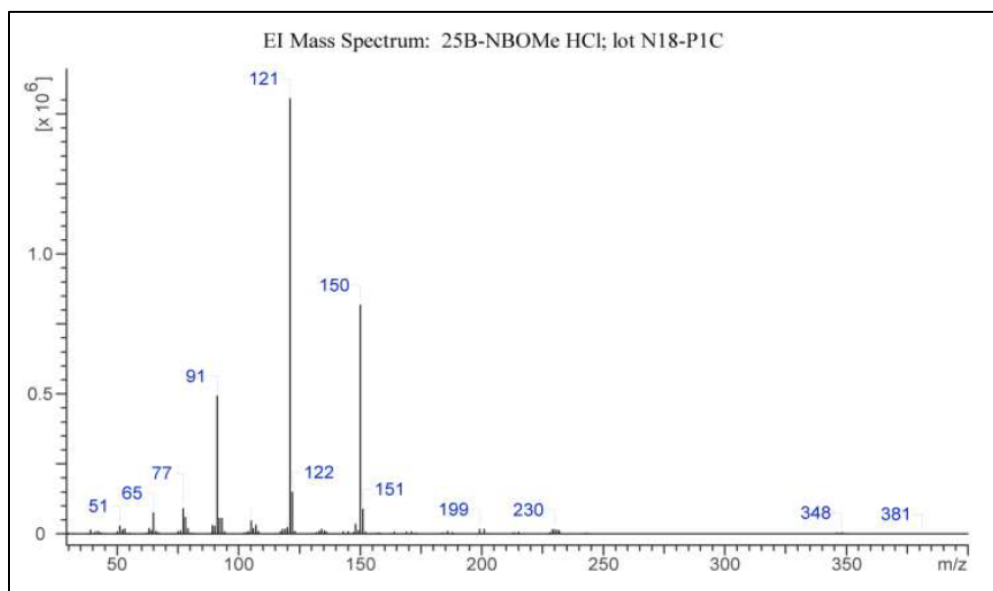


Figure 8 EI mass spectrum of 25B-NBOM HCL salt [95].

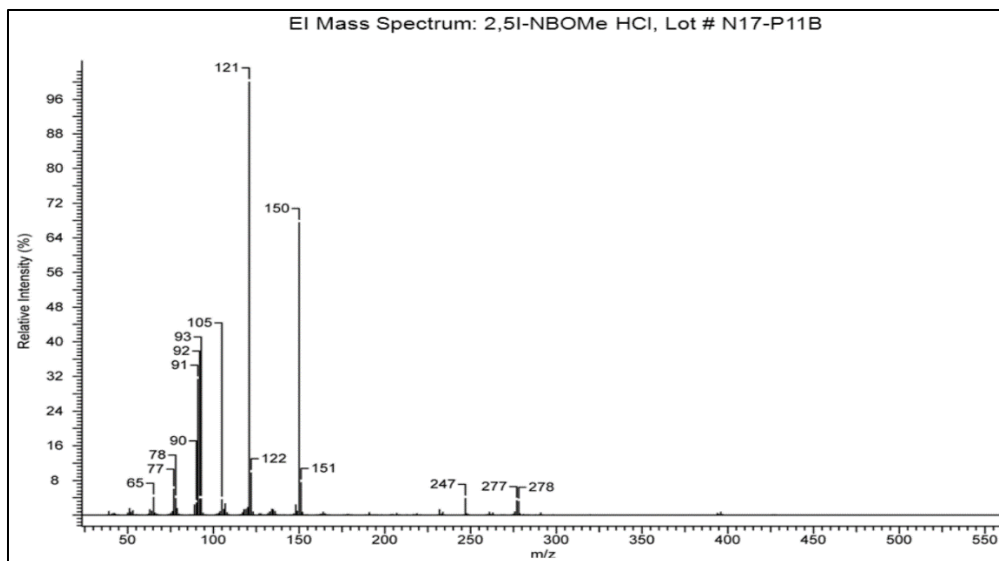


Figure 9 EI mass spectrum of 25I-NBOM HCL salt [96].

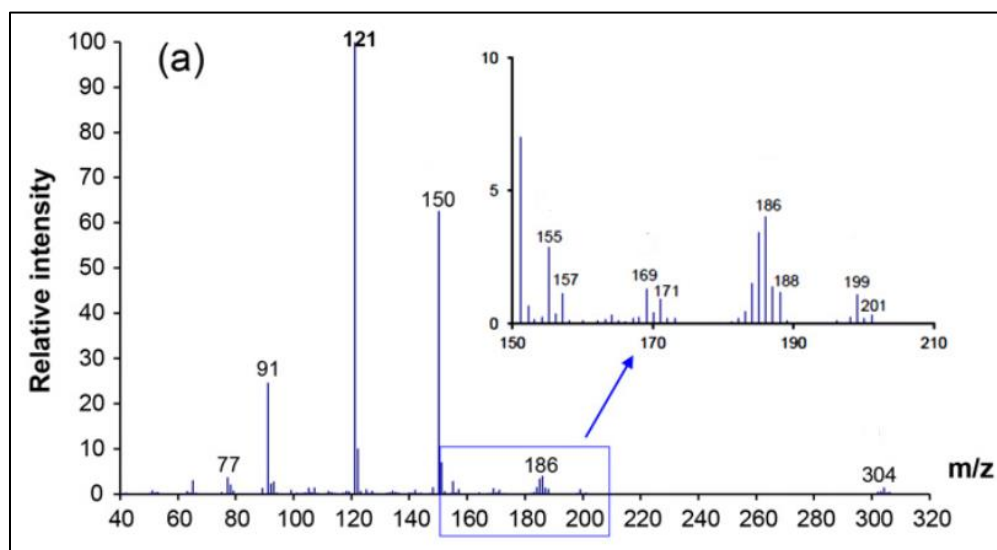
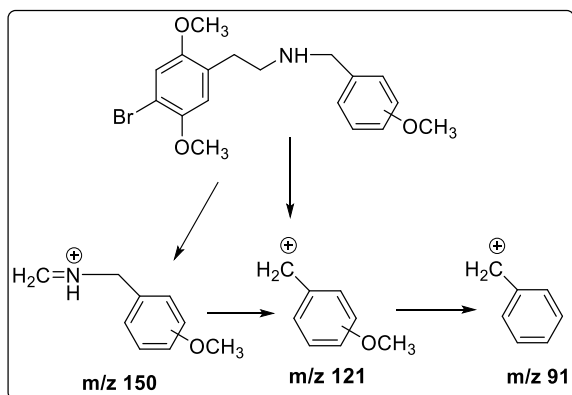


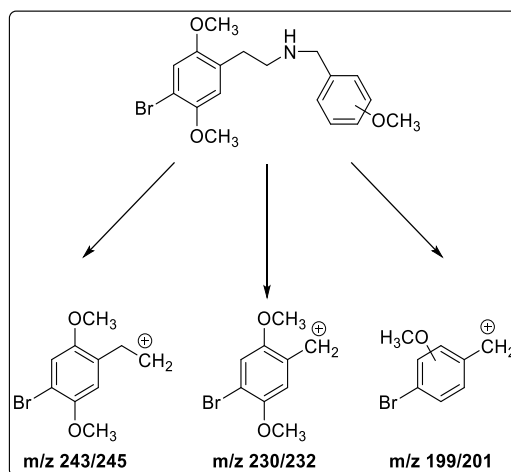
Figure 10 EI mass spectrum of 25C-NBOM HCL salt [28].

Interestingly, even though these compounds differ in the nature of the 4-substituent (Br, I, Cl) they yield very similar mass spectra with dominant ions observed at $m/z = 121$, 150 and 91, with the base peak at $m/z 121$. The EI-MS of these NBOMe derivatives do not show a molecular ion of significant abundance. The proposed fragmentation scheme for these compounds is shown in Scheme 2 and involves formation of ions of highest abundance from that portion of the NBOMe structure which is common to all three derivatives. The base peak $m/z 121$ appears to form by the cleavage of the N-C bond yielding the 2-methoxybenzyl cation. The ion at $m/z 150$ is likely the iminium cation formed by the dissociation of bond between α - and β -carbon atoms, a common

pathway for phenethylamine compounds. Finally, the ion at m/z 91 appears to have formed from loss of CH_2O from the methoxy benzyl cation. Thus, the EI-MS spectra of all three compounds are very similar. While none of the more abundant ions in the spectra of these distinct NBOMe compounds appeared to contain a halogen, there are halogen-containing minor fragments at the higher masses (> 180) which allow for differentiation of these compounds based on their 4-substituents. For example, based on masses and isotopic abundance, the bromo analogue contains minor fragments at m/z 199/201, 230/232, and 243/245 for the bromine-containing imine and benzyl cations shown in Scheme 3 and comparable higher mass fragments containing halogen are also present in the 4-iodo and 4-chloro NBOMe derivatives.



Scheme 2 Proposed EI-MS fragmentation pathway for the N-(monomethoxy)benzyl-4-bromo-2,5-dimethoxyphenethylamines.



Scheme 3 Proposed EI-MS fragmentation pathway for the N-(monomethoxy)benzyl-4-bromo-2,5-dimethoxyphenethylamines.

Casale and Hays synthesized and analyzed 11 commonly encountered NBOMes with differing 4-substituents as well their 3- and 4-methoxybenzyl regioisomers (Table 1) [97]. Again, the parent NBOMe compounds with differing 4-substituents (R_1) but a common N-2-methoxybenzyl R_2 group (compounds 1, 4, 7, 10, 13, 16, 19, 22, 25, 28, and 31) all yielded similar mass spectra with dominant ions observed at $m/z = 121$, 150 and 91 and with the base peak m/z 121. These 11 parent compounds could be differentiated by CI-MS based on differences in their molecular weight, as well as differences in their minor fragment ions in the higher mass regions of the spectra, fragments which vary depending on the nature of the 4-substituent as described above.

Differentiation of the individual regioisomeric 2', 3' and 4'-methoxybenzyl derivatives within each series of 4-substituted NBOMe compounds (i.e. compounds 4, 5 and 6) proved to be more challenging. For example, the EI-MS of the three 2', 3' and 4'-methoxybenzyl derivatives of 25B-NBOMe are shown in Figure 11. The MS spectra of all three of these regioisomers contain the same three dominant ions at $m/z = 121$ (base peak), 150 and 91, and same minor bromine-containing fragment ions in the higher mass regions of the spectra. The only difference in the MS spectra of these three regioisomers is the relative abundance ratios of the m/z 150 and 91 ions and these differences are relatively small. Therefore, specific differentiation and identification of regioisomeric derivatives within a single 4-substituted NBOMe class presents a greater analytical challenge, particularly if the benzyl group were to contain more complex substitution patterns where even more regioisomers were possible. Also, there are no mass spectra reported for NBOMe derivatives where the substitution pattern on the phenethyl ring is varied or derivatives with modifications in the ethyl side or nitrogen atom. Thus, it is unclear if these fragmentation patterns would be observed for a broader range of NBOMe derivatives that could emerge in the clandestine market in the days to come.

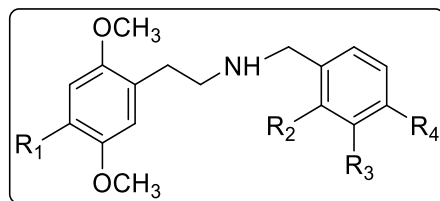


Table 1 Structural formula of NBOMe Derivatives [97].

Compound	R ₁	R ₂	R ₃	R ₄
25H-NB2OMe	H	OCH ₃	H	H
25H-NB3OMe	H	H	OCH ₃	H
25H-NB4OMe	H	H	H	OCH ₃
25B-NB2OMe	Br	OCH ₃	H	H
25B-NB3OMe	Br	H	OCH ₃	H
25B-NB4OMe	Br	H	H	OCH ₃
25C-NB2OMe	Cl	OCH ₃	H	H
25C-NB3OMe	Cl	H	OCH ₃	H
25C-NB4OMe	Cl	H	H	OCH ₃
25D-NB2OMe	CH ₃	OCH ₃	H	H
25D-NB3OMe	CH ₃	H	OCH ₃	H
25D-NB4OMe	CH ₃	H	H	OCH ₃
25E-NB2OMe	C ₂ H ₅	OCH ₃	H	H
25E-NB3OMe	C ₂ H ₅	H	OCH ₃	H
25E-NB4OMe	C ₂ H ₅	H	H	OCH ₃
25I-NB2OMe	I	OCH ₃	H	H
25I-NB3OMe	I	H	OCH ₃	H
25I-NB4OMe	I	H	H	OCH ₃
25N-NB2OMe	NO ₂	OCH ₃	H	H
25N-NB3OMe	NO ₂	H	OCH ₃	H
25N-NB4OMe	NO ₂	H	H	OCH ₃
25P-NB2OMe	CH ₂ CH ₂ CH ₃	OCH ₃	H	H
25P-NB3OMe	CH ₂ CH ₂ CH ₃	H	OCH ₃	H
25P-NB4OMe	CH ₂ CH ₂ CH ₃	H	H	OCH ₃
25T2-NB2OMe	CH ₃ CH ₂ S	OCH ₃	H	H
25T2-NB3OMe	CH ₃ CH ₂ S	H	OCH ₃	H
25T2-NB4OMe	CH ₃ CH ₂ S	H	H	OCH ₃
25T4-NB2OMe	(CH ₃) ₂ CHS	OCH ₃	H	H
25T4-NB3OMe	(CH ₃) ₂ CHS	H	OCH ₃	H
25T4-NB4OMe	(CH ₃) ₂ CHS	H	H	OCH ₃
25T7-NB2OMe	CH ₃ (CH ₂) ₂ S	OCH ₃	H	H
25T7-NB3OMe	CH ₃ (CH ₂) ₂ S	H	OCH ₃	H
25T7-NB4OMe	CH ₃ (CH ₂) ₂ S	H	H	OCH ₃

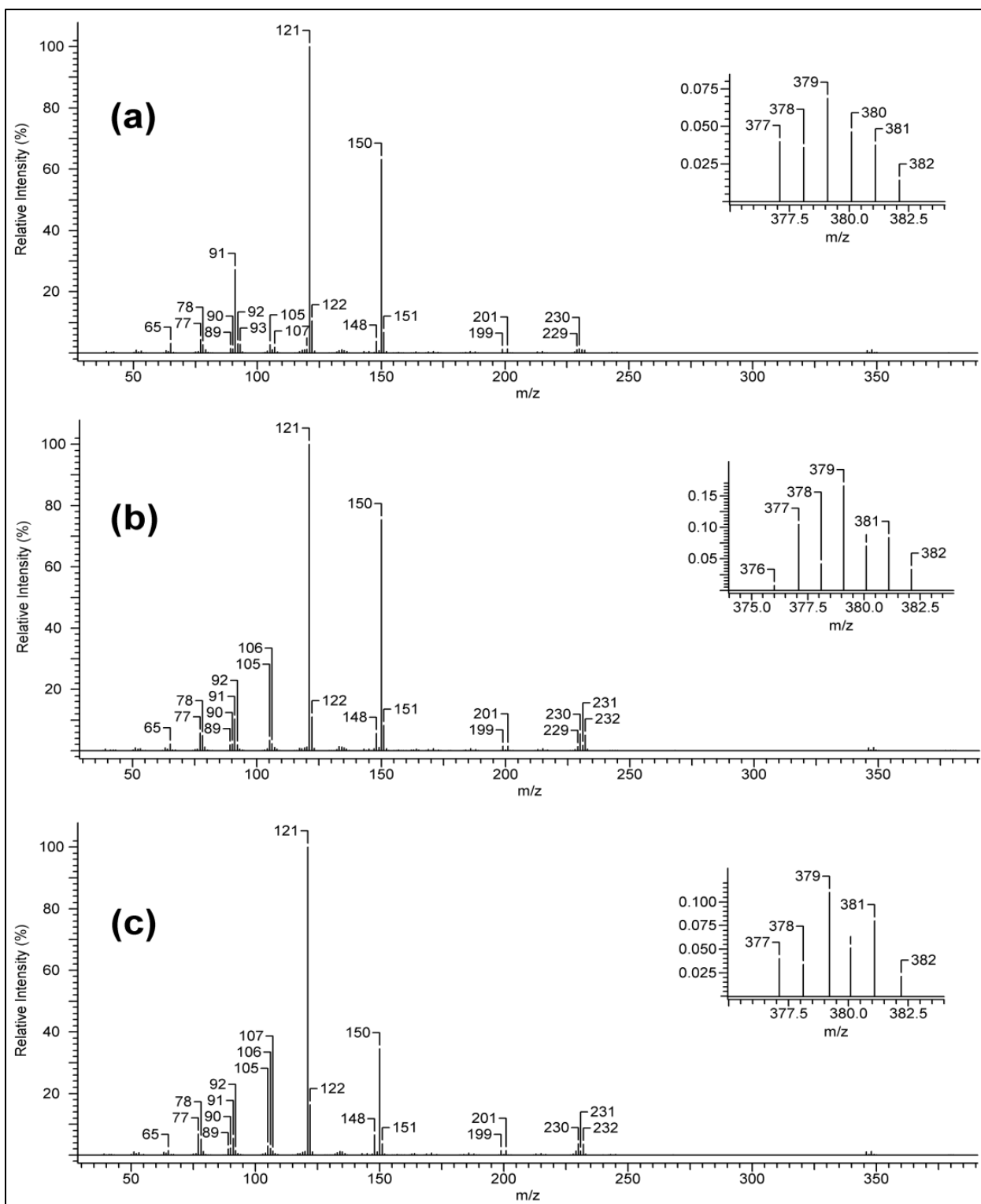


Figure 11 Mass spectra of (a) 2,5-dimethoxy-4-bromo-N-(2'-methoxy)benzyl-phenethylamine (25B-NB2OMe) 4, (b) 2,5-dimethoxy-4-bromo-N-(3'-methoxy)benzyl-phenethylamine (25B-NB3OMe) 5, and (c) 2,5-dimethoxy-4-bromo-N-(4'-methoxy)benzyl-phenethylamine (25B-NB4OMe) [93].

1.9 Gas chromatography with infrared detection (GC–IRD):

Mass spectrometry is usually the confirmatory piece of evidence for the chemical structure elucidation of many drugs in forensic laboratories [98]. One of the most important disadvantages of mass spectroscopy technique is the inability to differentiate closely related member of drugs with limited unique mass spectral characteristics [94, 98]. Infrared spectroscopy is considered as a useful tool for the identification of compounds with similar mass spectra such as positional [94] and geometric isomers [99] other than optical isomers [100]. The use of gas chromatography coupled to infrared detection (GC–IRD) provides the benefits of both instruments by combining separation power of gas chromatography with the identification power of infrared spectrometry [98]. Casale and Hays used FTIR to analyze 11 commonly encountered NBOMes with differing 4-substituents as well as their 3- and 4-methoxybenzyl regioisomers [97]. All of these compounds were analyzed as their HCl salts and each compound exhibited characteristic secondary amine HCl ion-pair absorbances between 2500-3000 cm^{-1} (Figure 12). They also noted that while NBOMe derivatives with different 4-substituents yielded similar IR spectra, there were characteristic differences in the 400-1600 cm^{-1} region of the spectra, allowing for compound differentiation. They also observed significant differences between the 2'-, 3' and 4'-methoxy regioisomers of NBOMEs with a common 4-substituent and that these were sufficient for isomer differentiation. At present there are only a few other studies on the IR properties of NBOMe derivatives [28, 29, 93, 97, 101].

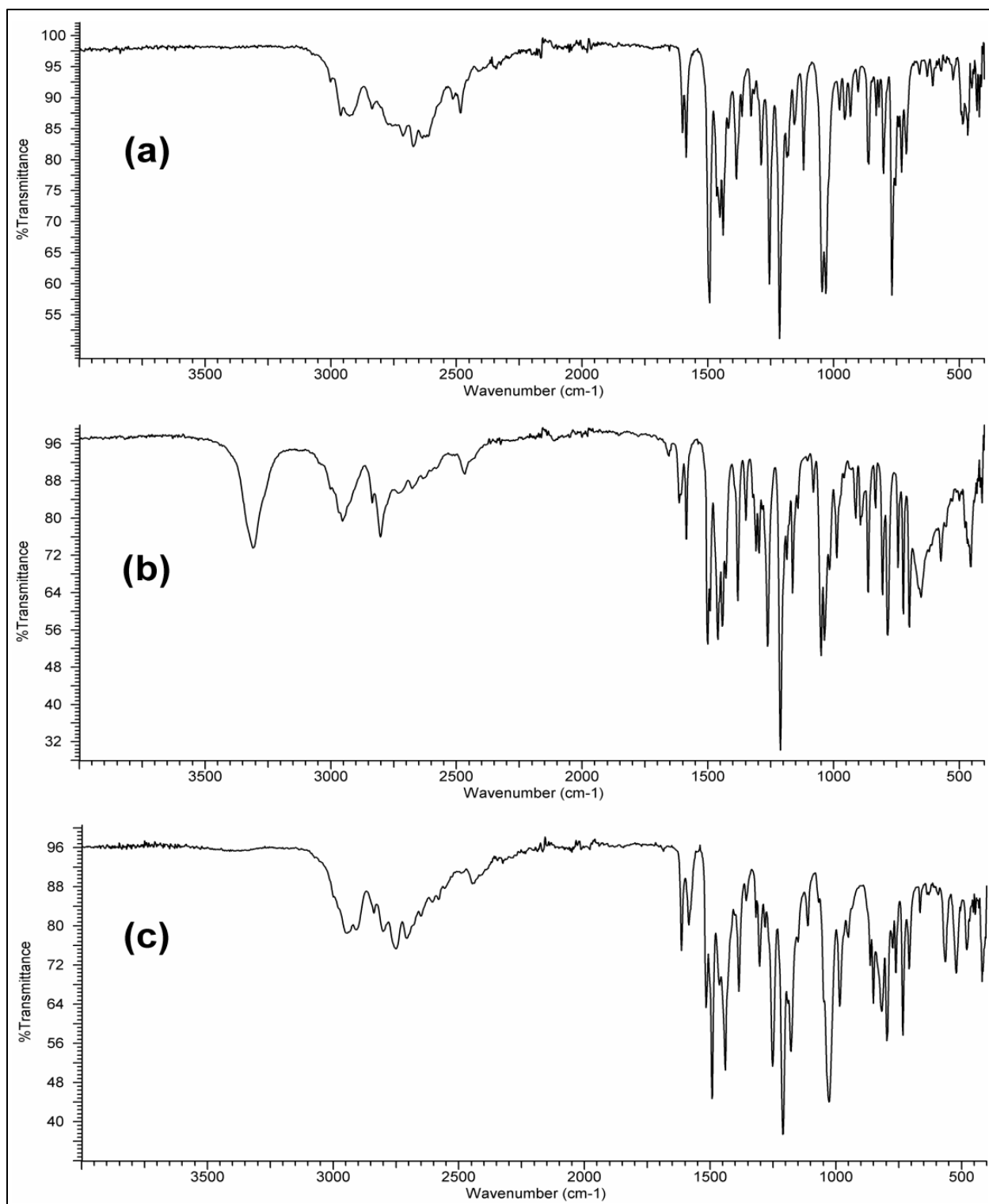


Figure 12 FTIR spectra of (a) 2,5-dimethoxy-4-bromo-N-(2'-methoxy)benzyl-phenethylamine HCl (25B-NB2OMe) 4, (b) 2,5-dimethoxy-4-bromo-N-(3'-methoxy)benzyl-phenethylamine HCl (25B-NB3OMe) 5, and (c) 2,5-dimethoxy-4-bromo-N-(4'-methoxy)benzyl-phenethylamine HCl (25B-NB4OMe) [97].

1.10 Nuclear magnetic resonance (NMR):

NMR spectroscopy can be very a very useful analytical instrument for structural identification of controlled substances. For example, it has the ability to distinguish between different stereoisomers and to analyze non-volatile materials [102], it can eliminate the need for sample derivatization to avoid thermal decomposition. It also allows the use of both forms of sample, salt and free base for sample analysis and it can estimate the percentage purity [103]. Furthermore, NMR has the capability of analyzing the chemical structure of a sample without destroying the compound [104, 105] as long the sample is stable in the solvent chosen for the analysis. This can allow for sample recovery for further analysis by other means [105].

However, in spite of its benefits for forensic analysis, NMR has its limitations, including lack of sensitivity. While mass spectrometry requires only nanograms or less of the sample to be tested, NMR usually requires micrograms or more for drug analysis. Therefore, this limitation does affect the ability of the NMR to be used in forensic sample analysis of bodily fluids and their metabolites [105] as they tend to have very small concentration of the drug. Among other reasons that limit NMR use in many forensic labs is the high cost to own it [105, 106].

Several reports have been published regarding NBOMe identification using NMR spectroscopy [28, 29, 101, 107-109]. The proton NMR spectra for all 25X-NBOMes reported to date are very similar and consistent with that of 25B-NBOMe shown in the Figure 13 below. There are six aromatic protons in a multiplet centered at 7.1 ppm and three singlets from 3.6-3.75 ppm for the three methoxy groups integrating for a total of nine protons. The four coupled protons of the ethyl side chain are centered at 3.1 ppm and the two benzylic protons at 4.15 ppm.

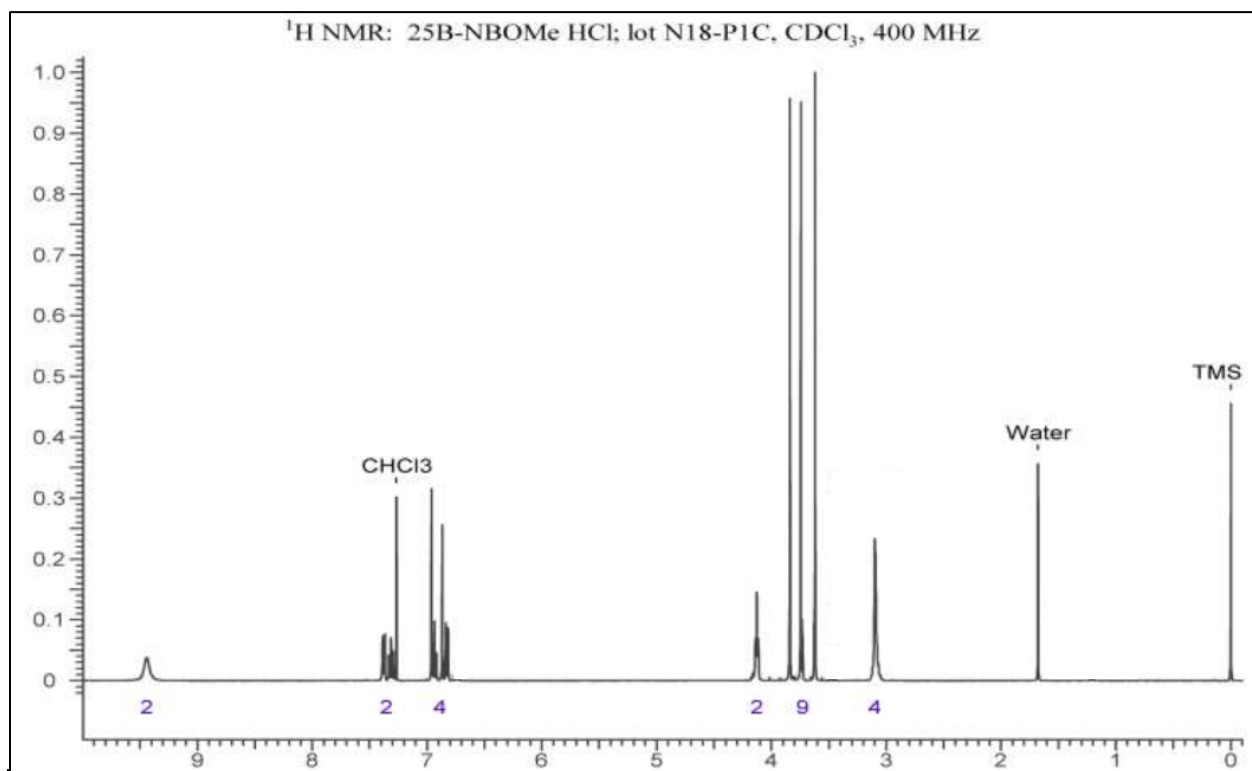


Figure 13 NMR spectrum of 25B-NBOMe HCl salt [95].

1.11 Synthesis and Chemistry of the NBOMes:

The NBOMe compounds are derivatives of the 2C-X hallucinogens with a N-2'-methoxybenzyl substituent. These compounds contain a single, basic nitrogen atom and therefore can be available in free base form or as salts of organic and inorganic acids. Both the free base forms and salt forms are solids. The NBOMes do not contain a chiral center and no stereoisomers exist.

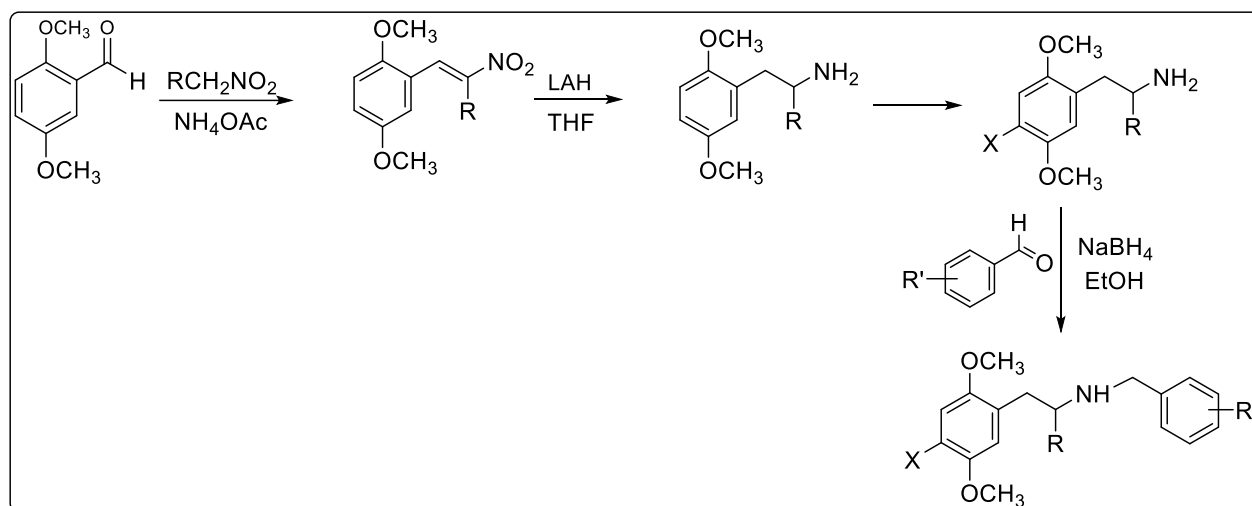
The IUPAC nomenclature for compounds of this structure class is 2-(4-halo-2,5-dimethoxyphenyl)-N-[(2-methoxyphenyl)methyl]ethanamine. They are also referred to by the following trivial chemical names:

- 2-(4-halo-2,5-dimethoxyphenyl)-N-(2-methoxybenzyl)ethanamine
- 2-(4-halo-2,5-dimethoxyphenyl)-N-(2-methoxybenzyl)ethan-1-amine
- 4-halo-2,5-dimethoxy-N-(2-methoxybenzyl)phenethylamine
- 4- halo -2,5-dimethoxy-N-(o-methoxybenzyl)phenethylamine
- 4- halo -2,5-dimethoxy-N-[(2-methoxyphenyl)methyl]-benzeneethanamine
- N-(2-methoxybenzyl)-2,5-dimethoxy-4-halophenethylamine
- N-(2-methoxybenzyl)-4- halo-2,5-dimethoxyphenethylamine

The synthesis of 25B-NBOMe and 25I-NBOMe was first described by Heim in 2003. It involved a stepwise reductive alkylation where first an imine was formed by reaction of 2-methoxybenzaldehyde and 2C-B in an alcohol solvent. The imine was then reduced by addition of sodium borohydride (NaBH₄). A number of NBOMes derivatives with varying 4-substituents (25X-NBOMes) have been prepared by this method using reaction of 2-methoxybenzaldehyde with different 2C-X intermediates.

The core structure of NBOMe molecules and the method used for their synthesis makes these drugs ideal candidates for designer modification. For example, the phenethyl aromatic ring is easily modified by simply preparing 2C-X precursors with differing ring substituents and substitution patterns. The synthesis of a large number of 2C-X compounds is reported in the literature and usually involves reaction of 2,5-dimethoxybenzaldehyde with nitromethane to form the 2,5-

dimethoxyphenyl-2-nitroethene intermediates which are then reduced to 2C by lithium aluminum hydride. The X-substituent are then added at the 4-position by a variety of functionalization reactions. Using this same basic synthetic approach but replacing nitromethane with other nitroalkanes, NBOMe analogs with substitutions in the ethyl side chain could also be generated. Also, NBOMe derivatives with modified N-benzyl substituents could be synthesized by using any of hundreds different commercially available or synthetically derived benzaldehyde or aromatic ketone derivatives. Finally, NBOMe designer analogs with additional N-substituents could be synthesized by simple N-substitution reactions of either NBOMe compounds themselves or 2C-X precursors. These types of modifications are illustrated by the generic synthetic scheme 4 shown below:



Scheme 4 general synthetic scheme for 25X-NBOMes.

1.12 Project Rationale and Specific Objectives:

A relative large number of NBOMe-type drugs of abuse have already been detected in forensic samples and clinical case reports from across the globe. Furthermore, it is anticipated that attempts to tighten legal control of the NBOMe compounds and the general interest in designer drug development will likely stimulate clandestine chemists to generate novel NBOMe derivatives in the future. Such designer drug activity has already been observed for many drugs of abuse class including the amphetamines, MDMA, bath salts and synthetic cannabinoids over the past several decades. The basic structure of the NBOMe molecules and the methods used for their synthesis makes these drugs ideal candidates for designer modification. Analytical studies with the NBOMe compounds reported to date have already highlighted the challenges in identifying compounds of this structural class, and especially differentiating individual NBOMe derivatives within a regioisomeric series. As noted, these compounds can exist in homologous and isomeric forms often sharing the same mass spectrum, the most common method of confirmation of drug identity in forensic drug analysis.

The goal of this work was to develop an analytical framework for the identification of individual substituted NBOMe or N-benzyl-phenethylamine derivatives to the exclusion of all other possible isomeric and homologous forms of these compounds. Generally, this analytical specificity was accomplished by the chemical synthesis of several series of substituted N-benzyl-phenethylamines which varied in their substitution pattern in all four regions of the core structure as described below, and generation of an analytical profile for each series of derivatives as well as the individual members of a series. Chromatographic studies were undertaken to separate and resolve all regioisomeric members of each N-benzyl-phenethylamine series that had overlapping analytical profiles. Also, based on initial results obtained during the course of the research, additional analogs were synthesized and derivatization studies were conducted to enhanced and validate analytical specificity. The approaches employed to accomplish these goals are described in more detail below.

1.13 Design and Synthesis of NBOMe derivatives:

The overall goal of this project was a comprehensive analytical study of isomeric and designer analogues of the substituted NBOMe derivatives of the N-benzyl-phenethylamine class of synthetic drugs. The availability of the necessary compounds to establish and validate structure-retention, structure-fragmentation and other structure-property analytical relationships was therefore the initial objective of this research. Figure 14 shows that novel NBOMe derivatives can readily be generated by changing the nature of precursors used in the synthesis or altering the synthetic approach. Such synthetic modifications would yield new derivatives which would vary from existing NBOMe compounds in four general regions of the molecule including the aromatic ring substituents on the phenethyl group (I: X, Y and Z), the aromatic ring substituents on the benzyl group (II: X' and Y'), alkyl substitution of the phenethyl chain (III: R) and additional alkyl substitution of the nitrogen (IV: R').

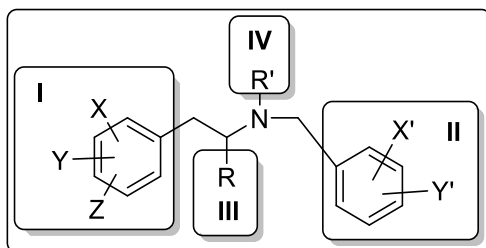


Figure 14 General skeleton of NBOMes derivatives.

Derivatives prepared included:

I: Modifications of the aromatic ring substituents on the phenethyl group included:

- Derivatives with no substituents ($X = Y = Z = H$)
- Regioisomeric 2-, 3- and 4-methoxy derivatives ($X = OCH_3$; $Y = Z = H$)
- Regioisomeric 2,3-, 2,4-, 2,5-, 2,6-, 3,4- and 3,5-dimethoxy derivatives ($X = Y = OCH_3$; $Z = H$)
- 4-Bromo-2,5-dimethoxy derivatives ($X = Y = 2,5-OCH_3$; $Z = 4-Br$)
- 4-Iodo-2,5-dimethoxy derivatives ($X = Y = 2,5-OCH_3$; $Z = 4-I$)

II: Modifications of the aromatic ring substituents on the benzyl group included:

- Derivatives with no substituents ($X = Y = Z = H$)
- Regioisomeric 2-, 3- and 4-methoxy derivatives ($X = OCH_3$; $Y = Z = H$)
- Regioisomeric 2,3-, 2,4-, 2,5-, 2,6-, 3,4- and 3,5-dimethoxy derivatives ($X = Y = OCH_3$; $Z = H$)
- Various bromo-dimethoxy derivatives ($X = Y = OCH_3$; $Z = Br$)

III. Modifications of phenethyl chain included methyl substitution ($R = CH_3$)

IV. Modifications of the substitution of the nitrogen ($R = CH_3$)

Initial Mass Spectral Analysis: Each of the NBOMe derivatives prepared was initially analyzed by CI-MS and EI-MS to establish molecular weight and characteristic fragment patterns. MS/MS studies were performed to identify the origin of the more abundant fragment ions

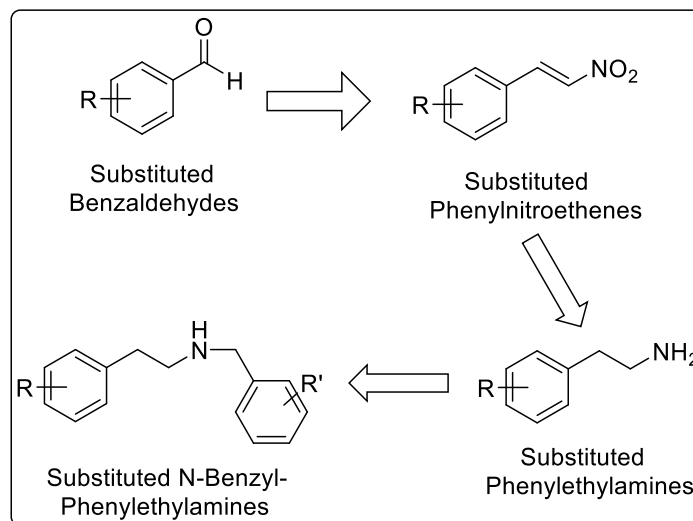
Secondary Mass Spectral Studies: MS/MS studies were performed to identify the origin of the more abundant fragment ions. Additional NBOMe derivatives including deuterium and ^{13}C -labeled analogs were prepared and analyzed to establish specific MS-fragment structures and elemental composition. TFA-derivatization studies were performed in an attempt to individualize mass spectra of regioisomeric derivatives

Chromatographic Separations: GC chromatographic conditions were explored to separate members of regioisomer series and their TFA-derivatives

2 Synthesis of the Target NBOMe Derivatives

2.1 Synthesis of N-(Methoxy)-, N-(Dimethoxy)- and N-(Methylenedioxyphenyl)benzyl-Substituted phenethylamines:

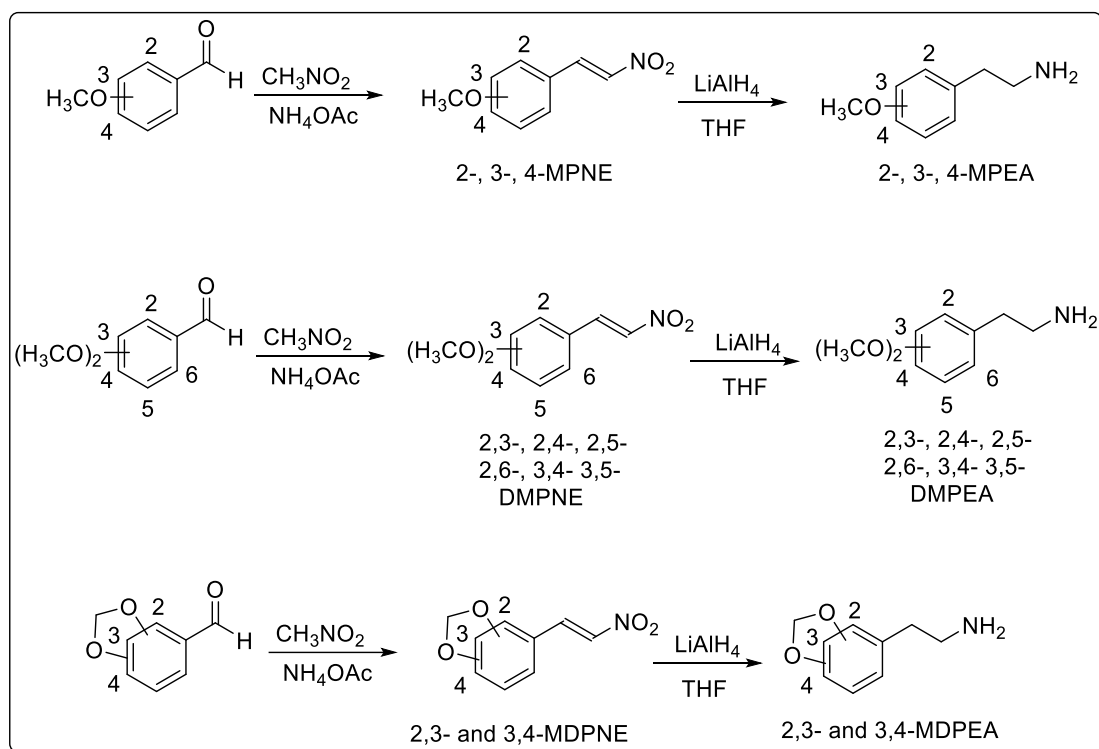
The compounds of this series are NBOMe derivatives where the 4-halogen has been eliminated from the phenethylamine portion of the base NBOME structure, and the methoxy group substitution pattern in the phenethyl and benzyl aromatic rings has been varied as described below. The approach for the synthesis of the methoxy-, dimethoxy- and methylenedioxy-substituted N-benzylphenethylamines series is shown in the Scheme 5 below and is based on standard methodology used to prepare compounds of the NBOMe structural class. This approach requires first the synthesis of substituted phenethylamines which are then subjected to reductive alkylation with substituted benzaldehydes to yield the desired products. The substituted phenethylamines are prepared by reaction of commercially available substituted benzaldehydes with nitromethane in a condensation reaction, followed by reduction of the intermediate phenylnitroethenes with lithium aluminum hydride (Scheme 5).



Scheme 5 Synthetic approach for the methoxy-, dimethoxy- and methylenedioxy-substituted N-benzylphenethylamines.

Reaction of the three commercially available methoxybenzaldehydes (2-, 3- and 4-methoxybenzaldehyde), six dimethoxybenzaldehydes (2, 3-, 2, 4-, 2, 5-, 2, 6-, 3, 4- and 3, 5-

dimethoxybenzaldehydes and two methylenedioxybenzaldehydes (2,3- and 3,4-) with nitromethane in the presence of anhydrous ammonium acetate provided the intermediate substituted-phenyl-2-nitroethenes (Scheme 6 and Table 2, abbreviated as substituted “PNE” for phenylnitroethenes). All of the nitroethene intermediates were crystallized and recrystallized from alcohol solvents or solvent mixtures and were obtained in adequate yield (except for the 2-MPNE isomer which required re-synthesis due to low yields) for subsequent reactions. The structures of all nitroethene intermediates were confirmed by mass spectroscopy and with NMR for selected members of this series. Figures 15-17 show the EI mass spectra of representative members of this series. Each structure type, the monomethoxyphenyl-2-nitroethenes (MPNE), dimethoxy-2-nitroethenes (DMPNE) and methylenedioxy-2-nitroethenes (MDPNE) gave a molecular ion (M⁺) of high relative abundance (MPNE *m/z* 179, DMPNE *m/z* 209 and MDPNE *m/z* 193) and fragment ions characteristic for this structural class based on our previous research.



Scheme 6 Synthetic approach for the methoxy-, dimethoxy- and methylenedioxy-substituted phenethylamine intermediates.

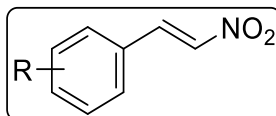


Table 2 Yields and Crystallization Solvents for the Methoxy (MPNEs)-, Dimethoxy (DMPNEs)- and Methyleneedioxy (MDPNEs)- phenylnitroethenes.

Product	Crude product forms	Crystallization solvent	Recrystallization solvent
2-MPNE	Orange oil	MeOH	iPrOH/Acetone (2.7 g)
3-MPNE	Orange oil	iPrOH	iPrOH (6.2 g)
4-MPNE	Dark red oil	iPrOH	MeOH (2.1 g)
2,3-DMPNE	Red oil	iPrOH	iPrOH (6.8 g)
2,4-DMPNE	Red oil	iPrOH	iPrOH (8.2 g)
2,5-DMPNE	Orange solid	iPrOH	iPrOH (8.7 g)
2,6-DMPNE	Yellow Solid	iPrOH	iPrOH (10.5 g)
3,4-DMPNE	Yellow Solid	iPrOH	iPrOH (10.8 g)
3,5-DMPNE	Yellow solid	iPrOH	iPrOH (6.6 g)
2,3-MDPNE	Yellow Solid	MeOH	MeOH (5.2 g)
3,4-MDPNE	Yellow Solid	iPrOH	iPrOH (7.2 g)

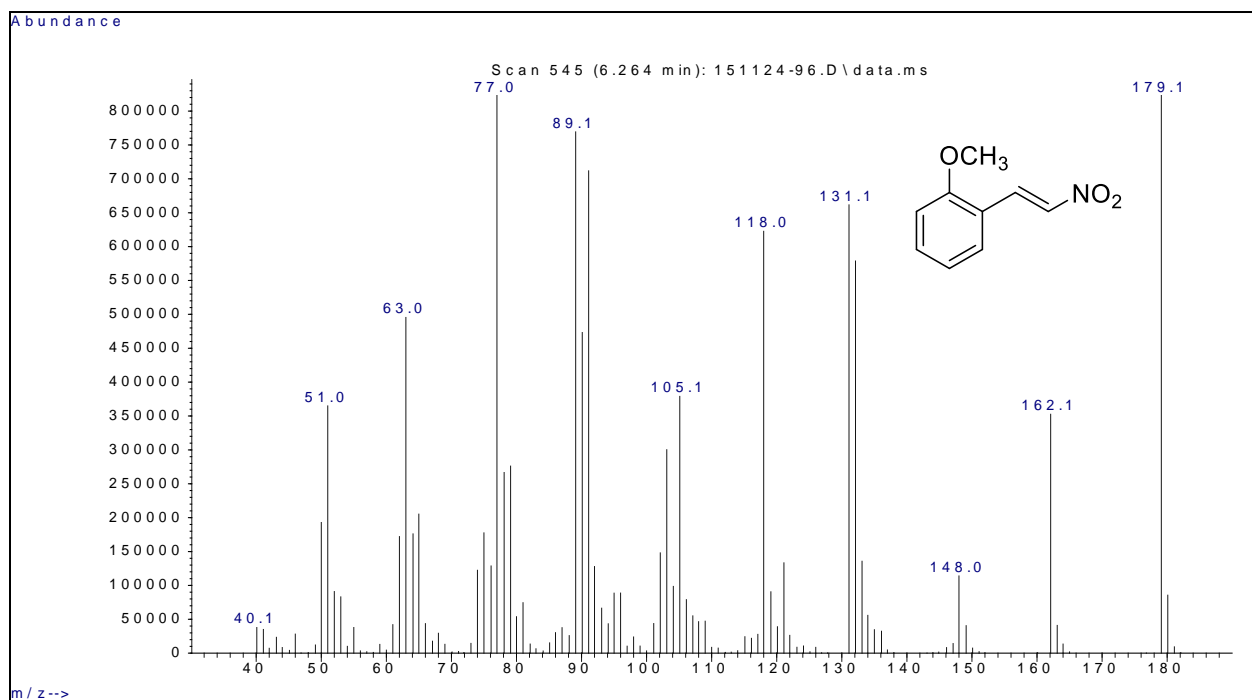


Figure 15 Mass Spectra of the 2-monomethoxy nitroethene.

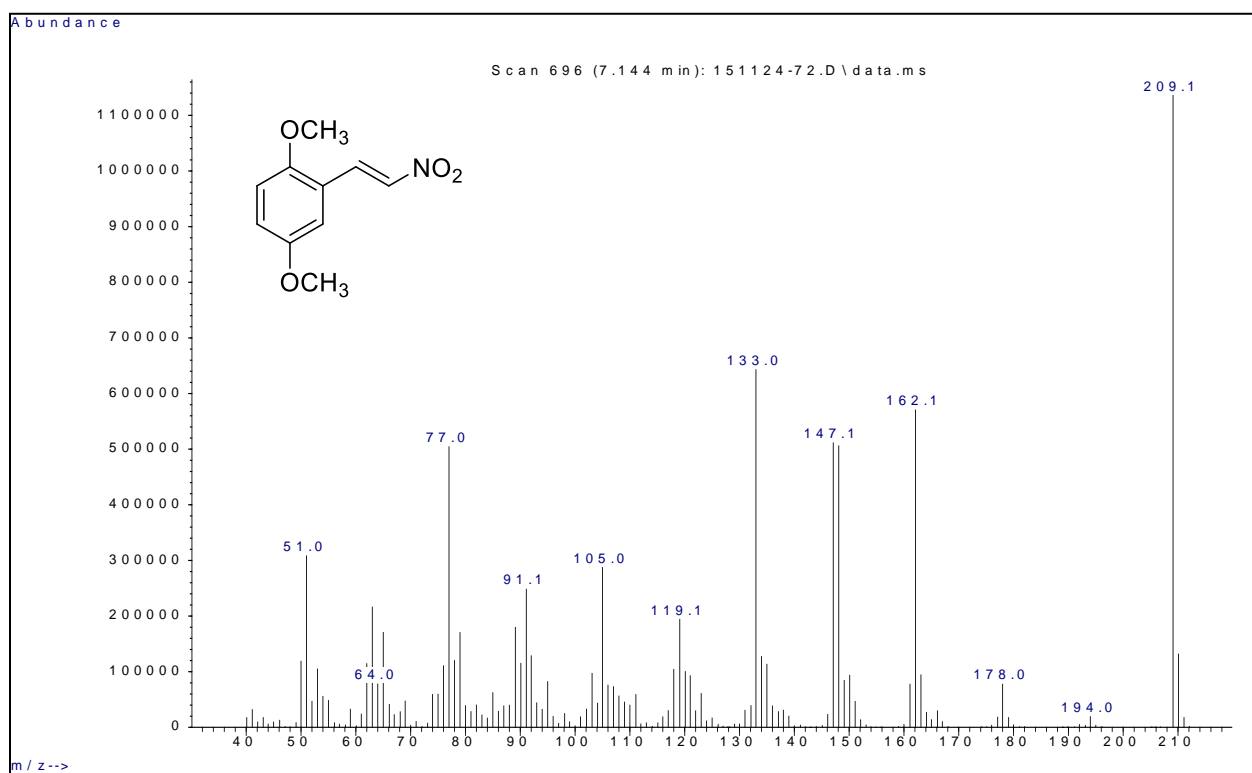


Figure 16 Mass Spectra of the 2,5-dimethoxy nitroethene.

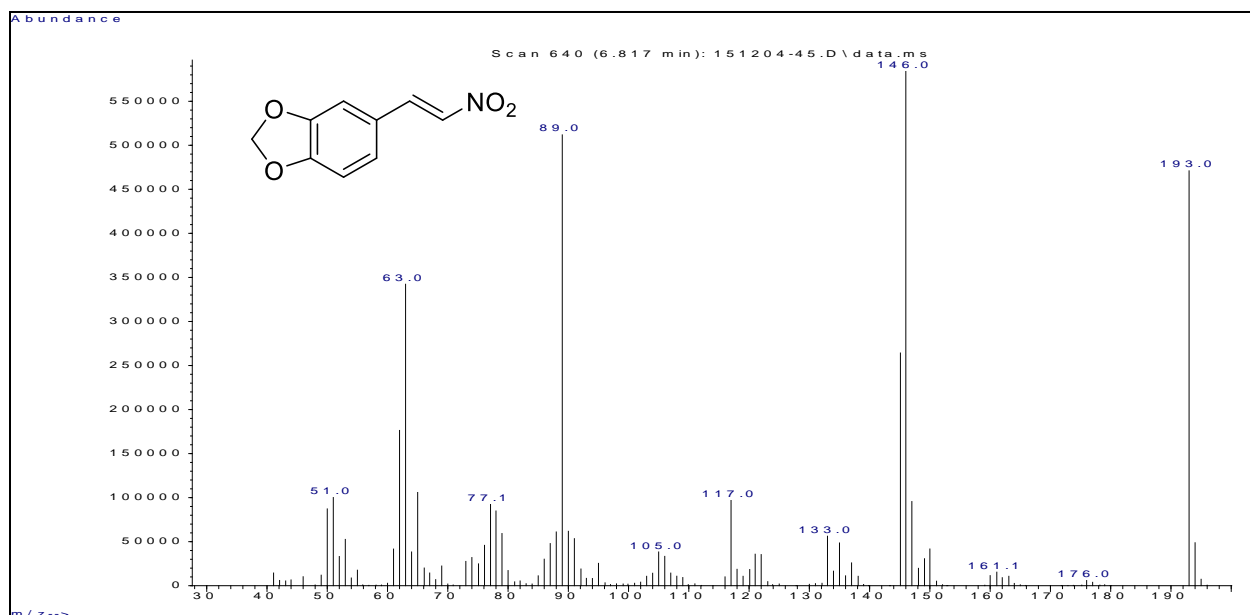


Figure 17 Mass Spectra of the 3,4-methylenedioxy nitroethene.

Figure 18 shows the proton NMR spectrum for the 2,5-dimethoxynitroethene (25DMPNE), a representative member of the PNE synthetic intermediates. The protons of the two methoxy groups appear as singlets at 3.8 and 3.9 ppm, characteristic for protons on an ether carbon, and the two coupled vinylic protons appear as doublets in the 7.8-7.9 and 8.10-8.15 ppm region.

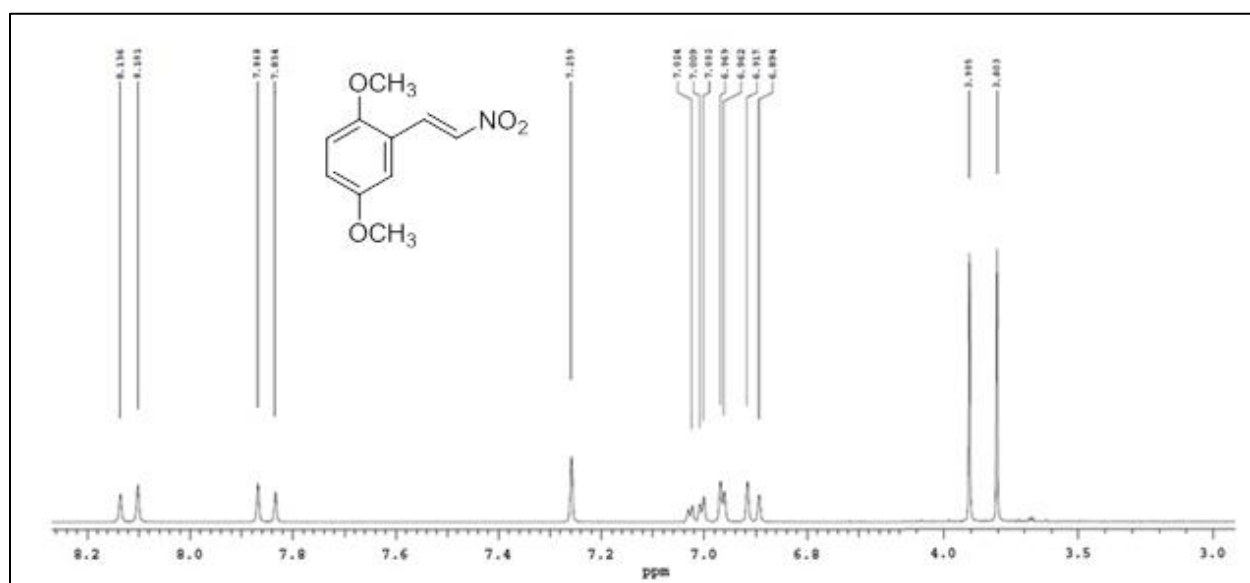


Figure 18 NMR Spectra of the 2,5-dimethoxy nitroethene.

The three aromatic protons are present at a multiplet from 6.9-7.1 ppm, all consistent with spectra obtained from this structural class in our previous studies and reported in the literature.

The recrystallized and dried nitroethenes were reduced with lithium aluminum hydride (LAH) in THF using standard literature protocol to give the three regioisomeric methoxyphenethylamines (2-, 3- and 4-MPEA), the six regioisomeric dimethoxyphenethylamines (2, 3-, 2, 4-, 2, 5-, 2, 6-, 3, 4- and 3, 5-DMPEA) and two regioisomeric methylenedioxyphenethylamines (2, 3- and 3,4-MDPEA). All of the phenethylamine intermediates, except the 2,3-DMPEA derivative, were converted to HCl salts for further purification by recrystallization. The products formed and their yields are shown in Table 3 below.

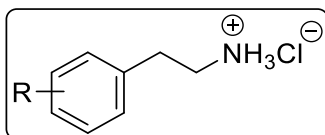


Table 3 Yields for the Methoxy (MPNEs)-, Dimethoxy (DMPNEs)- and Methylenedioxy- (MDPNEs)- Phenethylamines.

Product from reduction of 3 g of substituted PNE	Crude product base after extraction	Product yield of HCl salt
2-MPEA HCl	Oil	1.87 g
3-MPEA HCl	Oil	1.77 g
4-MPEA HCl	Oil	1.97 g
2,3-DMPEA	Oil	1.3 g (base)
2,4-DMPEA HCl	Oil	1.70 g
2,5-DMPEA HCl	Oil	1.48 g
2,6-DMPEA HCl	Oil	1.57 g
3,4-DMPEA HCl	Oil	0.92 g
3,5-DMPEA HCl	Oil	1.8 g
2,3-MDPEA HCl	Oil	1.190 g
3,4-MDPEA HCl	Oil	2.17 g

The structures of all phenethylamine intermediates were confirmed by mass spectroscopy and proton NMR. Figures 19-21 show the EI mass spectra of the representative members of this series including the 2-methoxy isomer (2MPEA), the 2,5-dimethoxy isomer (25DMPEA) and the 3,4-methylenedioxy isomer (34MDPEA). A molecular ion is observed for each of these compounds

(2MPEA $M = 151$, 25DMPEA $M = 181$, 34MDPEA $M = 165$), and each compound undergoes amine-dominated fragmentation to yield a benzyl cation base peak characteristic of the degree and nature of substitution on the aromatic ring and -29 mass units from the molecular ion (2MPEA $m/z = 122$, 25DMPEA $M = 152$, 34MDPEA $M = 136$). The immonium cation formed by an alpha-cleavage reaction is typically observed as the base peak for phenethylamines and would occur at m/z 30 for these isomers. However, the lower mass range limit for the scan range used was mass 40, thus the spectra do not show a peak for the immonium cation fragment. The mass spectral data obtained for these intermediates were completely consistent with data obtained for substituted phenethylamines in earlier studies in our laboratories.

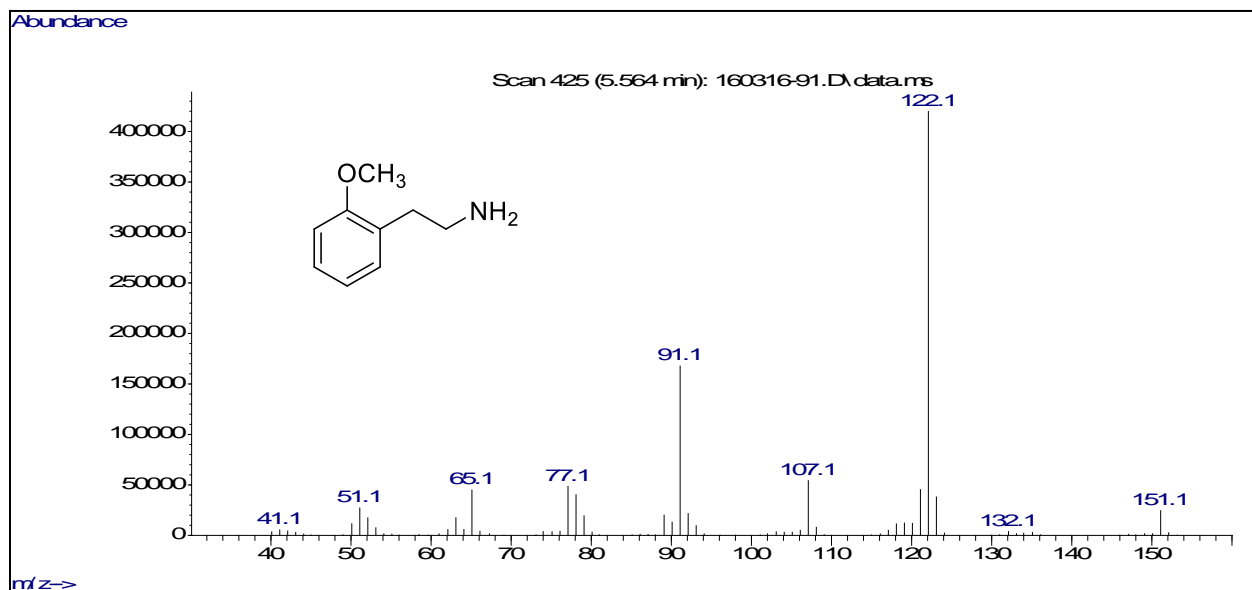


Figure 19 Mass Spectra of the 2-monomethoxyphenethylamine.

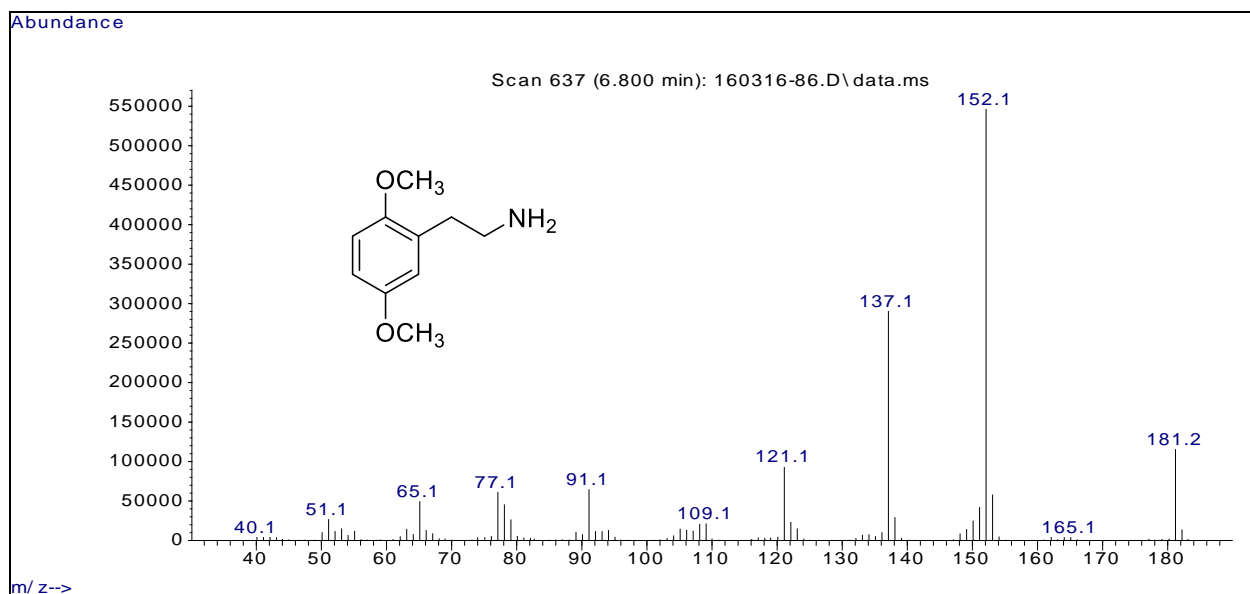


Figure 20 Mass Spectra of the 2,5-dimethoxyphenethylamine.

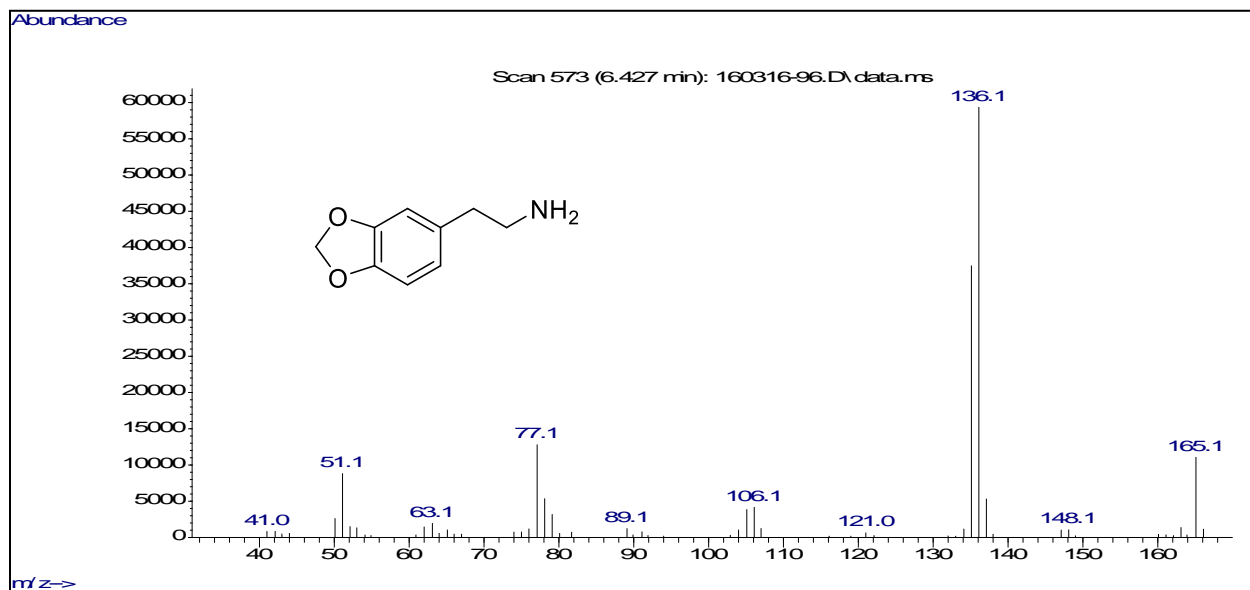


Figure 21 Mass Spectra of the 3,4-methylenedioxyphenethylamine.

Figure 22 shows the NMR spectrum for a selected member of the phenethylamine intermediate series, 2,5-dimethoxyphenethylamine. The two methoxy groups are present as singlets in the characteristic region of 3.7 and 3.8 ppm, and the two coupled methylene units are triplets at 2.8-2.9 ppm and 3.0-3.1 ppm. The three aromatic protons occur as a multiplet at 6.7-6.8 ppm and the

amine protons at 7.25 ppm. This proton NMR spectrum is characteristic for substituted phenethylamines synthesized previously in our laboratories.

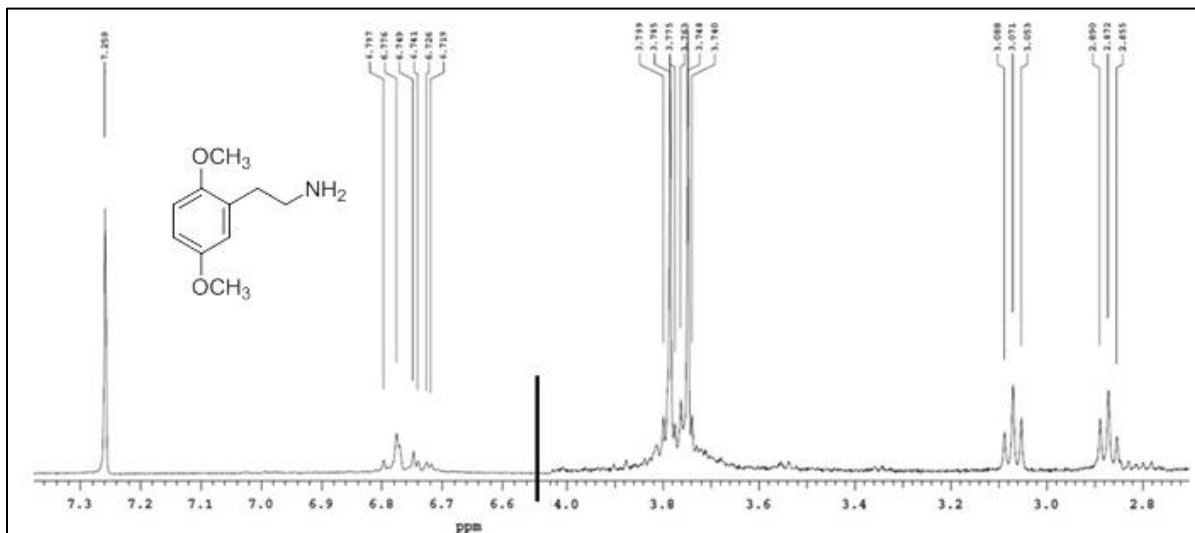


Figure 22 NMR Spectra of the 2,5-dimethoxyphenethylamine.

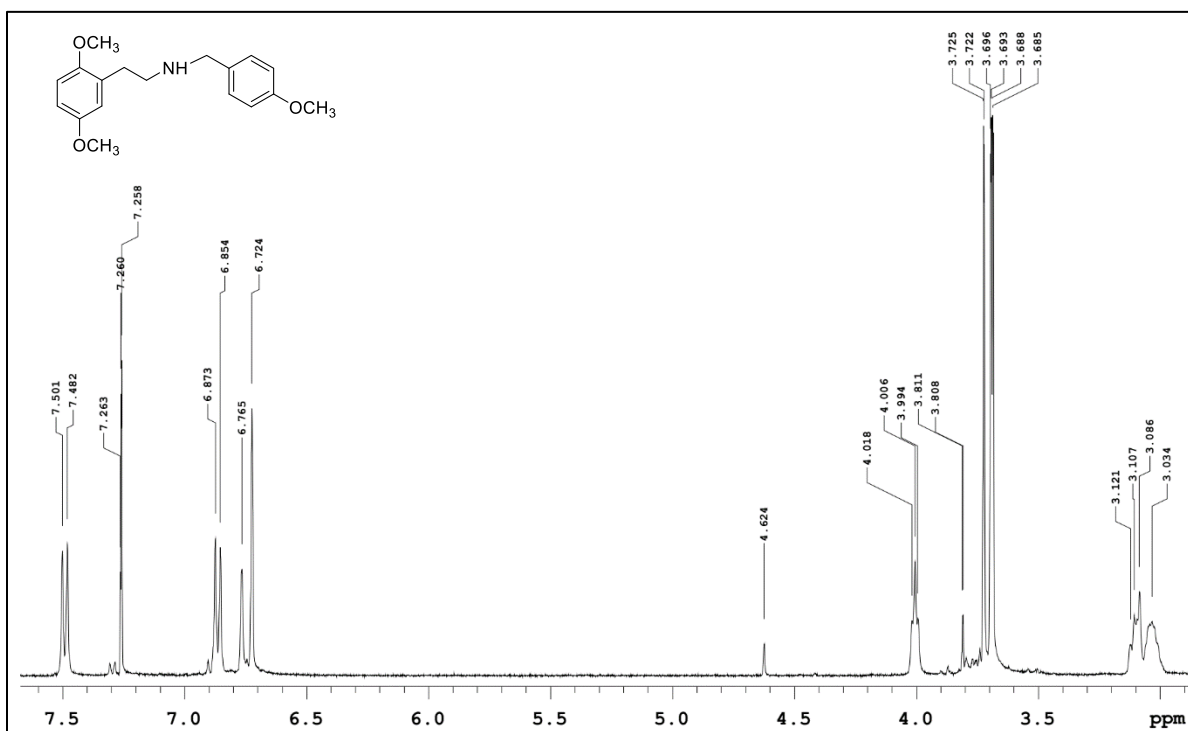
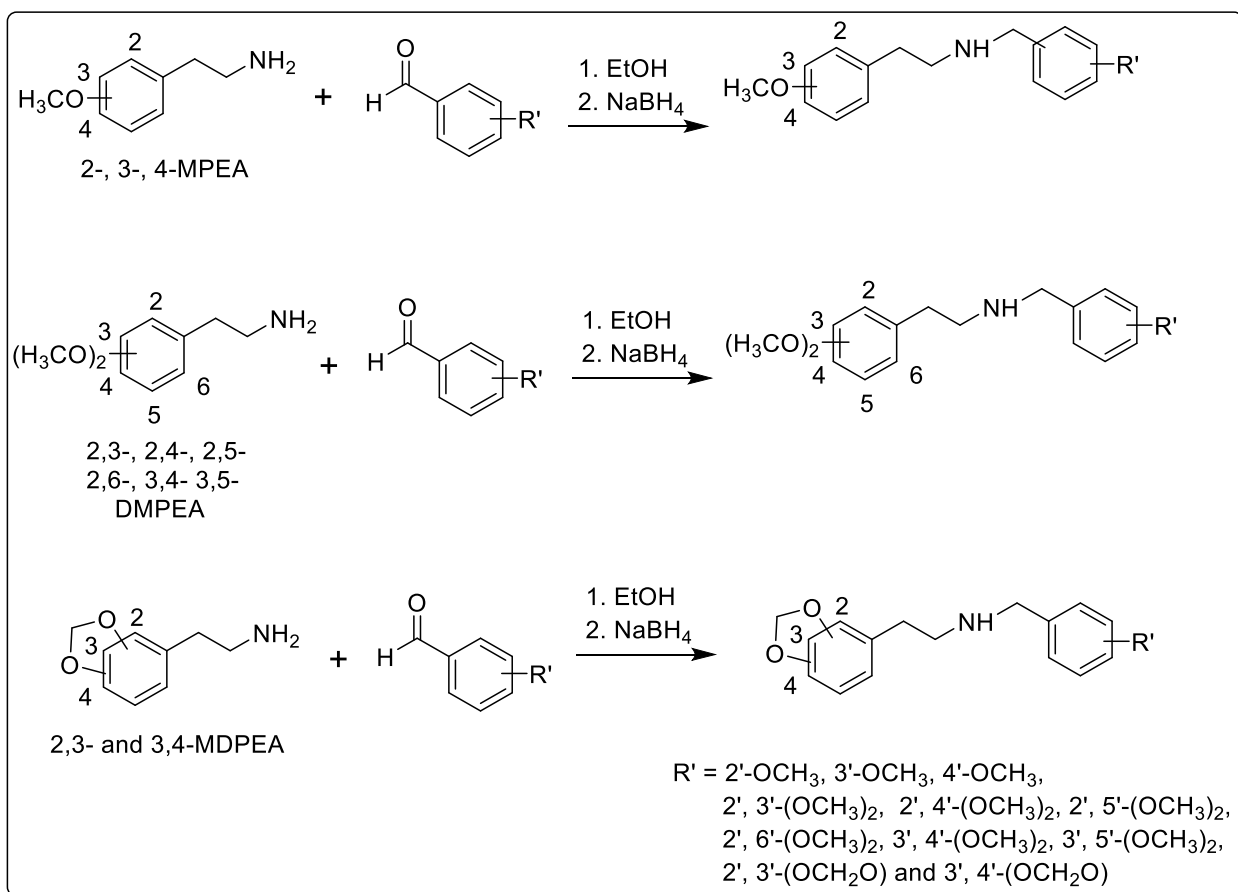


Figure 23 NMR spectrum of N-4-methoxybenzyl-2,5-Dimethoxyphenethylamines.

The three methoxy-, six dimethoxy- and two methylenedioxyphenethylamine hydrochloride salts were then used to prepare a large number of N-(substituted)benzyl-NBOMe derivatives, using the general reductive alkylation method shown in Scheme 7. The substituted benzaldehydes used for these reactions included the three commercially available methoxybenzaldehydes (2-, 3- and 4-methoxybenzaldehyde), six dimethoxybenzaldehydes (2, 3-, 2, 4-, 2, 5-, 2, 6-, 3, 4- and 3, 5-dimethoxybenzaldehydes and two methylenedioxybenzaldehydes (2,3- and 3,4-methylenedioxybenzaldehydes). Initially these reactions were attempted by combining the phenethylamine, appropriate benzaldehyde and sodium cyanoborohydride (NaBH_3CN) in ethanol as a single step reaction. However, this method afforded only very low yields, presumably due to slow formation of the intermediate imine. This approach also left relatively large quantities of unreacted primary amine (substituted phenethylamine) in the mixture with the product secondary amine which complicated purification. Therefore, these reactions were performed stepwise, involving imine formation first in hot ethanol, followed by reduction with sodium borohydride (NaBH_4) at room temperature. In this approach the substituted phenethylamine intermediates (1.0 mmolar scale) were heated for 2 hours with one equivalent of triethylamine and one equivalent of the desired commercially available aldehyde in ethanol to yield the intermediate imine (not isolated). After initial imine formation, the reaction mixture was cooled to room temperature and an excess of NaBH_4 (5.3 mmole) added and the resulting reaction mixture was stirred overnight at room temperature. The reactions were worked up by evaporation under reduced pressure and suspending the crude products in water which was neutralized by addition of a few drops of concentrated HCl. The products were extracted into dichloromethane (DCM) and the combined DCM extracts evaporated and dried under reduced pressure. All products were isolated in the free base form and were crystallized using the solvents listed in Tables 4-6 below. The specific products prepared are shown in Tables 4-6. The NMR of A representative member of NBOMes is shown in figure 23.



Scheme 7 Synthesis of the Methoxy-, Dimethoxy- and Methylenedioxy-N-Benzylphenethylamines.

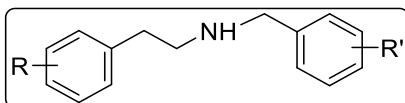


Table 4 Yields and Crystallization Solvents for the N-(Methoxy)benzyl-methoxyphenethylamines.

Compound abbreviation	Phenethyl ring substituent (R)	Benzyl ring substituent (R')	Yield, mg (1 st & 2 nd crop)	Crystallization solvent
PEAB	H	H	148	Ether
2MPEA2MB	2-MeO	2'-MeO	154.6	Ether
2MPEA3MB	2-MeO	3'-MeO	103.8	Ether
2MPEA4MB	2-MeO	4'-MeO	119.3	Ether
3MPEA2MB	3-MeO	2'-MeO	147.5	Ether
3MPEA3MB	3-MeO	3'-MeO	124.5	Ether
3MPEA4MB	3-MeO	4'-MeO	103.6	Ether
4MPEA2MB	4-MeO	2'-MeO	139.1	Ether
4MPEA3MB	4-MeO	3'-MeO	130.8	Ether
4MPEA4MB	4-MeO	4'-MeO	128.6	Ether

From 1 mmole amine HCl, + 1 mmole aldehyde and 1 mmole TEA and 200 mg NaBH₄.

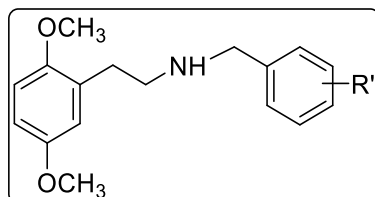


Table 5 Yields and Crystallization Solvents for the N-(dimethoxy)benzyl- and N-(methylenedioxy)benzyl-2,5-dimethoxyphenethylamines.

Compound abbreviation	Benzyl ring substituent (R')	Total yield (mg)	Crystallization solvent
25DMPEA23DMB	2',3'-DiMeO	117.6	Ether
25DMPEA24DMB	2',4'-DiMeO	86.5	Ether
25DMPEA25DMB	2',5'-DiMeO	158.4	Ether
25DMPEA26DMB	2',6'-DiMeO	25.4+oil	Ether/acetone
25DMPEA34DMB	3',4'-DiMeO	165.5	Ether
25DMPEA35DMB	3',5'-DiMeO	148.7	Ether
25DMPEA23MDB	2',3'-MD	68.6+oil	Ether/acetone
25DMPEA34MDB	3',4'-MD	5.3+oil	Ether/EtOH

*From 1 mmole amine HCl, + 1 mmole aldehyde and 1 mmole TEA and 200 mg NaBH₄.

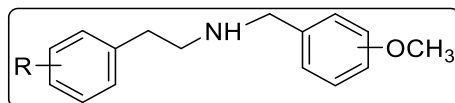


Table 6 Yields and Crystallization Solvents for the N-(methoxy)benzyl-dimethoxyphenethylamines.

Compound abbreviation	Phenethyl ring subst. (R)	Benzyl ring substituent (R')	Crystallization solvent	Total yield (mg)
23DMPEA2MB	2,3-DiMeO	2'-MeO	Benzene/Ether	124.0
23DMPEA3MB	2,3-DiMeO	3'-MeO	Ether	124.8
23DMPEA4MB	2,3-DiMeO	4'-MeO	Benzene	99.4
24DMPEA2MB	2,4-DiMeO	2'-MeO	Oil	Oil
24DMPEA3MB	2,4-DiMeO	3'-MeO	Ether	16.8
24DMPEA4MB	2,4-DiMeO	4'-MeO	Ether	70.6
25DMPEA2MB	2,5-DiMeO	2'-MeO	Ether/acetone	109.3
25DMPEA3MB	2,5-DiMeO	3'-MeO	Ether/acetone	126.8
25DMPEA4MB	2,5-DiMeO	4'-MeO	Ether/acetone	29.8
26DMPEA2MB	2,6-DiMeO	2'-MeO	Ether	142.9
26DMPEA3MB	2,6-DiMeO	3'-MeO	Ether	153.7
26DMPEA4MB	2,6-DiMeO	4'-MeO	Benzene	158.4
34DMPEA2MB	3,4-DiMeO	2'-MeO	Ether/EtOAc	25.4
34DMPEA3MB	3,4-DiMeO	3'-MeO	Ether	165.5
34DMPEA4MB	3,4-DiMeO	4'-MeO	Ether	148.7
35DMPEA2MB	3,5-DiMeO	2'-MeO	Ether	56.4
35DMPEA3MB	3,5-DiMeO	3'-MeO	Ether/benzene	75.4
35DMPEA4MB	3,5-DiMeO	4'-MeO	Ether	170.5
23MDPEA2MB	2,3-MD	2'-MeO	Ether	127.6
23MDPEA3MB	2,3-MD	3'-MeO	Ether	114.5
23MDPEA4MB	2,3-MD	4'-MeO	Ether	99.9
34MDPEA2MB	3,4-MD	2'-MeO	Ether/benzene	139.8
34MDPEA3MB	3,4-MD	3'-MeO	Ether	87.2
34MDPEA4MB	3,4-MD	4'-MeO	Ether	67.9

*From 1 mmole amine HCl, + 1 mmole aldehyde and 1 mmole TEA and 200 mg NaBH₄.

2.2 Synthesis of the N-(Substituted)benzyl-4-Bromo-2,5-Dimethoxyphenethylamines:

The compounds of this series are derivatives of N-(2'-methoxy)benzyl-4-bromo-2,5-dimethoxyphenethylamine (25B-NBOMe) where the substitution pattern on the aromatic ring of the N-benzyl substituent is modified yielding the 11 compounds shown in Figure 24. This series can be divided into three subsets. The first subset includes 25B-NBOMe and its 3'- and 4'-monomethoxy regioisomers (structures 1-3). In the second subset the N-benzyl aromatic ring is modified to include two methoxy groups at every possible position. Thus, this subset includes six regioisomeric compounds, the 2',3'-, 2',4'-, 2',5'-, 2',6'-, 3',4'- and 3',5'-dimethoxy regioisomers (structures 4-9). In the third subset in this series the N-benzyl aromatic ring is modified to contain the two possible methylenedioxy substitution patterns (structures 10-11). The N-benzyl substitution patterns selected for this series represent potential designer modifications since this functionality is commonly found in drugs of abuse.

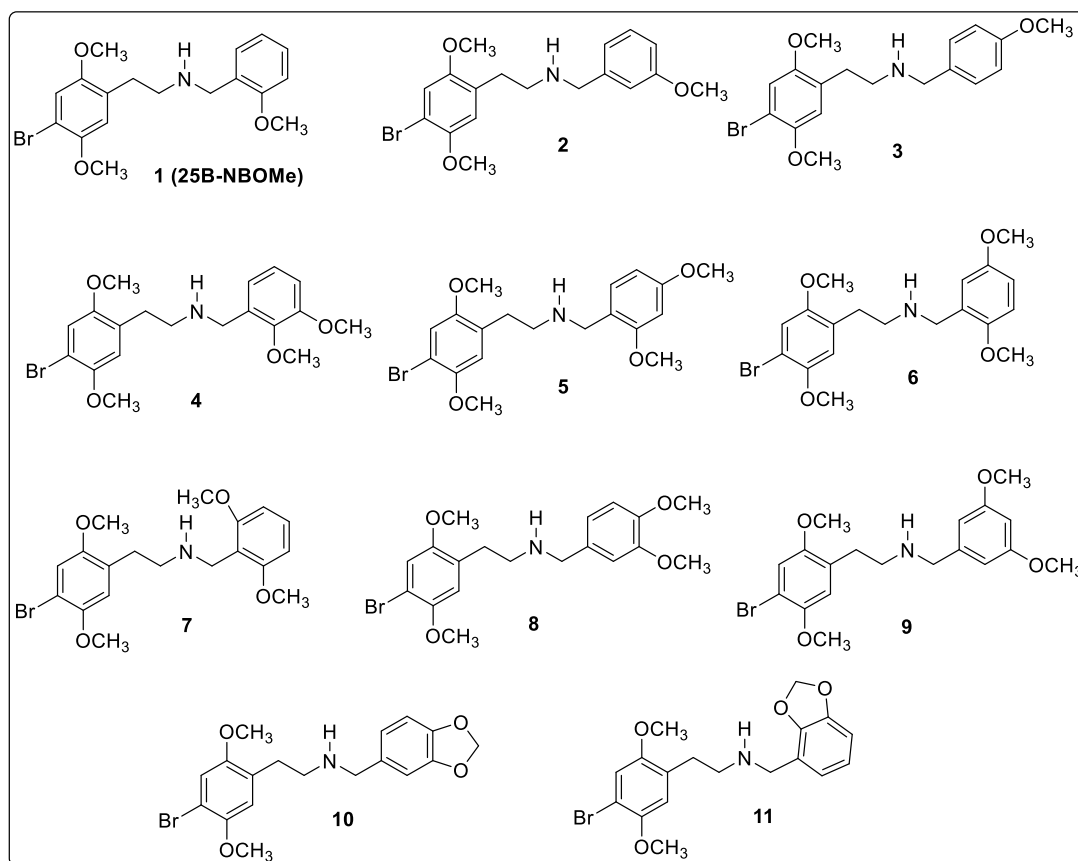
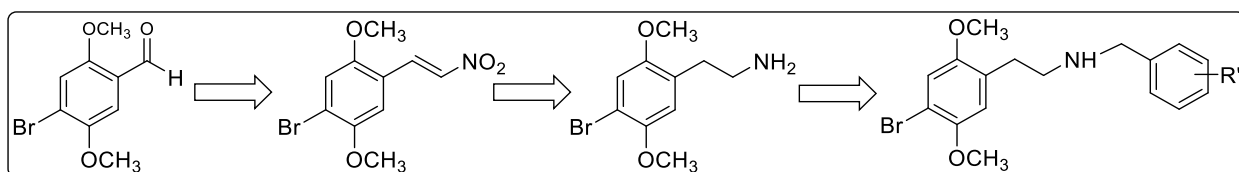


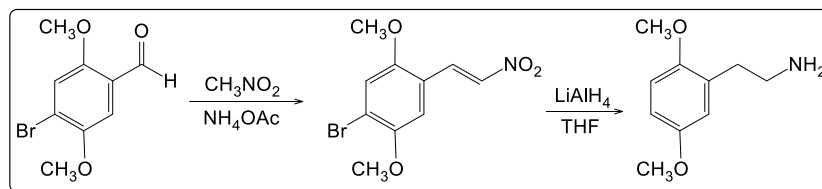
Figure 24 Structures of the N-(substituted)benzyl-4-bromo-2,5-dimethoxyphenethylamine Series.

The initial approach for the synthesis of compounds in this series is shown in the Scheme 8 below and is based on standard reaction sequence used to prepare compounds of the NBOMe series as described above. It was reasoned that commercially available 4-bromo-2,5-dimethoxybenzaldehyde could be converted to the nitroethene intermediate using standard condensation synthetic methodology, and reduction of this nitroethene with LAH would then provide the intermediate 4-bromo-2,5-dimethoxyphenethylamine. The 4-bromo-2,5-dimethoxyphenethylamine intermediate could then be used to make all eleven compounds of this series by reaction with commercially available substituted benzaldehydes under reductive amination conditions. Also, with this approach it was envisioned that additional regioisomeric derivatives could be prepared from other commercially available (bromo-dimethoxy)benzaldehydes.



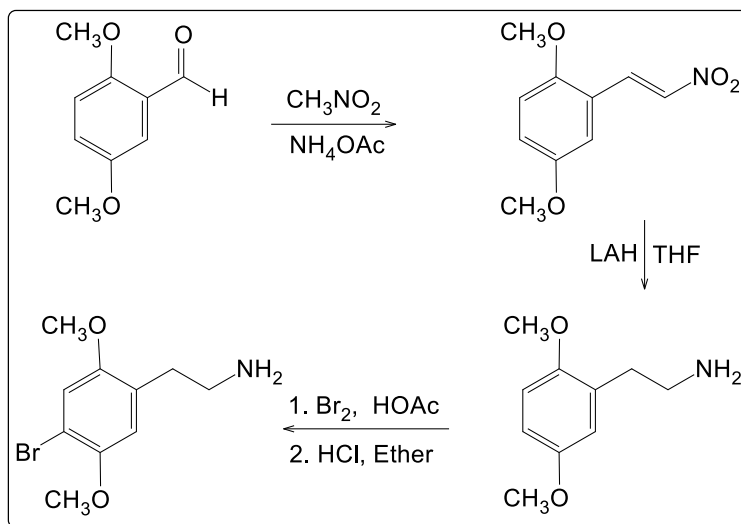
Scheme 8 Initial synthetic approach for the N-(substituted)benzyl-4-bromo-2,5-dimethoxyphenethylamine Series.

Thus, reaction of commercially available 4-bromo-2,5-dimethoxybenzaldehyde with nitromethane in the presence of anhydrous ammonium acetate provided the intermediate 1-(2,5-dimethoxyphenyl)-2-nitroethene in good yield. The recrystallized (iPrOH) and dried nitroethene was then reduced with lithium aluminum hydride (LAH) in THF using standard literature protocol. Analysis of the product of this reaction by EI-MS demonstrated that the nitroethene had reduced, but also the bromine atom was eliminated, presumably by reductive displacement (Scheme 9). A review of the literature revealed that this commonly occurs with aromatic bromine compounds when treated with LAH.



Scheme 9 Initial synthetic approach for the 4-bromo-2,5-dimethoxyphenethylamine intermediate.

While other reductive methods could have been explored to prepare the 4-bromo-2,5-dimethoxyphenethylamine intermediate, it was decided to incorporate the bromine atom after formation and reduction of the nitroethene as shown in Scheme 10 below and performed earlier in our laboratories. The nitroethene intermediate was prepared by reaction of commercially available 2,5-dimethoxybenzaldehyde with nitromethane as described before. The nitroethene was reduced in good yield to form the desired 2,5-dimethoxyphenethylamine intermediate using the standard LAH/THF reduction approach. Bromination of the 2,5-dimethoxyphenethylamine intermediate with bromine in acetic acid gave 4-bromo-2,5-dimethoxyphenethylamine in greater than 50% purified yield. The intermediate was isolated and purified as the HCl salt.



Scheme 10 Second synthetic approach for the 4-bromo-2,5-dimethoxyphenethylamine intermediate.

The position of bromination was confirmed by proton NMR in comparison to standard spectra in the literature. In the starting 2,5-dimethoxyphenethylamine the aromatic protons are found in the shift range of 6.7-6.8 and the protons at positions 3- and 4- are split as doublets with a coupling constant of 8.7 Hz (Figure 25). The 4-proton doublet is further split by meta coupling to the 6-proton ($J = 3.3$ Hz). In the final brominated product only two protons appear in the aromatic shift region and these are clearly not coupled by ortho or long range meta-coupling. The only way to obtain such a pattern in the proton NMR would be if the bromine atom was added to the 4-position. Furthermore, the NMR spectrum of the product obtained compared to literature spectra for the same compound (Figure 25).

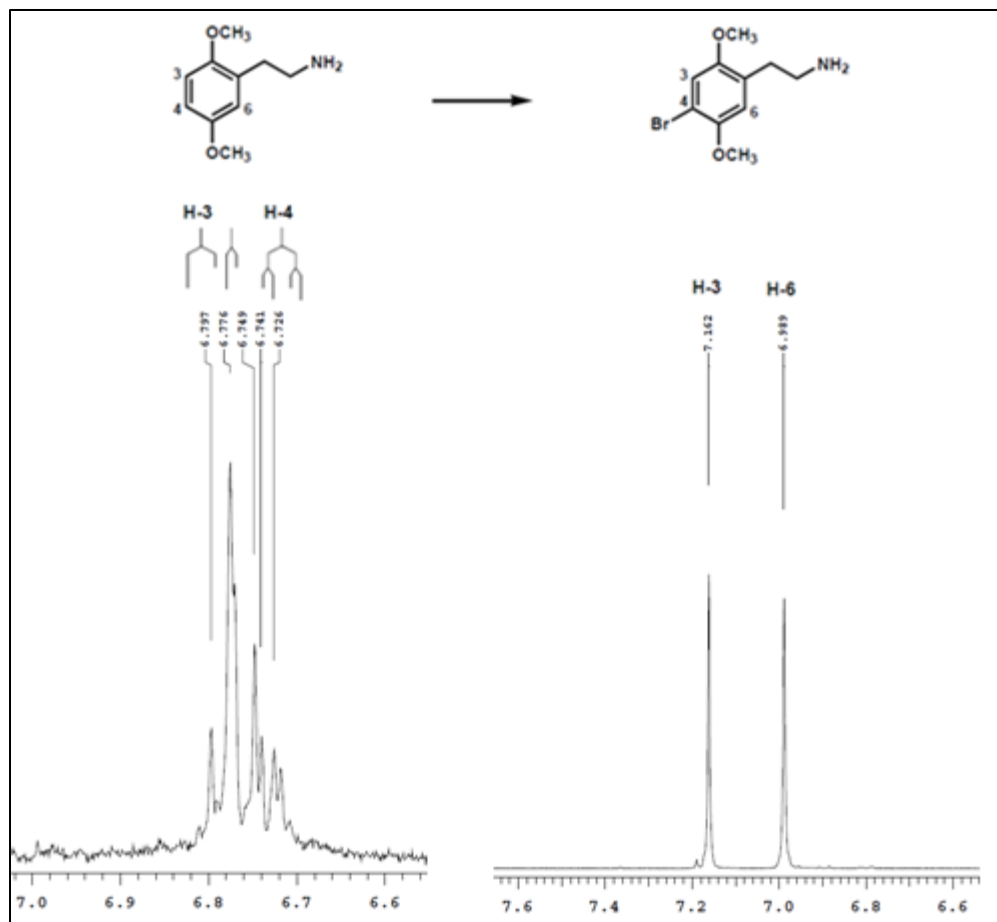
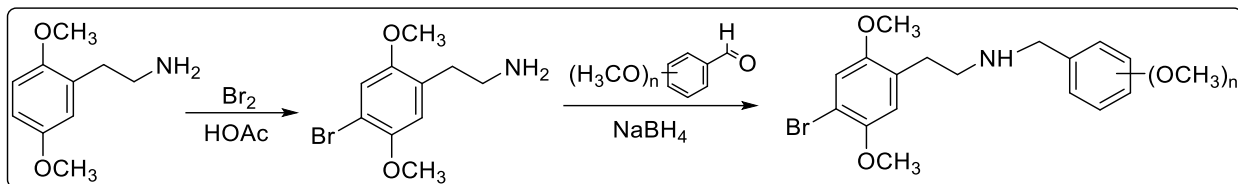


Figure 25 : Proton NMR of the 2,5-dimethoxyphenethylamine and 4-bromo-2,5-dimethoxyphenethyl-amine intermediates.

The 4-bromo-2,5-dimethoxyphenethylamine HCl intermediate was then used to prepare all three subsets of the N-(substituted)benzyl-4-bromo-2,5-dimethoxyphenethylamine series, using the general reductive alkylation method shown in Scheme 11. As for the unbrominated N-(substituted)benzyl-phenethylamines described earlier, these reactions were performed stepwise, involving imine formation first, followed by reduction with sodium borohydride (NaBH_4). In this approach the 4-bromo-2,5-dimethoxyphenethylamine HCl (1.0 mmolar scale) was heated for 2 hours with one equivalent of triethylamine and one equivalent of the desired commercially available aldehyde in ethanol to yield the intermediate imine (not isolated). After initial imine formation, the reaction mixture was cooled to room temperature and an excess of NaBH_4 (5.3 mmole) added and the reaction stirred overnight at room temperature.



Scheme 11 Synthesis of the N-(substituted)benzyl-4-bromo-2,5-dimethoxyphenethylamine Series.

All of the reductive alkylation reactions in this series were worked up by evaporation under reduced pressure and suspending the crude product in water which was neutralized by addition of a few drops of concentrated HCl. The products were extracted into dichloromethane (DCM) and the combined DCM extracts evaporated and dried under reduced pressure. The products in free base form were crystallized using the solvents listed in Table 7 below and isolated by filtration. The structures of all free base products were confirmed by standard spectroscopic means, and representative members were also evaluated by elemental analysis in their HCl salt forms. The HCl salts of each compound were prepared for pharmacological testing by dissolving 50-75 mg of the free base in 5 ml of dried absolute ethanol and bubbling HCl gas into the solution for 30-60 seconds. The ethanol solvent was then evaporated and the products dried thoroughly on a rotary evaporator. The resulting oils were crystallized from ether or mixtures of ether and ethanol as indicated in the table below. In addition to the compound listed in the table, the N-(3'-methoxy-4'-methyl) and N-(3'-methyl-4'-methoxy)benzyl derivatives were also prepared for mass spectral-derivative studies described in the chapters that follow.

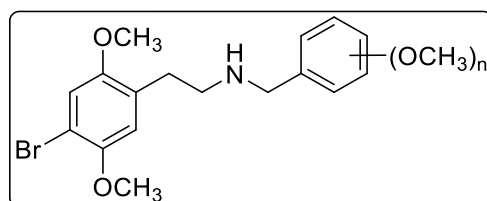


Table 7 Yields and Crystallization Solvents for The N-(Substituted)benzyl-4-Bromo-2,5-dimethoxyphenethylamines.

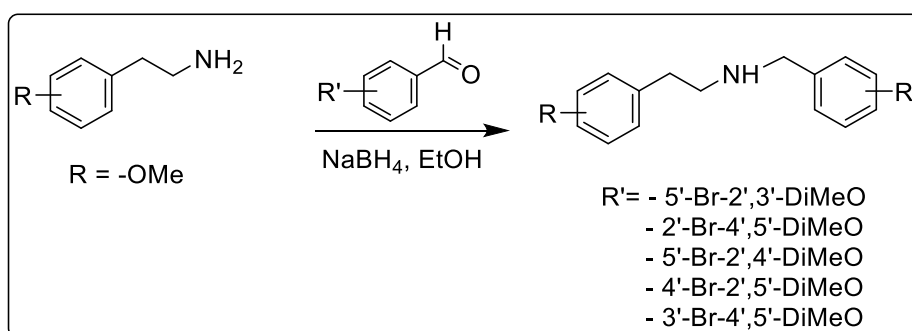
Compound abbreviation	Benzyl ring substituent (R')	Total yield (mg)	Crystallization solvent free base	MP, °C free base	Recrystallization solvent HCl salt
4Br25DMPEA2MB	2'-MeO	160	Ether	173-175	Ether*
4Br25DMPEA3MB	3'-MeO	180	Ether/Pet ether	124-126	Ether/EtOH
4Br25DMPEA4MB	4'-MeO	176	Ether	185-186	Ether*
4Br25DMPEA23DMB	2',3'-DiMeO	216	EtOH/Ether	86-87	Ether/EtOH
4Br25DMPEA24DMB	2',4'-DiMeO	255	Ether/pet ether	118-121	Ether/EtOH
4Br25DMPEA25DMB	2',5'-DiMeO	193	Ether/pet ether	117-118	Ether*
4Br25DMPEA26DMB	2',6'-DiMeO	141	Ether	164-166	Ether/EtOH
4Br25DMPEA34DMB	3',4'-DiMeO	136	Ether	165-167	Ether
4Br25DMPEA35DMB	3',5'-DiMeO	103	EtOAc/Pet ether	75-77	Ether/EtOH
4Br25DMPEA23MDB	2',3'-OCH ₂ O	271	EtOAc/ether	192-193	Ether
4Br25DMPEA23MDB	3',4'-OCH ₂ O	72	Ether	188-190	Ether/EtOH*

*From 1 mmole amine HCl, + 1 mmole aldehyde and 1 mmole TEA and 200 mg NaBH₄.

2.3 Synthesis of the N-(Bromo-Dimethoxysubstituted)benzyl-monomethoxyphenethylamines (eMOBNs):

The compounds of this series are derivatives of N-(2'-methoxy)benzyl-4-bromo-2,5-dimethoxyphenethylamine (25B-NBOMe) where the substitution pattern of the phenethylamine and benzylamine aromatic rings are reversed, and the bromo-dimethoxy substituents in the benzyl substituents are varied in their position. Therefore, the compounds of this series contain only a single methoxy substituent in the phenethyl aromatic ring, and a bromo-dimethoxy substitution pattern in the benzyl aromatic ring. We have designated these derivatives as “eMOBNs” based on the reversal of the ring substitution patterns. All of these compounds are regioisomers of the - (Substituted)benzyl-4-bromo-2,5-dimethoxyphenethylamine since they have identical atomic composition and only vary in the position of substituents.

These compounds could be prepared directly by reaction of 2-, 3- and 4-methoxyphenethylamines (synthesized as described earlier in this chapter or obtained commercially) with commercially available (bromo-dimethoxy)benzaldehydes in the presence of sodium borohydride in ethanol (Scheme 12). The only difference was the extended reaction time from 2 hours to overnight to allow for complete formation of the intermediate imine. This increase in reaction time was necessary due to the increased steric bulk of the halogenated benzaldehyde which reduces reactivity. The free base form of the final products was crystallized using the solvents listed in Table 8 below and isolated by filtration. The structures of all free base products were confirmed by standard spectroscopic means.



Scheme 12 Synthesis of the N-(bromo-dimethoxy)benzyl-monomethoxyphenethylamines.

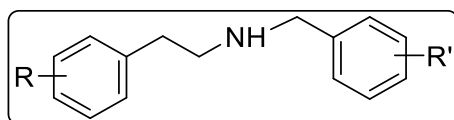


Table 8 Yields for the N-(bromo-dimethoxy)benzyl-monomethoxyphenethylamines.

Compound abbreviation	Phenethyl ring substituent (R)	Benzyl ring substituents (R')	Total yield (mg)	Crystallization solvent free base
2MPEA5Br23DMB	2-MeO	5'-Br-2',3'-DiMeO	292 mg	Ether/EtOH
3MPEA5Br23DMB	3-MeO	5'-Br-2',3'-DiMeO	151 mg	Ether/Benzene/iPrOH
4MPEA5Br23DMB	4-MeO	5'-Br-2',3'-DiMeO	92 mg	Ether
2MPEA2Br45DMB	2-MeO	2'-Br-4',5'-DiMeO	150 mg	Ether
3MPEA2Br45DMB	3-MeO	2'-Br-4',5'-DiMeO	92 mg	Ether
4MPEA2Br45DMB	4-MeO	2'-Br-4',5'-DiMeO	173 mg	Ether
2MPEA5Br24DMB	2-MeO	5'-Br-2',4'-DiMeO	100 mg	Ether
3MPEA5Br24DMB	3-MeO	5'-Br-2',4'-DiMeO	58 mg	Ether
4MPEA5Br24DMB	4-MeO	5'-Br-2',4'-DiMeO	75 mg	Ether
2MPEA4Br25DMB	2-MeO	4'-Br-2',5'-DiMeO	>100mg	EtOAc
3MPEA4Br25DMB	3-MeO	4'-Br-2',5'-DiMeO	>100mg	Ether
4MPEA4Br25DMB	4-MeO	4'-Br-2',5'-DiMeO	>100mg	Ether
2MPEA3Br45DMB	2-MeO	3'-Br-4',5'-DiMeO	28 mg	Ether/Pet.Ether/Benzene
3MPEA3Br45DMB	3-MeO	3'-Br-4',5'-DiMeO	150 mg	Ether
4MPEA3Br45DMB	4-MeO	3'-Br-4',5'-DiMeO	86 mg	Ether/Benzene

*From 1 mmole amine HCl, + 1 mmole aldehyde and 1 mmole TEA and 200 mg NaBH₄.

2.4 Synthesis of the N-(Substituted)benzyl-4-Iodo-2,5-Dimethoxyphenethylamines:

The compounds of this series are derivatives of N-(2'-methoxy)benzyl-4-iodo-2,5-dimethoxyphenethylamine (25I-NBOMe) where the substitution pattern on the aromatic ring of the N-benzyl substituent is modified yielding the 11 compounds in Figure 26. This series can be divided into three subsets. The first subset includes 25I-NBOMe and its 3'- and 4'-monomethoxy regioisomers (structures 1-3). In the second subset the N-benzyl aromatic ring is modified to include two methoxy groups at every possible position. Thus, this subset includes six regioisomeric compounds, the 2',3'-, 2',4'-, 2',5'-, 2',6'-, 3',4'- and 3',5'-dimethoxy regioisomers (structures 4-9). In the third subset in this series the N-benzyl aromatic ring is modified to contain the two possible methylenedioxy substitution patterns (structures 10-11). The N-benzyl substitution patterns selected for this series represent potential designer modifications since this functionality is commonly found in drugs of abuse.

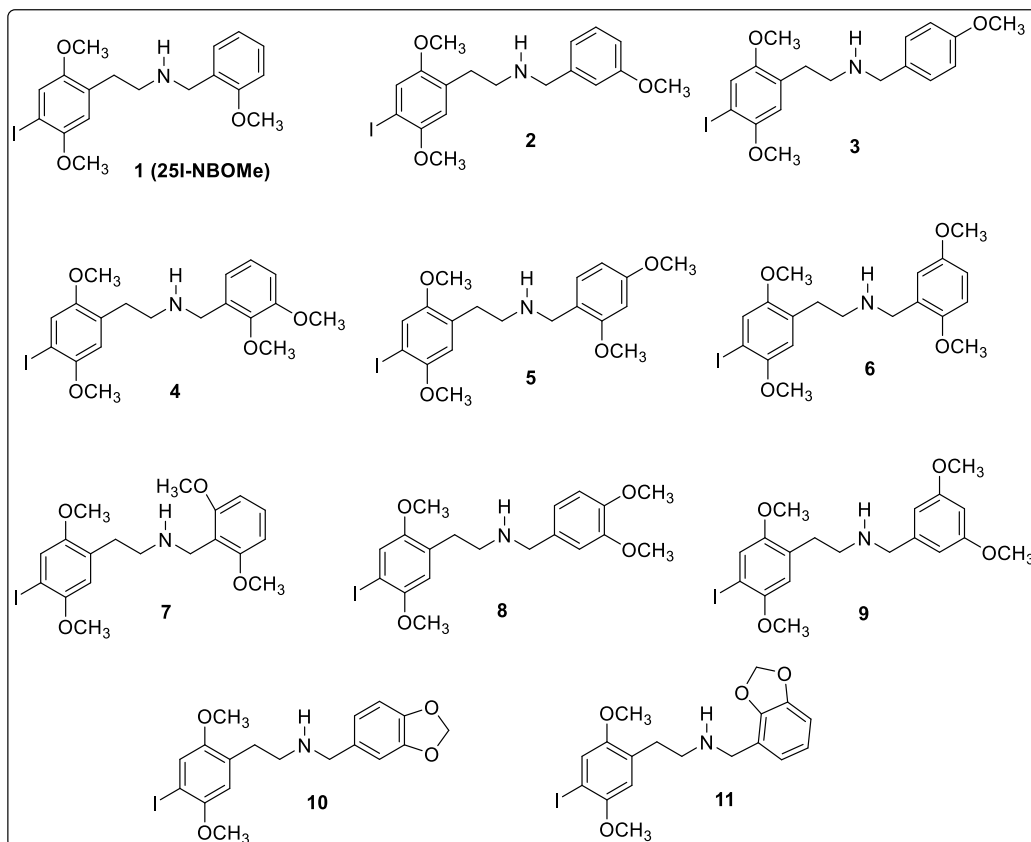
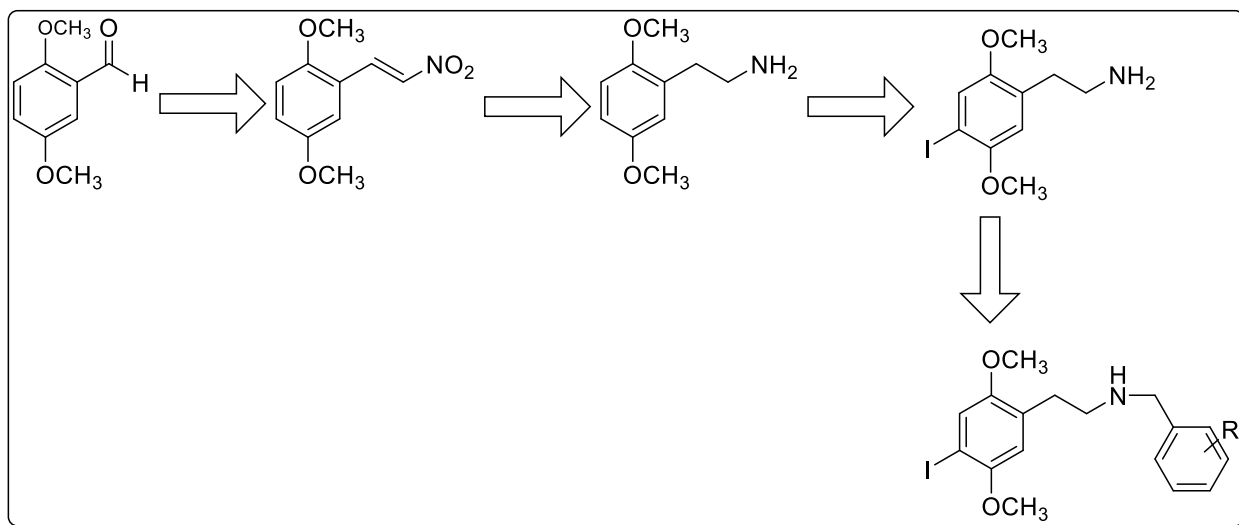


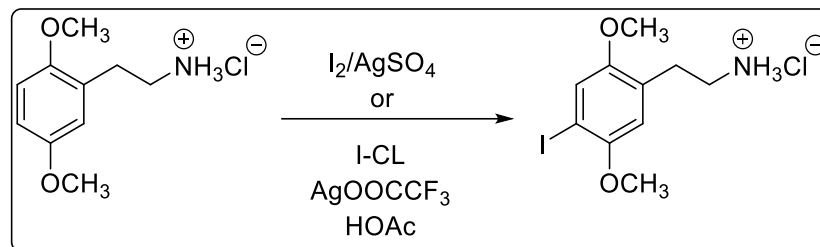
Figure 26 Structures of the N-(substituted)benzyl-4-iodo-2,5-dimethoxyphenethylamine Series.

The initial approach for the synthesis of compounds in this series is shown in the Scheme 13 below and is based on standard reaction sequence used to prepare compounds of the NBOMe series as described above. It was reasoned that commercially available 2,5-dimethoxybenzaldehyde could be converted to the nitroethene intermediate using standard condensation synthetic methodology, and reduction of this nitroethene with LAH would then provide the intermediate 2,5-dimethoxyphenethylamine. The 2,5-dimethoxyphenethylamine intermediate could be then converted to 4-iodo-2,5-dimethoxyphenethylamine by iodination reactions reported in the literature for methoxyphenethylamines, and the iodo intermediate could be then used to make all eleven compounds of this series by reaction with commercially available substituted benzaldehydes under reductive amination conditions.



Scheme 13 Initial synthetic approach for the N-(substituted)benzyl-4-iodo-2,5-dimethoxyphenethylamine Series.

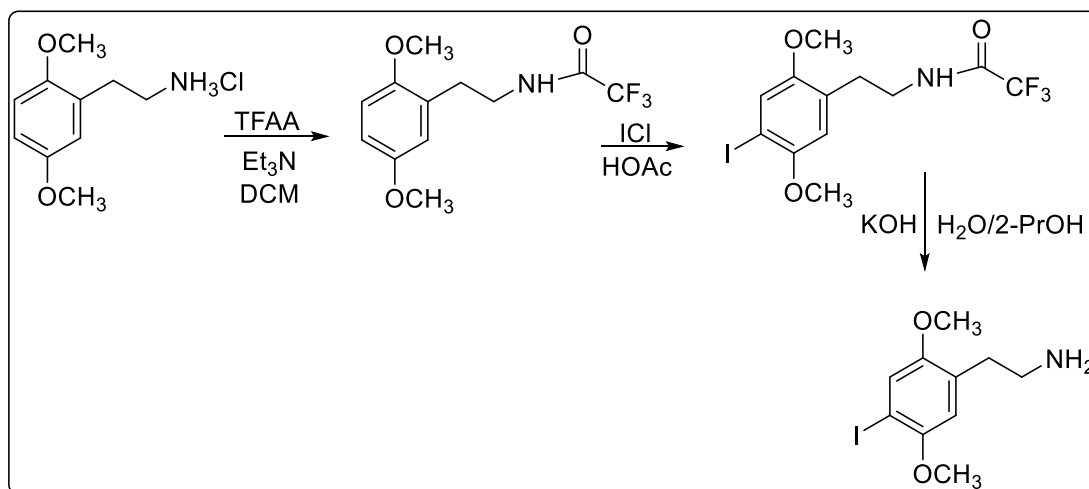
Thus, reaction of commercially available 2,5-dimethoxybenzaldehyde with nitromethane in the presence of anhydrous ammonium acetate provided the intermediate 1-(2,5-dimethoxyphenyl)-2-nitroethene in good yield. The recrystallized (iPrOH) and dried nitroethene was then reduced with lithium aluminum hydride (LAH) in THF using standard literature protocol. The iodination of the 2,5-dimethoxyphenethylamine with either $\text{ICl}/\text{AgOOCF}_3/\text{HOAc}$ [110] or $\text{I}_2/\text{Ag}_2\text{SO}_4$ [111] however proceeded in only very low yield (10%) and the product contained a number of contaminants (Scheme 14).



Scheme 14 Initial synthetic approach for the 4-iodo-2,5-dimethoxyphenethylamine intermediate.

While other iodination methods could have been explored to prepare the 4-iodo-2,5-dimethoxyphenethylamine, it was decided to protect the amino group of the dimethoxyphenethylamine intermediate as an amide prior to iodination. Then once the iodine was added, the amide intermediate could be deprotected to give the desired intermediate for the final reductive amination reactions.

Therefore, the amine functionality was protected as a trifluoroacetamide using trifluoroacetic anhydride and trimethylamine as shown in Scheme 15. Iodination of the protected phenethylamine with iodine monochloride in acetic acid gave 4-iodo-2,5-dimethoxyphenethylamine trifluoroacetamide in very good yield. This intermediate was purified by acid-base extraction and recrystallization from ethyl acetate. The trifluoroacetamide protecting group was then removed by hydrolysis in KOH/iPrOH/H₂O to give 4-iodo-2,5-dimethoxyphenethylamine in greater purified yield. The intermediate was isolated and purified as the HCl salt.



Scheme 15 Second synthetic approach for the 4-iodo-2,5-dimethoxyphenethylamine intermediate.

The position of iodination was confirmed by proton NMR in comparison to standard spectra in the literature. In the starting 2,5-dimethoxyphenethylamine the aromatic protons are found in the shift range of 6.7-6.8 and the protons at positions 3- and 4- are split as doublets with a coupling constant of 8.7 Hz (figure 27). The 4-proton doublet is further split by meta coupling to the 6-proton ($J = 3.3$ Hz). In the final iodinated product only two protons appear in the aromatic shift region and these are clearly not coupled by ortho or long range meta-coupling. The only way to obtain such a pattern in the proton NMR would be if the iodine atom was added to the 4-position. Furthermore, the NMR spectrum of the product obtained compared to literature spectra for the same compound (Figure 27).

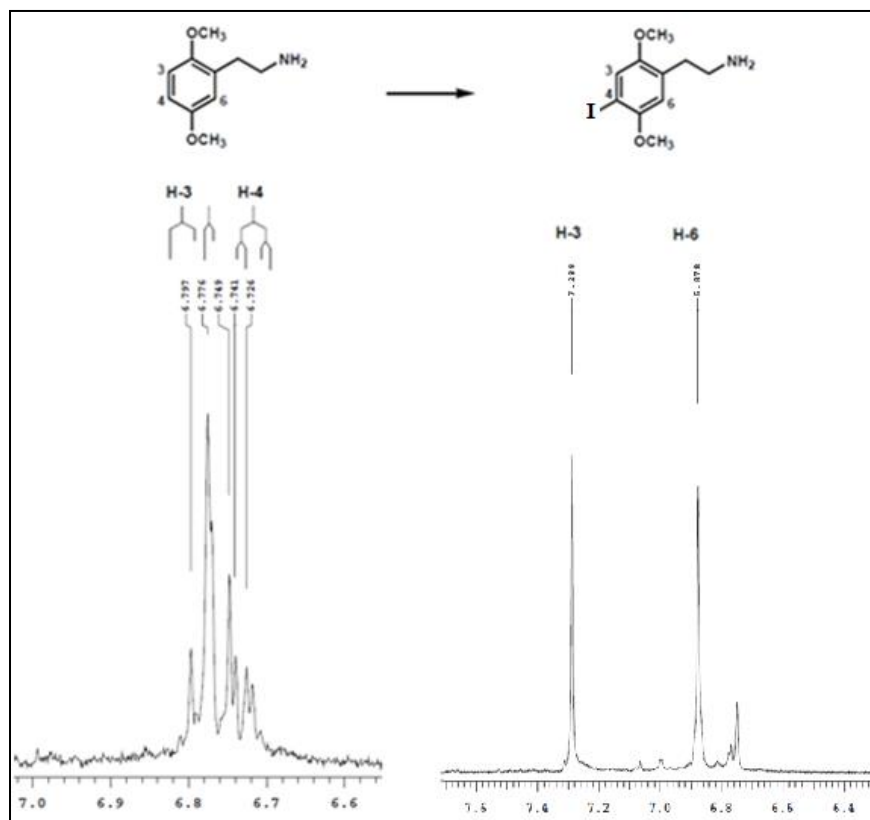
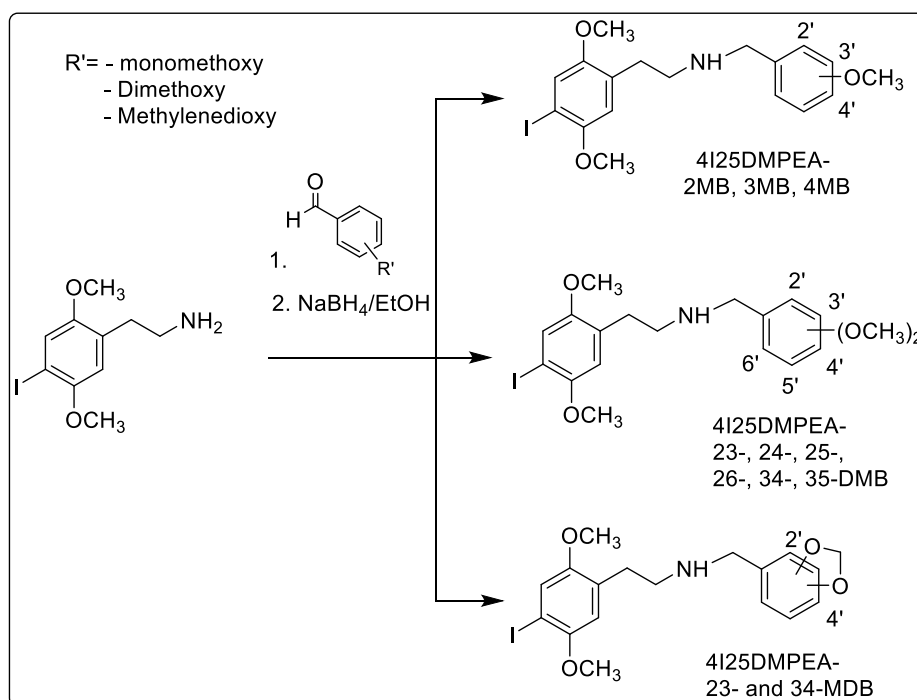


Figure 27 Proton NMR of the 2,5-dimethoxyphenethylamine and 4-iodo-2,5-dimethoxyphenethylamine intermediates.

The 4-iodo-2,5-dimethoxyphenethylamine HCl intermediate was then used to prepare all three subsets of the N-(substituted)benzyl-4-iodo-2,5-dimethoxyphenethylamine series, using the general reductive alkylation method shown in Scheme 16. These reactions were performed stepwise, as reported before, involving imine formation first, followed by reduction with sodium

borohydride (NaBH_4). In this approach the 4-iodo-2,5-dimethoxyphenethylamine HCl (1.0 mmolar scale) was heated for 2 hours with one equivalent of triethylamine and one equivalent of the desired commercially available aldehyde in ethanol to yield the intermediate imine (not isolated). After initial imine formation, the reaction mixture was cooled to room temperature and an excess of NaBH_4 (5.3 mmole) added and the reaction stirred overnight at room temperature. The reaction was worked up by evaporation of the solvent under reduced pressure and suspending the crude product in water which was neutralized by addition of a few drops of concentrated HCl. The products were extracted into dichloromethane (DCM) and the combined DCM extracts evaporated and dried under reduced pressure. The products in free base form were crystallized using the solvents listed in Table 9 below and isolated by filtration. The structures of all free base products were confirmed by standard spectroscopic means, and representative members were also evaluated by elemental analysis in their HCl salt forms. The HCl salts of each compound were prepared by dissolving 50-75 mg of the free base in 5 ml of dried absolute ethanol and bubbling HCl gas into the solution for 30-60 seconds. The ethanol solvent was then evaporated and the products dried thoroughly on a rotary evaporator. The resulting oils were crystallized from ether or mixtures of ether and ethanol as indicated in Table 9 below.



Scheme 16 Synthesis of the N-(substituted)benzyl-4-iodo-2,5-dimethoxyphenethylamine Series.

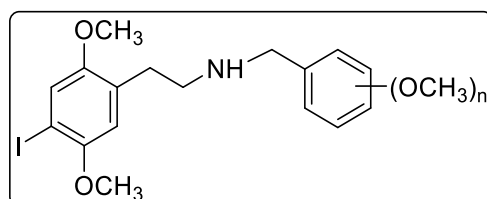


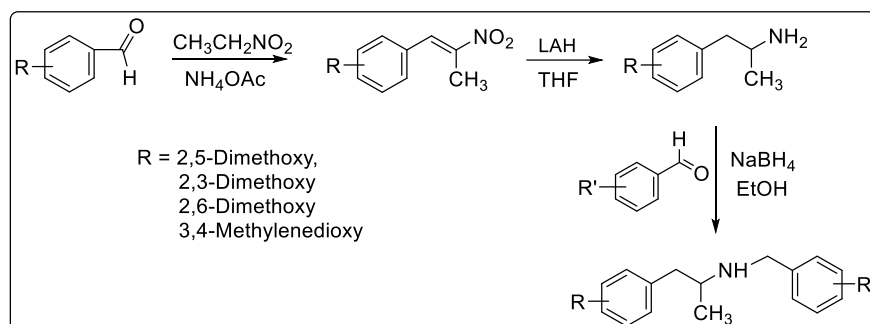
Table 9 Yields and Crystallization Solvents for the N-(Substituted)benzyl-4-iodo-2,5-dimethoxyphenethylamines.

Benzyl ring substituent	Yield, mg (1 st & 2 nd crop)	Crystallization solvent free base	Recrystallization solvent HCl salt
2'-MeO	165.7	EtOAc/PE	Ether/EtOH
3'-MeO	58 (+ oil)	Ether	Ether/EtOH*
4'-MeO	261.5	Ether	Ether/EtOH
2',3'-DiMeO	87 (+ oil)	Ether/PE	Ether/EtOAc
2',4'-DiMeO	265	Ether	Ether
2',5'-DiMeO	329	Ether	Ether
2',6'-DiMeO	175	Ether	Ether/acetone
3',4'-DiMeO	298	EtOAc/PE	Ether/acetone
3',5'-DiMeO	136 (+ oil)	Ether	Ether/acetone*
2',3'-MD	Oil	Ether	Ether*
3',4'-MD	Oil	Ether	Ether*

*From 1 mmole amine HCl, + 1 mmole aldehyde and 1 mmole TEA and 200 mg NaBH₄.

2.5 Synthesis of the N-(Substituted)benzyl-Dimethoxyphenpropylamines (DMPPAs):

The compounds of this series are derivatives of the NBOMes where the phenethylamine side chain is substituted with a methyl group alpha to the amine, and the substitution pattern on the aromatic ring is varied to contain a variety of dimethoxy (2,3-, 2,5- and 2,6-dimethoxy) or 3,4-methylenedioxy substituents. Also, the substitution pattern of the N-benzyl aromatic ring was modified to include monomethoxy (2'-, 3'- and 4'-methoxy), dimethoxy (2',3'-, 2',4'-, 2',5'-, 2',6'-, 3',4'- and 3',5'-dimethoxy) and methylenedioxy (2',3'- and 3',4'-) substituents. These derivatives can be considered as “amphetamine type” analogues of the NBOMes (see Table 11). The rationale for inclusion of this series compounds is discussed further in the analytical chapters of this dissertation.



Scheme 17 Synthesis of the N-(Substituted)benzyl-dimethoxy- and methylenedioxyphenpropylamines.

The approach for the synthesis of this series is the same as that described previously and is based on the same reaction sequence used to prepare other compounds of the NBOMe series. In this series commercially available 2,3-, 2,5-, 2,6-dimethoxy- and 3,4-methylenedioxybenzaldehydes were allowed to react with nitroethane and anhydrous ammonium acetate to provide the intermediate substituted phenyl-2-nitropropenes in good yield (Table 10). The nitropropene intermediates were then reduced to the corresponding amines with LAH/THF as described earlier. The substituted phenpropylamine intermediates were then subjected to reductive alkylation with sodium borohydride and substituted benzaldehydes to yield the final products (Scheme 17). The free base form of the final products was crystallized using the solvents listed in Table 11 below and isolated by filtration. The structures of all free base products were confirmed by standard spectroscopic means.

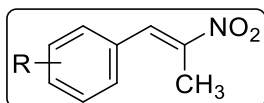


Table 10 Yields and Crystallization Solvents for the dimethoxy- and Methylenedioxyphenyl-2-nitropropenes.

PNP product	Phenethyl ring substituent (R)	Crude product form	Crystallization & recrystallization solvent	Total yield (g)
2,3-DMPNP	2,3-DiMeO	Oil (yellow)	iPrOH	8.6
2,5-DMPNP	2,5-DiMeO	Oil (yellow)	iPrOH	5.3
2,6-DMPNP	2,6-DiMeO	Oil (reddish)	iPrOH	9.1
3,4-MDPNP	3,4-OCH ₂ O-	Solid	iPrOH	8.6

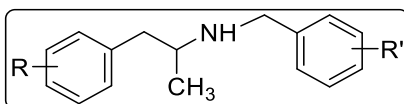


Table 11 Yields for the N-(Substituted)benzyl-phenpropylamines.

Compound abbreviation	Phenethyl ring substituent	Benzyl ring substituent	Total yield (mg)	Crystallization solvent free base
25DMPPA2MB	2,5-DiMeO	2'-MeO	169 mg	Ether
25DMPPA3MB	2,5-DiMeO	3'-MeO	173 mg	Ether
25DMPPA4MB	2,5-DiMeO	4'-MeO	119 mg	Ether/EtOAc/Pet Ether
25DMPPA23DMB	2,5-DiMeO	2',3'-DiMeO	128 mg	Ether/iPrOH
25DMPPA24DMB	2,5-DiMeO	2',4'-DiMeO	167 mg	Ether/EtOH
25DMPPA25DMB	2,5-DiMeO	2',5'-DiMeO	157 mg	Ether/EtOAc
25DMPPA26DMB	2,5-DiMeO	2',6'-DiMeO	159 mg	Ether
25DMPPA34DMB	2,5-DiMeO	3',4'-DiMeO	154 mg	Ether/EtOAc
25DMPPA35DMB	2,5-DiMeO	3',5'-DiMeO	50 mg	Ether/EtOAc/Pet Ether
25DMPPA23MDB	2,5-DiMeO	2',3'-MD	50 mg	Ether/EtOAc/Pet Ether
25DMPPA34MDB	2,5-DiMeO	3',4'-MD	126 mg	Ether
23DMPPA2MB	2,3-DiMeO	2'-MeO	146 mg	Ether/EtOAc
23DMPPA3MB	2,3-DiMeO	3'-MeO	109 mg	Ether/EtOAc
23DMPPA4MB	2,3-DiMeO	4'-MeO	160 mg	Ether/EtOAc
26DMPPA2MB	2,6-DiMeO	2'-MeO	15 mg	Ether/EtOAc
26DMPPA3MB	2,6-DiMeO	3'-MeO	95 mg	Ether/EtOH/EtOAc
26DMPPA4MB	2,6-DiMeO	4'-MeO	163 mg	Ether
34MDMPPA2MB	3,4-MD	2'-MeO	209 mg	Ether
34MDMPPA3MB	3,4-MD	3'-MeO	120 mg	Ether/Pet.Ether/EtOAc
34MDMPPA4MB	3,4-MD	4'-MeO	206 mg	Ether

*From 1 mmole amine HCl, + 1 mmole aldehyde and 1 mmole TEA and 200 mg NaBH₄.

2.6 Synthesis of the N-(Substituted)benzyl-Bromo-2,5-Dimethoxyphenylpropylamines:

The compounds of this series are derivatives of N-(2'-methoxy)benzyl-4-bromo-2,5-dimethoxyphenethylamine (25B-NBOMe) where the phenethylamine side chain is substituted with a methyl group alpha to the amine and the substitution pattern on the aromatic ring of the N-benzyl substituent is modified yielding the 11 compounds shown in in Figure 28. This series can be divided into three subsets. The first subset includes 25B-NBOMe and its 3'- and 4'-monomethoxy regioisomers (structures 1-3). In the second subset the N-benzyl aromatic ring is modified to include two methoxy groups at every possible position, including the 2',3',-, 2',4'-, 2',5'-, 2',6'-, 3',4'- and 3',5'-dimethoxy regioisomers (structures 4-9). In the third subset in this series the N-benzyl aromatic ring is modified to contain the two possible methylenedioxy substitution patterns (structures 10-11). The compounds of this series are basically “amphetamine-type” derivatives of the 25B-NBOMes which will also provide insights into analytical profiles and differentiation among the NBOME type designer drugs.

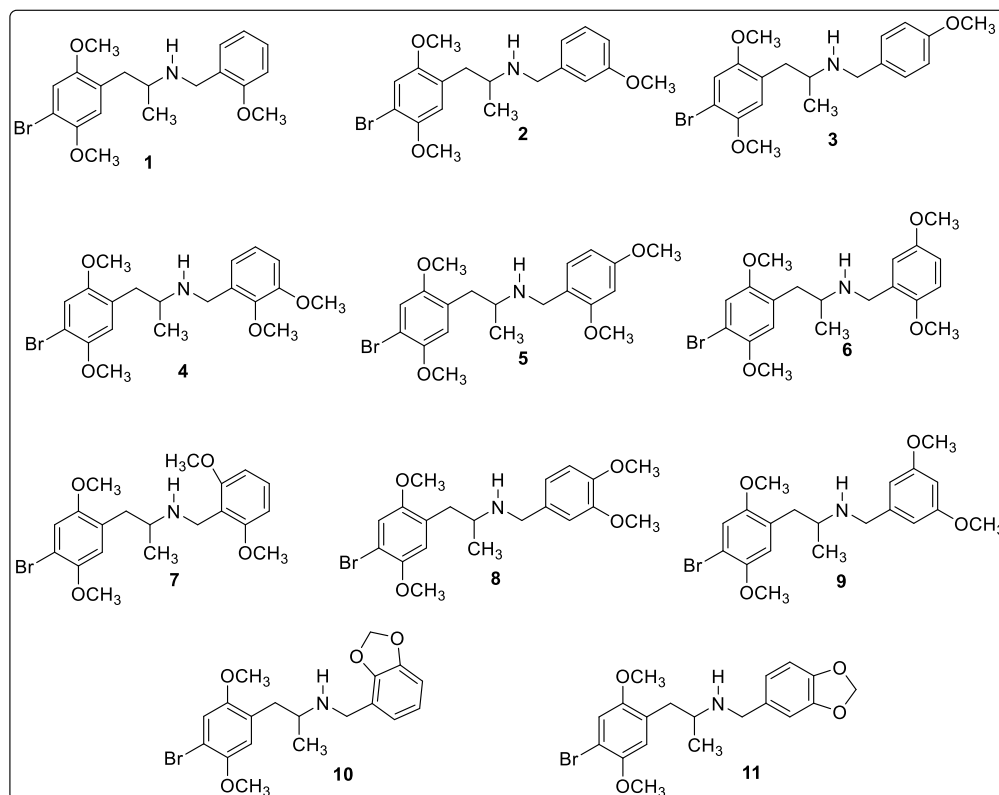


Figure 28 Structures of the N-(methoxy)benzyl-dimethoxyphenylpropylamine Series.

The original approach to synthesize the compounds of this series involved the same procedure used for the preparation of the N-(substituted)benzyl-4-bromo-2,5-dimethoxyphenethylamines described above. The 2,5-dimethoxyphenpropylamine precursor was prepared from 2,5-dimethoxybenzaldehyde as described in the previous section of this chapter. Direct bromination of 2,5-dimethoxyphenpropylamine with bromine in glacial acetic acid yielded a product mixture as shown by the chromatogram in Figure 29. The largest peak in this chromatogram is the desired amine intermediate as demonstrated by the molecular ion (m/z 230/232) and amine-dominated cleavage fragment (m/z /44). Based on their molecular ions and fragmentation patterns, the contaminants represented by peaks 1 and 2 in the chromatogram were determined to be ring brominated side products forming from oxidative deamination of the amine (compound 2) and bromine displacement (compound 3). These products are shown in Scheme 18.

In attempt to improve yields it was decided to use the method which provided the highest yields of the 4-iodo-2,5-dimethoxyphenethylamine intermediate, 4I-2,5-DMPEA. Thus the 2,5-dimethoxyphenpropylamine was first converted to the trifluoroacetamide by treatment with trifluoroacetic anhydride. The protected amide was obtained in very good yield with a simple acid-base workup (Scheme 19). The N-trifluoroacetyl-protected amine was allowed to react with bromine and acetic acid with heating to afford the 4-bromo-2,5-dimethoxyphenpropylamine trifluoroacetamide (Scheme 19). This product was contaminated with a small amount of a side product with an apparent mass 14 units lower than the desired product. Based on mass spectral fragmentation the side product was tentatively identified as a demethylated product, a phenol formed by cleavage on one of the two ether moieties. This phenol side product most likely formed as a result of HBr cleavage of one of the methyl ether groups. HBr-mediated cleavage has been reported by others using this method to brominate aromatic methyl ethers. Which phenol formed was not determined.

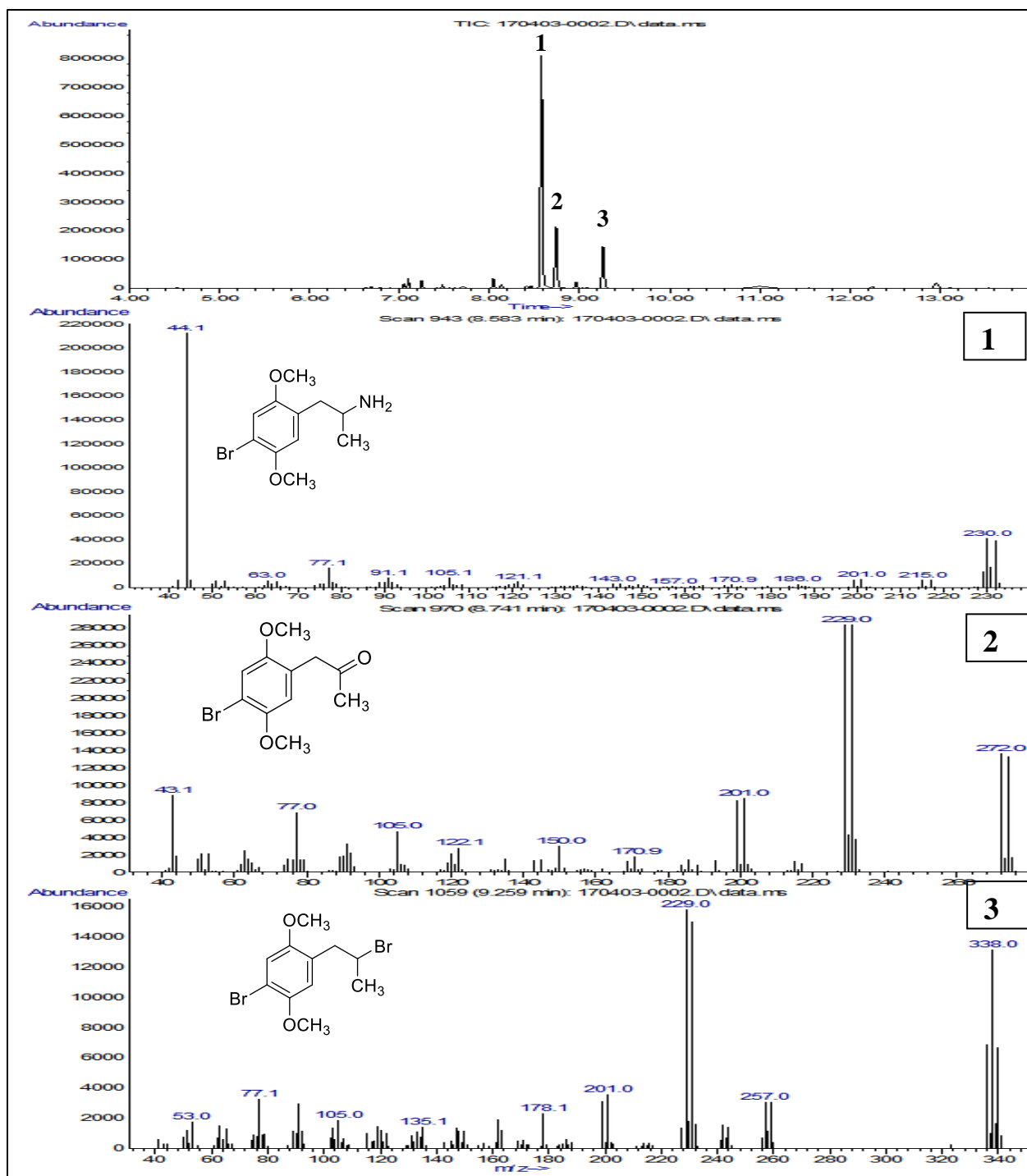
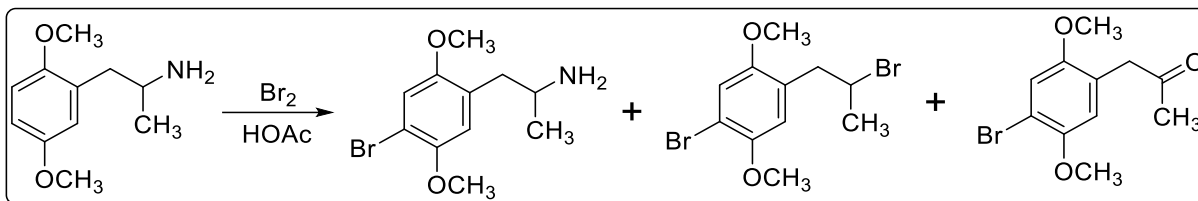
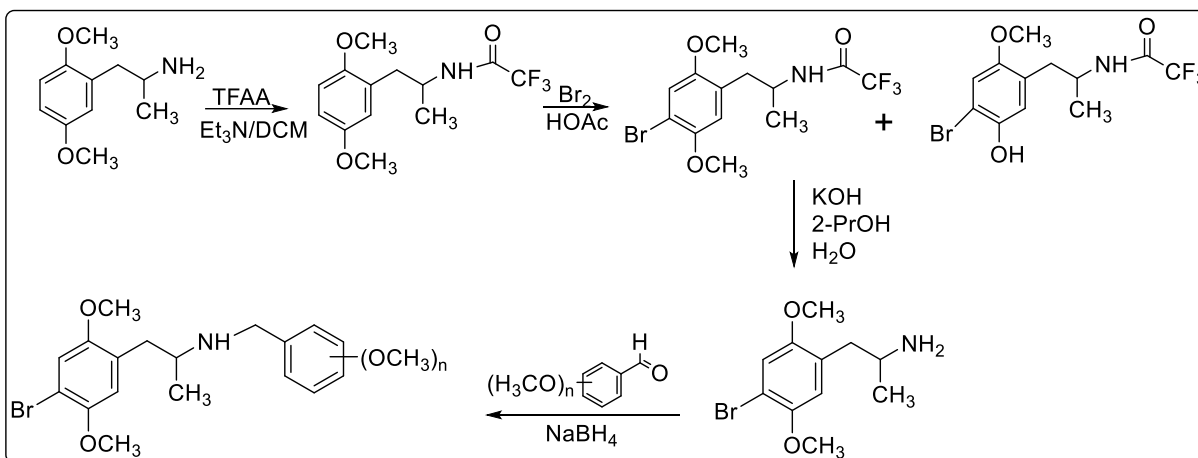


Figure 29 Gas chromatography and mass spectrometry of product obtained from reaction of 2,5-dimethoxyphenylpropylamine with bromine-acetic acid.



Scheme 18 Initial synthetic approach for the 4-bromo-2,5-dimethoxyphenylpropylamine intermediate.

The 4-bromo-2,5-dimethoxyphenylpropylamine trifluoroacetamide intermediate was purified by recrystallization with 2-propanol and then subjected to hydrolysis in propanol with aqueous KOH (Scheme 19). Acid-base workup of this reaction after evaporation of the 2-propanol gave the desired intermediate, 4-bromo-2,5-dimethoxyphenylpropylamine as the free base which crystallized upon standing.



Scheme 19 Synthesis of the N-(Substituted)benzyl-bromo-2,5-dimethoxyphenylpropylamines.

The 4-bromo-2,5-dimethoxyphenylpropylamine intermediate was subjected to reductive amination with the three monomethoxy-, six dimethoxy- and two methylenedioxybenzaldehydes using the method reported earlier. All products were isolated by ether extraction after evaporation and neutralization of the reaction mixture with HCl. The yields and crystallization solvents are listed in the table 12 below.

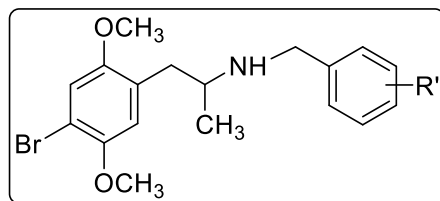


Table 12 Yields and Crystallization Solvents for the N-(Substituted)benzyl-4-bromo-2,5-dimethoxyphenethylamines.

Compound abbreviation	Benzyl ring substituent (R')	Yield, mg (1 st & 2 nd crop)	Crystallization solvent free base
4Br25DMPPA2MB	2'-MeO	174 mg	Ether/EtOAc/Pet.Ether
4Br25DMPPA3MB	3'-MeO	199 mg	Ether/EtOH
4Br25DMPPA4MB	4'-MeO	214 mg	Ether
4Br25DMPPA23DMB	2',3'-DiMeO	347 mg	EtOH/Ether
4Br25DMPPA24DMB	2',4'-DiMeO	230 mg	Ether/EtOH
4Br25DMPPA25DMB	2',5'-DiMeO	114 mg	Ether/Pet.Ether
4Br25DMPPA26DMB	2',6'-DiMeO	225 + 50 mg	Ether
4Br25DMPPA34DMB	3',4'-DiMeO	189 mg	Ether
4Br25DMPPA35DMB	3',5'-DiMeO	89 mg	Ether/EtOH/Pet.Ether
4Br25DMPPA23MDB	2',3'-MD	112 mg	Ether/EtOAc/EtOH
4Br25DMPPA34MDB	3',4'-MD	194 + 27 mg	Ether/EtOAc/EtOH

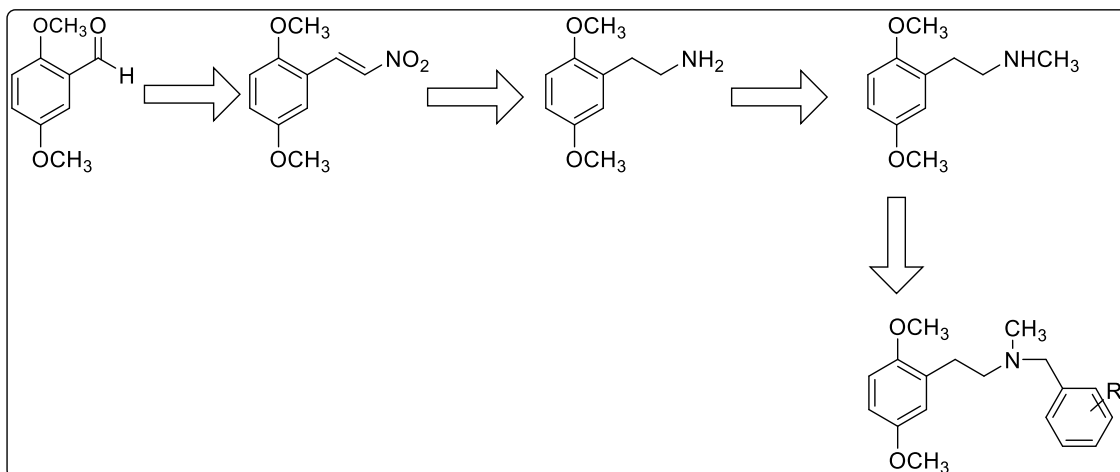
*From 1 mmole amine HCl, + 1 mmole aldehyde and 1 mmole TEA and 200 mg NaBH₄.

2.7 Synthesis of the N-(Substituted)benzyl-N-Methyl-2,5-Dimethoxyphenethylamines:

The compounds of this series are basically derivatives of the NBOMes and compounds described earlier in this chapter where the nitrogen is substituted with a methyl group. These derivatives were prepared primarily to aid in interpretation of data obtained from analytical studies described in the chapters that follow.

The initial approach for the synthesis of compounds in this series is shown in the Scheme 20 below and is based on standard reaction sequence used to prepare compounds of the NBOMe series as described above. The 2,5-dimethoxyphenethylamine could be prepared by from commercially available 2,5-dimethoxybenzylaldehyde via the intermediate 2,5-dimethoxyphenethyl-2-nitroethene as described previously. The 2,5-dimethoxyphenethylamine could then be converted to N-methyl-2,5-dimethoxyphenethylamine analogue via formamide derivative as reported in the

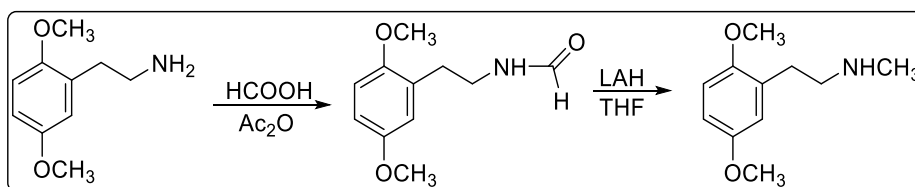
literature and performed previously in our laboratories. Finally, the N-methyl intermediate could be used to make all eleven compounds of this series by reaction with commercially available substituted benzaldehydes under reductive amination conditions to form the final product.



Scheme 20 Initial synthetic approach for the (substituted)benzyl-N-methyl-2,5-dimethoxyphenethylamines series.

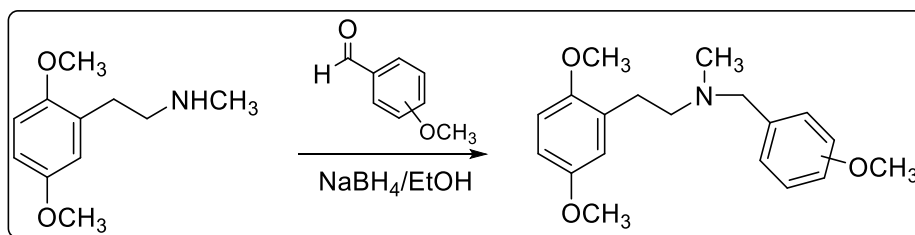
Thus, reaction of commercially available 2,5-dimethoxybenzaldehyde with nitromethane in the presence of anhydrous ammonium acetate provided the intermediate 1-(2,5-dimethoxyphenyl)-2-nitroethene in good yield. The recrystallized (iPrOH) and dried nitroethene was then reduced with lithium aluminum hydride (LAH) in THF using standard literature protocol. Treatment of the 2,5-dimethoxyphenethylamine a mixture of formic acid and acetic anhydride yielded the intermediate formamide in excellent yield. Reducing the formamide intermediate with LAH gave the required intermediate, N-methyl-2,5-dimethoxyphenethylamine (Scheme 21).

Reaction of N-methyl-2,5-dimethoxyphenethylamine with substituted benzaldehydes followed sodium borohydride reduction was not successful.



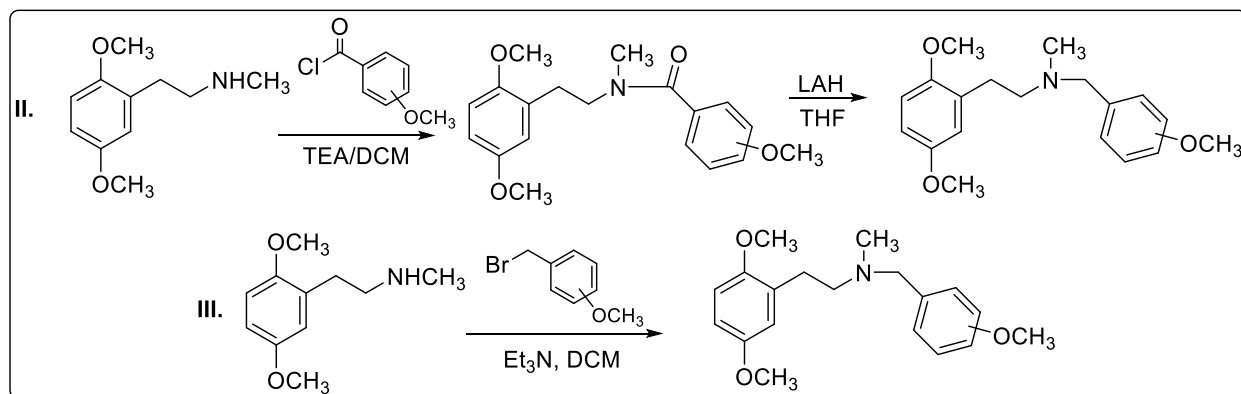
Scheme 21 Synthesis of the N-methyl-2,5-dimethoxyphenethylamine.

Analysis of the products from these reactions by EI-MS revealed not only very low yield of the desired product, but also the presence of a number of contaminants (Scheme 22). Increasing reaction times or performing the reaction under dehydration conditions (Dean-Starke) with acid catalysis (*p*-TsOH) did not improve yields. While other modifications of the reductive alkylation reaction described could have been explored to enhance product yields and purity, it was decided to pursue alternative synthetic strategies.



Scheme 22 Initial synthetic approach for the synthesis of (substituted)benzyl-N-methyl-2,5-dimethoxyphenethylamines.

One alternate method pursued involved first acylating the amino group of N-methyl-2,5-dimethoxyphenethylamine with the desired (substituted methoxy)benzoyl chloride to yield the benzamide intermediates, and then reduce these amides to the desired final products (Scheme 23-I). A second method investigated direct alkylation of the N-methyl-2,5-dimethoxyphenethylamine with selected substituted methoxy benzylbromide to make the final product (scheme 23-II). This second method was considered as a backup method in case of failure of the first method which involved using a substituted methoxy benzoyl chloride to make the intermediate amide.



Scheme 23 Synthesis of the (substituted)benzyl-N-methyl-2,5-dimethoxyphenethylamines.

First for the benzoylamide method, N-methyl-2,5-dimethoxyphenethylamine (1 mmole) and TEA (1 mmole) was reacted with 1 mmole of the desired substituted methoxy benzoyl chloride to make the benzoylamide intermediates which were purified by acid-base extraction. The pure and dry amides were then reduced with LAH in THF to yield the desired amine products. The products formed in this reaction are listed in Table 13 and were isolated in the free base form. The structures of all free base products were confirmed by standard spectroscopic means.

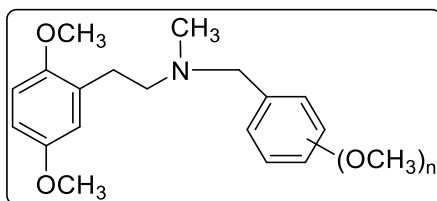


Table 13 Yields for the (substituted)benzyl-N-methyl-2,5-di-methoxyphenethylamines.

Benzyl Ring substituent	Yield, mg (1st & 2nd crop)	Crystallization solvent free base
2'-MeO	Oil	Ether/EtOH
3'-MeO	Oil	Ether/EtOH
4'-MeO	Oil	Ether/EtOH

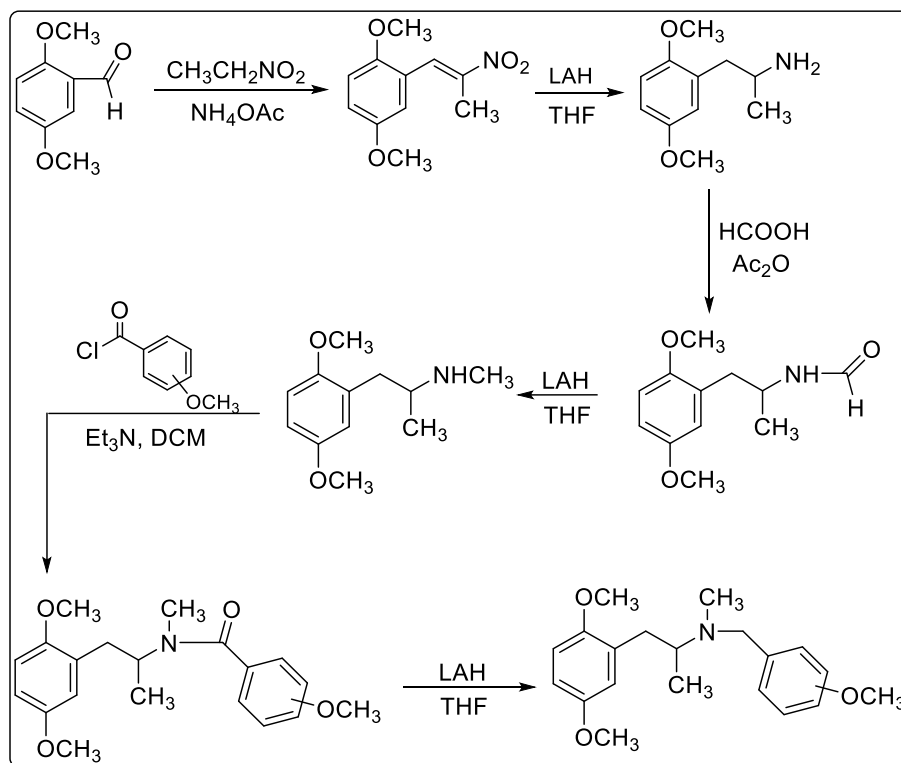
*From 1 mmole amine HCl, + 1 mmole aldehyde and 1 mmole TEA and 200 mg NaBH₄.

The alternative method to make the final products of this series involved direct alkylation of the N-methyl-2,5-dimethoxyphenethylamine with the desired substituted methoxy benzylbromide. In these reactions, the desired substituted methoxy benzylbromide (1 mole) was added to a mixture of N-methyl-2,5-dimethoxyphenethylamine (1 mmole) and TEA (1 mmole) in methylene chloride and the reaction allowed to proceed overnight at room temperature. The products were isolated and purified in free base form by acid-base extraction and structures of all products were confirmed by standard spectroscopic means. Both of the benzoylamide and direct alkylation methods provided purer products in higher yields and cleaner products than the original direct reductive alkylation method.

2.8 Synthesis of the (Substituted)benzyl-N-Methyl-2,5-Dimethoxyphenylamines:

The compounds of this series are basically derivatives of the NBOMes and earlier compounds described in this chapter where both the nitrogen and the phenethylamine alpha-carbon are substituted with a methyl group. These derivatives were prepared primarily to aid in interpretation of data obtained from analytical studies described in the chapters that follow.

The approach for the synthesis of this series was the same as those described previously involving the preparation of an alpha-methyl substituted phenethylamine (2,5-dimethoxyphenylpropylamine) and then N-methylating this intermediate (Scheme 24). The alpha-methyl-N-methyl intermediate was then converted to the desired products by forming the appropriately substituted benzoylamides and reducing these amides to the amines. All of these reactions were carried out as described previously in the same quantities. The products formed in these reactions were isolated in the free base form as listed in Table 14. The structures of all free base products were confirmed by standard spectroscopic means.



Scheme 24 Synthesis of the (substituted)benzyl-N-methyl-2,5-dimethoxyphenylamines.

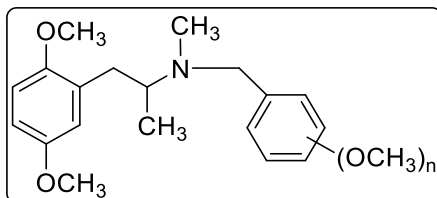


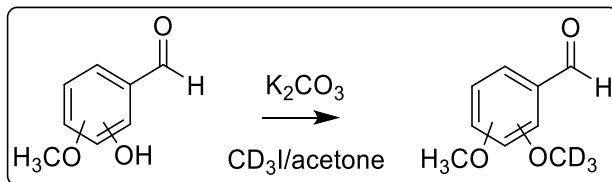
Table 14 Yields for the N-(methoxy)benzyl-N-methyl-2,5-dimethoxyphenylamines.

Benzyl Ring substituent	Yield, mg (1 st & 2 nd crop)	Crystallization solvent free base
2'-MeO	Oil	Ether/EtOH
3'-MeO	Oil	Ether/EtOH
4'-MeO	Oil	Ether/EtOH

*From 1 mmole amine HCl, + 1 mmole aldehyde and 1 mmole TEA and 200 mg NaBH₄.

2.9 Synthesis of the deuterium and ¹³C labeled 2,3-Dimethoxybenzaldehydes for mass spectral fragmentation studies.

To aid in interpretation of mass spectral data, several deuterium and ¹³C-labeled NBOME analogs were prepared. The 2-OCD₃ and 3-OCD₃ derivatives of 2,3-dimethoxybenzaldehyde were synthesized by treating the appropriate (hydroxyl-methoxy)benzaldehyde with d₃-methyl iodine with potassium carbonate in dry acetone at room temperature (Scheme 25).



Scheme 25 Synthesis of deuterated 2,3-dimethoxybenzaldehyde

The product was isolated by filtration and evaporation of the reaction solvent and used without further purification. The structures of the deuterated products were confirmed by GC-MS (Figure 30):

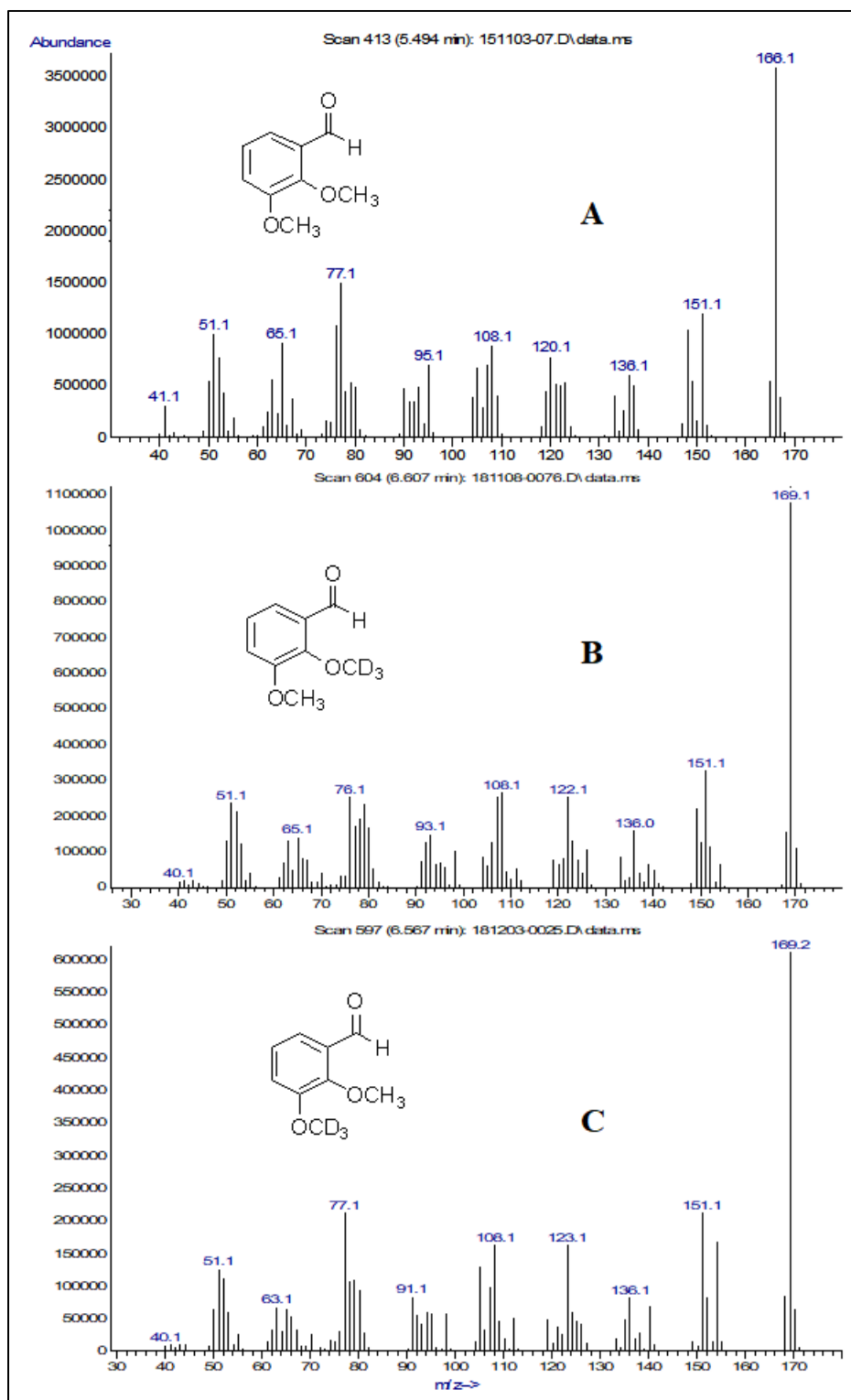
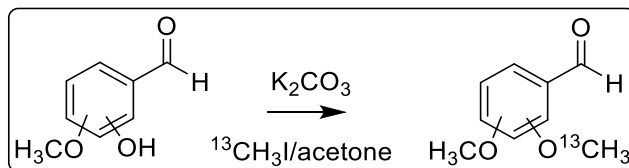


Figure 30 Mass spectra of A) 2,3-dimethoxybenzaldehyde, B) 2-OCD₃,3-methoxybenzaldehyde, C) 3-OCD₃,2-methoxybenzaldehyde.

The 2-O¹³CH₃ and 3-O¹³CH₃ derivatives of 2,3-dimethoxybenzaldehyde were synthesized by treating the appropriate (hydroxyl-methoxy)benzaldehyde with ¹³C-methyl iodide with potassium carbonate in dry acetone at room temperature (Scheme 26).



Scheme 26 Synthesis of deuterated 2,3-dimethoxybenzaldehyde.

The product was isolated by filtration and evaporation of the reaction solvent and used without further purification. The structures of the deuterated products were confirmed by GC-MS (Figure 31).

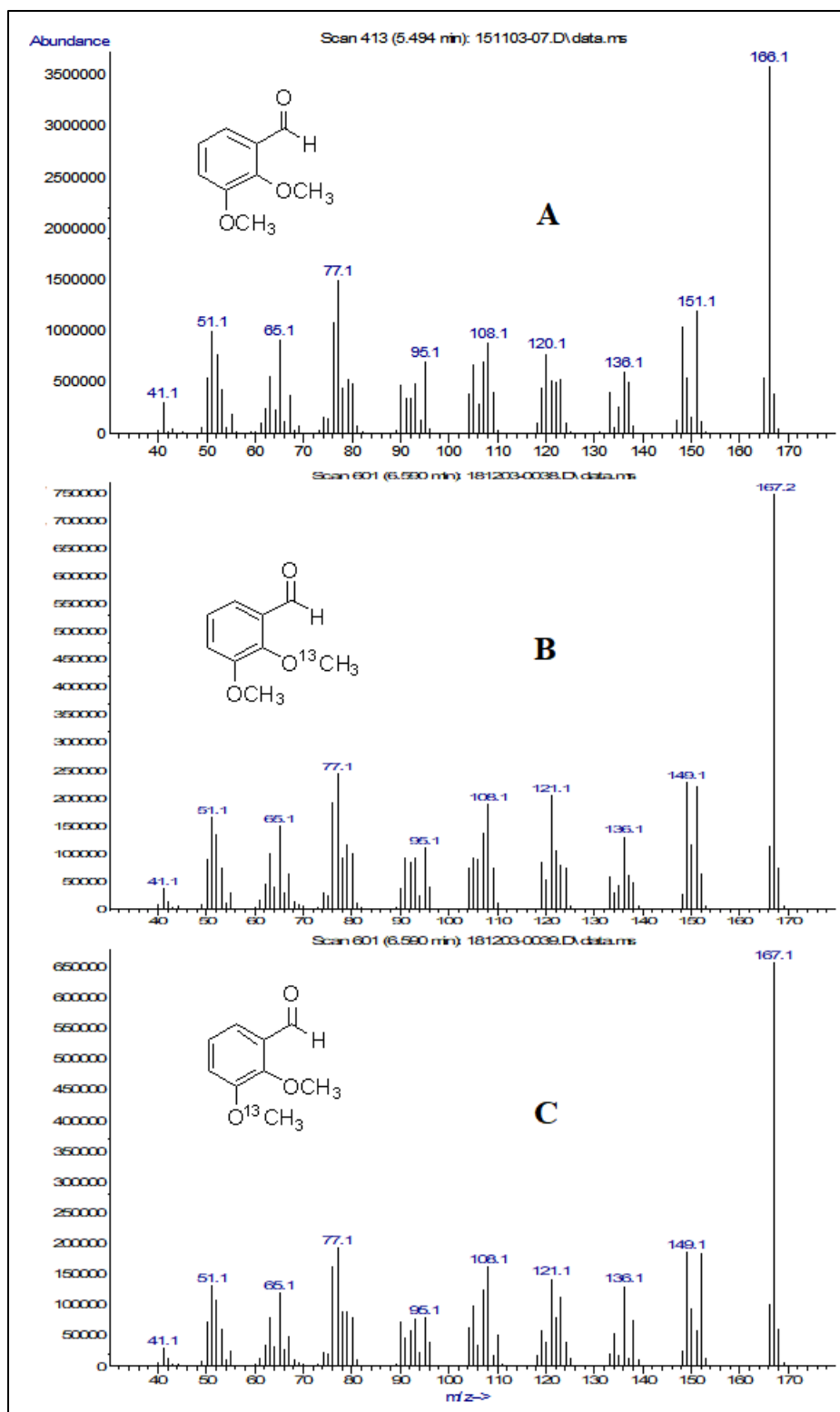


Figure 31 Mass spectra of A) 2,3-dimethoxybenzaldehyde, B) 2- O^{13}CH_3 ,3-methoxybenzaldehyde, C) 3- O^{13}CH_3 ,3-methoxybenzaldehyde.

3 Analysis of the N-(Methoxy)benzyl-methoxyphenethylamine Series

3.1 Introduction:

The compounds of this series (structures 1-9) are simplified derivatives of NBOMes where the halogen atom was deleted from the structure and there is a single methoxy substituent on each of the aromatic rings of the core NBOMe structure. Each aromatic ring of the base NBOMe structure has three positions that can be mono-substituted, the 2-, 3-, and 4-positions of the phenethyl aromatic ring and the 2', 3', and 4'-positions of the N-benzyl ring. Monomethoxy substitution at each of these positions on each ring gives rise to nine regioisomeric monomethoxy-monomethoxy derivatives as shown in Figure 32. The synthesis of these compounds was described in the previous chapter.

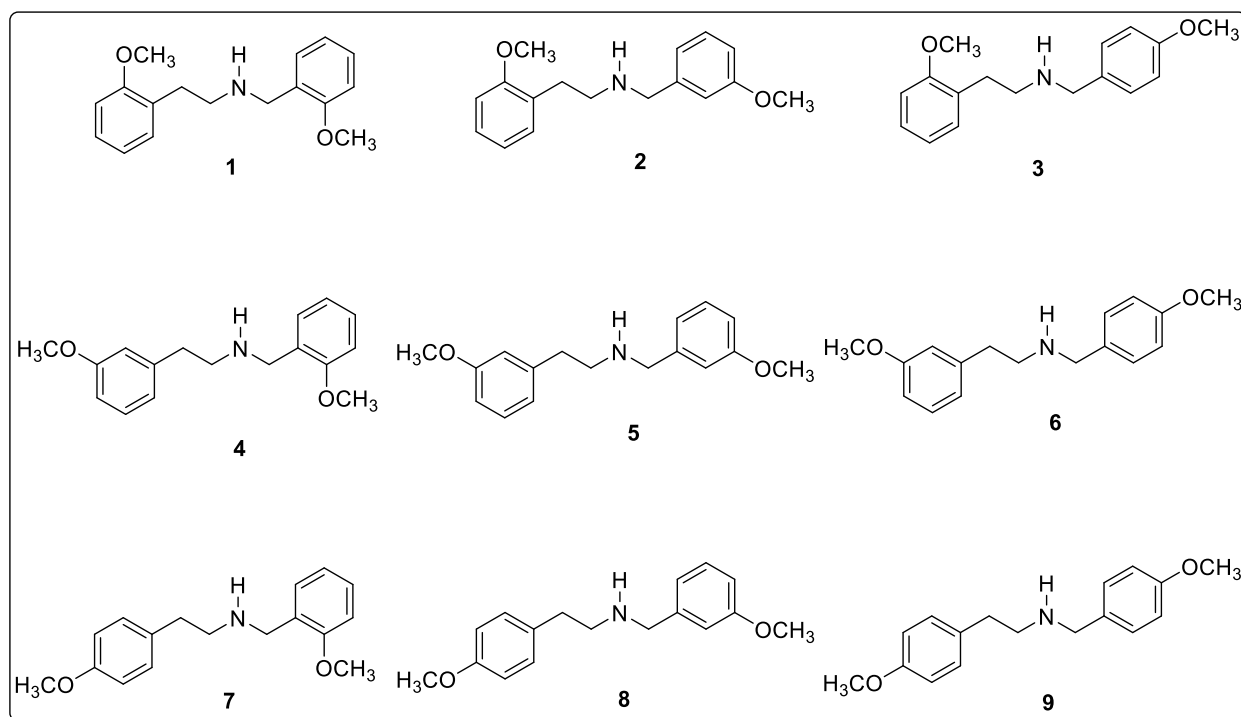


Figure 32 Structures of the N-(methoxy)benzyl-methoxyphenethylamine Series.

3.2 Mass Spectral Analysis:

All nine regioisomeric members yielded nearly identical mass spectra as shown in Figures 33-36. The molecular ion (MW = 271) is not apparent in the EI-MS spectrum of any of these compounds, however the molecular mass was confirmed by CI-MS as illustrated for the N-(2'-methoxy)benzyl-2-methoxyphenethylamine isomer in Figure 33 where a M+1 ion of 272 was present. As reported for other 25-NBOMe compounds and illustrated in Chapter 1, the dominant ions in EI-MS spectrum of all nine compounds in this series are observed at $m/z = 121$, 150 and 91, with the base peak m/z 121 (Figure 34-36). The m/z 91 ion was present in the highest abundance in the 2'-methoxy isomer and decreased in the 3'- and 4'-methoxy isomers. Other than the relative abundance of the m/z 91 ions, there are no other features in the mass spectra of these regioisomers which allows for specific differentiation.

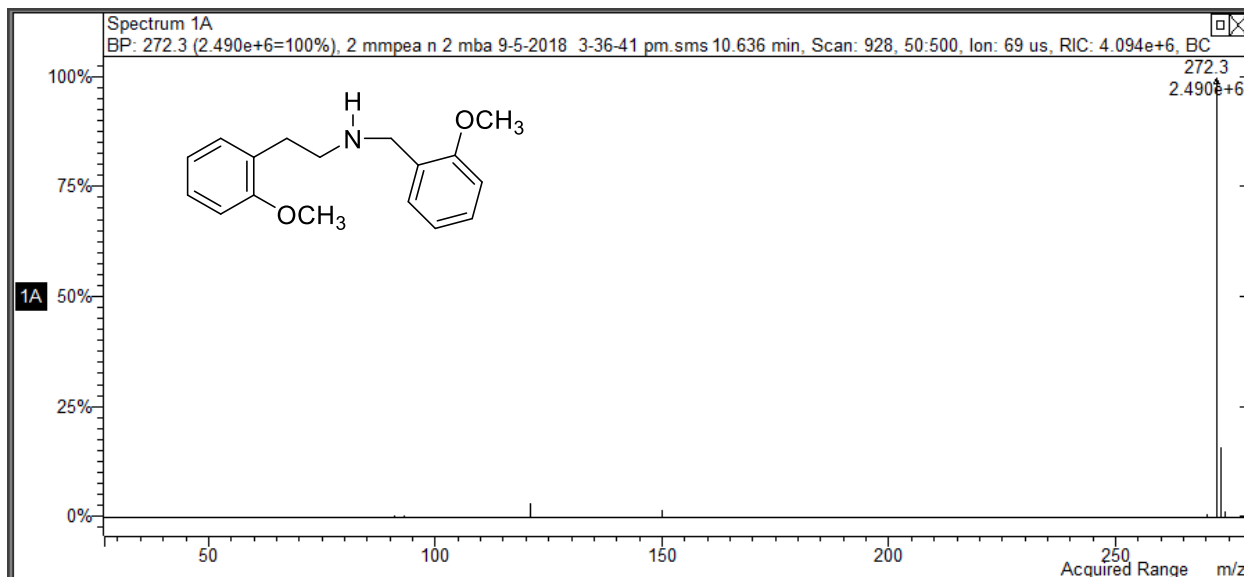


Figure 33 CI-MS of Mass Spectra of the N-2'-methoxybenzyl-2-methoxyphenethylamines.

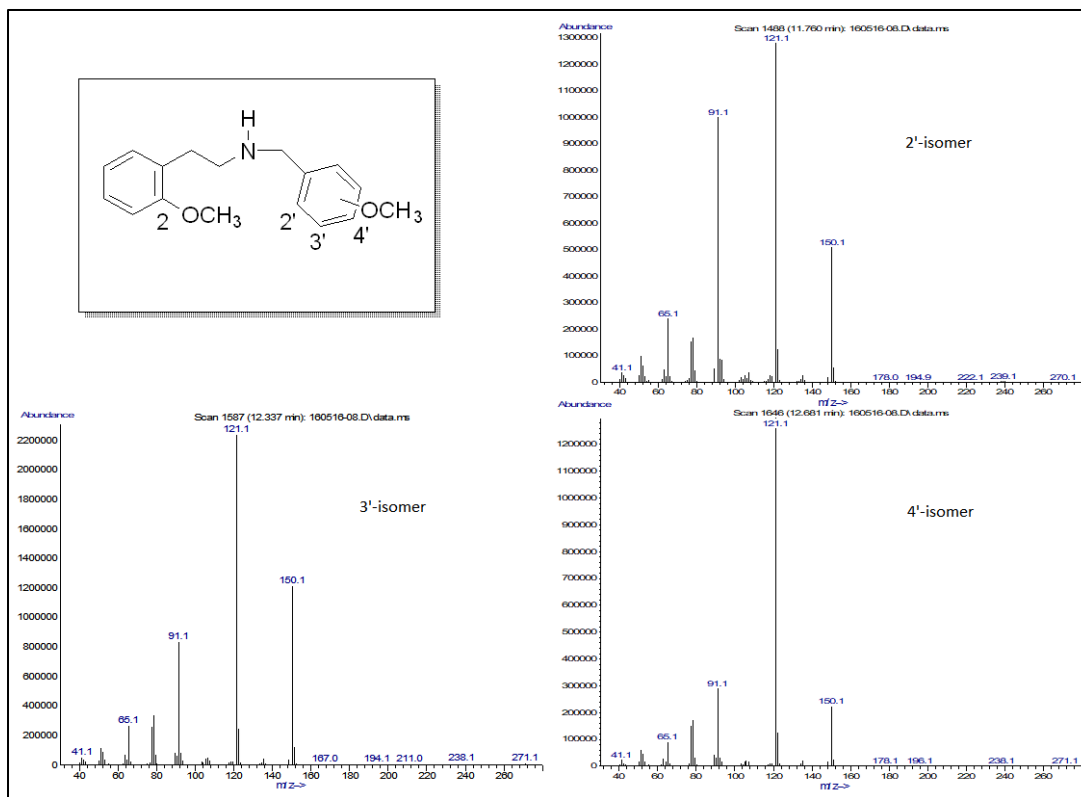


Figure 34 Mass Spectra of the N-(monomethoxy)benzyl-2-methoxyphenethylamines.

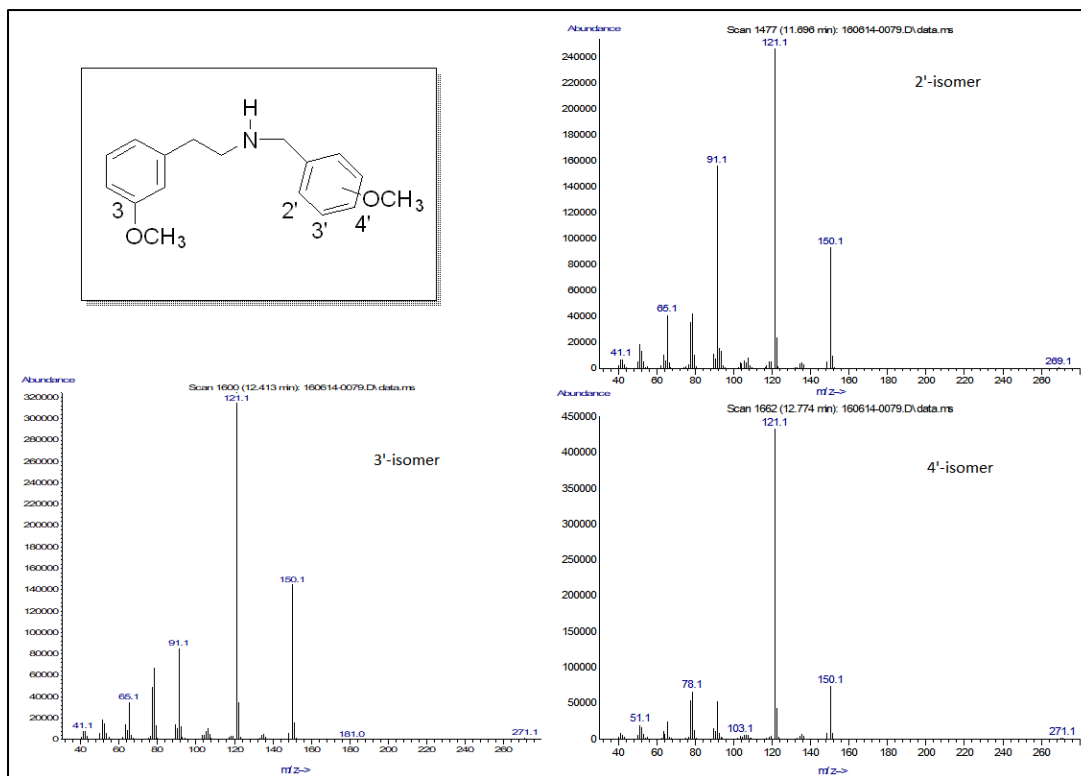


Figure 35 Mass Spectra of the N-(monomethoxy)benzyl-3-methoxyphenethylamines.

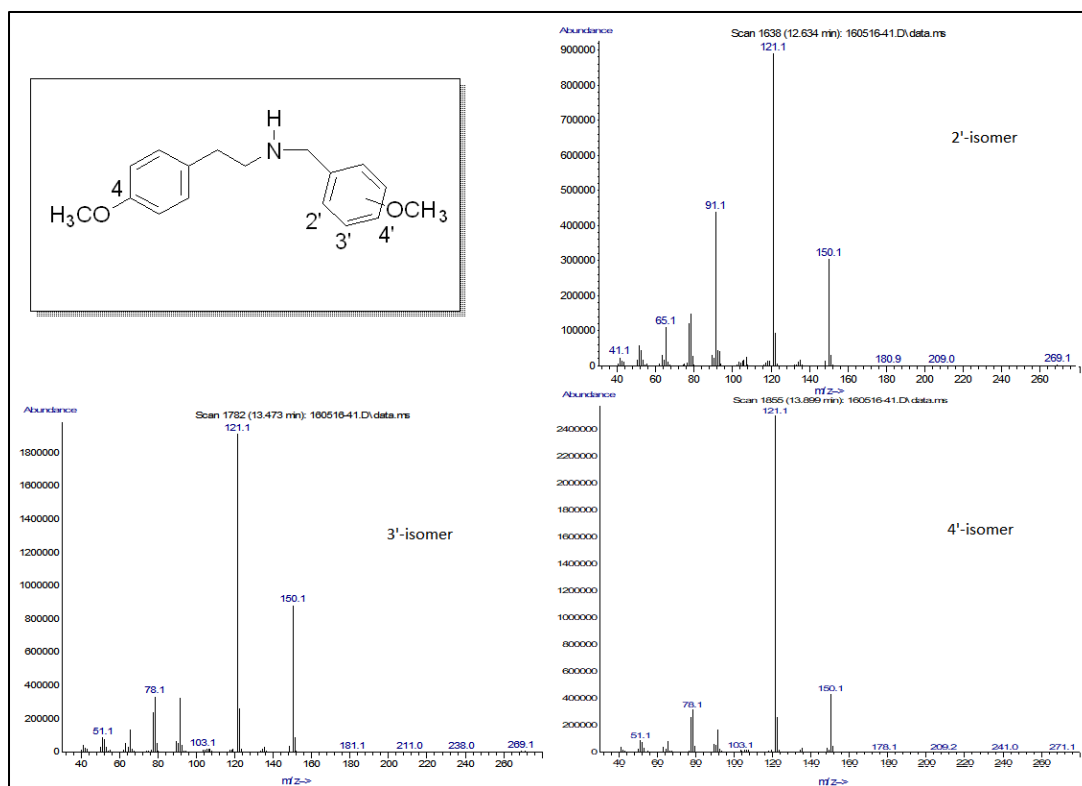
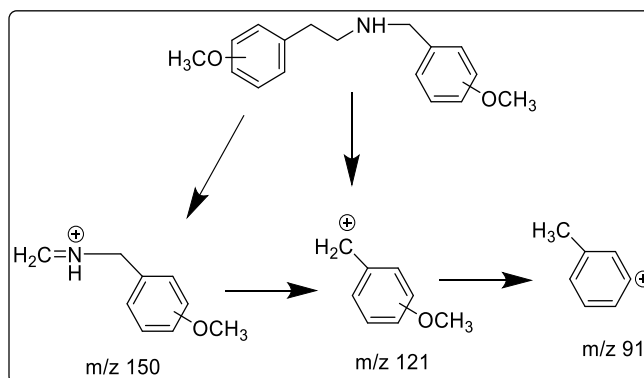


Figure 36 Mass Spectra of the N-(monomethoxy)benzyl-4-methoxyphenethylamines.

A proposed fragmentation pathway showing the dominant ions for the monomethoxy subseries of compounds is shown in Scheme 27. The ion at m/z 150 is likely the iminium cation formed by the dissociation of bond between α - and β -carbon atoms, a common pathway for phenethylamine compounds.



Scheme 27 Proposed EI-MS fragmentation pathway for the N-(methoxy)benzyl-methoxyphenethylamines.

The base peak m/z 121 can be formed by the cleavage of the N-C bond yielding 2-methoxybenzyl cation but could possibly form by cleavage of the C-C bond of the phenethyl side chain. Finally, the ion at m/z 91 appears to have formed from loss of CH_2O from the methoxy benzyl cation.

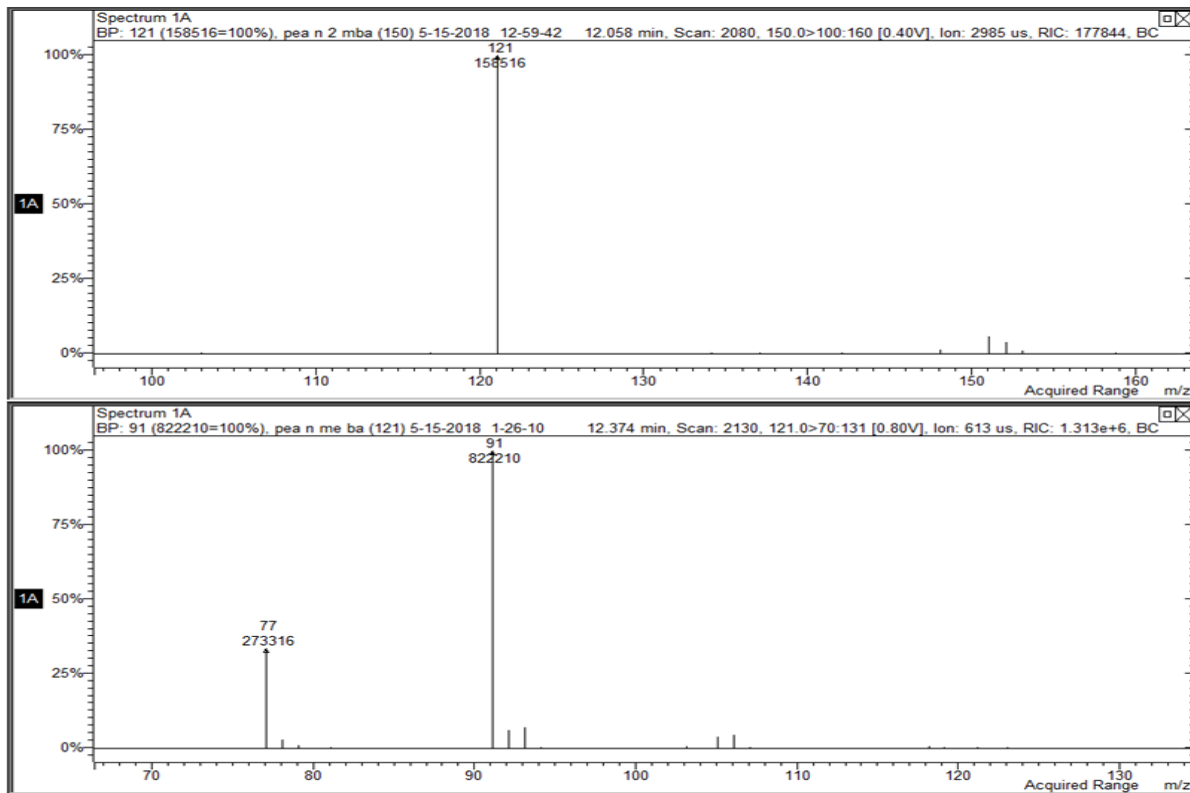


Figure 37 MS-MS of the 150 ion (top) and 121 ion (bottom) of the N-(methoxy)benzyl-methoxyphenethylamines.

Support for this fragmentation pathway was provided by MS-MS studies which demonstrate that the m/z 121 ion is formed from the m/z 150 fragment and m/z 91 ion is formed from the m/z 121 fragment as shown in Figure 37.

In an attempt to investigate the fragmentation pathways for this series of compounds in more detail a number of structurally simplified derivatives were prepared and analyzed. The derivatives prepared included compound 10 which contains no methoxy substituents, compounds 11 and 12 which contain only a single methoxy group in either the benzyl or phenethyl aromatic rings, compounds 13 and 14 where the nitrogen atom is substituted with a methyl group and lastly compound 15 which contains a single methoxy group in the benzyl aromatic ring with additional methyl group on the benzyl substituent (Figure 38).

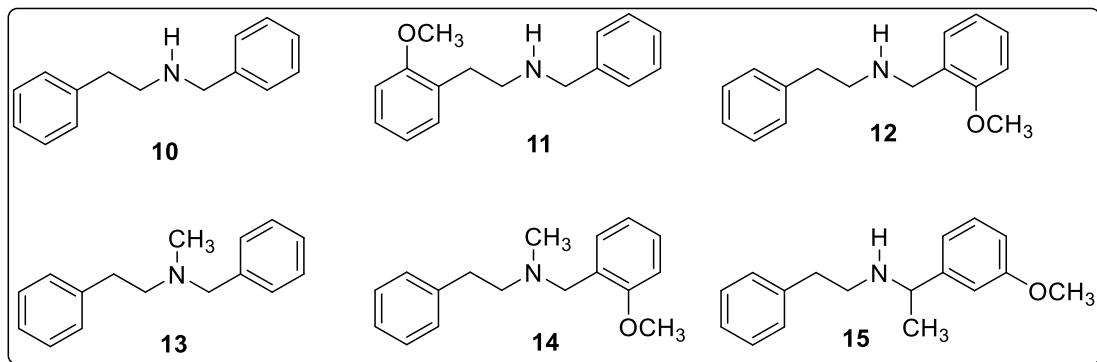
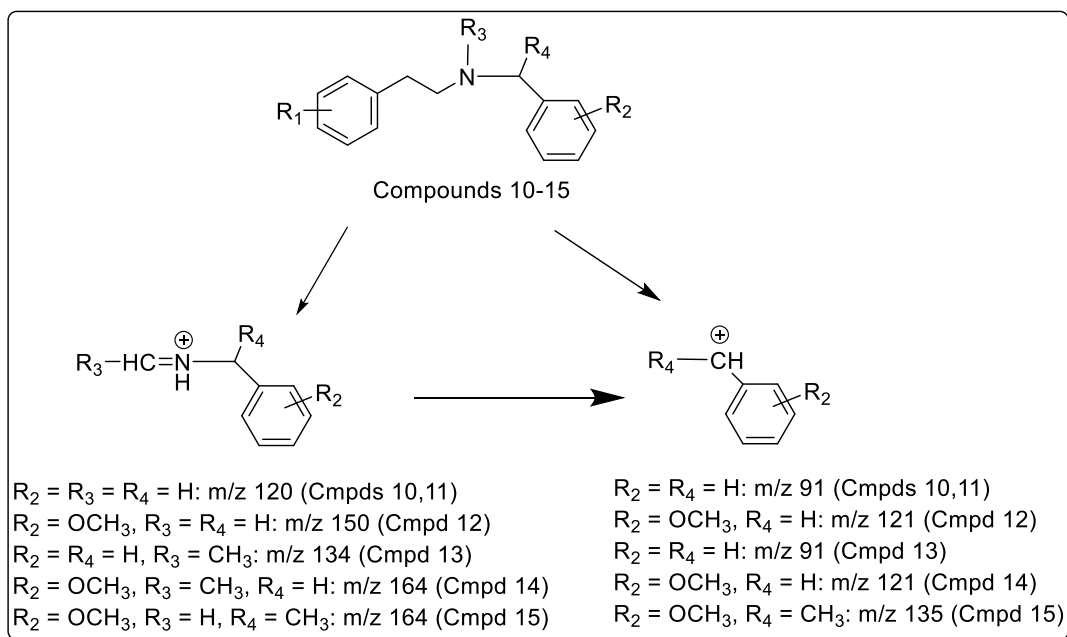


Figure 38 Structures of the simplified derivatives.

The EI-MS of these compounds are shown in Figures 39-44. If the fragmentation pathway shown in Scheme 27 is accurate and characteristic for compounds of this structure class, then compounds 10-15 would be expected to yield ions of high abundance as shown in Scheme 28. Since both compounds 10 and 11 lack a benzyl methoxy substituent they would be expected to give an iminium cation at m/z 120 by phenethyl side α -/ β -carbon bond dissociation, consistent with the fragmentation pathways in Schemes 27 and 28. This ion is present in the MS of both compounds 10 and 11 and is 30 mass units less than observed for derivatives containing a methoxy substituent in the benzyl ring (Figures 39 and 40). Similarly, compound 12 which contains a benzyl methoxy substituent like the nine regioisomers of this series would be expected to give an iminium cation at m/z 150, as is present in the EI-MS (Figure 41). The N-methyl derivative lacking a methoxy substituent (compound 13) should yield an iminium cation at m/z 134 (14 mass units higher than compound 10 - Figure 42), and the N-methyl derivative containing a benzyl methoxy group (compound 14) should yield an iminium ion at m/z 164 (30 mass units higher than compound 13 as shown in Figure 43). Again, both of these ions are present in the MS of compound 13 and 14. Finally, since compound 15 contains an additional methyl group on the α -carbon of the benzyl substituent, it is expected to generate iminium cation at m/z 164, similar to compound 14 (Figure 44), providing support for the original proposed fragmentation pathway.

The base peak m/z 121 ion present in the spectra of all nine N-(methoxy)benzyl-methoxyphenethylamines (compounds 1-9) was proposed to be the 2-methoxybenzyl cation formed by cleavage of the N-C bond. Again, if the original fragmentation pathway shown in Scheme 27 is accurate and characteristic for compounds of this structure class, then compounds 10-15 would be expected to give benzyl cation base peaks as shown in Scheme 28. Since

compounds 10, 11 and 13 lack a benzyl methoxy substituent, they would be expected to give a benzyl cation base peak at m/z 91. This ion is present in the MS of all three compounds 10, 11 and 13, and is 30 mass units less (m/z 121) than observed for nine regioisomers containing a methoxy substituent in the benzyl ring (Figures 39, 40 and 42). Similarly, compounds 12 and 14 which contain a benzyl methoxy substituent like the nine regioisomers of this series would be expected to give a benzyl cation base peak at m/z 121, as is present in the EI-MS (Figures 41 and 43). Furthermore, due to additional benzylic methyl group in compound 15 it would be expected to give a benzyl cation base peak at m/z 135, 14 mass units higher than observed for nine regioisomers containing only a methoxy substituent in the benzyl ring as is present in the EI-MS (Figure 44). Therefore EI-MS analysis of these structurally simplified derivatives supports the original fragmentation pathway proposed in Scheme 28 and demonstrates that compounds of this series undergo characteristic fragmentation.



Scheme 28 Proposed EI-MS fragmentation pathway for the ring and N-substituted-benzyl-methoxyphenethylamines.

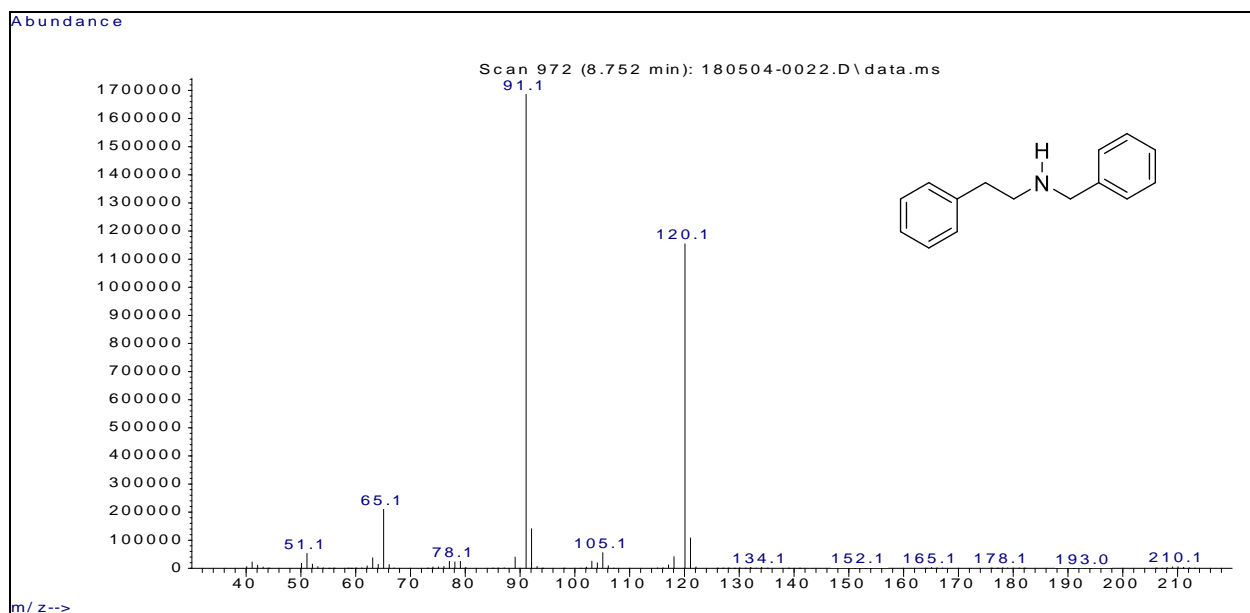


Figure 39 EI-MS of Mass Spectra of the N-benzyl-phenethylamine (Compound 10).

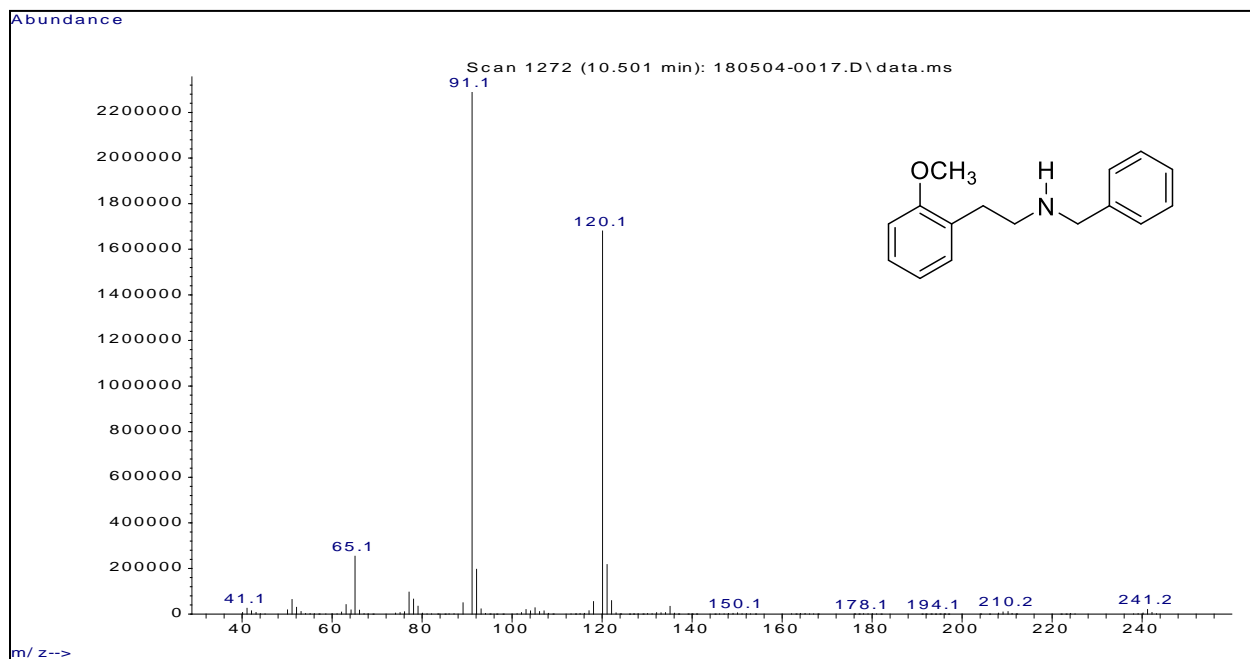


Figure 40 EI-MS of Mass Spectra of the N-benzyl-2-methoxyphenethylamine (Compound 11).

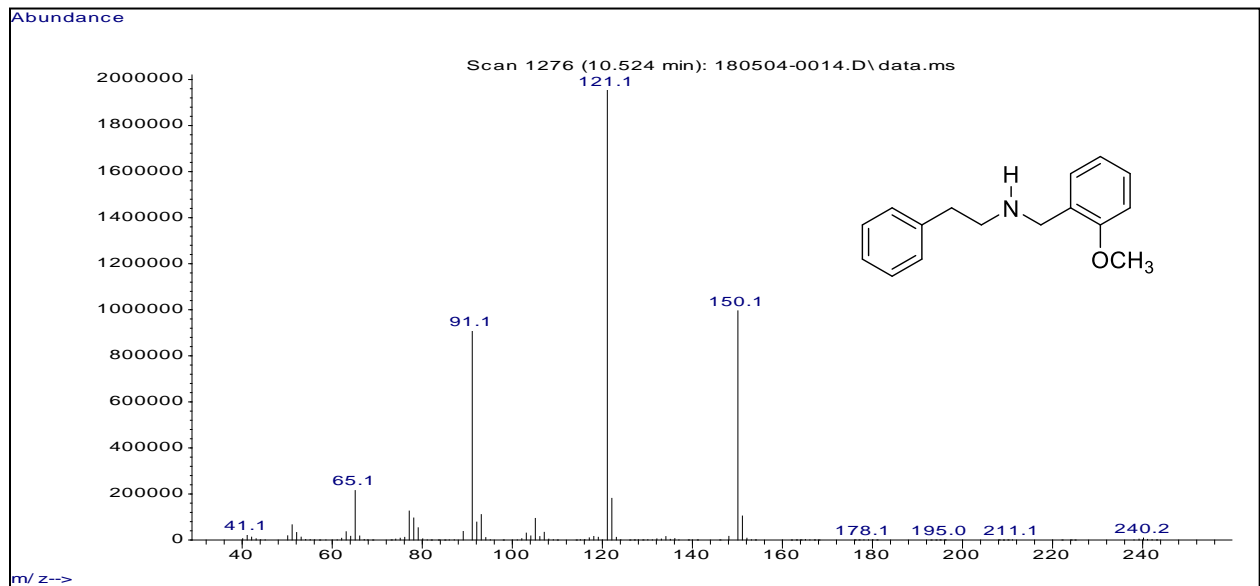


Figure 41 EI-MS of Mass Spectra of the N-(2'-methoxy)benzyl-phenethylamine (Compound 12).

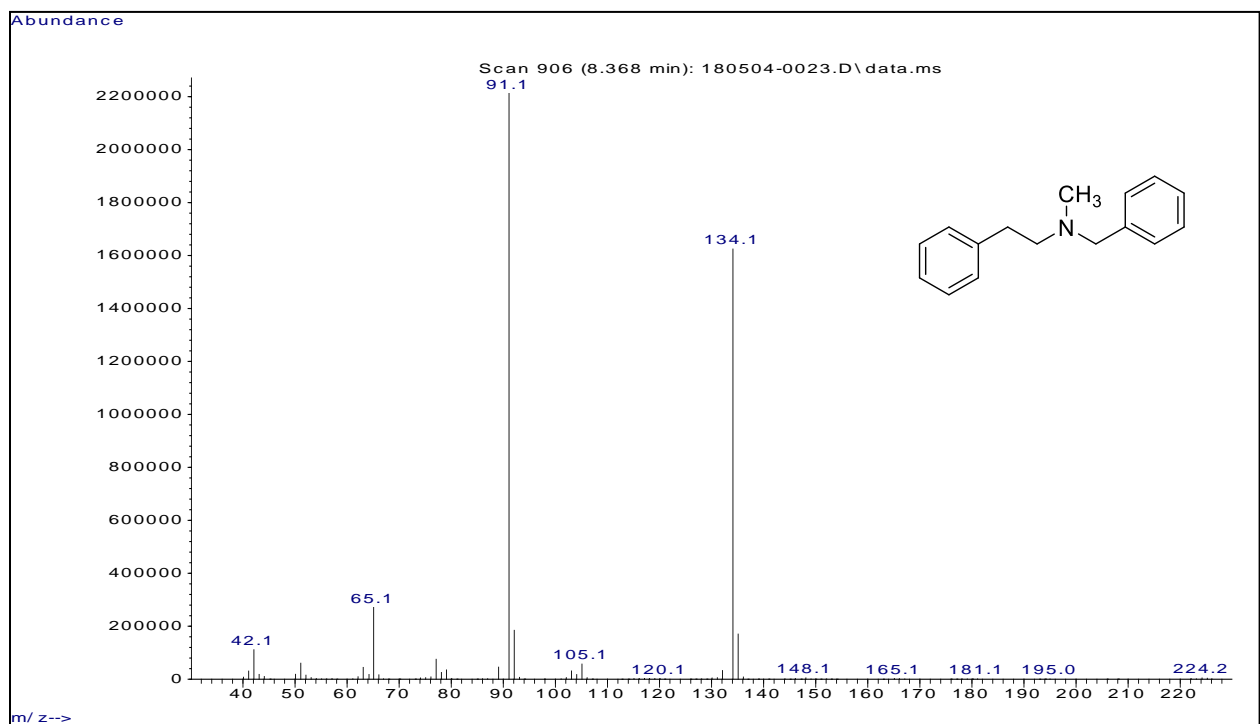


Figure 42 EI-MS of Mass Spectra of the N-benzyl-methylphenethylamine (Compound 13).

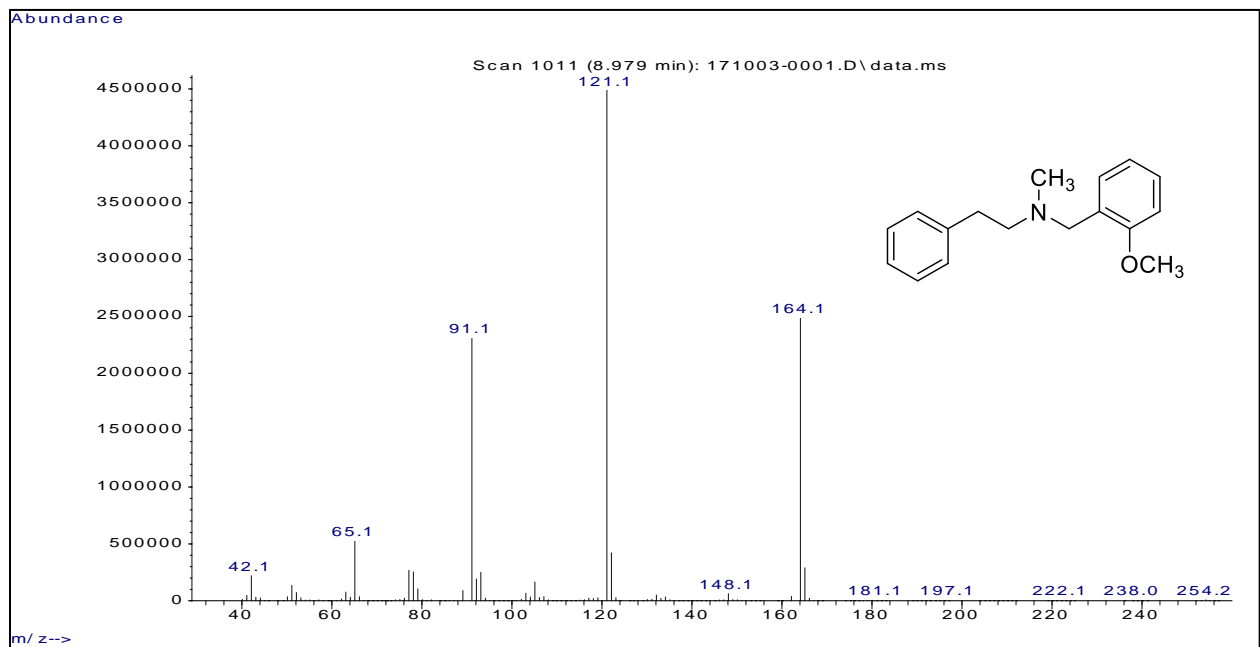


Figure 43 EI-MS of Mass Spectra of the (2'-methoxy)benzyl-N-methylphenethylamine (Compound 14).

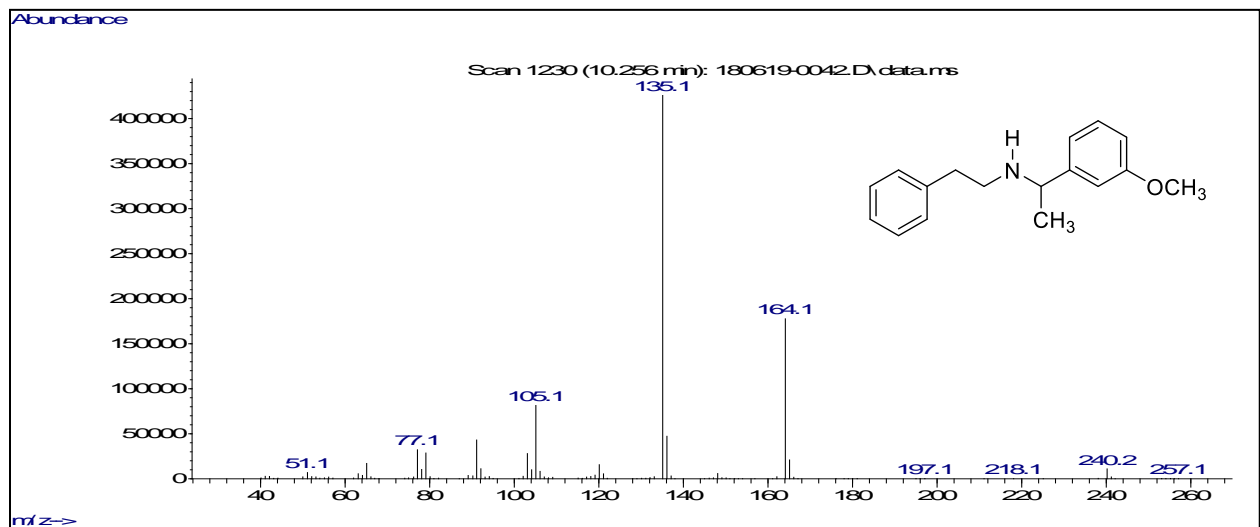


Figure 44 EI-MS of Mass Spectra of the N-2-(3'-methoxy)phenethyl-N-phenethylamine (Compound 15).

3.3 Gas Chromatographic Separations:

Gas chromatographic separations were performed in an attempt to further differentiate the nine regioisomers of this series. The compounds were divided into three subsets for initial separation studies, where the position of the methoxy group in the phenethyl ring was held constant while the methoxy group of benzyl ring was varied. Separations were accomplished on 30m x 0.25mm ID capillary column coated with 0.25 μm film of midpolarity Crossbond[®] silarylene phase containing a 50% phenyl and 50% dimethyl polysiloxane polymer (Rxi[®]-17Sil MS). Separations were achieved over 22 minutes starting from initial temperature of 70 °C held for 1 minute then gradually increased to reach terminal temperature at 250 °C at a rate of 30 °C/minute and held for 15 minutes with elution over a 1 minute window. This set of chromatographic conditions yielded an excellent separation of each subset of three compounds with the 2'-methoxy isomer eluting before the 3'-isomer, and the 3'-isomer before the 4'-isomer in each case (Figure 45).

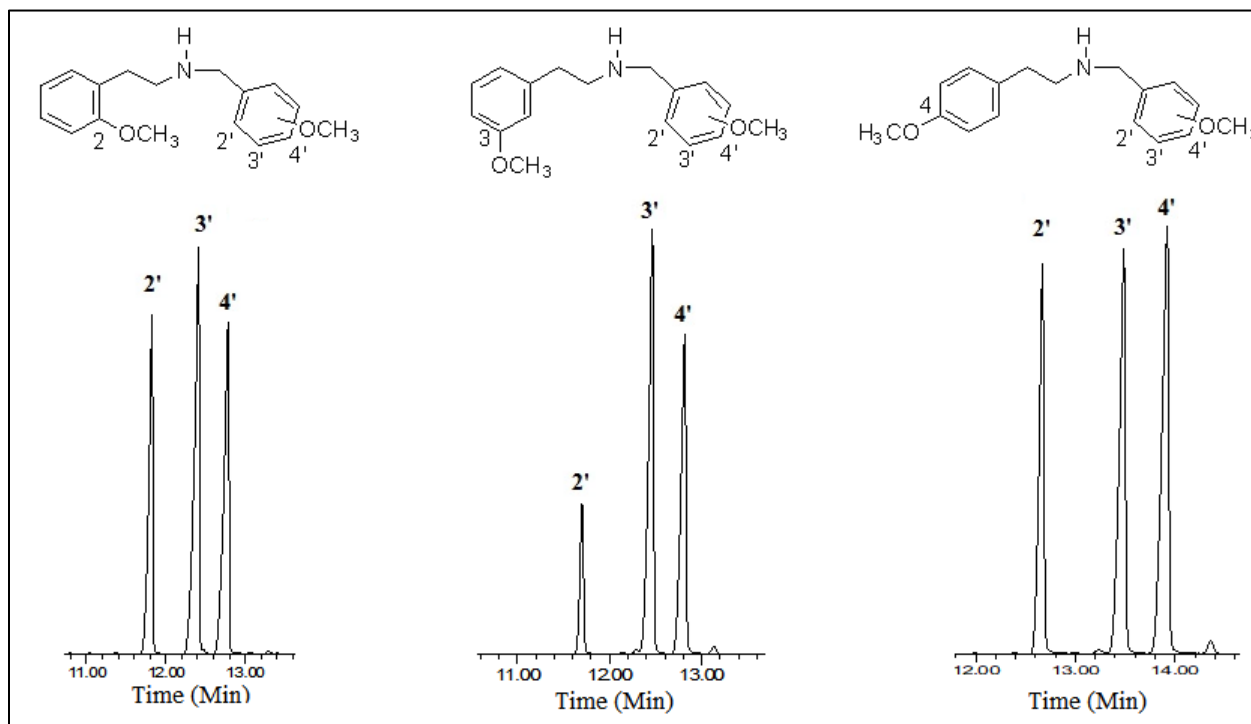


Figure 45 Gas chromatographic separation of the N-(monomethoxy)benzyl-methoxyphenethylamines.

A second series of separations was accomplished by dividing the nine regioisomers into three subsets where the position of the methoxy group in the phenethyl ring was varied while the methoxy group of phenethyl ring was varied (Figure 46). The same column and temperature program were used as above with similar elution order with the 2'-methoxy isomer eluting before the 3'-isomer, and the 3'-isomer before the 4'-isomer in each case. Attempts to separate all nine regioisomers were not successful, with multiple regioisomers co-eluting under a variety of chromatographic conditions. However, based on differences in chromatographic retention times and relative abundance of the m/z 91 ion, it is possible to differentiate members of each subset of the N-(monomethoxy)benzyl-methoxyphenethylamines.

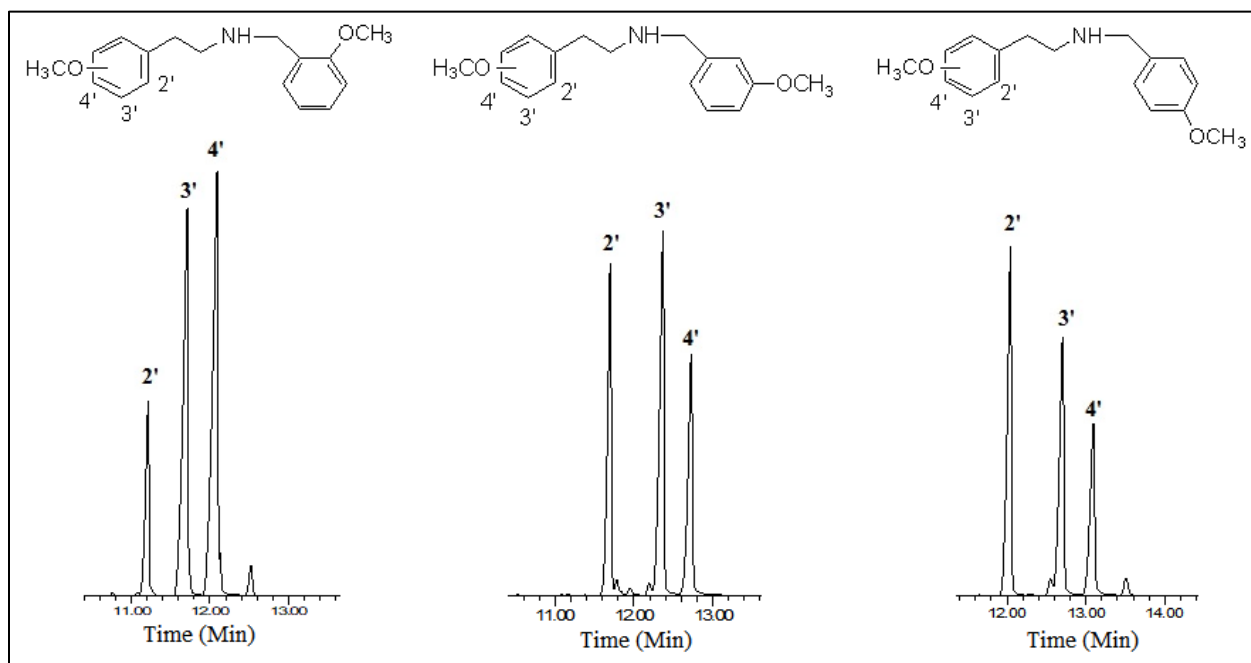


Figure 46 Gas chromatographic separation of the N-(monomethoxy)benzyl-methoxyphenethylamines.

4 Analysis of the N-(Methoxy)benzyl-dimethoxyphenethylamine and N-(Methoxy)benzyl-methylenedioxyphenethylamine Series

4.1 Introduction:

The compounds of N-(methoxy)benzyl-dimethoxyphenethylamines series are simplified derivatives of the NBOMes where the halogen atom is eliminated and there are two methoxy substituents on the phenethyl aromatic ring and a single methoxy substituent on the benzyl ring of the core NBOME structure. There are six possible dimethoxy substitution patterns and three possible monomethoxy substitution patterns, for a total of 18 regioisomeric compounds. This series can be divided into six subsets based primarily on the position of the dimethoxy substituents on the phenethyl aromatic ring (the 2,3-, 2,4-, 2,5-, 2,6-, 3,4- and 3,5-positions) and secondarily on the position of the single methoxy group on the benzyl aromatic ring (2'-, 3'-, and 4'-) as shown in Figure 47. All of these compounds were synthesized as described in the previous chapter.

The compounds of N-(methoxy)benzyl-methylenedioxyphenethylamine series are derivatives of the NBOMes where the halogen atom is eliminated and the dimethoxy substituents in the phenethyl aromatic ring are replaced with a methylenedioxy group. In the phenethyl aromatic ring there are two possible methylenedioxy substitution patterns, at positions 2,3- and 3,4- as shown in Figure 48. Combining these two possible methylenedioxy substitutions with substitution of a single methoxy group at each position of the benzyl aromatic ring gives rise to 6 regioisomeric compounds (Figure 48). These methylenedioxy derivatives were prepared because this substitution pattern is common in a number of drugs of abuse families including the MDMA and the cathinones.

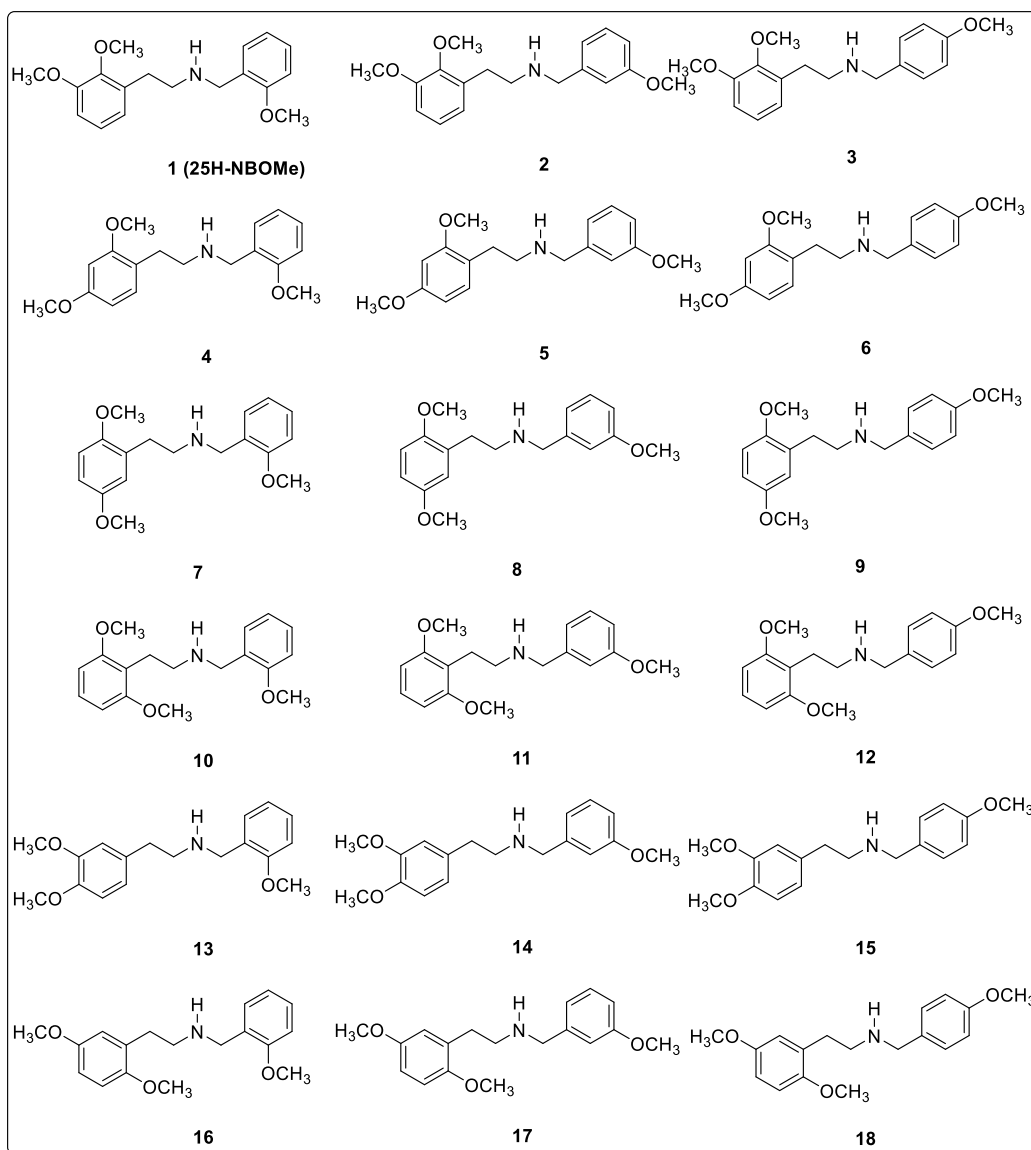


Figure 47 Structures of the N-(methoxy)benzyl-dimethoxyphenethylamine Series.

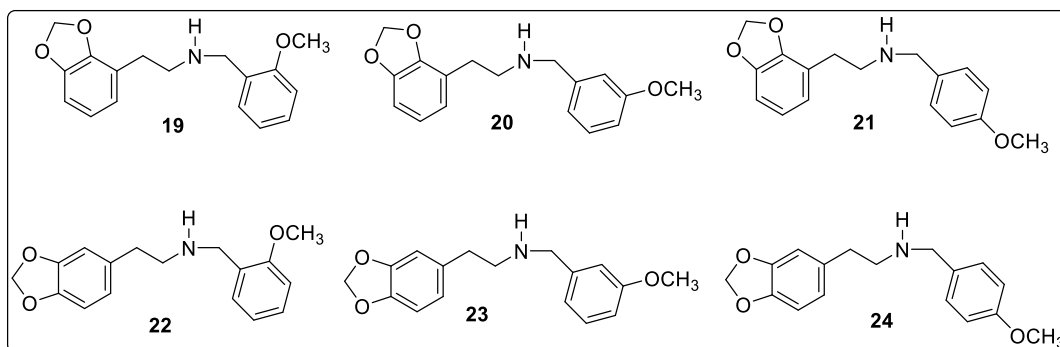


Figure 48 Structures of the N-(methoxy)benzyl-methylenedioxyphenethylamine Series.

4.2 Mass Spectral Analysis:

All eighteen regioisomeric N-(methoxy)benzyl-dimethoxyphenethylamine compounds (Structures 1-18) yielded nearly identical mass spectra as shown in Figures 49-52. The molecular ion (MW = 301) is not apparent in the EI-MS spectrum of any of these compounds, however the molecular mass was confirmed by CI-MS where a M+1 ion of 302 was present (Figure 49). As reported for the 25-NBOMe compounds and the N-(monomethoxy)benzyl-monomethoxyphenethylamines in the previous chapter, the dominant ions in GC-MS spectrum of all eighteen compounds in this series are observed at $m/z = 121$, 150 and 91, with the base peak m/z 121 (Figures 50-52). The m/z 91 ion was present in the highest abundance in the 2'-methoxy isomer and decreased in the 3'- and 4'-methoxy isomers as observed in the previous monomethoxy series. Other than the relative abundance of the m/z 91 ions, there are no other features in the mass spectra of these regioisomers which allows for specific differentiation.

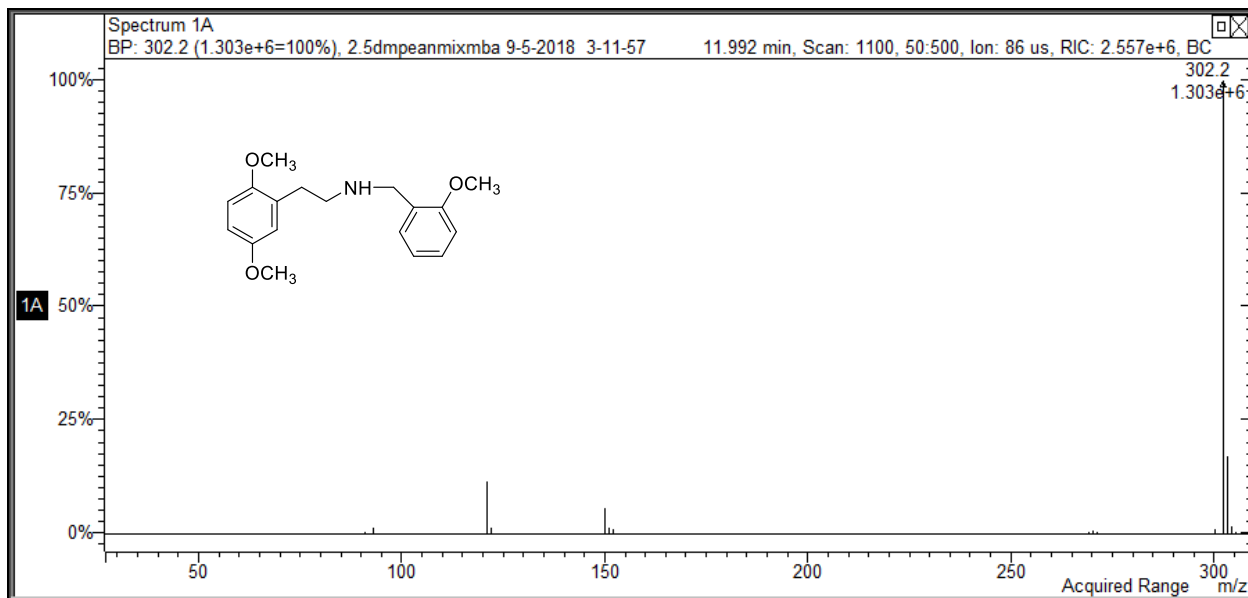


Figure 49 Representative CI-MS of Mass Spectra of the N-(2'-methoxy)benzyl-2,5-dimethoxyphenethylamines.

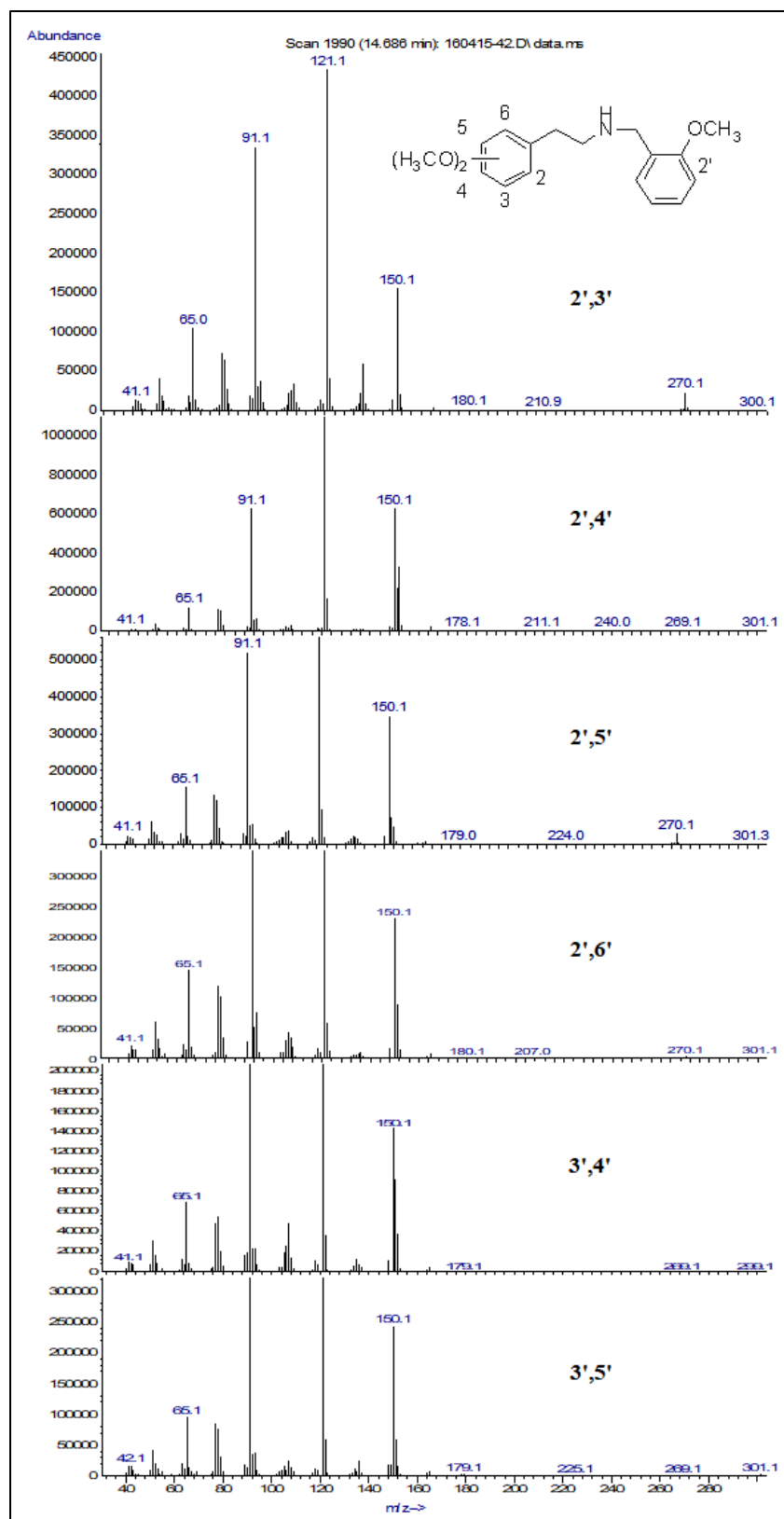


Figure 50 Mass Spectra of the N-(2'-methoxy)benzyl-dimethoxyphenethylamines.

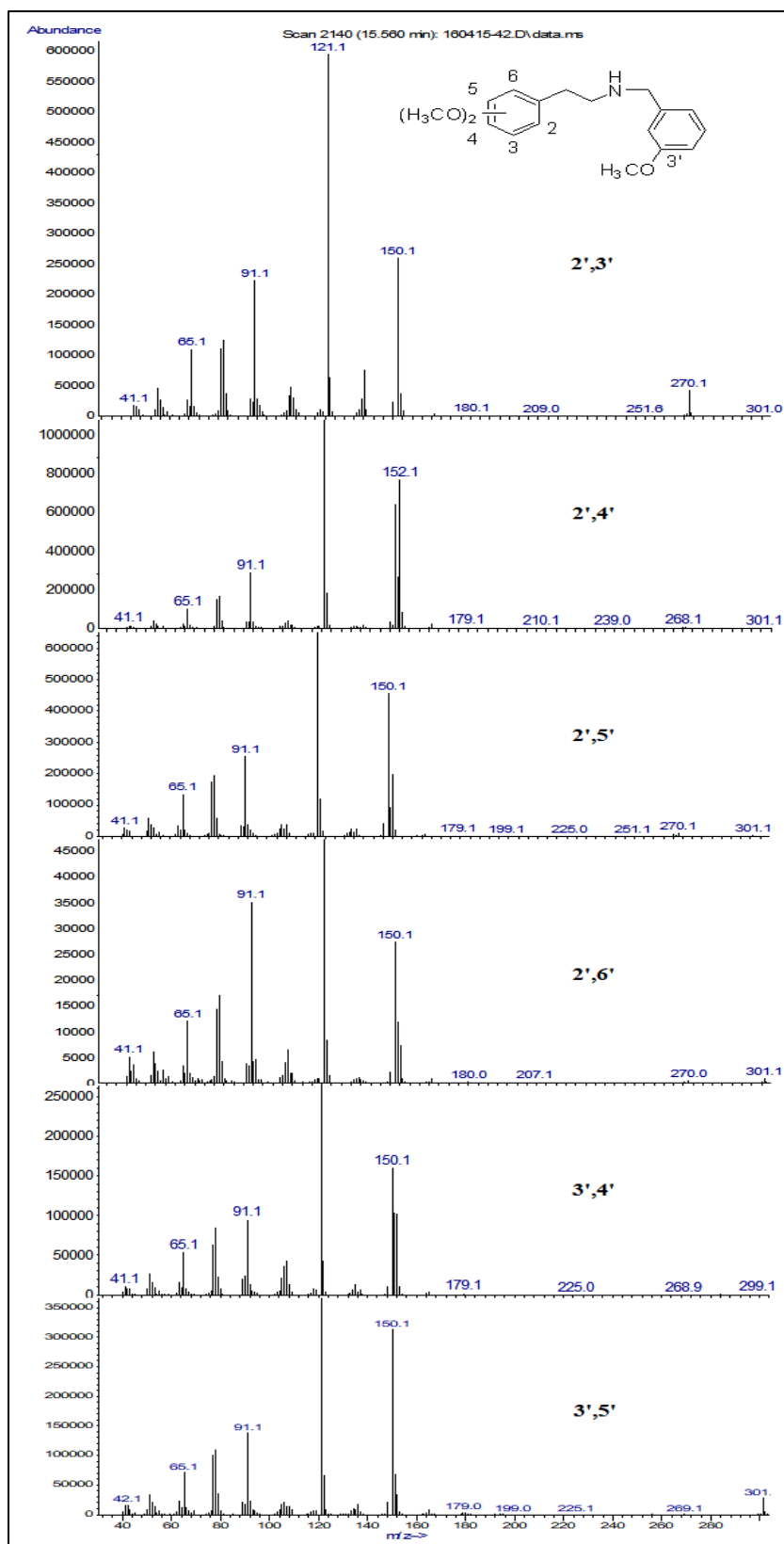


Figure 51 Mass Spectra of the N-(3'-methoxy)benzyl-dimethoxyphenethylamines.

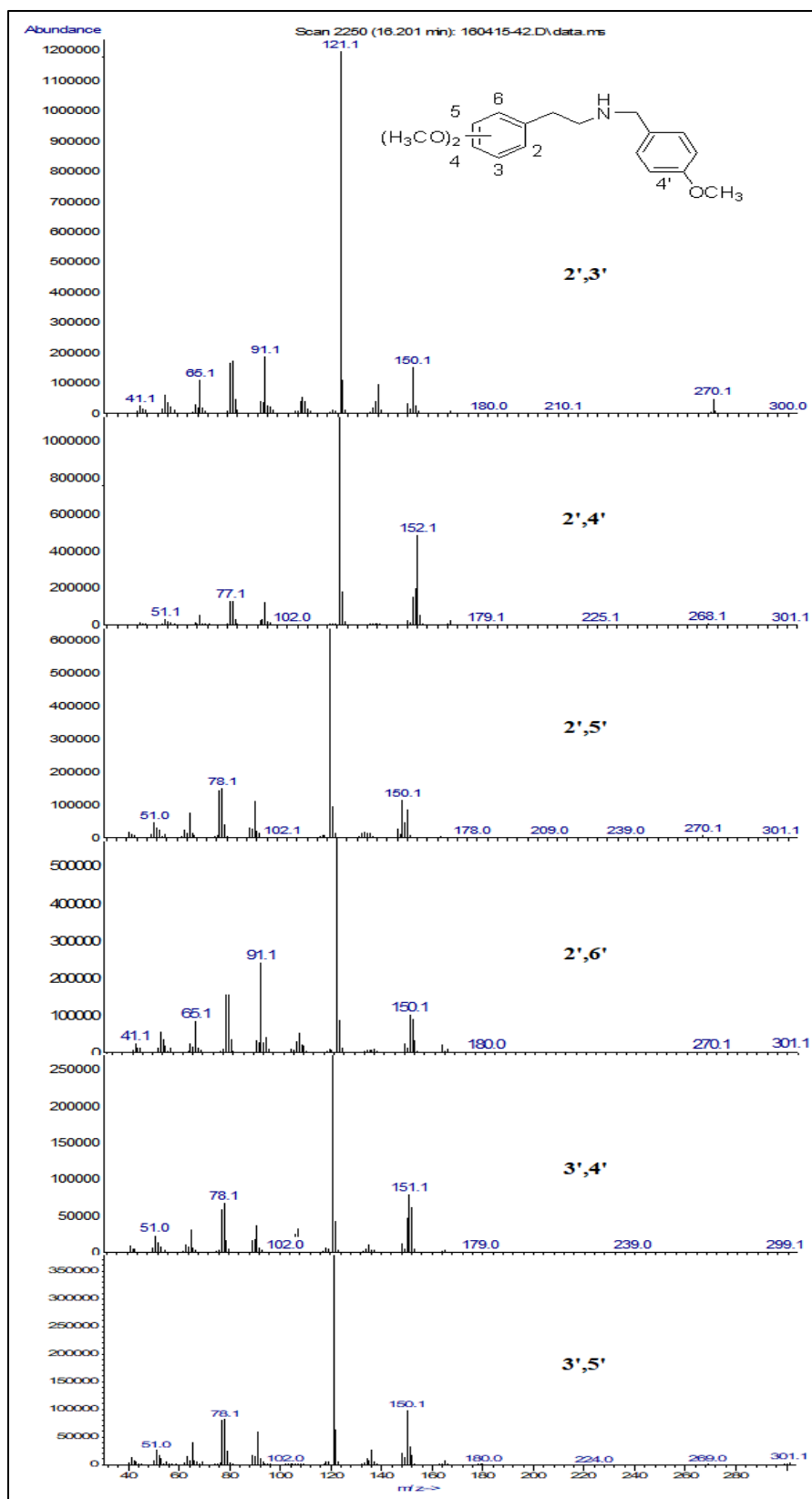
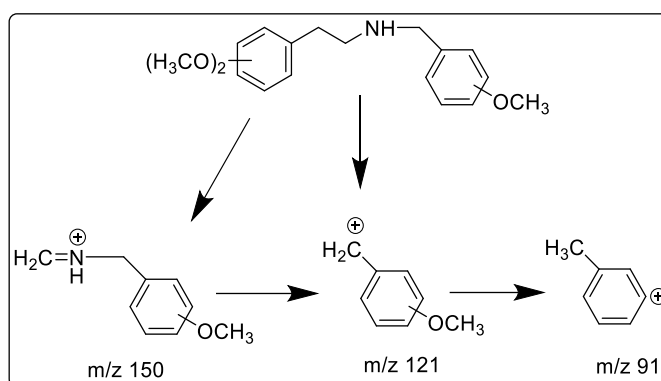


Figure 52 Mass Spectra of the N-(4'-methoxy)benzyl-dimethoxyphenethylamines.

A proposed fragmentation pathway showing the dominant ions for the N-(methoxy)benzyl-dimethoxyphenethylamine subseries of compounds is shown in Scheme 29 and is similar to that proposed for the N-(methoxy)benzyl-monomethoxyphenethylamines in the previous chapter. The base peak m/z 121 can be formed by the cleavage of the N-C bond yielding 2-methoxybenzyl cation. The ion at m/z 150 is likely the iminium cation formed by the dissociation of bond between α - and β -carbon atoms, a common pathway for phenethylamine compounds. Finally, the ion at m/z 91 appears to have formed from loss of CH_2O from the methoxy benzyl cation.



Scheme 29 Proposed EI-MS fragmentation pathway for the N-(monomethoxy)benzyl-dimethoxyphenethylamines.

Support for this fragmentation pathway was provided by tandem mass spectroscopy or MS-MS studies. With this technique, ions formed in the ion source during the first stage of mass spectrometry (MS1) are separated by their mass-to-charge ratio. Ions of a particular mass-to-charge ratio are then selected and secondary fragment ions or product ions formed from these ions are separated and detected in the second mass spectrometry stage (MS2). MS-MS experiments with the 23DMPEA2MB derivative yielded the results in Figures 53A-C showing that the m/z 121 ion is formed from the molecular ion (m/z 302) and the m/z 150 fragment ion, and that the m/z 91 ion is formed from the m/z 121 ion.

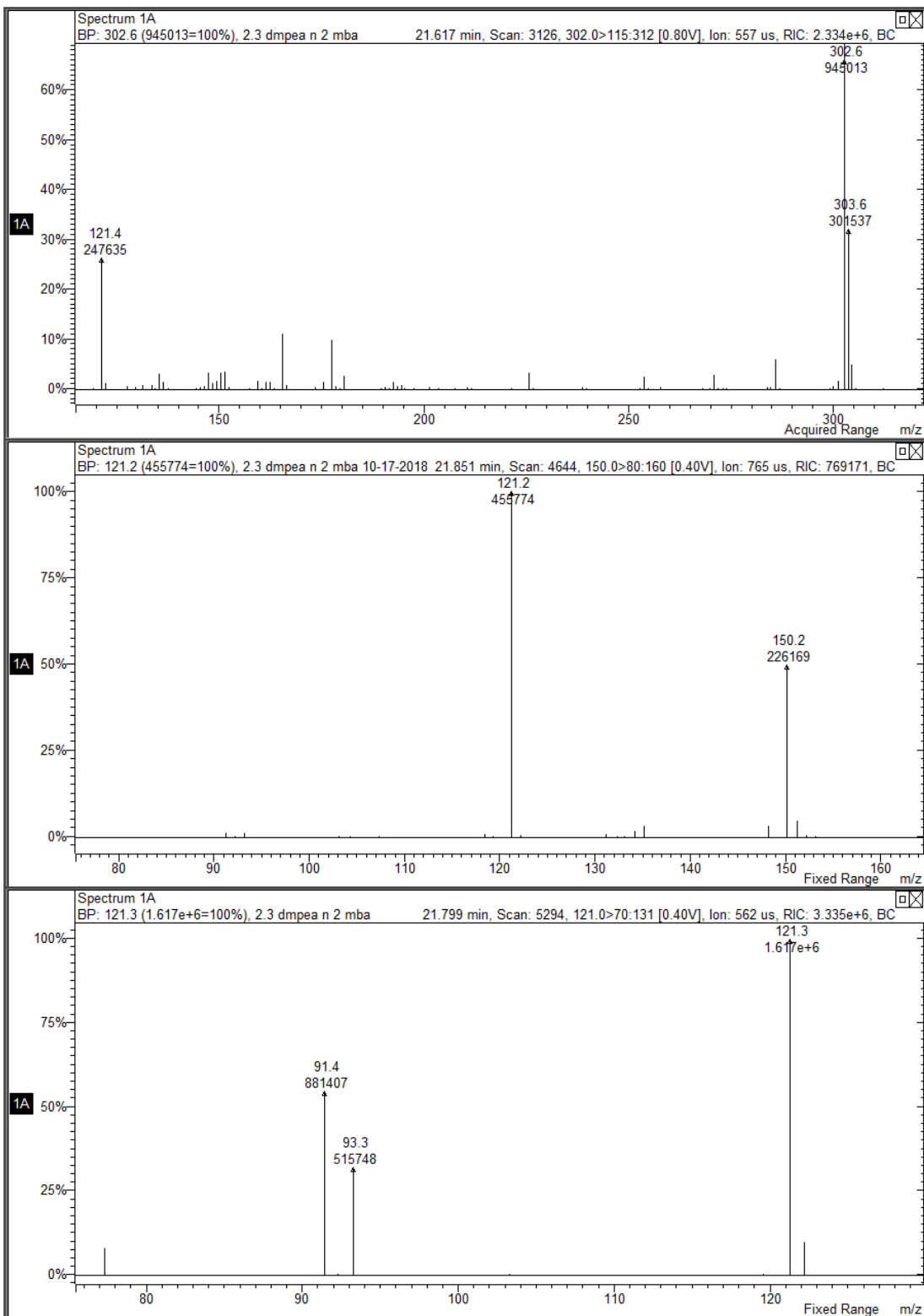


Figure 53 MS-MS results of for 23DMPEA2MB and fragment ions m/z 121 and 91.

In an attempt to investigate the fragmentation pathways for this series of compounds in more detail a number of structurally simplified derivatives were prepared and analyzed.

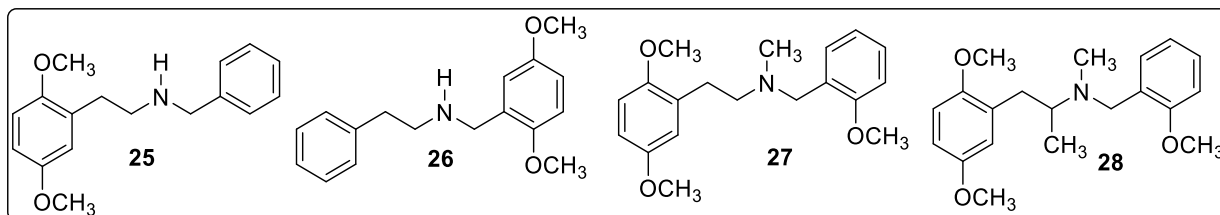


Figure 54 Structures of the simplified derivatives.

The derivatives prepared included compounds 25-26 which contain no methoxy substituents in either the benzyl or phenethyl aromatic rings, compound 27 where the nitrogen atom is substituted with a methyl group and a single methoxy group is present in the benzyl aromatic ring and two methoxy groups on the phenethyl aromatic ring, and compound 28 which is a derivative of compound 27 containing an additional methyl substituent at the beta-position of the phenethyl side chain (Figure 54).

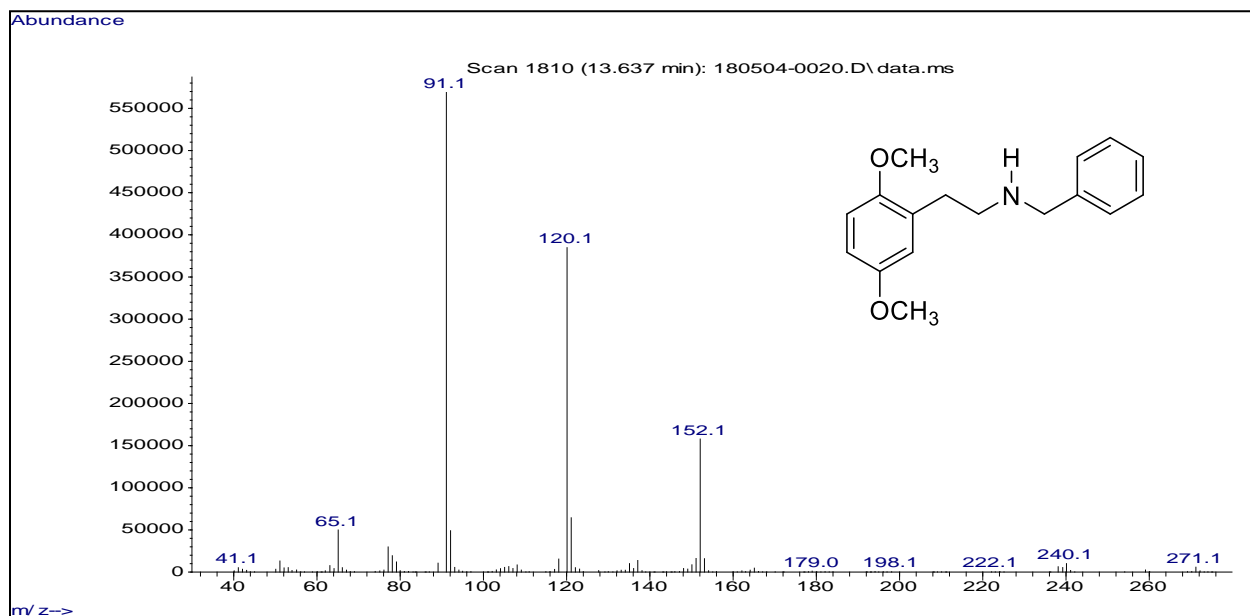


Figure 55 EI-MS of Mass Spectra of the N-benzyl-2,5-dimethoxyphenethylamine (Compound 25).

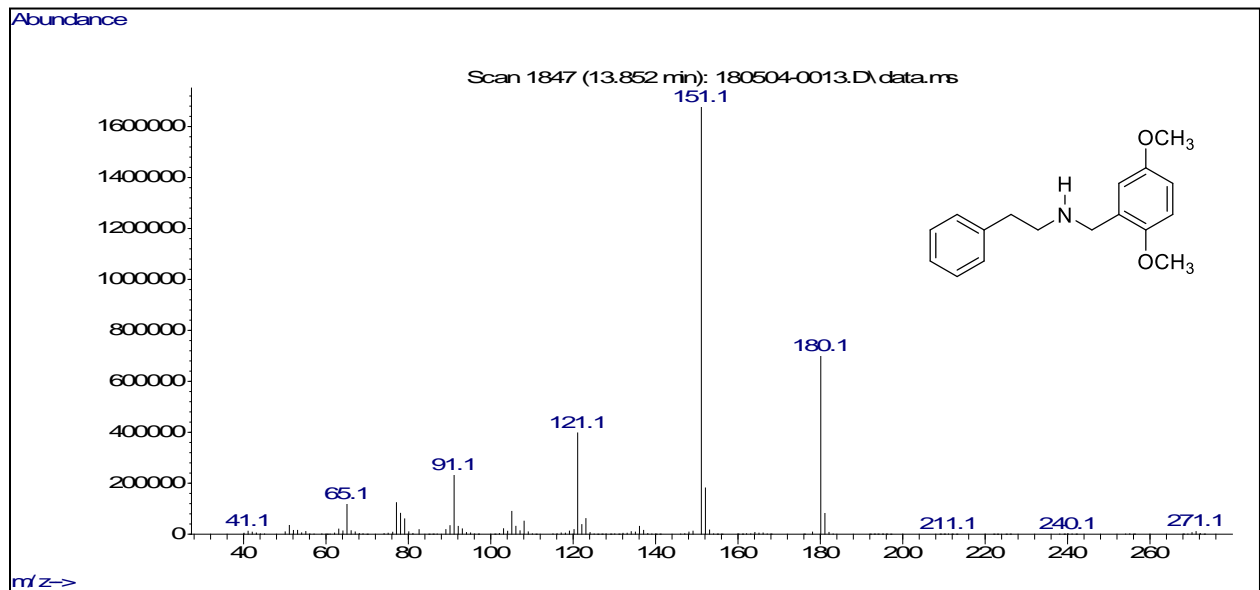


Figure 56 EI-MS of Mass Spectra of the N-(2',5'-dimethoxy)benzyl-phenethylamine (Compound 26).

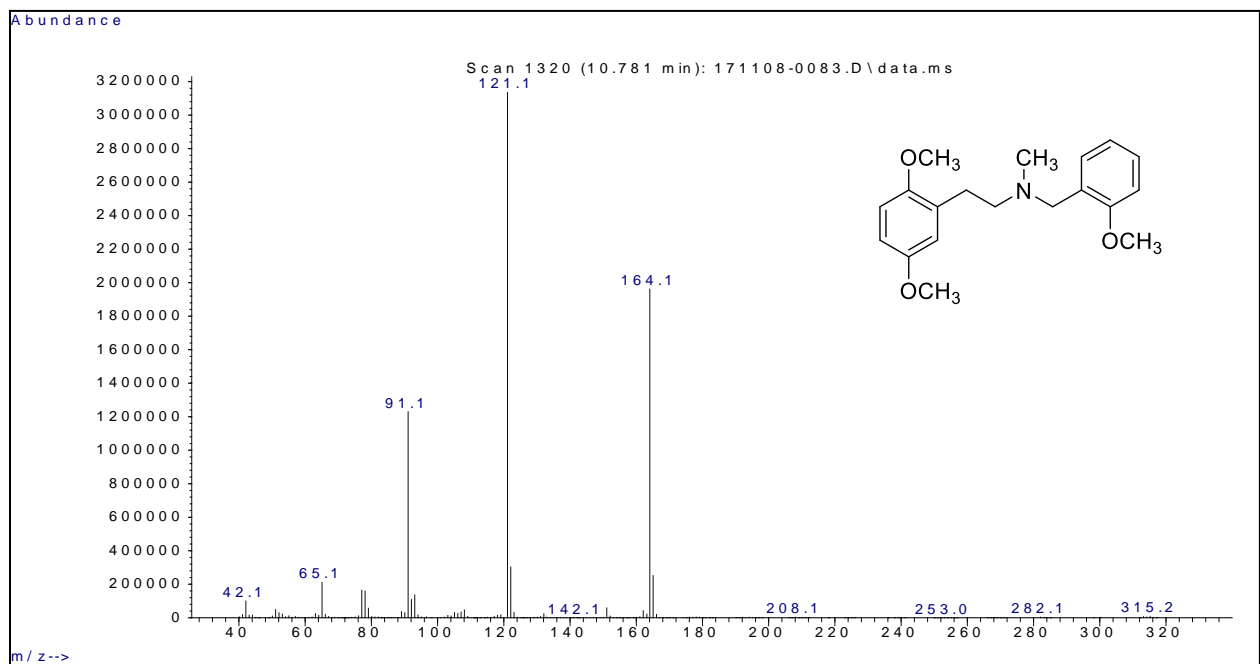


Figure 57 EI-MS of Mass Spectra of the (2'-monomethoxy)benzyl-N-methyl-2,5-dimethoxyphenethylamine (Compound 27).

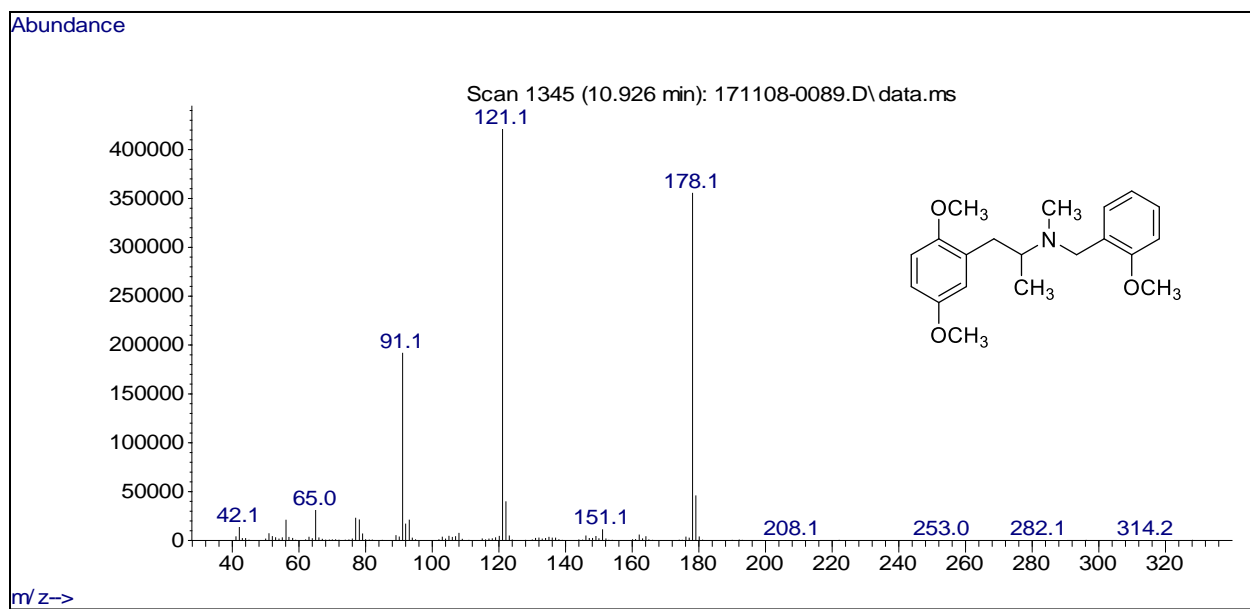
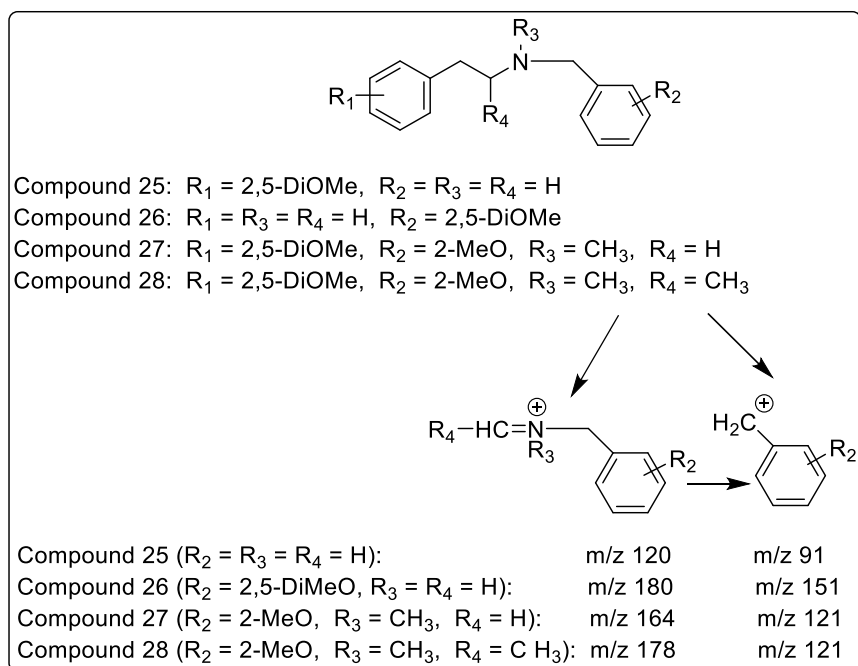


Figure 58 EI-MS of Mass Spectra of the (2'-monomethoxy)benzyl-N-methyl-2,5-dimethoxyphenpropylamine (Compound 28).

The EI-MS of compounds 25-28 are shown in Figures 55-58. If the fragmentation pathway shown in Scheme 29 is accurate and characteristic for compounds of this structure class, then compounds 25-28 would be expected to yield ions of high abundance as shown in Scheme 30. Since compound 25 lacks a benzyl methoxy substituent it would be expected to give an iminium cation at m/z 120 by phenethyl side α -/ β -carbon bond dissociation, consistent with the fragmentation pathways in Scheme 29 and 30. This ion is present in the MS of compound 25 and it is 30 mass units less than observed for derivatives containing a methoxy substituent in the benzyl ring (Figure 55). On the other hand, compound 26 which contains two methoxy substituents on the benzyl ring, would be expected to give an iminium cation at m/z 180, as is present in the EI-MS (Figure 56). For compound 27, since it contains both N-methyl group and a single methoxy benzyl substituent, it is expected to have iminium cation at m/z 164, 44 mass units higher than the corresponding ion from compound 25 (Figure 57). Finally, it would be expected for compound 28 to yield iminium cation at 178 m/z (14 mass units higher than compound 27) due to the additional methyl substituent on the alkyl side chain of the phenethyl aromatic rings (Figure 58), providing support for the original proposed fragmentation pathway.

The base peak m/z 121 ion present in the spectra of all eighteen N-(methoxy)benzyl-dimethoxyphenethylamines (compounds 1-18) was proposed to be the 2-methoxybenzyl cation formed by cleavage of the N-C bond yielding. Again, if the original fragmentation pathway shown in Scheme 29 is accurate and characteristic for compounds of this structure class, then compound 25 would be expected to give benzyl cation base peaks as shown in Scheme 30. Since compound 25 lacks a benzyl methoxy substituent, it would be expected to give a benzyl cation base peak at m/z 91. This ion is present in the EI-MS of compound 25 and it is 30 mass units less (m/z 121) than observed for 18 regioisomers containing a methoxy substituent in the benzyl ring (Figure 55). On the other hand, compound 26 contains two methoxy substituents in the benzyl ring. Therefore, it would be expected to give a benzyl cation base peak at m/z 151, 30 mass units higher than the eighteen compounds of the N-(methoxy)benzyl-dimethoxyphenethylamine series. However, since both compounds 27 and 28 have a single methoxy substituent on the benzyl aromatic ring, they should give a benzyl cation base peak at m/z 121, similar to the 18 compounds of the N-(methoxy)benzyl-dimethoxyphenethylamine series. Therefore EI-MS analysis of these structurally modified derivatives supports the original fragmentation pathway proposed in Scheme 29 and demonstrates that compounds of this series undergo characteristic fragmentation.



Scheme 30 Proposed EI-MS fragmentation pathway for Compounds 25-27.

In conclusion, since all the eighteen compounds of this series cannot be differentiated from each other by simple EI-MS, other analytical methods are required for specific compound identification.

The EI-MS for the all six regioisomeric N-(methoxy)benzyl-methylenedioxyphenethylamine compounds (Structures 19-24) yielded nearly identical mass spectra as shown in Figures 59-61. Again, the molecular ion (MW = 285) is not apparent in the EI-MS spectrum of any of these compounds, however the molecular mass was confirmed by CI-MS where a M+1 ion of 286 was present (Figure 59). As reported for the 25-NBOMe compounds and the eighteen regioisomers in the preceding section, the dominant ions in EI-MS spectrum of all six compounds in this series are observed at m/z = 121, 150 and 91, with the base peak m/z 121 (Figures 60-61). The m/z 91 ion was present in the highest abundance in the 2'-methoxy isomer and decreased in the 3'- and 4'-methoxy isomers. Other than the relative abundance of the m/z 91 ions, there are no other features in the mass spectra of these regioisomers which allows for specific differentiation.

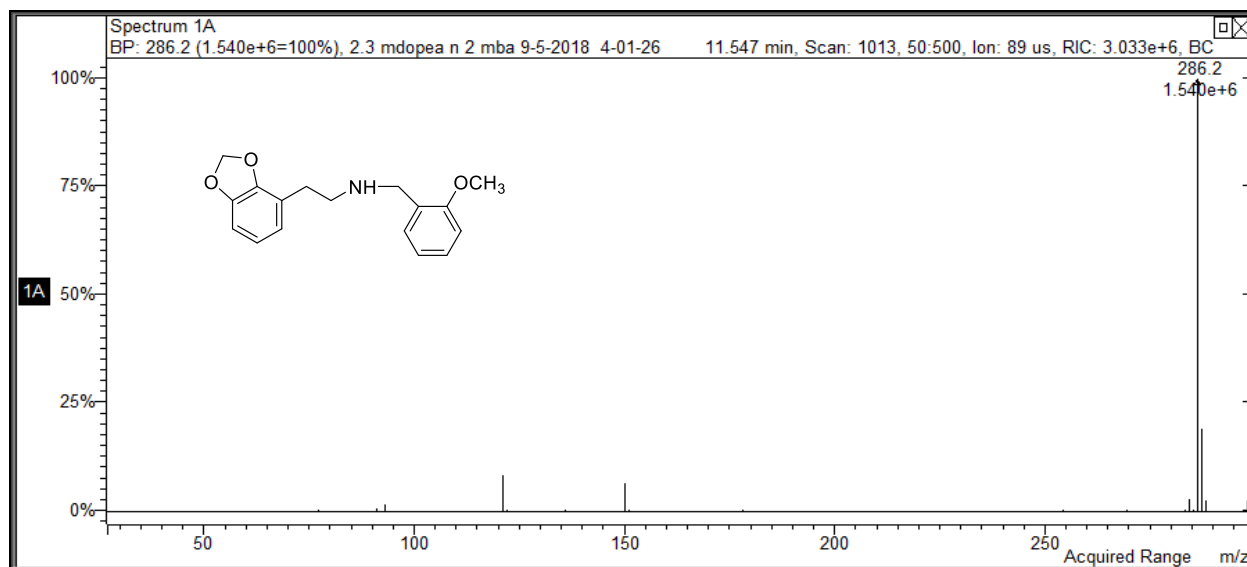


Figure 59 Representative CI-MS of Mass Spectra of the N-(2'-methoxy)benzyl-2,3-methylenedioxyphenethylamines.

The three most abundant ions in the EI-MS of this methylenedioxy series (m/z 121, 150 and 91) are the same as the most abundant ions of the N-(methoxy)benzyl-monomethoxyphenethylamine series reported in the previous chapter and the N-(methoxy)benzyl-dimethoxyphenethylamines series described earlier in this chapter. This similarity in MS fragmentation is a result of all of

these derivatives having the same core NBOME structure and common N-(methoxy)benzyl substitution patterns.

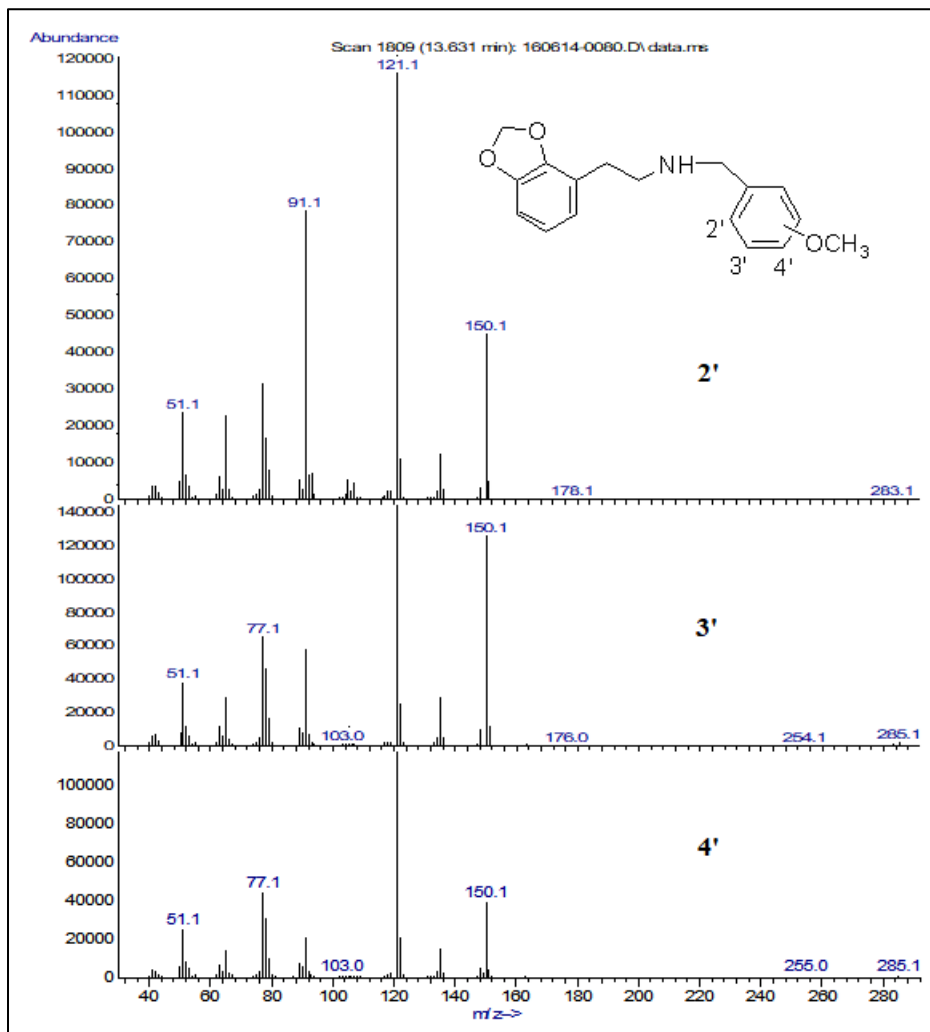


Figure 60 Mass Spectra of the N-(methoxy)benzyl-2,3-methylenedioxyphenethylamines.

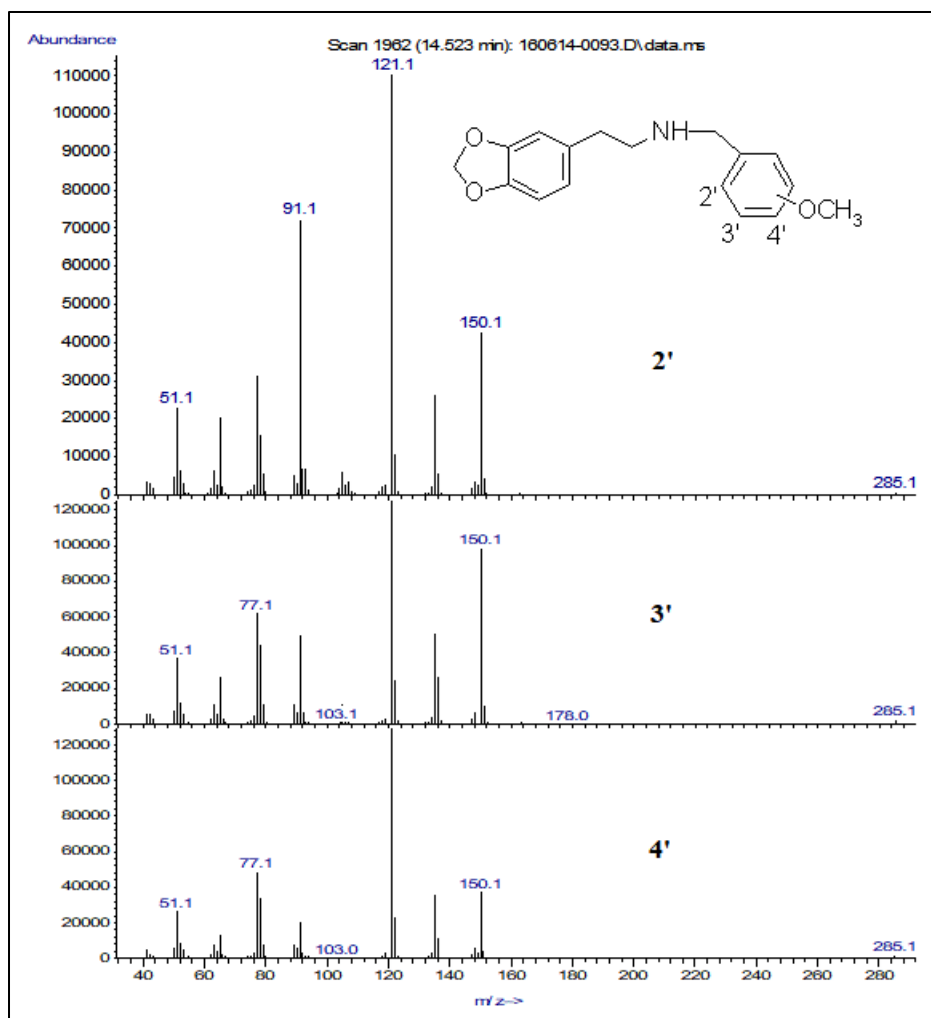
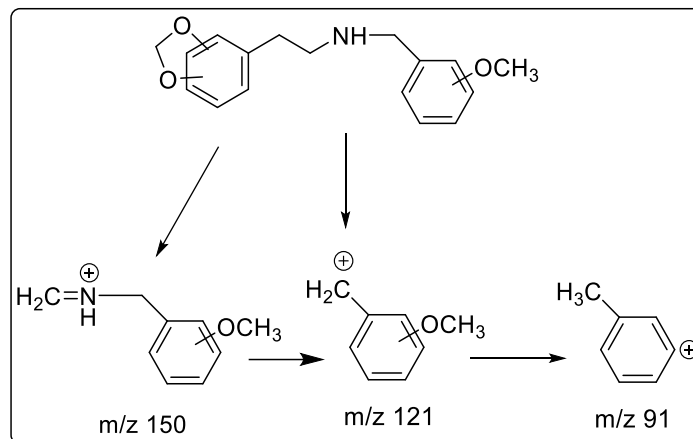


Figure 61 Mass Spectra of the N-(methoxy)benzyl-3,4-methylenedioxyphenethylamines.

Thus, it appears that the six methylenedioxy regioisomers undergo fragmentation under EI conditions similar to the N-(methoxy)benzyl-monomethoxyphenethylamine series reported in the previous chapter and the N-(methoxy)benzyl-dimethoxyphenethylamines described in this chapter as illustrated in Scheme 31. Again, the predominant ion at m/z 121 can be formed by the cleavage of the N-C bond yielding 2-methoxybenzyl cation and the ion at m/z 150 is likely the iminium cation formed by the dissociation of bond between α - and β -carbon atoms. Finally, the ion at m/z 91 appears to have formed from loss of CH_2O from the methoxy benzyl cation. The fragmentation pattern observed for these methylenedioxy derivatives also supports the fragmentation mechanisms proposed earlier in this chapter for the N-(methoxy)benzyl-dimethoxyphenethylamines and in the N-(methoxy)benzyl-monomethoxyphenethylamine series described in the previous chapter.



Scheme 31 Proposed EI-MS fragmentation pathway for the N-(methoxy)benzyl-monomethoxyphenethylamines.

In conclusion, all of the N-(methoxy)benzyl-methylenedioxyphenethylamines, as well as the N-(methoxy)benzyl-dimethoxyphenethylamines and N-(methoxy)-benzyl-monomethoxyphenethylamines appear to undergo the same fragmentation under EI-MS conditions and based on their common methoxybenzyl substitution pattern they cannot easily be differentiated from one another. Thus, other analytical methods including GC separations were explored for further differentiation within each regioisomeric subseries.

4.3 Gas Chromatographic Separations:

Gas chromatographic separations were performed in an attempt to further differentiate the eighteen dimethoxyphenethylamine regioisomers of this series. The compounds were divided into six subsets for initial separation studies, where the position of the dimethoxy group in the phenethyl ring was held constant while the methoxy group of benzyl ring was varied. Separations were accomplished on 30m x 0.25mm ID capillary column coated with 0.25 μm film of of midpolarity Crossbond[®] silarylene phase containing a 50% phenyl and 50% dimethyl polysiloxane polymer (Rxi[®]-17Sil MS). Separations were achieved over 22 minutes starting from initial temperature of 70 $^{\circ}\text{C}$ held for 1 minute then gradually increased to reach terminal temperature at 250 $^{\circ}\text{C}$ at a rate of 30 $^{\circ}\text{C}/\text{minute}$ and held for 15 minutes with elution over a 2 minute window. This set of chromatographic conditions yielded an excellent separation of each subset of three compounds

with the 2'-methoxy isomer eluting before the 3'-isomer, and the 3'-isomer before the 4'-isomer in each case. (Figure 62).

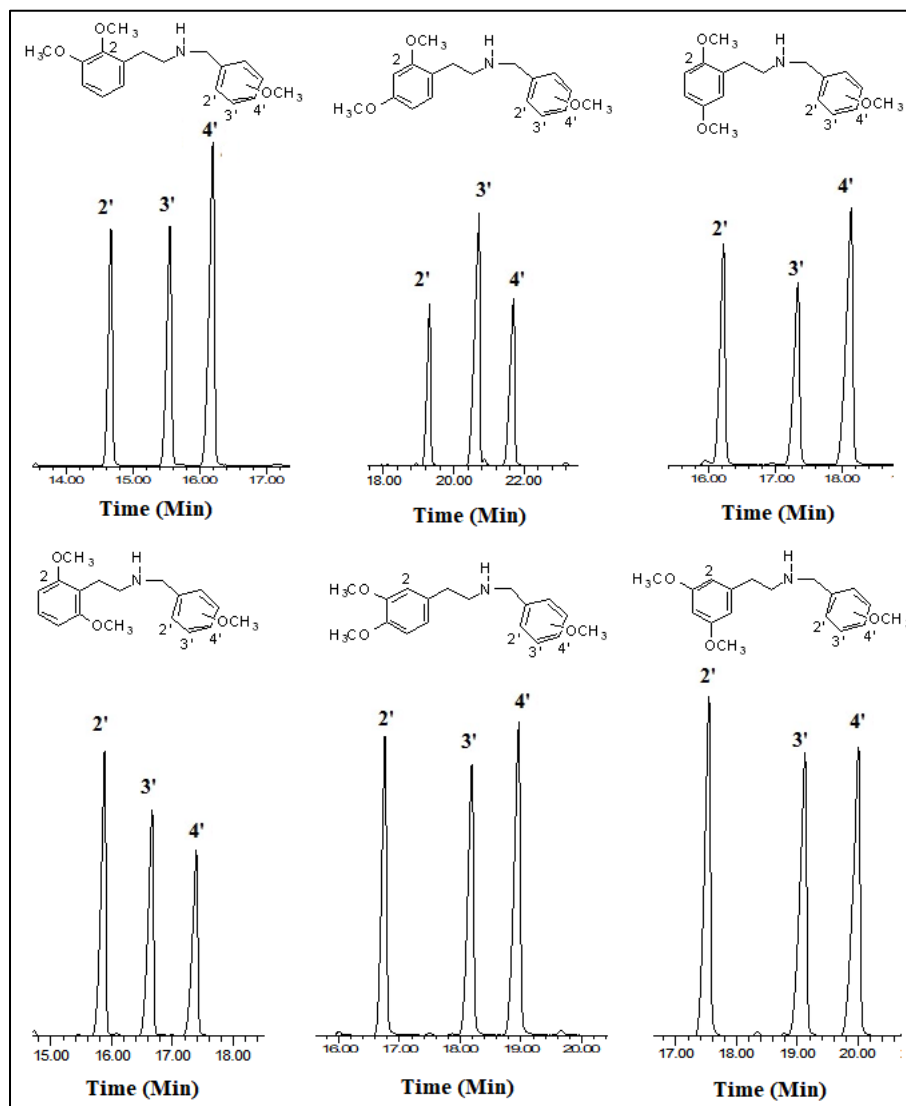


Figure 62 Gas chromatographic separation of the N-(monomethoxy)benzyl-dimethoxyphenethylamines.

Similar separations were achieved for all six of the methylenedioxyphenethylamine regioisomers. The compounds were divided into two subsets, based on the position of the methylenedioxy group in the phenethyl ring was held constant while the methoxy group of benzyl ring was varied for initial separation studies. The same capillary column was used with the same temperature program conditions and similar elution order of the compounds with the 2'-methoxy isomer eluting before the 3'-isomer, and the 3'-isomer before the 4'-isomer in each case. The compounds again eluted

over a 2 minute window as shown in Figure 63-64. This is the same elution pattern that was observed in the N-(monomethoxy)benzyl-monomethoxyphenethylamines series.

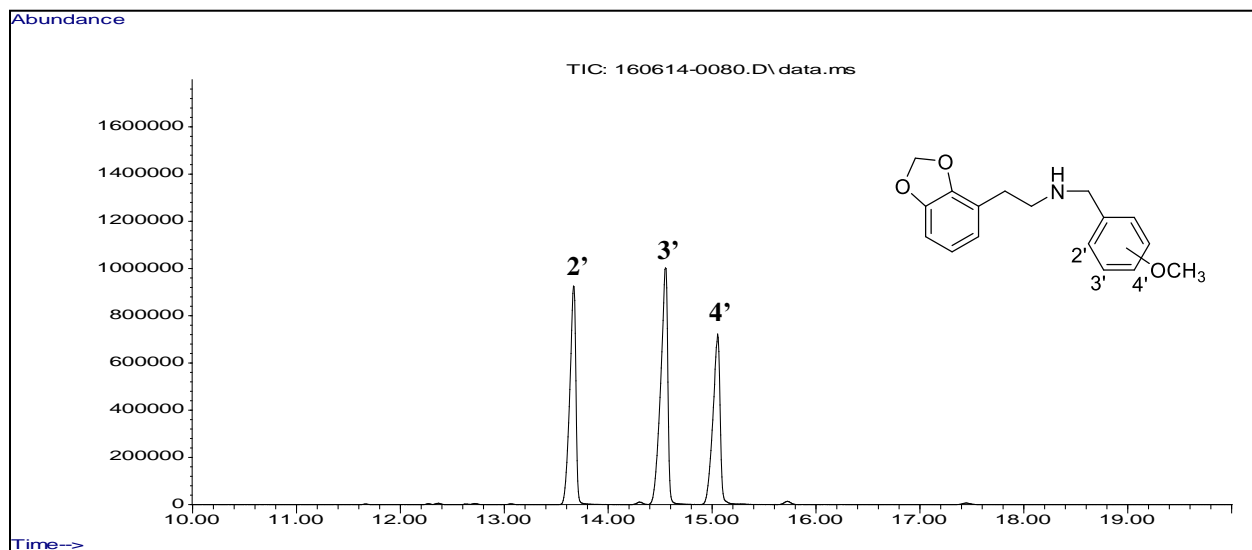


Figure 63 Gas chromatographic separation of the N-(monomethoxy)benzyl-2,3-methylenedioxyphenethylamines.

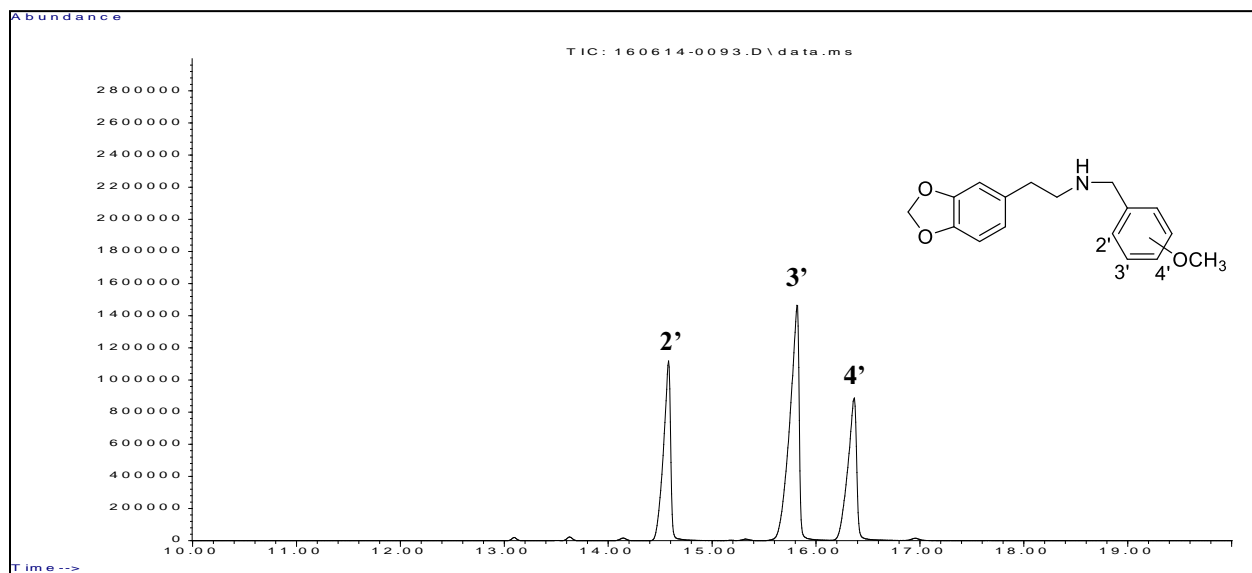


Figure 64 Gas chromatographic separation of the N-(monomethoxy)benzyl-3,4-methylenedioxyphenethylamines.

5 Analysis of the N-(dimethoxy)benzyl- and N-(methylenedioxy)benzyl-2,5-dimethoxyphenethylamine Series

5.1 Introduction:

The compounds of this series (structures 1-8) are simplified derivatives of NBOMes with the 2,5-dimethoxy substituents on the phenethyl aromatic ring but no halogen atoms, and either a dimethoxy or methylenedioxy substitution pattern on the benzylic ring of the core NBOME structure. This series can be divided into two subsets, with the six possible dimethoxybenzyl regioisomers (2',3'-, 2',4'-, 2',5'-, 2',6'-, 3',4'- and 3',5'-dimethoxy, structures 1-6) representing one subset and the 2,3-methylenedioxy and 3,4-methylenedioxy regioisomers representing the second subset (structures 7 and 8, Figure 65). All of these compounds were synthesized as described in the previous chapter.

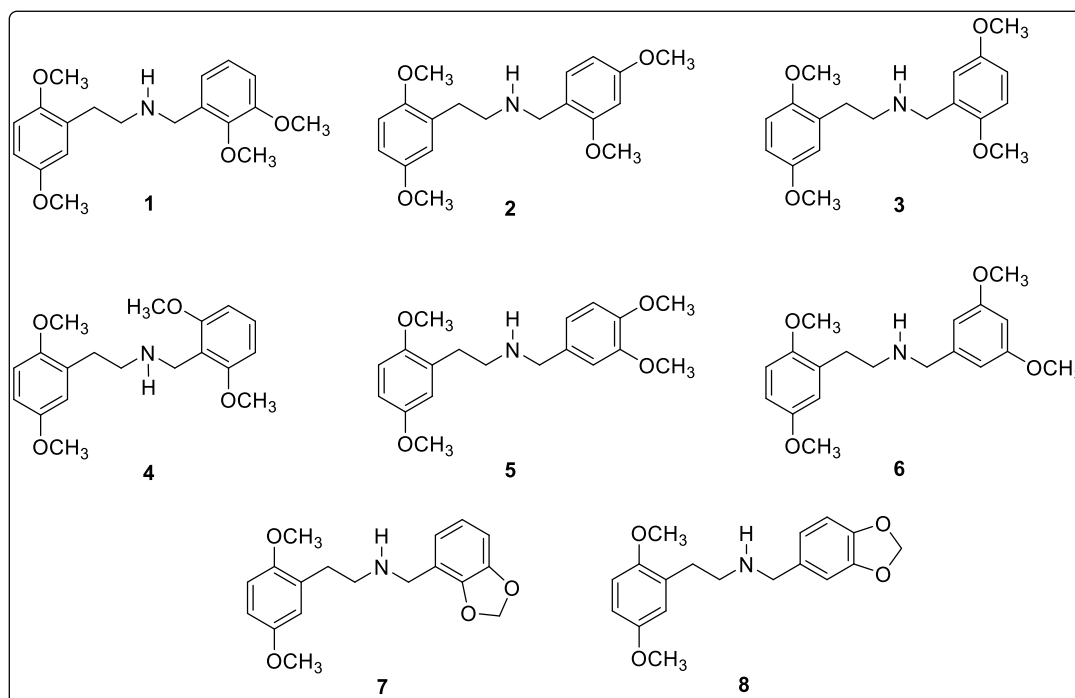


Figure 65 Structures of the N-(methoxy)benzyl-2,5-dimethoxyphenethylamine Series.

5.2 Mass Spectral Analysis of the N-(dimethoxy)benzyl-2,5-dimethoxyphenethylamine Series:

The EI-MS of all members of this series of compounds are shown in Figures 67. All six regioisomeric members of the dimethoxybenzyl subset of derivatives (compounds 1-6) yielded nearly identical mass spectra as shown in Figure 67. The molecular ion (M^+) also is not apparent in the EI-MS spectrum (MW 331), however the mass was confirmed by CI-MS (Figure 66) where a $M+1$ ion of 332. The dominant ions in GC-MS spectrum of the six dimethoxybenzyl regioisomeric subset are observed at $m/z = 151$, 180 and 121, with the base peak m/z 151 (Figure 67).

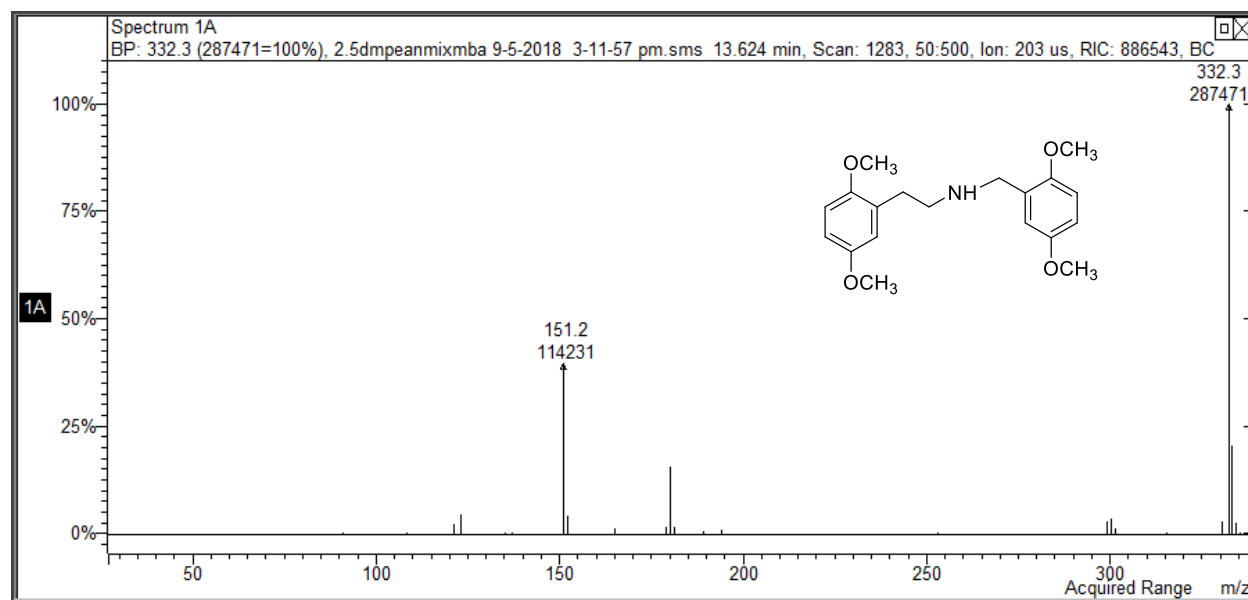


Figure 66 CI-MS of Mass Spectra of the N-2',5'-dimethoxybenzyl-2,5-dimethoxyphenethylamine.

A proposed fragmentation pathway showing the dominant ions for the monomethoxy subseries of compounds is shown in Scheme 32. The base peak m/z 151 can be formed by the cleavage of the N-C bond yielding dimethoxybenzyl cation. The ion at m/z 180 is likely the iminium cation formed by the dissociation of bond between α - and β -carbon atoms, a common pathway for phenethylamine compounds. Finally, the ion at m/z 121 appears to have formed from loss of CH_2O from the dimethoxy benzyl cation. These major fragments correspond to those observed in the previous section with NBOMes derivatives containing only a single methoxy group in the N-benzyl ring except now the masses are increased by 30 due to the presence of a second methoxy group.

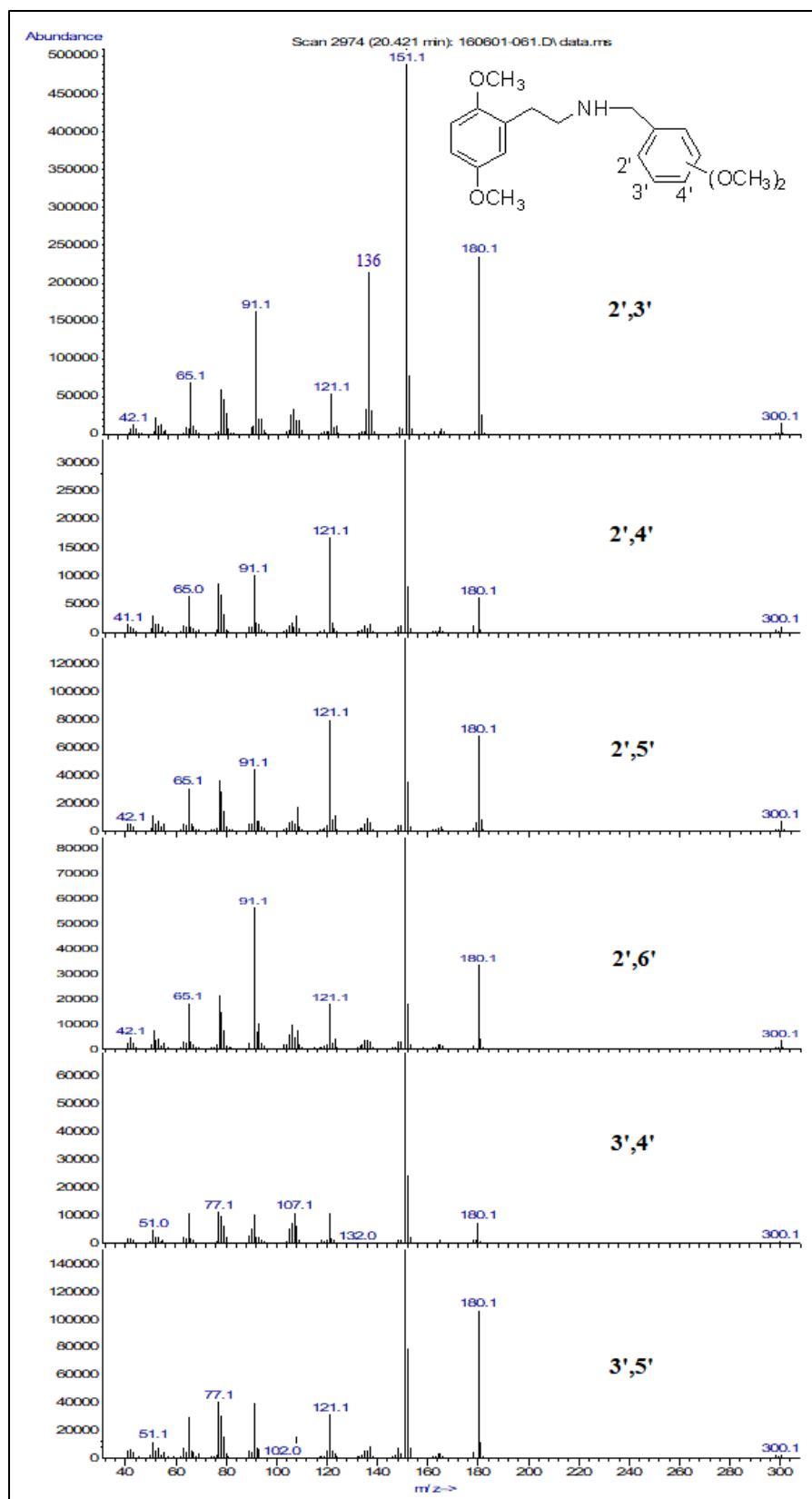
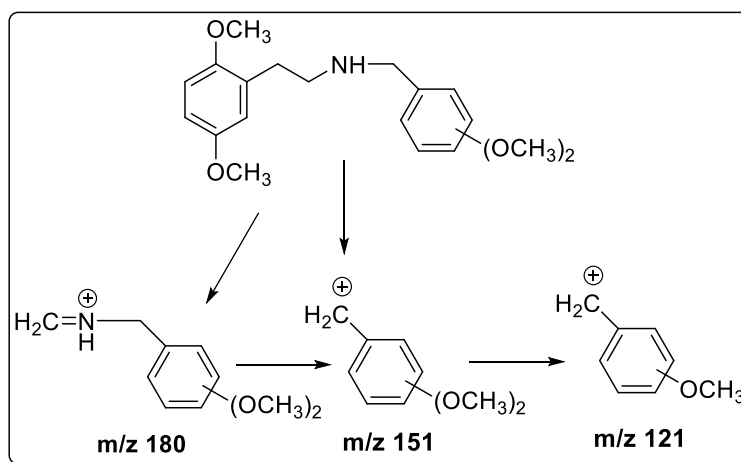


Figure 67 Mass Spectra of the N-(dimethoxy)benzyl-2,5-dimethoxyphenethylamines.



Scheme 32 Proposed EI-MS fragmentation pathway for the N-(dimethoxy)benzyl-2,5-dimethoxyphenethylamines.

The EI-MS obtained for the N-(methoxy)benzyl-methoxyphenethylamines and derivatives (Chapter 3), N-(dimethoxy)benzyl-methoxyphenethylamines (Chapter 4) and the N-(dimethoxy)benzyl-dimethoxyphenethylamines in this chapter show a consistent fragmentation pattern. For all derivatives of this general structural class the base peak in the EI-MS is derived from cleavage of the N-C bond yielding benzyl cation. The mass of this benzyl cation is determined by the nature and degree of substitution on the N-benzyl substituent as illustrated in Table 15 below. Ions of secondary abundance in the EI-MS of these compounds include the imine formed by the dissociation of bond between α - and β -carbon atoms, and a secondary benzyl cation which is derived from loss of CH_2O from those derivatives which contain at least methoxy group in the base peak benzyl cation. The varying nature and degree of benzyl ring substitution determines the masses of the base peak, the imine cation and secondary benzyl cation fragment ions in these derivatives and allows for general differentiation of structural types. However, these data do not allow for differentiation among regioisomers within a structural series such as all of the six N-(dimethoxy)benzyl-2,5-dimethoxyphenethylamines described in this chapter.

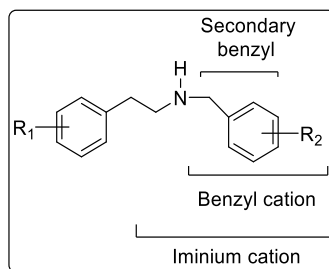


Table 15 Common Fragmentation Pathways for the methoxy/dimethoxy substituted NBOMe derivatives.

R ₁	R ₂	Base Peak Benzyl	Imine	Secondary Benzyl cation (loss of CH ₂ O from Benzyl Base Peak)
H	H	91	120	-----
CH ₃ O	H	91	120	-----
H	CH ₃ O	121	150	91
CH ₃ O	CH ₃ O	121	150	91
(CH ₃ O) ₂	CH ₃ O	121	150	91
(CH ₃ O) ₂	(CH ₃ O) ₂	151	180	121

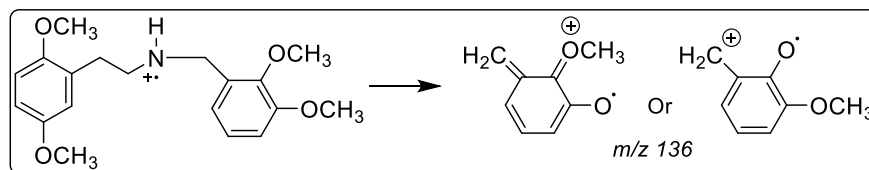
The discussion above highlights the similarities in the EI-MS of the N-(methoxy)benzyl-methoxyphenethylamines (Chapter 3), N-(dimethoxy)benzyl-methoxyphenethylamines (Chapter 4) and the N-(dimethoxy)benzyl-2,5-dimethoxyphenethylamines of this chapter. Analysis of the spectra of the individual regioisomers in the N-(dimethoxy)benzyl-2,5-dimethoxyphenethylamines series (Figure 67) revealed the presence unique ion at m/z 136 for the 2',3'-dimethoxy regioisomer. This ion differentiates this particular regioisomer from other members of the N-(dimethoxy)benzyl-2,5-dimethoxyphenethylamine series as well as derivatives of the previous series which contained only a single methoxy group in the N-benzyl substituent.

Mass	Calc. Mass	mDa	PPM	DBE	i-FIT	Formula
136.0513	136.0524	-1.1	-8.1	5.0	18.2	C8 H8 O2

Figure 68 Exact mass determination for the m/z 136 ion using high resolution mass spectrometry (HRMS).

Exact mass analysis using GC-TOF-MS confirmed the m/z 136 ion has an elemental composition of $C_8H_8O_2$ (degree of agreement between calculated and experimental results of -1.1mDa, 8.1 ppm) Figure 68. MS-MS studies showed that this fragment ion formed from the molecular ion, presumably as a result of bond cleavage between the nitrogen and benzylic carbon atom after loss of a methyl group radical as shown in Scheme 33. The fact that this fragment ion is only present in the EI-MS of the 2',3'-dimethoxy regioisomer strongly indicates that it formed from the N-2'3'-dimethoxybenzyl substituent rather than from the 2,5-dimethoxy ring of the phenethyl group. If the m/z 136 fragment formed from the 2,5-dimethoxyphenethyl portion on the molecule, then the mass spectra of all six regioisomers of this series, as well as dimethoxy phenethyl derivatives in the previous series (Chapter 4) would be expected to contain this ion. Since this compound contains two methoxy groups, it is possible that either the 2'- or 3'-methoxy methyl groups migrates in this fragmentation process.

To confirm the fragmentation pathway proposed in Scheme 33 and in attempt to identify which of the two methyl groups is lost in this pathway, derivatives of N-(2',3'-dimethoxy)benzyl-2,5-dimethoxyphenethylamine were prepared and analyzed where either the benzylic 2'- methoxy group ($2'\text{-}^{13}\text{CH}_3\text{O}$) or the 3'-methoxy ($3'\text{-}^{13}\text{CH}_3\text{O}$) group carbon atom was labeled with ^{13}C isotope.



Scheme 33 Proposed Mechanism for the formation of the m/z 136 ion.

Thus, each of these labeled derivatives had one mass unit added to the parent N-(2',3'-dimethoxy)benzyl-2,5-dimethoxyphenethylamine structure. The EI-MS of these two ^{13}C -labelled derivatives are shown in Figures 69 A-B. The base peak in these spectra, formed by the cleavage of the N-C bond to yield the dimethoxybenzyl cation, occurs at m/z 152, one mass unit higher than the corresponding ion in the unlabeled compound as shown above. Also, the fragment ion of

secondary abundance, the iminium cation formed by the dissociation of bond between α - and β -carbon atoms, now appears at m/z 182, one mass higher than the corresponding ion in the unlabeled compound.

Finally, each of the spectra for the ^{13}C -labeled derivatives contain a m/z 137 ion corresponding to the unique m/z 136 ion in the unlabeled compound. Taken together, these data provide support for the original fragmentation proposed in Scheme 32 and in earlier chapters.

The mass spectra for the ^{13}C labeled derivatives also provides some insight into the fragmentation pathway which results in formation of the m/z 136 ion present only in the N-(2',3'-dimethoxy)benzyl isomer of this series. If only the 2'-methoxy methyl group migrates in the formation of the m/z 136 ion, then the EI-MS of the labeled 2'- $^{13}\text{CH}_3\text{O}$ derivative would be expected to have a m/z 136 ion, while the spectrum of the 3'-methoxy (3'- $^{13}\text{CH}_3\text{O}$) derivative would have a m/z 137 ion. Conversely, if only the 3'-methoxy group methyl migrates in the formation of the m/z 136 ion, then the EI-MS of the labeled 2'- $^{13}\text{CH}_3\text{O}$ derivative would be expected to have a m/z 137 ion, while the spectrum of the 3'-methoxy (3'- $^{13}\text{CH}_3\text{O}$) derivative would have a m/z 136 ion. The mass spectra of each of these labeled derivatives show both m/z 136 and 137 ions, suggesting that either the 2'- or 3'-methoxy methyl group can migrate to form this unique ion. However, the relative abundance of these two ions suggests a preference for 3'-methoxy group migration since m/z 137 ion formation is greater than m/z 136 ion in the (2'- $^{13}\text{CH}_3\text{O}$) derivative, and m/z 136 ion formation is greater than m/z 137 ion in the 3'-methoxy (3'- $^{13}\text{CH}_3\text{O}$) derivative. The preference for 3'-methoxy group migration probably results from the greater electronic stability of this product ion.

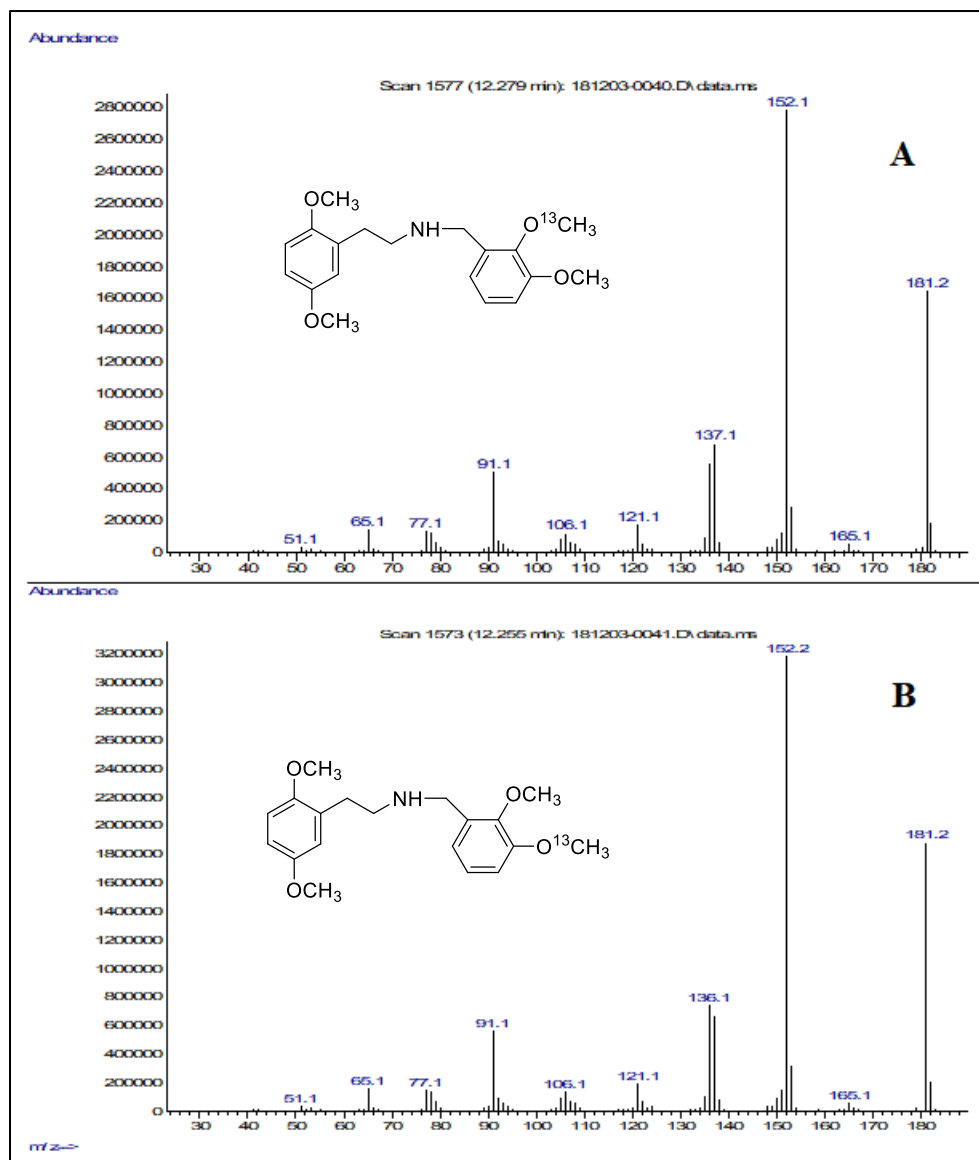


Figure 69 Mass Spectra of ^{13}C labeled N-(2',3'-dimethoxy)benzyl-2,5-dimethoxyphenethylamines.

5.3 Mass Spectral Analysis of the N-(methylenedioxy)benzyl-2,5-dimethoxyphenethylamine Series:

The EI-MS for the two methylenedioxy regioisomers in this series are shown in Figure 70. Once again both regioisomeric members of this subset of compounds derivatives (compounds 7-8) yielded nearly identical mass spectra. No molecular ion (M) was observed, however the molecular weight was confirmed by M+1 ion at 316 as shown in Figure 71. The dominant ions in this series were observed at $m/z = 135, 164$ and 105 , as observed in the dimethoxy subseries.

The three most abundant ions in the methylenedioxy series ($m/z 135, 164$ and 105), each represent fragments 16 mass units lower than the most abundant ions in the mass spectra of the dimethoxy subset ($m/z 151, 180$ and 121). The mass difference between each of these ions relative to the dimethoxy compounds is precisely the difference in mass corresponding to the molecular weight differences in these three series (a reduction in 16 mass units corresponds to the loss of a carbon and two hydrogen atoms relative to the dimethoxy compounds).

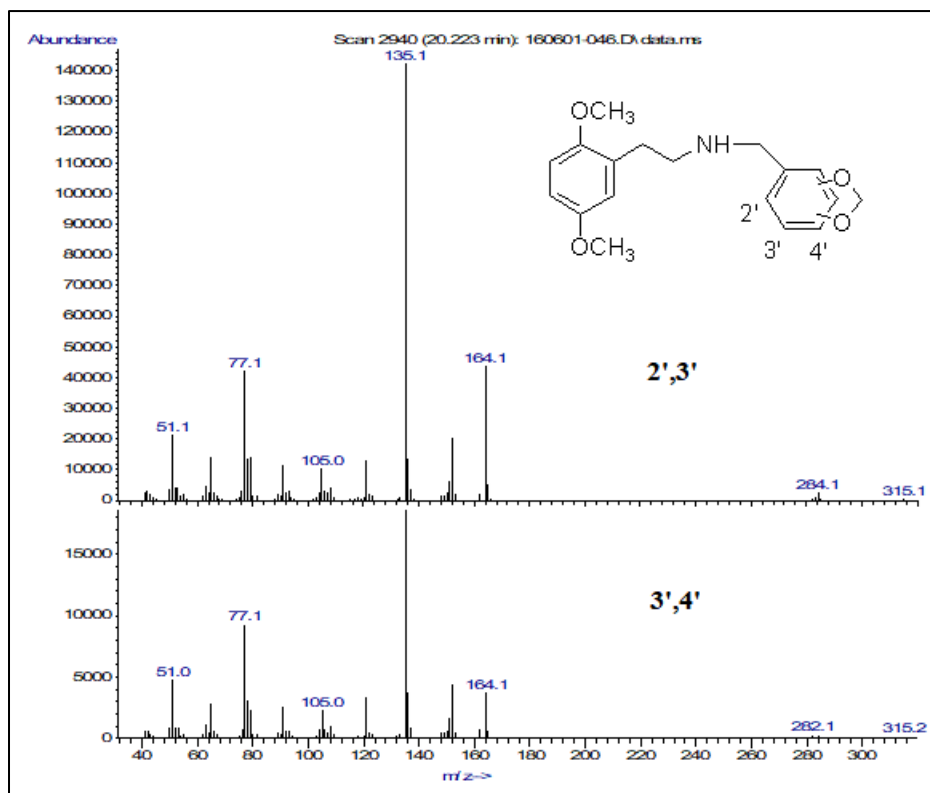


Figure 70 Mass Spectra of the N-(methylenedioxy)benzyl-2,5-dimethoxyphenethylamines.

Thus, it appears that the methylenedioxy regioisomers undergo fragmentation under EI conditions similar to the dimethoxy compounds as illustrated in Scheme 34. Again, the predominant ion at m/z 135 can be formed by the cleavage of the N-C bond yielding 2',3'-methylenedioxybenzyl cation and the ion at m/z 164 is likely the iminium cation formed by the dissociation of bond between α - and β -carbon atoms. Finally, the ion at m/z 105 appears to have formed from loss of CH_2O from the methylenedioxy benzyl cation.

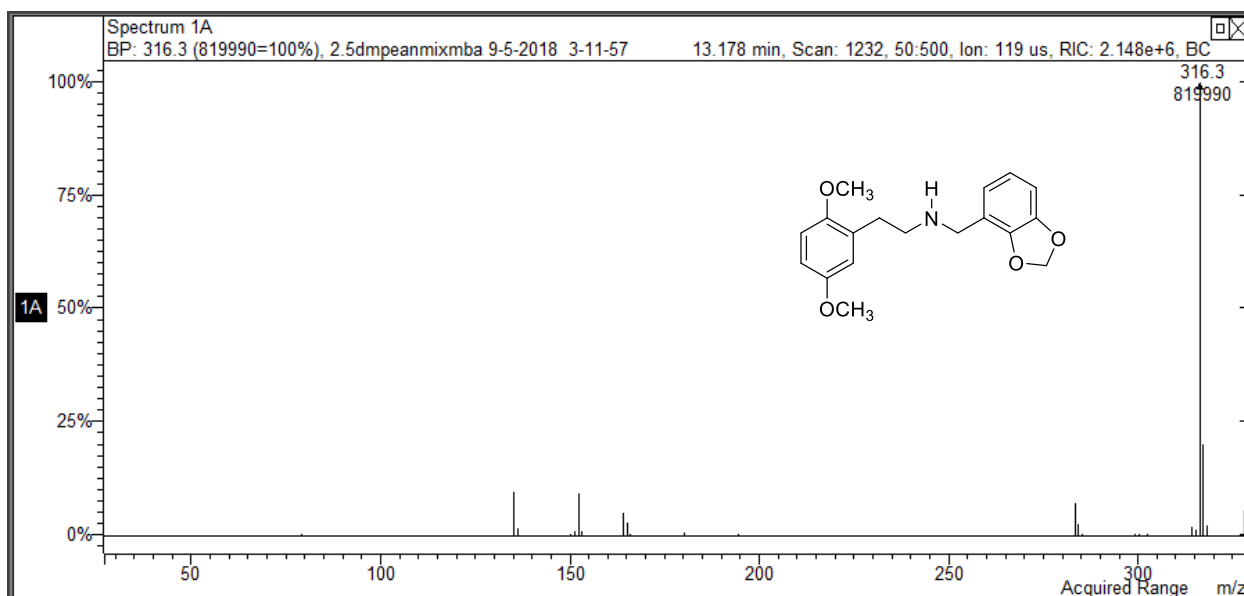
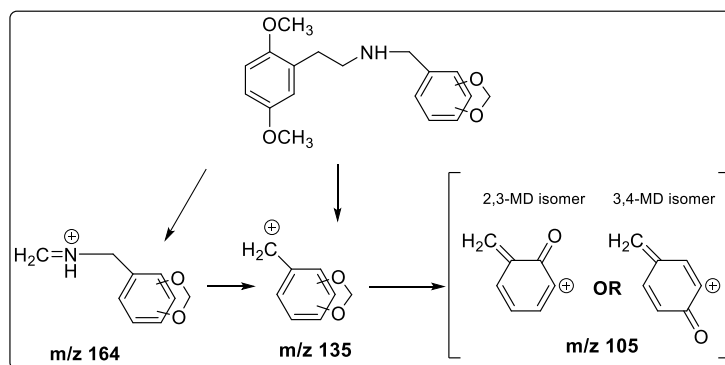


Figure 71 CI-MS of Mass Spectra of N-2',3'-methylenedioxybenzyl-2,5-dimethoxyphenethylamine.



Scheme 34 Proposed EI-MS fragmentation pathway for the N-(methylenedioxy)benzyl-2,5-dimethoxyphenethylamines.

5.4 Gas Chromatographic Separations:

Gas chromatographic separations were performed in an attempt to further differentiate the eight regioisomers of this series. The compounds were divided into two subsets for initial separation studies, where the position of the 2,5-dimethoxy group in the phenethyl ring was held constant while the methoxy group of benzyl ring was varied. In an attempt to differentiate the compounds in each of the six N-(dimethoxy)benzyl-2,5-dimethoxyphenethylamine subsets, gas chromatographic separations of dimethoxybenzyl regioisomers subset were performed on Rxi®-17Sil MS 30m x 0.25mm ID capillary column coated with 0.25 µm film of midpolarity Crossbond® silarylene phase containing a 50% phenyl and 50% dimethyl polysiloxane polymer.

Our initial attempt to separate them failed to separate all the six regioisomers since the chromatogram showed five peaks for the six regioisomers where two regioisomers co-eluted at the same retention time (2',4' and 3',4'-dimethoxybenzyl regioisomers). We identified the exact regioisomers based on previous injections for each isomer separately to record their unique retention time then a sample contains all the six regioisomers were prepared to separate them. Our best separation were achieved over 30 minutes starting form initial temperature of 70 °C held for 1 minute then gradually increased to reach 245 °C at a rate of 70 °C/minute and held for 5.5 minutes then ramped up again to reach 300 °C at a rate of 5 °C/minute which held again for 10 minutes with elution over a 3 minute window (figure 72).

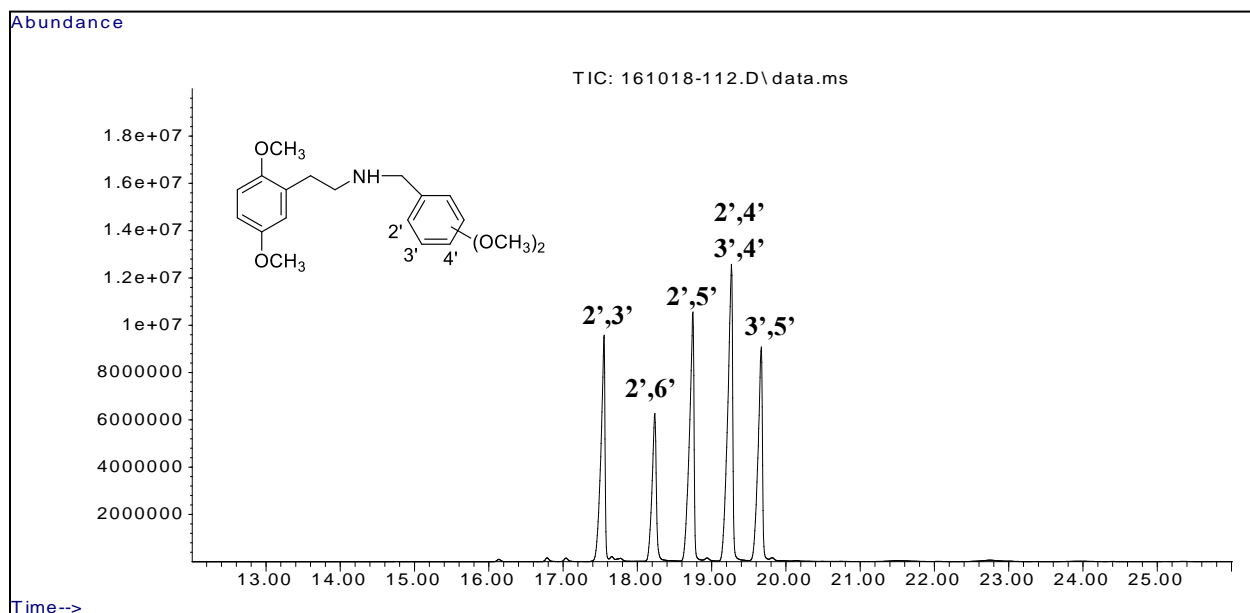
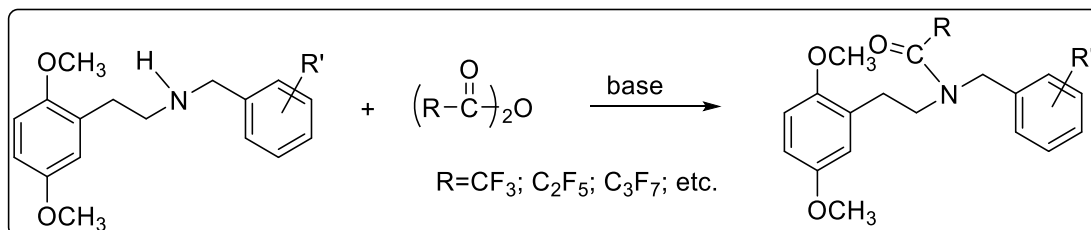


Figure 72 Gas chromatographic separation of the N-(dimethoxy)benzyl-2,5-dimethoxyphenethylamine regioisomers.

To improve the separation of the six regioisomers, a derivatization technique was applied. This technique is used in our lab to separate chromatographic challenging samples by micro-reacting the sample with perfluoro acid anhydride to make the perfluoroacetamide regioisomeric sample to separate them again (Scheme 35).



Scheme 35 Derivatization technique.

This set of chromatographic conditions yielded an excellent separation of all six regioisomers, using the same chromatographic condition as above with the 2',3'-elute first followed by 2',5'- then 3',5'- and the 3',4'- before the 2',6'- then finally the 2',4'-dimethoxy regioisomer (Figure 73).

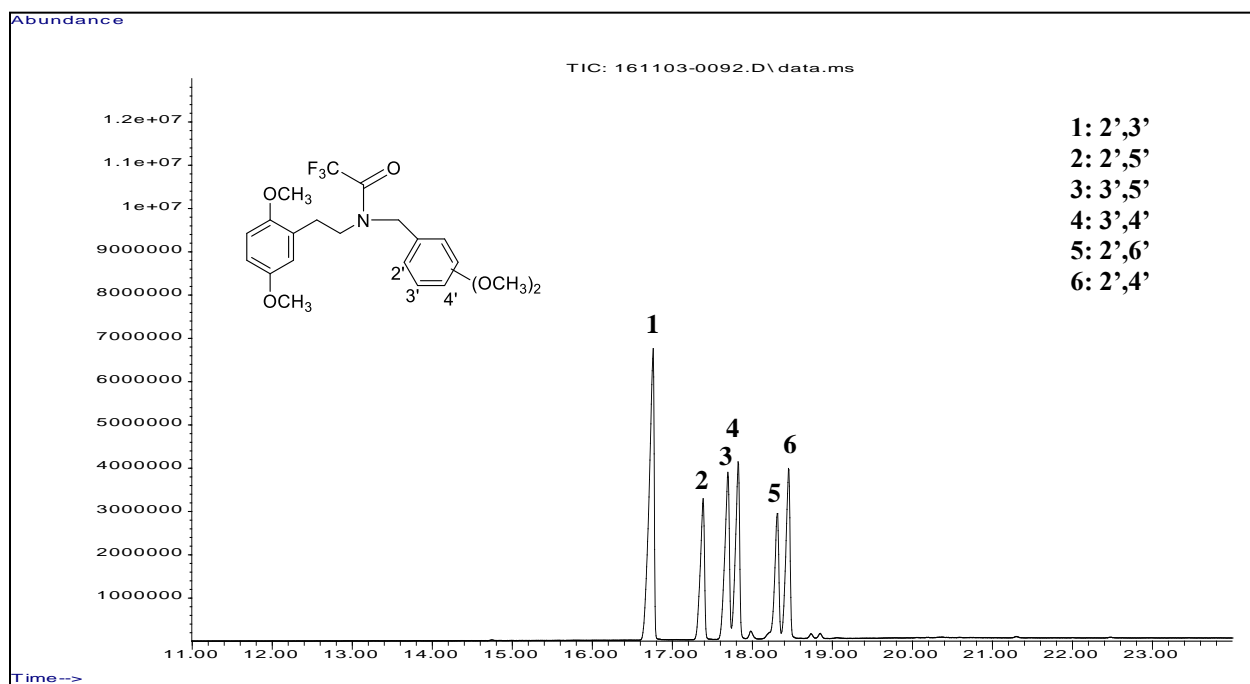


Figure 73 Gas chromatographic separation of the derivatized N-trifluoroacetamide-(dimethoxy)benzyl-2,5-dimethoxyphenethylamines.

Lastly, the last chromatogram (Figure 74) shows the separation of the two methylenedioxy regioisomers. The temperature program started with initial temperature of 70 °C held for 1 minute then gradually increased to reach a final temperature of 250 °C at a rate of 30 °C/minute with a total 32 minutes run time. In this series 2',3'-methylenedioxy eluted before 3',4'-methylenedioxy regioisomer the two regioisomers under similar separation condition as above. This is the same relative elution pattern that was observed in the dimethoxy bromo NBOME series.

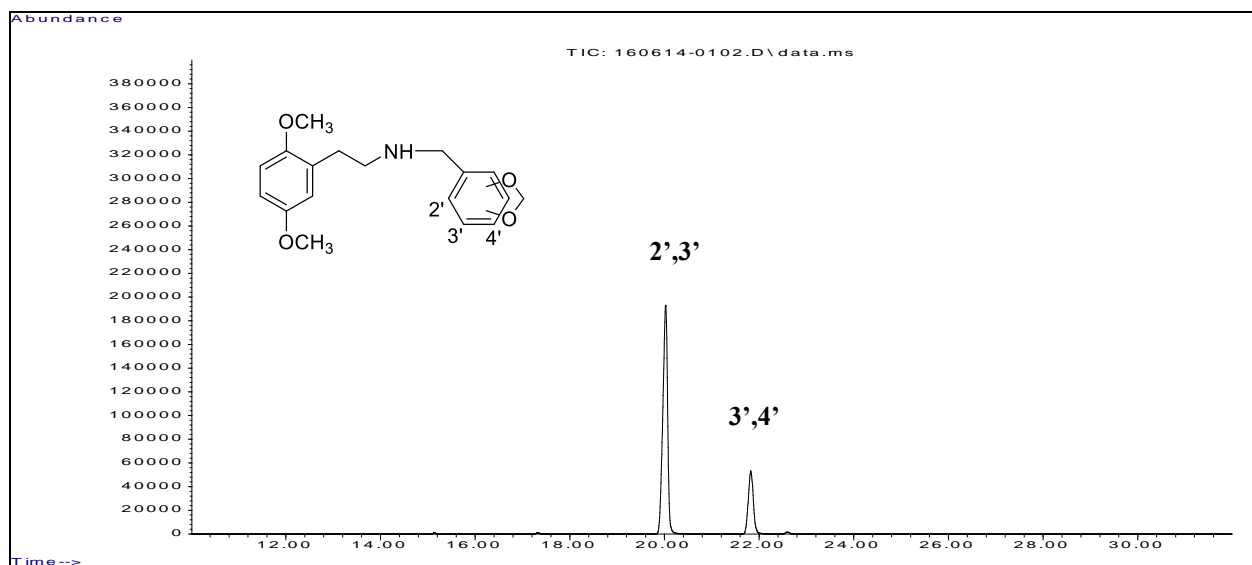


Figure 74 Gas chromatographic separation of the N-(methylenedioxy)benzyl-2,5-dimethoxyphenethylamines.

6 The N-(Substituted)benzyl-4-bromo-2,5-dimethoxyphenethylamine Series

6.1 Introduction:

The compounds of this series are derivatives of N-(2'-methoxy)benzyl-4-bromo-2,5-dimethoxyphenethylamine (25B-NBOMe) where the substitution pattern on the aromatic ring of the N-benzyl substituent is modified yielding the 11 compounds in Figure 75. This series can be divided into three subsets. The first subset includes 25B-NBOMe and its 3- and 4-monomethoxy regioisomers (structures 1-3). In the second subset the N-benzyl aromatic ring is modified to include two methoxy groups at every possible position. Thus, this subset includes six regioisomeric compounds, the 2,3-, 2,4-, 2,5-, 2,6-, 3,4- and 3,5-dimethoxy regioisomers (structures 4-9). In the third subset in this series the N-benzyl aromatic ring is modified to contain the two possible methylenedioxy substitution patterns (structures 10-11). The N-benzyl substitution patterns selected for this series represent potential designer modifications since this functionality is commonly found in drugs of abuse. All of these compounds were synthesized as described in the previous chapter.

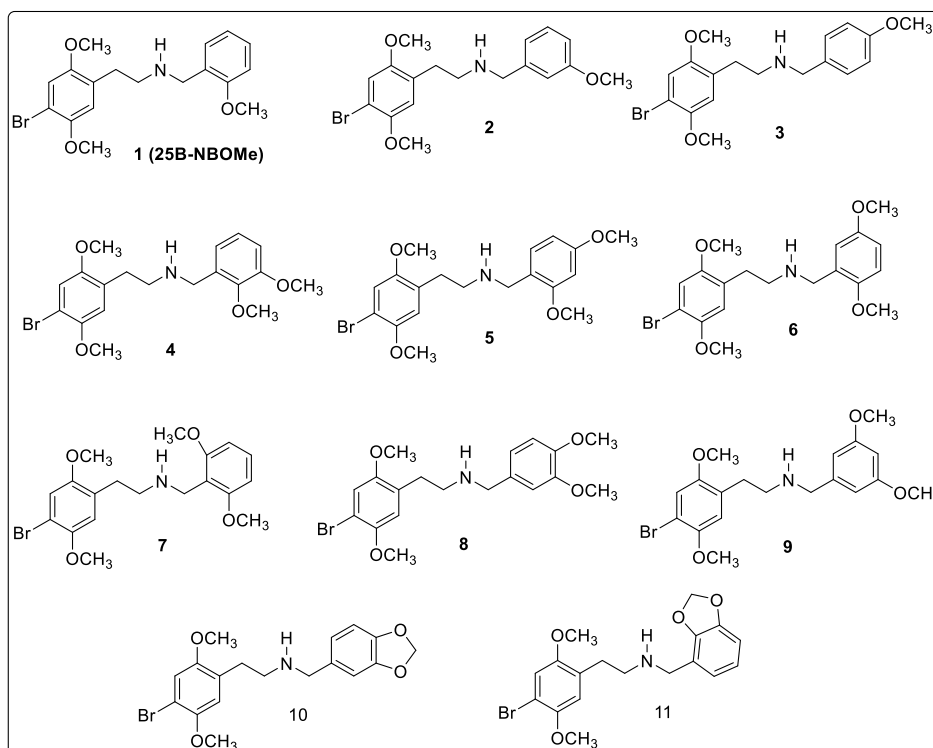


Figure 75 Structures of the N-(substituted)benzyl-4-bromo-2,5-dimethoxyphenethylamine Series.

6.2 Mass Spectral Analysis:

The EI-MS of all members of this series of compounds are shown in Figures 76-79 (2-5). All three regioisomeric members of the monomethoxybenzyl subset of derivatives (compounds 1-3) yielded nearly identical mass spectra as shown in Figure 76. As reported for other 25-NBOMe compounds, the dominant ions in GC-MS spectrum of the 2-, 3- and 4'-monomethoxy derivatives in this series are observed at $m/z = 121$, 150 and 91, with the base peak m/z 121 (Figure 76). The m/z 91 ion was present in the highest abundance in the 2'-methoxy isomer and decreased in the 3'- and 4'-methoxy isomers. It is interesting to note that none of the dominant ions in these spectra appeared to contain bromine.

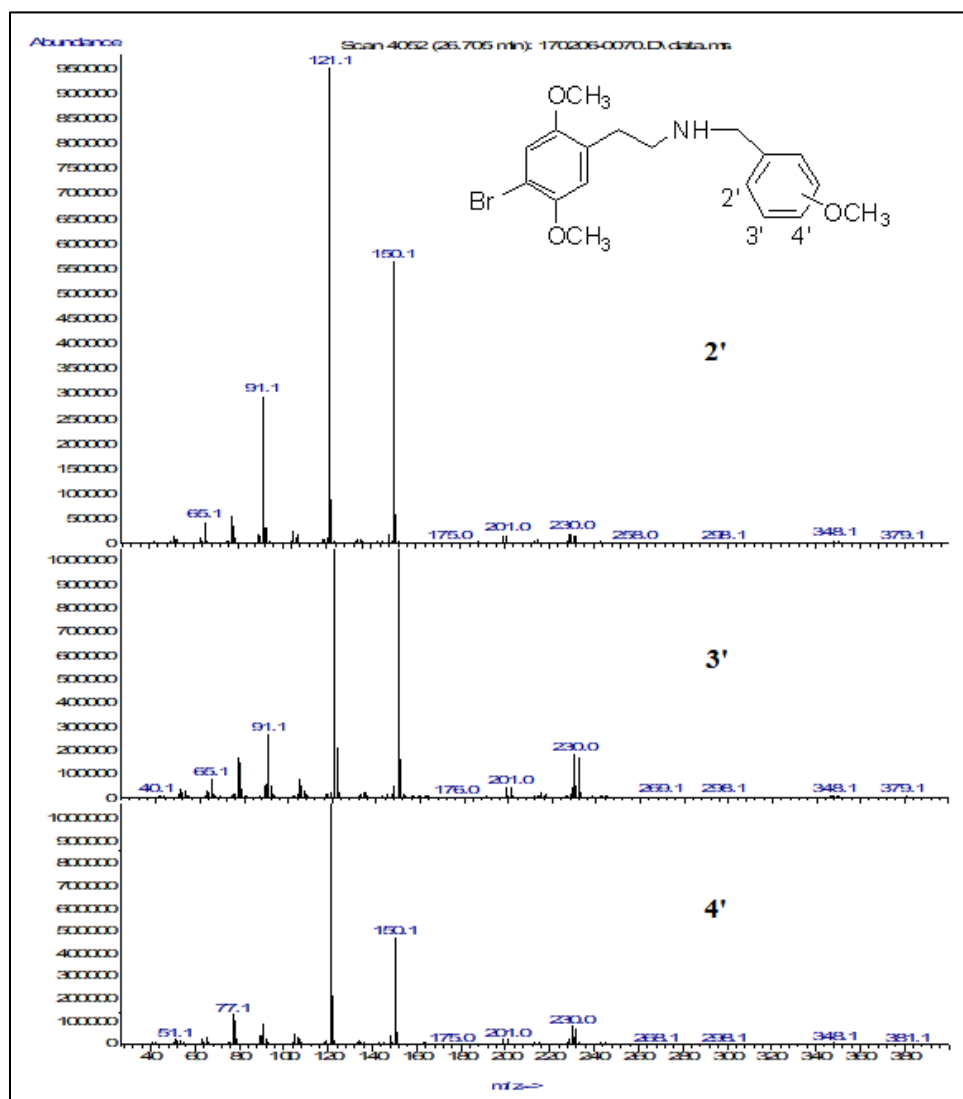


Figure 76 Mass Spectra of the N-(monomethoxy)benzyl-4-bromo-2,5-dimethoxyphenethylamines.

The molecular ion (M) also is not apparent in the EI-MS spectrum, however the mass was confirmed by CI-MS (Figure 77) where a M+1 ions of 380/382 (bromine isotope).

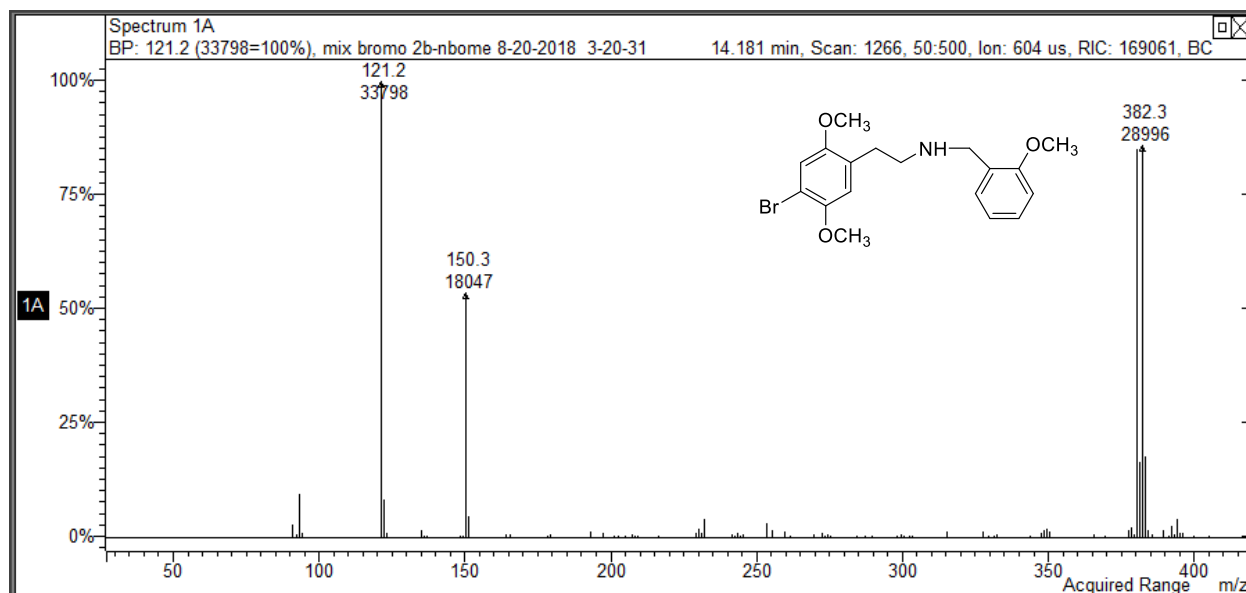
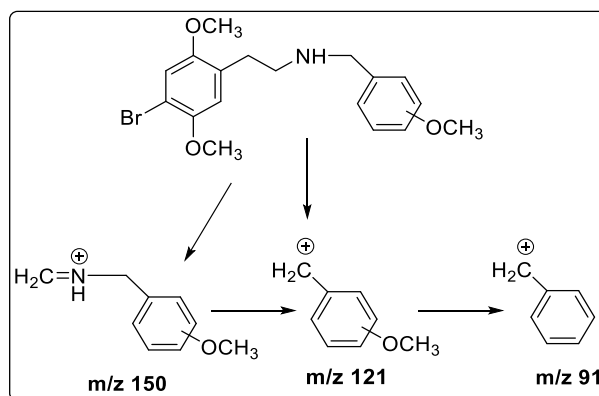


Figure 77 CI-MS of Mass Spectra of the N-2'-methoxybenzyl-4-bromo-2,5-dimethoxyphenethylamines.

A proposed fragmentation pathway showing the dominant ions for the monomethoxy subseries of compounds is shown in Scheme 36. The base peak m/z 121 can be formed by the cleavage of the N-C bond yielding 2-methoxybenzyl cation. The ion at m/z 150 is likely the iminium cation formed by the dissociation of the bond between the α - and β -carbon atoms, a common pathway for phenethylamine compounds. Finally, the ion at m/z 91 appears to have formed from loss of CH_2O from the methoxy benzyl cation.



Scheme 36 Proposed EI-MS fragmentation pathway for the N-(monomethoxy)benzyl-4-bromo-2,5-dimethoxyphenethylamines.

Support for this fragmentation pathway was provided by MS-MS studies which demonstrate that the m/z 91 ion is formed from the m/z 121 fragment as shown in Figure 78.

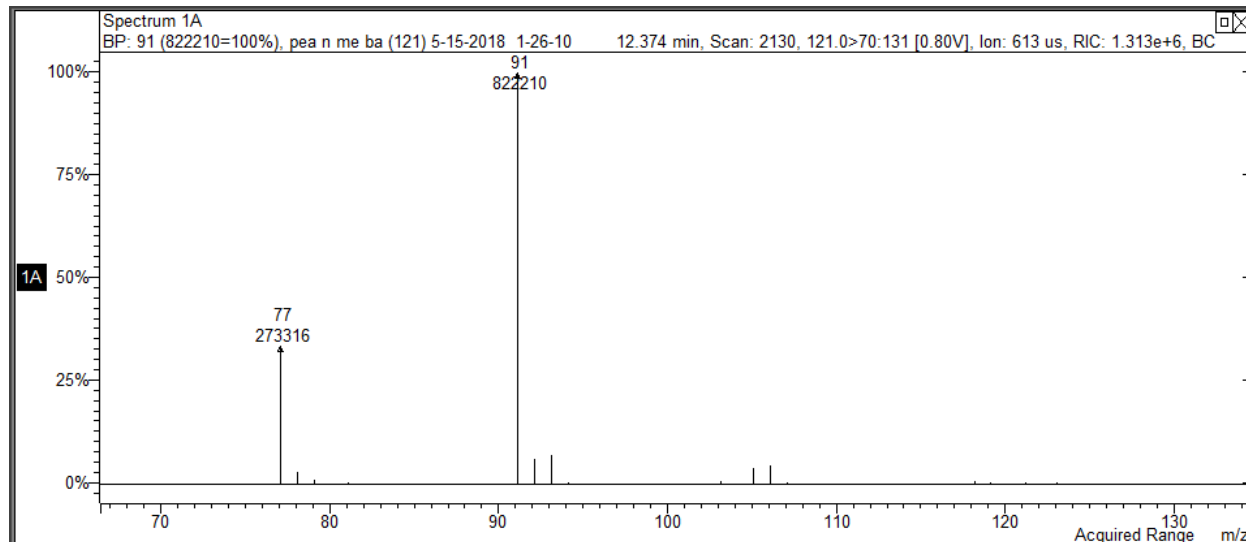


Figure 78 MS-MS of the 121 ion.

Additional support for this proposed fragmentation pathway of the monomethoxy regioisomers was derived from studies with isomers where the substitution pattern on the two aromatic rings of the monomethoxy NBOMe derivatives were reversed – the so-called “eMOBNs”. These compounds were prepared in a single step by a reductive alkylation procedure with commercially available methoxyphenethylamines and 4-bromo-2,5-dimethoxybenzaldehyde. A representative mass spectrum for the 2-methoxy eMOBN derivative is shown in Figure 79 below compared to the original 2-methoxy NBOMe compound. The dominant ions in the eMOBN derivative now occur at m/z 229/231 and 258/260. These ions clearly contain bromine as indicated by the isotopic multiplicity, and form by the same fragmentation noted in the scheme above for the parent 2-methoxy NBOMe compound. This fragmentation pathway is shown in Scheme 37.

A closer analysis of the m/z 200-400 range of the mass spectra of the monomethoxy series does reveal the presence of several ion fragments of very low abundance that do appear to contain bromine based on mass and isotopic abundances (Figure 80). There are two natural isotopes of bromine with nearly equal relative abundance, ^{79}Br (50.69% natural abundance) and ^{81}Br (49.31%

natural abundance). Thus, fragments containing these masses would appear at two m/z values with very similar abundance. The EI MS below shows such fragment ion pairs at m/z 243/245, 230/232 and 199/201. These fragment ions likely form by the fragment pathways shown in scheme 38 below:

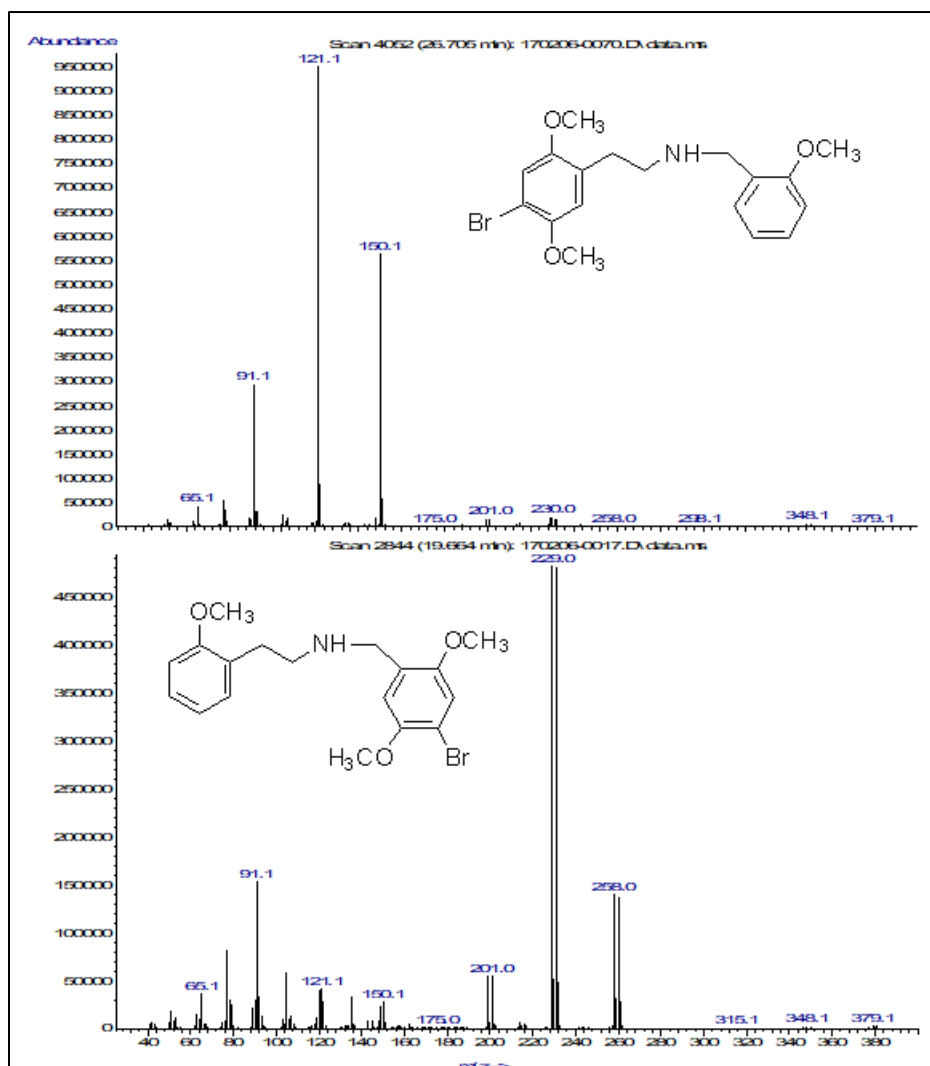
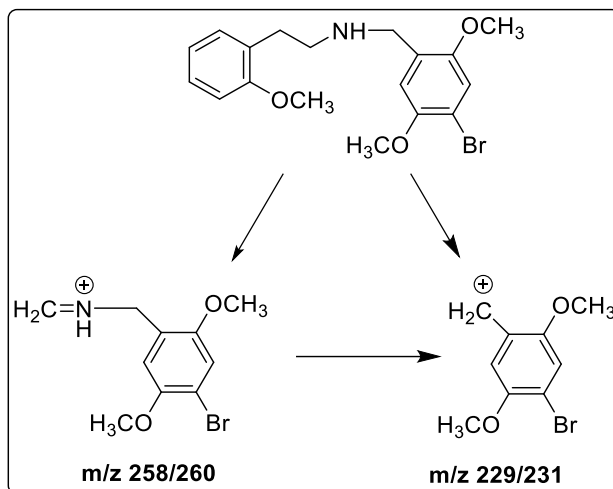


Figure 79 Fragmentation pathway of the 2-methoxy “eMOBN” Derivative.



Scheme 37 Proposed EI-MS fragmentation pathway for the N-(4'-bromo-2',5'-dimethoxy)benzyl-2-methoxyphenethylamine.

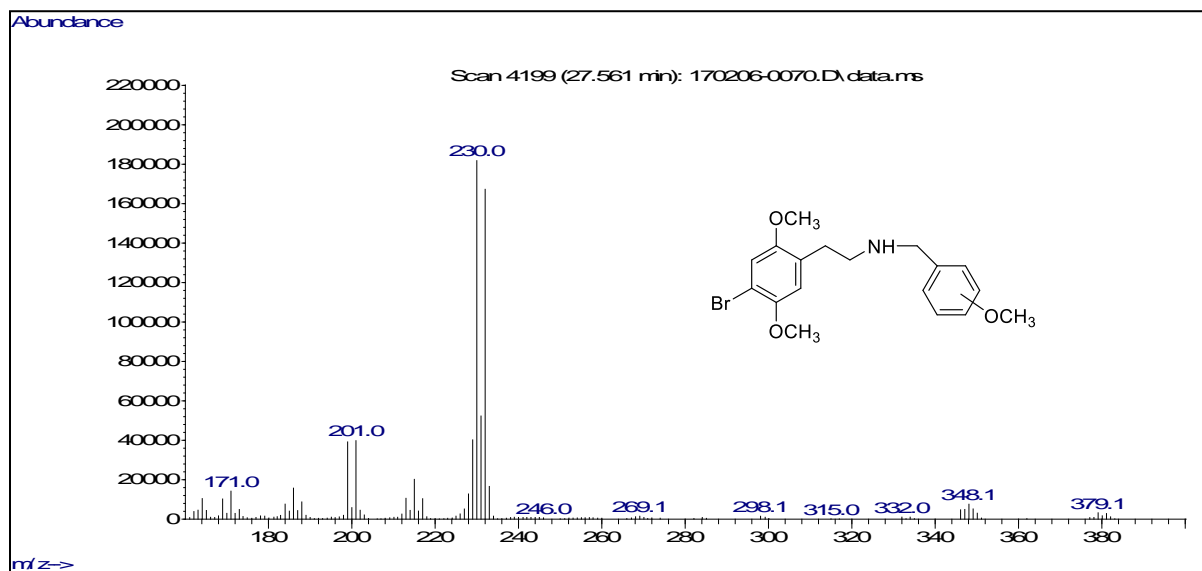
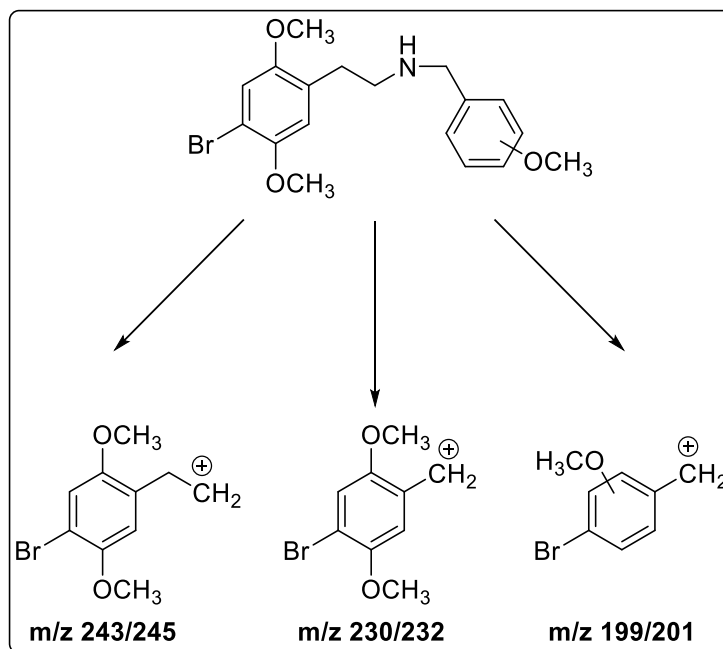


Figure 80 High mass region of bromine-containing fragment ions in the EI-MS of the N-(monomethoxy)benzyl-4-bromo-2,5-dimethoxyphenethylamines.



Scheme 38 Proposed EI-MS fragmentation pathway for the N-(monomethoxy)benzyl-4-bromo-2,5-dimethoxyphenethylamines.

The EI-MS for the six dimethoxy regioisomers in this series are shown in Figure 81. Once again, all regioisomeric members of this subset of compounds derivatives (compounds 4-9) yielded nearly identical mass spectra as shown in Figure 81. The dominant ions in this series were observed at $m/z = 151, 180$ and 121 and none of these ions appear to contain bromine, as observed in the monomethoxy subseries. Also, like the monomethoxy subset, no molecular ion (M) was observed, however the molecular weight was confirmed by M+1 ions at $410/412$ as shown in Figure 82.

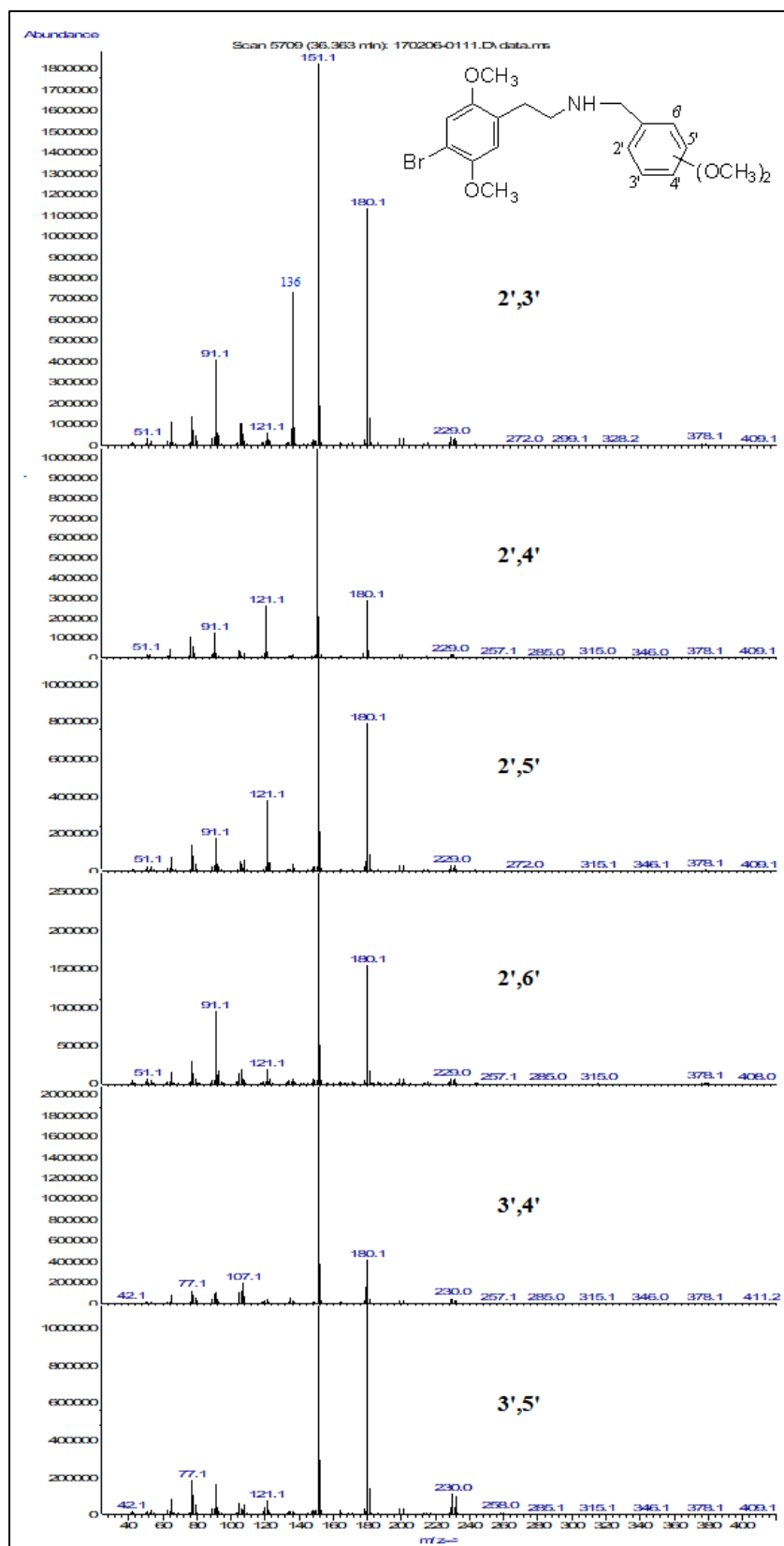


Figure 81 Mass Spectra of the N-(dimethoxy)benzyl-4-bromo-2,5-dimethoxyphenethylamines.

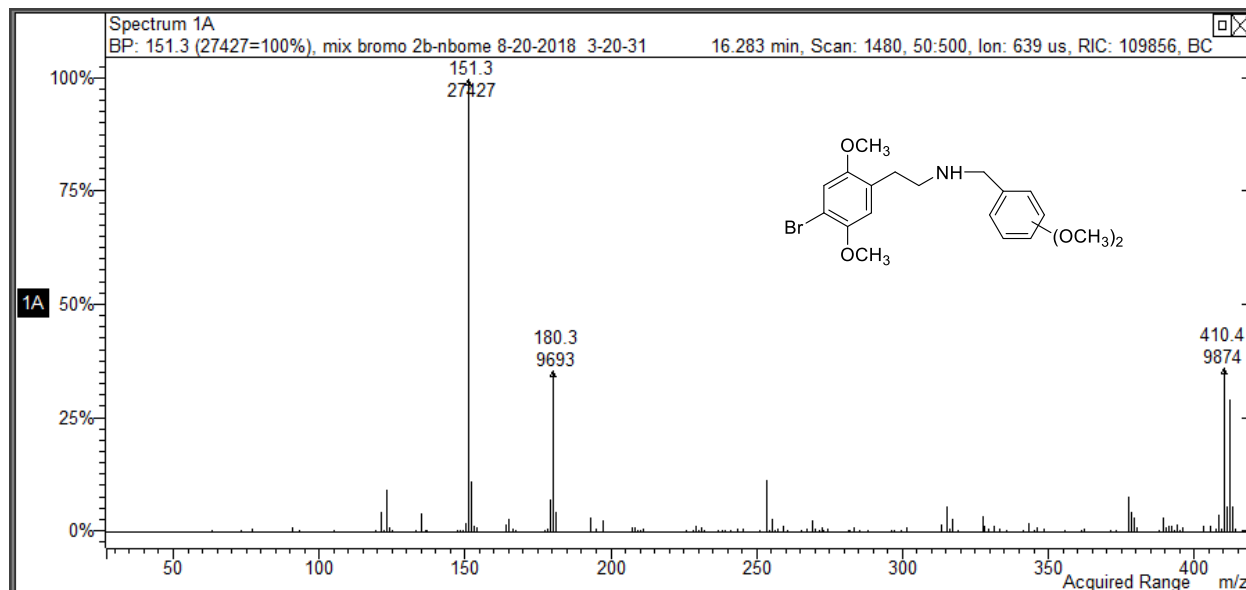
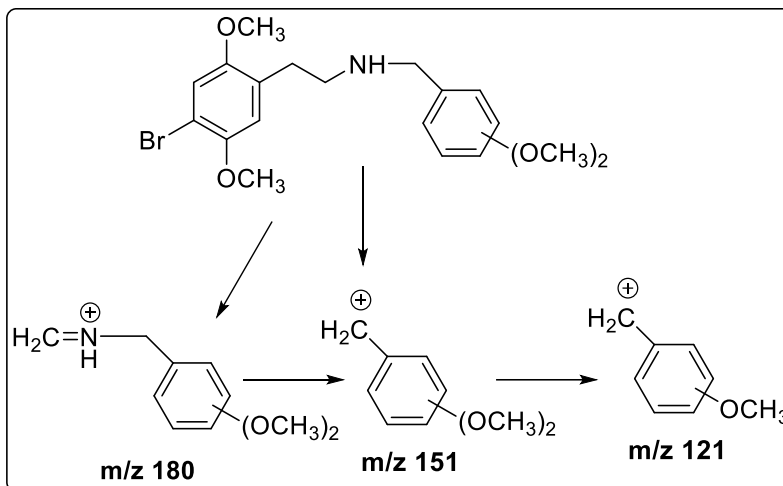


Figure 82 CI-MS of Mass Spectra of N-(dimethoxy)benzyl-4-bromo-2,5-dimethoxyphenethylamine.

The most abundant ions in the dimethoxy series at m/z 151, 180 and 121, each represent fragments 30 Da higher than the most abundant ions in the mass spectra of the monomethoxy compounds (m/z 121, 150 and 91). The mass difference between each of these ions is 30 Da, corresponding to the mass of a methoxy equivalent. Thus, it appears that the dimethoxy regioisomers undergo fragmentation under EI conditions similar to the monomethoxy compounds as illustrated in Scheme 39. The predominant ion at m/z 151 can be formed by the cleavage of the N-C bond yielding dimethoxybenzyl cation. The ion at m/z 180 is likely the iminium cation formed by the dissociation of bond between α - and β -carbon atoms. Finally, the ion at m/z 121 appears to have formed from loss of CH_2O from the dimethoxy benzyl cation.



Scheme 39 Proposed EI-MS fragmentation pathway for the N-(dimethoxy)benzyl-4-bromo-2,5-dimethoxyphenethylamines.

In this series only the 2',3'-dimethoxy regioisomer gave a significant fragment at m/z 136. This fragment ion was also observed in the unbrominated N-(dimethoxy)benzyl-2,5-dimethoxyphenethylamine series described in Chapter 5, and its structure was established by GC-TOF-MS and deuterium labeling studies described in Chapter 10.

The EI-MS for the two methylenedioxy regioisomers in this series are shown in Figure 83. Once again both regioisomeric members of this subset of compounds derivatives (compounds 10-11) yielded nearly identical mass spectra. The dominant ions in this series were observed at $m/z = 135$, 164 and 105 and none of these ions appear to contain bromine, as observed in the monomethoxy subseries. Also, like the monomethoxy and dimethoxy subsets, no molecular ion (M) was observed, however the molecular weight was confirmed by M+1 ions at 394/396 as shown in Figure 84.

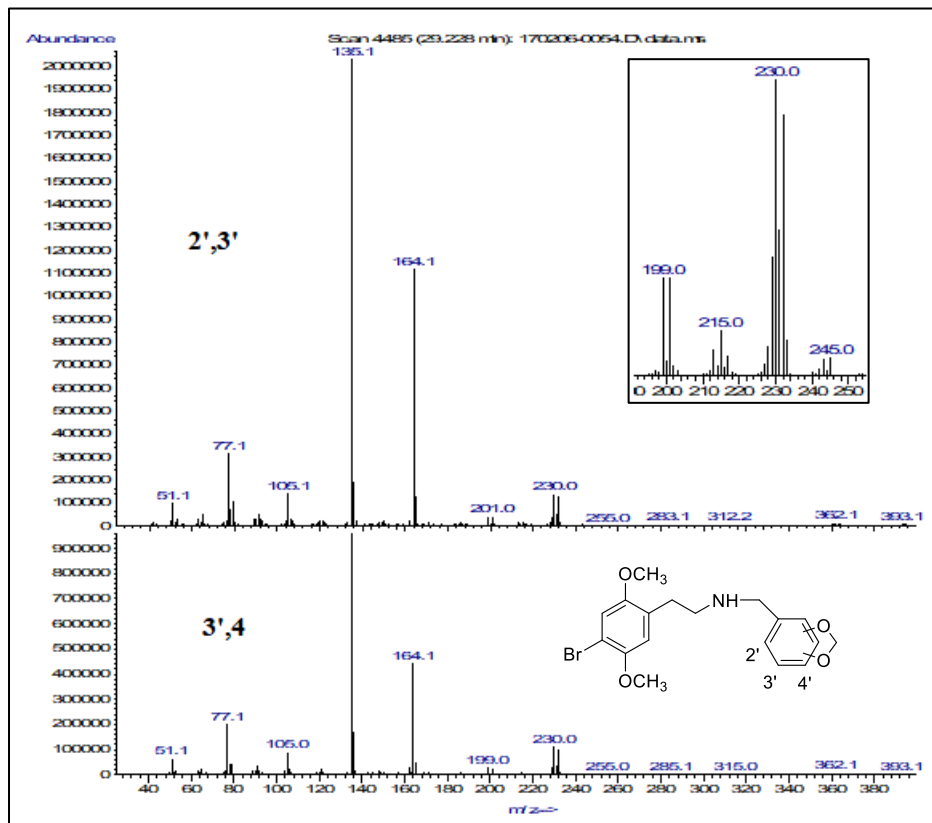


Figure 83 Mass Spectra of the N-(methylenedioxy)benzyl-4-bromo-2,5-dimethoxyphenethylamines.

The three most abundant ions in the methylenedioxy series (m/z 135, 164 and 105), each represent fragments 14 mass units higher than the most abundant ions in the mass spectra of the monomethoxy subset (m/z 121, 150 and 91) and 16 mass units lower than the most abundant ions in the mass spectra of the dimethoxy subset. The mass difference between each of these ions relative to the monomethoxy and dimethoxy compounds is precisely the difference in mass corresponding to the molecular weight differences in these three series (an additional 14 mass units corresponds to the addition of an oxygen atom with removal of two hydrogen atoms relative to the monomethoxy compounds, and a reduction in 16 mass units corresponds to the loss of a carbon and two hydrogen atoms relative to the dimethoxy compounds).

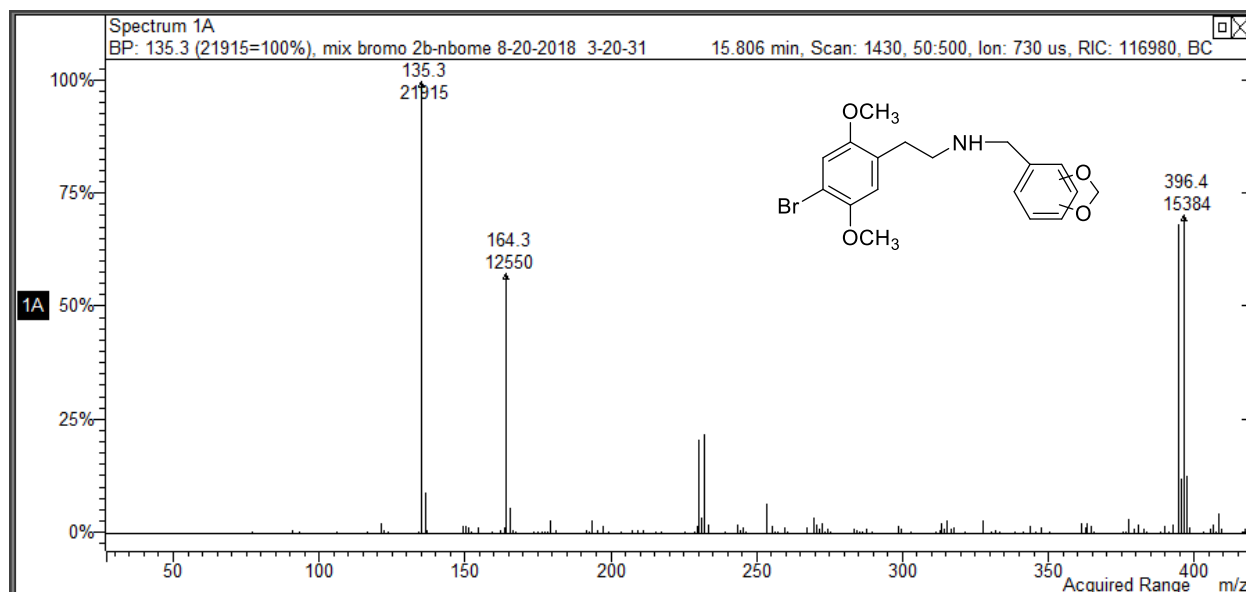
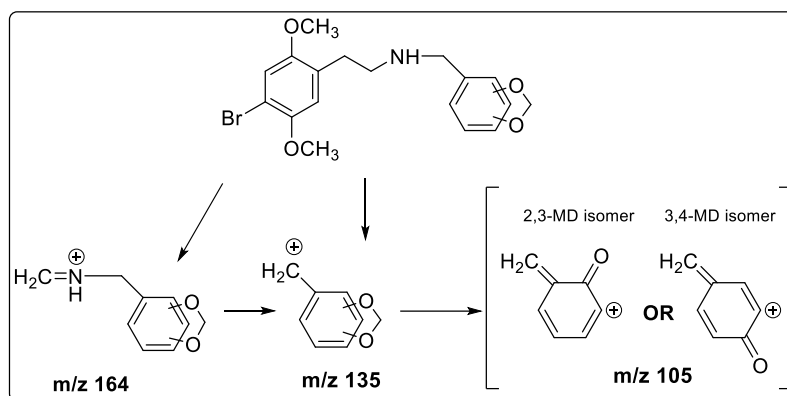


Figure 84 CI-MS of Mass Spectra N-(methylenedioxy)benzyl-4-bromo-2,5-dimethoxyphenethylamine series.

Thus, it appears that the methylenedioxy regioisomers undergo fragmentation under EI conditions similar to the monomethoxy compounds as illustrated in Scheme 40. Again, the predominant ion at m/z 135 can be formed by the cleavage of the N-C bond yielding 2-methylenedioxybenzyl cation and the ion at m/z 164 is likely the iminium cation formed by the dissociation of bond between α - and β -carbon atoms. Finally, the ion at m/z 105 appears to have formed from loss of CH_2O from the methylenedioxy benzyl cation.



Scheme 40 Proposed EI-MS fragmentation pathway for the N-(methylenedioxy)benzyl-4-bromo-2,5-dimethoxyphenethylamines.

The mass spectra for the 11 compounds of this series demonstrate that all members appear to undergo the same fragmentation and that each subset can be differentiated from the other two subsets by the most abundant ions based on differences in the degree of methoxy substitution or methylenedioxy substitution. These spectra also demonstrate that the individual members of each structural subset cannot be differentiated based on their mass spectra. Thus, other analytical methods including GC separations and FTIR spectral analysis were explored for further differentiation within each regioisomeric subseries.

6.3 Gas Chromatographic Separations:

In an attempt to further differentiate the compounds in each of the three N-(substituted)benzyl-4-bromo-2,5-dimethoxyphenethylamine subsets, gas chromatographic separations of (monomethoxy)benzyl regioisomers subset were performed on 30m x 0.25mm ID capillary column coated with 0.25 μm film of midpolarity Crossbond[®] silarylene phase containing a 50% phenyl and 50% dimethyl polysiloxane polymer (Rxi[®]-17Sil MS).

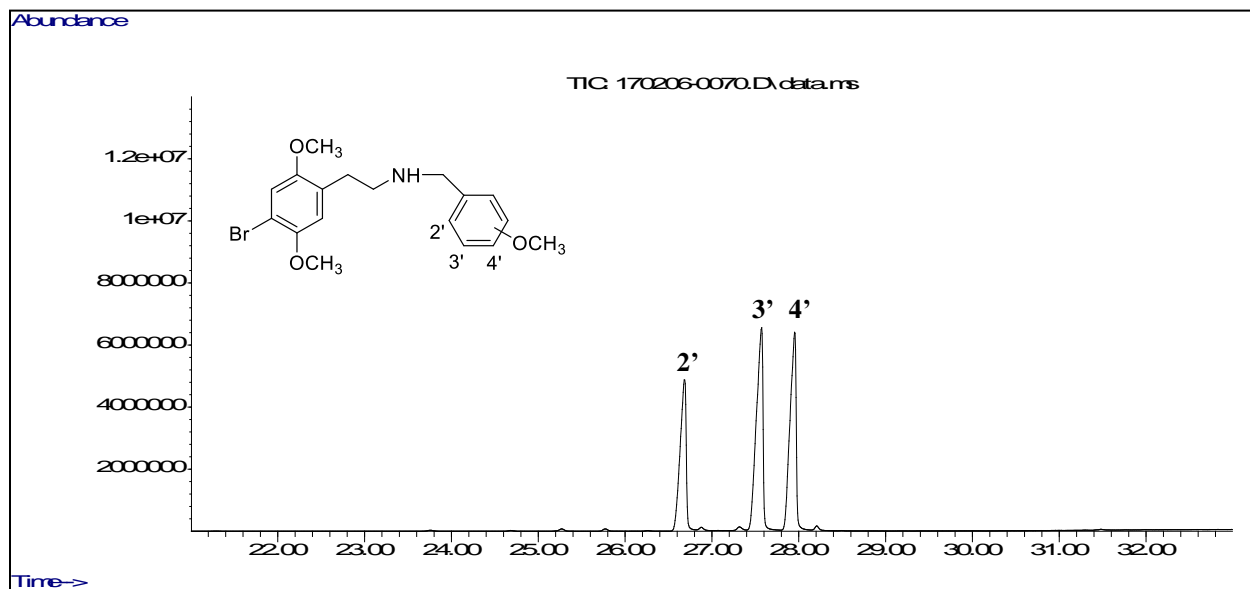


Figure 85 Gas chromatographic separation of the N-(monomethoxy)benzyl-4-bromo-2,5-dimethoxyphenethylamines.

Separations were achieved over 33 minutes starting from initial temperature of 70 °C held for 1 minute then gradually increased to reach 250 °C at a rate of 30 °C/minute and held for 15 minutes then ramped up again to reach 340 °C at a rate of 10 °C/minute which held again for 2 minutes with elution over a 2 minute window. This set of chromatographic conditions yielded an excellent separation of all three regioisomers, with the 2'-methoxy isomer eluting before the 3'-isomer, and the 3'-isomer before the 4'-isomer (Figure 85). Similar separations were achieved for all six of the dimethoxy regioisomers using the same capillary column but with different temperature program conditions. The temperature program started with initial temperature of 70 °C held for 1 minute then gradually increased to reach 250 °C at a rate of 30 °C/minute and held for 25 minutes then ramped up again to reach 340 °C at a rate of 15 °C/minute and held for 10 minutes with a total 48 minutes run time. The compounds eluted over a 2 minute window as shown in Figure 86. In this series those derivatives with a 2'-methoxy group (2',3'-, 2',4'-, 2',5'- and 2',6'-dimethoxy) eluted before the two regioisomers that did not contain a 2'-methoxy group. Also, the two derivatives with the greatest degree of steric crowding relative to the benzyl side chain (2,3- and 2,6-dimethoxy) eluted prior to all other members of the series.

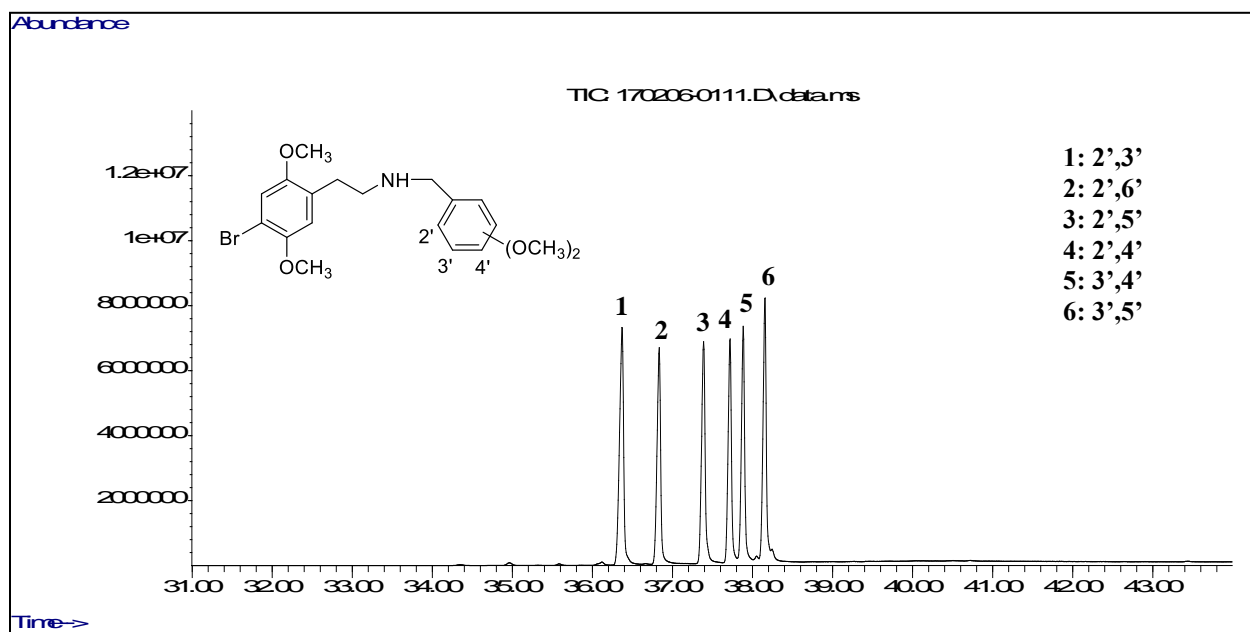


Figure 86 Gas chromatographic separation of the N-(dimethoxy)benzyl-4-bromo-2,5 dimethoxyphenethylamines.

Lastly, the last chromatogram (Figure 87) shows the separation of the two methylenedioxy regioisomers using the conditions described above in the separations of (monomethoxy)benzyl regioisomers. In this series 2',3'-methylenedioxy eluted before 3',4'-methylenedioxy regioisomer the two regioisomers under similar separation condition as above.

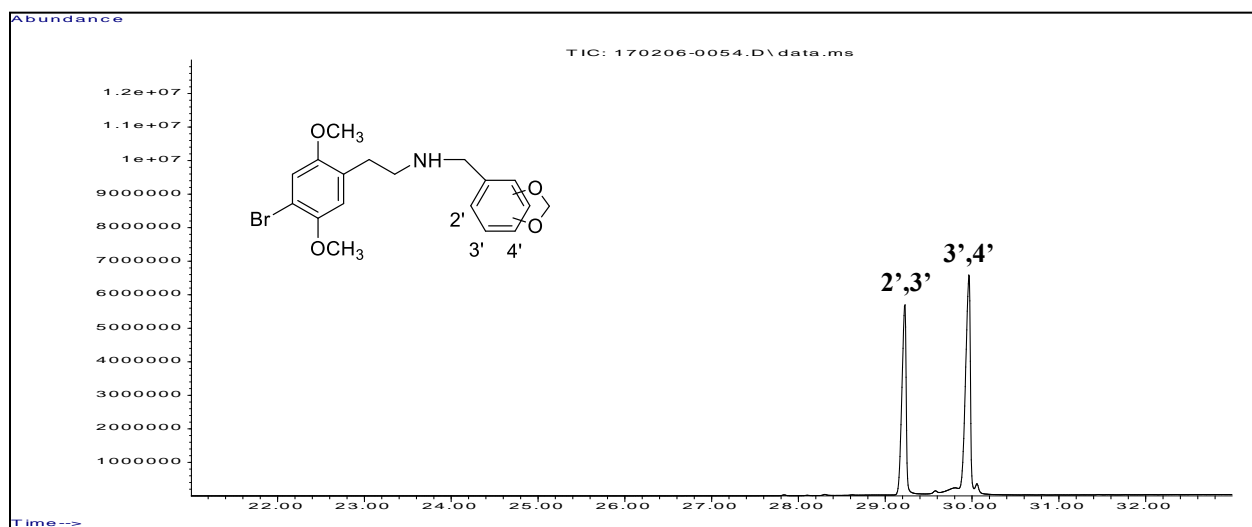


Figure 87 Gas chromatographic separation of the N-(methylenedioxy)benzyl-4-bromo-2,5-dimethoxyphenethylamines.

7 The N-(Bromo-Dimethoxy)benzyl-Monomethoxyphenethylamine Series (eMOBN)

7.1 Introduction:

The compounds of this series are derivatives of N-(2'-methoxy)benzyl-4-bromo-2,5-dimethoxyphenethylamine (25B-NBOMe) where the substitution pattern of the phenethylamine and benzylamine aromatic rings are reversed. Therefore, derivatives of this series contain only a single methoxy substituent in the phenethyl aromatic ring, and a bromo-dimethoxy substitution pattern in the benzyl aromatic ring and are referred to as "eMOBNs". In addition to the direct analogue of 25B-NBOMe (compound 10), other regioisomers were prepared where both the bromo-dimethoxy substitution pattern of the benzyl ring was varied as well as the methoxy substitution pattern in the phenethyl ring.

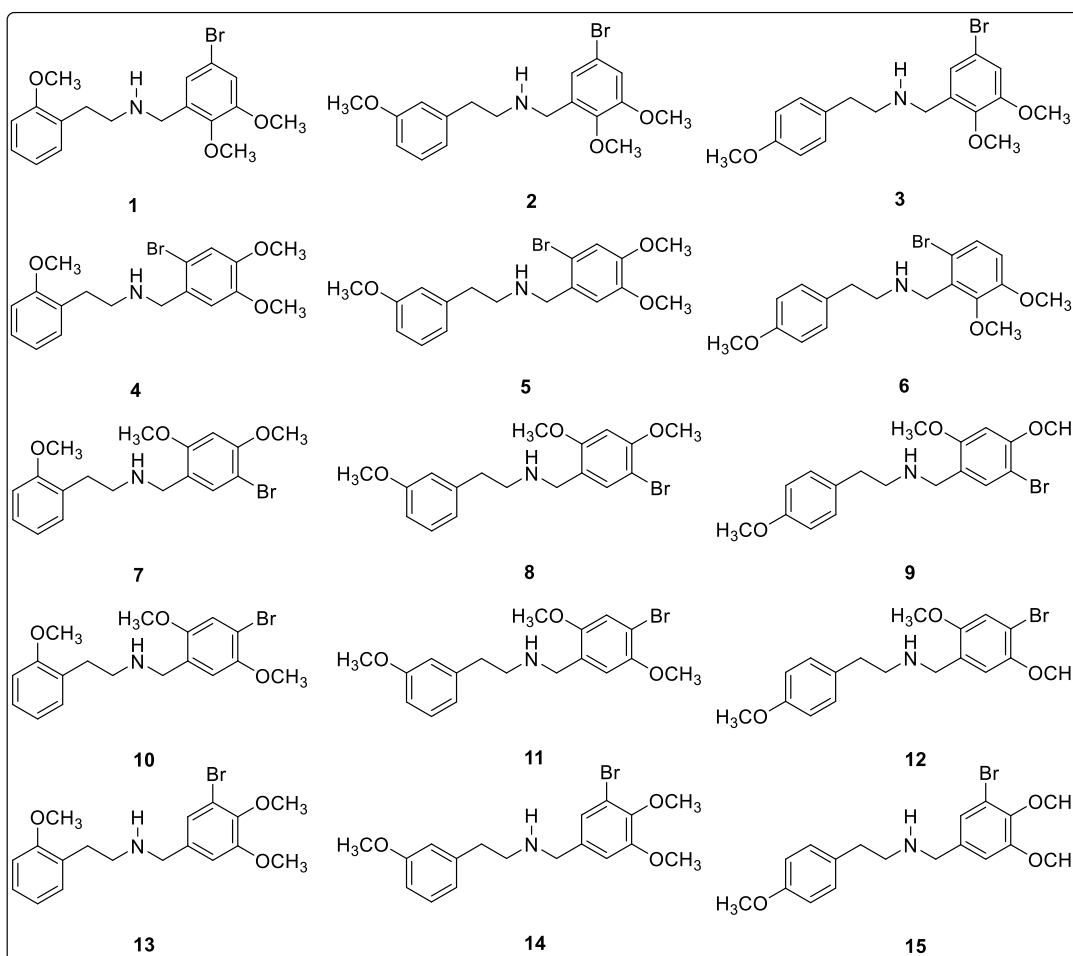


Figure 88 Structures of the N-(bromo-dimethoxy)benzyl-monomethoxyphenethylamine series.

The substitution patterns included in this series were based on the commercial availability of bromo-dimethoxy benzaldehydes. All of these derivatives were prepared as described in the previous chapter by direct reductive alkylation of 2-, 3- or 4-methoxyphenethylamine with 5'-Br-2',3'-DiMeO- 2'-Br-4',5'-DiMeO - 5'-Br-2',4'-DiMeO - 4'-Br-2',5'-DiMeO or 3'-Br-4',5'-DiMeO benzaldehyde. Based on available bromo-dimethoxy benzaldehydes this yielded five subsets of compounds as shown in Figure 88.

7.2 Mass Spectral Analysis:

As reported for the original NBOMe drugs of abuse and other NBOMe derivatives prepared in this research, compounds of this structural class typically do not display a molecular ion (MW 279/381) in the EI-MS spectrum. However, the molecular masses of these regioisomers were confirmed by CI-MS as illustrated for one member of this series in Figure 89 where a M+1 ions of m/z 380/382 was present. As reported for the 25B-NBOMe compound, two of the more abundant ions in EI-MS spectra of all fifteen of these regioisomers contained bromine based on isotopic distribution and were observed at $m/z = 229/231$ (base peak) and 258/260. Also fragments that did not contain bromine were present at m/z 91 and 121 in the spectra of all fifteen of these compounds.

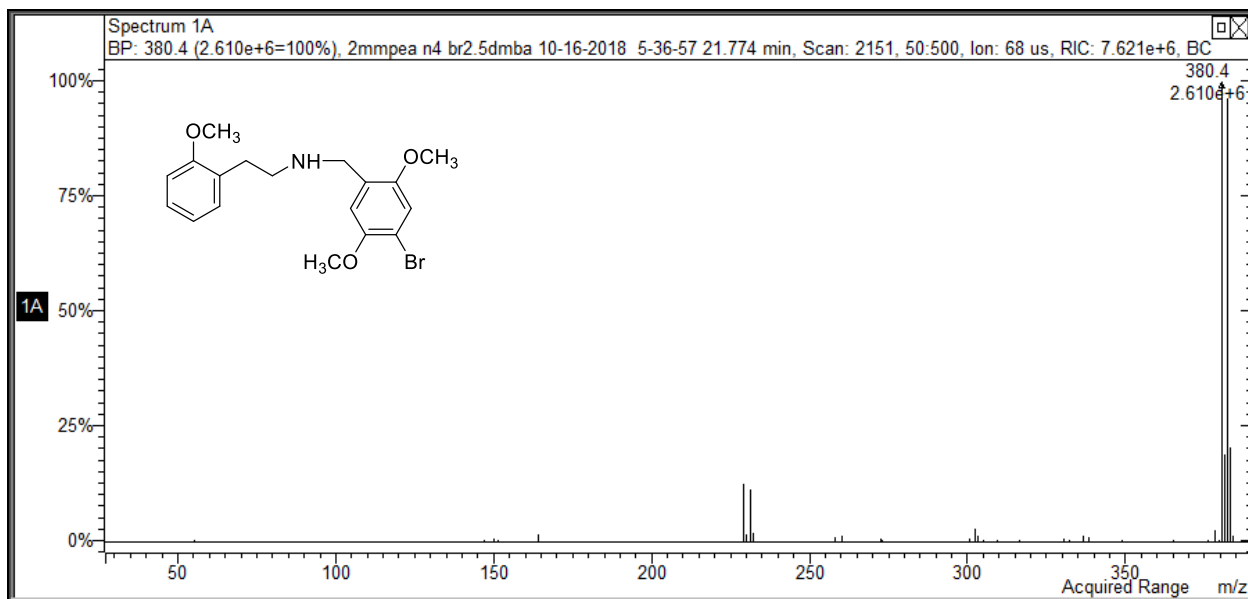
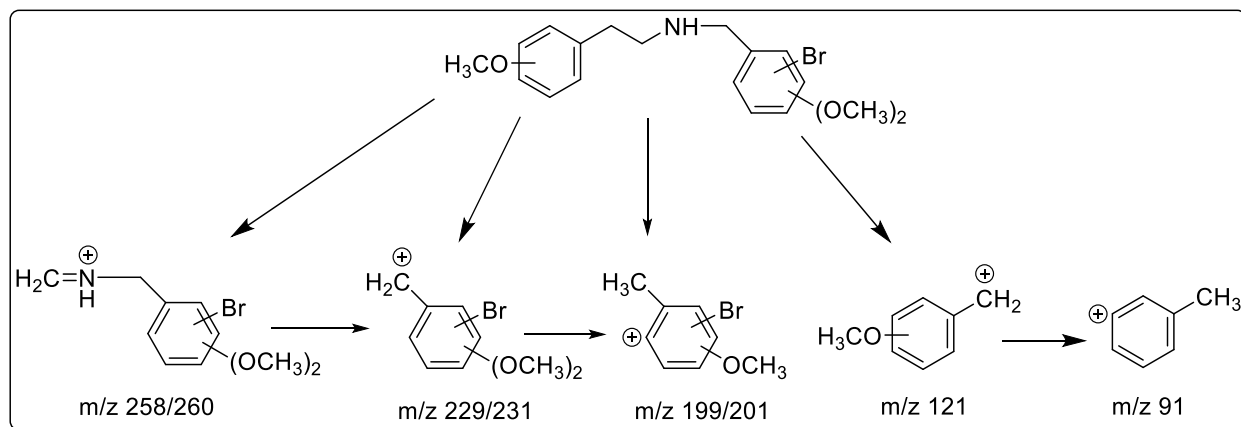


Figure 89 CI-MS of Mass Spectra of the N-(4'-bromo-2',5'-dimethoxy)benzyl-2-methoxyphenethylamines.

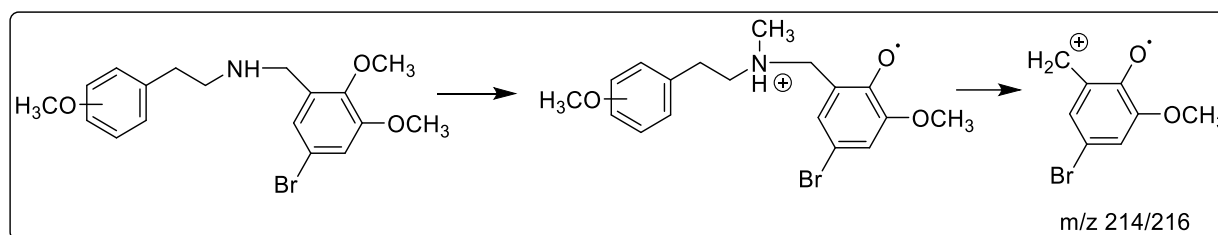
Within each subseries the relative abundance of the m/z 91 was highest for the 2-methoxy isomer and lowest for the 4-methoxy isomer. Also, within each subseries the relative abundance of the m/z 121 fragment was highest in the 4-methoxy isomer. A proposed fragmentation pathway for the four m/z ions noted above for all fifteen regioisomers is shown in Scheme 41. The ion at m/z 258/260 is likely the iminium cation formed by the dissociation of bond between α - and β -carbon atoms, a common pathway for phenethylamine compounds. The base peak at m/z 229/231 can be formed by the cleavage of the N-C bond yielding 2'-methoxy benzyl cation but could possibly form by cleavage of the C-C bond of the phenethyl side chain. Finally, the ions at m/z 91 and 121 likely are derived from fragmentation of the phenethyl side chain (121) and then loss of methoxy (-30) from the 121 ion. This fragmentation pathway is the same as all members of the basic NBOMe structural class as described in previous chapters.



Scheme 41 Proposed EI-MS fragmentation pathway for the N-(bromo-dimethoxy)benzyl-monomethoxy-phenethylamines.

While the EI-MS of all fifteen of the regioisomers in this series contained a number of common ions, there are significant differences in the mass spectra among the various subseries. For example, all three members of the 5'-bromo-2',3'-dimethoxy subseries gave a fragment of relatively high abundance at m/z 214/216 and this ion is present only in this subseries. This ion forms most likely by a methyl migration reaction after initial ionization as shown in scheme 42. A

similar fragment ion was observed in the mass spectra of all other 2',3'-dimethoxybenzyl NBOMes prepared in this research as noted in earlier chapters at m/z 136.



Scheme 42 Proposed formation of the m/z 214/216 ion from the N-(5'-bromo-2',3'-dimethoxy)benzyl-monomethoxyphenethylamines.

Also, the mass spectra of the 5'-bromo-2',4'-dimethoxy and 4'-bromo-2'5'-dimethoxy regioisomers contained an additional fragment ion containing bromine at 199/201 not present in the other subseries. The relative abundance of m/z 199/201 is nearly the same for each regioisomer in each subseries, whether it is 2'-, 3'-, or 4'-methoxyphenethylamine regioisomer.

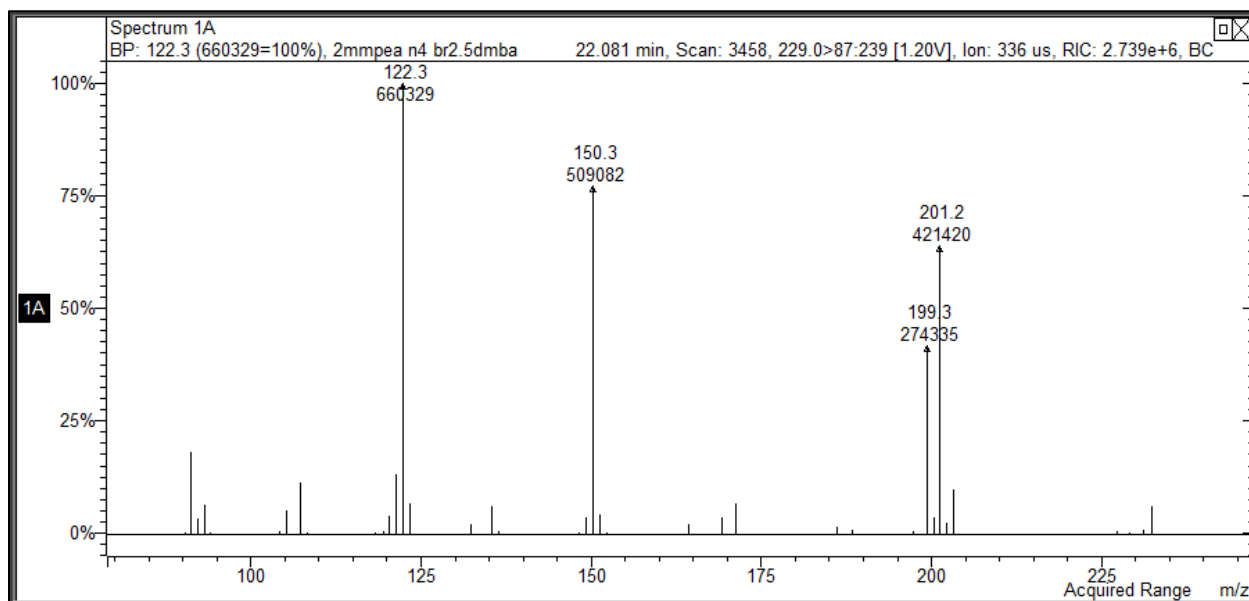


Figure 90 MS-MS of the m/z 229 ion.

Based on MS-MS studies shown in Figure 90, this ion appears to form by loss of a methoxy group (-30) from the m/z 229 benzyl cation. Interestingly, the m/z 199/201 ion appears to form only in subseries where there is a methoxy group positioned ortho to the benzylic carbon, with exception of the 5'-bromo-2',3'-dimethoxy isomer where methyl migration appears to predominate (m/z 214/216).

Thus, while there are similarities in the EI-MS of all fifteen of these eMOBN regioisomers (Figures 91 - 95), there are unique fragments between the subseries which allow for some degree of isomer differentiation. The 5'-bromo-2',3'-dimethoxy subseries can be differentiated from all other subseries by the presence of m/z 214/216 of high abundance, most likely the result of methyl migration. Also, the 5'-bromo-2',4'-dimethoxy and 4'-bromo-2',5'-dimethoxy regioisomeric subseries contain a m/z 199/201 fragment ion not present in the same abundance in the spectra of the other eMOBNs. Finally, within subseries, the 2-, 3- and 4-methoxyphenethyl isomers can be differentiated to some degree by the relative abundance of the m/z 91 and 121 ion.

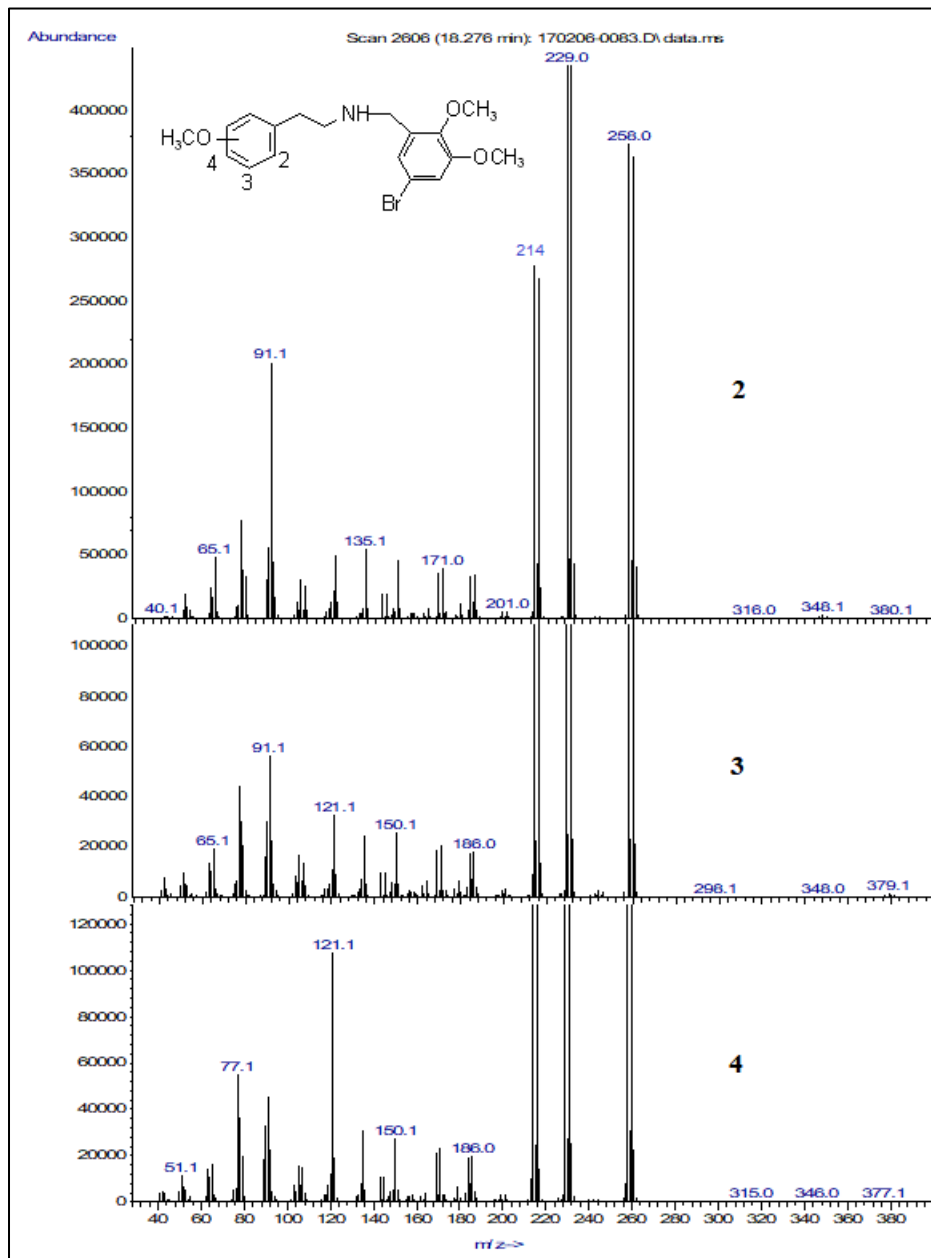


Figure 91 Mass Spectra of the N-(5'-bromo-2',3'-dimethoxy)benzyl-monomethoxyphenethylamines.

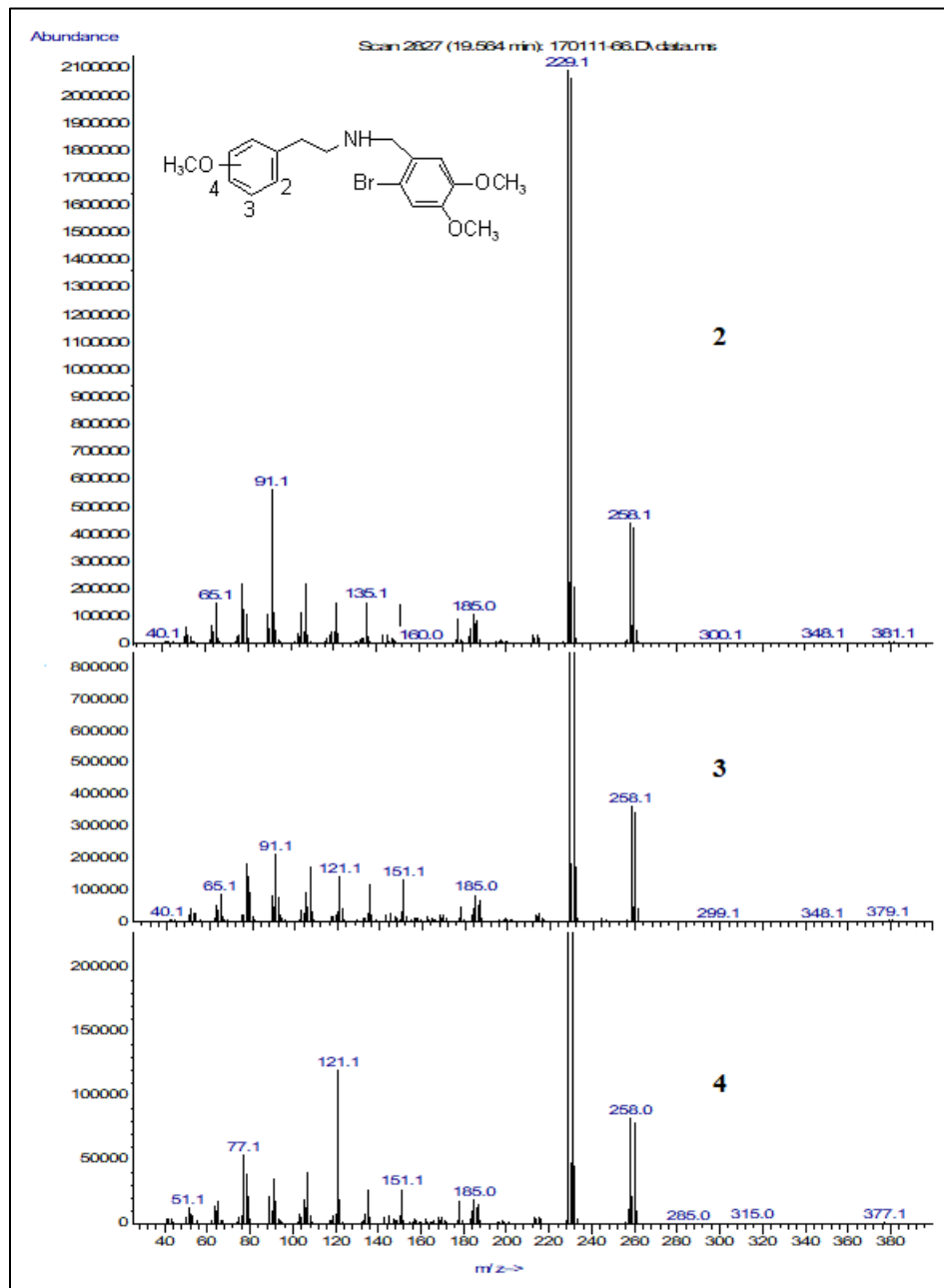


Figure 92 Mass Spectra of the N-(2'-bromo-4',5'-dimethoxy)benzyl-monomethoxyphenethylamines.

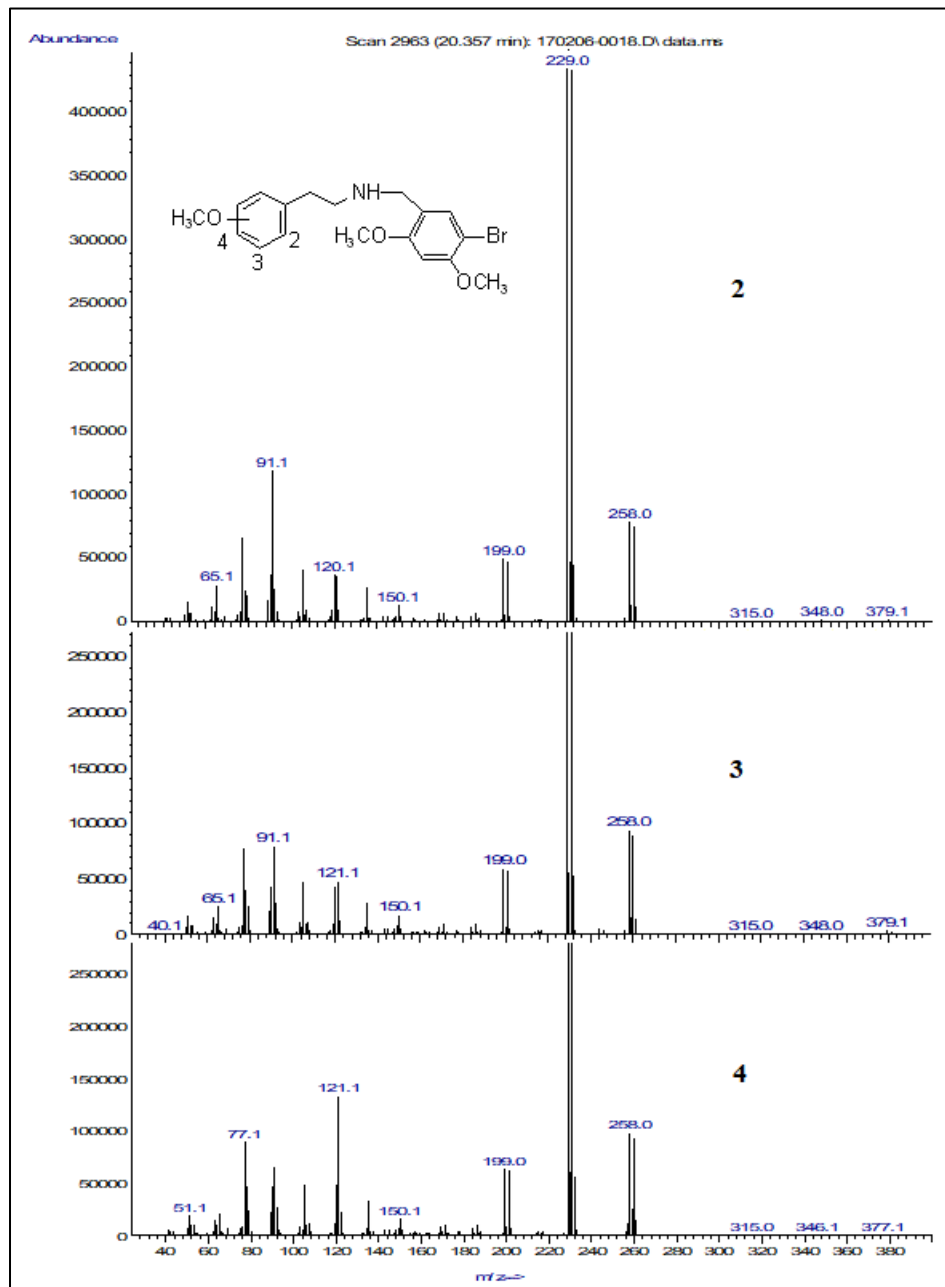


Figure 93 Mass Spectra of the N-(5'-bromo-2',4'-dimethoxy)benzyl-monomethoxyphenethylamines.

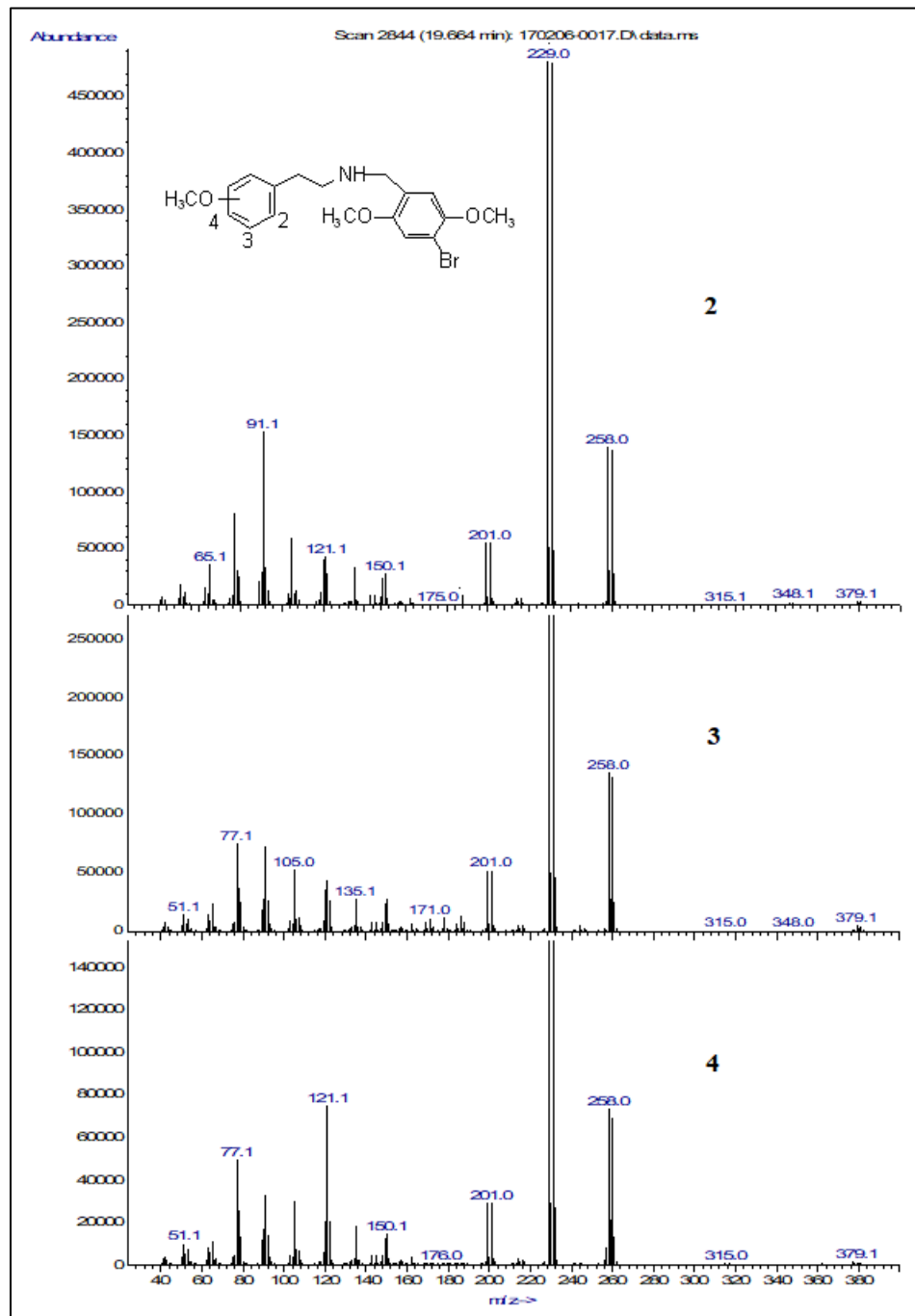


Figure 94 Mass Spectra of the N-(4'-bromo-2',5'-dimethoxy)benzyl-monomethoxyphenethylamines.

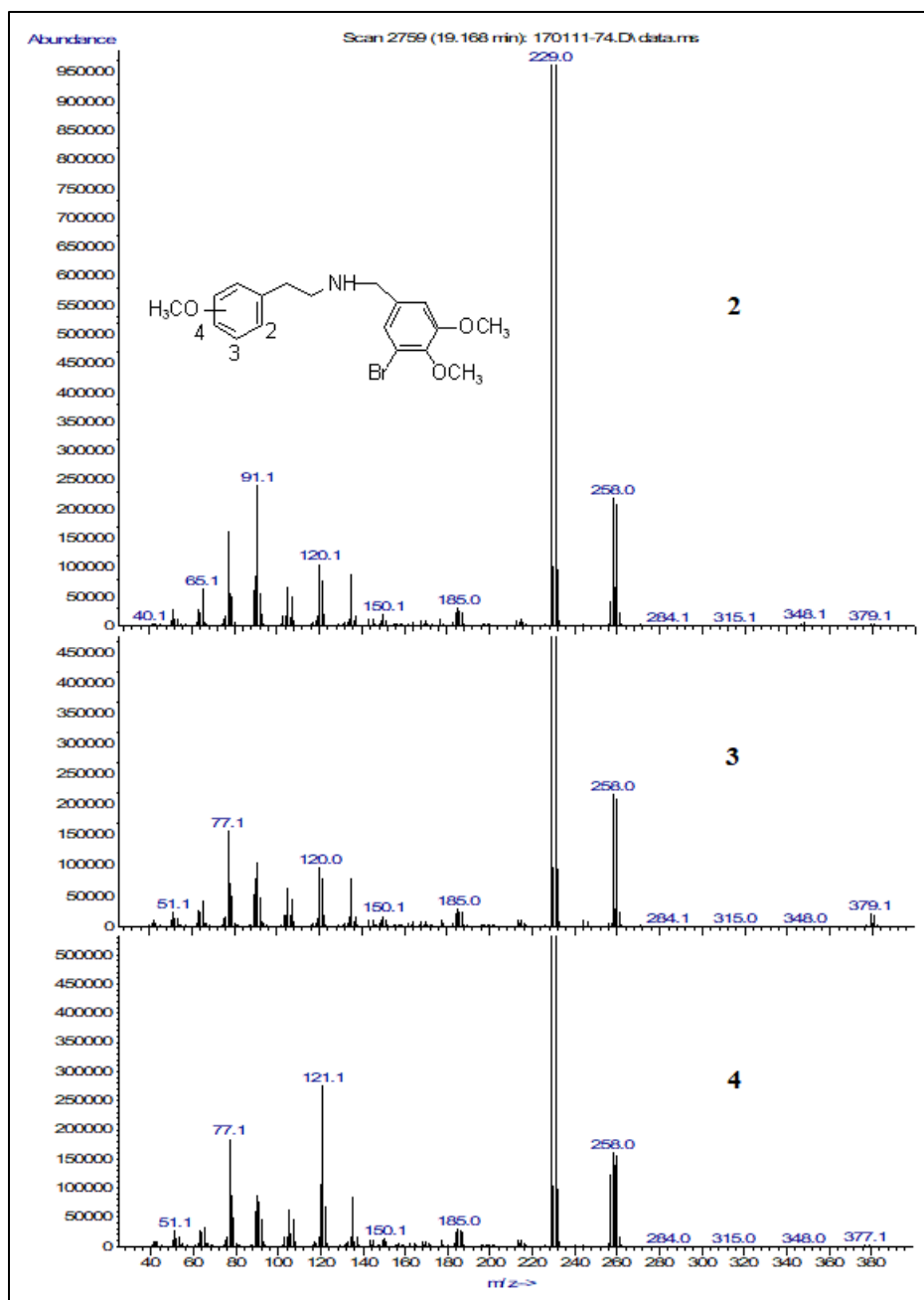


Figure 95 Mass Spectra of the N-(3'-bromo-4',5'-dimethoxy)benzyl-monomethoxyphenethylamines.

These spectra also demonstrate that some of individual members of each structural subset cannot be differentiated based on their mass spectra. Thus, other analytical methods such as GC separations is needed for further differentiation within each regioisomeric subseries.

7.3 Gas Chromatographic Separations:

In an attempt to further differentiate the compounds in each of the five N-(bromo-dimethoxy)benzyl-monomethoxyphenethylamines subsets, gas chromatographic separations of monomethoxyphenethylamine regioisomeric subsets were performed on 30m x 0.25mm ID capillary column coated with 0.25 μm film of midpolarity Crossbond[®] silarylene phase containing a 50% phenyl and 50% dimethyl polysiloxane polymer (Rxi[®]-17Sil MS). Separations were achieved over 30 minutes starting from initial temperature of 70 °C held for 1 minute then gradually increased to reach 245 °C at a rate of 70 °C/minute and held for 5.5 minutes then ramped up again to reach 300 °C at a rate of 5 °C/minute and held for 10 minutes. The compounds eluted over a 2 minute window as shown in Figure 96 - 100. This set of chromatographic conditions yielded an excellent separation of all three regioisomers, with the 2-methoxy isomer eluting before the 3-isomer, and the 3-isomer before the 4-isomer in each subseries (Figure 96 - 100). Attempts to separate more complex mixtures involving multiple subsets of the eMOBN regioisomers were not successful.

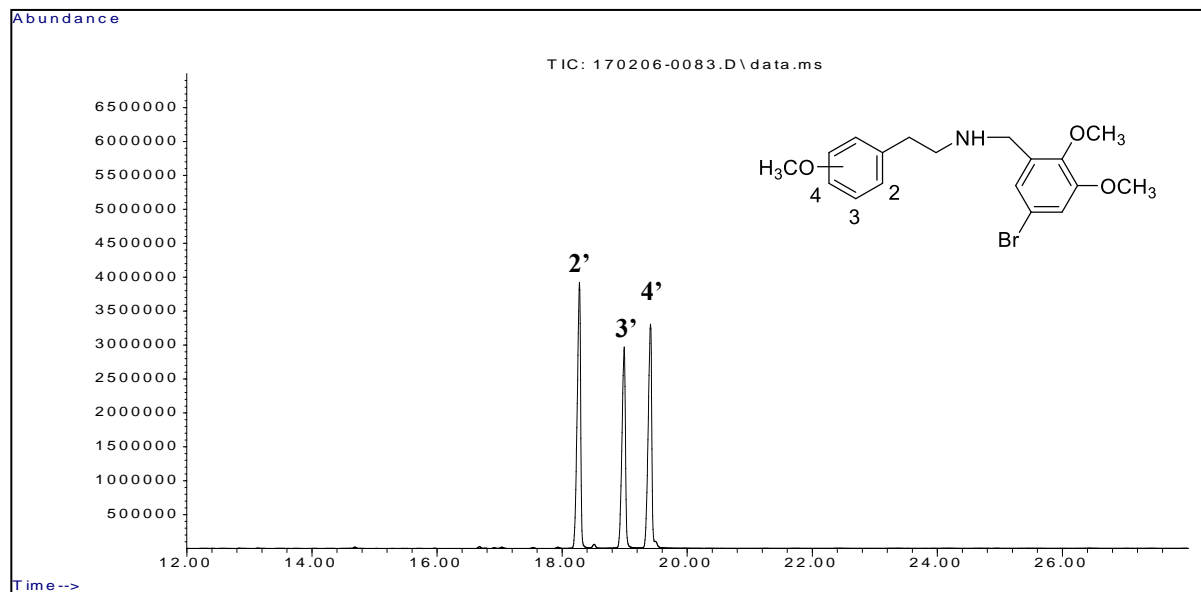


Figure 96 Gas chromatographic separation of the N-(5'-bromo-2',3'-dimethoxy)benzyl-monomethoxyphenethylamines.

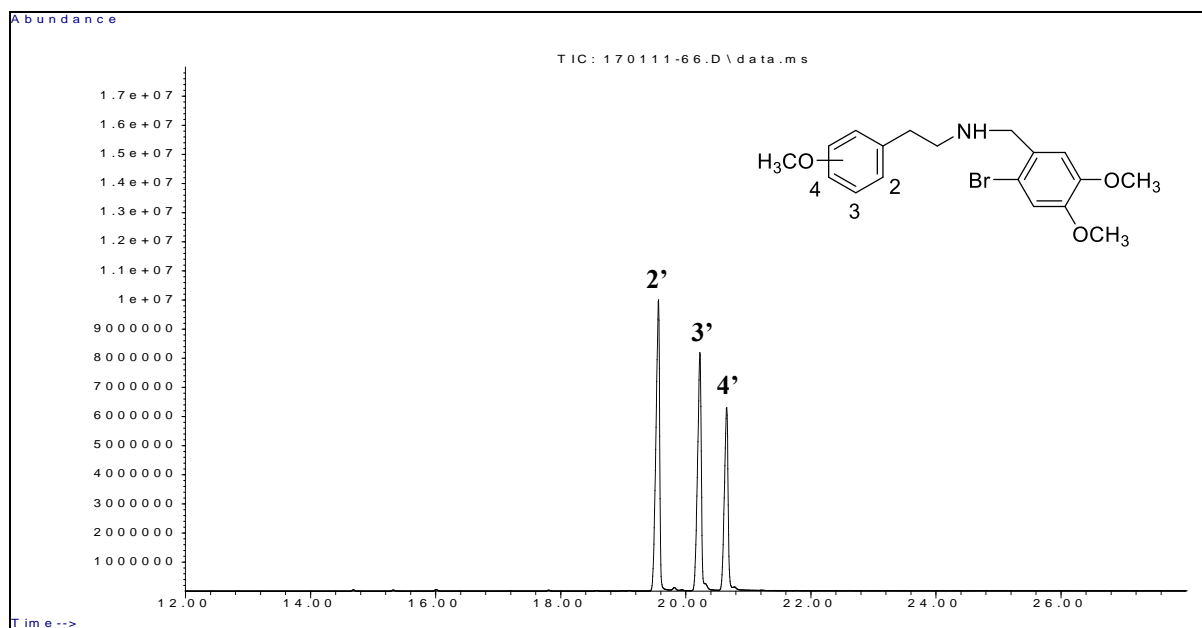


Figure 97 Gas chromatographic separation of the N-(2'-bromo-4',5'-dimethoxy)benzyl-monomethoxyphenethylamines.

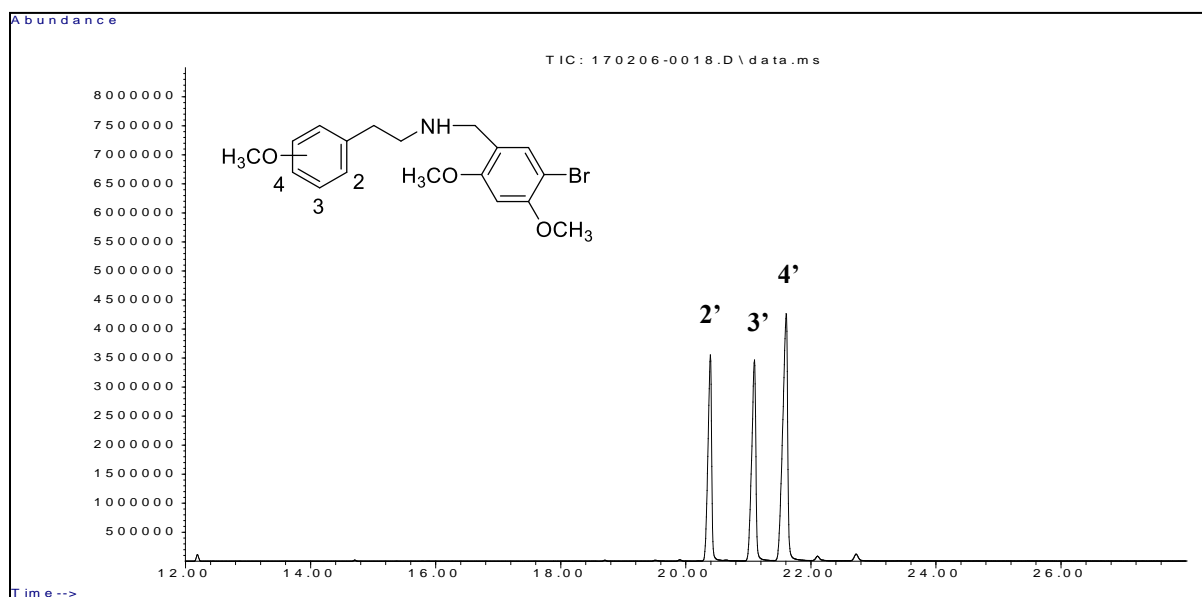


Figure 98 Gas chromatographic separation of the N-(5'-bromo-2',4'-dimethoxy)benzyl-monomethoxyphenethylamines.

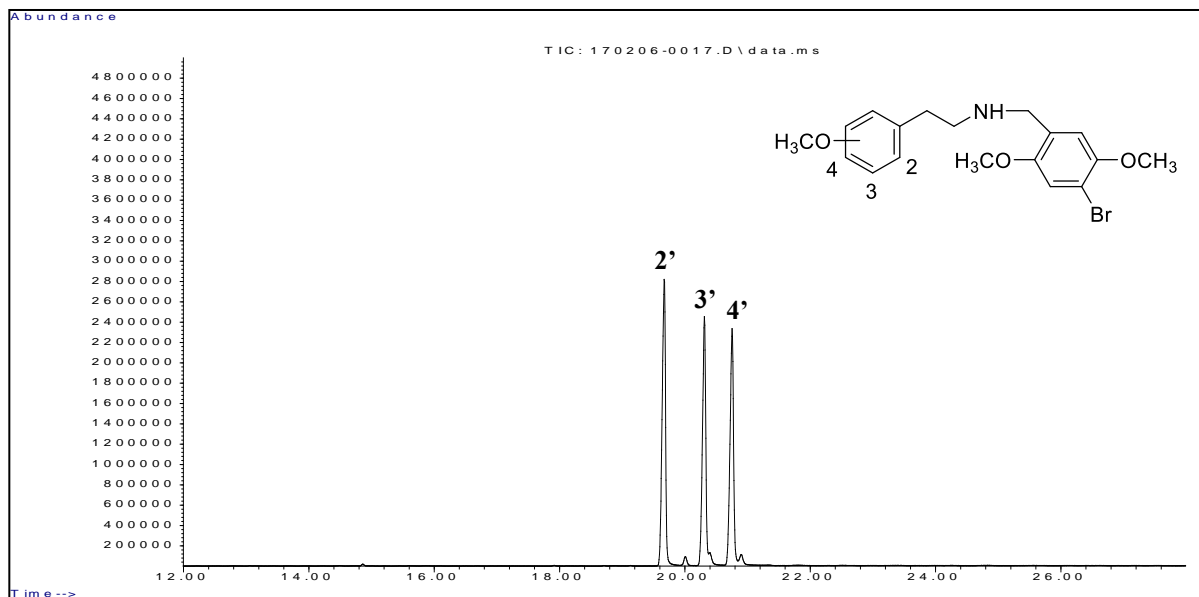


Figure 99 Gas chromatographic separation of the N-(4'-bromo-2',5'-dimethoxy)benzyl-monomethoxyphenethylamines.

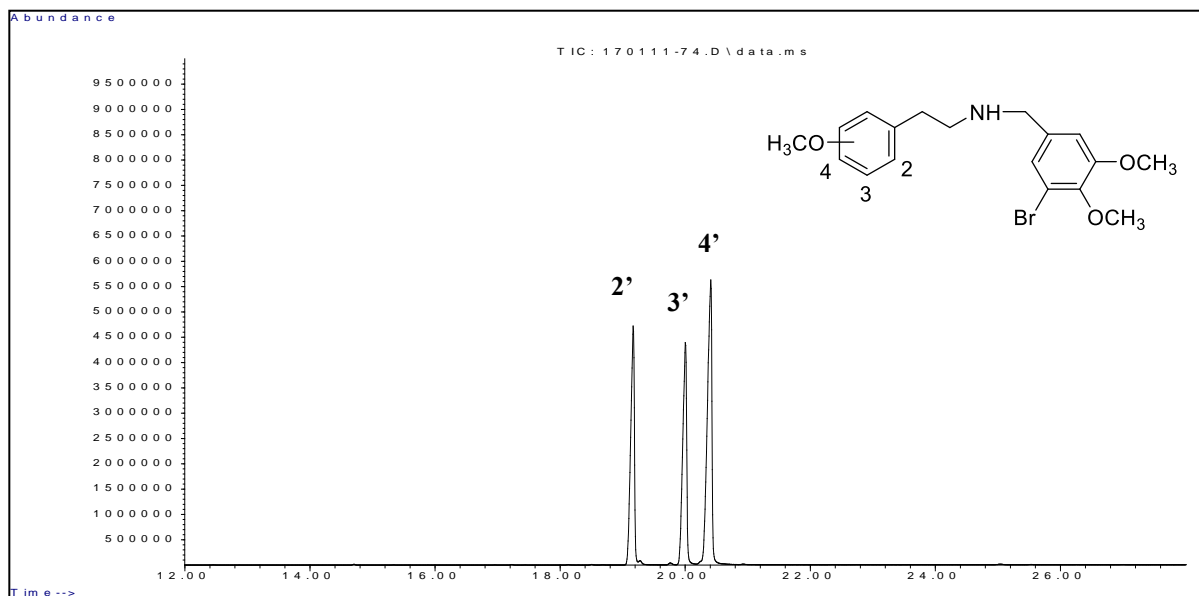


Figure 100 Gas chromatographic separation of the N-(3'-bromo-4',5'-dimethoxy)benzyl-monomethoxyphenethylamines.

8 The N-(Substituted)benzyl-4-iodo-2,5-dimethoxyphenethylamine Series

8.1 Introduction:

The compounds of this series are derivatives of N-(2'-methoxy)benzyl-4-iodo-2,5-dimethoxyphenethylamine (25I-NBOMe) where the substitution pattern on the aromatic ring of the N-benzyl substituent is modified yielding the 11 compounds in Figure 101. This series can be divided into three subsets. The first subset includes 25I-NBOMe and its 3- and 4-monomethoxy regioisomers (structures 1-3). In the second subset the N-benzyl aromatic ring is modified to include two methoxy groups at every possible position. Thus, this subset includes six regioisomeric compounds, the 2,3-, 2,4-, 2,5-, 2,6-, 3,4- and 3,5-dimethoxy regioisomers (structures 4-9). In the third subset in this series the N-benzyl aromatic ring is modified to contain the two possible methylenedioxy substitution patterns (structures 10-11).

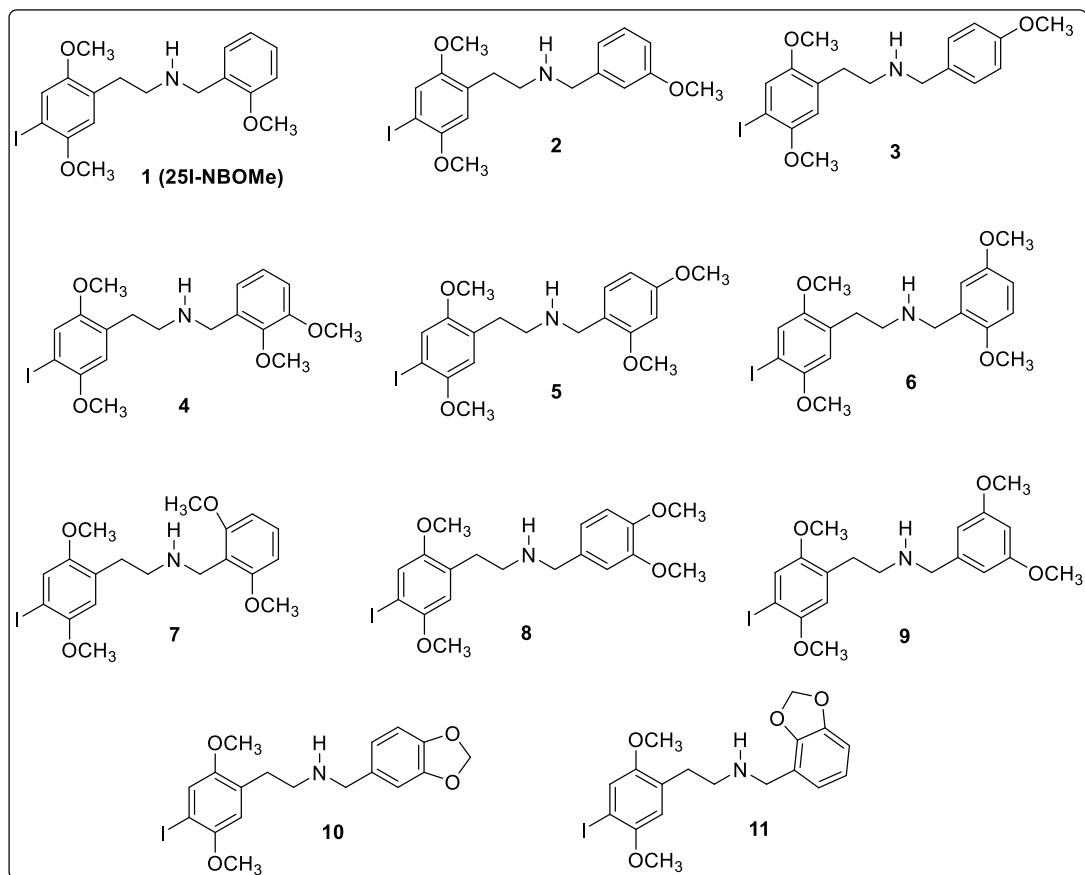


Figure 101 Structures of the N-(substituted)benzyl-4-iodo-2,5-dimethoxyphenethylamine Series.

The N-benzyl substitution patterns selected for this series represent potential designer modifications since this functionality is commonly found in drugs of abuse. All of these compounds were synthesized as described in the previous chapter.

8.2 Mass Spectral Analysis:

The EI-MS of all members of this series of compounds are shown in Figures 102 and 105. All three regioisomeric members of the (monomethoxy)benzyl subset of derivatives (compounds 1-3) yielded nearly identical mass spectra as shown in Figure 102.

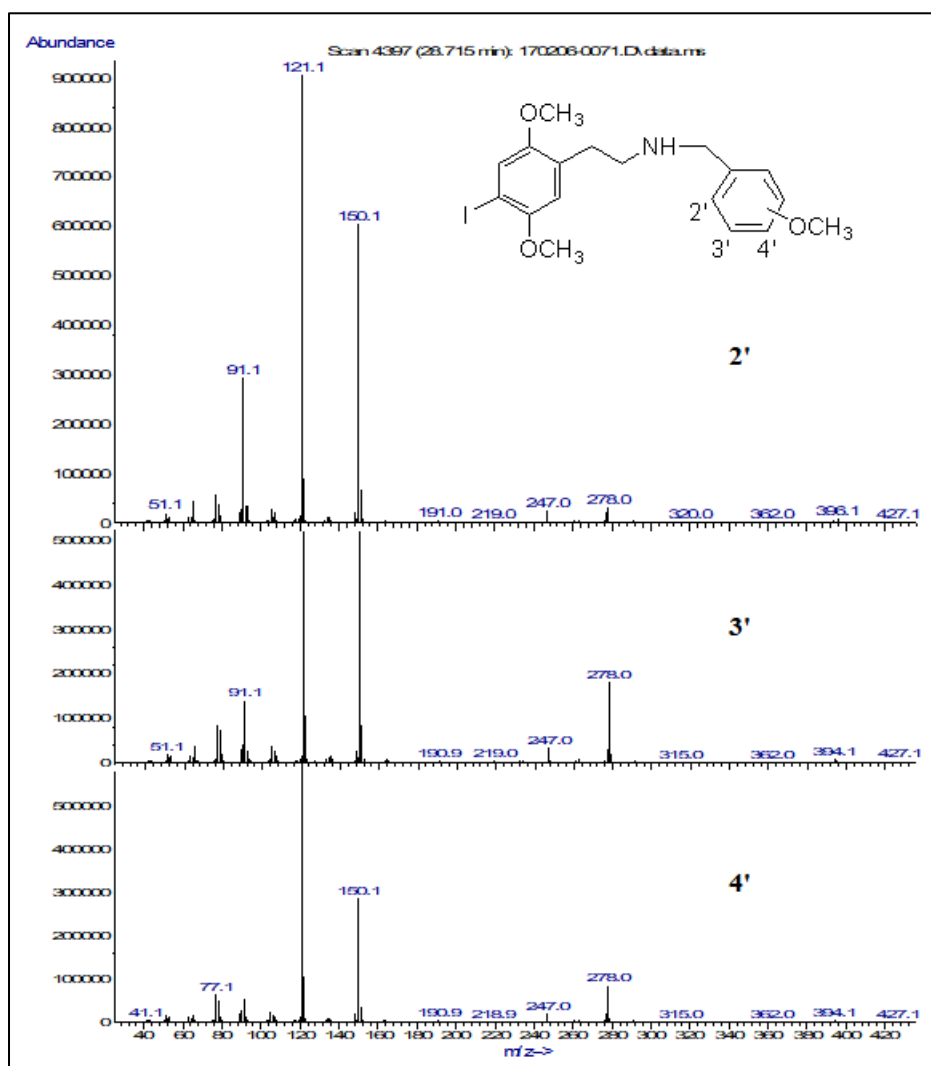


Figure 102 Mass Spectra of the N-(monomethoxy)benzyl-4-iodo-2,5-dimethoxyphenethylamines.

As reported for other 25-NBOME compounds, and the 2,5-bromo NBOME derivatives in the previous chapter, the dominant ions in GC-MS spectrum of the 2-, 3- and 4'-monomethoxy derivatives in this series are observed at $m/z = 121$, 150 and 91, with the base peak m/z 121 (Figure 102). The m/z 91 ion was present in the highest abundance in the 2'-methoxy isomer and decreased in the 3'- and 4'-methoxy isomers, a pattern also observed in the monomethoxy bromo NBOME series. It is interesting to note that none of the dominant ions in these spectra appeared to contain iodine. The molecular ion (M) also is not apparent in the EI-MS spectrum, however the mass was confirmed by CI-MS (Figure 103) where a M+1 ion of 428.

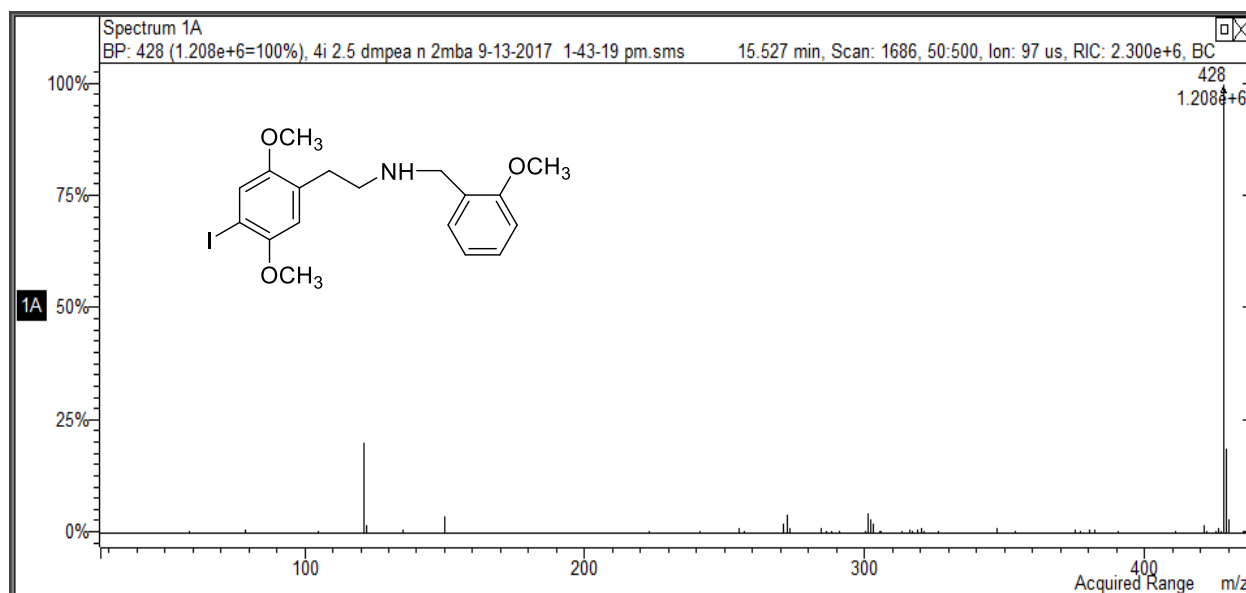
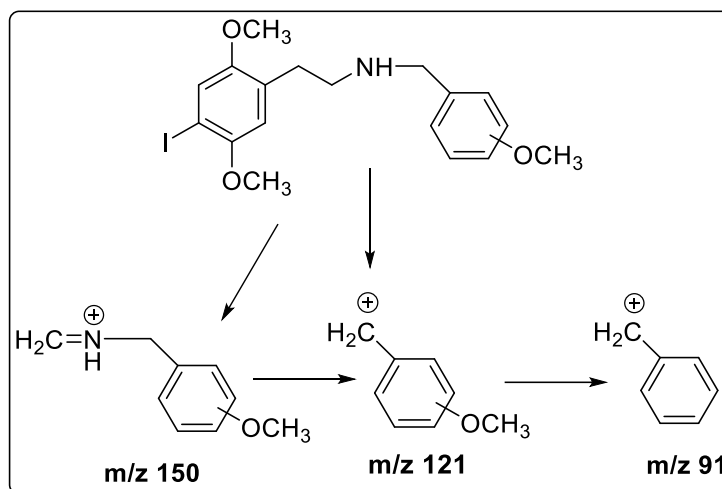


Figure 103 CI-MS of Mass Spectra of the N-2'-methoxybenzyl-4-iodo-2,5-dimethoxyphenethylamines.

A proposed fragmentation pathway showing the dominant ions for the monomethoxy subseries of compounds is shown in Scheme 43. The base peak m/z 121 can be formed by the cleavage of the N-C bond yielding 2-methoxybenzyl cation. The ion at m/z 150 is likely the iminium cation formed by the dissociation of bond between α - and β -carbon atoms, a common pathway for phenethylamine compounds. Finally, the ion at m/z 91 appears to have formed from loss of CH_2O from the methoxy benzyl cation.



Scheme 43 Proposed EI-MS fragmentation pathway for the N-(monomethoxy)benzyl-4-iodo-2,5-dimethoxyphenethylamines.

Support for this fragmentation pathway was provided by MS-MS studies which demonstrate that the m/z 91 ion is formed from the m/z 121 fragment as shown in Figure 104 as was observed in the monomethoxy bromo NBOME series

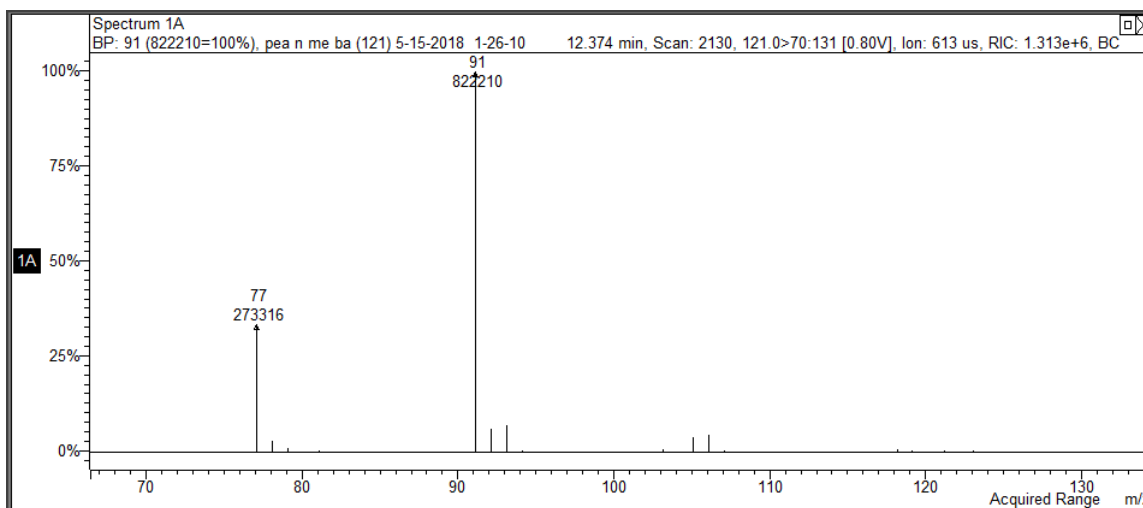


Figure 104 MS-MS of the 121 ion.

A closer analysis of the m/z 200-400 range of the mass spectra of the monomethoxy series does reveal the presence of several ion fragments of very low abundance that do appear to contain iodine based on mass abundances (Figure 105).

The EI MS below shows such fragment ion pairs at m/z 396, 278 and 247. These fragment ions likely form by the fragment pathways shown in scheme 44 below:

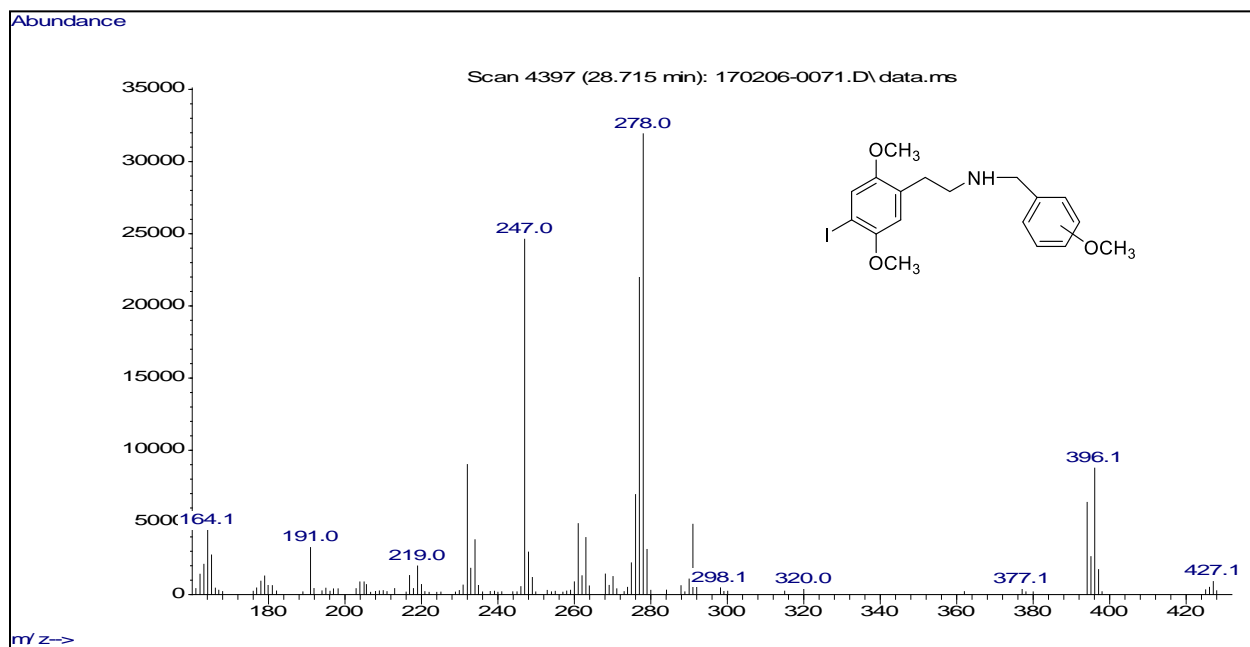
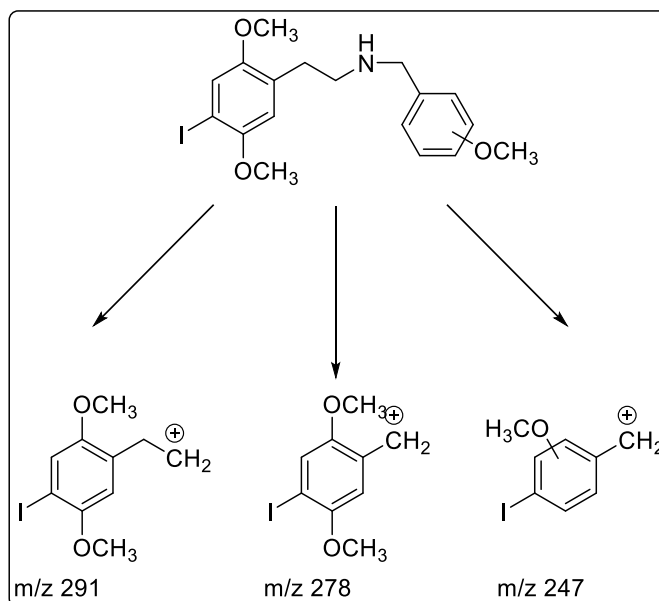


Figure 105 High mass region iodine-containing fragment ions in the EI-MS of the N-(monomethoxy)benzyl-4-iodo-2,5-dimethoxyphenethylamines.



Scheme 44 Proposed EI-MS fragmentation pathway for the N-(monomethoxy)benzyl-4-iodo-2,5-dimethoxyphenethylamines.

The EI-MS for the six dimethoxy regioisomers in this series are shown in Figure 106. Once again, all regioisomeric members of this subset of compounds derivatives (compounds 4-9) yielded nearly identical mass spectra as shown in Figure 106. The dominant ions in this series were observed at $m/z = 151$, 180 and 121 and none of these ions appear to contain iodine, as observed in the monomethoxy subseries and also the dimethoxy bromo NBOME series.

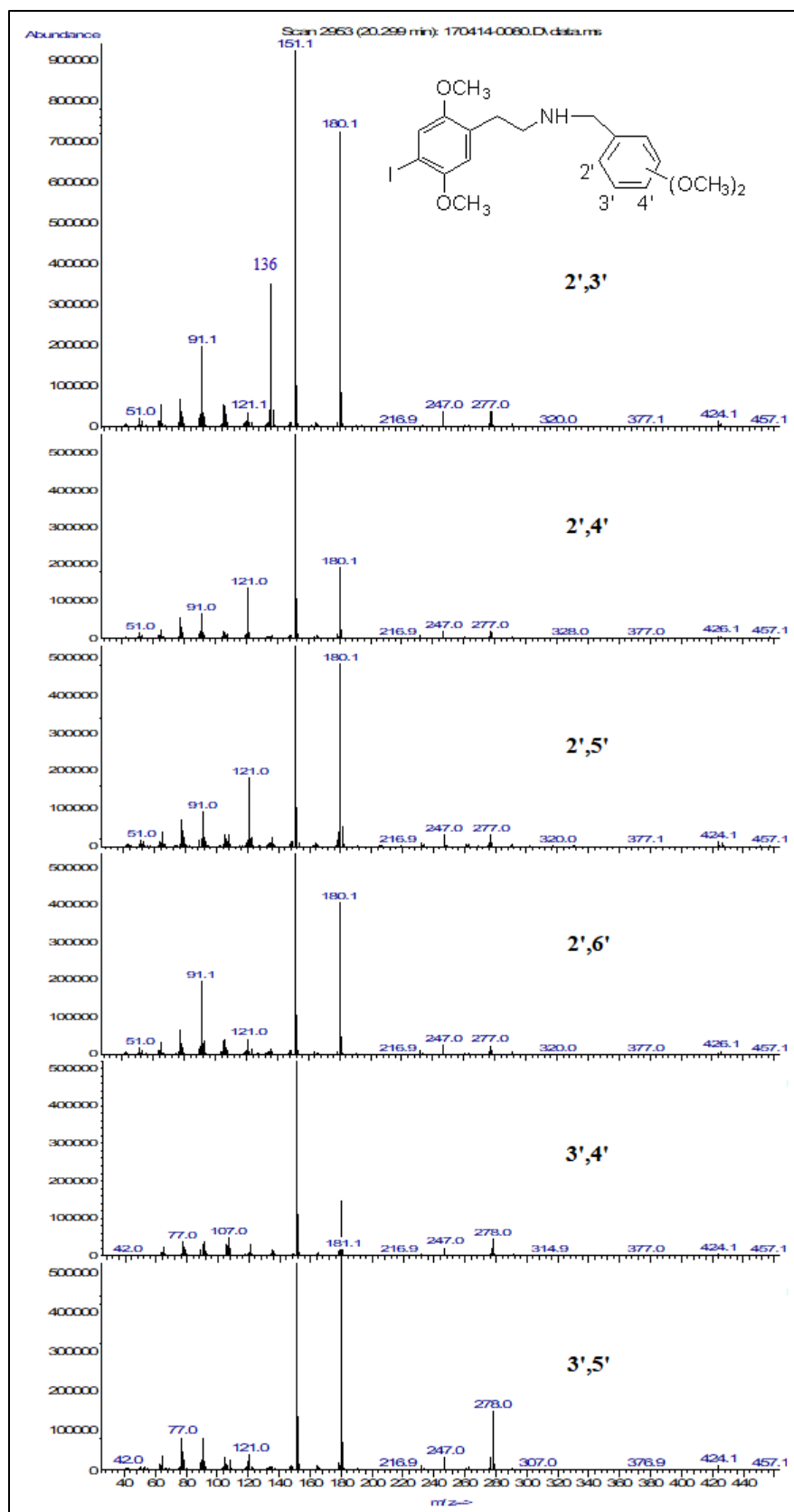


Figure 106 Mass Spectra of the N-(dimethoxy)benzyl-4-iodo-2,5-dimethoxyphenethylamines.

Also, like the monomethoxy subset, no molecular ion (M^+) was observed, however the molecular weight was confirmed by $M+1$ ion at 458 as shown in Figure 107.

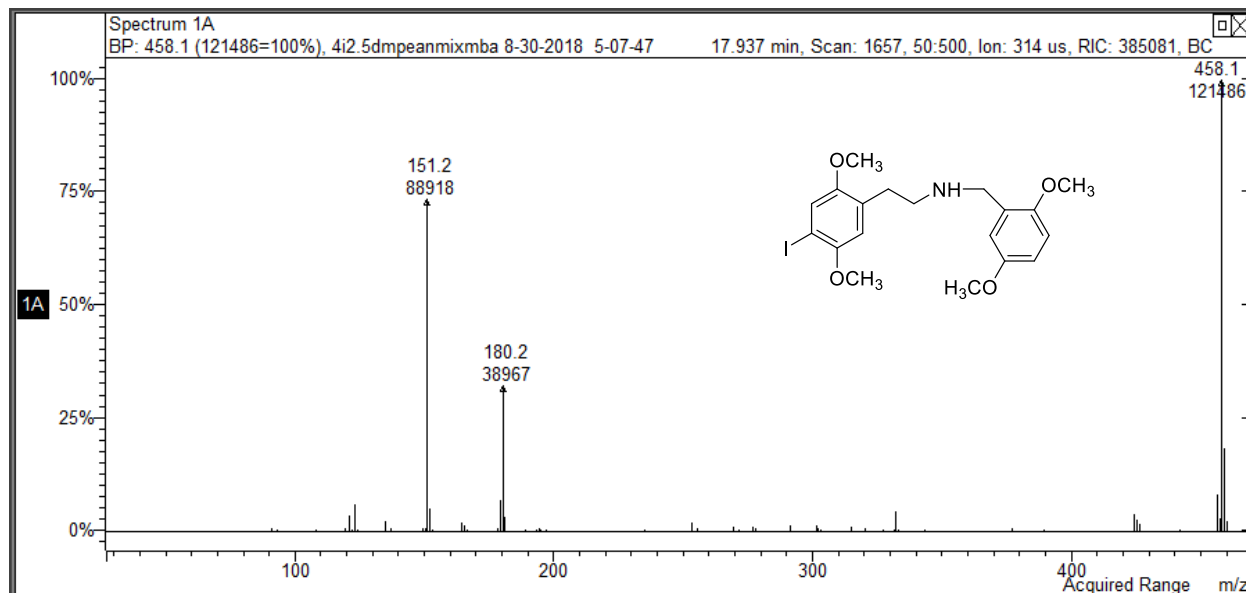
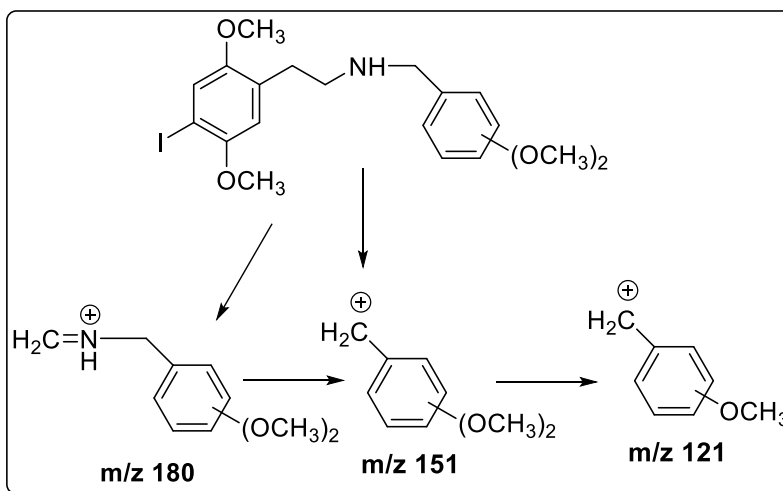


Figure 107 CI-MS of Mass Spectra of N-2,5-dimethoxybenzyl-4-iodo-2,5-dimethoxyphenethylamine.

The most abundant ions in the dimethoxy series at m/z 151, 180 and 121, each represent fragments 30 Da higher than the most abundant ions in the mass spectra of the monomethoxy compounds (m/z 121, 150 and 91). The mass difference between each of these ions is 30 Da, corresponding to the mass of a methoxy equivalent.



Scheme 45 Proposed EI-MS fragmentation pathway for the N-(dimethoxy)benzyl-4-iodo-2,5-dimethoxyphenethylamines.

Thus, it appears that the dimethoxy regioisomers undergo fragmentation under EI conditions similar to the monomethoxy compounds as illustrated in Scheme 45. The predominant ion at m/z 151 can be formed by the cleavage of the N-C bond yielding the dimethoxybenzyl cation. The ion at m/z 180 is likely the iminium cation formed by the dissociation of bond between α - and β -carbon atoms. Finally, the ion at m/z 121 appears to have formed from loss of CH_2O from the dimethoxy benzyl cation. In this series only the 2',3'-dimethoxy regioisomer gave a significant fragment at m/z 136. The structure of this fragment ion was discussed in Chapter 5.

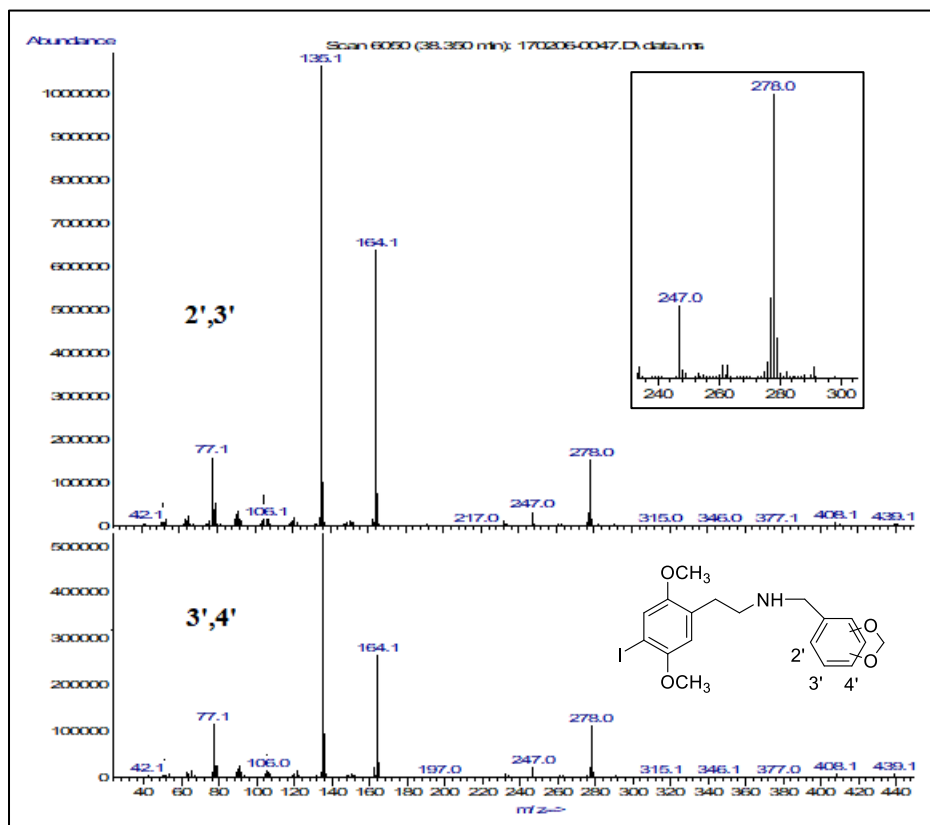


Figure 108 Mass Spectra of the N-(methylenedioxy)benzyl-4-iodo-2,5-dimethoxyphenethylamines.

The EI-MS for the two methylenedioxy regioisomers in this series are shown in Figure 108. Once again both regioisomeric members of this subset of compounds derivatives (compounds 10-11) yielded nearly identical mass spectra. The dominant ions in this series were observed at $m/z = 135$, 164 and 105 and none of these ions appear to contain iodine, as observed in the monomethoxy subseries.

Also, like the monomethoxy and dimethoxy subsets, no molecular ion (M) was observed, however the molecular weight was confirmed by M+1 ion at 442 as shown in Figure 109. The three most abundant ions in the methylenedioxy series (m/z 135, 164 and 105), each represent fragments 14 mass units higher than the most abundant ions in the mass spectra of the monomethoxy subset (m/z 121, 150 and 91) and 16 mass units lower than the most abundant ions in the mass spectra of the dimethoxy subset. The mass difference between each of these ions relative to the monomethoxy and dimethoxy compounds is precisely the difference in mass corresponding to the molecular weight differences in these three series (an additional 14 mass units corresponds to the addition of an oxygen atom with removal of two hydrogen atoms relative to the monomethoxy compounds, and a reduction in 16 mass units corresponds to the loss of a carbon and two hydrogen atoms relative to the dimethoxy compounds).

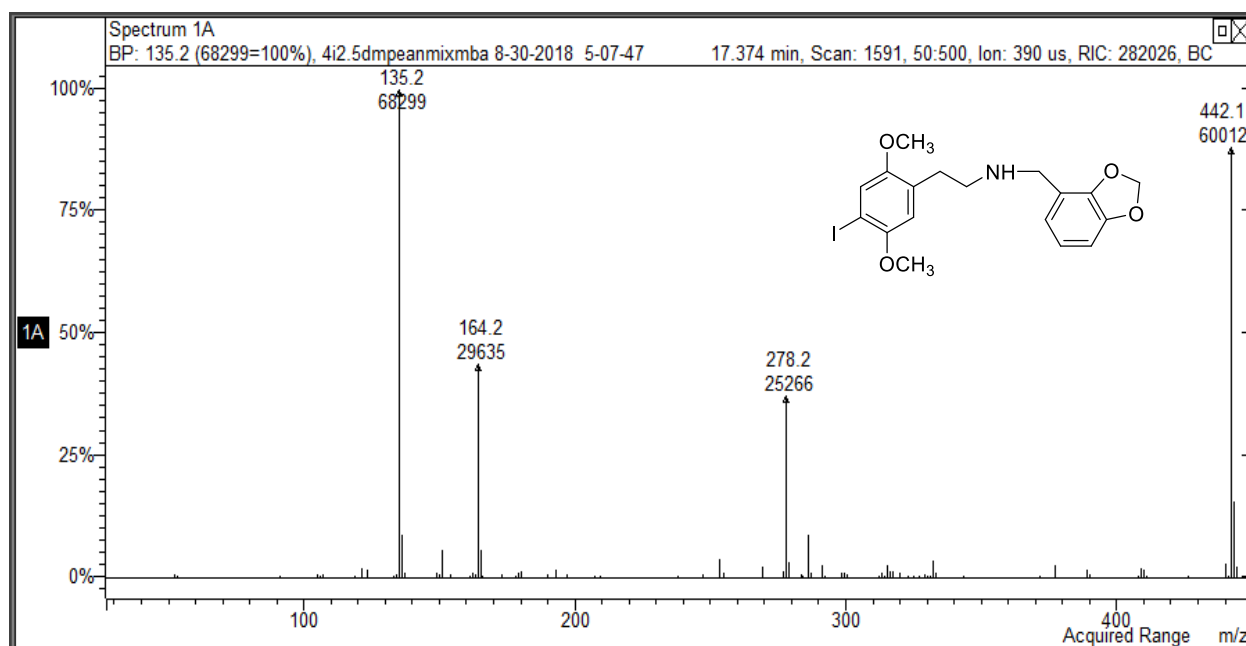
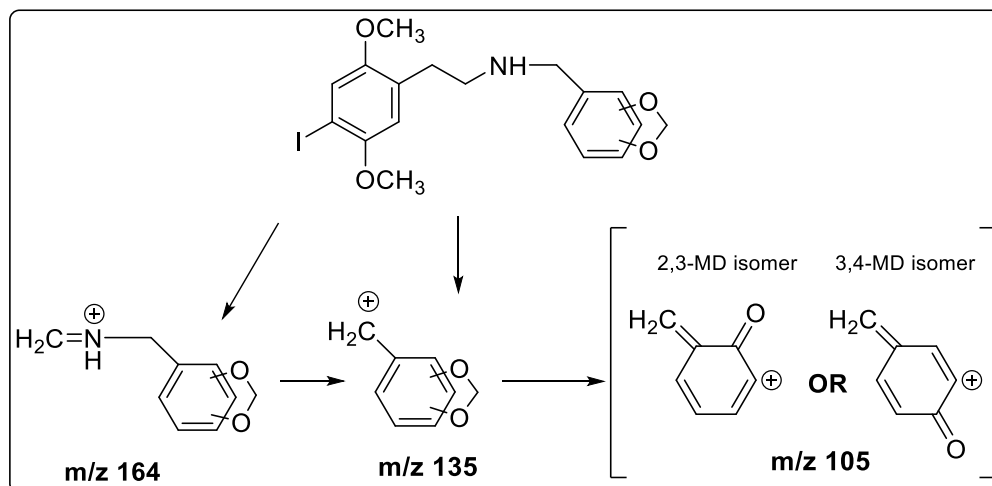


Figure 109 CI-MS of Mass Spectra N-(2,3-methylenedioxy)benzyl-4-iodo-2,5-dimethoxyphenethylamine series.

Thus, it appears that the methylenedioxy regioisomers undergo fragmentation under EI conditions similar to the monomethoxy compounds as illustrated in Scheme 46. Again, the predominant ion at m/z 135 can be formed by the cleavage of the N-C bond yielding 2-methylenedioxybenzyl cation and the ion at m/z 164 is likely the iminium cation formed by the dissociation of bond between α -

and β -carbon atoms. Finally, the ion at m/z 105 appears to have formed from loss of CH_2O from the methylenedioxy benzyl cation.



Scheme 46 Proposed EI-MS fragmentation pathway for the N-(methylenedioxy)benzyl-4-iodo-2,5-dimethoxyphenethylamines.

The mass spectra for the 11 compounds of this series demonstrate that all members appear to undergo the same fragmentation and that each subset can be differentiated from the other two subsets by the most abundant ions based on differences in the degree of methoxy substitution or methylenedioxy substitution. These spectra also demonstrate that the individual members of each structural subset cannot be differentiated based on their mass spectra. Thus, other analytical methods including GC separations and FTIR spectral analysis were explored for further differentiation within each regioisomeric subseries.

8.3 Gas Chromatographic Separations:

In an attempt to further differentiate the compounds in each of the three N-(substituted)benzyl-4-iodo-2,5-dimethoxyphenethylamine subsets, gas chromatographic separations of (monomethoxy)benzyl regioisomers subset were performed on Rxi[®]-17Sil MS 30m x 0.25mm ID capillary column. Separations were achieved over 33 minutes starting from initial temperature of

70 °C held for 1 minute then gradually increased to reach 250 °C at a rate of 30 °C/minute and held for 15 minutes then ramped up again to reach 340 °C at a rate of 10 °C/minute which held again for 2 minutes with elution over a 2 minute window. This set of chromatographic conditions yielded an excellent separation of all three regioisomers, with the 2'-methoxy isomer eluting before the 3'-isomer, and the 3'-isomer before the 4'-isomer (Figure 110). This same relative elution pattern was observed in the monomethoxy bromo NBOME series.

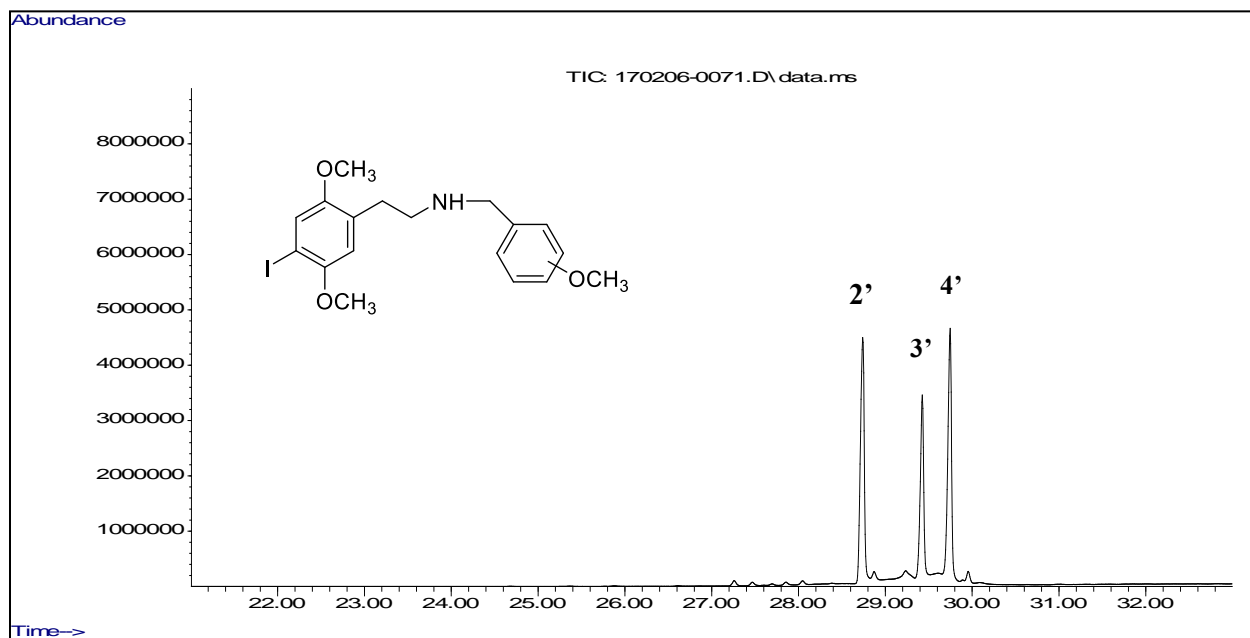


Figure 110 Gas chromatographic separation of the N-(monomethoxy)benzyl-4-iodo-2,5-dimethoxyphenethylamines.

Similar separations were achieved for all six of the dimethoxy regioisomers using the same capillary column but with different temperature program conditions. The temperature program started with initial temperature of 70 °C held for 1 minute then gradually increased to reach 290 °C at a rate of 30 °C/minute and held for 30 minutes with a total 38 minutes run time. The compounds eluted over a 5 minute window as shown in Figure 111. In this series those derivatives with a 2'-methoxy group (2',3'-, 2',4'-, 2',5'- and 2',6'-dimethoxy) eluted before the two regioisomers that did not contain a 2'-methoxy group. Also, the two derivatives with the greatest degree of steric crowding relative to the benzyl side chain (2,3- and 2,6-dimethoxy) eluted prior to all other members of the series. This is the same relative elution pattern that was observed in the dimethoxy bromo NBOME series.

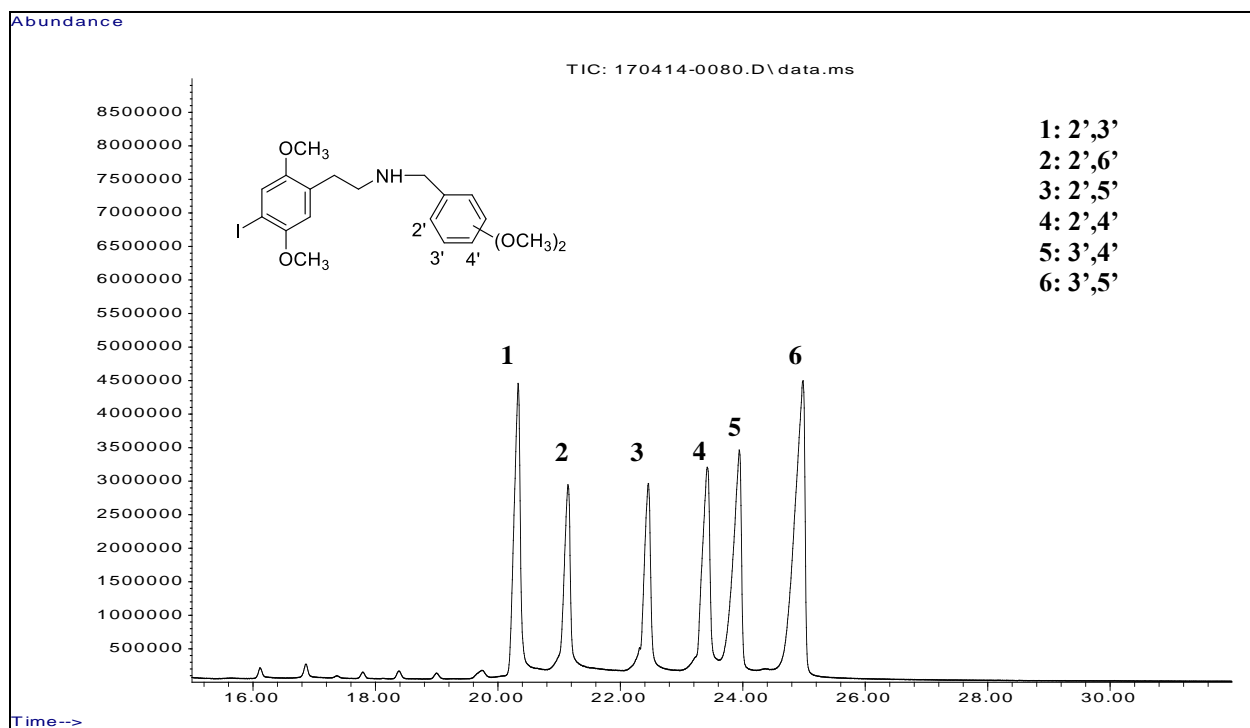


Figure 111 Gas chromatographic separation of the N-(dimethoxy)benzyl-4-iodo-2,5-dimethoxyphenethylamines.

Lastly, the last chromatogram (Figure 112) shows the separation of the two methylenedioxy regioisomers. The temperature program started with initial temperature of 70 °C held for 1 minute then gradually increased to reach 250 °C at a rate of 30 °C/minute and held for 25 minutes then ramped up again to reach 340 °C at a rate of 15 °C/minute and held for 10 minutes with a total 48 minutes run time. In this series 2',3'-methylenedioxy eluted before 3',4'-methylenedioxy regioisomer the two regioisomers under similar separation condition as above. This is the same relative elution pattern that was observed in the dimethoxy bromo NBOME series.

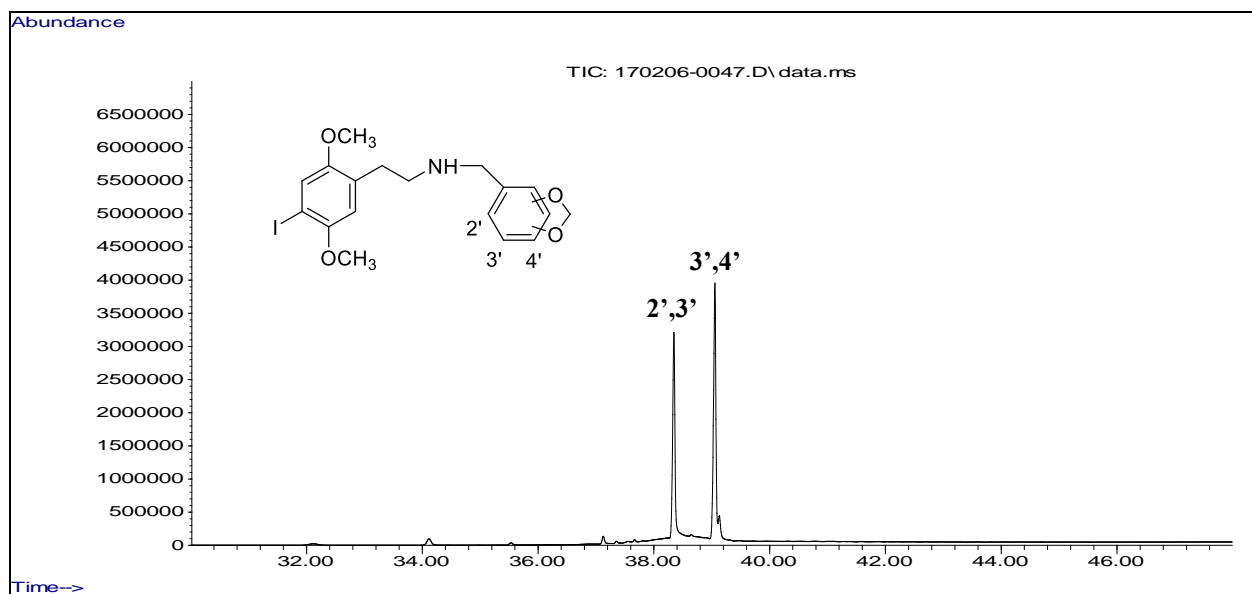


Figure 112 Gas chromatographic separation of the N-(methylenedioxy)benzyl-4-iodo-2,5-dimethoxyphenethylamines.

9 The N-(Methoxy)benzyl-, N-(Dimethoxy)benzyl- and N-(Methylenedioxy)benzyl-dimethoxyphenpropylamine Series

9.1 Introduction:

The primary compounds of N-(methoxy)benzyl-dimethoxyphenpropylamine series are simplified derivatives of the NBOMes where the halogen atom is eliminated from the structure and there are two methoxy substituents on 2 and 5 positions of the phenpropyl aromatic ring and the substitution pattern on the aromatic ring of the N-benzyl substituent is modified yielding the 11 compounds in Figure 113. This series can be divided into three subsets. The first subset includes 2-, 3-, and 4-monomethoxy regioisomers (structures 1-3).

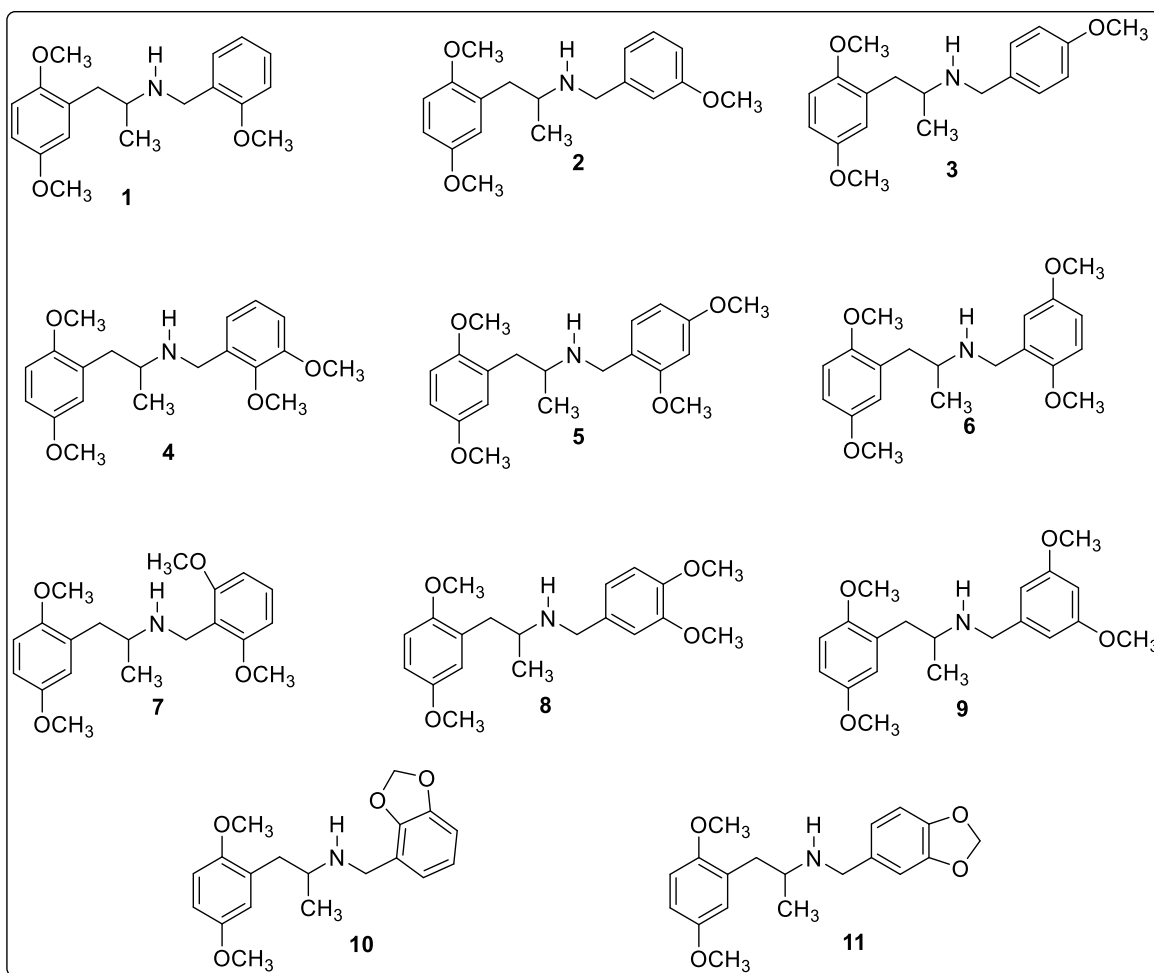


Figure 113 Structures of the N-(methoxy)benzyl-dimethoxyphenpropylamine Series.

In the second subset the N-benzyl aromatic ring is modified to include two methoxy groups at every possible position. Thus, this subset includes six regioisomeric compounds, the 2,3-, 2,4-, 2,5-, 2,6-, 3,4- and 3,5-dimethoxy regioisomers (structures 4-9). In the third subset in this series the N-benzyl aromatic ring is modified to contain the two possible methylenedioxy substitution patterns (structures 10-11). The N-benzyl substitution patterns selected for this series represent potential designer modifications since this functionality is commonly found in drugs of abuse.

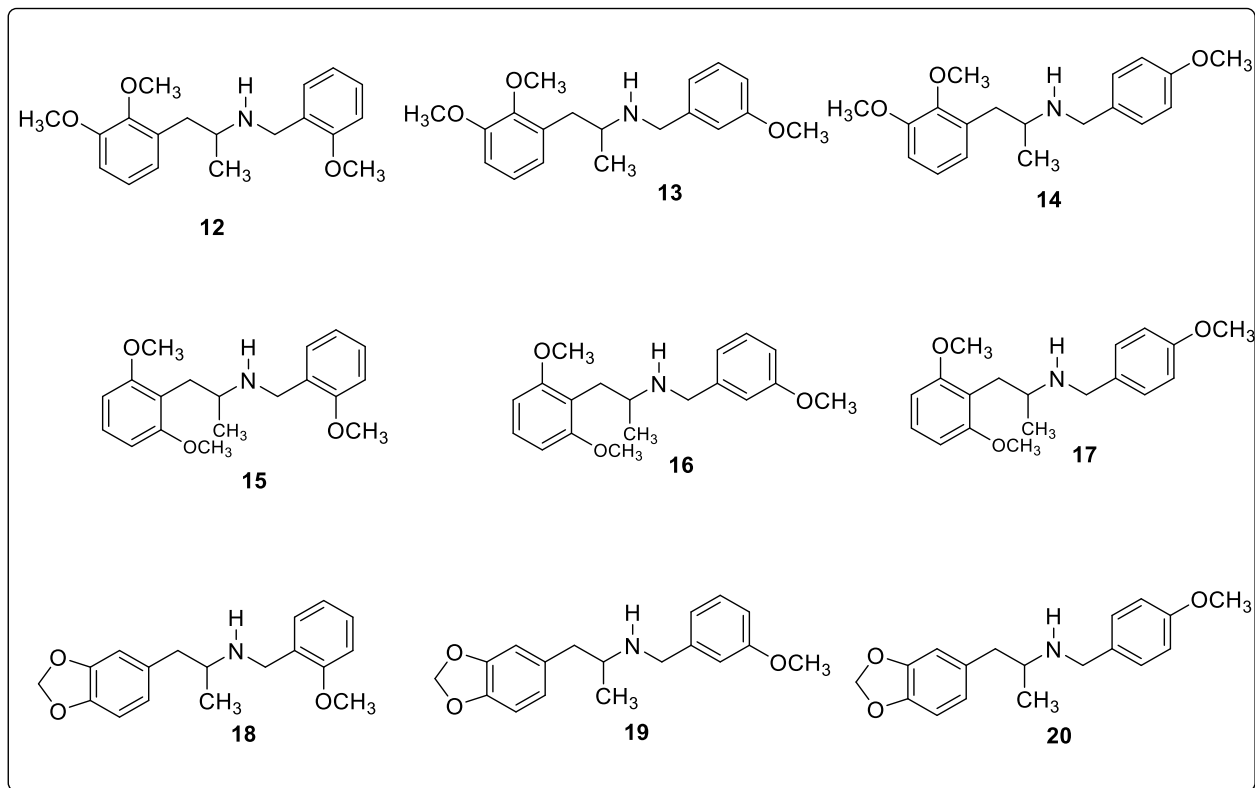


Figure 114 Structures of the N-(methoxy)benzyl-dimethoxyphenpropylamine and N-(methoxy)benzyl-methylenedioxyphenpropylamine Series.

Three additional subsets of derivatives of this basic structural class were also synthesized for analytical comparisons. The first and second subsets (compounds 12-17) of this additional series are a simplified derivatives of the NBOMes where the dimethoxy substitution pattern on the phenpropylamine aromatic ring was changed from the 2,5-positions to the 2,3- and 2,6- positions, respectively, while the substitution pattern on the aromatic ring of the N-benzyl substituent is modified to include only 2'-, 3'-, and 4'-monomethoxy regioisomers, yielding a total of 6 compounds (Figure 114). The third subset of derivatives (compounds 18-20) in this additional

series are also NBOMes analogues where the 2,5-dimethoxy substitution pattern on the phenpropylamine aromatic ring is replaced with a 3,4-methylenedioxy group, and the N-benzyl substituent contains a single methoxy group at the 2'-, 3'-, or 4'-positions, yielding three compounds (Figure 114). These methylenedioxy derivatives were prepared because this substitution pattern is common in a number of drugs of abuse families including the MDMA and the cathinones.

9.2 Mass Spectral Analysis:

The EI-MS of all members of this series of compounds are shown in Figures 115 – 117, 120, 122, 124. All three regioisomeric members of the (monomethoxy)benzyl subset of derivatives (compounds 1-3, 12-17) yielded nearly identical mass spectra as shown in Figure 115-117. As reported for other 25-NBOMe compounds, the dominant ions in GC-MS spectrum of the 2'-, 3'- and 4'-monomethoxy derivatives in this series are observed at $m/z = 121$, 164 and 91, with the base peak m/z 121 (Figure 115 - 117). The m/z 91 ion was present in the highest abundance in the 2'-methoxy isomer and decreased in the 3'- and 4'-methoxy isomers. The molecular ion (M) is not apparent in the EI-MS spectrum, however the mass was confirmed by CI-MS (Figure 118) where a M+1 ion of 315.

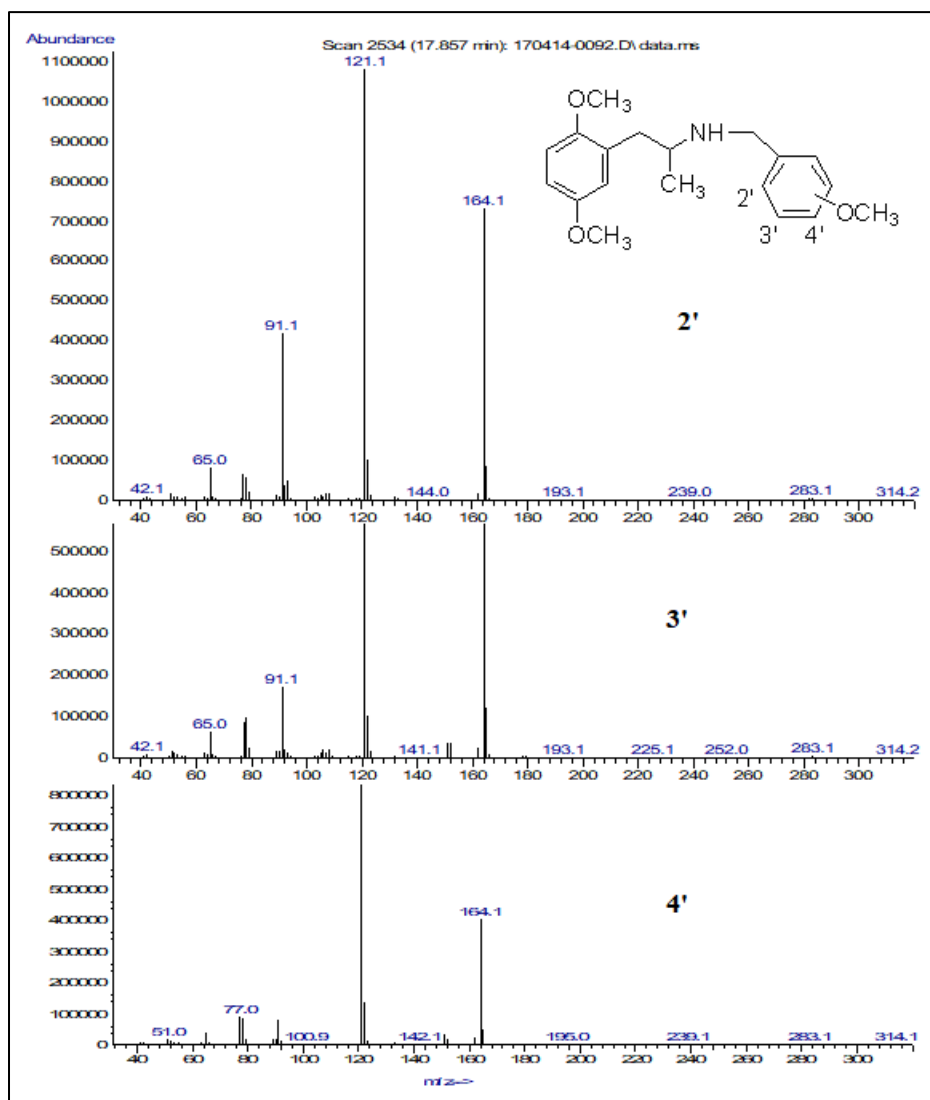


Figure 115 Mass Spectra of the N-(monomethoxy)benzyl-2,5-dimethoxyphenylpropylamines.

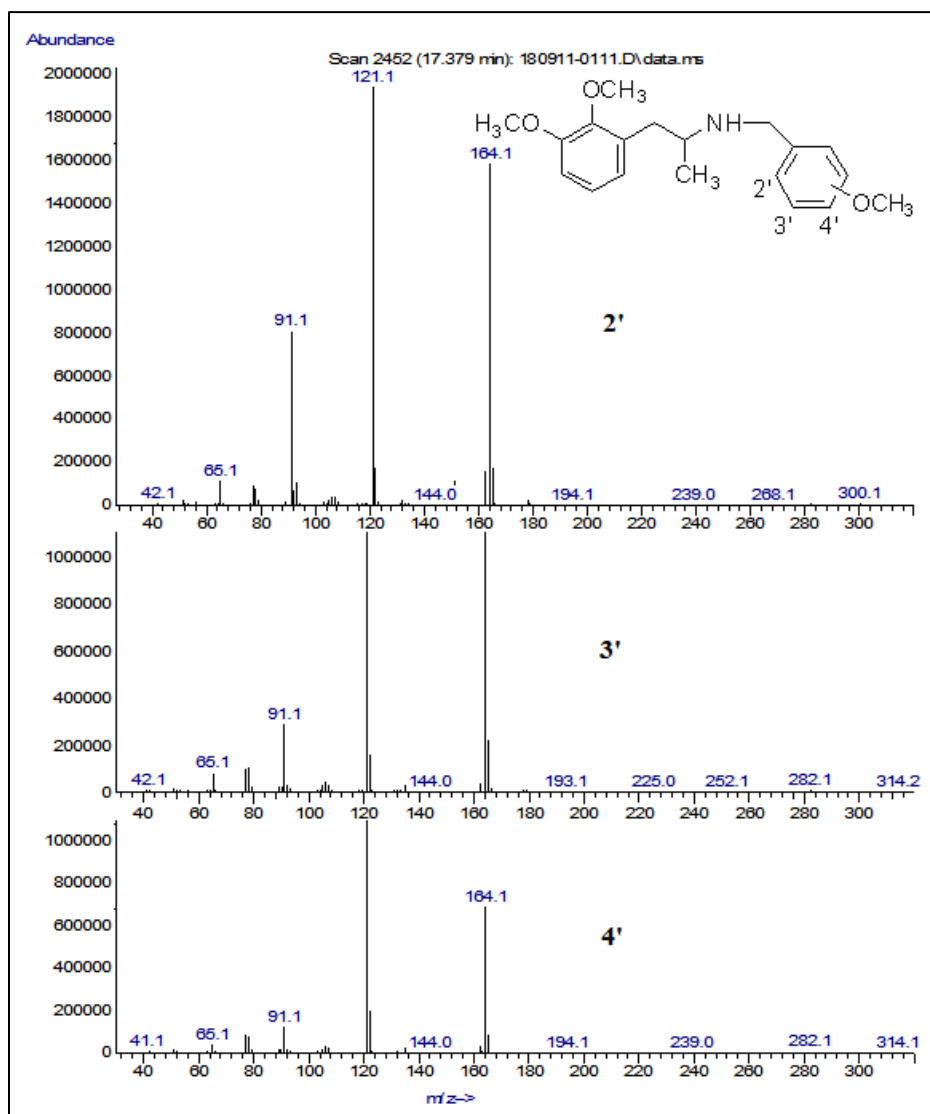


Figure 116 Mass Spectra of the N-(monomethoxy)benzyl-2,3-dimethoxyphenylpropylamines.

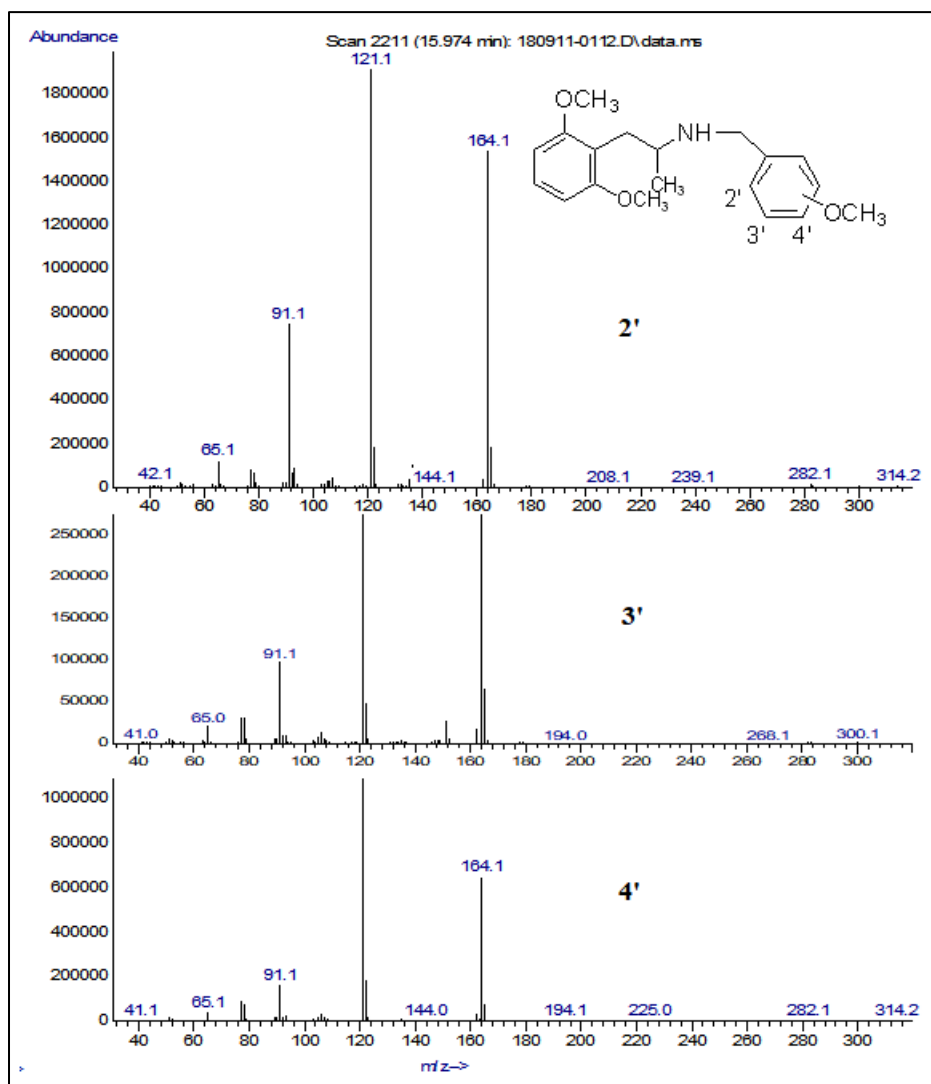


Figure 117 Mass Spectra of the N-(monomethoxy)benzyl-2,6-dimethoxyphenylpropylamines.

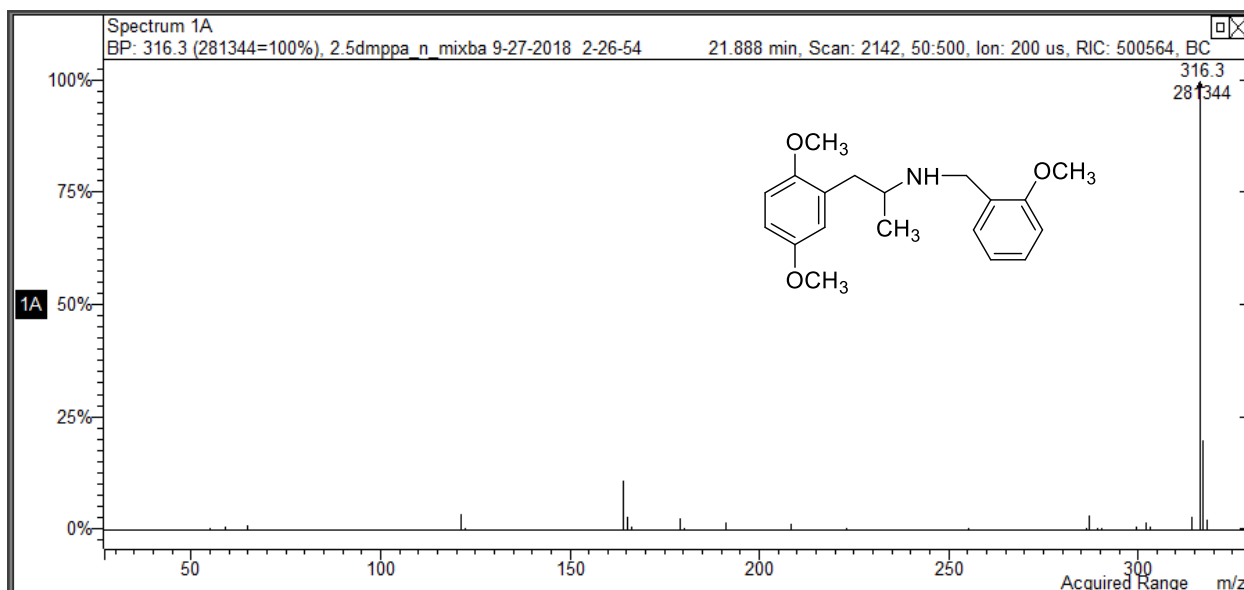
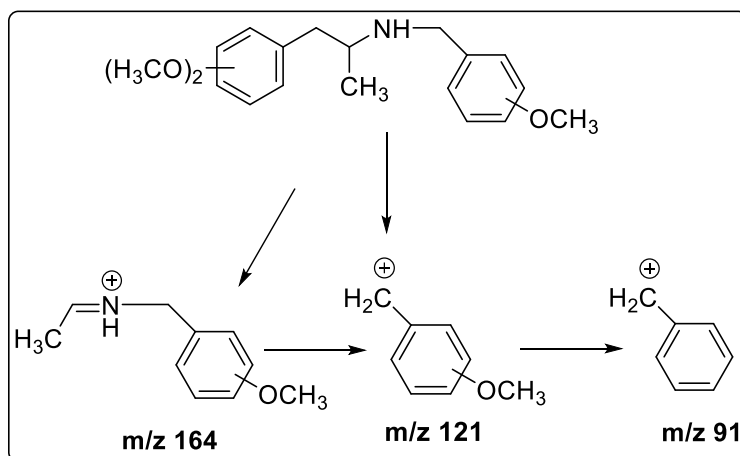


Figure 118 CI-MS of mass spectra of the N-2'-methoxybenzyl-2,5-dimethoxyphenpropylamines.

A proposed fragmentation pathway showing the dominant ions for the monomethoxy subseries of compounds is shown in Scheme 47 and is consistent with the NBOME derivatives reported in the previous chapters. The base peak m/z 121 can be formed by the cleavage of the N-C bond yielding 2-methoxybenzyl cation. The ion at m/z 164 is likely the iminium cation formed by the dissociation of bond between α - and β -carbon atoms, a common pathway for phenethylamine compounds. Finally, the ion at m/z 91 appears to have formed from loss of CH_2O from the methoxy benzyl cation.



Scheme 47 Proposed EI-MS fragmentation pathway for the N-(monomethoxy)benzyl-dimethoxyphenpropylamines.

Support for this fragmentation pathway was provided by MS-MS studies which demonstrate that the m/z 91 ion is formed from the m/z 121 fragment as shown in Figure 119.

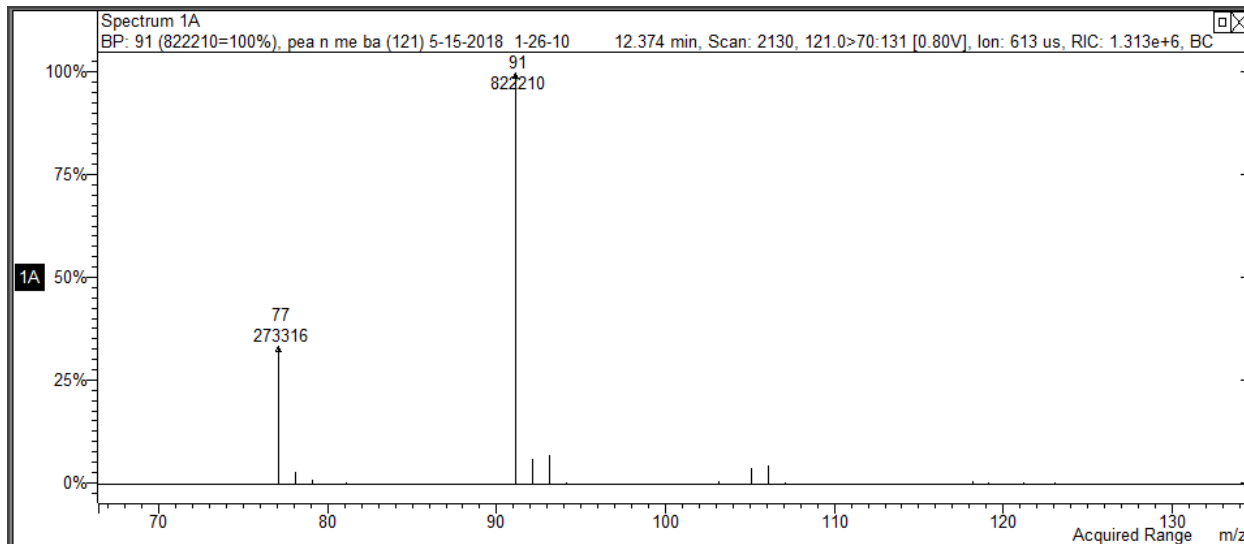


Figure 119 MS-MS of the 121 ion.

The EI-MS for the 3,4-methylenedioxy regioisomers in this series are shown in Figure 120. Once again both regioisomeric members of this subset of compounds derivatives (compounds 18-20) yielded nearly identical mass spectra. The dominant ions in this series were observed at $m/z = 121$, 164 and 91, as shown in Figures 120. The molecular ion (M) is not apparent in the EI-MS spectrum of any of these compounds, however the molecular mass was confirmed by CI-MS where a M+1 ion of 299 was present (Figure 121).

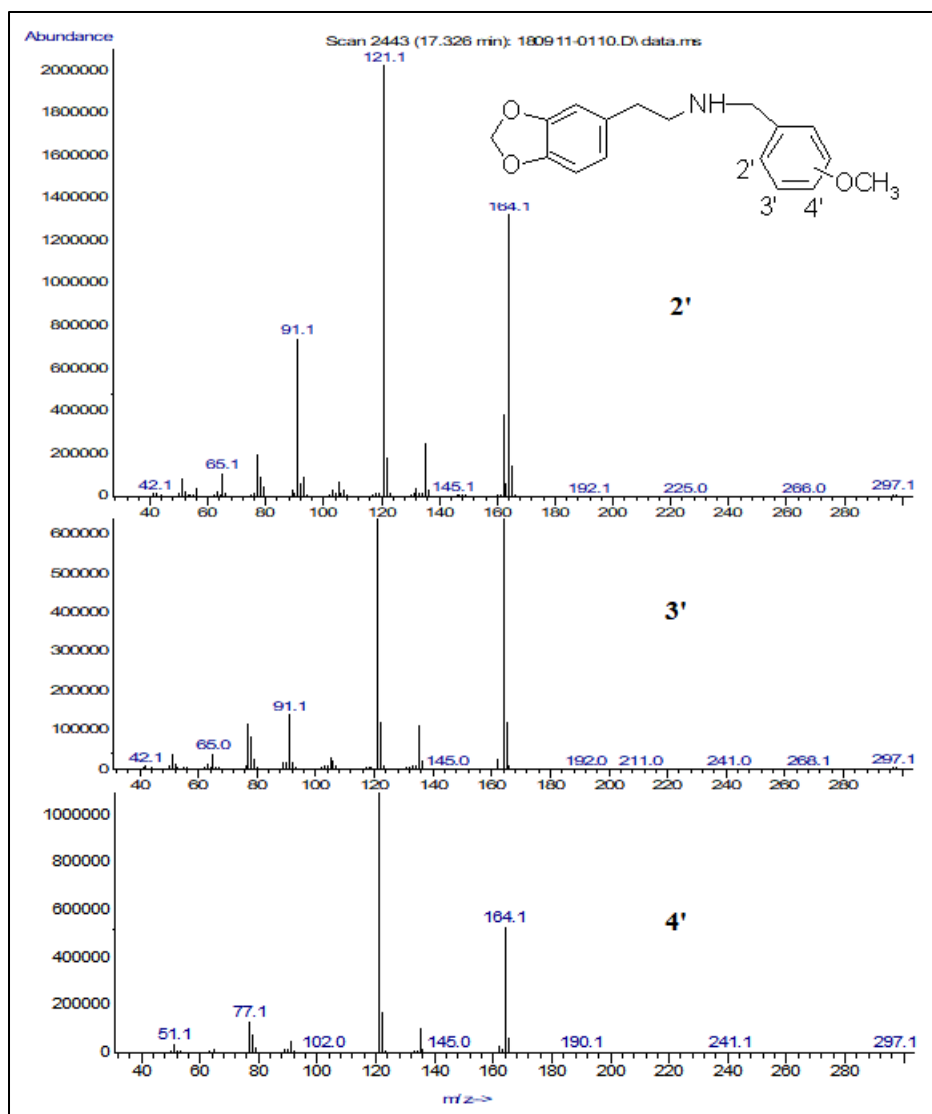


Figure 120 Mass Spectra of the N-(monomethoxy)benzyl-3,4-methylenedioxyphenylpropylamines.

As reported with the N-(monomethoxy)benzyl-dimethoxyphenylpropylamines compounds earlier the dominant ions in GC-MS spectrum of all three compounds in this series are almost identical at $m/z = 121$, 164 and 91, with the base peak m/z 121 (Figure 120). The m/z 91 ion was present in the highest abundance in the 2'-methoxy isomer and decreased in the 3'- and 4'-methoxy isomers. Other than the relative abundance of the m/z 91 ions, there are no other features in the mass spectra of these regioisomers which allows for specific differentiation.

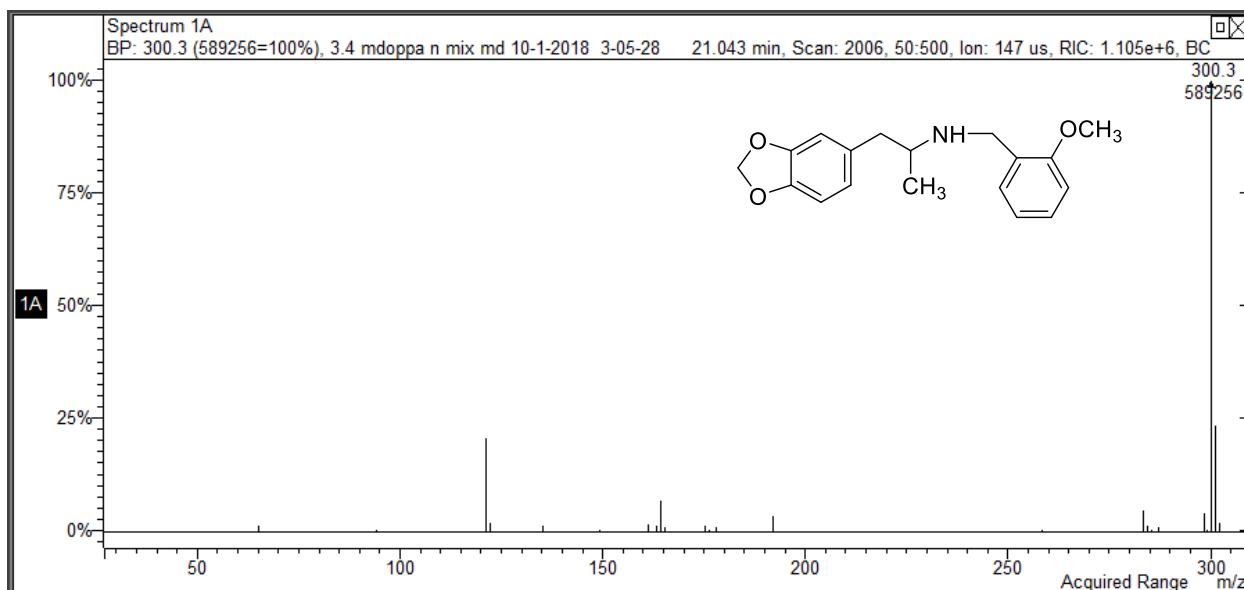
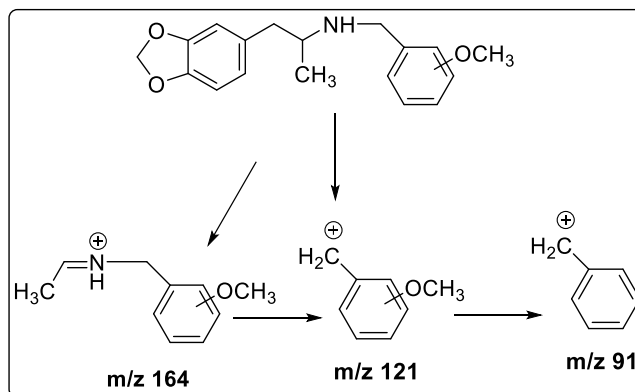


Figure 121 CI-MS of Mass Spectra N-(2'-methoxy)benzyl-3,4-methylenedioxyphenylamine series.

Thus, it appears that the methylenedioxy regioisomers undergo fragmentation under EI conditions similar to the dimethoxy compounds as illustrated in Scheme 48. Again, the predominant ion at m/z 121 can be formed by the cleavage of the N-C bond yielding 2-methoxybenzyl cation and the ion at m/z 164 is likely the iminium cation formed by the dissociation of bond between α - and β -carbon atoms. Finally, the ion at m/z 91 appears to have formed from loss of CH_2O from the methylenedioxy benzyl cation.



Scheme 48 Proposed EI-MS fragmentation pathway for the N-(monomethoxy)benzyl-3,4-methylenedioxyphenylamines.

In an attempt to investigate the fragmentation pathways for this series of compounds in more detail a number of structurally simplified derivatives were prepared and analyzed. The derivatives prepared included compound 21-23 which contains no methoxy substituents in either the benzyl or phenethyl aromatic rings (Figure 122).

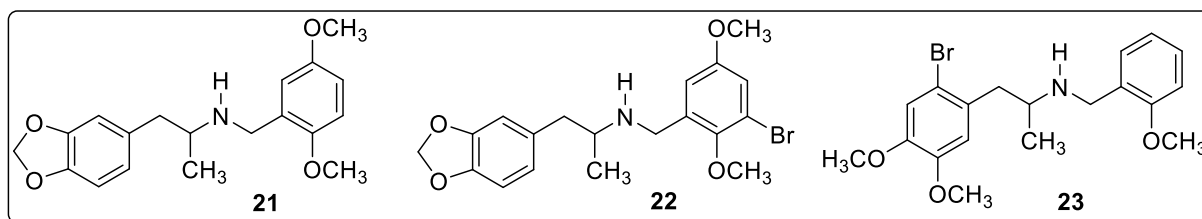


Figure 122 Structures of the simplified derivatives.

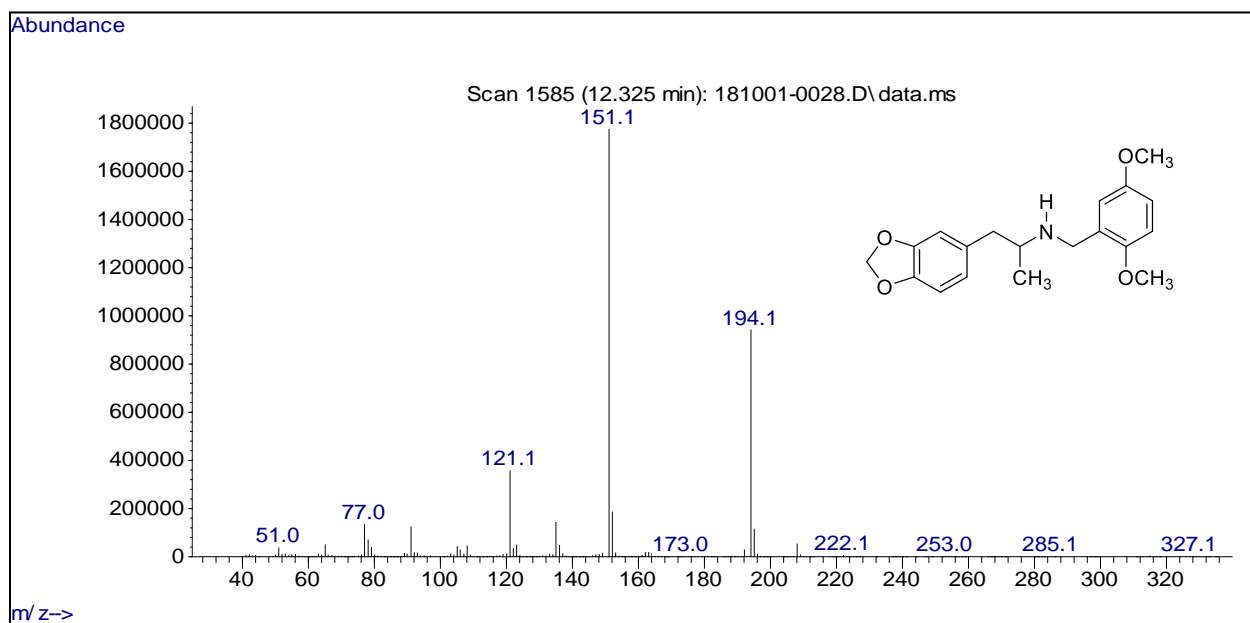


Figure 123 EI-MS of Mass Spectra of the N-(2',5'-dimethoxy)benzyl-3,4-methylenedioxyphenylamines (Compound 21).

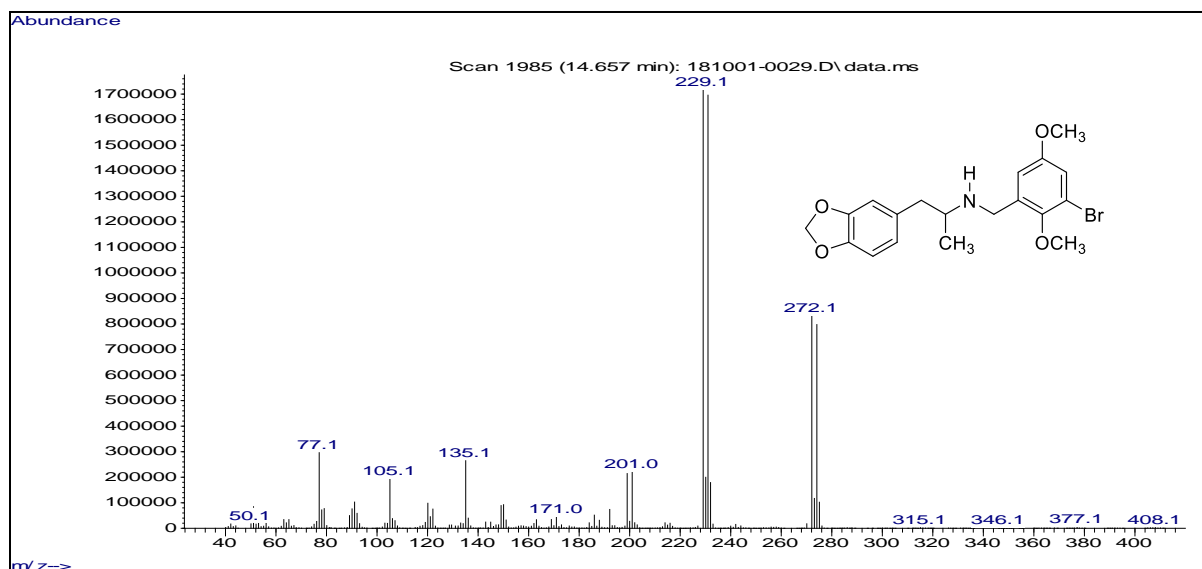


Figure 124 EI-MS of Mass Spectra of the N-(4'-Bromo-2',5'-dimethoxy)benzyl-3,4-methylenedioxyphenpropylamines (Compound 22).

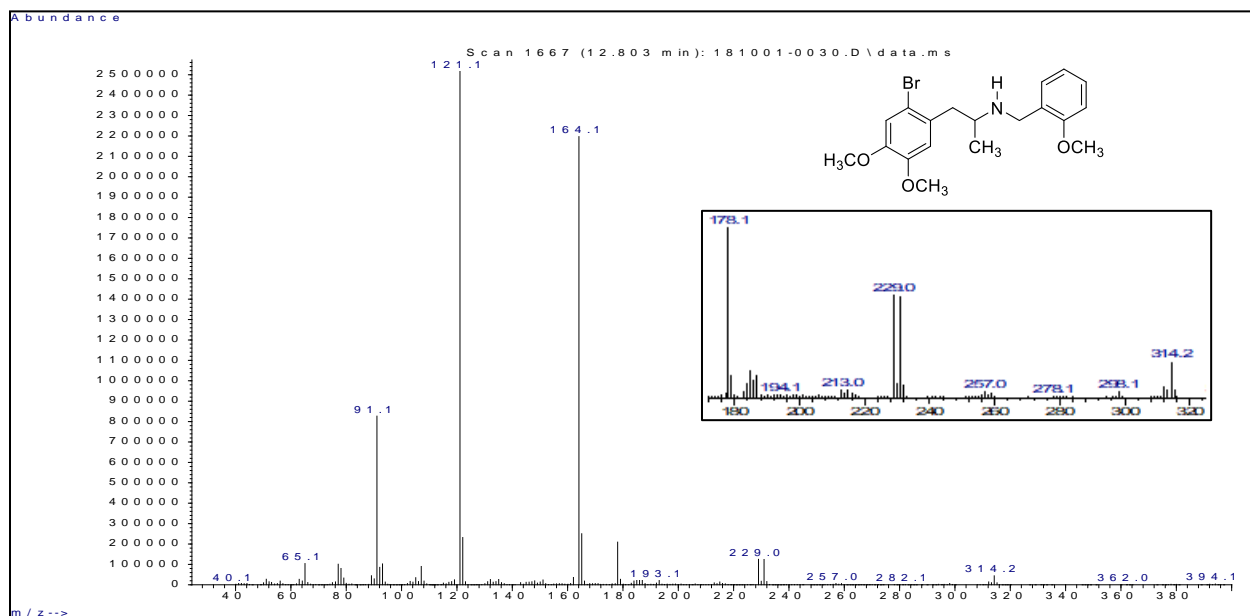
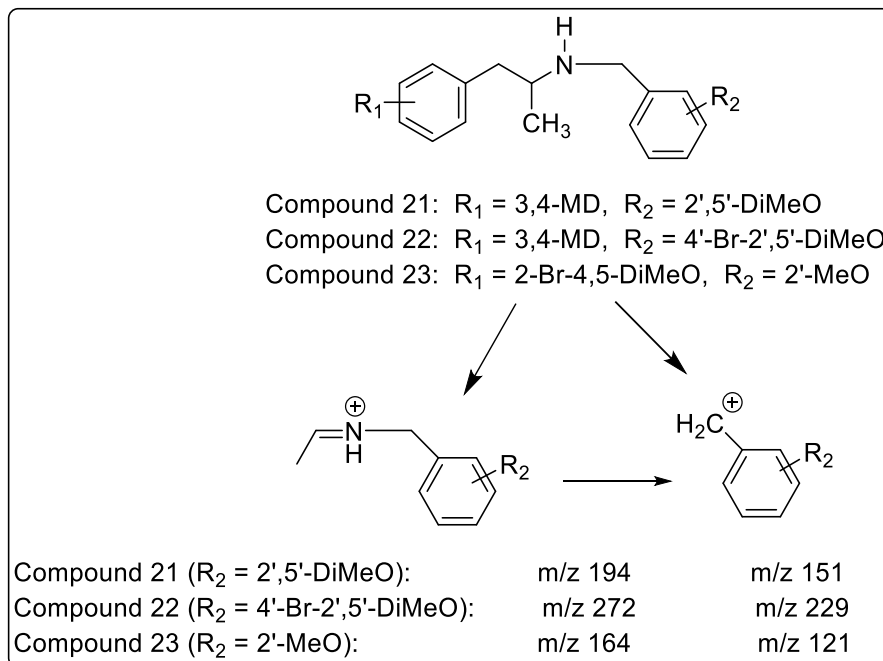


Figure 125 EI-MS of Mass Spectra of the N-(2'-monomethoxy)benzyl-2-Bromo-4,5-dimethoxyphenpropylamine (Compound 23).

The EI-MS of these compounds are shown in Figures 123-125. If the fragmentation pathway shown in Scheme 47 and 48 is accurate and characteristic for compounds of this structure class, then compounds 21-23 would be expected to yield ions of high abundance as shown in Scheme

49. Since compounds 21 have a benzyl dimethoxy substituent they would be expected to give an iminium cation at m/z 194 by phenethyl side α -/ β -carbon bond dissociation, consistent with the fragmentation pathways in Scheme 47-49. This ion is present in the MS of compounds 21 and it is 30 mass units higher than observed for derivatives containing a single methoxy substituent in the benzyl ring (Figures 123). On the other hand, 22 which contains one bromine atom and two benzyl methoxy substituents would be expected to give an iminium cation at m/z 272, as is present in the EI-MS (Figure 124). Finally, compounds 23 would be expected to show similar fragments to compounds 1-3,12-20 since they share the exact substitution pattern of a single methoxy substituent in the benzyl ring.

The base peak at m/z 121 ion present in the spectra of all twelve N-(methoxy)benzyl-dimethoxyphenpropylamines (compounds 1-3,12-20) was proposed to be the 2-methoxybenzyl cation formed by cleavage of the N-C bond. Again, if the original fragmentation pathway shown in Scheme 47-48 is accurate and characteristic for compounds of this structure class, then compounds 21 would be expected to give benzyl cation base peaks as shown in Scheme 49. Since compounds 21 have a benzyl dimethoxy substituent, they would be expected to give a benzyl cation base peak at m/z 121. This ion is present in the EI-MS of both compounds 21 and is 30 mass units higher (m/z 121) than observed for 12 regioisomers containing a methoxy substituent in the benzyl ring (Figures 123). On the other hand, compound 22 contains one bromine atom and two methoxy substituents in the benzyl ring. Therefore, it would be expected to give a benzyl cation base peak at m/z 229, 78 mass units higher than the 12 compounds of the N-(methoxy)benzyl-dimethoxyphenpropylamine series. Finally, compound 23 contains a single methoxy substituent in the benzyl ring. Therefore, it would be expected to give the same benzyl cation base peak at m/z 121 regardless of the substituents on the aromatic ring of the phenpropylamine. Therefore EI-MS analysis of these structurally modified derivatives supports the original fragmentation pathway proposed in Scheme 47-48 and demonstrates that compounds of this series undergo characteristic fragmentation.



Scheme 49 Proposed EI-MS fragmentation pathway for Compounds 25-27.

In conclusion, all the twelve compounds (Compounds 1-3, 12-20) of the N-(monomethoxy)benzyl series can't be distinguished from each other just by simply looking at their mass spectra. Therefore, other techniques are needed

The EI-MS for the six dimethoxy regioisomers in this series are shown in Figure 126. Once again, all regioisomeric members of this subset of compounds derivatives (compounds 4-9) yielded nearly identical mass spectra as shown in Figure 126. The dominant ions in this series were observed at $m/z = 151$, 194 and 121 and none of these ions appear to contain bromine, as observed in the monomethoxy subseries. Also, like the monomethoxy subset, no molecular ion (M) was observed, however the molecular weight was confirmed by M+1 ion at 345 as shown in Figure 127.

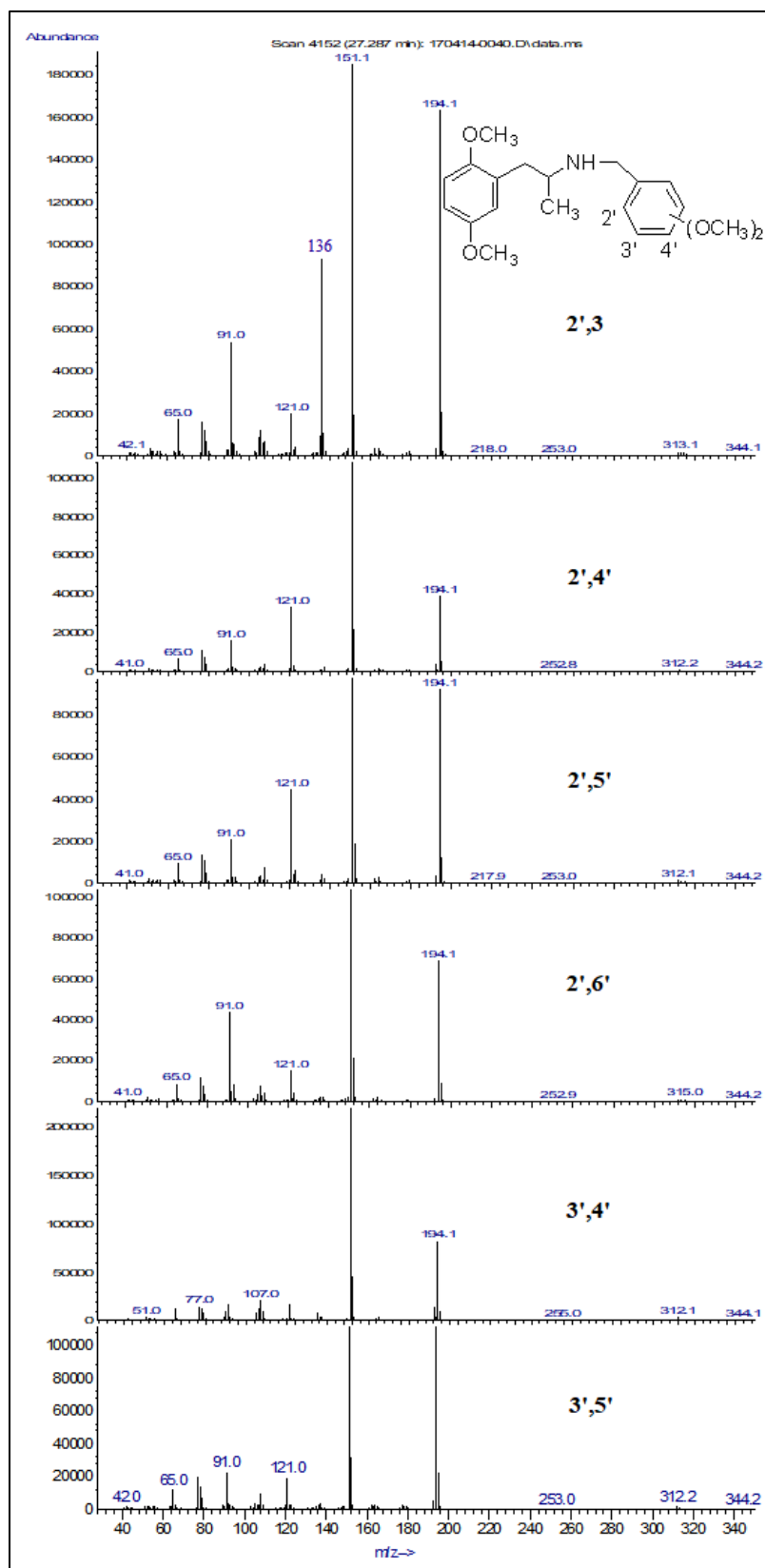


Figure 126 Mass Spectra of the N-(dimethoxy)benzyl-2,5-dimethoxyphenylamines.

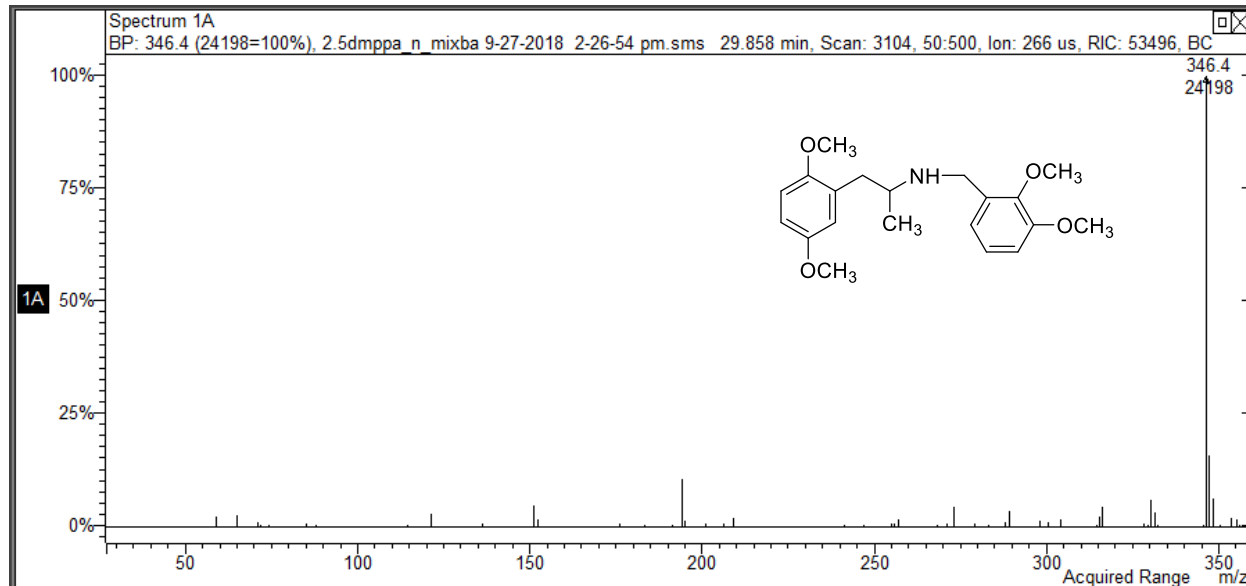
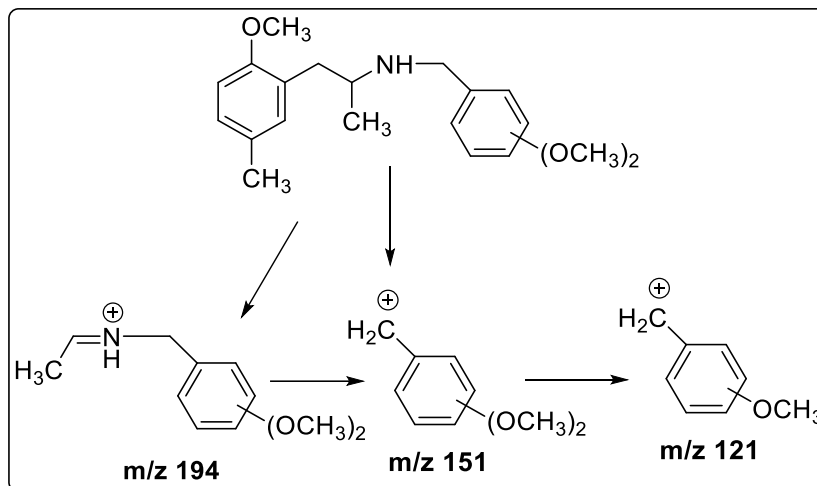


Figure 127 CI-MS of Mass Spectra of N-2,3-dimethoxybenzyl-2,5-dimethoxyphenpropylamine.

The most abundant ions in the dimethoxy series at m/z 151, 194 and 121, each represent fragments 30 Da higher than the most abundant ions in the mass spectra of the monomethoxy compounds (m/z 121, 164 and 91). The mass difference between each of these ions is 30 Da, corresponding to the mass of a methoxy equivalent. Thus, it appears that the dimethoxy regioisomers undergo fragmentation under EI conditions similar to the monomethoxy compounds as illustrated in Scheme 50. The predominant ion at m/z 151 can be formed by the cleavage of the N-C bond yielding the dimethoxybenzyl the cation. The ion at m/z 194 is likely the iminium cation formed by the dissociation of bond between α - and β -carbon atoms. Finally, the ion at m/z 121 appears to have formed from loss of CH_2O from the dimethoxy benzyl cation.



Scheme 50 Proposed EI-MS fragmentation pathway for the N-(dimethoxy)benzyl-2,5-dimethoxyphenpropylamines.

In this series only the 2',3'-dimethoxy regioisomer gave a significant fragment at m/z 136. This fragment ion was also observed in the N-(dimethoxy)benzyl-2,5-dimethoxyphenethylamine series as described in Chapter 5, as well as the corresponding 4-bromo- and 4-iodo derivatives (Chapters 6 and 8). The structure of this fragment ion was established by GC-TOF-MS and deuterium labeling studies described in Chapter 10.

Finally, The EI-MS for the two methylenedioxy regioisomers in this series are shown in Figure 128. Once again both regioisomeric members of this subset of compounds derivatives (compounds 10-11) yielded nearly identical mass spectra. The dominant ions in this series were observed at m/z = 135, 178 and 105, as observed in the monomethoxy subseries. Also, like the monomethoxy and dimethoxy subsets, no molecular ion (M) was observed, however the molecular weight was confirmed by an M+1 ion at 329 as shown in Figure 129.

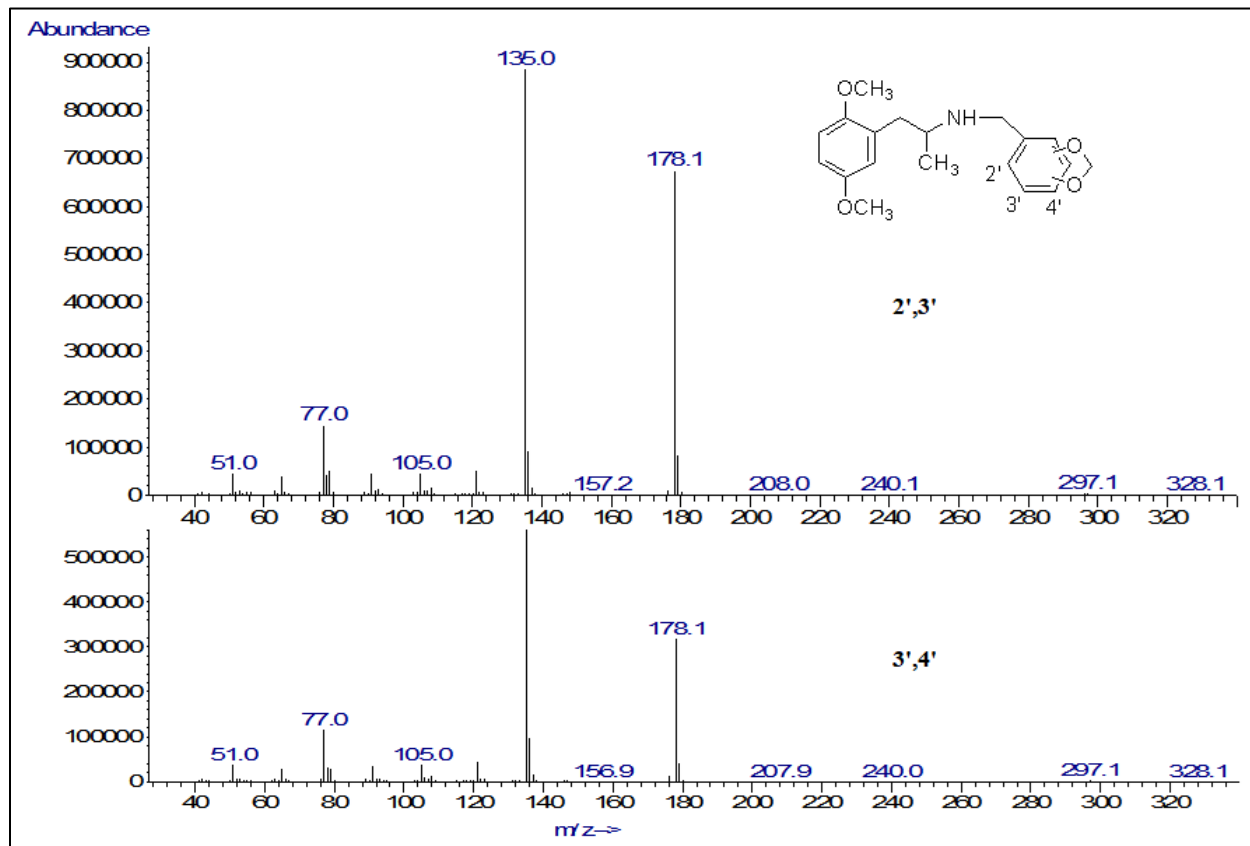


Figure 128 Mass Spectra of the N-(methylenedioxy)benzyl-2,5-dimethoxyphenylpropylamines.

The three most abundant ions in the methylenedioxy series (m/z 135, 178 and 105), each represent fragments 14 mass units higher than the most abundant ions in the mass spectra of the monomethoxy subset (m/z 121, 164 and 91) and 16 mass units lower than the most abundant ions in the mass spectra of the dimethoxy subset. The mass difference between each of these ions relative to the monomethoxy and dimethoxy compounds is precisely the difference in mass corresponding to the molecular weight differences in these three series (an additional 14 mass units corresponds to the addition of an oxygen atom with removal of two hydrogen atoms relative to the monomethoxy compounds, and a reduction in 16 mass units corresponds to the loss of a carbon and two hydrogen atoms relative to the dimethoxy compounds).

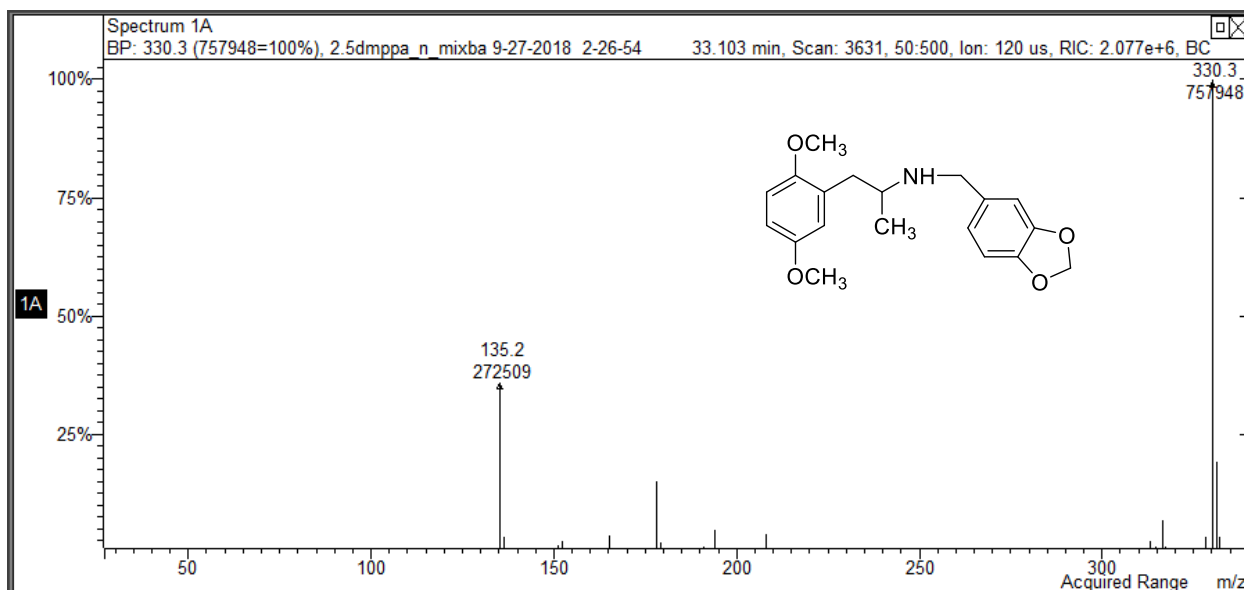
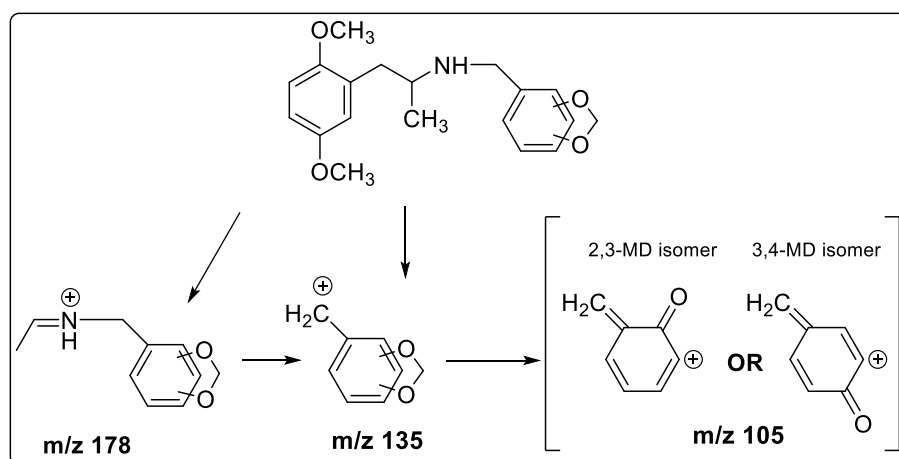


Figure 129 CI-MS of Mass Spectra N-3,4-methylenedioxybenzyl-2,5-dimethoxyphenpropylamine series.

Thus, it appears that the methylenedioxy regioisomers undergo fragmentation under EI conditions similar to the monomethoxy compounds as illustrated in Scheme 51. Again, the predominant ion at m/z 135 can be formed by the cleavage of the N-C bond yielding 2-methylenedioxybenzyl cation and the ion at m/z 178 is likely the iminium cation formed by the dissociation of bond between α - and β -carbon atoms. Finally, the ion at m/z 105 appears to have formed from loss of CH_2O from the methylenedioxy benzyl cation.



Scheme 51 Proposed EI-MS fragmentation pathway for the N-(methylenedioxy)benzyl- 2,5-dimethoxyphenpropylamines.

The mass spectra for the 20 compounds of this series demonstrate that all members appear to undergo the same fragmentation and that each subset can be differentiated from the other two subsets by the most abundant ions based on differences in the degree of methoxy substitution or methylenedioxy substitution. These spectra also demonstrate that the individual members of each structural subset cannot be differentiated based on their mass spectra. Thus, other analytical methods including GC separations and FTIR spectral analysis were explored for further differentiation within each regioisomeric subseries.

9.3 Gas Chromatographic Separations:

In an attempt to further differentiate the compounds in each of the three N-(substituted)benzyl-2,5-dimethoxyphenylpropylamine subsets, gas chromatographic separations of (monomethoxy)benzyl regioisomers subset were performed on 30m x 0.25mm ID capillary column coated with 0.25 μm film of midpolarity Crossbond[®] silylene phase containing a 50% phenyl and 50% dimethyl polysiloxane polymer (Rxi[®]-17Sil MS). Separations were achieved over 50 minutes starting from initial temperature of 70 °C held for 1 minute then gradually increased to reach 250 °C at a rate of 20 °C/minute and held for 40 minutes with elution over a 2 minute window.

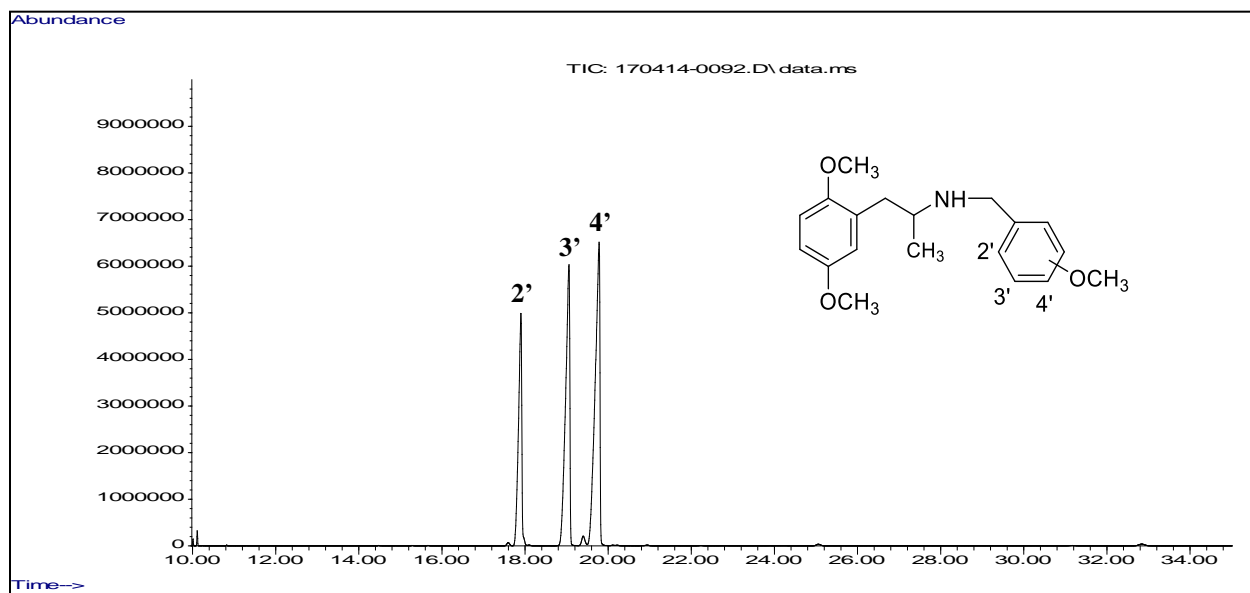


Figure 130 Gas chromatographic separation of the N-(monomethoxy)benzyl-2,5-dimethoxyphenylpropylamines.

This set of chromatographic conditions yielded an excellent separation of all three regioisomers, with the 2'-methoxy isomer eluting before the 3'-isomer, and the 3'-isomer before the 4'-isomer (Figure 130).

Similar to the N-(monomethoxy)benzyl-2,5-dimethoxyphenylpropylamines series, complete separation was achieved for the N-(substituted)benzyl-2,3-dimethoxyphenylpropylamine subsets, the N-(substituted)benzyl-2,6-dimethoxyphenylpropylamine subsets, and the N-(substituted)-benzyl-3,4-methylenedioxyphenylpropylamines using the following program with complete separations under 20 minutes, initial GC oven temperature was set to be 70 °C that held for 1 minute then gradually increased to reach 270 °C at a rate of 30 °C/minute and held for 40 minutes with a total of 48 minutes and elution window over 2 minutes (Figure 131-133). All The three subsets showed similar elution order as the N-(substituted)benzyl-2,5-dimethoxyphenylpropylamine subsets in which 2'-methoxy isomer eluted before the 3'-isomer, and the 3'-isomer before the 4'-isomer.

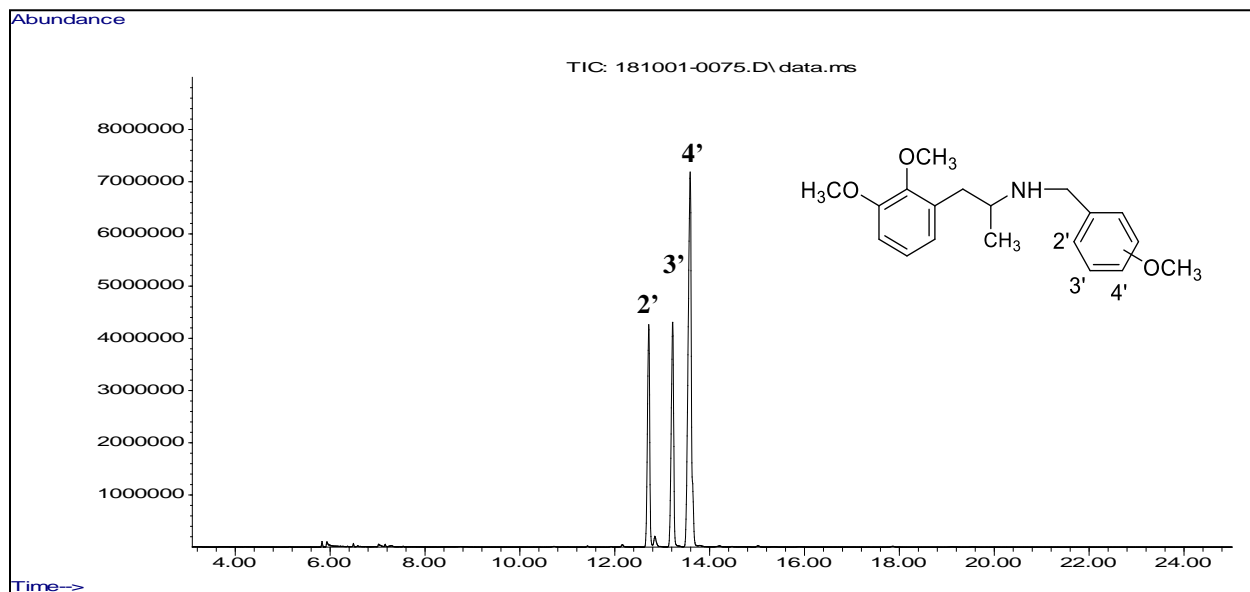


Figure 131 Gas chromatographic separation of the N-(monomethoxy)benzyl-2,3-dimethoxyphenylpropylamines.

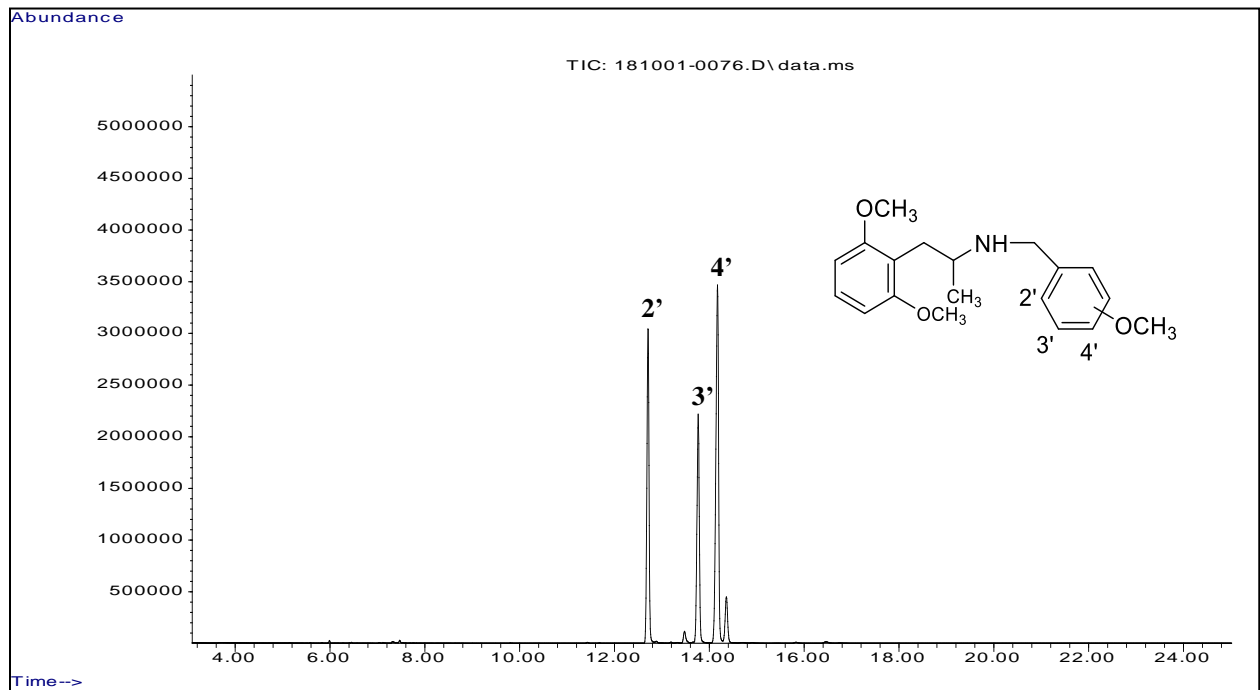


Figure 132 Gas chromatographic separation of the N-(monomethoxy)benzyl-2,6-dimethoxyphenpropylamines.

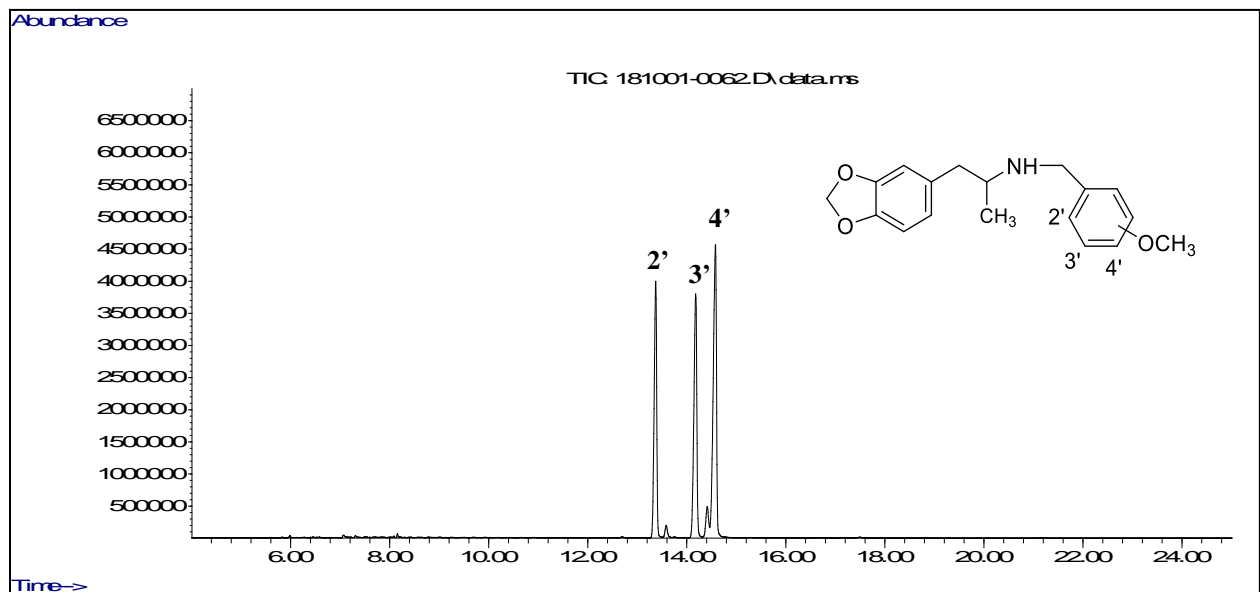


Figure 133 Gas chromatographic separation of the N-(monomethoxy)benzyl-3,4-methylenedioxyphenpropylamines.

In the case of all the six of the dimethoxy regioisomers, full separation was achieved using the same capillary column but with different temperature program conditions. The temperature program started with initial temperature of 70 °C held for 1 minute then gradually increased to reach 260 °C at a rate of 10 °C/minute and held for 40 minutes with a total 60 minutes run time. The compounds eluted over a 4 minute window as shown in Figure 134. In this series those derivatives with a 2'-methoxy group (2',3'-, 2',4'-, 2',5'- and 2',6'-dimethoxy) eluted before the two regioisomers that did not contain a 2'-methoxy group. Also, the two derivatives with the greatest degree of steric crowding relative to the benzyl side chain (2,3- and 2,6-dimethoxy) eluted prior to all other members of the series.

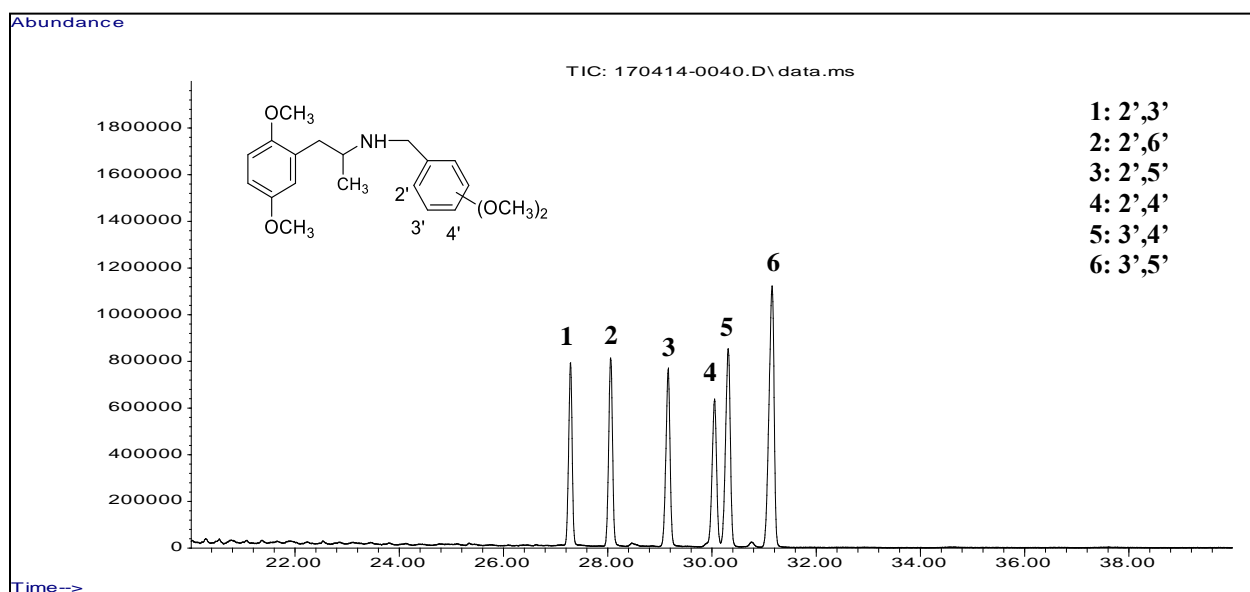


Figure 134 Gas chromatographic separation of the N-(dimethoxy)benzyl-2,5 dimethoxyphenyl-propylamines.

Lastly, the last chromatogram (Figure 135) shows the separation of the two methylenedioxy regioisomers using the conditions described above in the separations of (monomethoxy)benzyl regioisomers. In this series 2',3'-methylenedioxy eluted before 3',4'-methylenedioxy regioisomer the two regioisomers under similar separation condition as above.

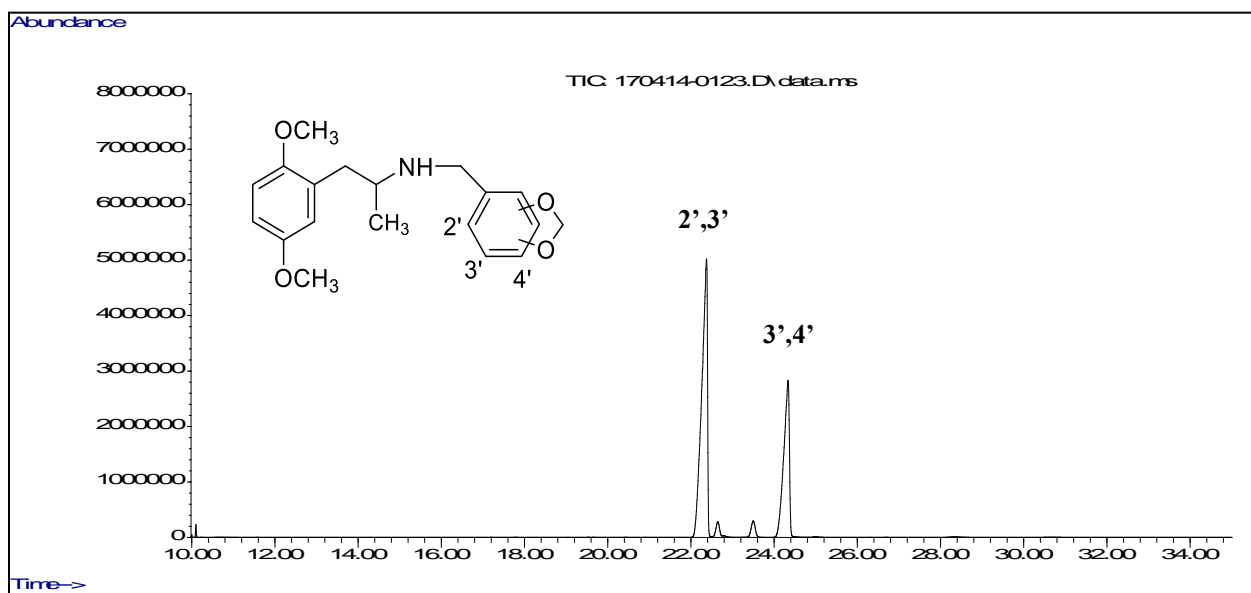


Figure 135 Gas chromatographic separation of the N-(methylenedioxy)benzyl-2,5-dimethoxyphenylamines.

10 GC-MS Analysis of Trifluoroacetamide Derivatives of the N-(Methoxy)benzyl-4-Bromo-2,5-dimethoxyphenethylamines, N-(Dimethoxy)benzyl-4-Bromo-2,5-dimethoxyphenethylamines and N-(Dimethoxy)benzyl-4-Iodo-2,5-dimethoxyphenethylamines

10.1 GC-MS of TFA Derivatives of the N-(Substituted)-4-X-2,5-Dimethoxyphenethylamines:

In an attempt to differentiate the three regioisomeric N-(methoxy)benzyl-4-bromo-2,5-dimethoxyphenethylamines and the six regioisomeric N-(dimethoxy)benzyl-4-bromo-2,5-dimethoxyphenethylamines derivatization studies were pursued.

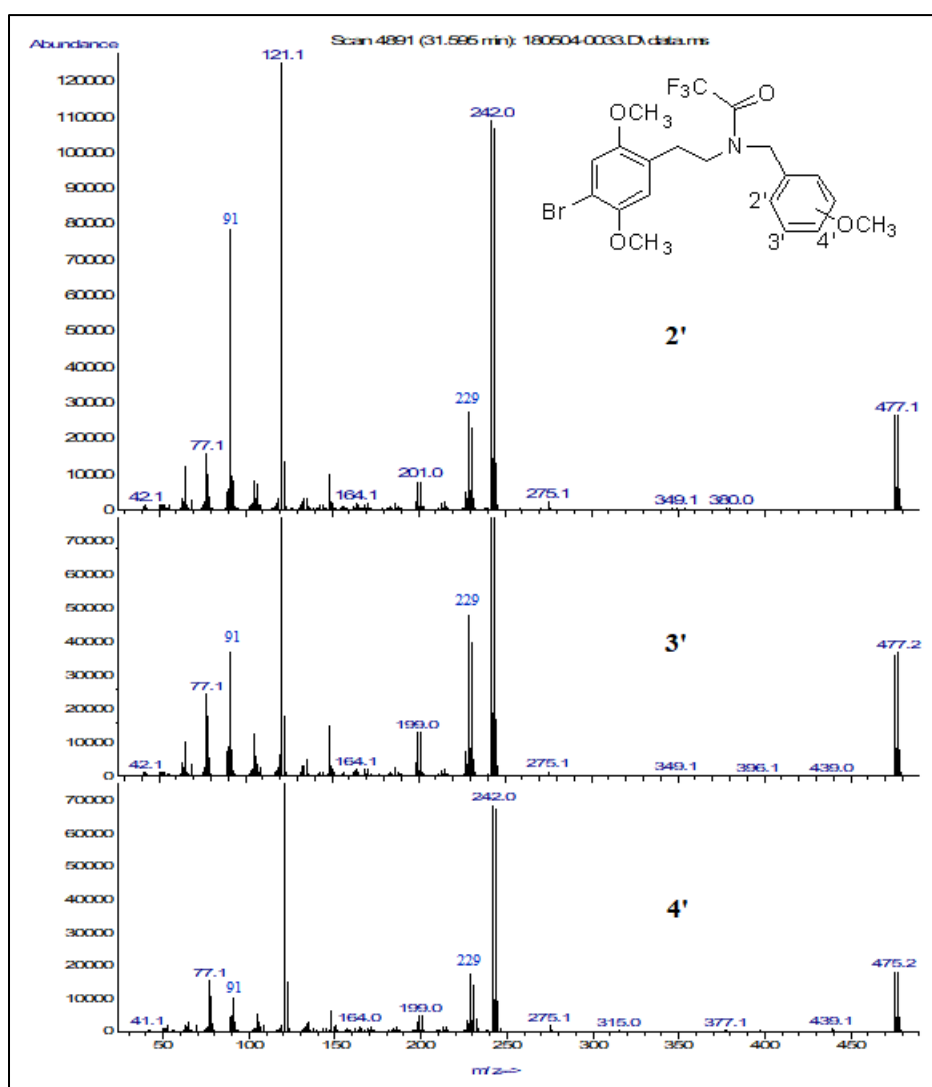
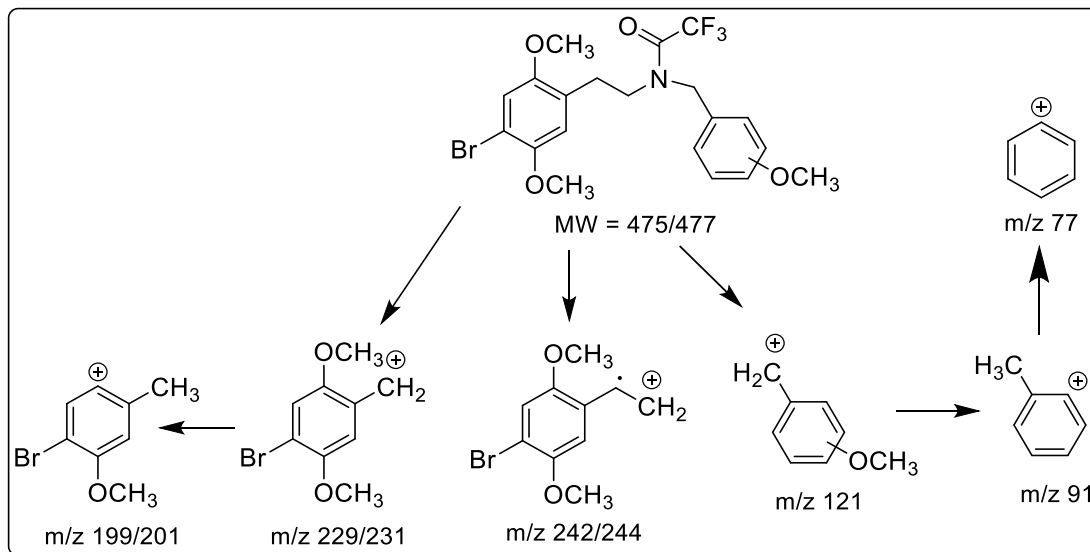


Figure 136 Mass Spectra of the N-(methoxy)benzyl-4-bromo-2,5-dimethoxyphenethyltrifluoroacetamide regioisomers.

It has been demonstrated that acylation of amines significantly lowers the basicity of the nitrogen atom and can allow other fragmentation pathways to play a more prominent role in the mass spectrum. Thus, each of the compounds in this series was converted to trifluoroacetamide (TFA) derivatives by treatment with trifluoroacetic anhydride and the derivatives analyzed by mass spectroscopy. The EI-MS of the three isomeric N-(methoxy)benzyl-4-bromo-2,5-dimethoxyphenethylamines are shown in Figure 136.

Each of the TFA derivatives gave a molecular ion of significant abundance at m/z 475/477, unlike the parent compounds where no molecular ion was observed. The base peak in each spectrum occurs at m/z 121 and forms by the cleavage of the N-C bond yielding the methoxybenzyl cation as observed with the parent underivatized compounds (Scheme 52). Also, each spectrum contained a significant m/z 91 which represents the loss of CH_2O from the methoxy benzyl cation. As observed with the underivatized parent compounds, the m/z 91 ion is present in highest abundance in the 2'-methoxy isomer and decreases in the 3'-isomer and further in the 4'-isomer. The other significant ions in the mass spectra of these isomers at m/z 242/244, m/z 229/231 and m/z 199/201 contain bromine based on isotopic abundance and comparable ions were not present in the underivatized compounds. The bromine-containing ion of highest abundance at m/z 242/244 is likely the phenethyl radical cation formed by H migration followed by the dissociation of N-C bond from the phenethyl side of the compound (Scheme 52). The ion at m/z 229/231 likely forms by the cleavage of the C-C bond of the phenethyl side chain yielding the 4-bromo-2,5-dimethoxybenzyl cation, and the m/z 199/201 ion appears to form by loss of a methoxy group (-30) from the m/z 229/231 benzyl cation (Scheme 52). The three regioisomers of this series can be differentiated based on the relative abundance of the lower mass fragment ions at m/z 91 and 77. The m/z 91 ion is present in higher abundance in the 2'-methoxy isomer than the 3'-isomer, and higher in the 3'-isomer than the 4'-methoxy isomer. Also, the ratio of the m/z 91 ion to the m/z 77 ion is the greatest for 2'-methoxy isomer, lesser in the 3'-isomer and lowest for the 4-methoxy isomer where it is actually more abundant than the m/z 91 ion. Thus, examination of the lower mass fragment ions in the EI-MS of the TFA derivatives of these compounds allows for the differentiation of these three regioisomers.



Scheme 52 Proposed EI-MS fragmentation pathway for the N-(methoxy)benzyl-4-bromo-2,5-dimethoxyphenethyltrifluoroacetamide.

The EI mass spectra for the TFA-derivatives of the six regioisomeric N-(dimethoxy)benzyl-4-bromo-2,5-dimethoxyphenethylamine series are shown in Figure 137. Each of the TFA derivatives gave a molecular ion of significant abundance at m/z 505/507, unlike the parent compounds where no molecular ion was observed. Two major fragment ions common in the spectra of all six regioisomeric derivatives occur at m/z 242/244 and m/z 151. The m/z 242/244 ion contains bromine and is likely the phenethyl radical cation formed by hydrogen migration followed by the dissociation of benzylic N-C bond from the phenethyl side of the compound (Scheme 53). The same fragment ion is present in the mass spectra of the N-(methoxy)benzyl-4-bromo-2,5-dimethoxyphenethyl-trifluoromethylamides described above (Figure 136, Scheme 52). The m/z 151 ion forms by the cleavage of the N-C bond yielding the methoxybenzyl cation as observed with the parent underivatized compounds. A comparable ion at m/z 121 ion (-30 mass units) was also present in the mass spectra of the three N-(methoxy)benzyl-4-bromo-2,5-dimethoxyphenethyl-trifluoro-methylamide regioisomers described above. The relative abundance of these ions is shown in Table 16.

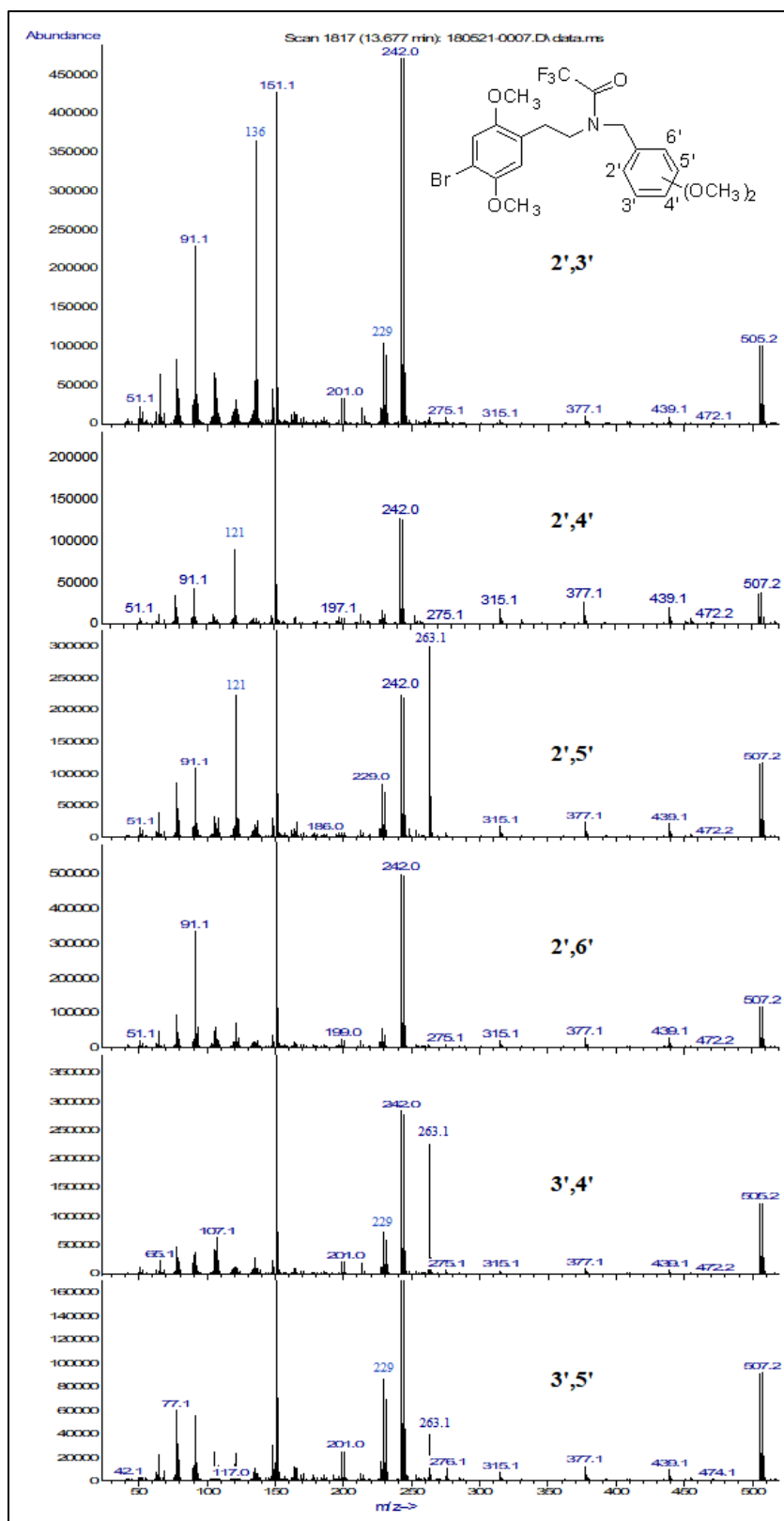
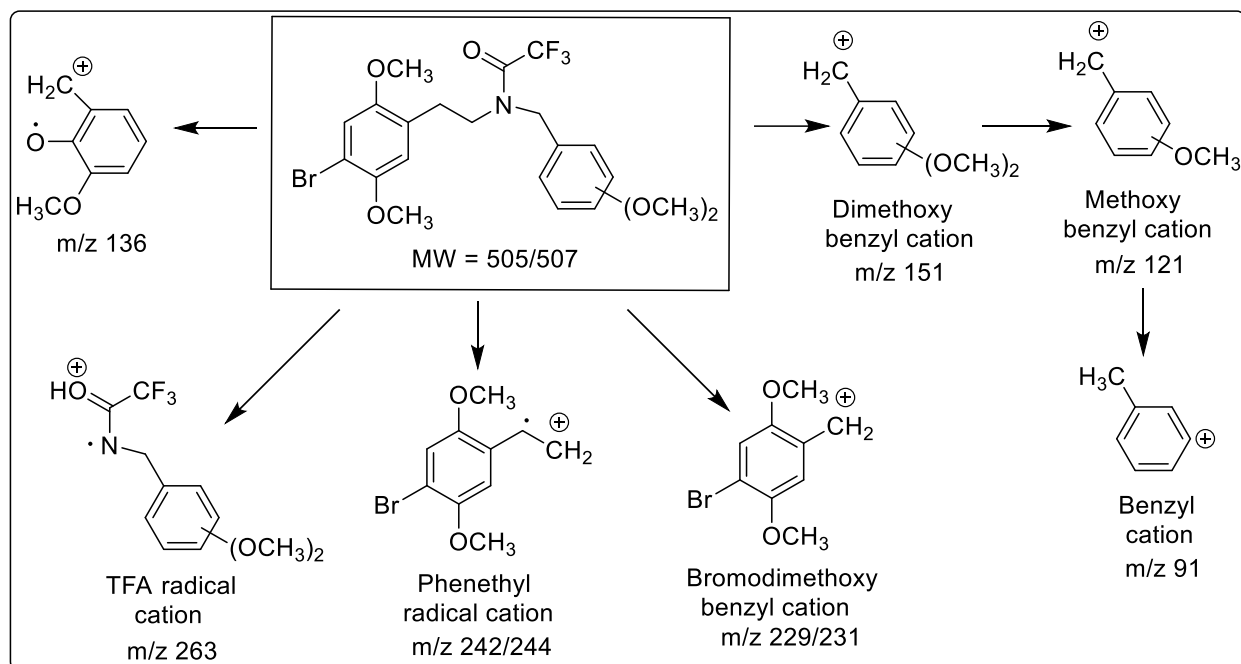


Figure 137 Mass Spectra of the N-(dimethoxy)benzyl-4-bromo-2,5-dimethoxyphenethyltrifluoroacetamide regioisomers.



Scheme 53 Proposed EI-MS fragmentation pathway for the N-(dimethoxy)benzyl-4-bromo-2,5-dimethoxyphenethyltrifluoroacetamide.

Table 16 Relative abundance of Fragment ions in the EI-MS of the N-(dimethoxy)benzyl-4-bromo-2,5-dimethoxyphenethyltrifluoroacetamide.

25B-NBOMe Regioisomers	Base Peak	2 nd Most Abundant Ion	3 rd Most Abundant Ion	4 th Most Abundant Ion
2',3'-Isomer	242/244	151	136*	91
2',4'-Isomer	151	242/244	121	91
2',5'-Isomer	151	263*	121 = 242/244	229/231
2',6'-Isomer	151	242/244	91	121
3',4'-Isomer	151	242/244	263*	229/231
3',5'-Isomer	242/244	151	229/231	91

While the m/z 242/244 and m/z 151 fragment ions are present in all six regioisomeric N-(dimethoxy)benzyl-4-bromo-2,5-dimethoxyphenethylamine TFA derivatives, a number of other ions varying in mass or relative abundance are present in these spectra and allow for some significant degree of differentiation. For example, only the 2',3'- and 3',5'-dimethoxy compounds have a base peak of m/z 242/244, setting them apart from the other four regioisomers (Figure 137). But only the 2',3'-dimethoxy isomer contains a m/z 136 ion of high abundance in its EI mass

spectrum, differentiating this compound from the 3',5'-dimethoxy isomer and the other four regioisomers of this series. This m/z 136 ion is also observed in the underivatized form of this isomer and distinguishes it from the other five regioisomers of this series and is derived from a methyl migration reaction from the parent compound in the EI-MS.

The 2',4'-, 2',5'-, 2',6'- and 3',4'-dimethoxy isomers all have a base peak at 151 m/z in their EI-MS (Figure 137). However, only the 2',5'-dimethoxy compound has an intense m/z 263 fragment ion second in abundance only to the base peak and in greater relative abundance than the m/z 242/244 ion. The 3',4'-isomer also contains a m/z 263 fragment ion in its spectrum, but its abundance is significantly lower than the base peak (m/z 151) and the m/z 242/244 ion. In addition to the m/z 263 ion, the 2',5'-dimethoxy compound has a m/z 121 ion of nearly equal intensity to the m/z 242/244 ion and an ion of this mass is not present in any significant abundance in the spectrum of the 3',4'-isomer. Therefore, the presence and relative abundance of the m/z 263 and m/z 121 fragment ions differentiates the 2',5'-isomer from all other regioisomers of this series. It should be noted that the mass spectrum of the 3',5'-isomer also contains a m/z 263 fragment ion of relatively low abundance (Figure 137). However, this isomer is differentiated based on its base peak of m/z 242/244 as noted above, and a more intense m/z 229/231 ion (third most abundant) than the other five isomers.

The remaining 2',4'- and 2',6'-dimethoxy isomers have a base peak at m/z 151 and a m/z 242/244 fragment ion of secondary abundance. The EI-MS of these two isomers lack significant fragment ions at m/z 136 and 263, distinguishing them from the other four members of this series. Their spectra also differ from the other four regioisomers in the relative abundance of the m/z 229/231 fragment ion. This ion is present in significantly greater abundance in the 2',3'-, 2',5'-, 3',4'- and 3',5'-isomers than in the 2',4'- and 2',6'-dimethoxy isomers. The mass spectra of the 2',4'- and 2',6'-dimethoxy regioisomers differ from each other in the relative abundance of significant ions at m/z 121 and m/z 91. In the case of the 2',4'-isomer, the m/z 121 ion is the third most abundant ion and is present in greater intensity than the m/z 91 ion. This is reversed in the 2',6'-isomers where the m/z 91 ion is the third most abundant ion and is present in greater intensity than the m/z 121 ion.

Thus, the combination of different base peak ions (m/z 151 or 242/244), unique fragment ions (m/z 136 and m/z 263), along with differences in the relative abundance of ions at m/z 121 and m/z 91, allows for differentiation and specific identification of all six of the regioisomers of the N-(dimethoxy)benzyl-4-bromo-2,5-dimethoxyphenethylamine series in their TFA-derivatized form. Also, all six of these regioisomers in their underivatized form were also successfully separated and identified using gas chromatographic methods as reported in Chapter 6.

To determine if this derivatization method could individualize the mass spectra of NBOMe-type compounds in general and allow for specific regioisomer identification, the TFA derivatives of the N-(dimethoxy)benzyl-4-iodo-2,5-dimethoxyphenethylamine series were analyzed also by EI-MS. The results of these analyses are shown in Figure 138 and Table 17.

Table 17 Relative abundance of Fragment ions in the EI-MS of the N-(dimethoxy)benzyl-4-iodo-2,5-dimethoxyphenethyl-trifluoroacetamide

25I-NBOME Regioisomers	Base Peak	2nd Most Abundant Ion	3rd Most Abundant Ion	4th Most Abundant Ion
2',3'-Isomer	290	151	136	91
2',4'-Isomer	151	290	121	91
2',5'-Isomer	151	290	263	121
2',6'-Isomer	151	290	91	121
3',4'-Isomer	151	290	263	277
3',5'-Isomer	290	151	277	91

As the results of the EI-MS analyses show for the N-(dimethoxy)benzyl-4-iodo-2,5-dimethoxyphenethylamine derivatives, again only the 2',3'- and 3',5'-dimethoxy isomers have a phenethyl radical base peak (m/z 290) which is +47 mass units from comparable base peak in these isomers in the 4-bromo series (m/z 242/244). Also, of these two compounds, only the 2',3'-dimethoxy isomer contains a significant m/z 136 fragment ion, as was observed in the 4-bromo series described above, allowing for differentiation.

The other four regioisomers in the 4-iodo series (2',4'-, 2',5'-, 2',6'- and 3',4'-dimethoxy isomers) have a base peak of m/z 151 ion resulting from cleavage of the N-C bond to yield the methoxybenzyl cation, precisely as observed in the 4-bromo series. Again only the 2',5'- and 3',4'-

dimethoxy isomers have a significant m/z 263 fragment ion differentiating these compounds from the other regioisomers in this series. Furthermore, the intensity of the m/z 263 ion is greater in the spectrum of the 2',5'-dimethoxy isomer than the 3',4'-isomer, and the 2',5'-isomer also contains a m/z 121 ion of significantly greater abundance than the 3',4'-isomer. These same trends were observed in the 4-bromo series and allows for the differentiation of these two regioisomers from each other and all other members of this series.

Finally, in the 4-iodo series the 2',4'- and 2'6'-dimethoxy isomers have a base peak at m/z 151 phenethyl radical at m/z 290. These two isomers differ from the other four regioisomers of the 4-iodo series by their base peak and the absence of m/z 136 and m/z 263 fragment ion. Furthermore, the mass spectra of the 2',4'- and 2'6'-dimethoxy regioisomers differ from each other in the relative abundance of significant ions at m/z 121 and m/z 91. In the case of the 2',4'-isomer, the m/z 121 ion is the third most abundant ion and is present in greater intensity than the m/z 91 ion. This is reversed in the 2'6'-isomers where the m/z 91 ion is the third most abundant ion and is present in greater intensity than the m/z 121 ion. Again, this same pattern of relative fragment ion intensities was observed in the 4-bromo series described above and demonstrates that the TFA derivatization method can be used to differentiate regioisomers of this general NBOMe structural class. Also, all six of these regioisomers in their underivatized form were also successfully separated and identified using gas chromatographic methods as reported in Chapter 8.

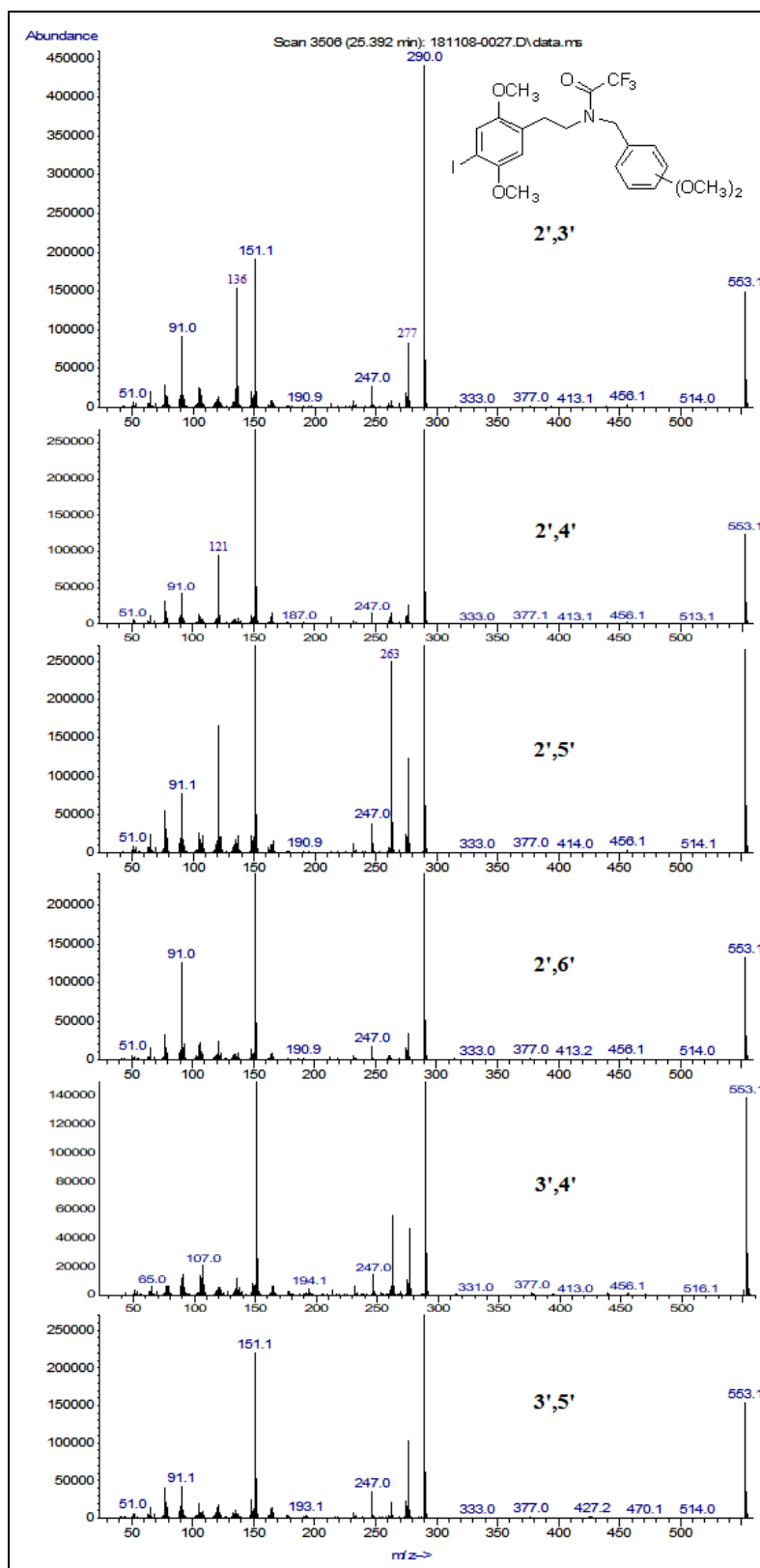
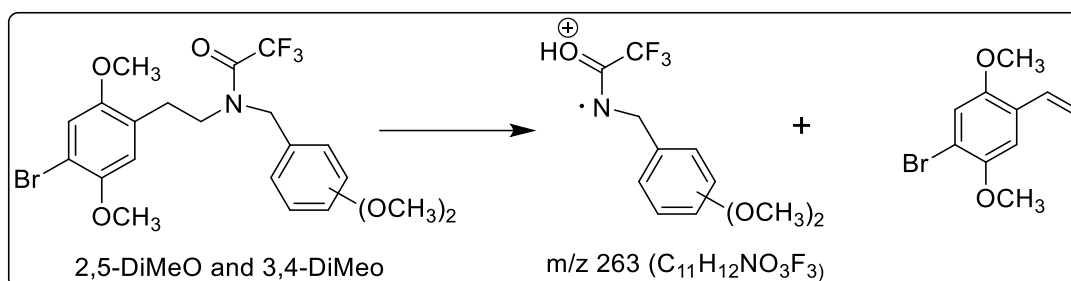


Figure 138 Mass Spectra of the N-(dimethoxy)benzyl-4-iodo-2,5-dimethoxyphenyltrifluoroacetamide regioisomers.

10.2 Structure-MS Studies and the m/z 263 Ion:

The presence of a m/z 263 fragment ion of high relative abundance in the EI-MS of TFA derivative of the 2',5'-dimethoxy isomer of this series prompted further studies to confirm its structure. This ion does not contain bromine and may form following initial H migration to the oxygen atom of the carbonyl group followed by cleavage of the N-C bond from the phenethyl side of the compound as shown in Scheme 54.



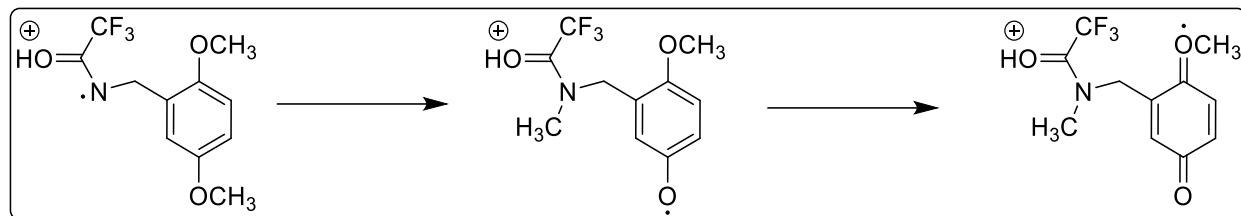
Scheme 54 Structure of the N-(2',5'-dimethoxy)benzyltrifluoroacetamide m/z 263 ion.

The elemental composition of m/z 263 ion determined by exact mass measurement using high resolution GC-EI/MS-TOF spectroscopy. Figure 139 shows the exact mass was found to be 263.0765 (263.0769 theoretical mass, -1.5 ppm), matching a formula of C₁₁H₁₂NO₃F₃ as proposed in Scheme 54. The second closest formula approximating this mass is C₉H₁₀N₄O₂F₃ (mass error of 3.4 PPM), which is clearly does not represent the m/z 263 fragment ion since the parent compound does not contain four nitrogen atoms in its structure.

Mass	Calc. Mass	mDa	PPM	DBE	Formula
263.0765	263.0769	-0.4	-1.5	5.0	C11 H12 N 03 F3

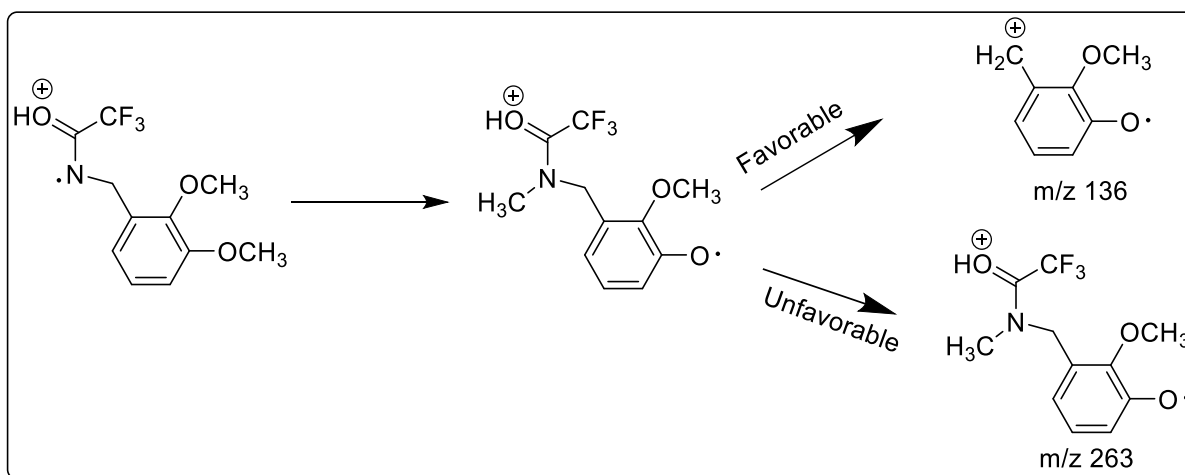
Figure 139 Exact mass determination for the m/z 263 ion using high resolution mass spectrometry (HRMS).

The high abundance of the m/z 263 ion in the TFA derivatives of the 2',5'- and 3',4'-dimethoxy derivatives may result from methoxy group conjugation in these isomers which would allow for stabilization of the radical species formed as shown in Scheme 55.



Scheme 55 Proposed conjugation for the N-2',5'-dimethoxybenzyltrifluoroacetamide.

The absence of this ion in the spectrum of the 2',3'-isomer where the methoxy groups are also conjugated may result from this isomer preferentially fragmenting to yield the unique m/z 136 fragment (Scheme 56).



Scheme 56 preferential fragmentation of m/z 136 over 263 ion.

To investigate the origin of the m/z 263 fragment ion in the mass spectra of the N-(2',5'-dimethoxy)benzyl-4-bromo-2,5-dimethoxyphenethylamine TFA derivative, additional derivatives and analogues of this compound were prepared and subjected to EI-MS analysis. Figure 140 shows the EI mass spectrum for the pentafluoropropylamide (PFPA) derivative of N-(2',5'-dimethoxy)benzyl-4-bromo-2,5-dimethoxyphenethylamine. This derivative contains an additional CF_2 unit (+50 mass units) relative to the TFA derivative, and thus should give rise to a m/z 313 ion by the fragment pathway shown in Scheme 54. As can be seen a m/z 313 ion is present in the spectrum of this PFPA derivative while other fragment ions are similar to those observed in the TFA derivative in terms of mass and intensities (m/z 151 > 313 > 242/244 = 121).

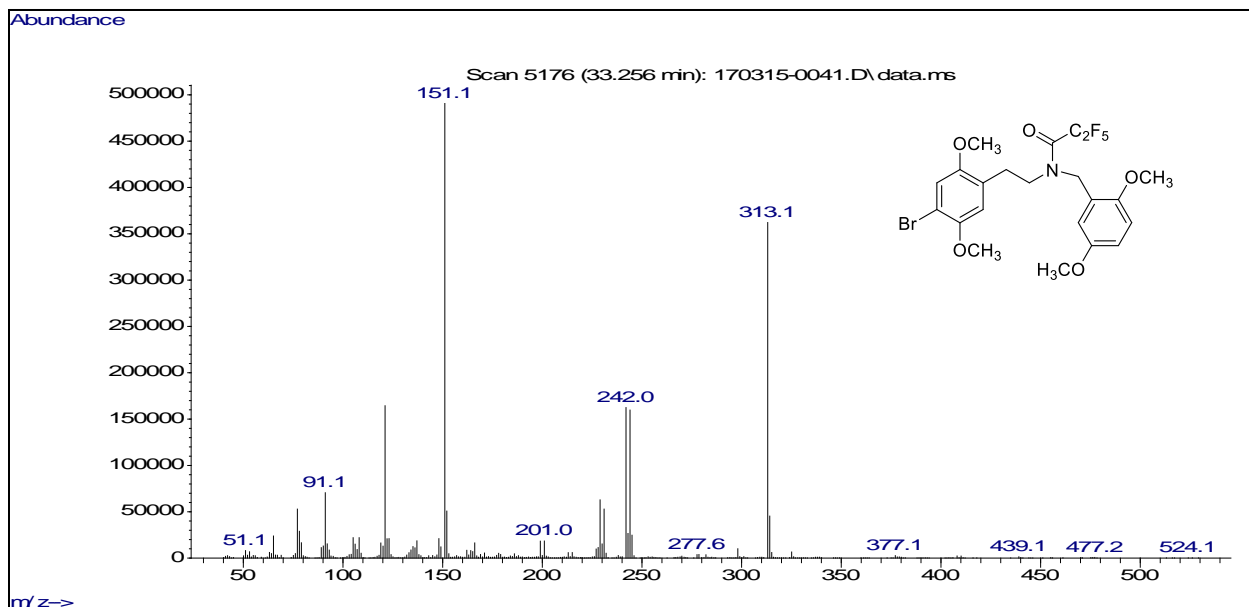


Figure 140 N-(2',5'-dimethoxy)benzyl-4-bromo-2,5-dimethoxyphenethylpentafluoropropionamide.

If the m/z 263 ion is characteristic for derivatives of this particular benzyl substitution pattern, then other 2',5'-dimethoxy-NBOMe analogues with varied substituents in the phenethyl ring or phenethyl side chain would also be expected to yield a m/z 263 ion in their mass spectra.

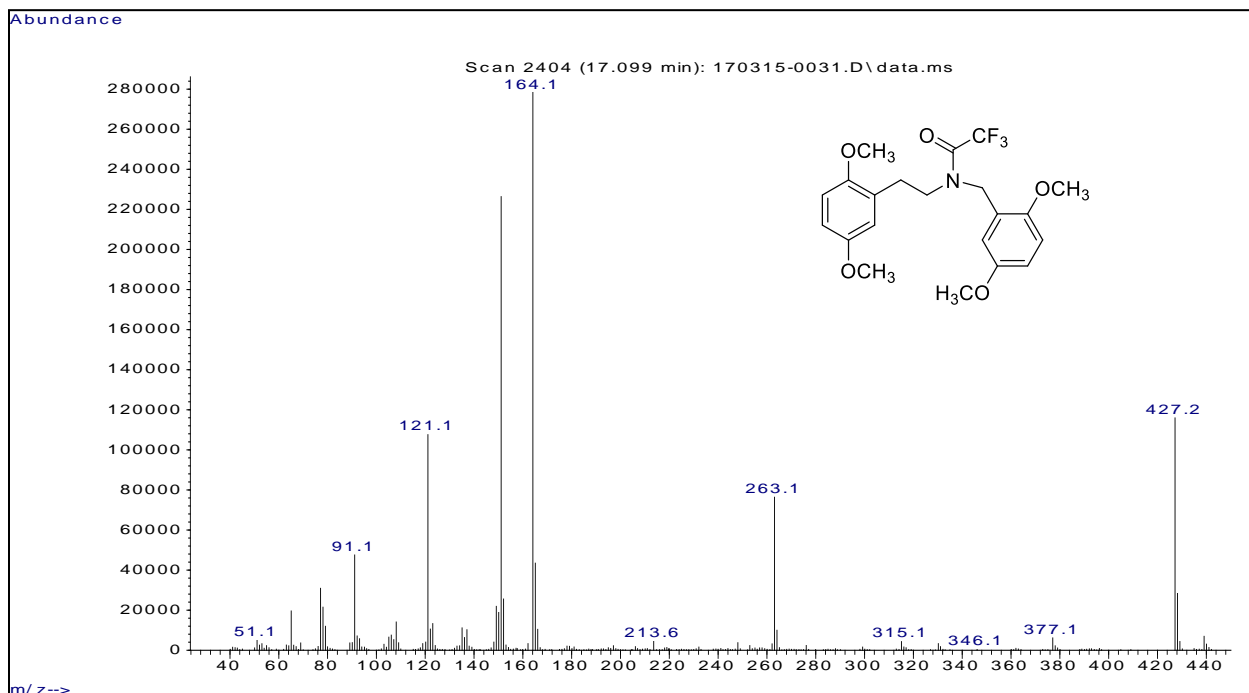


Figure 141 N-(2',5'-dimethoxy)benzyl-2,5-dimethoxyphenethyltrifluoroacetamide.

To explore this possibility the TFA derivative of the non-halogenated derivative (N-(2',5'-dimethoxy)benzyl-2,5-dimethoxyphenethylamine) and the 4-iodo derivative (4-iodo--(2',5'-dimethoxy)benzyl-4-bromo-2,5-dimethoxyphenethylamine) were prepared and subjected to EI-MS analysis. As shown in Figure 141 the non-halogenated derivative also yielded a m/z 263 fragment ion. The m/z 164 in the mass spectrum of this hydrogen derivative corresponds to the 242/244 ion in the spectrum of the bromine compound.

Figure 142 shows the mass spectrum of the N-(2',5'-dimethoxy)benzyl-4-bromo-2,5-dimethoxyphenethylamine TFA derivative. This compound differs from the parent compound only in the presence of a methyl group on alpha-carbon of the phenethyl side chain. This compound gives a m/z 263 as would be expected based on the mechanism above, albeit of relatively low abundance. The lower relative abundance of m/z 263 in this derivative may be a result of steric inhibition of the initial H migration from the phenethyl side to the amide carbonyl precedes cleavage of the N-C bond.

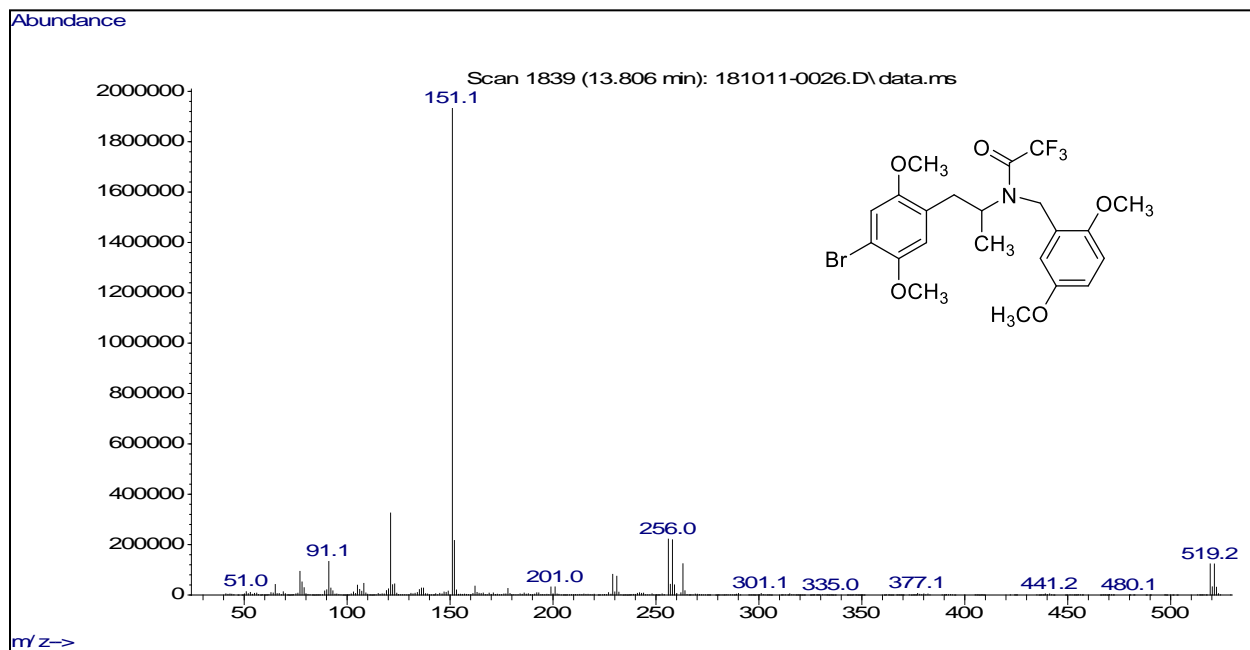


Figure 142 N-(2',5'-dimethoxy)benzyl-4-bromo-2,5-dimethoxyphenethyltrifluoroacetamide.

To examine the theory that the m/z 263 ion present in mass spectrum of the TFA derivative of N-(2',5'-dimethoxy)benzyl-4-bromo-2,5-dimethoxyphenylpropylamine forms as a result of stabilization of the intermediate oxygen radical species by conjugated methoxy groups, two additional derivatives were prepared and derivatized in which either the 3'- or 4'-methoxy group was replaced with a methyl group. It was reasoned that the TFA derivatives of these two methyl-methoxy analogues would not be able to fragment to yield give a comparable m/z 263 ion since a stabilized oxygen radical species could not form. If such a fragment ion did form with the TFA derivatives of these analogues it would occur at m/z 247 (16 mass units lower due to the elimination of one oxygen atom). As the mass spectra for the two TFA-derivatives of the methyl-methoxy compounds show (Figures 143 and 144), no “ m/z 263 equivalent” (m/z 247) fragment ions form, supporting the original hypothesis that this pathway is unique to NBOMe derivatives with conjugated 2',5'- or 3',4' dimethoxy substitution pattern in the N-benzyl substituent.

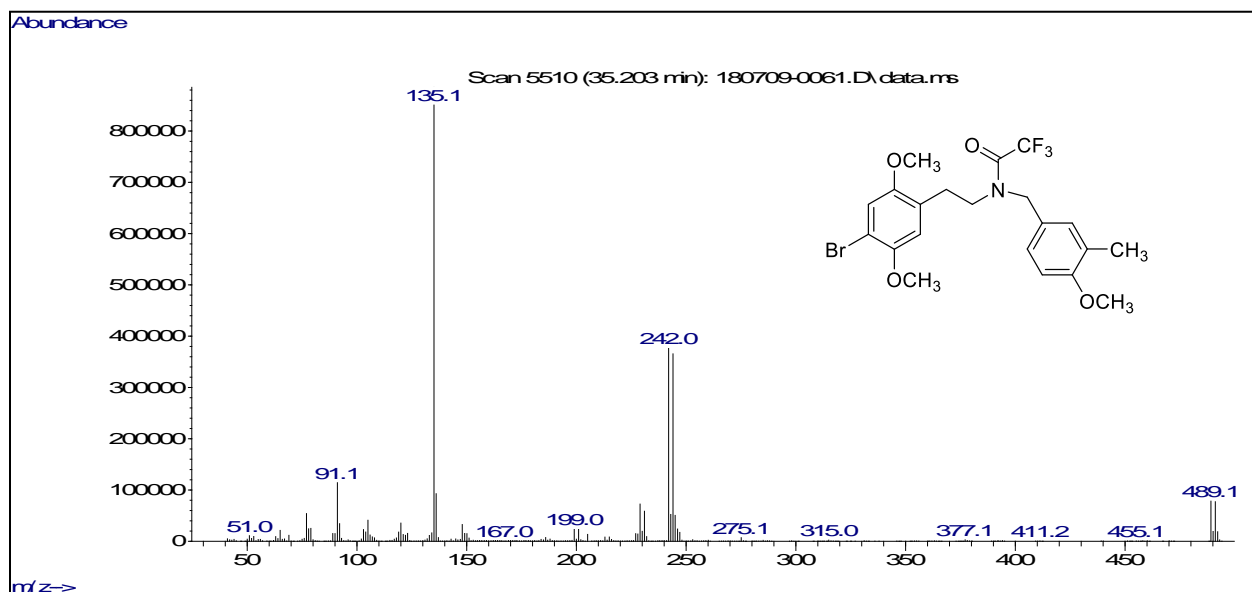


Figure 143 N-(3'-methyl-4'-methoxy)benzyl-4-bromo-2,5-dimethoxyphenethyltrifluoroacetamide.

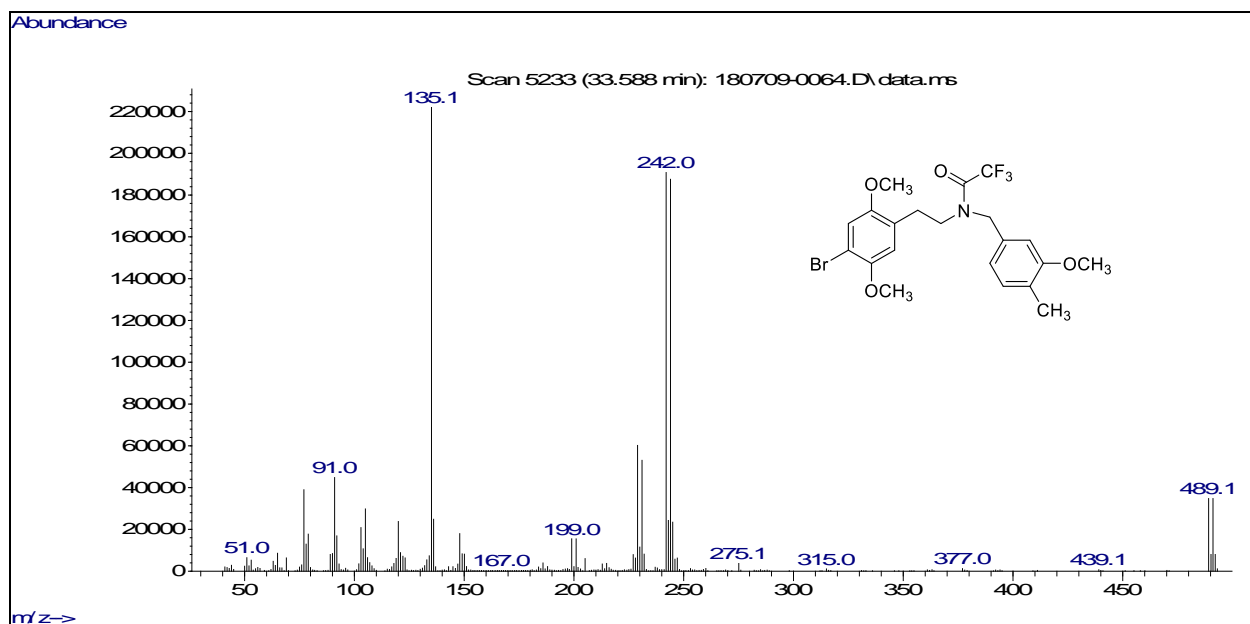
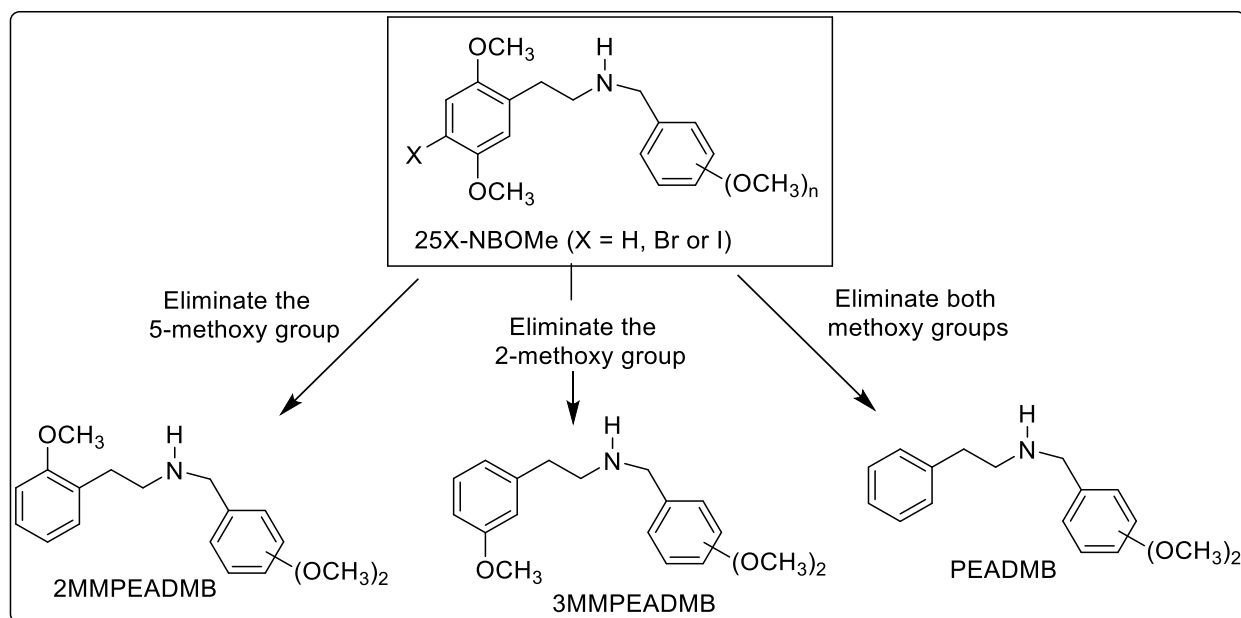


Figure 144 N-(3'-methoxy-4'-methyl)benzyl-4-bromo-2,5-dimethoxyphenethyltrifluoroacetamide.

10.3 GC-MS of TFA Derivatives of the N-(Substituted)-Methoxyphenethylamines:

The GC-MS studies with TFA derivatives described in the preceding section all involve NBOME analogs with the classic 2,5-dimethoxy substitution on the phenethyl aromatic ring (25X-NBOMes). For each series of compounds in these studies only the number and position of methoxy substituents in the N-benzyl ring were varied. Results from these studies demonstrated that derivatives with regioisomeric monomethoxy- or dimethoxy-substitution on the N-benzyl substituent of the core 25X-NBOME structure can be differentiated and specifically identified by MS analysis following TFA derivatization. To expand these studies and investigate structure-MS fragmentation pathways in more detail, additional NBOME analogs were prepared in which one or both of the methoxy groups in the phenethyl aromatic ring (along with the halogen) were removed as shown in Scheme 57. The 2MMPEADMB derivatives represent analogs where the 5-methoxy group was eliminated from the classic 25-NBOME structure, and the 3MMPEADMB derivatives represent analogs where the 2-methoxy group is eliminated. The PEADMB derivatives represent 25-NBOME analogs where both of the phenethyl ring methoxy groups are eliminated. For each of these three series all six regioisomeric dimethoxybenzyl substituted analogs (2',3'-, 2',4'-, 2',5'-, 2',6'-, 3',4'- and 3',5'-dimethoxy) were prepared and analyzed. These compounds were synthesized by reductive alkylation reactions with commercially available 2-methoxy, 3-methoxy-

or unsubstituted phenethylamines and the corresponding six regioisomeric dimethoxy benzaldehydes as described earlier. The mass spectra of the TFA derivatives of each of the 2MMPEADMB, 3MMPEADMB and PEADMB series are shown in Figures 145-147 and the relative abundance of fragment ions in Table 18.



Scheme 57 NBOMe derivatives with modified phenethyl aromatic ring substituents.

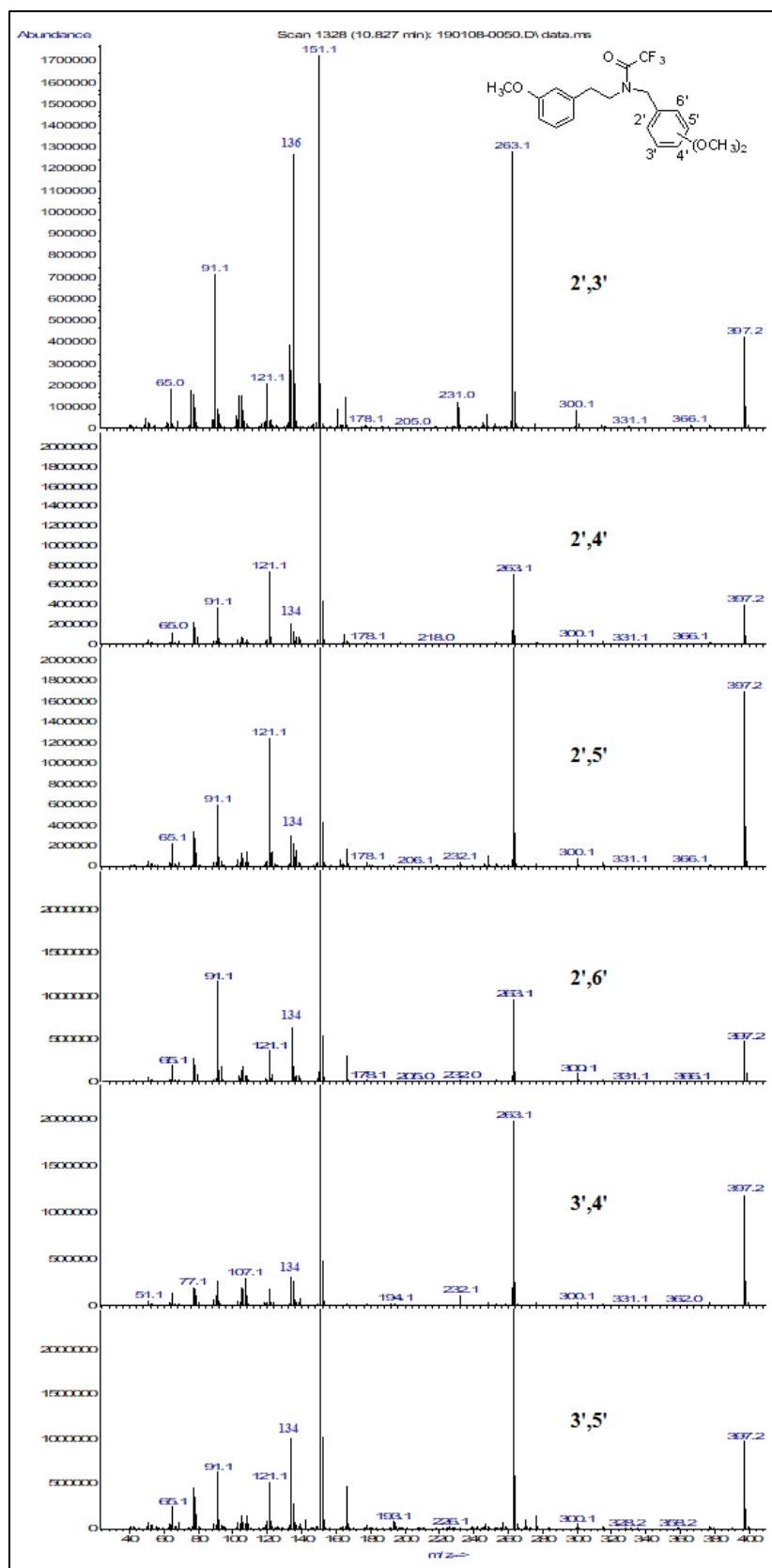


Figure 146 EI-MS of the 3MMPEADMB regioisomers.

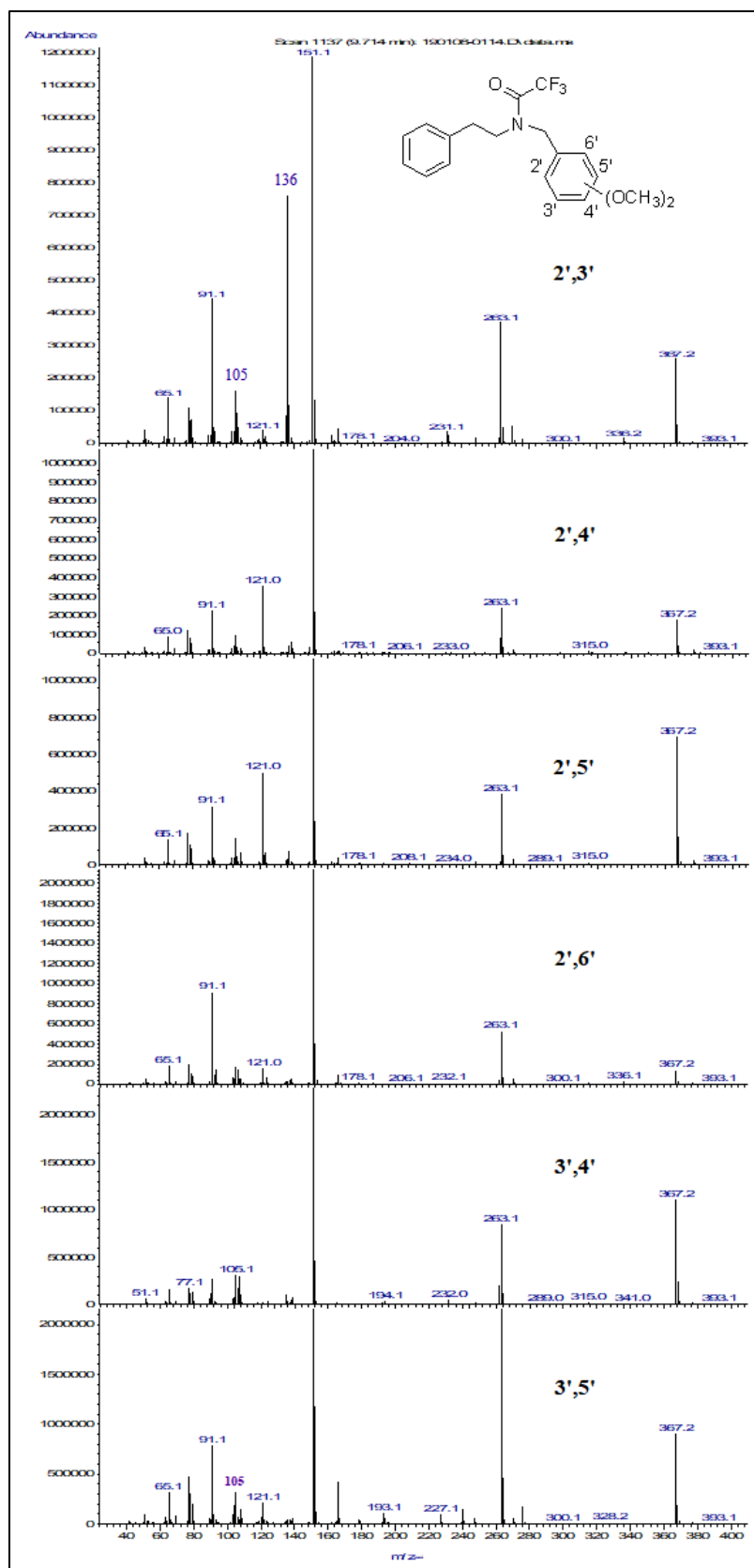
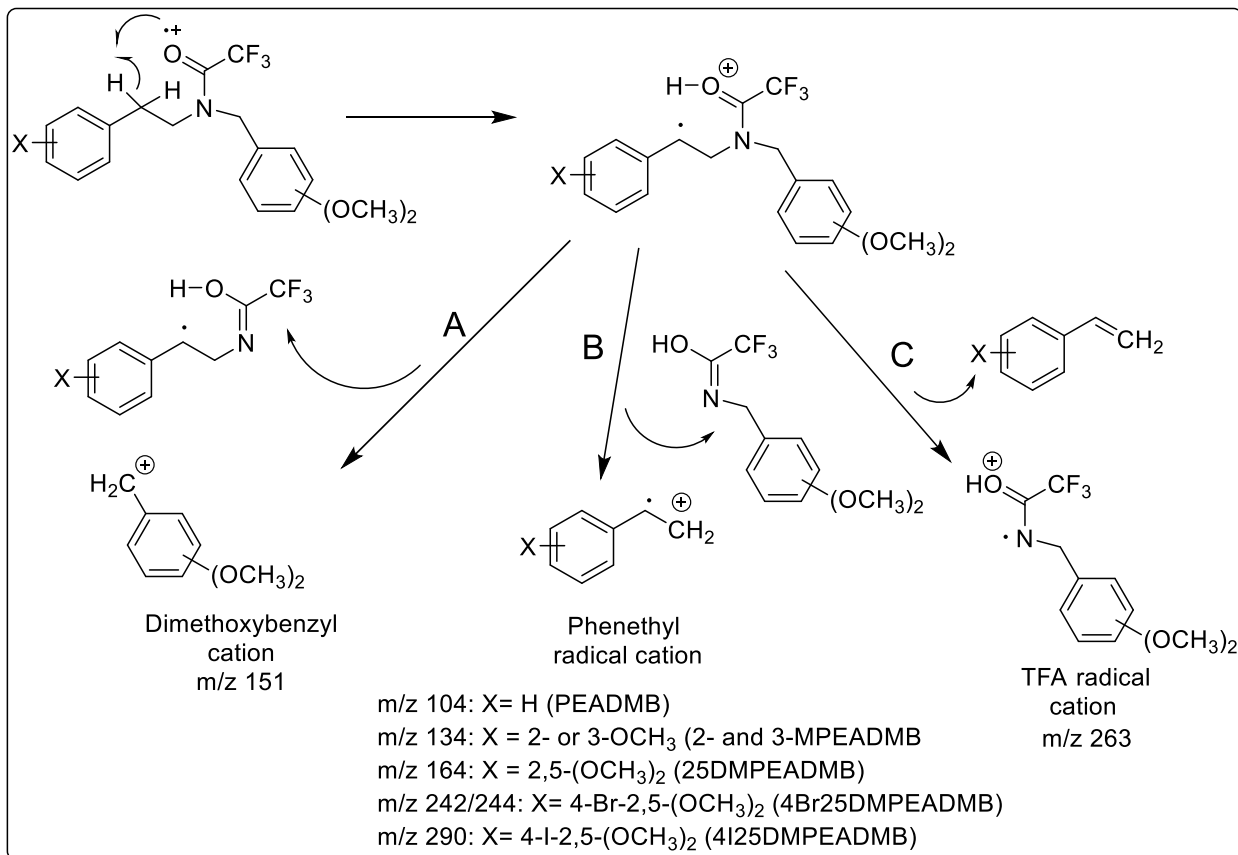


Figure 147 EI-MS of the PEADMB regioisomers.

Table 18 Relative abundance of fragment ions in the EI-MS of 2MMPEADMBs, 3MMPEADMBs and PEADMBs.

2MMPEADMB Regioisomers	Base Peak	2nd Most Abundant Ion	3rd Most Abundant Ion	4th Most Abundant Ion	5th Most Abundant Ion
2',3'-Isomer	263	151	91	136	134
2',4'-Isomer	151	263	121	91	134
2',5'-Isomer	151	263	121	91	134
2',6'-Isomer	151	91	134	263	121
3',4'-Isomer	151	263	91	121	134
3',5'-Isomer	263	151	91	121	134
3MMPEADMB Regioisomers					
3MMPEADMB Regioisomers	Base Peak	2nd Most Abundant Ion	3rd Most Abundant Ion	4th Most Abundant Ion	5th Most Abundant Ion
2',3'-Isomer	263	151	136	91	134
2',4'-Isomer	151	263	121	91	134
2',5'-Isomer	151	263	121	91	134
2',6'-Isomer	151	263	91	134	121
3',4'-Isomer	151	263	134	91	121
3',5'-Isomer	263	151	134	91	121
PEADMB Regioisomers					
PEADMB Regioisomers	Base Peak	2nd Most Abundant Ion	3rd Most Abundant Ion	4th Most Abundant Ion	5th Most Abundant Ion
2',3'-Isomer	151	136	91	263	105
2',4'-Isomer	151	121	263	91	105
2',5'-Isomer	151	121	263	91	105
2',6'-Isomer	151	91	263	105	121
3',4'-Isomer	151	263	104	91	121
3',5'-Isomer	151	263	91	105	121



Scheme 58 Mass spectral fragmentation pathways for TFA-derivatives of NBOMe analogs.

The major fragmentation in the EI-MS for these TFA derivatives appears to be limited to three pathways yielding the dimethoxybenzyl cation and the two radical cations (TFA radical cation and phenethyl radical cation) shown in Scheme 58. The dimethoxy benzyl cation at m/z 151 along with its likely product ions (m/z 121 and m/z 91) can occur following initial radical cation formation at the dimethoxyphenyl aromatic ring. Additionally, the m/z 151 dimethoxybenzyl cation can occur following initial hydrogen transfer to the carbonyl oxygen as shown for the distonic molecular radical cation in Scheme 58. The fragmentation of this species along pathway “A” could yield the m/z 151 cation. Fragmentation via pathway “B” yields the phenethyl radical cation occurring at various masses depending on the substituents on the phenethyl group. Decomposition of the common distonic radical cation along pathway “C” results in the formation of the m/z 263 radical cation.

While the m/z 151 cation could occur via several fragmentation pathways, the phenethyl radical cation and the m/z 263 ion appear to occur via common pathway from the distonic molecular radical cation. Previous studies have shown that the relative intensity of these three major fragments can be used to determine the dimethoxy groups substitution pattern on the aromatic ring of the N-benzyl group for TFA-25X-NBOMe compounds. All these observations were made based on the electron rich halogen containing 2,5-dimethoxyphenyl group on the phenethyl portion of the NBOMe structure. These electrons donating substituent groups appear to play a role in the ease of formation of the distonic molecular radical cation and its subsequent decomposition along the perhaps competing pathways especially the formation of the m/z 263 fragment and the substituted phenethyl radical cation.

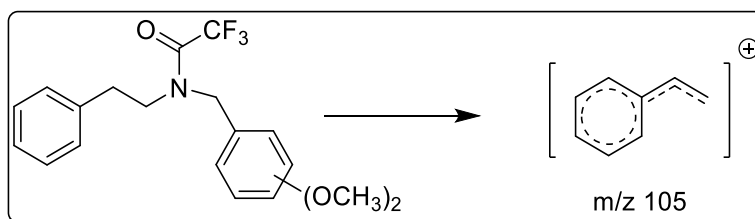
The electron rich substituted phenethyl radical cation fragments from pathway B are a major ion for many of the dimethoxy benzyl substitution patterns in the 4-substituted (H, Br, I)-2,5-dimethoxyphenethylamine derivatives (25X-NBOMes). The m/z 263 and the substituted phenethyl radical cations each form by cleavage of the same chemical bond, the nitrogen to aliphatic carbon of the phenethyl group. The homolytic cleavage of the bond yields the m/z 263 radical cation and the neutral substituted phenylalkene. Breaking the same bond in a heterolytic manner yields the substituted phenethyl radical cation and the neutral substituted benzyl trifluoroacetamide.

The systematic removal of the electron donating groups from the 2,5-dimethoxyphenyl structure of 25X-NBOMes to yield the 2-methoxyphenyl, 3-methoxyphenyl, and phenyl allowed an evaluation these structural effects on the formation of the phenethyl and m/z 263 radical cations. The EI-MS for these isomers are in Figures 145-147. As previously described, the 2,5-dimethoxyphenyl series of isomers showed a significant dimethoxybenzyl ion at m/z 151 as well as a significant peak for the phenethyl radical cation, the mass of which varies with the nature of the 4-substituent (m/z 164 for 4-H, m/z 242/244 for 4-Br and m/z 290 for 4-I in Scheme 58). In fact, the phenethyl radical cation is the base peak for three of the six isomers in the 25X-NBOMe series and m/z 151 is the base peak for the others, while the m/z 263 fragment is not a prominent peak in any of the six spectra for each of the 25X-NBOMe series (4 substituent = H, Br or I). However, in both the 2-MMPEADMB and 3-MMPEADMB series of isomers containing only one of the electrons donating methoxy groups in the phenethyl aromatic ring, the m/z 263 radical cation

becomes a more prominent fragment ion and the methoxyphenethyl radical cation at m/z 134 is relatively insignificant (see Figures 145-147 and Table 18). These results suggest the homolytic cleavage of the N-C bond is the favored pathway leading to the formation of m/z 263 and the neutral 2- or 3-methoxyphenethylene. This is further confirmed by the EI-MS of the unsubstituted phenethyl PEADMB series (Figure 147) with no phenylalkene radical cation at m/z 104. The m/z 151 is the base peak in all six spectra of the PEADMBs and its product ions at m/z 121 and 91 are prominent ions in this series. The presence of the m/z 263 radical cation shows that the distonic molecular radical cation continues to form in this unsubstituted phenethylamine series. However, these results suggest that the decomposition of this species favors formation of the m/z 263 species with the elimination of the neutral phenylethene molecule. Furthermore, the addition of electron donating groups to the aromatic ring of the phenethyl group as in the NBOMe-type molecules shifts the decomposition of the corresponding distonic molecular radical cation to favor the formation of the electron rich substituted phenethyl radical cation.

The mass spectra of the 2',3'-dimethoxy isomers of 2MMPEADMB, 3MMPEADMB and PEADMB each contain a m/z 136 fragment ion which is not present in the mass spectra of the other five N-(dimethoxy)benzyl regioisomers in each series. This unique ion was also observed in the spectra of all 2',3'-dimethoxy isomers of the 25X-NBOMe series as described previously and appears to form in a fragmentation process resulting from loss of a methyl group from one of the methoxy groups on the benzyl ring. In the 25X-NBOMe series (where X is 4-H, 4-Br or 4-I), the m/z 136 ion is the third most abundant after the phenethyl cation (most abundant) and dimethoxybenzyl cation (second most abundant). For the 2',3'-dimethoxy isomers of the 2- and 3-MMPEADMB series, the m/z 136 ion is less abundant than the TFA radical cation (m/z 263) and dimethoxybenzyl cation (m/z 151). However, in the mass spectra of the 2',3'-dimethoxy isomer of the PEADMB series only the dimethoxybenzyl cation (m/z 151) is more abundant than the m/z 136 ion, and the TFA radical cation (m/z 263) is formed in relatively low abundance. These data suggest that the relative abundance of unique m/z 136 ion is related to which fragmentation pattern predominates after formation of the molecular ion or distonic radical cation.

The intent of the EI-MS studies with the MMPEADMBs and PEADMB series was investigate the influence of substituents on the phenethyl aromatic ring of NBOMe derivatives on EI-MS fragmentation pathways. Analysis of the mass spectra of these compounds suggests it is possible to differentiate the regioisomeric members in each of these series based on relative fragment ion abundances, and unique ions not observed in 25X-NBOMe derivatives. For example, most of the spectra of the PEADMB compounds contain a m/z 105 ion (Scheme 59) which appears to be a phenethyl cation fragment, perhaps unique to NBOMe-type compounds lacking substituents in the phenethyl aromatic ring.



Scheme 59 The m/z 105 fragment.

Using mass spectrometry alone, even with TFA derivatization, it is not possible to readily differentiate and identify each of the six dimethoxy regioisomers in MMPEADMB or PEADMB series. For example, in both the 2-MMPEADMB and 3-MMPEADMB series the 2',4'- and 2',5'-dimethoxy regioisomers have the same five most abundant fragment ions in order with m/z 151 > 263 > 121 > 91 > 134 (Table 18). The only difference between these regioisomers is the relative abundance of the m/z 263 ion compared to the base peak (m/z 151). The same is observed for the 2',4'- and 2',5'-dimethoxy regioisomers in the PEADMB series, and in this case the m/z 263 ion of both isomers is present in essentially equal abundance relative to the base peak and other ions of high abundance (Table 18). It was possible to separate and identify the six dimethoxy regioisomers in the PEADMB series by gas chromatography as illustrated by the sample chromatogram in Figure 148 below. However, the utility of chromatographic separations for specific regioisomer identification is limited because it is dependent upon the availability of known standards for retention time correlations.

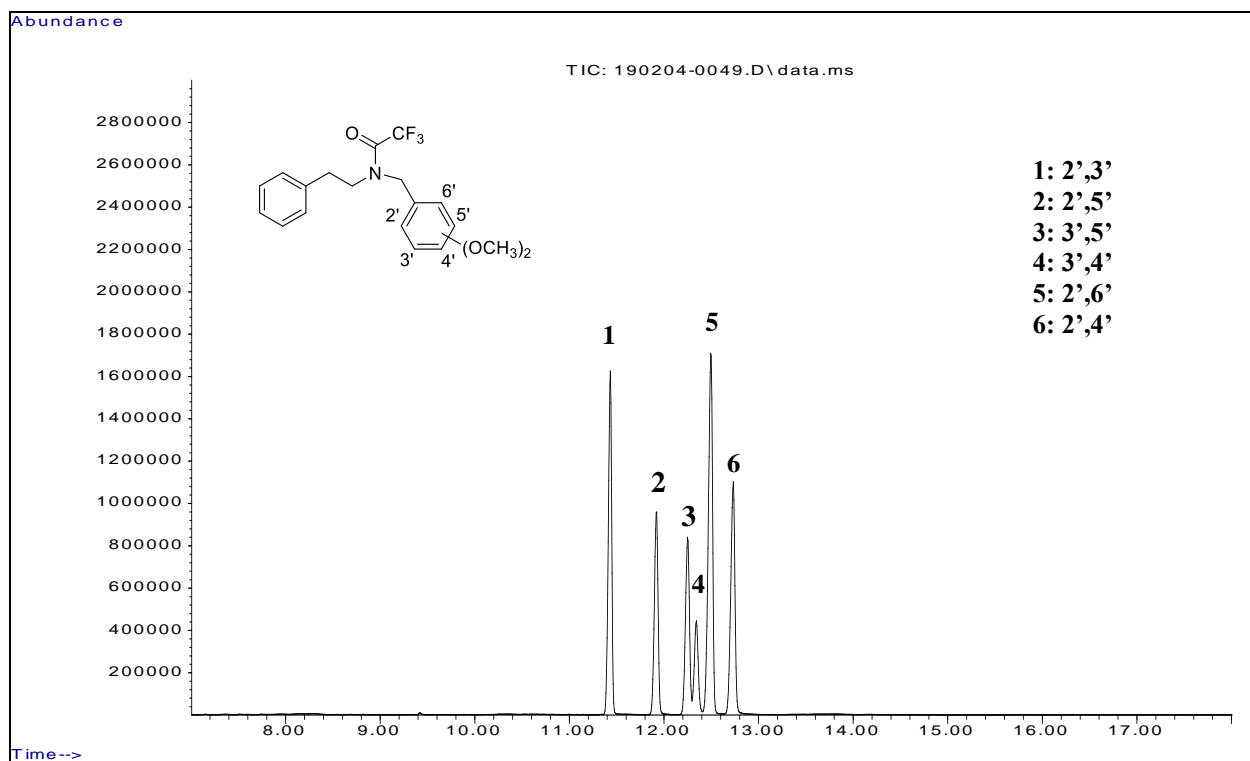


Figure 148 Gas chromatographic separation of the derivatized N-trifluoroacetamide-N-(dimethoxy)benzylphenethylamines.

11 Pharmacology

11.1 Experimental Procedure and Data Analysis:

A number of the NBOMe compounds reported in this dissertation were selected for screening in neurotransmitter receptor and transporter assays by the University of North Carolina's Psychoactive Drug Screening Program (PDSP). The receptors and transporters included in this screening are shown in Table 19 along with the cell lines used to prepare membrane pallets for the binding assays. All clones were stable lines, while transient cells are marked with an asterisk. Most clones are of human origin unless noted, such as (rat) behind receptor name. Detailed information about media is included in the PDSP Protocol Manual [112].

All compounds were converted to their corresponding HCl salts prior to testing to enhance water solubility in the receptor assays. A solution of the compound to be tested was prepared as a 1-mg/ml stock in Standard Binding Buffer or DMSO according to its solubility. A similar stock of a reference compound (positive control) was also prepared. Eleven dilutions (5 x assay concentration) of the test and reference compounds are prepared in standard binding buffer by serial dilution: 0.05 nM, 0.5 nM, 1.5 nM, 5 nM, 15 nM, 50 nM, 150 nM, 500 nM, 1.5 μ M, 5 μ M, 50 μ M (thus, the corresponding assay concentrations span from 10 pM to 10 μ M and include semilog points in the range where high-to-moderate affinity ligands compete with radioligand for binding sites). The standard binding buffer was composed of 50 mM Tris HCl, 10 mM MgCl₂, 0.1 mM EDTA, pH 7.4.

Radioligand (see Tables that follow for each the radioligand used for receptor subtype) was diluted to five times the assay concentration in Standard Binding Buffer. Typically, the assay concentration of radioligand was a value between one half the *KD* and the *KD* of a particular radio ligand at its target. Aliquots (50 μ l) of radioligand were dispensed into the wells of a 96-well plate (see Figure 149) containing 100 μ l of standard binding buffer (described above). Then, duplicate 50- μ l aliquots of the test and reference compound dilutions were added. Finally, crude membrane fractions of cells expressing recombinant target were resuspended in 3 ml of chilled Standard Binding Buffer and homogenized by several passages through a 26 gauge needle, then 50 μ l were dispensed into each well (Figure 149).

The 250- μ l reactions were incubated at room temperature and shielded from light (to prevent photolysis of light-sensitive ligands) for 1.5 hours, then harvested by rapid filtration onto Whatman GF/B glass fiber filters pre-soaked with 0.3% polyethyleneimine using a 96-well Brandel harvester. Four rapid 500- μ l washes were performed with chilled Standard Binding Buffer to reduce non-specific binding. Filters were placed in 6-ml scintillation tubes and allowed to dry overnight. The next day, 4 ml of EcoScint scintillation cocktail were added to each tube. The tubes were capped, labeled, and counted by liquid scintillation counting. For higher throughput assays, bound radioactivity is harvested onto 0.3% polyethyleneimine-treated, 96-well filter mats using a 96-well Filtermate harvester. The filter mats were dried, then scintillant was melted onto the filters and the radioactivity retained on the filters was counted in a Microbeta scintillation counter.

Table 19 Cell lines used to prepare membrane pallets for the binding assays

Receptor	Note	Parental cells	Media (see details below the table)
Serotonin (5HT)			
5-HT _{1A}		stable CHO	500 G418
5-HT _{1B}		stable HEK	500 G418
5-HT _{1D}	*	HEKT	COS/HEK
5-HT _{1E}		stable HEK	500 G418
5-HT _{2A} (rat)		stable 3T3	500 G418
5-HT _{2A}	*	HEKT	COS/HEK
5-HT _{2B}		stable HEK	2 µg/ml Puromycin
5-HT _{2C}		HEK T	COS/HEK
5-HT ₃	*	HEKT	COS/HEK
5-HT ₄		HEK T	COS/HEK
5-HT _{5A}		Flp-In CHO	DMEM/F-12 200 µg/ml Hygromycin B
5-HT ₆		stable HEK	500 G418
5-HT _{7A}		Stable HEK	2 µg/ml Puromycin
Dopamine			
D ₁	*	HEKT	COS/HEK
D ₂		stable fibroblast	COS/HEK
D _{2L}		stable CHO	F-12/10%FBS 400G418
D ₃ (rat)	*	HEKT	COS/HEK
D ₃	*	HEKT	COS/HEK
D ₄		Stable HEK	DMEM/F12 10% CS Fe+
D ₅	*	HEKT	COS/HEK
Opioid			
DOR		stable HEK	200 G418
MOR		stable HEK	200 G418
KOR (rat)		stable HEK	500 G418
KOR		stable HEK	500 G418
NOP	*	HEKT	COS/HEK
Neurotransmitter Transporters			
SERT		stable HEK	500 G418
NET		stable HEK	hNET (250 G418)
DAT		stable HEK	hDAT (350 G418)
Adrenergic			
α _{1A}		stable	500 G418
α _{1B}	*	HEKT	
α _{1D}		stable	500 G418
α _{2A}		stable MDCK	500 G418
α _{2B}	*	HEKT	COS/HEK
α _{2C}		stable MDCK	500 G418
β ₁		CHO Flp-In	DMEM/F12 200 µg/ml Hygromycin B
β ₂		HEK Flp-In	DMEM 100 µg/ml Hygromycin B
β ₃		HEK Flp-In	DMEM 100 µg/ml Hygromycin B
Muscarinic acetylcholine			
M ₁		stable CHO	250 G418
M ₂		stable CHO	500 G418
M ₃		stable CHO	500 G418
M ₄		stable CHO	10% FBS F12
M ₄ D (DREADD)		HEKT	COS/HEK
M ₅		stable CHO	250 G418
Histamine			
H ₁		stable HEK	500 G418
H ₂		Stable HEK	In Progress
H ₃		HEK Flp-In	DMEM 100 µg/ml Hygromycin B
H ₄		HEK T	COS/HEK
Sigma1	*	HEKT	
Sigma2	*	HEKT	

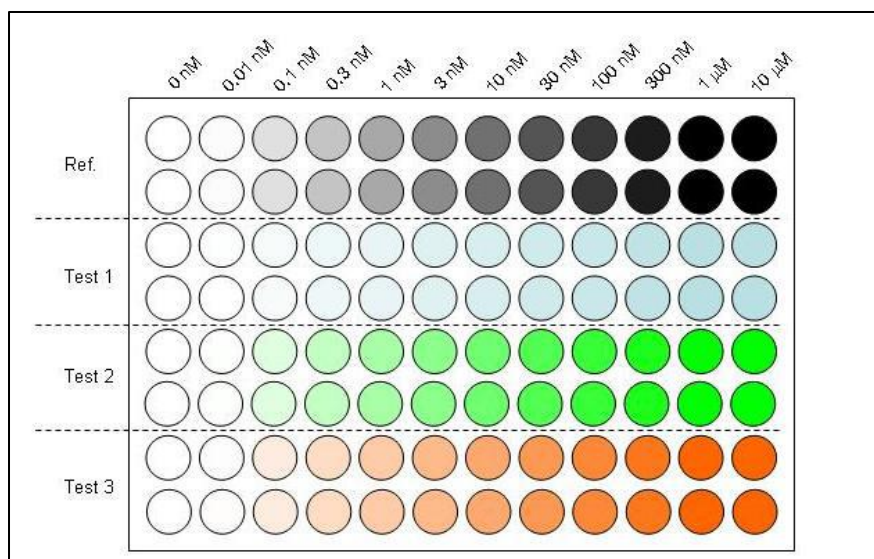


Figure 149 Schematic of binding assay plate. Increasing concentrations (0.01 nM to 10 μ M, from left to right) of reference or test compound are added (50 μ L aliquots, in duplicate) from 5x stocks to wells containing 50 μ L of 5x radioligand (fixed concentration, prepared in buffer) and 100 μ L of buffer. Finally, 50 μ L of receptor-containing membrane homogenate (5x suspension in buffer) are added to achieve a final assay volume of 250 μ L.

Raw data (dpm) representing total radioligand binding (*i.e.*, specific + non-specific binding) were plotted as a function of the logarithm of the molar concentration of the competitor (*i.e.*, test or reference compound). Non-linear regression of the normalized (*i.e.*, percent radioligand binding compared to that observed in the absence of test or reference compound) raw data were performed in Prism 4.0 (GraphPad Software) using the built-in three parameter logistic model describing ligand competition binding to radioligand-labeled sites as follows:

$$y = \text{bottom} + [(\text{top}-\text{bottom})/(1 + 10^{\text{x}-\log\text{IC50}})]$$

where bottom equals the residual radioligand binding measured in the presence of 10 μ M reference compound (*i.e.*, non-specific binding) and top equals the total radioligand binding observed in the absence of competitor.

The log IC₅₀ (*i.e.*, the log of the ligand concentration that reduces radioligand binding by 50%) was thus estimated from the data and used to obtain the *K_i* by applying the Cheng-Prusoff

approximation shown below. K_i values were converted to pK_i values ($-\log K_i$) in the tables that follow:

$$K_i = IC_{50}/(1 + [ligand]/K_D)$$

where [ligand] equals the assay radioligand concentration and K_D equals the affinity constant of the radioligand for the target receptor. Examples of dose-response plots obtained and the resultant K_i values (as pK_i values) are presented in the sections that follow.

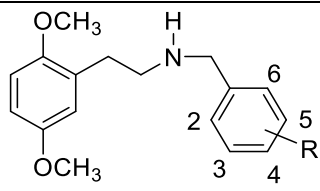
11.2 Serotonin 5-HT₁ Receptor Binding Profiles:

The sub-classification and physiologic functions of serotonin receptor subtypes were described in the Review of the Literature (Chapter 1). The experimental conditions used to determine receptor binding profiles of the NBOMe compounds at serotonin receptor subtypes are detailed in Table 20 below. The reference standards for the 5-HT₁ receptor subtypes have pK_i values (-log K_i) ranging from 8.05 (8.82 nM) for ergotamine at 5-HT_{1E} receptors to 9.18 (0.66 nM) for 8-OH-DPAT at 5-HT_{1A} receptors. Previous studies have shown that 25B-NBOMe and 25I-NBOMe have relatively low affinity for all of the 5-HT₁ receptor subtypes with pK_i values < 6.5 (K_i 250 nM) [18, 21].

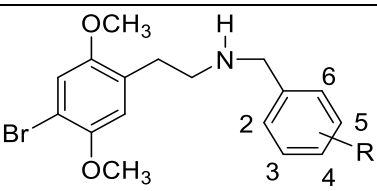
Table 20 Experimental conditions used to determine receptor binding profiles of the NBOMe compounds at serotonin receptor subtypes.

5-HT receptors			
Standard BB (SBB): 50 mM Tris HCl, 10 mM MgCl ₂ , 0.1 mM EDTA, pH 7.4, RT			
Standard WB (SWB): 50 mM Tris HCl, pH 7.4, cold			
Target	Radioligand pK _d ± SEM (K _d , nM)	Radioligand used (nM)	Reference Ligand pK _i ± SEM (K _i , nM)
5-HT _{1A}	[³ H]-Way100635 9.30 ± 0.04 (0.50)	0.5 – 1.0	8-OH-DPAT 9.18 ± 0.02 (0.66)
5-HT _{1B}	[³ H]5-CT 9.06 ± 0.09 (0.87)	0.6 – 1.5	Ergotamine 8.84 ± 0.03 (1.44)
5-HT _{1D}	[³ H]5-CT 9.06 ± 0.06 (0.86)	1.0 – 2.0	Ergotamine 8.32 ± 0.02 (4.83)
5-HT _{1E}	[³ H]5-HT 8.42 ± 0.06 (3.82)	2.1 – 5.0	5-HT 8.05 ± 0.03 (8.82)
5-HT _{1F}			

The data in Tables 21-23 demonstrate that the 5-HT₁ receptor subtypes also have very low affinity for the 3'- and 4'-methoxy regioisomers, as well as all dimethoxy and methylenedioxy regioisomers of the 4H, 4Br and 4I-DMPEA series prepared in this study, all pK_i values below 7 (100 nM). The 4I25-DMPEAs generally had higher affinities than their corresponding 4H25-DMPEA and 4Br25-DMPEA derivatives at these receptor subtypes, but even all of these compounds have significantly lower affinity than the reference standards. Also, the MPEABrDMBz (reverse NBOMes or “eMOBN”) isomers have minimal affinity at 5-HT_{1B-E} receptors subtypes and only modest affinity for 5-HT_{1A} receptors with pK_i values ranging from <5 to 7.32 for the 2MPEA4Br25DMBzHCl isomer (tables 24). The differences in activity between the NBOMe compounds and the reference standards are further highlighted by the dose-response curves in Figure 150.

Table 21 Binding Affinity of the 4H25-DMPEA Series at 5-HT₁ Receptor Subtypes.


PDSP ID Number (4H25-DMPEAs)	5-HT_{1A}, pKi (SE)	5-HT_{1B}, pKi (SE)	5-HT_{1D}, pKi (SE)	5-HT_{1E}, pKi (SE)
48238 (25DMPEA2MBzHCl)	5.61±0.08	<5 (ND)	<5 (ND)	<5 (ND)
48239 (25DMPEA3MBzHCl)	6.1±0.1	<5 (ND)	<5 (ND)	<5 (ND)
48240 (25DMPEA4MBzHCl)	5.88±0.08	<5 (ND)	<5 (ND)	<5 (ND)
48241 (25DMPEA23DMBzHCl)	5.57±0.09	<5 (ND)	<5 (ND)	<5 (ND)
48242 (25DMPEA24DMBzHCl)	5.66±0.06	<5 (ND)	<5 (ND)	<5 (ND)
48243 (25DMPEA25DMBzHCl)	<5 (ND)	<5 (ND)	<5 (ND)	<5 (ND)
48244 (25DMPEA26DMBzHCl)	5.75±0.09	<5 (ND)	<5 (ND)	<5 (ND)
48257 (25DMPEA34DMBzHCl)	<5 (ND)	5.5±0.1	<5 (ND)	<5 (ND)
48258 (25DMPEA35DMBzHCl)	6.08±0.05	<5 (ND)	<5 (ND)	<5 (ND)
48245 (25DMPEA23MDBzHCl)	6.0±0.1	<5 (ND)	5.2±0.1	<5 (ND)
48259 (25DMPEA34MDBzHCl)	6.26±0.05	<5 (ND)	<5 (ND)	<5 (ND)

Table 22 Binding Affinity of the 4Br25-DMPEA Series at 5-HT₁ Receptor Subtypes.


PDSP ID Number (4Br25-DMPEAs)	5-HT_{1A}, pKi (SE)	5-HT_{1B}, pKi (SE)	5-HT_{1D}, pKi (SE)	5-HT_{1E}, pKi (SE)
48246 (4Br25DMPEA2MBzHCl)	6.15±0.09	<5 (ND)	<5 (ND)	<5 (ND)
48247 (4Br25DMPEA3MBzHCl)	5.75±0.09	<5 (ND)	5.8±0.1	<5 (ND)
48248 (4Br25DMPEA4MBzHCl)	6.04±0.09	<5 (ND)	<5 (ND)	5.3±0.1
48249 (4Br25DMPEA23DMBzHCl)	6.02±0.09	6.1±0.1	5.7±0.1	5.3±0.1
48250 (4Br25DMPEA24DMBzHCl)	6.0±0.1	5.4±0.1	<5 (ND)	5.3±0.1
48251 (4Br25DMPEA25DMBzHCl)	6.2±0.1	5.8±0.1	<5 (ND)	<5 (ND)
48252 (4Br25DMPEA26DMBzHCl)	6.3±0.1	5.5±0.1	5.3±0.1	<5 (ND)
48253 (4Br25DMPEA34DMBzHCl)	6.1±0.1	<5 (ND)	5.3±0.1	5.5±0.1
48254 (4Br25DMPEA35DMBzHCl)	5.9±0.09	<5 (ND)	5.5±0.1	5.56±0.09
48255 (4Br25DMPEA23MDBzHCl)	5.9±0.1	<5 (ND)	5.5±0.1	5.78±0.09
48256 (4Br25DMPEA34MDBzHCl)	6.05±0.09	5.7±0.1	5.8±0.1	<5 (ND)

Table 23 Binding Affinity of the 4I25-DMPEA Series at 5-HT₁ Receptor Subtypes.

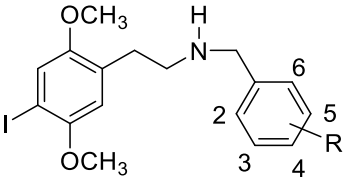
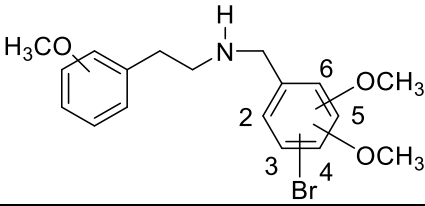
				
PDSP ID Number (4I25-DMPEAs)	5-HT_{1A}, pKi (SE)	5-HT_{1B}, pKi (SE)	5-HT_{1D}, pKi (SE)	5-HT_{1E}, pKi (SE)
48260 (4I25DMPEA2MBzHCl)	6.1±0.1	5.4±0.1	5.63±0.08	<5 (ND)
48261 (4I25DMPEA3MBzHCl)	6.1±0.1	<5 (ND)	5.90±0.08	<5 (ND)
48262 (4I25DMPEA4MBzHCl)	6.2±0.1	<5 (ND)	5.51±0.08	<5 (ND)
48263 (4I25DMPEA23DMBzHCl)	6.73±0.05	<5 (ND)	5.79±0.09	<5 (ND)
48264 (4I25DMPEA24DMBzHCl)	6.65±0.05	<5 (ND)	5.92±0.09	<5 (ND)
48265 (4I25DMPEA25DMBzHCl)	6.8±0.05	<5 (ND)	5.75±0.08	<5 (ND)
48266 (4I25DMPEA26DMBzHCl)	6.89±0.05	6.44±0.09	6.40±0.07	6.7±0.1
48267 (4I25DMPEA34DMBzHCl)	6.42±0.06	<5 (ND)	<5 (ND)	<5 (ND)
48268 (4I25DMPEA35DMBzHCl)	6.48±0.05	<5 (ND)	<5 (ND)	<5 (ND)
48269 (4I25DMPEA23MDBzHCl)	6.65±0.05	<5 (ND)	<5 (ND)	<5 (ND)
48270 (4I25DMPEA34MDBzHCl)	6.54±0.05	6.04±0.09	6.05±0.07	6.0±0.1

Table 24 Binding Affinity of MPEABrDMBz (“eMOBN”) Series at 5-HT₁ Receptor Subtypes.

				
PDSP ID Number (MPEABrDMBzs)	5-HT_{1A}, pKi (SE)	5-HT_{1B}, pKi (SE)	5-HT_{1D}, pKi (SE)	5-HT_{1E}, pKi (SE)
48271 (2MPEA4Br25DMBzHCl)	7.32±0.05	<5 (ND)	<5 (ND)	<5 (ND)
48272 (3MPEA4Br25DMBzHCl)	6.97±0.05	<5 (ND)	<5 (ND)	<5 (ND)
48273 (4MPEA4Br25DMBzHCl)	6.75±0.05	<5 (ND)	<5 (ND)	<5 (ND)
48274 (2MPEA2Br45DMBzHCl)	5.73±0.08	<5 (ND)	<5 (ND)	<5 (ND)
48275 (3MPEA2Br45DMBzHCl)	6.00±0.08	<5 (ND)	<5 (ND)	<5 (ND)
48276 (4MPEA2Br45DMBzHCl)	<5 (ND)	<5 (ND)	<5 (ND)	<5 (ND)

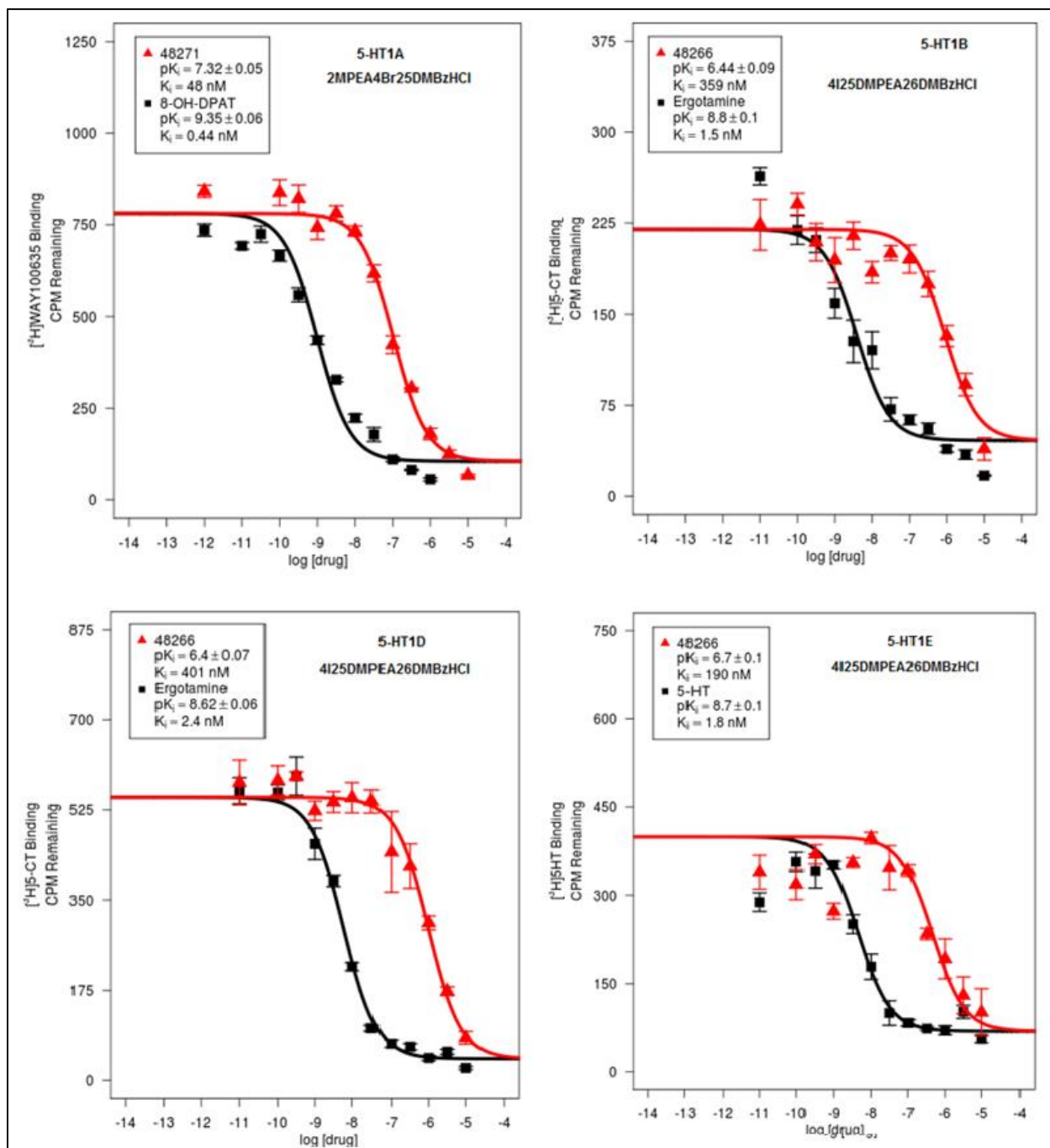


Figure 150 Dose response curves for the most potent 4X25DMPEA derivatives at 5-HT₁ receptor subtypes.

11.3 Serotonin 5-HT₂ Receptor Binding Profiles:

The experimental conditions used to determine receptor binding profiles of the NBOMe compounds at all serotonin receptor subtypes are detailed in Table 25. The reference standards for the 5-HT₂ receptor types include clozapine with a pK_i of 8.23 (K_i 5.91 nM) at 5-HT_{2A} receptors, SB206553 with a pK_i of 7.84 (K_i 14.4 nM) at 5-HT_{2B} receptors and ritanserin with a pK_i of 8.84 (K_i 1.44 nM) at 5-HT_{2C} receptors. Previous studies have shown that 5-HT_{2A} and 5-HT_{2C} receptors have very high affinities for 25X-NBOMe with a pK_i of 9.58 for 25B-NBOMe and 10.09 for 25I-NBOMe (K_is < 1.0 nM) [18, 21].

Table 25 Experimental conditions used to determine receptor binding profiles of the NBOMe compounds at serotonin receptor subtypes 2.

5-HT receptors			
Standard BB (SBB): 50 mM Tris HCl, 10 mM MgCl ₂ , 0.1 mM EDTA, pH 7.4, RT Standard WB (SWB): 50 mM Tris HCl, pH 7.4, cold			
Target	Radioligand pK _d ± SEM (K _d , nM)	Radioligand used (nM)	Reference Ligand pK _i ± SEM (K _i , nM)
5-HT _{2A}	[³ H]-Ketanserin 8.92 ± 0.04 (1.20)	1.2 – 2.4	Clozapine 8.23 ± 0.01 (5.91)
5-HT _{2B}	[³ H]-LSD 8.93 ± 0.03 (1.19)	1.0 – 2.0	SB206553 7.84 ± 0.01 (14.39)
5-HT _{2C}	[³ H]-Mesulergine 5.85 ± 0.06 (2.66)	1.0 – 2.5	Ritanserin 8.84 ± 0.02 (1.44)

The 5-HT₂ receptor binding profiles for the compounds synthesized in this study are shown in Tables 26-29 and dose response curves for the most potent ligand at each receptor subtype are shown in Figure 151.

As the data in the Tables 26-28 indicate, the relative 5-HT₂ receptor subtype binding profile for most of the 4X25-DMPEA (X = H, Br or I) derivatives prepared in this study is 5-HT_{2A} > 5-HT_{2B} > 5-HT_{2C}. The exceptions include the 3,4-dimethoxy, 3,5-dimethoxy and 3,4-methylenedioxy members in these series which have higher affinity for 5-HT_{2B} receptors than 5-HT_{2A} and 5-HT_{2C}

subtypes. These data suggest that 5-HT₂ receptor subtype selectivity in this series can be altered by varying substitution on the on N-benzyl ring.

Analysis of the receptor binding data at the 5-HT_{2A} and 5-HT_{2C} receptor subtype for each series of 4X25-DMPEA derivatives illustrates a number of interesting trends. At 5-HT_{2A} receptor subtypes, generally the 4I25-DMPEA derivatives have higher affinities than their corresponding 4Br25-DMPEA derivatives, and the 4Br25-DMPEA derivatives have higher affinities than their corresponding 4H25-DMPEA derivatives. This is illustrated by comparing the 2'-methoxy derivatives of each series where the 4I25-DMPEA2MBz has a higher pKi (10.0) than the corresponding 4Br25-DMPEA2MBz derivative (pKi 9.54) which has a higher pKi (7.84) than the unsubstituted 4H25-DMPEA2MBz derivative. Furthermore, this is consistent with structure-activity data reported earlier for NBOMe compounds where 4-bromo substitution and 4-iodo substitution resulted in increased 5-HT_{2A} receptor affinity [18, 21].

Analysis of the receptor binding data at the 5-HT_{2A} receptor subtype for each series of 4X25-DMPEA derivatives also illustrates several consistent structure-activity trends. For example, for each series of monomethoxy 4X25-DMPEAMBz derivatives, the 2'-methoxy derivative displays higher 5-HT_{2A} affinity than the 3'-methoxy derivative, and the 3'-methoxy derivative higher affinity than the 4'-methoxy analog. This is illustrated by comparing the pKi values for the most potent 4I25-DMPEAMBz series where the 2'-methoxy isomer (4I25-DMPEA2MBz) has a pKi of 10.0, the 3'-methoxy (4I25-DMPEA3MBz) a pKi of 9.5 and the 4'-methoxy (4I25-DMPEA4MBz) isomer a pKi of 7.8. Also, in all three 4X25-DMPEA series, the 2',3'-methylenedioxy derivatives (4X25MPEA23MDBzs) have higher 2-HT2A receptor affinities than the corresponding 3',4'-methoxydioxy isomers (4X25-DMPEA34MDBzs). For example, 4I25-DMPEA23MBz has a pKi 9.4 at this receptor subtype while 4I25-DMPEA34MDBz has a pKi of 8.6. Also, the 2'-methoxy derivatives (4X25-DMPEA2MBz) in each series and 2',3'-methylenedioxy (4X25-DMPEA23MDB) derivatives are more potent any of the corresponding dimethoxy derivatives (4X25-DMPEADMBzs). Also, structure-activity trends among the dimethoxy derivatives (4X25-DMPEADMBzs) in each of these series are less consistent. This is illustrated in the 4H25-

DMPEADMBz series where the 2',6'-dimethoxy isomer has the highest 5-HT_{2A} receptor affinity and the 2',4'-dimethoxy isomer the lowest.

But in the more potent 4Br25-DMPEADMBz and 4I25-DMPEADMBz series the 2'3'- and 2'4'-dimethoxy isomers have the highest affinity at 5-HT_{2A}, while the 2',6'-dimethoxy isomers have among the lowest affinities. These data may suggest that 4-halogenated NBOMe derivatives (4Br25-DMPEAs and 4I25-DMPEAs) may interact with 5-HT_{2A} receptors differently than 4-unsubstituted NBOMe derivatives such as the 25DMPEAs.

Table 26 Binding Affinity of the 4H25-DMPEA Series at 5-HT₂ Receptor Subtypes.

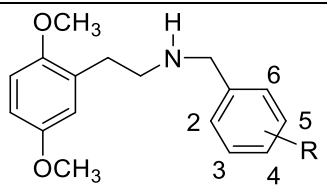
			
PDSP ID Number (4H25-DMPEAs)	5-HT_{2A}, pKi (SE)	5-HT_{2B}, pKi (SE)	5-HT_{2C}, pKi (SE)
48238 (25DMPEA2MBzHCl)	7.84±0.07	7.57±0.08	7.2±0.1
48239 (25DMPEA3MBzHCl)	7.32±0.07	7.06±0.07	6.58±0.08
48240 (25DMPEA4MBzHCl)	6.93±0.07	6.51±0.06	5.89±0.08
48241 (25DMPEA23DMBzHCl)	6.31±0.07	7.09±0.06	6.24±0.08
48242 (25DMPEA24DMBzHCl)	5.86±0.07	<5 (ND)	<5 (ND)
48243 (25DMPEA25DMBzHCl)	6.33±0.08	<5 (ND)	<5 (ND)
48244 (25DMPEA26DMBzHCl)	7.61±0.08	7.22±0.06	6.44±0.08
48257 (25DMPEA34DMBzHCl)	6.2±0.1	7.04±0.07	6.3±0.1
48258 (25DMPEA35DMBzHCl)	6.0±0.1	7.01±0.07	6.2±0.1
48245 (25DMPEA23MDBzHCl)	7.17±0.07	6.85±0.06	6.65±0.09
48259 (25DMPEA34MDBzHCl)	6.7±0.1	8.56±0.08	6.3±0.1

Table 27 Binding Affinity of the 4Br25-DMPEA Series at 5-HT₂ Receptor Subtypes.

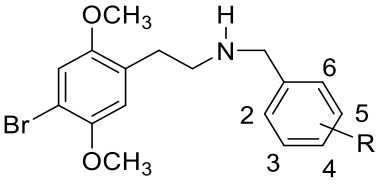
			
PDSP ID Number (4Br25-DMPEAs)	5-HT_{2A}, pKi (SE)	5-HT_{2B}, pKi (SE)	5-HT_{2C}, pKi (SE)
48246 (4Br25DMPEA2MBzHCl)	9.54±0.07	8.97±0.06	8.93±0.08
48247 (4Br25DMPEA3MBzHCl)	9.14±0.07	8.18±0.06	8.39±0.08
48248 (4Br25DMPEA4MBzHCl)	7.95±0.07	7.52±0.06	7.3±0.1
48249 (4Br25DMPEA23DMBzHCl)	8.49±0.07	8.20±0.09	7.8±0.1
48250 (4Br25DMPEA24DMBzHCl)	7.71±0.07	8.0±0.1	7.7±0.1
48251 (4Br25DMPEA25DMBzHCl)	7.38±0.08	7.2±0.1	7.3±0.1
48252 (4Br25DMPEA26DMBzHCl)	6.69±0.09	9.09±0.07	8.3±0.1
48253 (4Br25DMPEA34DMBzHCl)	7.2±0.1	7.94±0.07	6.9±0.1
48254 (4Br25DMPEA35DMBzHCl)	7.54±0.09	7.74±0.07	7.22±0.07
48255 (4Br25DMPEA23MDBzHCl)	9.7±0.1	8.92±0.07	8.4±0.1
48256 (4Br25DMPEA34MDBzHCl)	8.8±0.1	9.28±0.07	7.8±0.1

Table 28 Binding Affinity of the 4I25-DMPEA Series at 5-HT₂ Receptor Subtypes.

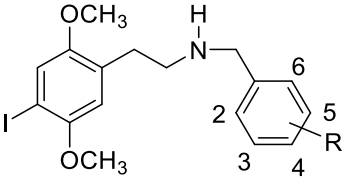
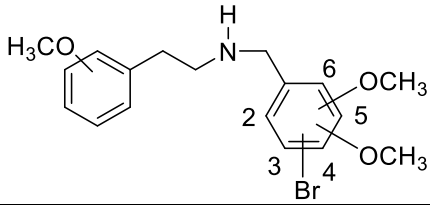
			
PDSP ID Number (4I25-DMPEAs)	5-HT_{2A}, pKi (SE)	5-HT_{2B}, pKi (SE)	5-HT_{2C}, pKi (SE)
48260 (4I25DMPEA2MBzHCl)	10.0±0.1	8.5±0.1	9.09±0.04
48261 (4I25DMPEA3MBzHCl)	9.5±0.1	8.2±0.1	8.30±0.04
48262 (4I25DMPEA4MBzHCl)	7.8±0.1	8.0±0.1	7.51±0.04
48263 (4I25DMPEA23DMBzHCl)	8.9±0.1	7.88±0.07	8.18±0.05
48264 (4I25DMPEA24DMBzHCl)	8.1±0.1	8.0±0.1	8.28±0.05
48265 (4I25DMPEA25DMBzHCl)	7.8±0.1	7.34±0.08	7.79±0.05
48266 (4I25DMPEA26DMBzHCl)	7.9±0.1	9.10±0.03	8.51±0.05
48267 (4I25DMPEA34DMBzHCl)	7.6±0.1	8.06±0.03	7.07±0.07
48268 (4I25DMPEA35DMBzHCl)	7.6±0.1	7.91±0.03	7.17±0.07
48269 (4I25DMPEA23MDBzHCl)	9.4±0.1	8.97±0.03	8.52±0.07
48270 (4I25DMPEA34MDBzHCl)	8.6±0.1	9.26±0.04	7.84±0.09

Table 29 Binding Affinity of MPEABrDMBz (“eMOBN”) Series at 5-HT₂ Receptor Subtypes.

			
PDSP ID Number (MPEABrDMBzs)	5-HT_{2A}, pKi (SE)	5-HT_{2B}, pKi (SE)	5-HT_{2C}, pKi (SE)
48271 (2MPEA4Br25DMBzHCl)	7.4±0.1	7.49±0.04	7.02±0.09
48272 (3MPEA4Br25DMBzHCl)	7.6±0.1	8.23±0.03	7.17±0.08
48273 (4MPEA4Br25DMBzHCl)	6.9±0.2	7.89±0.06	6.57±0.08
48274 (2MPEA2Br45DMBzHCl)	5.9±0.2	7.29±0.06	5.96±0.06
48275 (3MPEA2Br45DMBzHCl)	6.1±0.1	7.79±0.06	5.81±0.06
48276 (4MPEA2Br45DMBzHCl)	<5 (ND)	7.66±0.06	ND

Analysis of the receptor binding data at the 5-HT_{2C} receptor subtype for each series of 25X-DMPEA derivatives illustrates the same basic structure-activity trends observed for 5-HT_{2A} receptors. To summarize, again for three series (4X25-DMPEAMBzs where X = H, Br or I), the 2'-methoxy derivative displays higher 5-HT_{2C} affinity than the 3'-methoxy derivative, and the 3'-methoxy derivative higher affinity than the 4'-methoxy analog. Also, in all three 4X25-DMPEA series, the 2',3'-methylenedioxy derivatives (4X25-DMPEA23MDBzs) have higher 5-HT_{2C} receptor affinities than the corresponding 3',4'-methoxydioxy isomers (4X25-DMPEA34MDBzs). Unlike the activity pattern at 5-HT_{2A} receptors, the binding profiles for the dimethoxy isomers (4X25-DMPEADMBzs) at 5-HT_{2C} receptors were more consistent across series. At 5-HT_{2C} receptors the 2',6'- and 2',3'-dimethoxy isomers were among the most potent, while 2',5'-, 3',4'- and 3',5'-dimethoxy isomers were least potent. These data may suggest that 5-HT_{2A} versus 5-HT_{2C} receptor selectivity could be achieved by modification of the substitution pattern in the N-benzyl portion of the aromatic ring of NBOMe compounds.

Finally, Table 29 shows the 5-HT₂ receptor subtype binding profiles for the MPEABrDMBz or “reversed 25Br-NBOMes” (eMOBNs). In these compounds the traditional bromo-dimethoxy substitution pattern is moved from the phenethyl aromatic ring to the N-benzyl ring, and the single methoxy group present in 25Br-NBOMe (4Br25DMPEAMBzs) is moved from the N-benzyl aromatic ring to the phenethyl ring. All of these derivatives display significantly reduced affinity at all 5-HT₂ receptor subtypes compared to their 25X-NBOMe or 4Br25DMPEAMBz analogs.

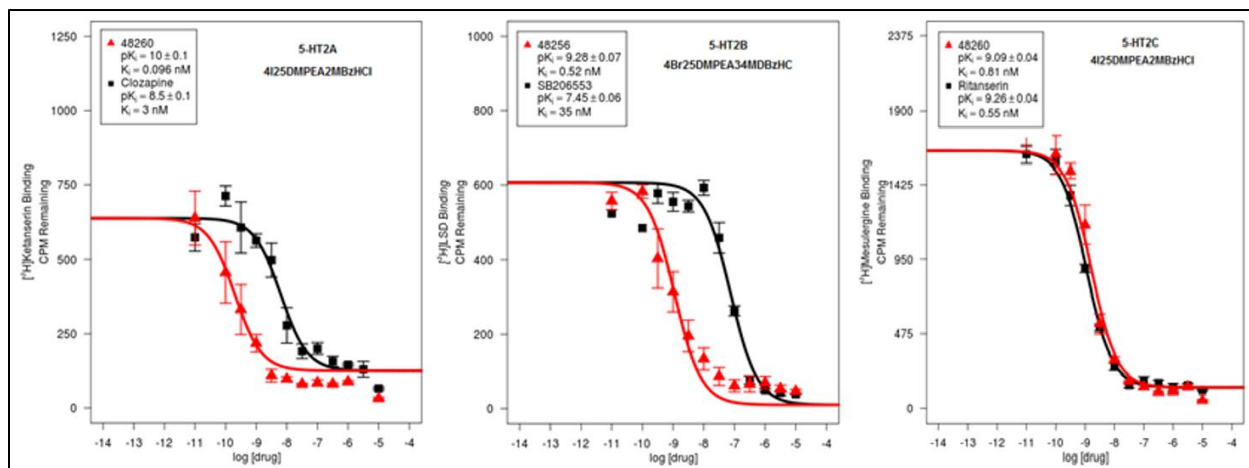


Figure 151 Dose response curves for the most potent 4X25DMPEA derivatives at 5-HT₂ receptor subtypes.

11.4 Serotonin 5-HT₃₋₇ Receptor Binding Profiles:

The experimental conditions used to determine receptor binding profiles of the 4x25-DMPEA - NBOMe compounds at serotonin receptor subtypes are detailed in Table 30. The reference standards for these receptor subtypes have pK_i values ranging from 9.23 (K_i 0.58 nM) for zacopride at 5-HT₃ receptor subtypes to 7.61 (K_i 24.6 nM) for ergotamine at 5-HT_{5A} receptors. Previous studies have shown that 25B-NBOMe and 25I-NBOMe have very low affinity at 5-HT₃, 5-HT_{5A} and 5-HT₇ receptor subtypes with pK_i values < 6.5 (K_i > 250 nM) [18, 21]. The binding data obtained is presented in Table 31-34 below.

Table 30 Experimental conditions used to determine receptor binding profiles of the NBOMe compounds at different serotonin receptor.

5-HT receptors			
Standard BB (SBB): 50 mM Tris HCl, 10 mM MgCl ₂ , 0.1 mM EDTA, pH 7.4, RT			
Standard WB (SWB): 50 mM Tris HCl, pH 7.4, cold			
Target	Radioligand pK _d ± SEM (K _d , nM)	Radioligand used (nM)	Reference Ligand pK _i ± SEM (K _i , nM)
5-HT ₃	[³ H]GR65630 8.46 ± 0.14 (3.48)	1.0 – 2.0	Zacopride 9.23 ± 0.02 (0.58)
5-HT ₄	[³ H]GR113808 8.66 ± 0.17 (2.19)	0.5 – 2.0	SDZ205557 7.94 ± 0.09 (11.44)
5-HT _{5A}	[³ H]-LSD 8.72 ± 0.03 (1.91)	2.0 - 3.3	Ergotamine 7.61 ± 0.03 (24.60)
5-HT ₆	[³ H]-LSD 8.37 ± 0.04 (4.27)	2.0 – 4.0	Clozapine 8.28 ± 0.02 (5.27)
5-HT _{7A}	[³ H]-LSD 8.13 ± 0.06 (7.48)	5.0 – 6.0	Clozapine 7.99 ± 0.02 (10.33)

The 5-HT receptor binding profiles for the compounds synthesized in this study are shown in Tables 31-34 and dose response curves for the most potent ligand at each receptor subtype are shown in Figure 152.

As the data in Table 31-33 demonstrate, the 5-HT₃, 5-HT_{5A} and 5-HT₇ receptors all have relatively low affinity for the of the methoxy-, dimethoxy- and methylenedioxy-regioisomers of the 4H25-DMPEA, 4Br25-DMPEA and 4I25-DMPEA series with pK_i values below 7 (K_i > 100 nM). Most

derivatives in the 4Br25-DMPEA and 4I25-DMPEA series displayed weak binding at 5-HT₆ receptor subtypes with pK_is in the 6-7 range (K_is < 100 nM).

In general, the 4Br25-DMPEA and 4I25-DMPEA derivatives displayed higher affinities at 5-HT₆ receptors, with the most potent compounds being the 2'-methoxy (4Br- and 4I25-DMPEA2MBz) and most of the dimethoxy isomers (4Br- and 4I25-DMPEADMBzs) having pK_is > 7 (100 nM). However even these most active derivatives had affinities approximately 20-fold lower than the reference compound clozapine (pK_i 8.28, K_i 5.3 nM).

As the data in Table 34 demonstrate, none of the MPEABrDMBz (“eMOBN”) compounds have significant affinity (pK_is > 6 or >1000 nM) for the 5-HT₃, 5a, 6, 7 receptors

Table 31 Binding Affinity of the 4H25-DMPEA Series at 5-HT_{3,7} Receptor Subtypes.

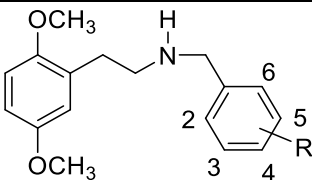
	5-HT ₃	5-HT _{5A}	5-HT ₆	5-HT ₇
	pK _i (SE)	pK _i (SE)	pK _i (SE)	pK _i (SE)
48238 (25DMPEA2MBzHCl)	<5 (ND)	5.20±0.1	5.7±0.1	<5 (ND)
48239 (25DMPEA3MBzHCl)	<5 (ND)	5.30±0.1	5.8±0.1	5.89±0.09
48240 (25DMPEA4MBzHCl)	<5 (ND)	5.60±0.1	<5 (ND)	<5 (ND)
48241 (25DMPEA23DMBzHCl)	<5 (ND)	<5 (ND)	<5 (ND)	<5 (ND)
48242 (25DMPEA24DMBzHCl)	<5 (ND)	<5 (ND)	<5 (ND)	<5 (ND)
48243 (25DMPEA25DMBzHCl)	<5 (ND)	<5 (ND)	5.8±0.1	5.74±0.08
48244 (25DMPEA26DMBzHCl)	<5 (ND)	<5 (ND)	<5 (ND)	6.2±0.1
48257 (25DMPEA34DMBzHCl)	<5 (ND)	<5 (ND)	<5 (ND)	6.1±0.2
48258 (25DMPEA35DMBzHCl)	<5 (ND)	5.76±0.07	5.8±0.1	5.9±0.1
48245 (25DMPEA23MDBzHCl)	<5 (ND)	<5 (ND)	<5 (ND)	5.77±0.08
48259 (25DMPEA34MDBzHCl)	<5 (ND)	5.73±0.06	5.84±0.07	6.4±0.1

Table 32 Binding Affinity of the 4Br25-DMPEA Series at 5-HT₃₋₇ Receptor Subtypes.

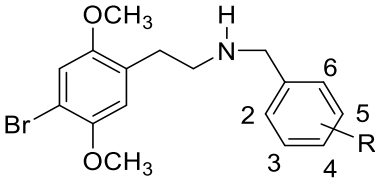
				
PDSP ID Number (4Br25-DMPEAs)	5-HT₃ pKi (SE)	5-HT_{5A} pKi (SE)	5-HT₆ pKi (SE)	5-HT₇ pKi (SE)
48246 (4Br25DMPEA2MBzHCl)	<5 (ND)	<5 (ND)	7.39±0.08	<5 (ND)
48247 (4Br25DMPEA3MBzHCl)	<5 (ND)	<5 (ND)	6.82±0.08	<5 (ND)
48248 (4Br25DMPEA4MBzHCl)	<5 (ND)	<5 (ND)	6.58±0.08	<5 (ND)
48249 (4Br25DMPEA23DMBzHCl)	<5 (ND)	<5 (ND)	6.68±0.09	<5 (ND)
48250 (4Br25DMPEA24DMBzHCl)	<5 (ND)	<5 (ND)	7.13±0.09	<5 (ND)
48251 (4Br25DMPEA25DMBzHCl)	<5 (ND)	<5 (ND)	7.11±0.09	<5 (ND)
48252 (4Br25DMPEA26DMBzHCl)	<5 (ND)	<5 (ND)	6.93±0.09	6.4±0.2
48253 (4Br25DMPEA34DMBzHCl)	<5 (ND)	5.53±0.09	6.2±0.1	6.2±0.1
48254 (4Br25DMPEA35DMBzHCl)	<5 (ND)	5.62±0.08	6.9±0.1	6.0±0.1
48255 (4Br25DMPEA23MDBzHCl)	<5 (ND)	6.23±0.08	6.1±0.1	5.7±0.1
48256 (4Br25DMPEA34MDBzHCl)	<5 (ND)	5.91±0.06	6.4±0.1	6.0±0.1

Table 33 Binding Affinity of the 4I25-DMPEA Series at 5-HT₃₋₇ Receptor Subtypes.

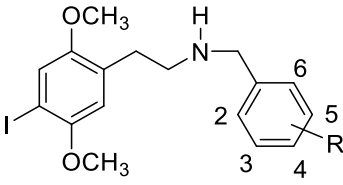
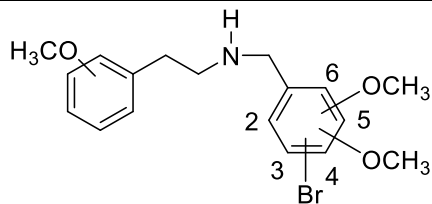
				
PDSP ID Number (4I25-DMPEAs)	5-HT₃ pKi (SE)	5-HT_{5A} pKi (SE)	5-HT₆ pKi (SE)	5-HT₇ pKi (SE)
48260 (4I25DMPEA2MBzHCl)	<5 (ND)	<5 (ND)	7.34±0.08	5.3±0.2
48261 (4I25DMPEA3MBzHCl)	<5 (ND)	<5 (ND)	5.64±0.04	<5 (ND)
48262 (4I25DMPEA4MBzHCl)	<5 (ND)	5.94±0.08	7.20±0.04	6.24±0.09
48263 (4I25DMPEA23DMBzHCl)	<5 (ND)	<5 (ND)	6.48±0.05	<5 (ND)
48264 (4I25DMPEA24DMBzHCl)	<5 (ND)	<5 (ND)	6.56±0.06	<5 (ND)
48265 (4I25DMPEA25DMBzHCl)	5.63±0.06	<5 (ND)	7.00±0.05	<5 (ND)
48266 (4I25DMPEA26DMBzHCl)	<5 (ND)	<5 (ND)	7.03±0.06	6.09±0.09
48267 (4I25DMPEA34DMBzHCl)	<5 (ND)	<5 (ND)	6.15±0.06	<5 (ND)
48268 (4I25DMPEA35DMBzHCl)	<5 (ND)	<5 (ND)	7.11±0.06	<5 (ND)
48269 (4I25DMPEA23MDBzHCl)	<5 (ND)	<5 (ND)	6.10±0.06	<5 (ND)
48270 (4I25DMPEA34MDBzHCl)	<5 (ND)	5.60±0.1	6.87±0.04	<5 (ND)

Table 34 Binding Affinity of MPEABrDMBz (“eMOBN”) Series at 5-HT₃₋₇ Receptor Subtypes.

PDSP ID Number (MPEABrDMBzs)	5-HT₃ pKi (SE)	5-HT_{5A} pKi (SE)	5-HT₆ pKi (SE)	5-HT₇ pKi (SE)
48271 (2MPEA4Br25DMBzHCl)	<5 (ND)	<5 (ND)	5.72±0.06	5.8±0.1
48272 (3MPEA4Br25DMBzHCl)	<5 (ND)	<5 (ND)	5.96±0.06	5.60±0.08
48273 (4MPEA4Br25DMBzHCl)	<5 (ND)	<5 (ND)	6.59±0.06	5.85±0.09
48274 (2MPEA2Br45DMBzHCl)	<5 (ND)	<5 (ND)	6.26±0.06	<5 (ND)
48275 (3MPEA2Br45DMBzHCl)	<5 (ND)	<5 (ND)	6.08±0.06	<5 (ND)
48276 (4MPEA2Br45DMBzHCl)	<5 (ND)	<5 (ND)	6.36±0.06	<5 (ND)



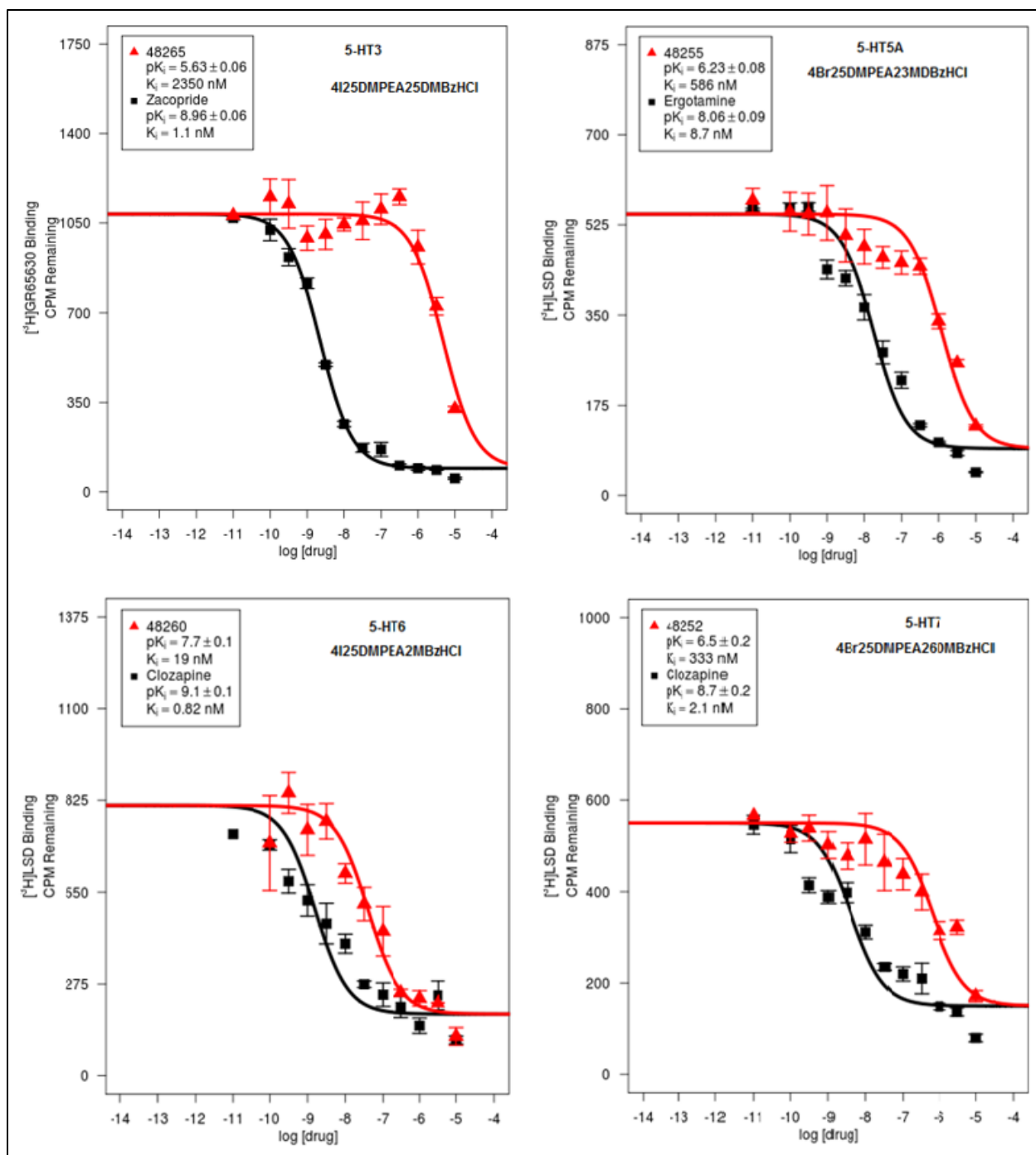


Figure 152 Dose response curves for the most potent 4X25DMPEA derivatives at 5-HT₃₋₇ receptor subtypes.

11.5 Dopamine D₁-D₅ Receptor Binding Profiles:

Dopamine receptors are implicated in many neurological processes, including motivation, pleasure, cognition, memory, learning, and fine motor control, as well as modulation of neuroendocrine signaling. Abnormal dopamine receptor signaling and dopaminergic nerve function is implicated in several neuropsychiatric disorders. Therefore, dopamine receptors are common neurologic drug targets including the antipsychotic drugs most of which are dopamine receptor antagonists, and Parkinson drugs which are dopamine receptor agonists. There are at least five subtypes of dopamine receptors designated as D₁, D₂, D₃, D₄, and D₅. The D₁ and D₅ receptor subtypes are members of the D₁-like family of dopamine receptors which are coupled to G_s-proteins, while the D₂, D₃ and D₄ receptor subtypes are members of the D₂-like family coupled to G_i-proteins.

The experimental conditions used to determine receptor binding profiles of the NBOMe compounds at dopamine receptor subtypes are detailed in Table 35 below. The reference standards for these receptor subtypes have pK_i values ranging from 8.6 (K_i 2.6 nM) for SKF38393 at D₅ receptors to 7.5 (K_i 32.6 nM) for chlorpromazine at D₄ receptors. Previous studies have shown that 25B-NBOMe and 25I-NBOMe have relatively low affinity for all of these receptor subtypes with pK_i values < 6.0 (K_is > 1000 nM) [18, 21]. The binding data obtained is presented in Table 36-39 below.

Table 35 Experimental conditions used to determine receptor binding profiles of the 4X25-DMPEA compounds at dopamine receptor subtypes.

Dopamine receptors			
Dopamine Binding Buffer: 50 mM HEPES, 50 mM NaCl, 5 mM MgCl ₂ , 0.5mM EDTA, pH 7.4, RT			
Standard Wash Buffer: 50 mM Tris HCl, pH 7.4, cold			
Target	Radioligand pK _d ± SEM (K _d , nM)	Radioligand used (nM)	Reference Ligand pK _i ± SEM (K _i , nM)
D ₁	[³ H]-SCH23390 9.13 ± 0.05 (0.74)	0.6 – 1.3	(+)-Butaclamol 8.51 ± 0.02 (3.07)
D ₂	[³ H]-N-methylspiperone 9.33 ± 0.06 (0.47)	0.4 – 1.0	Haloperidol 8.15 ± 0.02 (7.15)
D ₃	[³ H]-N-methylspiperone 9.44 ± 0.09 (0.36)	0.5 – 1.8	Chlorpromazine 7.99 ± 0.02 (10.30)
D ₄	[³ H]-N-methylspiperone 9.07 ± 0.06 (0.86)	0.6 – 1.7	Chlorpromazine 7.49 ± 0.02 (32.62)
D ₅	[³ H]-SCH23390 8.69 ± 0.05 (2.03)	2.0 – 3.0	SKF38393 8.59 ± 0.02 (2.59)

The dopamine receptor binding profiles for the compounds synthesized in this study are shown in Tables 36-39 and dose response curves for the most potent ligand at each receptor subtype are shown in Figure 153.

As the data in Tables 36-38 demonstrate, none of the 4-X25DMPEA derivatives assayed demonstrated any significant affinity at the D₁-family of receptors (D₁ and D₅) with pK_is < 5 (K_i > 10 μm). Also, only the 3'-methoxy, 4'-methoxy and 3',4'-methylenedioxy derivatives of the 4I25-DMPEA series had pK_is above 6 in the D₂ receptor assays.

At D₃ receptor subtypes the 4Br25-DMPEA and 4I25-DMPEA series demonstrated higher receptor affinities (pK_is ranging from 5.5 to 7.8) than the compounds of the 4H25-DMPEA series (all pK_is < 5.8), suggesting 4-halogenation enhances affinity for these receptors. However, most of the 4X25-DMPEA compounds prepared in this study had significantly lower affinity than the standard chlorpromazine (pK_i 8.0) at D₃ receptors. Only the 4'-methoxy derivative of the 4Br25-DMPEA series (4Br25DMPEA4MBz, pK_i 7.8) and the 3',4'-methylenedioxy derivatives of the 4I25-DMPEA series (4I25-DMPEA34MDBz, pK_i 7.4) have affinities approaching the standard

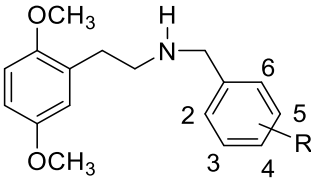
and these compounds have higher affinity than reported for 25I-NBOMe ($pK_i < 6.3$, $K_i > 500$) at D_3 receptors [18, 21].

The 4Br25-DMPEA and 4I25-DMPEA compounds do display consistent structure-activity relationships at D_3 receptor subtypes. For example, the relative D_3 receptor binding affinity for the monomethoxy derivatives in both the 4-bromo and 4-iodo series (4X25-DMPEAMBzs) is 4'-methoxy > 3'-methoxy > 2'-methoxy. Also, the relative D_3 receptor binding affinity for the methylenedioxy derivatives in both the 4-bromo and 4-iodo series (4X25-DMPEAMDBzs) is 3',4'-methylenedioxy > 2',3'-methylenedioxy (Tables 37 and 38). Finally, all the dimethoxy derivatives in both the 4-bromo and 4-iodo series (4X25-DMPEADMBzs) have very similar D_3 affinities over narrow pK_i range (5.5-6.4) and lower affinities than the 4'-methoxy (4X25-DMPEA4MB) and 3',4'-methylenedioxy (4X25-DMPEA34MDBz) compounds.

The 4X25-DMPEA compounds display higher affinity at D_4 receptors (pK_i s 5.5-7.0) than D_1 or D_5 receptors as noted above, but lower than the D_4 receptor reference standard chlorpromazine (pK_i 7.5). Also, in the 4Br25DMPEA series, most compounds have higher affinity for D_3 than D_4 receptors. But in the 4I25-DMPEA series most derivatives have higher affinity at D_4 versus D_3 receptors. As a result, structure-activity relationships in general are not consistent for the 4-bromo and 4-iodo series (4X25-DMPEAs) series of compounds at D_4 receptors, suggesting that 4-halogenation may have at least an impact on the mode of receptor binding.

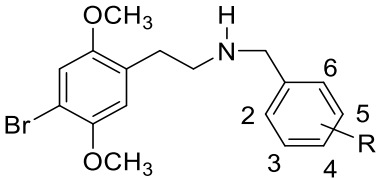
Finally, Table 39 shows the dopamine receptor subtype binding profiles for the MPEABrDMBz or "reversed 25Br-NBOMe" (eMOBN) derivatives. Almost all of these derivatives (except 4MPEA4Br25DMBz at D_3 receptors) display minimal affinity for D_1 , D_2 , D_4 and D_5 receptors. However, the MPEA4Br25DMBz derivatives do display modest affinity at D_4 receptors with affinity constants (pK_i s) comparable to the 4Br25-DMPEAs and 4I25-DMPEAs (pK_i s 6.3-6.5), but an order of magnitude less than the reference standard chlorpromazine (pK_i 7.5).

Table 36 Binding Affinity of 4H25-DMPEA Series at Dopamine Receptor Subtypes.



PDSP ID Number (4H25-DMPEAs)	D₁, pKi (SE)	D₂, pKi (SE)	D₃, pKi (SE)	D₄, pKi (SE)	D₅, pKi (SE)
48238 (25DMPEA2MBzHCl)	<5 (ND)	<5 (ND)	<5 (ND)	<5 (ND)	<5 (ND)
48239 (25DMPEA3MBzHCl)	<5 (ND)	<5 (ND)	<5 (ND)	5.70±0.09	<5 (ND)
48240 (25DMPEA4MBzHCl)	<5 (ND)	<5 (ND)	6.6±0.1	5.73±0.07	<5 (ND)
48241 (25DMPEA23DMBzHCl)	<5 (ND)	<5 (ND)	<5 (ND)	<5 (ND)	<5 (ND)
48242 (25DMPEA24DMBzHCl)	<5 (ND)	<5 (ND)	<5 (ND)	<5 (ND)	<5 (ND)
48243 (25DMPEA25DMBzHCl)	<5 (ND)	<5 (ND)	5.8±0.1	<5 (ND)	<5 (ND)
48244 (25DMPEA26DMBzHCl)	<5 (ND)	<5 (ND)	5.7±0.1	<5 (ND)	<5 (ND)
48257 (25DMPEA34DMBzHCl)	<5 (ND)	<5 (ND)	<5 (ND)	5.6±0.1	<5 (ND)
48258 (25DMPEA35DMBzHCl)	<5 (ND)	<5 (ND)	<5 (ND)	5.6±0.1	<5 (ND)
48245 (25DMPEA23MDBzHCl)	<5 (ND)	<5 (ND)	5.41±0.09	<5 (ND)	<5 (ND)
48259 (25DMPEA34MDBzHCl)	<5 (ND)	<5 (ND)	<5 (ND)	5.8±0.1	<5 (ND)

Table 37 Binding Affinity of 4Br25-DMPEA Series at Dopamine Receptor Subtypes.



PDSP ID Number (4Br25-DMPEAs)	D₁, pKi (SE)	D₂, pKi (SE)	D₃, pKi (SE)	D₄, pKi (SE)	D₅, pKi (SE)
48246 (4Br25DMPEA2MBzHCl)	<5 (ND)	<5 (ND)	5.92±0.09	5.78±0.07	<5 (ND)
48247 (4Br25DMPEA3MBzHCl)	<5 (ND)	<5 (ND)	6.19±0.09	6.31±0.07	<5 (ND)
48248 (4Br25DMPEA4MBzHCl)	<5 (ND)	<5 (ND)	7.84±0.09	6.38±0.08	<5 (ND)
48249 (4Br25DMPEA23DMBzHCl)	<5 (ND)	<5 (ND)	5.92±0.09	5.8±0.1	<5 (ND)
48250 (4Br25DMPEA24DMBzHCl)	<5 (ND)	<5 (ND)	6.2±0.09	5.8±0.1	<5 (ND)
48251 (4Br25DMPEA25DMBzHCl)	<5 (ND)	<5 (ND)	6.30±0.09	5.74±0.08	<5 (ND)
48252 (4Br25DMPEA26DMBzHCl)	<5 (ND)	<5 (ND)	6.1±0.1	5.5±0.1	<5 (ND)
48253 (4Br25DMPEA34DMBzHCl)	<5 (ND)	<5 (ND)	5.91±0.07	5.7±0.1	<5 (ND)
48254 (4Br25DMPEA35DMBzHCl)	<5 (ND)	<5 (ND)	5.95±0.07	6.09±0.08	<5 (ND)
48255 (4Br25DMPEA23MDBzHCl)	<5 (ND)	<5 (ND)	5.70±0.06	6.8±0.1	<5 (ND)
48256 (4Br25DMPEA34MDBzHCl)	<5 (ND)	<5 (ND)	6.48±0.07	6.4±0.1	<5 (ND)

Table 38 Binding Affinity of 4I25-DMPEA Series at Dopamine Receptor Subtypes.

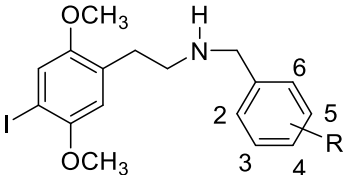
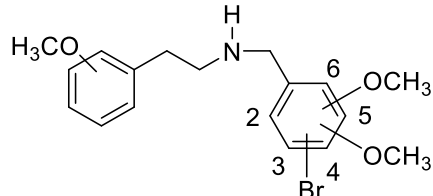
					
PDSP ID Number (4I25-DMPEAs)	D₁, pKi (SE)	D₂, pKi (SE)	D₃, pKi (SE)	D₄, pKi (SE)	D₅, pKi (SE)
48260 (4I25DMPEA2MBzHCl)	<5 (ND)	<5 (ND)	5.8±0.2	6.2±0.1	<5 (ND)
48261 (4I25DMPEA3MBzHCl)	<5 (ND)	6.14±0.08	6.90±0.09	6.86±0.07	<5 (ND)
48262 (4I25DMPEA4MBzHCl)	<5 (ND)	7.37±0.08	7.16±0.09	6.65±0.07	<5 (ND)
48263 (4I25DMPEA23DMBzHCl)	<5 (ND)	<5 (ND)	6.0±0.1	6.86±0.07	<5 (ND)
48264 (4I25DMPEA24DMBzHCl)	<5 (ND)	<5 (ND)	6.3±0.1	6.47±0.06	<5 (ND)
48265 (4I25DMPEA25DMBzHCl)	<5 (ND)	<5 (ND)	6.2±0.1	6.3±0.1	<5 (ND)
48266 (4I25DMPEA26DMBzHCl)	<5 (ND)	<5 (ND)	5.53±0.09	5.89±0.09	<5 (ND)
48267 (4I25DMPEA34DMBzHCl)	<5 (ND)	<5 (ND)	6.2±0.1	6.15±0.09	<5 (ND)
48268 (4I25DMPEA35DMBzHCl)	<5 (ND)	<5 (ND)	6.4±0.1	6.87±0.09	<5 (ND)
48269 (4I25DMPEA23MDBzHCl)	<5 (ND)	<5 (ND)	6.1±0.1	6.77±0.09	<5 (ND)
48270 (4I25DMPEA34MDBzHCl)	<5 (ND)	6.32±0.08	7.4±0.1	7.0±0.1	<5 (ND)

Table 39 Binding Affinity of MPEABrDMBz (“eMOBN”) Series at Dopamine Receptor Subtypes.

					
PDSP ID Number (NBOMe Derivative)	D₁, pKi (SE)	D₂, pKi (SE)	D₃, pKi (SE)	D₄, pKi (SE)	D₅, pKi (SE)
48271 (2MPEA4Br25DMBzHCl)	<5 (ND)	<5 (ND)	<5 (ND)	6.5±0.1	<5 (ND)
48272 (3MPEA4Br25DMBzHCl)	<5 (ND)	<5 (ND)	<5 (ND)	6.3±0.1	<5 (ND)
48273 (4MPEA4Br25DMBzHCl)	<5 (ND)	<5 (ND)	6.7±0.1	6.3±0.1	<5 (ND)
48274 (2MPEA2Br45DMBzHCl)	5.50±0.1	<5 (ND)	<5 (ND)	5.7±0.1	<5 (ND)
48275 (3MPEA2Br45DMBzHCl)	<5 (ND)	<5 (ND)	<5 (ND)	<5 (ND)	<5 (ND)
48276 (4MPEA2Br45DMBzHCl)	<5 (ND)	<5 (ND)	<5 (ND)	5.6±0.1	<5 (ND)

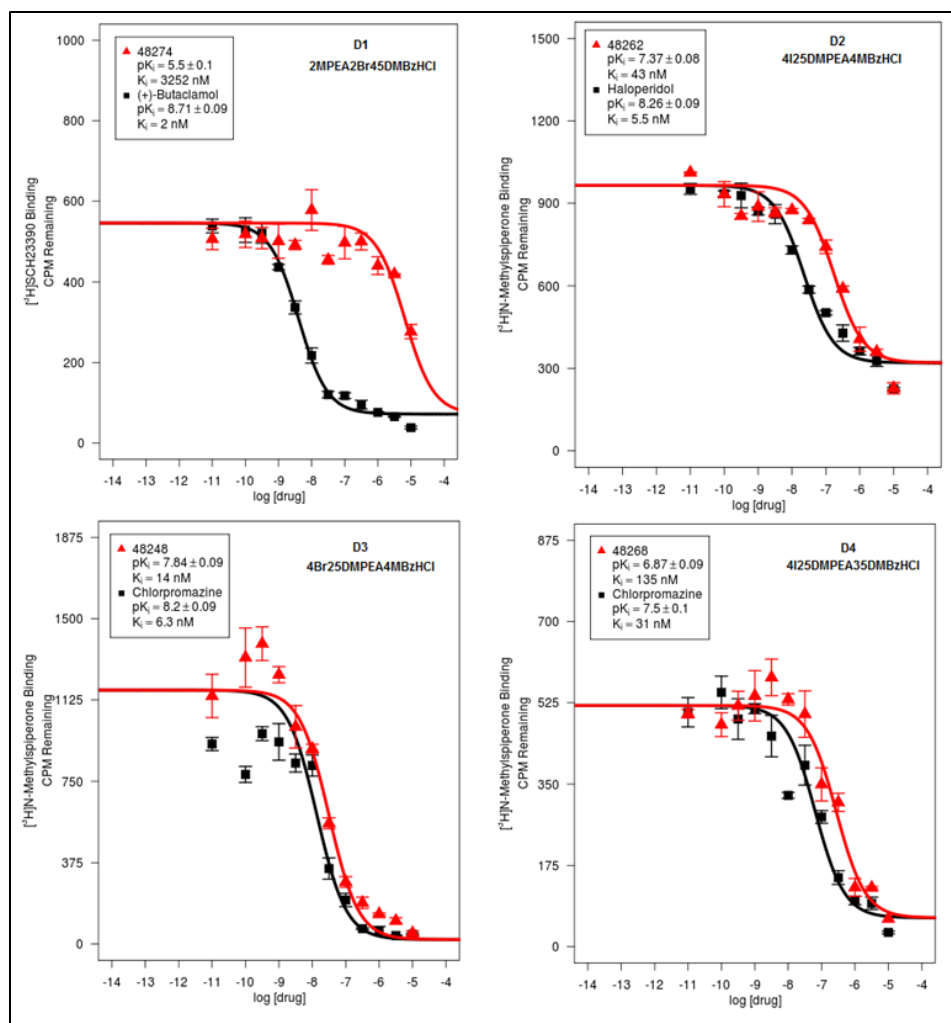


Figure 153 Dose response curves for the most potent 4X25DMPEA derivatives at dopamine receptor subtypes.

11.6 Adrenergic Receptor Binding Profiles:

Adrenergic receptors are expressed on virtually every cell type in the body and are the receptors for epinephrine and norepinephrine within the sympathetic nervous system and central nervous system. Adrenergic receptors serve critical roles in maintaining homeostasis in normal physiologic settings as well as pathologic states. These receptors are also targets for therapeutically administered agonists and antagonists. Currently, nine adrenergic receptors have been cloned, and they have been divided into two general subpopulations – the alpha with six subtypes, and beta-receptors with three subtypes. The experimental conditions used to determine receptor binding profiles of the 4X25-DMPEA - NBOMe compounds at adrenergic receptor subtypes are detailed in Table 40 below. The reference standards for these receptor subtypes have pKi values ranging

from 9.2 (0.63 nM) for prazosin at α_{1D} receptors to 7.38 (41.6 nM) for oxymetazoline at α_{2C} receptors. Previous studies have shown that 25B-NBOMe and 25I-NBOMe have relatively low affinity for α_1 and beta-receptor subtypes with pK_i values < 6.0 ($K_i > 1000$ nM), and only modest affinity for α_2 receptor subtypes (pK_i 6-7) [18, 21]. The binding data obtained is presented in Tables 41-44 below.

Table 40 Experimental conditions used to determine receptor binding profiles of the 4X25-DMPEA compounds at adrenergic receptor subtypes.

Adrenergic receptors			
α_1 Binding Buffer: 20 mM Tris HCl, 145 mM NaCl, pH 7.4, RT			
α_2 Binding Buffer: 50 mM Tris HCl, 5 mM MgCl ₂ , pH 7.7, RT			
Target	Radioligand $pK_d \pm SEM (K_d, nM)$	Radioligand used (nM)	Reference ligand $pK_i \pm SEM (K_i, nM)$
α_{1A}	[³ H]-Prazosin 9.36 \pm 0.07 (0.43)	0.2 - 1.0	Prazosin 9.16 \pm 0.03 (0.70)
α_{1B}	[³ H]-Prazosin 9.23 \pm 0.29 (0.58)	0.3 - 1.0	Prazosin 9.05 \pm 0.03 (0.88)
α_{1D}	[³ H]-Prazosin 9.21 \pm 0.07 (0.62)	0.3 - 1.0	Prazosin 9.20 \pm 0.03 (0.63)
α_{2A}	[³ H]-Rauwolscine 8.46 \pm 0.16 (3.47)	1.0 - 3.0	Oxymetazoline 8.35 \pm 0.02 (4.51)
α_{2B}	[³ H]-Rauwolscine 8.74 \pm 0.13 (1.81)	1.5 - 2.0	Yohimbine 8.24 \pm 0.02 (5.81)
α_{2C}	[³ H]-Rauwolscine 9.02 \pm 0.10 (0.96)	0.5 - 1.0	Oxymetazoline 7.38 \pm 0.02 (41.6)
Target	Radioligand $pK_d \pm SEM (K_d, nM)$	Radioligand used (nM)	Reference ligand $pK_i \pm SEM (K_i, nM)$
β_1	[¹²⁵ I]-Pindolol 10.06 \pm 0.09 (0.10)	0.1 - 0.2	Alprenolol 8.73 \pm 0.03 (1.85)
β_2	[³ H]-CGP12177 9.15 \pm 0.16 (0.71)	0.5 - 1.0	Alprenolol 8.79 \pm 0.03 (1.61)
β_3	[³ H]-CGP12177 7.50 \pm 0.16 (31.8)	20	
β_3	[¹²⁵ I]-Pindolol 9.45 \pm 0.15 (0.36)	0.2 - 0.5	Alprenolol 7.64 \pm 0.03 (23.0)

Table 41 Binding Affinity of the 4H25-DMPEA Series at Adrenergic-2 Receptor Subtypes.

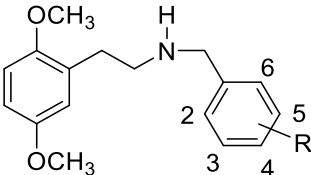
			
PDSP ID Number (4H25-DMPEA)	α_{2A} , pKi (SE)	α_{2B} , pKi (SE)	α_{2C} , pKi (SE)
48238 (25DMPEA2MBzHCl)	6.1 ±0.1	6.9±0.1	6.47±0.07
48239 (25DMPEA3MBzHCl)	6.3±0.1	6.3±0.1	5.94±0.07
48240 (25DMPEA4MBzHCl)	6.4±0.1	6.0±0.1	6.47±0.08
48241 (25DMPEA23DMBzHCl)	6.2±0.1	6.2±0.1	<5 (ND)
48242 (25DMPEA24DMBzHCl)	6.5±0.09	6.2±0.1	6.54±0.08
48243 (25DMPEA25DMBzHCl)	5.8±0.1	5.7±0.2	6.22±0.08
48244 (25DMPEA26DMBzHCl)	5.95±0.09	5.8±0.1	6.59±0.07
48257 (25DMPEA34DMBzHCl)	6.3±0.1	6.05±0.07	6.97±0.06
48258 (25DMPEA35DMBzHCl)	6.0±0.1	6.23±0.07	6.59±0.06
48245 (25DMPEA23MDBzHCl)	6.0±0.1	5.7±0.1	6.38±0.07
48259 (25DMPEA34MDBzHCl)	6.1±0.1	5.95±0.06	6.49±0.06

Table 42 Binding Affinity of the 4Br25-DMPEA Series at Adrenergic-2 Receptor Subtypes.

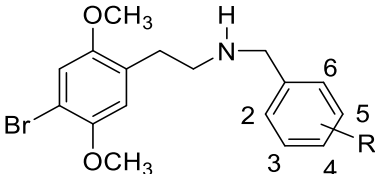
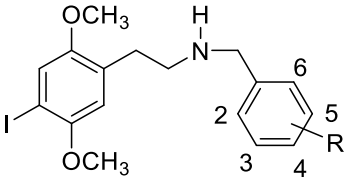
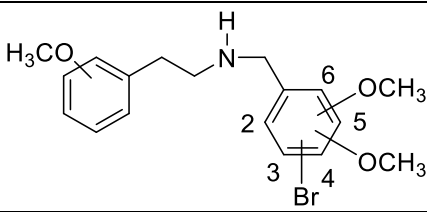
			
PDSP ID Number 4Br25-DMPEA	α_{2A} , pKi (SE)	α_{2B} , pKi (SE)	α_{2C} , pKi (SE)
48246 (4Br25DMPEA2MBzHCl)	6.5±0.1	5.9±0.1	6.60±0.08
48247 (4Br25DMPEA3MBzHCl)	6.7±0.1	6.2±0.2	6.27±0.08
48248 (4Br25DMPEA4MBzHCl)	6.3±0.1	5.7±0.1	6.52±0.06
48249 (4Br25DMPEA23DMBzHCl)	6.24±0.09	5.91±0.08	6.22±0.08
48250 (4Br25DMPEA24DMBzHCl)	6.3±0.1	6.02±0.08	6.31±0.05
48251 (4Br25DMPEA25DMBzHCl)	6.11±0.09	6.04±0.07	6.51±0.05
48252 (4Br25DMPEA26DMBzHCl)	6.3±0.1	6.35±0.08	6.53±0.05
48253 (4Br25DMPEA34DMBzHCl)	7.0±0.1	6.38±0.07	6.95±0.06
48254 (4Br25DMPEA35DMBzHCl)	6.8±0.1	6.19±0.07	6.63±0.05
48255 (4Br25DMPEA23MDBzHCl)	6.6±0.1	6.04±0.07	6.78±0.07
48256 (4Br25DMPEA34MDBzHCl)	6.6±0.1	6.40±0.07	6.30±0.07

Table 43 Binding Affinity of the IBr25DMPEA Series at Adrenergic-2 Receptor Subtypes.

			
PDSP ID Number (4IH25-DMPEA)	α_{2A} , pKi (SE)	α_{2B} , pKi (SE)	α_{2C} , pKi (SE)
48260 (4I25DMPEA2MBzHCl)	6.5±0.1	6.10±0.06	6.91±0.07
48261 (4I25DMPEA3MBzHCl)	6.7±0.1	6.21±0.06	6.69±0.06
48262 (4I25DMPEA4MBzHCl)	6.4±0.1	5.60±0.06	6.13±0.06
48263 (4I25DMPEA23DMBzHCl)	6.5±0.1	6.61±0.08	6.45±0.06
48264 (4I25DMPEA24DMBzHCl)	6.5±0.1	6.15±0.08	6.47±0.06
48265 (4I25DMPEA25DMBzHCl)	6.3±0.1	6.18±0.07	6.62±0.06
48266 (4I25DMPEA26DMBzHCl)	6.9±0.1	6.65±0.08	6.66±0.06
48267 (4I25DMPEA34DMBzHCl)	7.0±0.1	6.49±0.08	6.82 ±0.07
48268 (4I25DMPEA35DMBzHCl)	6.6±0.1	6.36±0.08	6.72±0.05
48269 (4I25DMPEA23MDBzHCl)	6.4±0.1	6.21±0.08	6.42±0.06
48270 (4I25DMPEA34MDBzHCl)	7.1±0.2	6.35±0.05	6.63±0.05

None of the 4X25-DMPEA compounds screened displayed any significant affinity (all pKis < 6) at any α_1 receptor subtype or beta-receptor subtype (data not shown), consistent with reported data for 25B-NBOMe and 25I-NBOMe. The 4X25-DMPEA compounds display weak affinity at α_2 receptor populations as shown in Tables 41-43 with most pKis in the 6-7 range (Kis 100-1000 nM). There are no significant differences in affinity or clear structure-activity patterns across α_2 receptor lines in each 4X25-DMPEA series. Comparing across structural series, the 4Br- and 4I25-DMPEA compounds appear to have modestly higher affinity at α_{2A} receptors than the 4H25-DMPEA series, suggesting that 4-halogenation may produce a modest increase in binding (5 to 10-fold increase) at these receptors. However, the affinity constants (pKis) at α_{2B} and α_{2C} receptor subtypes for all 4X25-DMPEA compounds all fall within a very narrow range, suggesting that halogenation has minimal impact on affinity at these receptors. Interestingly all of the MPEABrDMBzs or “reversed NBOMe” derivatives also display affinities over a very narrow range and do not differ significantly from the 4X25-DMPEA compounds (Table 44).

Table 44 Binding Affinity of MPEABrDMBz (“eMOBN”) Series at Adrenergic-2 Receptor Subtypes.

	α_{2A} ,	α_{2B} ,	α_{2C} ,
	pKi (SE)	pKi (SE)	pKi (SE)
48271 (2MPEA4Br25DMBzHCl)	6.3±0.1	6.94±0.05	6.57±0.05
48272 (3MPEA4Br25DMBzHCl)	6.2±0.1	6.21±0.05	6.34±0.05
48273 (4MPEA4Br25DMBzHCl)	6.2±0.1	6.17±0.05	6.36±0.05
48274 (2MPEA2Br45DMBzHCl)	6.2±0.1	6.49±0.05	6.26±0.05
48275 (3MPEA2Br45DMBzHCl)	6.0±0.1	6.0±0.1	5.6±0.1
48276 (4MPEA2Br45DMBzHCl)	<5 (ND)	5.8±0.2	<5 (ND)

11.7 Histamine Receptor Binding Profiles:

The four known histamine receptor subtypes are H₁, H₂, H₃, and H₄. H₁ receptors are found throughout the body and are involved in evoking pain and pruritus, vascular dilatation, vascular permeability, bronchoconstriction, and stimulation of cough receptors. H₂ receptors are widely distributed as well and have functions similar to those of the H₁ receptors, with increased activity in the gastrointestinal system leading to higher secretion of gastric acid and mucus. In allergic processes, H₂ receptors act indirectly by altering the cytokine milieu. H₃ and H₄ receptors have been described, and their expression appears to be limited to neural and hematopoietic tissues, respectively.

The experimental conditions used to determine receptor binding profiles of the 4X25-DMPEA - NBOMe compounds at histamine receptor subtypes are detailed in Table 45 below. The reference standards for these receptor subtypes have pKi values ranging from 9.05 (0.90 nM) for ORG-5222 at H₂ receptors to 6.60 (250 nM) for clozapine at H₄ receptors. Previous studies have shown that 25B-NBOMe and 25I-NBOMe have very low affinity for H₂ and H₃ receptor subtypes with pKi values < 6.3 (K_is > 500 nM), and only modest affinity at H₁ receptors (pK_is 6.5-6.6) [18, 21]. The binding data obtained is presented in Table 46-49 below.

Table 45 Experimental conditions used to determine receptor binding profiles of the 4X25-DMPEA compounds at histamine receptor subtypes.

Histamine receptors			
Histamine Binding Buffer: 50 mM Tris HCl, 0.5 mM EDTA, pH 7.4, RT			
Standard Wash Buffer: 50 mM Tris HCl, pH 7.4, cold			
Filter: GF/B			
Target	Radioligand pK _d ± SEM (K _d , nM)	Radioligand used (nM)	Reference Ligand pK _i ± SEM (K _i , nM)
H ₁	[³ H]-Pyrilamine 9.01 ± 0.05 (0.97)	0.6 – 2.0	Chlorpheniramine 8.78 ± 0.02 (1.64)
H ₂	[¹²⁵ I]-Iodo-aminopotentidine 10.47 ± 0.12 (0.03)	0.02 – 0.05	ORG-5222 9.05 ± 0.04 (0.90)
H ₃	[³ H]-α-methylhistamine 9.11 ± 0.07 (0.78)	0.5 – 1.0	Histamine 8.30 ± 0.03 (4.99)
H ₄	[³ H]-Histamine 8.26 ± 0.08 (5.46)	1.0 – 5.0	Clozapine 6.60 ± 0.06 (250)

Table 46 Binding Affinity of the 4H25-DMPEA Series at Histamine Receptor Subtypes.

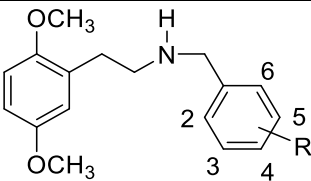
PDSP ID Number (4H25-DMPEA)				
	H ₁ pK _i (SE)	H ₂ pK _i (SE)	H ₃ pK _i (SE)	H ₄ pK _i (SE)
48238 (25DMPEA2MBzHCl)	<5 (ND)	5.94±0.06	<5 (ND)	<5 (ND)
48239 (25DMPEA3MBzHCl)	<5 (ND)	6.16±0.06	<5 (ND)	<5 (ND)
48240 (25DMPEA4MBzHCl)	<5 (ND)	6.30±0.06	<5 (ND)	<5 (ND)
48241 (25DMPEA23DMBzHCl)	<5 (ND)	5.99±0.05	<5 (ND)	<5 (ND)
48242 (25DMPEA24DMBzHCl)	<5 (ND)	6.47±0.04	<5 (ND)	<5 (ND)
48243 (25DMPEA25DMBzHCl)	5.44±0.09	6.10±0.04	<5 (ND)	<5 (ND)
48244 (25DMPEA26DMBzHCl)	<5 (ND)	6.88±0.04	<5 (ND)	<5 (ND)
48257 (25DMPEA34DMBzHCl)	<5 (ND)	6.13±0.04	<5 (ND)	<5 (ND)
48258 (25DMPEA35DMBzHCl)	<5 (ND)	6.41±0.04	<5 (ND)	<5 (ND)
48245 (25DMPEA23MDBzHCl)	<5 (ND)	6.77±0.04	<5 (ND)	<5 (ND)
48259 (25DMPEA34MDBzHCl)	<5 (ND)	6.75±0.04	<5 (ND)	<5 (ND)
48259 (25DMPEA34MDBzHCl)	<5 (ND)	6.73±0.04	<5 (ND)	<5 (ND)

Table 47 Binding Affinity of the 4Br25-DMPEA Series at Histamine Receptor Subtypes.

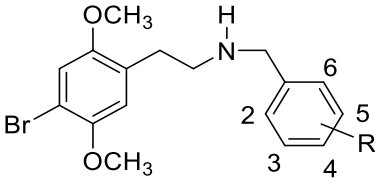
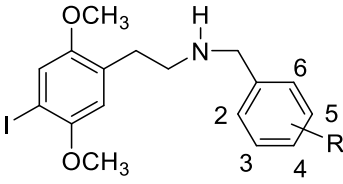
				
PDSP ID Number (4Br25-DMPEA)	H₁ pKi (SE)	H₂ pKi (SE)	H₃ pKi (SE)	H₄ pKi (SE)
48246 (4Br25DMPEA2MBzHCl)	6.87±0.09	6.64±0.04	<5 (ND)	<5 (ND)
48247 (4Br25DMPEA3MBzHCl)	6.83±0.09	6.90±0.04	<5 (ND)	<5 (ND)
48248 (4Br25DMPEA4MBzHCl)	5.82±0.09	7.28±0.04	<5 (ND)	<5 (ND)
48249 (4Br25DMPEA23DMBzHCl)	6.59±0.09	6.67±0.04	<5 (ND)	<5 (ND)
48250 (4Br25DMPEA24DMBzHCl)	6.80±0.2	7.36±0.04	<5 (ND)	<5 (ND)
48251 (4Br25DMPEA25DMBzHCl)	<5 (ND)	6.79±0.04	<5 (ND)	<5 (ND)
48252 (4Br25DMPEA26DMBzHCl)	6.30±0.1	7.28±0.04	<5 (ND)	<5 (ND)
48253 (4Br25DMPEA34DMBzHCl)	5.90±0.1	6.57±0.04	<5 (ND)	<5 (ND)
48254 (4Br25DMPEA35DMBzHCl)	6.20±0.1	6.93±0.04	<5 (ND)	<5 (ND)
48255 (4Br25DMPEA23MDBzHCl)	7.10±0.1	7.12±0.04	<5 (ND)	<5 (ND)
48256 (4Br25DMPEA34MDBzHCl)	6.70±0.1	7.22±0.04	<5 (ND)	<5 (ND)

Table 48 Binding Affinity of the 4I25-DMPEA Series at Histamine Receptor Subtypes.

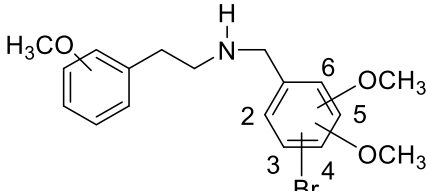
				
PDSP ID Number (4I25-DMPEA)	H₁ pKi (SE)	H₂ pKi (SE)	H₃ pKi (SE)	H₄ pKi (SE)
48260 (4I25DMPEA2MBzHCl)	7.30±0.2	6.79±0.03	<5 (ND)	<5 (ND)
48261 (4I25DMPEA3MBzHCl)	6.00±0.2	6.93±0.04	<5 (ND)	<5 (ND)
48262 (4I25DMPEA4MBzHCl)	6.10±0.1	7.29±0.03	<5 (ND)	<5 (ND)
48263 (4I25DMPEA23DMBzHCl)	6.30±0.2	6.81±0.05	<5 (ND)	<5 (ND)
48264 (4I25DMPEA24DMBzHCl)	6.40±0.2	7.45±0.05	<5 (ND)	<5 (ND)
48265 (4I25DMPEA25DMBzHCl)	5.70±0.1	6.82±0.05	<5 (ND)	<5 (ND)
48266 (4I25DMPEA26DMBzHCl)	6.50±0.1	7.22±0.05	<5 (ND)	<5 (ND)
48267 (4I25DMPEA34DMBzHCl)	6.20±0.1	6.71±0.05	<5 (ND)	<5 (ND)
48268 (4I25DMPEA35DMBzHCl)	6.50±0.1	6.78±0.05	<5 (ND)	<5 (ND)
48269 (4I25DMPEA23MDBzHCl)	6.44±0.09	7.09±0.05	<5 (ND)	<5 (ND)
48270 (4I25DMPEA34MDBzHCl)	7.20±0.1	7.18±0.06	<5 (ND)	<5 (ND)

As the data in Tables 46-48 illustrate, the 4X25-NBOMe compounds prepared in this study displayed minimal affinity at H₃ and H₄ receptor subtypes with pK_is < 5, but most compounds had modest affinity at H₁ and H₂ receptors (most pK_is > 6 at H₂ receptors). Most of the 4X25-DMPEA compounds had higher affinity at H₂ receptors than H₁ receptors, with exception of the 2'-methoxy derivatives 4Br25-DMPEAMBz and 4I25-DMPEAMBz. The higher affinity of many of these compounds at H₂ versus H₁ receptors differs from that observed for the 25X-NBOMes and may suggest that additional methoxy group substitution on at the N-benzyl ring can enhances H₂ receptor affinity.

When comparing across 4X25-DMPEA series, the 4Br- and 4I25-DMPEA compounds displayed higher H₂ receptor affinity than their corresponding unsubstituted 4H25-DMPEA derivatives. The 4Br- and 4I25-DMPEA compounds had very similar affinities, suggesting that halogenation increases affinity at H₂ receptors and that a 4-bromine or 4-iodine substituent can contribute equally to enhanced binding. Also, structure-activity relationships were consistent in the 4Br- and 4I25-DMPEA series since the 2'-methoxy, 2',4'-dimethoxy and 2',6'-dimethoxy compounds in both series had the highest affinities at H₂ receptors.

When comparing across 4X25-DMPEA series, the 4Br- and 4I25-DMPEA compounds also displayed higher H₁ receptor affinity than their corresponding unsubstituted 4H25-DMPEA derivatives, again suggesting that 4-halogenation enhances affinity at this receptor. At the H₂, however, there are no structure-activity consistencies when comparing comparably substituted 4Br- and 4I25-DMPEA derivatives. All compounds in the 4Br- and 4I25-DMPEA series had affinities over a very narrow range of 5.7 to 7.3, suggesting that variation in the degree or position of methoxy substitution has little impact on H₂ receptor binding.

Table 49 Binding Affinity of MPEABrDMBz (“eMOBN”) Series at Histamine Receptor Subtypes.

				
PDSP ID Number (MPEABrDMBz)	H1 pKi (SE)	H2 pKi (SE)	H3 pKi (SE)	H4 pKi (SE)
48271 (2MPEA4Br25DMBzHCl)	7.10±0.1	6.86±0.06	<5 (ND)	<5 (ND)
48272 (3MPEA4Br25DMBzHCl)	7.30±0.2	7.00±0.06	<5 (ND)	<5 (ND)
48273 (4MPEA4Br25DMBzHCl)	6.70±0.2	7.19±0.06	<5 (ND)	<5 (ND)
48274 (2MPEA2Br45DMBzHCl)	<5 (ND)	6.26±0.06	<5 (ND)	<5 (ND)
48275 (3MPEA2Br45DMBzHCl)	<5 (ND)	6.23±0.06	<5 (ND)	<5 (ND)
48276 (4MPEA2Br45DMBzHCl)	<5 (ND)	6.40±0.06	<5 (ND)	<5 (ND)

11.8 Opioid Receptor Binding Profiles:

The experimental conditions used to determine receptor binding profiles of the 4X25-DMPEA - NBOMe compounds at opioid receptor subtypes are detailed in Table 50 below. The reference standards for these receptor subtypes have pKi values ranging from 9.30 (0.50 nM) for naltrindole at delta (DOR) receptors to 8.53 (2.98 nM) for salvinorin A at kappa (KOR) receptors. The opioid receptor affinity of 25X-NBOMe compounds has only been reported for 25I-NBOMe where it was reported to have significant affinity for mu (MOR) receptors with a Ki of 82 nM and modest affinity at kappa (KOR) receptors with a Ki of 288 nM. Although, The 25I-NBOMe compound had minimal affinity at delta (DOR) receptors (pKi < 6.3, Ki > 500) [18, 21]. The binding data obtained is presented in Table 51-54 below.

Table 50 Experimental conditions used to determine receptor binding profiles of the 4X25-DMPEA compounds at opioid receptor subtypes.

Opioid receptors			
Standard Binding Buffer: 50 mM Tris HCl, 10 mM MgCl ₂ , 0.1 mM EDTA, pH 7.4, RT Standard Wash Buffer: 50 mM Tris HCl, pH. 7.4, 4 °C to 8 °C			
Target	Radioligand pK _d ± SEM (K _d , nM)	Radioligand used (nM)	Reference Ligand pK _i ± SEM (K _i , nM)
DOR	[³ H]-DADLE 8.57 ± 0.05 (2.69)	1.0 – 2.0	Naltrindole 9.30 ± 0.02 (0.50)
KOR	[³ H]-U69593 9.08 ± 0.04 (0.83)	0.6 – 1.2	Salvinorin A 8.53 ± 0.02 (2.98)
MOR	[³ H]-DAMGO 8.92 ± 0.05 (1.20)	1.0 – 2.0	DAMGO 8.75 ± 0.02 (1.76)

All of the 4X25-DMPEA compounds displayed very little affinity at DOR receptors with pK_is < 6 (1000 nM). Many of the 4Br25-DMPEA and 4I25-DMPEA compounds had higher affinities at KOR receptors than the 4H25-DMPEAs, but with pK_is ranging from 5.7 to 7.2 for the most part. Interestingly, the most active compound in each 4X25-DMPEA series at KOR receptors was the 2',4'-dimethoxy derivative, suggesting some structure-activity consistency across series.

The monomethoxy derivatives (4X25-DMPEAMBzs) generally displayed higher affinities at MOR than KOR receptors, consistent with the trends reported earlier for 25X-NBOMe compounds (affinities: MOR > KOR > DOR). And the monomethoxy derivatives of the 4Br25-DMPEAMBz series had higher affinity at MOR receptors than the corresponding 4IX25-DMPEAMBzs compounds. However, most of the dimethoxy (4X25-DMPEADMBzs) and methylenedioxy derivatives (4X25-DMPEAMDBzs) of the 4-bromo and 4-iodo series had higher affinity at KOR receptors than MOR receptors, counter to the trend observed for 25X-NBOMes. Also, most of the 4I25-DMPEA dimethoxy derivatives had higher affinities at MOR receptors than the corresponding 4Br25-DMPEA dimethoxy compounds, although the magnitude of the difference was relatively small (less than 10-fold). In the MPEABrDMBz or reversed NBOMe series the relative opioid receptor affinity was KOR > MOR > DOR, consistent with the dimethoxy 4X25-DMPEADMBz series, and different from the 25X-NBOMes.

Table 51 Binding Affinity of the 4H25-DMPEA Series at Opioid Receptor Subtypes.

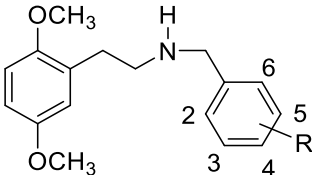
			
PDSP ID Number (4H25-DMPEA)	DOR, pKi (SE)	KOR, pKi (SE)	MOR, pKi (SE)
48238 (25DMPEA2MBzHCl)	<5 (ND)	<5 (ND)	<5 (ND)
48239 (25DMPEA3MBzHCl)	<5 (ND)	<5 (ND)	5.9±0.07
48240 (25DMPEA4MBzHCl)	<5 (ND)	5.54±0.07	5.73±0.07
48241 (25DMPEA23DMBzHCl)	<5 (ND)	<5 (ND)	5.71±0.07
48242 (25DMPEA24DMBzHCl)	<5 (ND)	6.11±0.07	6.13±0.07
48243 (25DMPEA25DMBzHCl)	<5 (ND)	5.73±0.07	6.03±0.07
48244 (25DMPEA26DMBzHCl)	<5 (ND)	5.94±0.07	6.38±0.08
48257 (25DMPEA34DMBzHCl)	<5 (ND)	<5 (ND)	<5 (ND)
48258 (25DMPEA35DMBzHCl)	<5 (ND)	<5 (ND)	<5 (ND)
48245 (25DMPEA23MDBzHCl)	<5 (ND)	6.02±0.07	6.25±0.08
48259 (25DMPEA34MDBzHCl)	<5 (ND)	5.76±0.08	<5 (ND)

Table 52 Binding Affinity of the 4Br25-DMPEA Series at Opioid Receptor Subtypes.

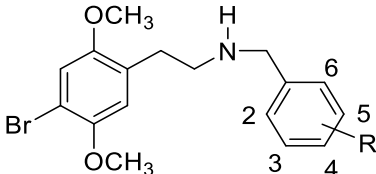
			
PDSP ID Number (4Br25-DMPEA)	DOR, pKi (SE)	KOR, pKi (SE)	MOR, pKi (SE)
48246 (4Br25DMPEA2MBzHCl)	<5 (ND)	6.45±0.05	6.83±0.06
48247 (4Br25DMPEA3MBzHCl)	<5 (ND)	5.97±0.08	6.27±0.07
48248 (4Br25DMPEA4MBzHCl)	5.03±0.1	6.08±0.08	6.18±0.07
48249 (4Br25DMPEA23DMBzHCl)	5.40±0.1	6.09±0.08	6.36±0.07
48250 (4Br25DMPEA24DMBzHCl)	5.64±0.05	7.15±0.07	6.41±0.07
48251 (4Br25DMPEA25DMBzHCl)	<5 (ND)	6.50±0.1	5.99±0.07
48252 (4Br25DMPEA26DMBzHCl)	<5 (ND)	6.50±0.1	6.2±0.1
48253 (4Br25DMPEA34DMBzHCl)	<5 (ND)	5.70±0.1	<5 (ND)
48254 (4Br25DMPEA35DMBzHCl)	<5 (ND)	6.20±0.1	5.69±0.07
48255 (4Br25DMPEA23MDBzHCl)	<5 (ND)	6.20±0.1	5.89±0.07
48256 (4Br25DMPEA34MDBzHCl)	<5 (ND)	6.20±0.1	5.94±0.07

Table 53 Binding Affinity of the IBr25DMPEA Series at Opioid Receptor Subtypes.

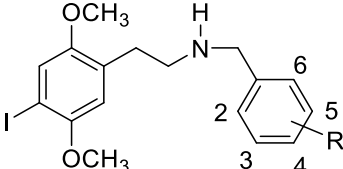
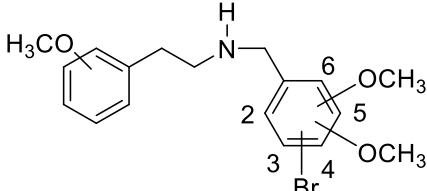
			
PDSP ID Number (4I25-DMPEA)	DOR, pKi (SE)	KOR, pKi (SE)	MOR, pKi (SE)
48260 (4I25DMPEA2MBzHCl)	<5 (ND)	6.32±0.08	6.70±0.07
48261 (4I25DMPEA3MBzHCl)	<5 (ND)	5.99±0.07	5.58±0.09
48262 (4I25DMPEA4MBzHCl)	<5 (ND)	<5 (ND)	6.3±0.1
48263 (4I25DMPEA23DMBzHCl)	<5 (ND)	5.88±0.07	5.9±0.1
48264 (4I25DMPEA24DMBzHCl)	5.41±0.07	7.26±0.06	6.1±0.1
48265 (4I25DMPEA25DMBzHCl)	5.76±0.07	6.91±0.07	6.3±0.1
48266 (4I25DMPEA26DMBzHCl)	5.66±0.08	7.20±0.1	7.3±0.1
48267 (4I25DMPEA34DMBzHCl)	<5 (ND)	5.90±0.1	5.7±0.1
48268 (4I25DMPEA35DMBzHCl)	<5 (ND)	6.20±0.1	5.9±0.1
48269 (4I25DMPEA23MDBzHCl)	<5 (ND)	6.20±0.1	6.44±0.09
48270 (4I25DMPEA34MDBzHCl)	<5 (ND)	6.40±0.1	6.00±0.09

Table 54 Binding Affinity of MPEABrDMBz (“eMOBN”) Series at Opioid Receptor Subtypes.

			
PDSP ID Number (NBOMe Derivative)	DOR, pKi (SE)	KOR, pKi (SE)	MOR, pKi (SE)
48271 (2MPEA4Br25DMBzHCl)	<5 (ND)	6.50±0.1	6.11±0.09
48272 (3MPEA4Br25DMBzHCl)	<5 (ND)	6.80±0.1	6.09±0.07
48273 (4MPEA4Br25DMBzHCl)	<5 (ND)	7.00±0.1	6.0±0.1
48274 (2MPEA2Br45DMBzHCl)	<5 (ND)	6.30±0.1	5.91±0.09
48275 (3MPEA2Br45DMBzHCl)	<5 (ND)	6.82±0.07	6.61±0.04

11.9 Transporter Binding Profiles:

The experimental conditions used to determine the binding profiles of the 4X25-DMPEA - NBOMe compounds at DAT, NET and SERT transporters detailed in Table 55 below along with a standard reference compound. GBR12909 was used as the reference standard for the DAT and it had a pKi of 8.33 (4.73 nM). Desipramine was the reference standard for the NET transporter with a pKi of 8.65 (2.24 nM). Amitriptyline was the reference standard for the SERT transporter with a pKi of 8.26 (5.53 nM). 25I-NBOMe is reported to have a pKi < 6.3 (>500 nM) at DAT and SERT transporters [18, 21]. The binding data obtained is presented in Table 56-59 below.

Table 55 Experimental conditions used to determine receptor binding profiles of the 4X25-DMPEA compounds at transporter subtypes.

Neurotransmitter transporters			
Transporter Binding Buffer: 10 mM HEPES, 135 mM NaCl, 5 mM KCl, 0.8 mM MgCl ₂ , 1 mM ETGA, pH 7.4, RT			
Transporter Wash Buffer: Transporter binding buffer, pH 7.4, cold			
Target	Radioligand pK _d ± SEM (K _d , nM)	Radioligand used (nM)	Reference Ligand pK _i ± SEM (K _i , nM)
DAT	[³ H]-Win35428 8.02 ± 0.04 (9.47)	3.6 – 16.0	GBR12909 8.33 ± 0.02 (4.73)
NET	[³ H]-Nisoxetine 8.42 ± 0.06 (3.83)	1.3 – 5.0	Desipramine 8.65 ± 0.01 (2.24)
SERT	[³ H]-Citalopram 8.58 ± 0.11 (2.63)	1.5 – 2.0	Amitriptyline 8.26 ± 0.02 (5.53)

As the data in Tables 56-59 demonstrate, none of the 4X25-DMPEA or MPEABrDMBz (“eMOBN”) compounds have significant affinity (pKis > 6 or >1000 nM) for the NET or DAT transporters. Compounds of the 4I25-DMPEA (Table 58) had weak affinity for SERT transporters with pKis over a narrow range of 5.7-6.3. In general, the 4I25-DMPEA compounds displayed slightly higher affinity at SERT transporters than the 4Br25-DMPEA and 4H25-DMPEA compounds which had pKi ranging from <5 to 5.9. But all of the 4X25-DMPEA compounds had significantly lower SERT affinity than the reference compound, amitriptyline (pKi 8.26). These results are generally consistent with data reported from binding studies with 25I-NBOMe where this compound had a pKi >6.3 at DAT and SERT transporters [21].

Table 56 Binding Affinity of the 4H25-DMPEA Series at Transporters.

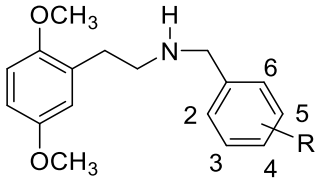
			
PDSP ID Number (4H25-DMPEA)	NET, pKi (SE)	DAT, pKi (SE)	SERT, pKi (SE)
48238 (25DMPEA2MBzHCl)	5.6±0.1	<5 (ND)	5.6±0.1
48239 (25DMPEA3MBzHCl)	<5 (ND)	<5 (ND)	<5 (ND)
48240 (25DMPEA4MBzHCl)	<5 (ND)	5.6±0.1	5.8±0.1
48241 (25DMPEA23DMBzHCl)	<5 (ND)	<5 (ND)	5.9±0.2
48242 (25DMPEA24DMBzHCl)	<5 (ND)	<5 (ND)	<5 (ND)
48243 (25DMPEA25DMBzHCl)	<5 (ND)	<5 (ND)	<5 (ND)
48244 (25DMPEA26DMBzHCl)	<5 (ND)	<5 (ND)	<5 (ND)
48257 (25DMPEA34DMBzHCl)	<5 (ND)	<5 (ND)	±0.07
48258 (25DMPEA35DMBzHCl)	<5 (ND)	5.6±0.1	<5 (ND)
48245 (25DMPEA23MDBzHCl)	<5 (ND)	<5 (ND)	<5 (ND)
48259 (25DMPEA34MDBzHCl)	<5 (ND)	<5 (ND)	5.41±0.07

Table 57 Binding Affinity of the 4Br25-DMPEA Series at Transporters.

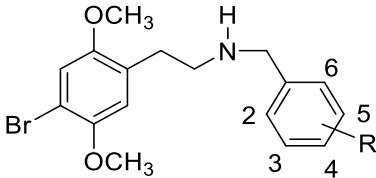
			
PDSP ID Number (4Br25-DMPEA)	NET, pKi (SE)	DAT, pKi (SE)	SERT, pKi (SE)
48246 (4Br25DMPEA2MBzHCl)	<5 (ND)	<5 (ND)	5.82±0.06
48247 (4Br25DMPEA3MBzHCl)	<5 (ND)	5.8±0.2	5.6±0.1
48248 (4Br25DMPEA4MBzHCl)	5.6±0.1	5.4±0.2	5.3±0.1
48249 (4Br25DMPEA23DMBzHCl)	<5 (ND)	<5 (ND)	5.3±0.1
48250 (4Br25DMPEA24DMBzHCl)	<5 (ND)	<5 (ND)	5.5±0.1
48251 (4Br25DMPEA25DMBzHCl)	5.6±0.1	<5 (ND)	5.6±0.1
48252 (4Br25DMPEA26DMBzHCl)	5.8±0.1	<5 (ND)	5.9±0.1
48253 (4Br25DMPEA34DMBzHCl)	<5 (ND)	<5 (ND)	5.82±0.07
48254 (4Br25DMPEA35DMBzHCl)	5.2±0.2	5.8±0.2	<5 (ND)
48255 (4Br25DMPEA23MDBzHCl)	<5 (ND)	5.6±0.1	5.41±0.08
48256 (4Br25DMPEA34MDBzHCl)	<5 (ND)	5.9±0.1	5.43±0.07

Table 58 Binding Affinity of the IBr25DMPEA Series at Transporters.

PDSP ID Number (4I25-DMPEA)	NET, pKi (SE)	DAT, pKi (SE)	SERT, pKi (SE)
48260 (4I25DMPEA2MBzHCl)	<5 (ND)	5.5±0.2	5.66±0.06
48261 (4I25DMPEA3MBzHCl)	<5 (ND)	5.6±0.2	5.9±0.1
48262 (4I25DMPEA4MBzHCl)	6.0±0.2	<5 (ND)	6.1±0.1
48263 (4I25DMPEA23DMBzHCl)	<5 (ND)	5.1±0.3	6.0±0.1
48264 (4I25DMPEA24DMBzHCl)	<5 (ND)	<5 (ND)	6.3±0.1
48265 (4I25DMPEA25DMBzHCl)	<5 (ND)	5.6±0.1	6.1±0.1
48266 (4I25DMPEA26DMBzHCl)	5.65±0.09	5.6±0.1	6.6±0.2
48267 (4I25DMPEA34DMBzHCl)	<5 (ND)	<5 (ND)	6.4±0.2
48268 (4I25DMPEA35DMBzHCl)	5.8±0.2	5.7±0.1	6.2±0.2
48269 (4I25DMPEA23MDBzHCl)	5.6±0.2	<5 (ND)	6.0±0.1
48270 (4I25DMPEA34MDBzHCl)	5.4±0.2	NA	6.2±0.2

Table 59 Binding Affinity of MPEABrDMBz (“eMOBN”) Series at Transporters.

PDSP ID Number (MPEABrDMBz)	NET, pKi (SE)	DAT, pKi (SE)	SERT, pKi (SE)
48271 (2MPEA4Br25DMBzHCl)	6.0±0.1	NA	6.0±0.2
48272 (3MPEA4Br25DMBzHCl)	6.4±0.1	NA	5.9±0.06
48273 (4MPEA4Br25DMBzHCl)	6.0±0.1	NA	6.0±0.1
48274 (2MPEA2Br45DMBzHCl)	<5 (ND)	NA	5.4±0.1
48275 (3MPEA2Br45DMBzHCl)	<5 (ND)	NA	5.73±0.09
48276 (4MPEA2Br45DMBzHCl)	<5 (ND)	NA	NA

11.10 Other Receptors:

Selected members of the 4X25-DMPEA compounds synthesized in this study were also assayed to characterize their binding profiles at GABA, benzodiazepine (BDZ) and muscarinic (M1-M5) receptor subtypes. None of the 4X25-DMPEA compounds were found to have significant affinity (all $pK_{is} < 6$) in any of these receptor lines (data not presented). These results are generally consistent with data reported from binding studies with 25X-NBOMe compounds at these receptors.

12 Summary and Conclusions

The potential for designer analogue synthesis in the NBOMe series of drugs of abuse is very high based on the methods used to synthesize this structural class of compounds, and the availability of a wide variety of precursor chemicals which would allow for significant structural variation. Also, since derivatives and isomers of the NBOMe class of drugs are difficult to differentiate by routine analytical methods, the production of designer analogues would pose significant challenges for those involved in drug detection and identification. In this study several series of NBOMe derivatives and regioisomers (Figure 154) were synthesized with varying substituents and substitution patterns in the phenethyl aromatic ring (sites A and B), the N-benzyl aromatic ring (Site C), the ethyl side chain (Site D) and nitrogen atom (Site E). Analytical methods were then explored to identify the specific NBOMe derivatives and differentiate individual compounds regioisomers within a regioisomeric series.

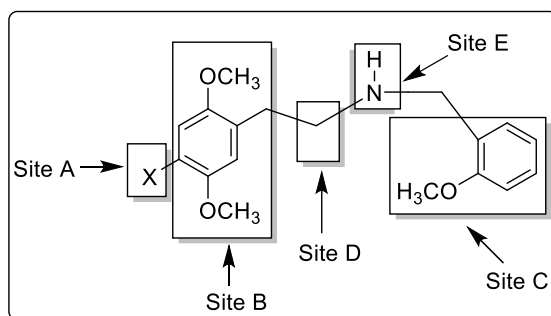


Figure 154 NBOMe derivatives.

The NBOMe derivatives and regioisomers were synthesized by reaction of commercially available substituted benzaldehydes with a nitroalkane to yield substituted phenylnitroalkene intermediates, then reduction of the phenylnitroalkene intermediates to substituted phenethylamines, and finally addition of various N-benzyl substituents to the phenethylamines by reductive alkylation. In the case of the 4-halogenated derivatives (4-Br and 4-I), the halogen was introduced by electrophilic substitution at the phenethylamine intermediate stage.

The first series of compounds, the N-(monomethoxy)benzyl-monomethoxyphenethylamines (Figure 155), represent simplified derivatives of NBOMes where the halogen atom was deleted from the structure and only a single methoxy substituent was included on each of the aromatic rings (modification of Site A and B). Each aromatic ring of the base NBOME structure has three positions that can be mono-substituted, the 2-, 3-, and 4-positions of the phenylethyl aromatic ring and the 2'-, 3'-, and 4'-positions of the N-benzyl ring. Thus, substitution at each of these aromatic positions yielded nine regioisomeric derivatives. All nine regioisomers of this series yielded nearly identical EI-mass spectra with a base peak of m/z 121 and other fragment ions of relatively high abundance at m/z 150 and 91. The base peak at m/z 121 formed by the cleavage of the N-C bond yielding 2-methoxybenzyl cation. The ion at m/z 150 was determined to be the iminium cation formed by the dissociation of bond between α - and β -carbon atoms, a common pathway for phenethylamine compounds. Finally, the ion at m/z 91 formed from loss of CH_2O from the methoxybenzylcation. A molecular ion ($\text{MW} = 271$) was not apparent in the EI-MS spectra of any of the compounds of this series, however the molecular mass was confirmed by CI-MS.

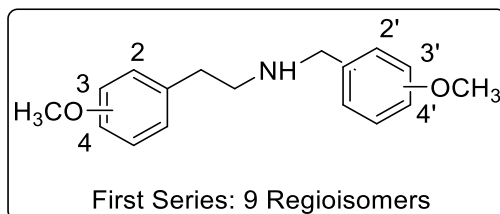


Figure 155 N-(monomethoxy)benzyl-monomethoxyphenethylamine series.

Based on the similarity in their mass spectra it was not possible to differentiate all nine regioisomers of the N-(monomethoxy)benzyl-monomethoxyphenethylamine series using EI-MS. However, some degree of differentiation was possible within subsets of this series where the methoxy group in the phenethyl ring was held at a constant position and the N-benzyl methoxy group varied from the 2'-, 3'- and 4'-positions. Within these subsets, the m/z 91 ion was present in the highest abundance in the 2'-methoxy isomer and decreased in abundance in the 3'-isomer and further in the 4'-methoxy isomer. However, regioisomers where the position of the methoxy group on the N-benzyl ring is held constant and the position of the methoxy group on the phenethyl

ring is varied could not be differentiated by EI-MS, and no other features in the mass spectra of these regioisomers allowed for specific differentiation of one isomer from another. It was possible to separate and identify subsets of the N-(monomethoxy)benzyl-monomethoxyphenethylamine series by gas chromatography using a midpolarity Crossbond® silarylene phase containing a 50% phenyl and 50% dimethyl polysiloxane polymer (Rxi®-17Sil MS). This set of chromatographic conditions yielded an excellent separation of each subset of three compounds with the 2'-methoxy isomer eluting before the 3'-isomer, and the 3'-isomer before the 4'-isomer in each case.

The second series of compounds, the N-(monomethoxy)benzyl-dimethoxyphenethylamines, represent simplified derivatives of the NBOMes where the halogen atom is eliminated (Site A) and there are two methoxy substituents on the phenethyl aromatic ring (Site B) with only a single methoxy substituent on the benzyl ring (Site C) of the core NBOME structure. There are six possible dimethoxy phenethyl substitution patterns and three possible N-benzyl monomethoxy substitution patterns, giving rise to a total of 18 regioisomeric compounds in this series (Figure 156). For purposes of analysis this series was divided into six subsets based primarily on the position of the dimethoxy substituents on the phenethyl aromatic ring (the 2,3-, 2,4-, 2,5-, 2,6-, 3,4- and 3,5-positions) and secondarily on the position of the single methoxy group on the benzyl aromatic ring (2'-, 3'-, and 4'-positions).

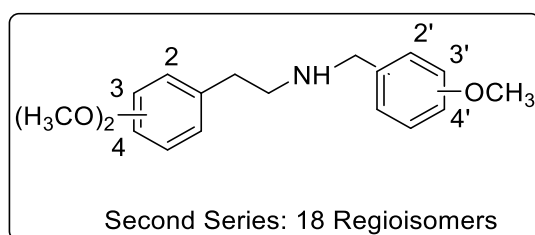


Figure 156 N-(monomethoxy)benzyl-dimethoxyphenethylamine series.

All eighteen regioisomeric N-(monomethoxy)benzyl-dimethoxyphenethylamine compounds of this series yielded nearly identical EI-mass spectra with base peak at m/z 121 and other high abundance fragment ions at m/z 150 and 91. Thus the N-(monomethoxy)benzyl-

dimethoxyphenethylamines of this second series fragment by the same mechanisms in the EI-MS as the N-(monomethoxy)benzyl-monomethoxyphenethylamines of the first series, giving rise to fragment ions of the same mass. Since the N-(monomethoxy)benzyl-dimethoxyphenethylamine derivatives have an additional methoxy group and molecular weights 30 units higher, they were readily differentiated from compounds of the N-(monomethoxy)benzyl-monomethoxyphenethylamine series by CI-MS.

Based on the similarity in the EI-mass spectra it was not possible to differentiate all 18 regioisomers of the N-(monomethoxy)benzyl-dimethoxyphenethylamine series. However, subsets of these regioisomers where the dimethoxy substitution pattern was held constant and the position of the N-benzyl methoxy group was varied could be differentiated based on the relative abundance of the m/z 91 benzyl cation. Again, as observed in the N-(monomethoxy)benzyl-monomethoxyphenethylamine series, the m/z 91 ion was present in the highest abundance in the 2'-methoxy isomer and decreased in the 3'- and 4'-methoxy isomers. Other than the relative abundance of the m/z 91 ions, there are no other features in the mass spectra of these regioisomers which allows for specific differentiation. It was possible to separate and identify regioisomers in each of the six subsets of the N-(monomethoxy)benzyl-dimethoxyphenethylamine series by gas chromatography using a midpolarity Crossbond® silarylene phase containing a 50% phenyl and 50% dimethyl polysiloxane polymer (Rxi®-17Sil MS). These chromatographic conditions yielded an excellent separation of each subset of three compounds with the 2'-methoxy isomer eluting before the 3'-isomer, and the 3'-isomer before the 4'-isomer in each case. This was the same elution order trend observed in the N-(monomethoxy)benzyl-monomethoxyphenethylamine series.

The third series of compounds, the N-(dimethoxy)benzyl-2,5-dimethoxyphenethylamines (25H-NBOMes), represent simplified derivatives of NBOMes where the 2,5-dimethoxy substitution pattern on the phenylethyl aromatic is retained, the halogen atom at the 4-position eliminated, and an additional methoxy group added on the benzylic ring of the core NBOME structure. There are six possible dimethoxy substitution patterns on the N-benzyl ring (2',3'-, 2',4'-, 2',5'-, 2',6'-, 3',4'- and 3',5'-dimethoxy) giving rise to six regioisomers in this series (Figure 157). All six

regioisomeric members of this series yielded nearly identical mass spectra, with the base peak m/z 151 and major fragment ions at m/z 180 and 121. Each of these fragment ions is 30 mass units higher than the corresponding most abundant ions in the EI-MS of the N-(monomethoxy)benzyl-monomethoxyphenethylamine and N-(monomethoxy)benzyl-dimethoxyphenethylamine series (first and second series), consistent with the presence of an additional methoxy group in the N-benzyl ring. Therefore, all three of these series appear to undergo the same predominant EI-MS fragmentation pathway. However the six regioisomers of this N-(dimethoxy)benzyl-2,5-dimethoxyphenethylamine series are readily differentiated from all members of the first (N-(monomethoxy)benzyl-monomethoxyphenethylamine and all members of the second (N-(monomethoxy)benzyl-dimethoxyphenethylamine series by their higher molecular weight as determined by CI-MS.

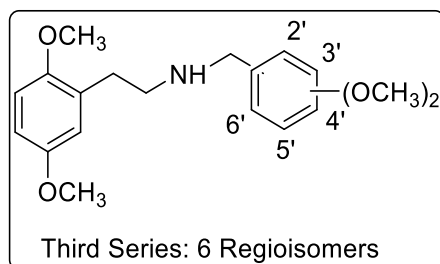


Figure 157 N-(dimethoxy)benzyl-2,5-dimethoxyphenethylamines.

Based on the similarity in the EI-mass spectra it was not possible to specifically identify and differentiate all six regioisomers of the N-(dimethoxy)benzyl-dimethoxyphenethylamine series. The 2',3'-dimethoxy regioisomer had a unique fragment ion at m/z 136 which distinguishes this compound from the other five regioisomers of the series as well as derivatives of the previous series which contained only a single methoxy group in the N-benzyl substituent (first and second series). The structure of this unique ion was confirmed by labeling studies. Attempts to separate these six regioisomers under a variety of gas chromatographic conditions were also unsuccessful, with the 2',4' and 3',4'-dimethoxybenzyl regioisomers co-eluting under most conditions. Thus the six regioisomers of this N-(dimethoxy)benzyl-2',5'-dimethoxyphenethylamine series could not be specifically differentiated by direct EI-MS or gas chromatographic analysis.

The fourth series of compounds, the N-(monomethoxy)benzyl- and N-(dimethoxy)benzyl-4-bromo-2,5-dimethoxyphenethylamine represent derivatives of 25B-NBOMe where the 4-bromo-2,5-dimethoxy substitution pattern on the phenethyl ring is retained, but the substitution pattern on the aromatic ring of the N-benzyl substituent is modified to include the three possible monomethoxy isomers, and the six possible dimethoxy derivatives (Figure 158). All three of the monomethoxy-benzyl regioisomers yielded nearly identical EI-mass spectra with base peak at m/z 121 and other high abundance fragment ions at m/z 150 and 91, as observed for the N-benzylmonomethoxy derivatives of the first and second series. None of the dominant ions in the EI-mass spectra of these compounds contained bromine. Also, as observed for the N-benzylmonomethoxy derivatives of the first and second series, the three monomethoxy regioisomers could be differentiated by the relative abundance of the m/z 91 fragment ion, being present in the highest abundance in the 2'-methoxy isomer and decreasing in abundance in the 3'- and 4'-methoxy isomers. These data confirm that the primary fragmentation pathways for the NBOMe derivatives with a single methoxy group in the benzyl ring involve cleavage of the benzylic C-N bond yielding 2-methoxybenzyl cation base peak, dissociation of bond between α - and β -carbon atoms to form iminium cation, and loss of CH_2O from the methoxybenzyl cation to form the benzyl cation. Furthermore, the relative abundance of the benzyl cation is dependent upon position of the methoxy group on the N-benzyl ring and this allows for specific regioisomer identification. These fragmentation pathways predominate for monomethoxy-N-benzyl NBOMe derivatives irrespective of the substitution pattern in the phenethyl aromatic ring. Of course the N-(monomethoxy)benzyl-4-bromo-2,5-dimethoxyphenethylamines of this series were readily differentiated from corresponding monomethoxy derivatives of the first and second series by molecular mass differences $(\text{M}+\text{H})^+$ determined by CI-MS.

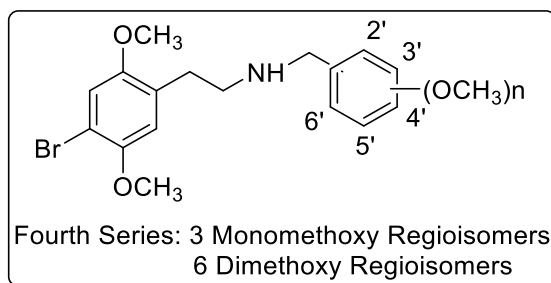


Figure 158 N-(monomethoxy)benzyl- and N-(dimethoxy)benzyl-4-bromo-2,5-dimethoxyphenethylamine series.

The EI-mass spectra of the six N-(dimethoxy)benzyl-4-bromo-2,5-dimethoxyphenethylamine regioisomers of series four were nearly identical with a base peak at m/z 151 and ions of high abundance at m/z 180 and 121. Furthermore, these spectra were very similar to those obtained for the 4-unsubstituted-N-(dimethoxy)benzyl-2,5-dimethoxyphenethylamines of the third series (25H-NBOMes), again suggesting a common fragmentation pathway independent of the substituents in the phenethyl ring. Also, as observed in the 4-unsubstituted-N-(dimethoxy)-benzyl-2,5-dimethoxyphenethylamine series, the 2',3'-dimethoxy regioisomer in this 4-bromo series had a unique fragment ion at m/z 136 which distinguishes this compound from the other five regioisomers of the series. Other than this unique ion, there were no significant differences in the spectra of these regioisomers to allow for specific differentiation. However, these six regioisomers were separated and identified by gas chromatographic methods. Also, the N-(dimethoxy)benzyl-4-bromo-2,5-dimethoxyphenethylamines of this series were readily differentiated from corresponding dimethoxy N-benzyl derivatives of the third series by molecular mass differences determined by CI-MS.

The fifth series of compounds, the N-(monomethoxy)benzyl- and N-(dimethoxy)benzyl-4-iodo-2,5-dimethoxyphenethylamines, represent derivatives of 25I-NBOMe where the 4-iodo-2,5-dimethoxy substitution pattern on the phenethyl ring is retained, but the substitution pattern on the aromatic ring of the N-benzyl substituent is modified to include the three possible monomethoxy isomers, and the six possible dimethoxy derivatives (Figure 159). EI-MS analysis of these compounds yielded the same results observed for the 4-unsubstituted-N-(dimethoxy)benzyl-2,5-dimethoxyphenethylamines of the third series and 4-bromo-N-(dimethoxy)benzyl-2,5-dimethoxyphenethylamines of the fourth series, again illustrating the characteristic fragmentation pathways for these structurally related series, and the inability to differentiate between dimethoxy N-benzyl regioisomers. It was possible to separate and differentiate all six N-(dimethoxy)benzyl-4-iodo-2,5-dimethoxyphenethylamine regioisomers by gas chromatography, but this method does not readily lend itself to specific identification of regioisomers in the absence of reference standards.

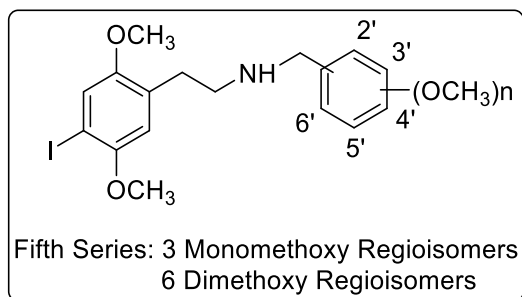


Figure 159 N-(monomethoxy)benzyl- and N-(dimethoxy)benzyl-4-iodo-2,5-dimethoxyphenethylamine series.

The regioisomers of the N-(dimethoxy)benzyl-2,5-dimethoxyphenethylamine series (Series 3), N-(dimethoxy)benzyl-4-bromo-2,5-dimethoxyphenethylamine series (Series 4) and N-(dimethoxy)benzyl-4-iodo-2,5-dimethoxyphenethylamine series (Series 5) were successfully differentiated by EI-MS following derivatization as trifluoroacetamides (TFA-acetamides – Figure 160). Differentiation and specific identification of all six regioisomers within each series (Series 3-5) as TFA-acetamide derivatives was possible based on a combination of different base peak ions, unique fragment ions (m/z 136 and m/z 263), along with differences in the relative abundance of benzyl cations at m/z 121 and m/z 91. TFA derivatization also improved gas chromatographic resolution for the six regioisomers in the 4-unsubstituted-N-(dimethoxy)benzyl-2,5-dimethoxyphenethylamines series (Series 4)

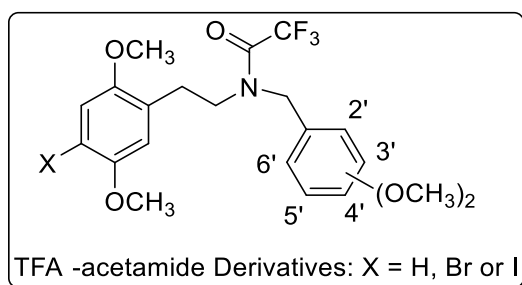


Figure 160 TFA-acetamide derivatives of the 4-unsubstituted, 4-bromo- and 4-iodo- N-benzyl-dimethoxy regioisomers of series 3, 4 and 5.

Additional NBOMe derivatives were prepared in each series (Series 3-5) where the N-benzyl aromatic ring was substituted with a 2',3'- or 3', 4'-methylenedioxy ring (Figure 161). These analogues undergo the same fragmentation pathways as other NBOMe derivatives, but the benzyl cation base peak (m/z 135) and abundant iminium cation (m/z 164) fragments have unique masses allowing for differentiation from all monomethoxy- and dimethoxy-N-benzyl NBOMe derivatives. These methylenedioxy derivatives also were readily differentiated by CI-MS from all other N-benzyl substituted NBOMe derivatives based on the differences in molecular weights. The two methylenedioxy regioisomers in each series (Series 3-5) were readily separated and identified by gas chromatography.

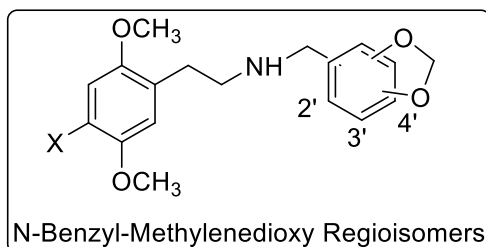


Figure 161 2',3'- or 3', 4'-methylenedioxy N-Benzyl ring Substituted NBOMe derivatives.

In addition to the NBOMe derivatives where the substitution pattern on the phenethyl and N-benzyl ring were modified, a number of analogues of series 3-5 were synthesized with methyl substitution in the ethylamine connecting chain at either the α -carbon, the nitrogen atom or both positions (Figure 162). All derivatives of this type underwent fragmentation in the EI-MS to give base peaks and fragment ions of high abundance analogous to those observed for NBOMe derivatives lacking an α -methyl or N-methyl group. In each case the base peak formed by the cleavage of the benzylic C-N bond to yield a peak with the same mass for all derivatives with a common N-benzyl substituent (R'). Also, in each case the iminium cation was the second most abundant fragment ion in the EI-MS, and all α -methyl derivatives and N-methyl derivatives with a common N-benzyl substituent (R') gave an iminium ion of the same mass. Thus EI-MS does not allow for differentiation of similarly substituted α -methyl or N-methyl NBOMe regioisomers. However, regioisomers of this type can be differentiated by other analytical methods including

proton NMR by chemical shifts and multiplicity, and infrared spectroscopy by absorbance differences between secondary and tertiary amines. Finally, those derivatives which contained both an α -methyl and N-methyl had the same benzyl cation base peak in their EI-MS as other NBOMe analogues with the same N-benzyl substituent (R'). But these compounds gave an iminium cation 14 mass units higher than NBOMe derivatives containing only an α -methyl or N-methyl substituent.

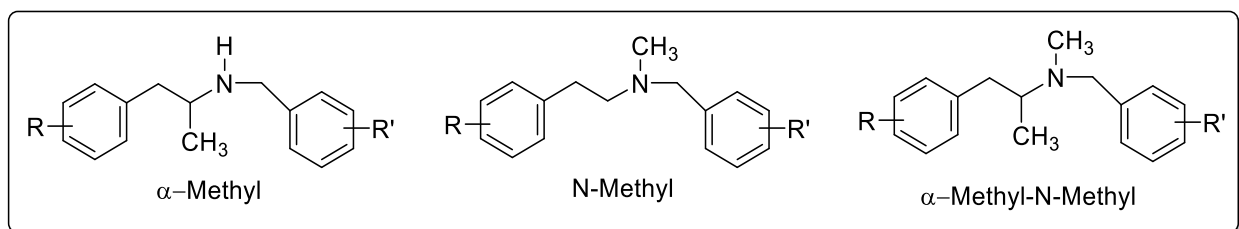


Figure 162 Alpha and N-methyl substituted NBOMe derivatives.

The new NBOMe compounds synthesized were tested for their receptor affinities in a variety of assays and several were found to have nanomolar affinities and high selectivity for 5-HT₂ receptor subtypes.

13 Experimental - Synthesis

13.1 Synthesis of deuterated vanillin:

Methyl iodide (369.04 mg, 2.6 mmol) was added to a reaction mixture of 2-hydroxy-3-methoxybenzaldehyde (*o*-vanillin, 152.15 mg, 1 mmol) and potassium carbonate (359.35 mg, 0.26 mmol) in dry acetone (50 ml). The reaction mixture was stirred overnight at room temperature. The next day, the reaction mixture was gravity filtered and the residue was washed with acetone (3x 5 ml) then the filtrate was evaporated under reduced pressure at 65 °C on a rotary evaporator to give 2,3-dimethoxybenzaldehyde. The structure of the product was confirmed by GC-MS. This same process was used to prepare the 3-OCD₃ labelled aldehyde precursor from 2-methoxy-3-hydroxybenzaldehyde, and the ¹³C labelled aldehyde precursors from both 2-hydroxy-3-methoxybenzaldehyde and 2-methoxy-3-hydroxybenzaldehyde.

13.2 Synthesis of 2,5-dimethoxyphenylnitroethene (2,5-DMPNE):

Commercially available 2,5-dimethoxybenzaldehyde (10g, 0.06 moles), nitromethane (22g, 0.36 moles - 1:6 ratio) and anhydrous ammonium acetate (1 g, 0.013 moles) were added to a round bottom flask and heated at reflux with stirring for 2-3 hours. The reaction mixture was cooled to room temperature and the excess nitromethane removed under reduced pressure at 80 °C on a rotary evaporator. The resulting dark colored oil was suspended in 100 ml of isopropyl alcohol (iPrOH) and heated to obtain a solution. The solution was allowed to cool to room temperature, and then placed in an ice bath resulting in the formation of product as needle shaped crystals. The product was isolated by vacuum filtration, washed with a small amount of cold iPrOH and recrystallized from 100 ml of iPrOH. After cooling at 4 °C in the refrigerator the purified product formed as large, yellow needles. The 2,5-dimethoxynitroethene product crystals were isolated by filtration, air dried on filter paper at room temperature, and then dried in an oven at 70 °C for 30 minutes. The structure of the product was confirmed by GC-MS and NMR spectroscopy and comparison to analytical data obtained for these compounds as prepared previously in our laboratories. All of the three of the monomethoxy- (2-, 3- and 4-methoxy), six dimethoxy- (2,3-, 2,4-, 2,6-, 3,4- and 3,5-) and both methylenedioxy (2,3- and 3,4-)-phenylnitroethenes (PNEs) and

were prepared by this method as shown in the table below. Also, the 2,3-, 2,5-, 2,6-dimethoxy- and 3,4-methylenedioxy-phenylnitropropenes (PNPs) were also prepared using this same method and nitroethane (27 g, 0.36 moles) in place of nitromethane. Yields and crystallization solvents for each nitroalkene intermediate are reported in Tables 60 and 61 below.

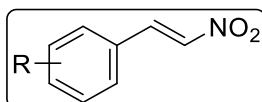


Table 60 Yields and Crystallization Solvents for the Methoxy (MPNEs)-, Dimethoxy (DMPNEs)- and Methylenedioxy- (MDPNEs)- phenylnitroethenes.

Product	Phenethyl ring substituent (R)	Crude product form	Crystallization solvent	Total yield (g)
2MPNE	2-MeO	Orange oil	iPrOH/Acetone	2.7
3MPNE	3-MeO	Orange oil	iPrOH	6.2
4MPNE	4-MeO	Dark red oil	MeOH	2.1
2,3DMPNE	2,3-DiMeO	Red oil	iPrOH	6.8
2,4DMPNE	2,4-DiMeO	Red oil	iPrOH	8.2
2,5DMPNE	2,5-DiMeO	Orange solid	iPrOH	8.7
2,6DMPNE	2,6-DiMeO	Yellow Solid	iPrOH	10.5
3,4DMPNE	3,4-DiMeO	Yellow Solid	iPrOH	10.8
3,5DMPNE	3,5-DiMeO	Yellow solid	iPrOH	6.6
2,3MDPNE	2,3-OCH ₂ O-	Yellow Solid	MeOH	5.2
3,4MDPNE	3,4-OCH ₂ O-	Yellow Solid	iPrOH	7.2

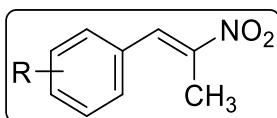


Table 61 Yields and Crystallization Solvents for the dimethoxy- and Methylenedioxyphenyl-2-nitropropenes.

PNP Product	Phenethyl ring substituent (R)	Crude product form	Crystallization / Recrystallization solvent	Total yield (g)
2,3DMPNP	2,3-DiMeO	Oil (yellow)	iPrOH	8.6
2,5DMPNP	2,5-DiMeO	Oil (yellow)	iPrOH	5.3
2,6DMPNP	2,6-DiMeO	Oil (reddish)	iPrOH	9.1
3,4MDPNP	3,4-OCH ₂ O-	Solid	iPrOH	8.6

13.3 Synthesis of 2,5-dimethoxyphenethylamine (25DMPEA):

Lithium aluminum hydride (LAH, 1.5 g, 40 mmole) was placed in a 500 mL dry round bottom flask and dry tetrahydrofuran (THF, 20-30 ml) added over a period of 5-10 minutes at room temperature. A solution of 2,5-dimethoxynitroethene (3.0 g, 14.4 mmole) in dry THF (20-30 ml) was then added to the THF-LAH suspension at room temperature over a period of 5-10 minutes using addition funnel. The reaction mixture was then stirred at reflux for 2-3 hours, then at room temperature overnight. The next day, the reaction mixture was cooled in an ice bath for 30 minutes and the LAH neutralized by successive dropwise addition of THF in water (1.5 ml THF in 7.5 ml water), 10% sodium hydroxide (3 ml) and finally water (4.5 ml). Methanol (10 ml) was then added to the quenched reaction mixture and stirred for 10 minutes. The quenched reaction mixture was then filtered through a scintered glass funnel of medium porosity and washed with additional methanol. The filtrate and washings were then evaporated under reduced pressure using a rotary evaporator with heating to 50 °C. The remaining crude product oil was dissolved in 2N HCl (120 ml) and washed with diethyl ether (2X120 ml) to remove any unreacted starting material. The aqueous acid extract was cooled in an ice bath and made alkaline by addition of sodium hydroxide pellets to pH 12. This aqueous basic suspension was then extracted with dichloromethane (DCM, 2X100 ml). The combined DCM extracts were evaporated under reduced pressure using a rotary evaporator at 50 °C, and the remaining product oil dried azeotropically with absolute ethanol. The dried product oil was dissolved in anhydrous ether (50 ml) and HCl gas added to form the hydrochloride salt as a gummy solid. Simple scratching of the inside wall of the round bottom flask with a spatula followed by stirring overnight yielded the product as a yellow solid. The product was isolated by gravity filtration and air dried. All of the three of the monomethoxy- (2-, 3- and 4-methoxy), six dimethoxy- (2,3-, 2,4-, 2,6-, 3,4- and 3,5-) and both methylenedioxy- (2,3- and 3,4-)-phenethylamines (PEAs) and were prepared by this method. The methoxy- and dimethoxy- and methylenedioxyphenylnitropropenes were also prepared using this same method and quantities. The HCl salts of these products were crystallized using the solvents listed in Table 62 below.

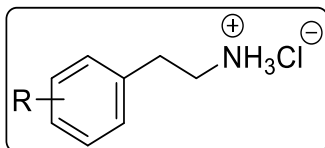


Table 62 Yields for the Methoxy (MPNEs)-, Dimethoxy (DMPNEs)- and Methylenedioxy (MDPNEs)- Phenethylamines.

PNE product, HCl Salt	Phenethyl ring substituent (R)	Crude product after extraction (free base)	Total Yield (g)
2MPEA HCl	2-MeO	Oil	1.87
3MPEA HCl	3-MeO	Oil	1.77
4MPEA HCl	4-MeO	Oil	1.97
23DMPEA (base)	2,3-DiMeO	Oil	1.3 (base)
24DMPEA HCl	2,4-DiMeO	Oil	1.70
25DMPEA HCl	2,5-DiMeO	Oil	1.48
26DMPEA HCl	2,6-DiMeO	Oil	1.57
34DMPEA HCl	3,4-DiMeO	Oil	0.92
35DMPEA HCl	3,5-DiMeO	Oil	1.8
23MDPEA HCl	2,3-OCH ₂ O-	Oil	1.19
34MDPEA HCl	3,4-OCH ₂ O-	Oil	2.17

13.4 Synthesis of N-(2'-methoxy)benzyl-2,5-dimethoxyphenethylamine (25DMPEA2MB):

A mixture of 2,5-dimethoxyphenethylamine HCl (217 mg, 1 mmole), 2-methoxybenzaldehyde (136 mg, 1 mmole) and triethylamine (101 mg, 1 mmole) in absolute ethanol (10 ml) in a 100 ml round bottom flask was heated at 70 °C for two hours to form the intermediate imine. The reaction mixture (yellow) was then cooled to room temperature and sodium borohydride NaBH₄ (200 mg, 5.3 mmoles) added and stirred at room temperature overnight. On the next day, the reaction solvent was evaporated under reduced pressure on a rotary evaporator at 50 °C. The resulting solid was suspended in water (20 ml) and neutralized (pH 7) by addition of a few drops of concentrated HCl. This aqueous suspension was then extracted with DCM (2 X 40 ml) and the combined DCM extracts evaporated under reduced pressure and dried azeotropically with absolute ethanol (5 ml, twice) at 65 °C. The products in the free base form was crystallized from ether and isolated by gravity filtration. All of the N-(methoxy)benzyl-dimethoxyphenethylamine, N-(2',5'-dimethoxy)benzyl-dimethoxyphenethylamine, N-(methylenedioxy)benzyl-methoxyphenethylamine and N-(methoxy)benzyl-dimethoxy- and methylenedioxyphenethylamine products

(MPEAs and DMPEAs), in the reagent quantities described above. The structures of the products were confirmed by standard spectroscopic methods and the yields and crystallization solvents are listed in Tables 63-65 below.

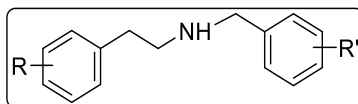


Table 63 Yields and Crystallization Solvents for the N-(Methoxy)benzyl-methoxyphenethylamines.

Compound abbreviation	Phenethyl Ring substituent (R)	Benzyl ring substituent (R')	Yield, mg (1 st & 2 nd crop)	Crystallization solvent (base)
PEAB	H	H	148	Ether
2MPEA2MB	2-MeO	2'-MeO	154.6	Ether
2MPEA3MB	2-MeO	3'-MeO	103.8	Ether
2MPEA4MB	2-MeO	4'-MeO	119.3	Ether
3MPEA2MB	3-MeO	2'-MeO	147.5	Ether
3MPEA3MB	3-MeO	3'-MeO	124.5	Ether
3MPEA4MB	3-MeO	4'-MeO	103.6	Ether
4MPEA2MB	4-MeO	2'-MeO	139.1	Ether
4MPEA3MB	4-MeO	3'-MeO	130.8	Ether
4MPEA4MB	4-MeO	4'-MeO	128.6	Ether

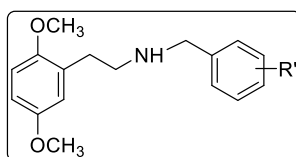


Table 64 Yields and Crystallization Solvents for the N-(dimethoxy)benzyl- and N-(methylenedioxy)benzyl-2,5-dimethoxyphenethylamines.

Compound abbreviation	Benzyl ring substituent (R')	Total yield (mg)	Crystallization solvent
25DMPEA23DMB	2',3'-DiMeO	117.6	Ether
25DMPEA24DMB	2',4'-DiMeO	86.5	Ether
25DMPEA25DMB	2',5'-DiMeO	158.4	Ether
25DMPEA26DMB	2',6'-DiMeO	25.4+oil	Ether/acetone
25DMPEA34DMB	3',4'-DiMeO	165.5	Ether
25DMPEA35DMB	3',5'-DiMeO	148.7	Ether
25DMPEA23MDB	2',3'-MD	68.6+oil	Ether/acetone
25DMPEA34MDB	3',4'-MD	5.3+oil	Ether/EtOH

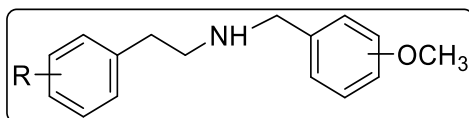


Table 65 Yields and Crystallization Solvents for the N-(methoxy)benzyl-dimethoxy-phenethylamines.

Compound abbreviation	Phenethyl ring substituent (R)	Benzyl ring substituent (R')	Crystallization solvent	Total yield (mg)
23DMPEA2MB	2,3-DiMeO	2'-MeO	Benzene/Ether	124.0
23DMPEA3MB	2,3-DiMeO	3'-MeO	Ether	124.8
23DMPEA4MB	2,3-DiMeO	4'-MeO	Benzene	99.4
24DMPEA2MB	2,4-DiMeO	2'-MeO	Oil	Oil
24DMPEA3MB	2,4-DiMeO	3'-MeO	Ether	16.8
24DMPEA4MB	2,4-DiMeO	4'-MeO	Ether	70.6
25DMPEA2MB	2,5-DiMeO	2'-MeO	Ether/acetone	109.3
25DMPEA3MB	2,5-DiMeO	3'-MeO	Ether/acetone	126.8
25DMPEA4MB	2,5-DiMeO	4'-MeO	Ether/acetone	29.8
26DMPEA2MB	2,6-DiMeO	2'-MeO	Ether	142.9
26DMPEA3MB	2,6-DiMeO	3'-MeO	Ether	153.7
26DMPEA4MB	2,6-DiMeO	4'-MeO	Benzene	158.4
34DMPEA2MB	3,4-DiMeO	2'-MeO	Ether/EtOAc	25.4
34DMPEA3MB	3,4-DiMeO	3'-MeO	Ether	165.5
34DMPEA4MB	3,4-DiMeO	4'-MeO	Ether	148.7
35DMPEA2MB	3,5-DiMeO	2'-MeO	Ether	56.4
35DMPEA3MB	3,5-DiMeO	3'-MeO	Ether/benzene	75.4
35DMPEA4MB	3,5-DiMeO	4'-MeO	Ether	170.5
23MDPEA2MB	2,3-MD	2'-MeO	Ether	127.6
23MDPEA3MB	2,3-MD	3'-MeO	Ether	114.5
23MDPEA4MB	2,3-MD	4'-MeO	Ether	99.9
34MDPEA2MB	3,4-MD	2'-MeO	Ether/benzene	139.8
34MDPEA3MB	3,4-MD	3'-MeO	Ether	87.2
34MDPEA4MB	3,4-MD	4'-MeO	Ether	67.9

13.5 Synthesis of 4-bromo-2,5-dimethoxyphenethylamine (4Br25DMPEA):

A solution of bromine (0.66 g, 4.1 mmol) in glacial acetic acid (2 ml) was added over a period of minute to a solution of 2,5-dimethoxyphenethylamine HCl (0.89 g, 4.1 mmol) in glacial acetic acid (2 ml) at room temperature. After the addition was complete the reaction mixture was stirred at room temperature an additional hour, resulting in the formation of a yellow precipitate. The yellow precipitate was isolated by filtration and washed with anhydrous ether. The solid product

was then dissolved in water (15 ml) and made alkaline (pH 12) by addition of NaOH pellets to yield a suspension. The aqueous base suspension was extracted with DCM (2 X 15 ml) and the combined DCM extracts evaporated at 50 °C on a rotary evaporator under vacuum to yield the product in free base form. The product base was dried azeotropically with ethanol (5 X 10 ml) and then dissolved in anhydrous ether (15-20 ml). HCl gas was bubbled into the ether solution yielding the product amine HCl salt as an off-white solid. The structure of the product was confirmed by GC-MS and NMR spectroscopy and comparison to analytical data obtained for these compounds as prepared previously in our laboratories.

13.6 Synthesis of N-(2'-methoxy)benzyl-4-bromo-2,5-dimethoxyphenethylamine (4Br25DMPEA2MB):

A solution of 4-bromo-2,5-dimethoxyphenethylamine HCl (295 mg, 1.0 mmole), triethylamine (101 mg, 1 mmole) and 2-methoxybenzaldehyde (136 mg, 1 mmole) in absolute ethanol (10 ml) was heated at reflux for 2 hours. The reaction mixture was cooled to room temperature and NaBH₄ (200 mg, 5.3 mmoles) added and the reaction mixture stirred at room temperature for 24 hours. The reaction mixture was then evaporated to dryness at 50 °C on rotary evaporator under vacuum to yield a yellow solid which was suspended in water (20 ml) and neutralized (pH 7) by addition of a few drops of conc. HCl. This solution was extracted with DCM (2 X 20 ml) and the combined DCM extracts evaporated and dried under reduced pressure to yield the product as a free base. To ensure complete drying of the product, 5 ml of absolute EtOH was added to the product and then evaporated in preheated, 65 °C rotary evaporator under vacuum twice. All of the three of the monomethoxy- (2'-, 3'- and 4'-methoxy), six dimethoxy- (2',3'-, 2',4'-, 2',6'-, 3',4'- and 3',5'-) and both methylenedioxy- (2',3'- and 3',4'-) products were prepared by this method using the molar quantities listed above. The products in free base form were crystallized using the solvents listed in Table 66 below and isolated by simple filtration. The structures of the products were confirmed by GC-MS spectroscopy and comparison to analytical data obtained for these compounds as prepared previously in our laboratories. Samples of all eleven compounds in this series were also converted to HCl salts using ethereal HCl and these samples were purified for submission for receptor binding assays.

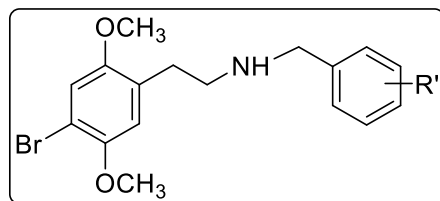


Table 66 Yields and Crystallization Solvents for the N-(Substituted)benzyl-4-Bromo-2,5-dimethoxyphenethylamines.

Compound abbreviation	Benzyl ring substituent (R')	Total yield (mg)	Crystallization solvent free base	MP, °C free base	Recrystallization solvent HCl salt
4Br25DMPEA2MB	2'-MeO	160	Ether	173-175	Ether*
4Br25DMPEA3MB	3'-MeO	180	Ether/Pet ether	124-126	Ether/EtOH
4Br25DMPEA4MB	4'-MeO	176	Ether	185-186	Ether*
4Br25DMPEA23DMB	2',3'-DiMeO	216	EtOH/Ether	86-87	Ether/EtOH
4Br25DMPEA24DMB	2',4'-DiMeO	255	Ether/pet ether	118-121	Ether/EtOH
4Br25DMPEA25DMB	2',5'-DiMeO	193	Ether/pet ether	117-118	Ether*
4Br25DMPEA26DMB	2',6'-DiMeO	141	Ether	164-166	Ether/EtOH
4Br25DMPEA34DMB	3',4'-DiMeO	136	Ether	165-167	Ether
4Br25DMPEA35DMB	3',5'-DiMeO	103	EtOAc/Pet ether	75-77	Ether/EtOH
4Br25DMPEA23MDB	2',3'-OCH ₂ O	271	EtOAc/ether	192-193	Ether
4Br25DMPEA23MDB	3',4'-OCH ₂ O	72	Ether	188-190	Ether/EtOH*

13.7 Synthesis of the N-(5'-Bromo-2',3'-dimethoxysubstituted)benzyl-2-methoxyphenethylamine (2MPEA5Br23DMB - eMOBNs):

A solution of 2-methoxyphenethylamine (188 mg, 1.0 mmole) and 5-bromo-2,3-dimethoxybenzaldehyde (245 mg, 1.0 mmole) in absolute ethanol (10 ml) was heated at reflux for 2 hours. The reaction mixture was cooled to room temperature and NaBH₄ (200 mg, 5.3 mmoles) added and the reaction mixture stirred at room temperature overnight. The reaction mixture was then evaporated to dryness at 50 °C on rotary evaporator under vacuum to yield a yellow solid which was suspended in water (20 ml) and neutralized (pH 7) by addition of a few drops of conc. HCl. This solution was extracted with DCM (2 X 20 ml) and the combined DCM extracts evaporated and dried under reduced pressure to yield the product as a free base. To ensure complete drying of the product, 5 ml of absolute EtOH was added to the product and then evaporated in preheated, 65 °C rotary evaporator under vacuum twice. The product in its free base form was crystallized using the solvent listed in table below and isolated by gravity filtration. The structure

of the product was confirmed by standard spectroscopic methods. This same method was used to synthesize all of the N-(bromo-dimethoxysubstituted)benzyl-2-methoxyphenethylamines (eMOBNs) listed in Table 67 below.

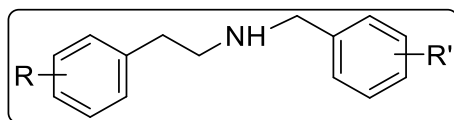


Table 67 Yields for the N-(bromo-dimethoxy)benzyl-monomethoxyphenethylamines.

Compound abbreviation	Phenethyl ring substituent (R)	Benzyl ring substituents (R')	Total yield (mg)	Crystallization solvent free base
2MPEA5Br23DMB	2-MeO	5'-Br-2',3'-DiMeO	292 mg	Ether/EtOH
3MPEA5Br23DMB	3-MeO	5'-Br-2',3'-DiMeO	151 mg	Ether/Benzene/iPrOH
4MPEA5Br23DMB	4-MeO	5'-Br-2',3'-DiMeO	92 mg	Ether
2MPEA2Br45DMB	2-MeO	2'-Br-4',5'-DiMeO	150 mg	Ether
3MPEA2Br45DMB	3-MeO	2'-Br-4',5'-DiMeO	92 mg	Ether
4MPEA2Br45DMB	4-MeO	2'-Br-4',5'-DiMeO	173 mg	Ether
2MPEA5Br24DMB	2-MeO	5'-Br-2',4'-DiMeO	100 mg	Ether
3MPEA5Br24DMB	3-MeO	5'-Br-2',4'-DiMeO	58 mg	Ether
4MPEA5Br24DMB	4-MeO	5'-Br-2',4'-DiMeO	75 mg	Ether
2MPEA4Br25DMB	2-MeO	4'-Br-2',5'-DiMeO	>100mg	EtOAc
3MPEA4Br25DMB	3-MeO	4'-Br-2',5'-DiMeO	>100mg	Ether
4MPEA4Br25DMB	4-MeO	4'-Br-2',5'-DiMeO	>100mg	Ether
2MPEA3Br45DMB	2-MeO	3'-Br-4',5'-DiMeO	28 mg	Ether/Pet.Ether/Benzene
3MPEA3Br45DMB	3-MeO	3'-Br-4',5'-DiMeO	150 mg	Ether
4MPEA3Br45DMB	4-MeO	3'-Br-4',5'-DiMeO	86 mg	Ether/Benzene

13.8 Synthesis of the N-(Substituted)benzyl-4-Iodo-2,5-dimethoxyphenethylamines by the ICl/AgOCCF₃ Method

A solution of iodine monochloride (0.94 ml, 2.92 g, 17.99 mmoles) in glacial acetic acid (10 ml) was added to a solution of 2,5-dimethoxyphenethylamine HCl (3.0 g, 13.8 mmole) and silver trifluoroacetate (AgOCCF₃, 4.8 g, 21.7 mmoles) in glacial acetic acid (50 ml) at room temperature over a period of 10 minutes. After the addition was complete the reaction mixture was stirred at room temperature for 1 hour until a yellow-brown precipitate formed. Anhydrous ether

(30 ml) was added to the reaction mixture and the resulting solid isolated by suction filtration using a scintered glass funnel (medium porosity). The solid was then dissolved in water (100 mL) and the aqueous solution made alkaline (pH 12) by addition of NaOH pellets. The resulting aqueous base suspension was extracted with DCM (2 X 100 ml) and the combined DCM extracts evaporated to dryness at 50 °C using a rotary evaporator under vacuum. To ensure complete drying of the product, 5 ml of absolute EtOH was added to the product and then evaporated in preheated at 65 °C rotary evaporator under vacuum twice. The HCl salt of the product was formed by dissolving the base in anhydrous ether (60 ml) and bubbling in HCl gas. The HCl salt was isolated by gravity filtration, yielding only a small quantity of the desired product (<200 mg) which was contaminated with several by-products by GC.MS.

13.9 Synthesis of N-(Substituted)benzyl-4-Iodo-2,5-dimethoxyphenethylamines by the I₂/Ag₂SO₄ Method:

Iodine (5.08 g, 20 mmole) was added to a suspension of 2,5-dimethoxyphenethylamine (1.83 g, 10 mmoles) and silver sulfate (Ag₂SO₄, 6.22 g, 20 mmoles) in absolute EtOH (100 ml). An addition quantity of EtOH (50 ml) was added and the suspension stirred overnight at room temperature. The reaction mixture was filtered and the solids washed with EtOH (3 X 10 ml). The combined EtOH filtrate and washings were evaporated at 65 °C on a rotary evaporator under vacuum to give golden-brown solid. This solid was suspended in DCM (200 ml) and 5% NaOH (200 ml) added and the two layers were stirred together until all of the solid had partitioned between the solvent layers (15 minutes). This mixture was then transferred to a separatory funnel and the solvent layers allowed to separate. The DCM solvent was isolated, washed with water (2 X 100 ml) and dried over anhydrous sodium sulfate (Na₂SO₄). The drying agent was removed by filtration and the DCM solvent evaporated at 50 °C on a rotary evaporator under vacuum and dried from any residual water using absolute EtOH to yield the product free base as a dark thick oil in low yield. GC-MS analysis revealed the presence of the desired product as well as a number of unidentified contaminants.

13.10 Synthesis of 2,5-dimethoxyphenethylamine-N-trifluoroacetamide (Protection):

A solution of trifluoroacetic anhydride (TFA, 4.2 ml, 6.3 g, 30 mmol) in DCM (100 ml) was added over a period of 5-10 minutes to a solution of 2,5-dimethoxyphenethylamine HCl (2.17 g, 10 mmol) and triethylamine (1.01 g, 10 mmol) in DCM (40 ml) at room temperature. After the addition was complete the reaction mixture was stirred at room temperature for 30 minutes, then at reflux for an additional 30 minutes. The reaction mixture was then cooled in an ice bath, transferred to a separatory funnel and washed successively with water (1 X 50 ml), saturated sodium bicarbonate (1 X 50 ml) and 1N HCl (1 X 50 ml). The DCM solvent was then removed by evaporation at 50 °C on a rotary evaporator under vacuum and dried azeotropically twice with EtOH (2 X 5 ml) to yield the product as a dark red oil. The product crystallized upon standing at room temperature. The structure of the product was confirmed by standard spectroscopic methods.

13.11 Synthesis of 4-iodo-2,5-dimethoxyphenethylaminetrifluoroacetamide:

A solution of iodine monochloride (ICl, 0.6 ml, 12 mmol) in glacial acetic acid (20 ml) was added over a period of 5-10 minutes to a solution of 2,5-dimethoxyphenethylamine trifluoroacetamide (2.77 g, 10 mmol) in acetic acid (20 ml) at room temperature with stirring. After the addition was complete the reaction mixture was stirred for 45 minutes at room temperature, then an additional 45 minutes with heating. The reaction mixture was cooled to room temperature and quenched by the addition of water (200 ml). The aqueous solution was extracted with DCM (2 X 100 ml) and the combined DCM extracts washed carefully with saturated sodium bicarbonate solution to neutralize the residual acetic acid in the DCM extracts. The DCM solution was then washed with water (2 X 100 ml) and evaporated at 50 °C on a rotary evaporator under vacuum, and dried azeotropically using absolute EtOH to give the product as a dark golden solid. This solid was recrystallized from a minimal volume of hot ethyl acetate and then ether and isolated by gravity filtration. The structure of the product was confirmed by standard spectroscopic methods.

13.12 Synthesis of 4-iodo-2,5-dimethoxyphenethylamine (Deprotection):

A solution of 2N potassium hydroxide (7.5 ml) was added over a period of 2-3 minutes to a solution of 4-iodo-2,5-dimethoxyphenethylamine trifluoroacetamide (1.44 g, 3.57 mmoles) in 2-propanol (50 ml) stirring at room temperature. The reaction mixture was warmed until all reactants dissolved, then stirred at room temperature overnight. The reaction mixture was then evaporated at 65 °C on a rotary evaporator under vacuum and the resulting product oil suspended in water (50 ml) and made alkaline (pH 12) by addition of NaOH pellets. The aqueous base suspension was extracted with DCM (2 X 50 ml) and the combined DCM extracts washed with water (50 ml) and evaporated to dryness at 50 °C on a rotary evaporator under vacuum, and dried azeotropically with using absolute EtOH to yield the product as a dark oil. The oil was dissolved in anhydrous ether and HCl gas bubbled into the ether solution to yield the product amine HCl salt as an off-white solid. The structure of the product was confirmed by NMR and GC-MS.

13.13 Synthesis of N-(2'-methoxy)benzyl-4-iodo-2,5-dimethoxyphenethylamine (4I25DMPEA2MB):

A solution of 4-iodo-2,5-dimethoxyphenethylamine HCl (343 mg, 1.0 mmole), triethylamine (101 mg, 1 mmole) and 2-methoxybenzaldehyde (136 mg, 1 mmole) in absolute ethanol (10 ml) was heated at reflux for 2 hours. The reaction mixture was cooled to room temperature and NaBH₄ (200 mg, 5.3 mmoles) added and the reaction mixture stirred at room temperature overnight. The reaction mixture was then evaporated to dryness at 50 °C on rotary evaporator under vacuum to yield a yellow solid which was suspended in water (20 ml) and neutralized (pH 7) by addition of a few drops of conc. HCl. This solution was extracted with DCM (2 X 20 ml) and the combined DCM extracts evaporated and dried under reduced pressure to yield the product as a free base. To ensure complete drying of the product, 5 ml of absolute EtOH was added to the product and then evaporated in preheated, 65 °C rotary evaporator under vacuum twice. All of the three of the monomethoxy- (2'-, 3'- and 4'-methoxy), six dimethoxy- (2',3'-, 2',4'-, 2',6'-, 3',4'- and 3',5'-) and both methylenedioxy- (2',3'- and 3',4'-) products were prepared by this method using the molar quantities listed above. The products in free base form were crystallized using the solvents listed in Table 68 below and isolated by simple filtration. The structures of the products were confirmed by GC-MS spectroscopy and comparison to analytical data obtained for these

compounds as prepared previously in our laboratories. Samples of all eleven compounds in this series were also converted to HCl salts using ethereal HCl and these samples were purified for submission for receptor binding assays.

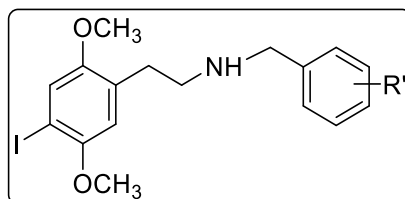


Table 68 Yields and Crystallization Solvents for the N-(Substituted)benzyl-4-iodo-2,5-dimethoxyphenethylamines.

Compound abbreviation	Benzyl ring substituent (R')	Total yield (mg)	Crystallization solvent free base	Recrystallization solvent HCl salt
4I25DMPEA2MB	2'-MeO	165.7	EtOAc/PE	Ether/EtOH
4I25DMPEA3MB	3'-MeO	58 (+ oil)	Ether	Ether/EtOH*
4I25DMPEA4MB	4'-MeO	261.5	Ether	Ether/EtOH
4I25DMPEA23DMB	2',3'-DiMeO	87 (+ oil)	Ether/PE	Ether/EtOAc
4I25DMPEA24DMB	2',4'-DiMeO	265	Ether	Ether
4I25DMPEA25DMB	2',5'-DiMeO	329	Ether	Ether
4I25DMPEA26DMB	2',6'-DiMeO	175	Ether	Ether/acetone
4I25DMPEA34DMB	3',4'-DiMeO	298	EtOAc/PE	Ether/acetone
4I25DMPEA35DMB	3',5'-DiMeO	136 (+ oil)	Ether	Ether/acetone*
4I25DMPEA23MDB	2',3'-MD	Oil	Ether	Ether*
4I25DMPEA23MDB	3',4'-MD	Oil	Ether	Ether*

13.14 Synthesis of 2,5-dimethoxyphenpropylamine (25DMPPA):

Lithium aluminum hydride (LAH, 1.5 g, 40 mmole) was placed in a 500 ml dry round bottom flask and dry tetrahydrofuran (THF, 20-30 ml) added over a period of 5-10 minutes at room temperature. A solution of 2,5-dimethoxynitropropene (3.0 g, 14.5 mmole) in dry THF (20-30 ml) was then added to the THF-LAH suspension at room temperature over a period of 5-10 minutes using addition funnel. The reaction mixture was then stirred at reflux for 2-3 hours, then at room temperature overnight. The next day, the reaction mixture was cooled in an ice bath for 30 minutes and the LAH neutralized by successive dropwise addition of THF in water (1.5 ml THF in 7.5 ml water), 10% sodium hydroxide (3 ml) and finally water (4.5 ml). Methanol (10 ml) was then added to the quenched reaction mixture and stirred for 10 minutes. The quenched reaction mixture was then filtered through a scintered glass funnel of medium porosity and washed with additional methanol. The filtrate and washings were then evaporated under reduced pressure using a rotary evaporator with heating to 50 °C. The remaining crude product oil was dissolved in 2N HCl (120 ml) and washed with diethyl ether (2X120 ml) to remove any unreacted starting material. The aqueous acid extract was cooled in an ice bath and made alkaline (pH 12) by addition of sodium hydroxide pellets. This aqueous basic suspension was then extracted with dichloromethane (DCM, 2X100 ml). The combined DCM extracts were evaporated under reduced pressure using a rotary evaporator at 50 °C, and the remaining product oil dried azeotropically with absolute ethanol. The dried product oil was dissolved in anhydrous ether (50 ml) and HCl gas added to form the hydrochloride salt as a gummy solid. Simple scratching of the inside wall of the round bottom flask with a spatula followed by stirring overnight yielded the product as a yellow solid. The product was isolated by gravity filtration and air dried. The 2,6-dimethoxyphenpropylamine and 3,4-methylenedioxyphenpropylamine intermediates using this same procedure and molar quantities. The structures of the products were confirmed by GC-MS spectroscopy and comparison to analytical data obtained for these compounds as prepared previously in our laboratories.

13.15 Synthesis of the N-(2'-methoxy)benzyl-2,5-dimethoxyphenpropylamine (25DMPPA2MB):

A solution of 2,5-dimethoxyphenpropylamine HCl (231 mg (1 mmole), triethylamine (101 mg, 1 mmole) and 2-methoxybenzaldehyde (136 mg, 1 mmole) in absolute ethanol (10 ml) was heated at reflux for 2 hours. The reaction mixture was cooled to room temperature and NaBH₄ (200 mg, 5.3 mmoles) added and the reaction mixture stirred at room temperature overnight. The reaction mixture was then evaporated to dryness at 50 °C on rotary evaporator under vacuum to yield a yellow solid which was suspended in water (20 ml) and neutralized (pH 7) by addition of a few drops of conc. HCl. This solution was extracted with DCM (2 X 20 ml) and the combined DCM extracts evaporated and dried under reduced pressure to yield the product as a free base. To ensure complete drying of the product, 5 ml of absolute EtOH was added to the product and then evaporated in preheated, 65 °C rotary evaporator under vacuum twice. All of the N-benzyl monomethoxy- (2'-, 3'- and 4'-methoxy), dimethoxy- (2',3'-, 2',4'-, 2',6'-, 3',4'-) and 3',5'-) and methylenedioxy- (2',3'- and 3',4'-)- 2,5-dimethoxy-phenpropylamine products were prepared by this method using the molar quantities listed above, as well as the three N-(methoxy)benzyl-substituted-2,6-dimethoxy-phenpropylamine and N-(methoxy)benzyl-substituted-3,4-methylenedioxyphenpropylamine isomers. The products in free base form were crystallized using the solvents listed in Table 69 below and isolated by simple filtration. The structures of the products were confirmed by GC-MS spectroscopy and comparison to analytical data obtained for these compounds as prepared previously in our laboratories. Samples of all eleven of the N-(substituted)benzyl-2,5-dimethoxyphenpropylamine compounds in this series were also converted to HCl salts using ethereal HCl and these samples were purified for submission for receptor binding assays.

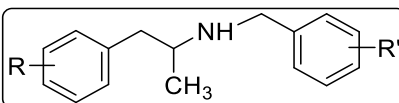


Table 69 Yields for the N-(Substituted)benzyl-substituted-phenpropylamines.

Compound abbreviation	Phenethyl ring substituent (R)	Benzyl ring substituent (R')	Total yield (mg)	Crystallization solvent free base
25DMPPA2MB	2,5-DiMeO	2'-MeO	169 mg	Ether
25DMPPA3MB	2,5-DiMeO	3'-MeO	173 mg	Ether
25DMPPA4MB	2,5-DiMeO	4'-MeO	119 mg	Ether/EtOAc/Pet Ether
25DMPPA23DMB	2,5-DiMeO	2',3'-DiMeO	128 mg	Ether/iPrOH
25DMPPA24DMB	2,5-DiMeO	2',4'-DiMeO	167 mg	Ether/EtOH
25DMPPA25DMB	2,5-DiMeO	2',5'-DiMeO	157 mg	Ether/EtOAc
25DMPPA26DMB	2,5-DiMeO	2',6'-DiMeO	159 mg	Ether
25DMPPA34DMB	2,5-DiMeO	3',4'-DiMeO	154 mg	Ether/EtOAc
25DMPPA35DMB	2,5-DiMeO	3',5'-DiMeO	50 mg	Ether/EtOAc/Pet Ether
25DMPPA23MDB	2,5-DiMeO	2',3'-MD	50 mg	Ether/EtOAc/Pet Ether
25DMPPA34MDB	2,5-DiMeO	3',4'-MD	126 mg	Ether
23DMPPA2MB	2,3-DiMeO	2'-MeO	146 mg	Ether/EtOAc
23DMPPA3MB	2,3-DiMeO	3'-MeO	109 mg	Ether/EtOAc
23DMPPA4MB	2,3-DiMeO	4'-MeO	160 mg	Ether/EtOAc
26DMPPA2MB	2,6-DiMeO	2'-MeO	15 mg	Ether/EtOAc
26DMPPA3MB	2,6-DiMeO	3'-MeO	95 mg	Ether/EtOH/EtOAc
26DMPPA4MB	2,6-DiMeO	4'-MeO	163 mg	Ether
34MDMPPA2MB	3,4-MD	2'-MeO	209 mg	Ether
34MDMPPA3MB	3,4-MD	3'-MeO	120 mg	Ether/Pet.Ether/EtOAc
34MDMPPA4MB	3,4-MD	4'-MeO	206 mg	Ether

13.16 Synthesis of 4-bromo-2,5-dimethoxyphenpropylamine Method A (4Br25DMPPA):

A solution of bromine (0.66 g, 4.1 mmol) in glacial acetic acid (2 ml) was added over a period of minute to a solution of 2,5-dimethoxyphenethylamine HCl (0.89 g, 4.1 mmol) in glacial acetic acid (2 ml) at room temperature. After the addition was complete the reaction mixture was stirred at room temperature an additional hour, resulting in the formation of a yellow precipitate. The yellow precipitate was isolated by filtration and washed with anhydrous ether. The solid product was then dissolved in water (15 ml) and made alkaline (pH 12) by addition of NaOH pellets to

yield a suspension. The aqueous base suspension was extracted with DCM (2 X 15 ml) and the combined DCM extracts evaporated at 50 °C on a rotary evaporator under vacuum to yield the product in free base form. The product base was dried azeotropically with ethanol (5 X 10 ml). Analysis of the product by GC-MS revealed that it consisted of a mixture of the desired product and several contaminants indicative of oxidative side reactions and methyl ether cleavage. This product was not purified further.

13.17 Synthesis of 2,5-dimethoxyphenpropylamine-trifluoroacetamide (Protection): Method B:

A solution of trifluoroacetic anhydride (TFA, 4.2 ml, 6.3 g, 30 mmol) in DCM (10 ml) was added over a period of 5-10 minutes to a solution of 2,5-dimethoxyphenethylamine HCl (2.32 g, 10 mmol) and triethylamine (1.01 g, 10 mmol) in DCM (40 ml) at room temperature. After the addition was complete the reaction mixture was stirred at room temperature for 30 minutes, then at reflux for an additional 30 minutes. The reaction mixture was then cooled in an ice bath, transferred to a separatory funnel and washed successively with water (1 X 50 ml), saturated sodium bicarbonate (1 X 50 ml) and 1N HCl (1 X 50 ml). The DCM solvent was then removed by evaporation at 50 °C on a rotary evaporator under vacuum and dried azeotropically twice with EtOH (2 X 5 ml) to yield the product as a dark red oil. The product crystallized upon standing at room temperature. The structure of the product was confirmed by standard spectroscopic methods.

13.18 Synthesis of 4-bromo-2,5-dimethoxyphenpropylamine-trifluoroacetamide:

A solution of bromine (1.92 g, 12.0 mmol) in glacial acetic acid (20 ml) was added over a period of 1-10 minutes to a solution of 2,5-dimethoxyphenpropylamine trifluoroacetamide (2.91 g, 10.0 mmol) in glacial acetic acid (20 ml). After the addition was complete the reaction mixture was stirred at room temperature for 45 minutes and then with warming for an additional 45 minutes. The reaction mixture was cooled to room temperature and quenched with water (200 ml) and extracted with DCM (2 X 100 ml). The combined DCM extracts were washed carefully with saturated sodium bicarbonate (2 X 100 ml) and then water (2 X 100 ml). The combined DCM extracts evaporated at 50 °C on a rotary evaporator under vacuum to yield the product as a dark

golden solid which was crystallized from ethyl acetate and washed with ether. The structure of the product was confirmed by GC-MS and NMR spectroscopy and comparison to analytical data obtained for these compounds as prepared previously in our laboratories.

13.19 Synthesis of 4-bromo-2,5-dimethoxyphenpropylamine (Deprotection):

A solution of 2N potassium hydroxide (7.5 ml) was added over a period of 2-3 minutes to a solution of 4-iodo-2,5-dimethoxyphenpropylamine trifluoroacetamide (1.32 g, 3.57 mmoles) in 2-propanol (50 ml) stirring at room temperature. The reaction mixture was warmed until all reactants dissolved, then stirred at room temperature overnight. The reaction mixture was then evaporated at 65 °C on a rotary evaporator under vacuum and the resulting product oil suspended in water (50 ml) and made alkaline (pH 12) by addition of NaOH pellets. The aqueous base suspension was extracted with DCM (2 X 50 ml) and the combined DCM extracts washed with water (50 ml) and evaporated to dryness at 50 °C on a rotary evaporator under vacuum, and dried azeotropically with using absolute EtOH to yield the product as a dark oil. The oil was dissolved in anhydrous ether and HCl gas bubbled into the ether solution to yield the product amine HCl salt as an off-white solid. The structure of the product was confirmed by NMR and GC-MS.

13.20 Synthesis of N-(2'-methoxy)benzyl-4-bromo-2,5-dimethoxyphenpropylamine:

A solution of 4-bromo-2,5-dimethoxyphenpropylamine HCl (311 mg, 1.0 mmole), triethylamine (101 mg, 1.0 mmole) and 2-methoxybenzaldehyde (136 mg, 1 mmole) in absolute ethanol (10 ml) was heated at reflux for 2 hours. The reaction mixture was cooled to room temperature and NaBH₄ (200 mg, 5.3 mmoles) added and the reaction mixture stirred at room temperature overnight. The reaction mixture was then evaporated to dryness at 50 °C on rotary evaporator under vacuum to yield a yellow solid which was suspended in water (20 ml) and neutralized (pH 7) by addition of a few drops of conc. HCl. This solution was extracted with DCM (2 X 20 ml) and the combined DCM extracts evaporated and dried under reduced pressure to yield the product as a free base. To ensure complete drying of the product, 5 ml of absolute EtOH was added to the product and then evaporated in preheated, 65 °C rotary evaporator under vacuum twice. All of the N-benzyl monomethoxy- (2'-, 3'- and 4'-methoxy), dimethoxy- (2',3'-, 2',4'-, 2',6'-, 3',4'-) and 3',5'-) and

methylenedioxy- (2',3'- and 3',4'-)-4-bromo-2,5-dimethoxy-phenpropylamine products were prepared by this method using the molar quantities listed above. The products in free base form were crystallized using the solvents listed in Table 70 below and isolated by simple filtration. The structures of the products were confirmed by GC-MS spectroscopy and comparison to analytical data obtained for these compounds as prepared previously in our laboratories. Samples of all eleven of the N-(substituted)benzyl-substituted-4-bromo-2,5-dimethoxyphenpropylamine compounds in this series were also converted to HCl salts using ethereal HCl and these samples were purified for submission for receptor binding assays.

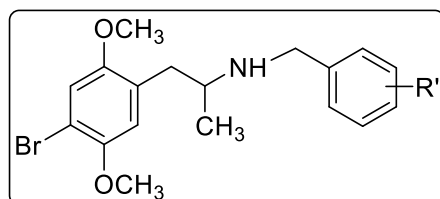


Table 70 Yields and Crystallization Solvents for the N-(Substituted)benzyl-4-bromo-2,5-dimethoxyphenpropylamines.

Compound abbreviation	Benzyl ring substituent (R')	Total yield, mg (1 st & 2 nd crop)	Crystallization solvent free base
4Br25DMPPA2MB	2'-MeO	174 mg	Ether/EtOAc/Pet.Ether
4Br25DMPPA3MB	3'-MeO	199 mg	Ether/EtOH
4Br25DMPPA4MB	4'-MeO	214 mg	Ether
4Br25DMPPA23DMB	2',3'-DiMeO	347 mg	EtOH/Ether
4Br25DMPPA24DMB	2',4'-DiMeO	230 mg	Ether/EtOH
4Br25DMPPA25DMB	2',5'-DiMeO	114 mg	Ether/Pet.Ether
4Br25DMPPA26DMB	2',6'-DiMeO	275 mg	Ether
4Br25DMPPA34DMB	3',4'-DiMeO	189 mg	Ether
4Br25DMPPA35DMB	3',5'-DiMeO	89 mg	Ether/EtOH/Pet.Ether
4Br25DMPPA23MDB	2',3'-MD	112 mg	Ether/EtOAc/EtOH
4Br25DMPPA34MDB	3',4'-MD	194 mg	Ether/EtOAc/EtOH

*From 1 mmole amine HCl, + 1 mmole aldehyde and 1 mmole TEA and 200 mg NaBH₄.

13.21 Synthesis of N-Methyl-2,5-dimethoxyphenethylamine:

A mixture of acetic anhydride (5 ml) and formic acid (5 ml) was stirred at room temperature for 30 minutes and then added over a period of 10 minutes to 2,5-dimethoxyphenethylamine (1.0 g, 5.5 mmoles). The reaction mixture was stirred at room temperature for 1-2 hours and then quenched by addition of crushed ice (20 ml). After the ice melted the reaction mixture was extracted with DCM (2 X 50 ml) and the combined DCM extracts washed successively with water (50 ml) and 2 N HCl (2 X 50 ml). Evaporation of the DCM solvent at 50 °C on a rotary evaporator under vacuum and drying azeotropically with ethanol (2 X 5ml) yielded the intermediate N-formamide-2,5-dimethoxyphenethylamine. The structure of the product was confirmed by GC-MS.

A solution of N-formamide-2,5-dimethoxyphenethylamine (209 mg, 1.0 mmoles) in dry THF (10 ml) was added over a period of 5-10 minutes to a stirred suspension of LAH (0.5 g, 13.2 mmoles) in dry THF (15 ml) at room temperature. After the addition was complete the reaction mixture was stirred at reflux for 2-3 hours and then at room temperature overnight. The reaction mixture was then cooled in an ice bath and quenched by successive addition of water (0.5 ml) in THF (2.5 ml), 10% NaOH (1.0 ml) and water (1.5 ml). Methanol (10 ml) was added to the quenched reaction mixture and the resulting suspension stirred at room temperature before filtering through a scintered glass funnel (medium porosity) under reduced pressure. The filtrate was evaporated at 50 °C on a rotary evaporator under reduced pressure to yield the crude product as an oil. The product oil was dissolved in 2 N HCl (20 ml) and washed with diethyl ether (2 X 20 ml) to eliminate any unreduced amide. The aqueous acid solution was made alkaline (pH 12) by addition of NaOH pellets with cooling, and the resulting suspension extracted with DCM (2X 20 ml). The combined DCM extracts were evaporated at 50 °C on a rotary evaporator under reduced pressure to yield the product free base as an oil which was dried azeotropically with ethanol (2 X 5 ml). The free base was dissolved in anhydrous ether (50 ml) and HCl gas bubbled into the ether solution for 30 seconds to form the HCl salt of the product as a dark, gummy oil. The oil was converted to a solid by cooling the ether-HCl salt mixture in an ice bath and scratching of the flask with a spatula and stirring. The solid product was isolated by gravity filtration and dried. The structure of the product was confirmed by GC-MS.

13.22 Synthesis of (2'-methoxy)benzyl-N-methyl-2,5-dimethoxyphenethylamine: Method A (Reductive Amination):

A solution of N-methyl-2,5-dimethoxyphenethylamine HCl (232 mg, 1.0 mmole), 2-methoxybenzaldehyde (136 mg, 1.0 mmoles) and triethylamine (101 mg, 1.0 mmoles) in absolute ethanol (10 ml) was heated at 70 °C for two hours. The reaction mixture was cooled to room temperature and sodium borohydride (200 mg, 5.3 mmoles) added and then stirred overnight at room temperature. The reaction mixture was evaporated at 50 °C on a rotary evaporator under vacuum to yield the crude product as a yellowish solid. This solid was suspended in water (20 ml) and neutralized by addition of a few drops of concentrated HCl. The resulting suspension was extracted with DCM (2 X 40 ml) and the combined DCM extracts evaporated under reduced pressure and dried azeotropically with absolute ethanol (2 X 5 ml) at 65 °C. GC.MS analysis of the product revealed the presence of unreacted starting amine and a very small amount of the desired product. Repeating the reaction with longer reaction times or under dehydrating conditions (Dean-Stark) with acid catalysis, para toluene sulfonic acid (*p*-TsOH), did not improve yields. Thus, this method was abandoned as a synthetic approach.

13.23 Synthesis of (2'-Methoxy)benzyl-N-methyl-2,5-dimethoxyphenethylamine: Method B (via intermediate benzoyl amides):

A solution of 2-methoxybenzoyl chloride (340 mg, 2.0 mmoles) in dry DCM (20 ml) was added to a solution of N-methyl-2,5-dimethoxyphenethylamine (270 mg, 2.0 mmoles) and triethylamine (202 mg, 2.0 mmoles) in dry DCM (20 ml) over a period of 15 minutes at room temperature. After the addition was complete the reaction mixture was heated for 2-3 hours, then stirred at room temperature overnight. The DCM reaction solution was then washed successively with 2N HCl (40 ml), water (40 ml) and saturated sodium bicarbonate (40ml). The DCM was then evaporated at 50 °C on a rotary evaporator under vacuum and dried using an absolute EtOH azeotrope.

A solution of N-benzoyl-2,5-dimethoxyphenethylamine (299 mg, 1.0 mmoles) in dry THF (10 ml) was added over a period of 5-10 minutes to a stirred suspension of LAH (0.5 g, 13.2 mmoles) in dry THF (15 ml) at room temperature. After the addition was complete the reaction mixture was stirred at reflux for 2-3 hours and then at room temperature overnight. The reaction mixture was then cooled in an ice bath and quenched by successive addition of water (0.5 ml) in THF (2.5 ml), 10% NaOH (1.0 ml) and water (1.5 ml). Methanol (10 ml) was added to the quenched reaction mixture and the resulting suspension stirred at room temperature before filtering through a sintered glass funnel (medium porosity) under reduced pressure. The filtrate was evaporated at 50 °C on a rotary evaporator under reduced pressure to yield the crude product as an oil. The product oil was dissolved in 2 N HCl (20 ml) and washed with diethyl ether (2 X 20 ml) to eliminate any unreduced amide. The aqueous acid solution was made alkaline (pH 12) by addition of NaOH pellets with cooling, and the resulting suspension extracted with DCM (2X 20 ml). The combined DCM extracts were evaporated at 50 °C on a rotary evaporator under reduced pressure to yield the product free base as an oil which was dried azeotropically with ethanol (2 X 5 ml). The structure of the product was confirmed by GC-MS.

13.24 Synthesis of N-(2'-methoxy)benzyl-N-methyl-2,5-dimethoxyphenethylamine, Method C (Direct displacement):

The 2-methoxybenzyl bromide (201 mg, 1.0 mmoles) was added over a period of 5-10 minutes to a solution of N-methyl-2,5-dimethoxyphenethylamine (135 mg, 1.0 mmoles) and triethylamine (101 mg, 1.0 mmoles) in DCM (20 ml) at room temperature and the reaction mixture was stirred overnight. The reaction mixture was then evaporated at 50 °C on a rotary evaporator under vacuum and the resulting oil dissolved in 2 N HCl (20 ml). The aqueous acid solution was washed with ether (2 X 20 ml) and then made alkaline (pH 12) by addition of NaOH pellets with cooling. The resulting alkaline suspension was extracted with DCM (2 X 20 ml) and the combined DCM extracts evaporated at 50 °C on a rotary evaporator under vacuum and dried azeotropically with absolute ethanol (2 X 5 ml) to yield the product in free base form. The structure of the product was confirmed by NMR and GC-MS.

13.25 Derivatization of amines with (trifluoroacetic anhydride or pentafluoropropionic anhydride):

A large excess of the derivatizing reagent (TFAA, PFPA, 50-100 μ l) is added to small amount of the free base amine (approximately 0.1 mg) dissolved in HPLC grade acetonitrile (1 ml). The reaction mixture was heated at 170-210°C for 15-30 minutes to concentrate the total volume to 0.5 ml. The samples were then directly analyzed by GC-MS.

14 Experimental

14.1 Materials:

Most of the precursor (benzaldehydes/chemical reagents) but 2,3-methylenedioxybenzaldehyde were purchased from Aldrich chemical company (Milwaukee, WI) including: 2-methoxybenzaldehyde, 3-methoxybenzaldehyde, 4-methoxybenzaldehyde, 2,3-dimethoxybenzaldehyde, 2,4-dimethoxybenzaldehyde, 2,5-dimethoxybenzaldehyde, 2,6-dimethoxybenzaldehyde, 3,4-dimethoxybenzaldehyde, 3,5-dimethoxybenzaldehyde, 2,3-methylenedioxy benzaldehyde 3,4-methylenedioxy benzaldehyde, 5-bromo-2,3-dimethoxybenzaldehyde,, 5-bromo-2,4-dimethoxybenzaldehyde, 4-bromo-2,5-dimethoxybenzaldehyde, 3-bromo-4,5-dimethoxybenzaldehyde, 4-methoxy-3-methylbenzaldehyde, 2-Hydroxy-3-methoxybenzaldehyde (*o*-vanilline), benzaldehyde, 2-hydroxybenzaldehyde (salicylaldehyde), 2'-methoxyacetophenone, nitromethane, nitroethane, ammonium acetate, 2-phenylethylamine, N-methyl phenethylamine, 2-(2-methoxyphenyl)ethylamine, 2-(3-methoxyphenyl)ethylamine, 2-(4-methoxyphenyl)ethylamine, benzylamine , 2-methoxy benzylamine 3-methoxy benzylamine , 4-methoxy benzylamine, triethylamine, 2-methoxybenzoyl chloride (*o*-Anisoyl chloride), 3-methoxybenzoyl chloride (*m*-Anisoyl chloride), 4-methoxybenzoyl chloride (*p*-Anisoyl chloride), iodine monochloride, ¹³C Iodomethane, Iodomethane d3, trifluoroacetic anhydride, pentafluoroacetic anhydride, reducing agents such as: sodium borohydride, sodium triacetoxyborohydride, lithium aluminum hydride.

The rest of the chemicals were bought from other vendors including bromine, benzyl amine, 2-bromo-4,5-dimethoxybenzaldehyde (6-Bromoveratraldehyde), acetic anhydride, silver sulfate, and silver trifluoroacetate from Alfa Aesar (MA), potassium hydroxide and glacial acetic acid from Fisher Scientific (Fair Lawn, NJ), sodium sulfate and sodium hydroxide from EMD Millipore (NJ), formic acid from VWR (PA), hydrochloric acid from Avantor (USA), 2-Hydroxy-3-methoxybenzaldehyde from Combi block (CA), 3-methoxy-4-methylbenzaldehyde from AOBchem(China), sodium bicarbonate from Ward's science (NY), hydrogen chloride gas from Praxair(CT).

In addition to the chemical reagents listed above, organic solvents such as methanol (ACS grade), isopropanol (ACS grade), tetrahydrofuran (ACS grade), acetone (ACS grade), ethyl acetate (ACS grade), dichloromethane (ACS grade), petroleum ether (ACS grade) were purchased from VWR (PA), tetrahydrofuran (anhydrous stabilized), benzene (ACS grade) from EMD Millipore (NJ), HPLC grade acetonitrile from Fisher Scientific, (Atlanta, GA), ethanol (ACS grade) from Mallinckrodt chemical (NJ), diethyl ether from (ACS grade) Avantor (USA). (For the/the) 2,3-methylenedioxybenzaldehyde, 4-methoxybenzoyl chloride, were bought from Tokyo Chemical Industry (TCI). Finally, (For /regarding) deuterated /chemical such as both chloroform-D, dimethyl sulfoxide-D6 are from Cambridge isotope laboratories, Inc. (MA)

14.2 Instruments:

Three different instruments were used in this study, the first instrument consisted of GC-MS system from Agilent Technologies (Santa Clara, CA) 7890A gas chromatograph and an Agilent 7683B auto injector coupled with a 5975C VL Agilent mass selective detector.

GC-MS System 1 consisted of an Agilent Technologies (Santa Clara, CA) 7890A gas chromatograph and an Agilent 7683B auto injector coupled with a 5975C VL Agilent mass selective detector. Sample injection volume was 1 μ l which was dissolved in high-performance liquid chromatography grade acetonitrile. Each sample was introduced to the system by auto injector with splitless option for the injection mode through helium (ultra-high purity, grade 5, 99.999%) as carrier gas with flow rate of 0.48 ml/minute and both front inlet, GC injector port, temperature and transfer line temperature of 230°C. Column head pressure was maintained at 10 psi. For the MS portion of the instrument, electron ionization (EI) mode was selected as ionization mode for the compounds with scan rate of 2.86 scans/s and ionization voltage of 70 eV. The MS source and quad temperature was 230°C and 150°C respectively. Due to the ionization of solvent, solvent peak effect, the mass spectrum filament was turned off during the first three minutes of each run

For the GC-MS system 2, it was operated under two different ionization modes, EI and CI. GC-MS System 2 consisted of an Agilent Technologies (Santa Clara, CA) 7890A gas chromatograph and an Agilent 7683B auto injector coupled with a 240 Agilent Ion Trap mass spectrometer (MS/MS). Sample injection volume was 1 μ l which was dissolved in high-performance liquid chromatography grade acetonitrile. Each sample was introduced to the system by auto injector with splitless option for the injection mode for the EI mode and split option mode with split ratio of 20:1 for the CI mode through ultra-high purity helium gas (grade 5, 99.999%) as carrier gas. The carrier gas flow rate was 1 ml/minute with injection port temperature of 230°C and transfer line temperature of 280°C. Column head pressure was maintained at 8.8085 psi. For the MS portion of the instrument, when electron ionization (EI) mode was selected as ionization mode in EI-MS studies, the number of scans was 2 μ scans with target TIC count of 20000 and maximum

ionization time of 25000 μsec . Ion trap temperature was 150°C. When the instrument performed MS/MS experiments in the EI mode, the type of scan selected was Automated Method Development function (AMD) with isolation window of 3 m/z , ionization storage level of 35 m/z , and finally the MS/MS excitation amplitude was ranged from 0 to 1.80 volts.

In the case of CI mode was operated in CI-MS studies, the number of scans was 3 μ scans with target TIC count of 5000 and maximum ionization time of 2500 μsec . The reagent gas used in CI-MS studies was 99.9% methanol. Due to the ionization of solvent, the mass spectrum filament was turned off during the first three minutes of each run

The third type of instruments is the GC-IR system from Hewlett-Packard 6890 Series gas chromatograph and a Hewlett-Packard 7683 series auto-injector for the GC and IRD-3 detector obtained from Analytical Solutions and Providers (ASAP), Covington, Kentucky for the detector. The GC-IR system was operated under the following condition: sample injection volume was 1 μl which was dissolved in high-performance liquid chromatography grade acetonitrile. Each sample was introduced to the system by auto injector with either split mode with split ratio of 10:1 or splitless modes through ultra-high purity helium gas (grade 5, 99.999%) as carrier gas. The carrier gas flow rate was 2 ml/minute with GC injector port temperature of 250°C and transfer line (A & B) and pipe line temperature of 250°C. Column head pressure was maintained at 2.62 psi in split mode or 5.83 psi in splitless mode. For the vapor phase infrared detector (IRD) detector portion of the instrument, the spectra scan ranged from 550 to 4000 cm^{-1} with selected resolution of 16 cm^{-1} and scan rate of. The temperature of the IRD flow cell temperatures was set at 250°C.

14.3 GC-Columns:

A number of GC capillary columns were used during the period of this study which are listed in table 71, these capillary columns were mainly purchased from Restek Corporation (Bellefonte, PA) with only one column from SGE analytical science (Victoria, Australia).

Table 71 List of columns used and their composition.

Column name	Composition	Length (m)	ID (mm)	Film thickness (μm)	Temperature ($^{\circ}\text{C}$)
Rxi®-35Sil MS	Midpolarity phase; similar to 35% phenyl, 65% dimethyl polysiloxane	30	0.25	0.50	360
Rxi®-17Sil MS	Midpolarity Crossbond® silarylene phase; similar to 50% phenyl, 50% dimethyl polysiloxane	30	0.25	0.25	360
Rtx®-5 MS	Crossbond® 5% diphenyl, 95% dimethyl polysiloxane	15	0.32	0.25	350
BPX5	5% Phenyl Polysilphenylene-siloxane	6	0.32	1	370

14.4 Temperature Programs:

Table 72-74 listed the best temperature program that achieved the best separation results , resolution and analysis time, throughout the period of this study.

Table 72 List of temperature programs used for system 1.

System	Program setup	#
(mass selective detector) Ionization mode: EI Injection type: Splitless Injector temperature: 230°C Transfer line temperature: 230°C	Initial temperature at 70°C held for 1 min, then temperature increased at rate of 30°C /min to reach 250°C followed by holding the temperature for 15 min	1
	Initial temperature at 70°C held for 1 min, then the temperature increased at rate of 70°C /min to reach 245°C which held for 5.5 min then followed by ramping the temperate at rate of 5°C /min to reach 300°C which held for 10 min.	2
	Initial temperature at 70°C held for 1 min, then the temperature increased at rate of 30°C /min to reach 250°C which held for 15 min then followed by ramping the temperate at rate of 10°C /min to reach 340°C which held for 2 min.	3
	Initial temperature at 70°C held for 1 min, then the temperature increased at rate of 30°C /min to reach 250°C which held for 25 min then followed by ramping the temperate at rate of 15°C /min to reach 340°C which held for 10 min.	4
	Initial temperature at 70°C held for 1 min, then temperature increased at rate of 30°C /min to reach 290°C followed by holding the temperature for 30 min	5
	Initial temperature at 70°C held for 1 min, then temperature increased at rate of 20°C /min to reach 250°C followed by holding the temperature for 40 min	6
	Initial temperature at 70°C held for 1 min, then temperature increased at rate of 30°C /min to reach 270°C followed by holding the temperature for 40 min	7
	Initial temperature at 70°C held for 1 min, then temperature increased at rate of 10°C /min to reach 260°C followed by holding the temperature for 40 min	8
	Initial temperature at 70°C held for 1 min, then the temperature increased at rate of 30°C /min to reach 250°C which held for 15 min then followed by ramping the temperate at rate of 20°C /min to reach 340°C which held for 2 min.	9
	Initial temperature at 80°C held for 1 min, then the temperature increased at rate of 30°C /min to reach 300°C which held for 0.5 min then followed by ramping the temperate at rate of 5°C /min to reach 340°C which held for 5 min.	10
	Initial temperature at 70°C held for 1 min, then temperature increased at rate of 30°C /min to reach 260°C followed by holding the temperature for 40 min	11

Table 73 List of temperature programs used for system 2.

System	Program setup
(Ion trap)	Initial temperature at 70°C held for 1 min, then temperature increased at rate of 30°C /min to reach 250°C followed by holding the temperature for 15 min
Ionization modes: EI & CI	Initial temperature at 80°C held for 1 min, then the temperature increased at rate of 30°C /min to reach 300°C which held for 0.5 min then followed by ramping the temperature at rate of 5°C /min to reach 330°C which held for 5 min.
Injections types: Splitless for EI & Split for CI	Initial temperature at 70°C held for 1 min, then temperature increased at rate of 30°C /min to reach 250°C followed by holding the temperature for 15 min
Injector temperature: 230°C	Initial temperature at 80°C held for 1 min, then the temperature increased at rate of 30°C /min to reach 300°C which held for 0.5 min then followed by ramping the temperature at rate of 5°C /min to reach 330°C which held for 5 min.
Transfer line temperature: 280°C	

Table 74 List of temperature programs used for system 3.

System	Type	Program setup
(IR)	Split	Initial temperature at 70°C held for 1 min, then temperature increased at rate of 25°C /min to reach 250°C followed by holding the temperature for 6.8 min
Spectroscopic mode: IR	Split	Initial temperature at 70°C held for 1 min, then temperature increased at rate of 25°C /min to reach 340°C followed by holding the temperature for 1.8 or 3.8 min
Injector temperature: 250°C	Splitless	Initial temperature at 70°C held for 1 min, then temperature increased at rate of 25°C /min to reach 250°C followed by holding the temperature for 6.8 min
Transfer line temperature: 250°C		

Group	Sample name	date	Expected column	#
Mono-mono	2-mix Mono	160516-08	Rxi-17 Sil MS	1
Mono-mono	3-mix Mono	160614-0079	Rxi-17 Sil MS	1
Mono-mono	4-mix Mono	160516-41	Rxi-17 Sil MS	1
Mono-mono	Mix Mono-2	160919-0068	Rxi-17 Sil MS	1
Mono-mono	mix Mono-3	160919-0069	Rxi-17 Sil MS	1
Mono-mono	Mix Mono-4	160919-0070	Rxi-17 Sil MS	1
di-mono	2.3-mix Mono	160415-42	Rxi-17 Sil MS	1
di-mono	2.4-mix Mono	170111-67	Rxi-17 Sil MS	1
di-mono	2.5-mix Mono	160415-105	Rxi-17 Sil MS	1
di-mono	2.6-mix Mono	160415-28	Rxi-17 Sil MS	1
di-mono	3.4-mix Mono	160415-106	Rxi-17 Sil MS	1
di-mono	3.5-mix Mono	160516-14	Rxi-17 Sil MS	1
mdo-mono	2.3-mix Mono	160614-0080	Rxi-17 Sil MS	1
mdo-mono	3.4-mix Mono	160614-0093	Rxi-17 Sil MS	1
2,5-di-di (UN-DERIVATISED)	2.5-mix Di	161018-112	Rxi-17 Sil MS	2
2,5-di-di (DERIVATISED)	2.5-mix Di	161103-0092	Rxi-17 Sil MS	2
2,5-di-mdo	2.5-mix MDO	160614-102	Rxi-17 Sil MS	1a
Br	mix Mono	170206-0070	Rxi-17 Sil MS	3
Br	mix Di	170206-0111	Rxi-17 Sil MS	4
Br	mix MDO	170206-0054	Rxi-17 Sil MS	3
eMOBN	Mix-3-Br-5,6	170206-0083	Rxi-17 Sil MS	2
eMOBN	Mix-2-Br-4,5	170111-66	Rxi-17 Sil MS	2
eMOBN	Mix-3-Br-4,6	170206-0018	Rxi-17 Sil MS	2
eMOBN	Mix-4-Br-2,5	170206-0017	Rxi-17 Sil MS	2
eMOBN	Mix-3-Br-4,5	170111-74	Rxi-17 Sil MS	2
I	mix Mono	170206-0071	Rxi-17 Sil MS	3

I	mix Di	170414-0080	Rxi-17 Sil MS	5
I	mix MDO	170206-0047	Rxi-17 Sil MS	4
2.5-PPA	2.5Di-mix Mono	170414-0092	Rxi-17 Sil MS	6
2.5-PPA	2.3Di-mix Mono	181001-0075	Rxi-17 Sil MS	7
2.5-PPA	2.6Di-mix Mono	181001-0076	Rxi-17 Sil MS	7
2.5-PPA	3.4MDO-mix Mono	181001-0062	Rxi-17 Sil MS	7
2.5-PPA	mix Di	170414-0040	Rxi-17 Sil MS	8
2.5-PPA	mix MDO	170414-0123	Rxi-17 Sil MS	6
4-Br-2,5-PPA	mix Mono	170508-0049	Rxi-17 Sil MS	8
4-Br-2,5-PPA	mix Di	170525-0078	Rxi-17 Sil MS	9
4-Br-2,5-PPA	mix MDO	170607-0001	Rxi-17 Sil MS	10
PEA (Derivatised)	mix Di	190204-0049	Rxi-17 Sil MS	11

References:

1. *World Drug Report Press Release*. 2018; Available from: https://www.unodc.org/doc/wdr2018/WDR_2018_Press_ReleaseENG.PDF.
2. Hondebrink, L., A. Zwartsen, and R.H. Westerink, *Effect fingerprinting of new psychoactive substances (NPS): What can we learn from in vitro data?* *Pharmacology & therapeutics*, 2018. **182**: p. 193-224.
3. *World Drug Report*. 2018; Available from: https://www.unodc.org/wdr2018/prelaunch/WDR18_Booklet_1_EXSUM.pdf.
4. UNODC. *UNODC Early Warning Advisory on NPS*. 2019 03-05-2019]; Available from: <https://www.unodc.org/LSS/Page/NPS>.
5. Rychert, M. and C. Wilkins, *What products are considered psychoactive under New Zealand's legal market for new psychoactive substances (NPS, 'legal highs')? Implications for law enforcement and penalties*. *Drug testing and analysis*, 2016. **8**(8): p. 768-778.
6. *European Drug Report 2018: Trends and Developments*. 2018; Available from: http://www.emcdda.europa.eu/system/files/publications/8585/20181816_TDAT18001ENN_PDF.pdf.
7. UNODC. *UNODC-SMART: Almost 900 NPS reported to UNODC from 119 countries and territories*. 2018 03-05-2019]; Available from: <https://www.unodc.org/LSS/Announcement/Details/eff8dc38-7ab0-42b0-8cd9-753b89953fcc>.
8. UNODC. *UNODC-SMART: Most new psychoactive substances are stimulants and synthetic cannabinoid receptor agonists, however opioids are on the rise*. 2019 03-05-2019]; Available from: <https://www.unodc.org/LSS/Announcement/Details/cfbdf979-0547-40d5-a1d1-5e8e3a7ba91f>.
9. Nikolaou, P., et al., *2C-I-NBOMe, an "N-bomb" that kills with "Smiles". Toxicological and legislative aspects*. *Drug Chem Toxicol*, 2015. **38**(1): p. 113-9.
10. Zawilska, J.B. and D. Andrzejczak, *Next generation of novel psychoactive substances on the horizon—A complex problem to face*. *Drug and Alcohol Dependence*, 2015. **157**: p. 1-17.
11. Kyriakou, C., et al., *NBOMe: new potent hallucinogens--pharmacology, analytical methods, toxicities, fatalities: a review*. *Eur Rev Med Pharmacol Sci*, 2015. **19**(17): p. 3270-81.
12. Chung, H., J. Lee, and E. Kim, *Trends of novel psychoactive substances (NPSs) and their fatal cases*. *Forensic Toxicology*, 2016. **34**(1): p. 1-11.
13. *The Challenge of New Psychoactive Substances*. 2013; Available from: https://www.unodc.org/documents/scientific/NPS_Report.pdf.
14. Halberstadt, A.L., *Pharmacology and Toxicology of N-Benzylphenethylamine ("NBOMe") Hallucinogens*. *Curr Top Behav Neurosci*, 2017. **32**: p. 283-311.
15. Assi, S., et al., *Profile, effects, and toxicity of novel psychoactive substances: A systematic review of quantitative studies*. *Human Psychopharmacology: Clinical and Experimental*, 2017. **32**(3): p. e2607.
16. Fantegrossi, W.E., et al., *Hallucinogen-like effects of 2-([2-(4-cyano-2, 5-dimethoxyphenyl) ethylamino] methyl) phenol (25CN-NBOH), a novel N-benzylphenethylamine with 100-fold selectivity for 5-HT_{2A} receptors, in mice*. *Psychopharmacology*, 2015. **232**(6): p. 1039-1047.
17. Halberstadt, A.L. and M.A. Geyer, *Effects of the hallucinogen 2,5-dimethoxy-4-iodophenethylamine (2C-I) and superpotent N-benzyl derivatives on the head twitch response*. *Neuropharmacology*, 2014. **77**: p. 200-7.
18. Heim, R., *Synthese und Pharmakologie Potenter 5-HT_{2A}Rezeptoragonisten mit N-2-Methoxybenzyl-Partialstruktur*. 2004, Freie Universität Berlin.
19. Braden, M.R., et al., *Molecular interaction of serotonin 5-HT_{2A} receptor residues Phe339 (6.51) and Phe340 (6.52) with super-potent N-benzyl phenethylamine agonists*. *Molecular Pharmacology*, 2006.

20. Papoutsis, I., et al., *25B-NBOMe and its precursor 2C-B: modern trends and hidden dangers*. Forensic Toxicology, 2015. **33**(1): p. 1-11.
21. Nichols, D.E., et al., *High specific activity tritium-labeled N-(2-methoxybenzyl)-2, 5-dimethoxy-4-iodophenethylamine (INBMeO): a high-affinity 5-HT 2A receptor-selective agonist radioligand*. Bioorganic & medicinal chemistry, 2008. **16**(11): p. 6116-6123.
22. Ettrup, A., et al., *Radiosynthesis and in vivo evaluation of a series of substituted 11 C-phenethylamines as 5-HT 2A agonist PET tracers*. European journal of nuclear medicine and molecular imaging, 2011. **38**(4): p. 681-693.
23. Ettrup, A., et al., *Radiosynthesis and evaluation of 11C-CIMBI-5 as a 5-HT2A receptor agonist radioligand for PET*. Journal of Nuclear Medicine, 2010. **51**(11): p. 1763.
24. Ettrup, A., et al., *Preclinical safety assessment of the 5-HT 2A receptor agonist PET radioligand [11 C] Cimbi-36*. Molecular imaging and biology, 2013. **15**(4): p. 376-383.
25. Tang, M., et al., *Two cases of severe intoxication associated with analytically confirmed use of the novel psychoactive substances 25B-NBOMe and 25C-NBOMe*. Clinical Toxicology, 2014. **52**(5): p. 561-565.
26. Rickli, A., et al., *Receptor interaction profiles of novel N-2-methoxybenzyl (NBOMe) derivatives of 2, 5-dimethoxy-substituted phenethylamines (2C drugs)*. Neuropharmacology, 2015. **99**: p. 546-553.
27. Shulgin, A. and A. Shulgin, *Pihkal: A Chemical Love Story*. 1991.
28. Zuba, D., K. Sekuła, and A. Buczek, *25C-NBOMe—new potent hallucinogenic substance identified on the drug market*. Forensic science international, 2013. **227**(1-3): p. 7-14.
29. Zuba, D. and K. Sekula, *Analytical characterization of three hallucinogenic N-(2-methoxy)benzyl derivatives of the 2C-series of phenethylamine drugs*. Drug Test Anal, 2013. **5**(8): p. 634-45.
30. Forrester, M.B., *NBOMe designer drug exposures reported to Texas poison centers*. Journal of addictive diseases, 2014. **33**(3): p. 196-201.
31. Lawn, W., et al., *The NBOMe hallucinogenic drug series: patterns of use, characteristics of users and self-reported effects in a large international sample*. Journal of Psychopharmacology, 2014. **28**(8): p. 780-788.
32. *25I-NBOMe, 25C-NBOMe, and 25B-NBOMe (Street names: N-bomb, Smiles, 25I, 25C, 25B)*. 2018 12-02-2018]; Available from: https://www.deadiversion.usdoj.gov/drug_chem_info/nbome.pdf.
33. *25C-NBOMe Critical Review Report*. 2014; Available from: https://www.who.int/medicines/areas/quality_safety/4_18_review.pdf.
34. *25B-NBOMe Critical Review Report*. 2014; Available from: https://www.who.int/medicines/areas/quality_safety/4_17_review.pdf.
35. *25I-NBOMe Critical Review Report*. 2014; Available from: https://www.who.int/medicines/areas/quality_safety/4_19_review.pdf.
36. *NBOMe Series Legal Status*. 2016 12-16-2018]; Available from: https://www.erowid.org/chemicals/nbome/nbome_law.shtml.
37. *EMCDDA—Europol Joint Report on a new psychoactive substance 4-iodo-2,5-dimethoxy-N-(2-methoxybenzyl)phenethylamine (25I-NBOMe)*. 2014; Available from: http://www.emcdda.europa.eu/system/files/publications/817/TDAS14003ENN_466654.pdf.
38. *Report on the risk assessment of 2-(4-iodo-2,5-dimethoxyphenyl)-N-(2-methoxybenzyl)ethanamine (25I-NBOMe) in the framework of the Council Decision on new psychoactive substances*. 2014; Available from: http://www.emcdda.europa.eu/system/files/publications/772/TDAK14001ENN_480887.pdf.
39. J. Lovett, C., et al., *Awareness and use of the NBOMe novel psychoactive substances is lower than those of mephedrone in a high drug using population*. Vol. 52. 2014. 361-361.
40. *Spotlight on NBOMes*, in *Erowid Extracts*. 2013, Erowid
41. Wood, D.M., et al., *Prevalence of use and acute toxicity associated with the use of NBOMe drugs*. Clin Toxicol (Phila), 2015. **53**(2): p. 85-92.

42. Kimmel, H.L., F.I. Carroll, and M.J. Kuhar, *Locomotor stimulant effects of novel phenyltropanes in the mouse*. Drug and alcohol dependence, 2001. **65**(1): p. 25-36.
43. Volkow, N., et al., *Imaging dopamine's role in drug abuse and addiction*. Neuropharmacology, 2009. **56**: p. 3-8.
44. Liechti, M.E., *Novel psychoactive substances (designer drugs): overview and pharmacology of modulators of monoamine signalling*. Swiss medical weekly, 2015. **145**: p. w14043.
45. Howell, L.L. and H.L. Kimmel, *Monoamine transporters and psychostimulant addiction*. Biochemical pharmacology, 2008. **75**(1): p. 196-217.
46. Koob, G.F. and N.D. Volkow, *Neurocircuitry of addiction*. Neuropsychopharmacology, 2010. **35**(1): p. 217.
47. Wee, S., et al., *Relationship between the serotonergic activity and reinforcing effects of a series of amphetamine analogs*. Journal of Pharmacology and Experimental Therapeutics, 2005. **313**(2): p. 848-854.
48. Juncosa, J.I., Jr., et al., *Extensive rigid analogue design maps the binding conformation of potent N-benzylphenethylamine 5-HT_{2A} serotonin receptor agonist ligands*. ACS Chem Neurosci, 2013. **4**(1): p. 96-109.
49. Hansen, M., et al., *Synthesis and structure–activity relationships of N-benzyl phenethylamines as 5-HT_{2A/2C} agonists*. ACS chemical neuroscience, 2014. **5**(3): p. 243-249.
50. Giulietti, M., et al., *How much do we know about the coupling of G-proteins to serotonin receptors?* Molecular Brain, 2014. **7**(1): p. 49.
51. Nichols, D.E. and C.D. Nichols, *Serotonin Receptors*. Chemical Reviews, 2008. **108**(5): p. 1614-1641.
52. Hansen, M., et al., *Synthesis and pharmacological evaluation of N-benzyl substituted 4-bromo-2, 5-dimethoxyphenethylamines as 5-HT_{2A/2C} partial agonists*. Bioorganic & medicinal chemistry, 2015. **23**(14): p. 3933-3937.
53. Glennon, R.A., et al., *Binding of phenylalkylamine derivatives at 5-HT_{1C} and 5-HT₂ serotonin receptors: evidence for a lack of selectivity*. Journal of medicinal chemistry, 1992. **35**(4): p. 734-740.
54. Heller, W.A. and J.M. Baraban, *Potent agonist activity of DOB at 5-HT₂ receptors in guinea pig trachea*. European journal of pharmacology, 1987. **138**(1): p. 115-117.
55. Sanders-Bush, E., K.D. Burris, and K. Knoth, *Lysergic acid diethylamide and 2, 5-dimethoxy-4-methylamphetamine are partial agonists at serotonin receptors linked to phosphoinositide hydrolysis*. Journal of Pharmacology and Experimental Therapeutics, 1988. **246**(3): p. 924-928.
56. Seggel, M.R., et al., *A structure-affinity study of the binding of 4-substituted analogs of 1-(2, 5-dimethoxyphenyl)-2-aminopropane at 5-HT₂ serotonin receptors*. Journal of medicinal chemistry, 1990. **33**(3): p. 1032-1036.
57. Barnett, G., M. Trsic, and R. Willette, *Progress with several models for the study of the SAR of hallucinogenic agents*. Quantitative Structure Activity Relationships of Analgesics, Narcotic Antagonists, and Hallucinogens, 1978: p. 159.
58. Klopman, G. and O.T. Macina, *Use of the computer automated structure evaluation program in determining quantitative structure-activity relationships within hallucinogenic phenylalkylamines*. Journal of theoretical biology, 1985. **113**(4): p. 637-648.
59. Thakur, M., A. Thakur, and P.V. Khadikar, *QSAR studies on psychotomimetic phenylalkylamines*. Bioorganic & medicinal chemistry, 2004. **12**(4): p. 825-831.
60. Neuvonen, K., H. Neuvonen, and F. Fülöp, *Effect of 4-substitution on psychotomimetic activity of 2, 5-dimethoxy amphetamines as studied by means of different substituent parameter scales*. Bioorganic & medicinal chemistry letters, 2006. **16**(13): p. 3495-3498.
61. Braden, M.R., *Towards a biophysical understanding of hallucinogen action*. 2007, Citeseer.
62. Silva, M.E., et al., *Theoretical studies on the interaction of partial agonists with the 5-HT_{2A} receptor*. Journal of computer-aided molecular design, 2011. **25**(1): p. 51-66.

63. Nichols, D.E., et al., *N-Benzyl-5-methoxytryptamines as potent serotonin 5-HT₂ receptor family agonists and comparison with a series of phenethylamine analogues*. ACS chemical neuroscience, 2015. **6**(7): p. 1165-1175.
64. Suzuki, J., et al., *Toxicities associated with NBOMe ingestion-a novel class of potent hallucinogens: a review of the literature*. Psychosomatics, 2015. **56**(2): p. 129-39.
65. Kelly, A., et al. *Case series of 25I-NBOMe exposures with laboratory confirmation*. in *Clinical Toxicology*. 2012. INFORMA HEALTHCARE 52 VANDERBILT AVE, NEW YORK, NY 10017 USA.
66. Rose, S.R., J.L. Poklis, and A. Poklis, *A case of 25I-NBOMe (25-I) intoxication: a new potent 5-HT_{2A} agonist designer drug*. Clin Toxicol (Phila), 2013. **51**(3): p. 174-7.
67. Rose, R.S., et al. *Severe poisoning following self-reported use of 25-I, a novel substituted amphetamine*. in *Clinical Toxicology*. 2012. INFORMA HEALTHCARE 52 VANDERBILT AVE, NEW YORK, NY 10017 USA.
68. Hill, S.L., et al., *Severe clinical toxicity associated with analytically confirmed recreational use of 25I-NBOMe: case series*. Clinical Toxicology, 2013. **51**(6): p. 487-492.
69. Stellpflug, S.J., et al., *2-(4-Iodo-2,5-dimethoxyphenyl)-N-[(2-methoxyphenyl)methyl]ethanamine (25I-NBOMe): clinical case with unique confirmatory testing*. J Med Toxicol, 2014. **10**(1): p. 45-50.
70. Poklis, J.L., et al., *Determination of 4-bromo-2,5-dimethoxy-N-[(2-methoxyphenyl)methyl]-benzeneethanamine (25B-NBOMe) in serum and urine by high performance liquid chromatography with tandem mass spectrometry in a case of severe intoxication*. Drug Test Anal, 2014. **6**(7-8): p. 764-9.
71. Poklis, J.L., D.J. Clay, and A. Poklis, *High-performance liquid chromatography with tandem mass spectrometry for the determination of nine hallucinogenic 25-NBOMe designer drugs in urine specimens*. Journal of analytical toxicology, 2014. **38**(3): p. 113-121.
72. Walterscheid, J.P., et al., *Pathological findings in 2 cases of fatal 25I-NBOMe toxicity*. Am J Forensic Med Pathol, 2014. **35**(1): p. 20-5.
73. Bersani, F.S., et al., *25C-NBOMe: preliminary data on pharmacology, psychoactive effects, and toxicity of a new potent and dangerous hallucinogenic drug*. BioMed Research International, 2014. **2014**.
74. Poklis, J.L., et al., *Identification of Metabolite Biomarkers of the Designer Hallucinogen 25I-NBOMe in Mouse Hepatic Microsomal Preparations and Human Urine Samples Associated with Clinical Intoxication*. J Anal Toxicol, 2015. **39**(8): p. 607-16.
75. Caspar, A.T., et al., *Studies on the metabolism and toxicological detection of the new psychoactive designer drug 2-(4-iodo-2,5-dimethoxyphenyl)-N-[(2-methoxyphenyl)methyl]ethanamine (25I-NBOMe) in human and rat urine using GC-MS, LC-MS(n), and LC-HR-MS/MS*. Anal Bioanal Chem, 2015. **407**(22): p. 6697-719.
76. Nielsen, L.M., et al., *Characterization of the hepatic cytochrome P450 enzymes involved in the metabolism of 25I-NBOMe and 25I-NBOH*. Drug Test Anal, 2017. **9**(5): p. 671-679.
77. Richter, L.H.J., H.H. Maurer, and M.R. Meyer, *New psychoactive substances: Studies on the metabolism of XLR-11, AB-PINACA, FUB-PB-22, 4-methoxy-alpha-PVP, 25-I-NBOMe, and meclonazepam using human liver preparations in comparison to primary human hepatocytes, and human urine*. Toxicol Lett, 2017. **280**: p. 142-150.
78. Leth-Petersen, S., et al., *Metabolic Fate of Hallucinogenic NBOMes*. Chem Res Toxicol, 2016. **29**(1): p. 96-100.
79. Boumrah, Y., et al., *In vitro characterization of potential CYP- and UGT-derived metabolites of the psychoactive drug 25B-NBOMe using LC-high resolution MS*. Drug Test Anal, 2016. **8**(2): p. 248-56.
80. Soh, Y.N. and S. Elliott, *An investigation of the stability of emerging new psychoactive substances*. Drug Test Anal, 2014. **6**(7-8): p. 696-704.

81. Temporal, K.H., et al., *Metabolic Profile Determination of NBOMe Compounds Using Human Liver Microsomes and Comparison with Findings in Authentic Human Blood and Urine*. J Anal Toxicol, 2017. **41**(7): p. 646-657.
82. Grafinger, K.E., et al., *In vitro phase I metabolism of three phenethylamines 25D-NBOMe, 25E-NBOMe and 25N-NBOMe using microsomal and microbial models*. Drug Test Anal, 2018. **10**(10): p. 1607-1626.
83. Caspar, A.T., et al., *Metabolic fate and detectability of the new psychoactive substances 2-(4-bromo-2,5-dimethoxyphenyl)-N-[(2-methoxyphenyl)methyl]ethanamine (25B-NBOMe) and 2-(4-chloro-2,5-dimethoxyphenyl)-N-[(2-methoxyphenyl)methyl]ethanamine (25C-NBOMe) in human and rat urine by GC-MS, LC-MS(n), and LC-HR-MS/MS approaches*. J Pharm Biomed Anal, 2017. **134**: p. 158-169.
84. Seo, H., et al., *Metabolic profile determination of 25N-NBOMe in human liver microsomes by liquid chromatography-quadrupole time-of-flight mass spectrometry*. Int J Legal Med, 2018.
85. Wohlfarth, A., et al., *25C-NBOMe and 25I-NBOMe metabolite studies in human hepatocytes, in vivo mouse and human urine with high-resolution mass spectrometry*. Drug Test Anal, 2017. **9**(5): p. 680-698.
86. Andreasen, M.F., et al., *A fatal poisoning involving 25C-NBOMe*. Forensic science international, 2015. **251**: p. e1-e8.
87. Caspar, A.T., et al., *LC-high resolution-MS/MS for identification of 69 metabolites of the new psychoactive substance 1-(4-ethylphenyl)-N-[(2-methoxyphenyl)methyl]propane-2-amine (4-EA-NBOMe) in rat urine and human liver S9 incubates and comparison of its screening power with further MS techniques*. Analytical and bioanalytical chemistry, 2018. **410**(3): p. 897-912.
88. Leth-Petersen, S., et al., *Correlating the metabolic stability of psychedelic 5-HT 2A agonists with anecdotal reports of human oral bioavailability*. Neurochemical research, 2014. **39**(10): p. 2018-2023.
89. Davies, B. and T. Morris, *Physiological parameters in laboratory animals and humans*. Pharmaceutical research, 1993. **10**(7): p. 1093-1095.
90. Sekuła, K. and D. Zuba, *Structural elucidation and identification of a new derivative of phenethylamine using quadrupole time-of-flight mass spectrometry*. Rapid Communications in Mass Spectrometry, 2013. **27**(18): p. 2081-2090.
91. Pasin, D., S. Bidny, and S. Fu, *Analysis of new designer drugs in post-mortem blood using high-resolution mass spectrometry*. Journal of analytical toxicology, 2014. **39**(3): p. 163-171.
92. Armenian, P. and R.R. Gerona, *The electric Kool-Aid NBOMe test: LC-TOF/MS confirmed 2C-C-NBOMe (25C) intoxication at Burning Man*. Am J Emerg Med, 2014. **32**(11): p. 1444.e3-5.
93. Neto, J.C., *Rapid detection of NBOMe's and other NPS on blotter papers by direct ATR-FTIR spectrometry*. Forensic science international, 2015. **252**: p. 87-92.
94. Shipman, R., et al., *Forensic Drug Identification by Gas Chromatography-Infrared Spectroscopy*. 2013: Vermont Forensic Laboratory Waterbury, USA.
95. *25B-NBOMe monograph*. 2013 03-04-2019]; Available from: <http://www.swgdrug.org/monographs/25b-nbome.pdf>.
96. *25I-NBOMe monograph*. 2013 03-04-2019]; Available from: <http://www.swgdrug.org/monographs/25i-nbome.pdf>.
97. Casale, J.F. and P.A. Hays, *Characterization of eleven 2, 5-dimethoxy-N-(2-methoxybenzyl)phenethylamine (NBOMe) derivatives and differentiation from their 3-and 4-methoxybenzyl analogues—part I*. Microgram Journal, 2012. **9**(2): p. 84-109.
98. Al-Hossaini, A.M., et al., *GC-MS and GC-IRD analysis of ring and side chain regioisomers of ethoxyphenethylamines related to the controlled substances MDEA, MDMMA and MBDB*. Forensic science international, 2010. **200**(1-3): p. 73-86.
99. Kempfert, K., *Forensic drug analysis by GC/FT-IR*. Applied Spectroscopy, 1988. **42**(5): p. 845-849.

100. Awad, T., et al., *Comparison of GC–MS and GC–IRD methods for the differentiation of methamphetamine and regioisomeric substances*. Forensic science international, 2009. **185**(1-3): p. 67-77.
101. Westphal, F., U. Girreser, and D. Waldmüller, *Analytical characterization of four new ortho-methoxybenzylated amphetamine-type designer drugs*. Drug testing and analysis, 2016. **8**(9): p. 910-919.
102. Lee, G.S., et al., *High-resolution solid state ¹³C nuclear magnetic resonance spectra of 3, 4-methylenedioxyamphetamine hydrochloride and related compounds and their mixtures with lactose*. Solid state nuclear magnetic resonance, 2000. **16**(4): p. 225-237.
103. Alotaibi, M.R., S.M. Husbans, and I.S. Blagbrough, *¹H, ¹³C, ¹⁵N HMBC, and ¹⁹F NMR spectroscopic characterisation of seized flephedrone, cut with benzocaine*. Journal of pharmaceutical and biomedical analysis, 2015. **107**: p. 535-538.
104. Zhong, Y., et al., *The Application of a Desktop NMR Spectrometer in Drug Analysis*. International journal of analytical chemistry, 2018. **2018**.
105. Dawson, B., *Nuclear Magnetic Resonance Spectroscopy for the Detection and Quantification of Abused Drugs*. Encyclopedia of Analytical Chemistry: Applications, Theory and Instrumentation, 2006.
106. Burns, D.T., R.J. Lewis, and P. Stevenson, *Determination of 3, 4-methylenedioxyamphetamine analogues (“ecstasy”) by proton nuclear magnetic resonance spectrometry*. Analytica chimica acta, 1997. **339**(3): p. 259-263.
107. Hays, P.A. and J.F. Casale, *Characterization of Eleven 2,5-Dimethoxy-N-(2-methoxybenzyl)phenethylamine (NBOMe) Derivatives and Differentiation from their 3- and 4-Methoxybenzyl Analogues - Part II*. Microgram Journal, 2014. **11**(1-4): p. 3-22.
108. Liu, C., et al., *Identification of five substituted phenethylamine derivatives 5-MAPDB, 5-AEDB, MDMA methylene homolog, 6-Br-MDMA, and 5-APB-NBOMe*. Drug testing and analysis, 2017. **9**(2): p. 199-207.
109. Shevyrin, V., et al., *Mass spectrometric properties of N-(2-methoxybenzyl)-2-(2, 4, 6-trimethoxyphenyl) ethanamine (2, 4, 6-TMPEA-NBOMe), a new representative of designer drugs of NBOMe series and derivatives thereof*. Journal of Mass Spectrometry, 2016. **51**(10): p. 969-979.
110. Glennon, R.A., et al., *Behavioral and serotonin receptor properties of 4-substituted derivatives of the hallucinogen 1-(2, 5-dimethoxyphenyl)-2-aminopropane*. Journal of medicinal chemistry, 1982. **25**(10): p. 1163-1168.
111. Wing-Wah, S., *Iodination of methoxyamphetamines with iodine and silver sulfate*. Tetrahedron letters, 1993. **34**(39): p. 6223-6224.
112. Roth, B., *National Institute of Mental Health’s Psychoactive Drug Screening Program (NIMH PDSP)*. Assay protocol book, Department of Pharmacology, University of North Carolina at Chapel Hill, Chapel Hill, NC.